

REVIEW



Guidelines for the use and interpretation of assays for monitoring autophagy (4th edition)[†]

- Daniel J. Klionsky^{1,2}, Amal Kamal Abdel-Aziz²³⁶¹, Sara Abdelfatah⁵³⁶, Mahmoud Abdellatif¹⁷⁸⁸, Asghar Abdoli²⁴⁰⁸,
5 Steffen Abel³, Hagai Abeliovich⁴, Marie H Abildgaard^{621,2346}, Yakubu Princely Abudu¹⁰⁵³, Abraham Acevedo-Arozena⁵,
Iannis E Adamopoulos⁶, Khosrow Adeli⁷, Timon E. Adolph⁹, Annagrazia Adornetto¹⁰, Elma Aflaki¹¹, Galila Agam¹²,
Anupam Agarwal¹³, Bharat Aggarwal¹⁴, Maria Agnello¹⁵, Patrizia Agostinis¹⁶, Javed N Agrewala¹⁷, Alexander Agrotis¹⁸,
Patricia Aguilar¹⁹, S Tariq Ahmad²⁰, Zubair M. Ahmed²¹, Ulises Ahumada-Castro^{264,2347}, Sonja Aits²¹, Shu Aizawa²²,
Yunus Akkoc⁷⁰², Tonia Akoumianaki^{306,2348}, Hafize Aysin Akpinar²³, Ahmed M Al-Abd²⁴, Lina Al-Akra¹⁶⁵⁸, Abeer Al-
10 Gharaibeh²⁵, Moulay A. Alaoui-Jamali²⁶, Simon Alberti²⁷, Elísabet Alcocer-Gómez²⁸, Cristiano Alessandri²⁹,
Muhammad Ali¹⁶⁵⁴, Md Abdul Alim Al-Bari³⁰, Saeb Aliwaini³¹, Javad Alizadeh³², Eugènia Almacellas³³,
Alexandru Almasan³⁴, Alicia Alonso³⁵, Guillermo D Alonso³⁶, Nihal Altan-Bonnet³⁷, Dario C Altieri³⁸, Élide Álvarez³⁹,
Cristine Alves da Costa⁴⁰, Mazen Alzaharna⁴¹, Marialaura Amadio⁴², Consuelo Amantini⁴³, Cristina Amaral⁴⁴,
Susanna Ambrosio⁴⁵, Amal Amer⁴⁶, Veena Ammanathan⁴⁷, Zhenyi An⁴⁸, Stig Andersen⁴⁹, Sabrina Angelini⁵⁰,
15 Shaida Andrabi⁵¹, Magaiver Andrade-Silva^{257,2349}, Allen M Andres¹⁹⁴⁹, David K Ann⁵², Uche C. Anozie⁵³,
Mohammad Y. Ansari⁵⁴, Pedro Antas⁵⁵, Adam Antebi⁵⁶, Zuriñe Anton⁵⁷, Tahira Anwar⁵⁸, Lionel Apetoh⁵⁹,
Nadezda Apostolova⁶⁰, Toshiyuki Araki⁶¹, Yasuhiro Araki⁶², Kohei Arasaki⁶³, Wagner L. Araújo⁶⁴, Jun Araya⁶⁵,
Catherine Arden⁶⁶, Esperanza Arias⁶⁷, Hirokazu Arimoto⁶⁸, Aileen Ariosa⁶⁹, Maria Angeles Arevalo⁷⁰,
Sandro Arguelles⁷¹, Jyothi Arikath⁷², Darius Armstrong-James⁷³, Laetitia Arnauné-Pelloquin⁷⁴, Angeles Aroca⁷⁵,
20 Daniela S Arroyo⁷⁶, Ivica Arsov⁷⁷, Rubén Artero⁷⁸, Dalia Maria Lucia Asaro⁷⁹, Michael Aschner⁸⁰, Milad Ashrafizadeh⁸¹,
Osnat Ashur-Fabian⁸², Atanas G Atanasov⁸³, Alicia K. Au⁸⁴, Patrick Auberger⁸⁵, Holger W Auner⁸⁶, Laure Aurelian⁸⁷,
Riccardo Autelli⁸⁸, Laura Avagliano⁸⁹, Yennifer Ávalos⁹⁰, Sanja Aveic⁹¹, Tamar Avin-Wittenberg⁹², Yucel Aydin⁹³,
Scott Ayton⁹⁴, Srinivas Ayyadevara⁹⁵, Maria Azzopardi⁹⁶, Misuzu Baba⁹⁷, Jonathan M Backer⁹⁸, Steven Backues⁹⁹, Dong-
Hun Bae¹⁰⁰, Ok-Nam Bae¹⁰¹, Soo Han Bae¹⁰², Eric Baehrecke¹⁰³, Ahruem Baek¹⁰⁴, Seung-Hoon Baek¹⁰⁵, Sung Hee Baek¹⁰⁶,
25 Giacinto Bagetta¹⁰⁷, Agnieszka Bagniewska-Zadworna¹⁰⁸, Hua Bai¹⁰⁹, Jie Bai¹¹⁰, Xiyuan Bai¹¹¹, Yidong Bai¹¹²,
Nandadulal Bairagi¹¹³, Shounak Baksi¹¹⁴, Teresa Balbi¹¹⁵, Cosima T Baldari¹¹⁶, Walter Balduini¹¹⁷, Andrea Ballabio¹¹⁸,
Maria Ballester¹¹⁹, Salma Balazadeh¹²⁰, Rena Balzan¹²¹, Rina Bandopadhyay¹²², Sreeparna Banerjee¹²³,
Sulagna Banerjee¹²⁴, Yan Bao¹²⁵, Ágnes Bánréti¹²⁶, Mauricio S Baptista¹²⁷, Alessandra Baracca¹²⁸, Cristiana Barbati¹²⁹,
Ariadna Bargiela¹³⁰, Daniela Barilà¹³¹, Peter G. Barlow¹³², Sami Barmada¹³³, Esther Barreiro¹³⁴, George E. Barreto¹³⁵,
30 Jiri Bartek¹³⁶, Bonnie Bartel¹³⁷, Alberto Bartolome¹³⁸, Gaurav R. Barve¹³⁹, Suresh Basagoudanavar¹⁴⁰, Diane C Bassham¹⁴¹,
Robert C Jr Bast¹⁴², Alakananda Basu¹⁴³, Henri Batoko¹⁴⁴, Isabella Batten¹⁴⁵, Etienne E. Baulieu¹⁴⁶, Bradley Baumgarner¹⁴⁷,
Jagadeesh Bayry¹⁴⁸, Rupert Beale¹⁴⁹, Isabelle Beau¹⁵⁰, Florian Beaumatin¹⁵¹, Luiz Bechara¹⁵², George Beck¹⁵³,
Michael Beers¹⁵⁴, Jakob Begun¹⁵⁵, Georg M. N. Behrens¹⁵⁶, Christian Behrends¹⁵⁷, Christian Behl¹⁵⁸, Roberto Bei¹⁵⁹,
Eloy Bejarano¹⁶⁰, Shai Bel¹⁶¹, Amine Belaid¹⁶², Naïma Belgareh-Touzé¹⁶³, Cristina Bellarosa¹⁶⁴, Francesca Belleudi¹⁶⁵,
35 Melissa Belló Pérez¹⁶⁶, Raquel Bello-Morales¹⁶⁷, Jackeline Soares de Oliveira Beltran¹⁶⁸, Sebastián Beltran¹⁶⁹,
Doris Mangiaracina Benbrook¹⁷⁰, Mykolas Bendorius¹⁷¹, Bruno A. Benitez¹⁷², Irene Benito-Cuesta¹⁷³, Julien Bensalem¹⁷⁴,
Martin W. Berchtold¹⁷⁵, Sabina Berezowska¹⁷⁶, Matteo Bergami¹⁷⁷, Daniele Bergamaschi¹⁷⁸, Andreas Bergmann¹⁷⁹,
Laura Berliocchi¹⁸⁰, Clarisse Berlioz-Torrent¹⁸¹, Amelie Bernard¹⁸², Lionel Berthoux¹⁸³, Cagri Besirli¹⁸⁴, Sebastien Besteiro¹⁸⁵,
Virginie Betin¹⁸⁶, Rudi Beyaert¹⁸⁷, Bezbradica. Jelena¹⁸⁸, Kiran Bhaskar¹⁸⁹, Ingrid Bhatia-Kissova¹⁹⁰, Resham Bhattacharya¹⁹¹,
40 Sujoy Bhattacharya¹⁹², Shalmoli Bhattacharyya¹⁹³, Md Shenuarin Bhuiyan¹⁹⁴, Sujit Kumar Bhutia¹⁹⁵, Ianrong Bi¹⁹⁶,
Xiaolin Bi¹⁹⁷, Trevor J Biden¹⁹⁸, Krikor Bijian¹⁹⁹, Viktor A. Billes²⁰⁰, Nadine Binart²⁰¹, Claudia Bincotto²⁰²,
Asa Birna Birgisdottir²⁰³, Geir Bjorkoy²⁰⁴, Gonzalo Blanco²⁰⁵, Ana Blas-Garcia²⁰⁶, Janusz Blasiak²⁰⁷, Robert Blomgran²⁰⁸,
Klas Blomgren²⁰⁹, Janice. S Blum²¹⁰, Emilio Boada-Romero²¹¹, Mirta Boban²¹², K Boesze-Battaglia²¹³, Philippe Boeuf²¹⁴,
Barry Boland²¹⁵, Pascale Bomont²¹⁶, Paolo Bonaldo²¹⁷, Srinivasa Reddy Bonam²¹⁸, Laura Bonfili²¹⁹, Juan S. Bonifacino²²⁰,
45 Brian A Boone²²¹, Martin Bootman²²², Matteo Bordini²²³, Christoph Borner²²⁴, Beat Bornhauser²²⁵, Gautam Borthakur²²⁶,
Jurgen Bosch²²⁷, Santanu Bose²²⁸, Chantal M Boulanger²²⁹, Michael E Boulton²³⁰, Guilhem Bousquet²³¹, Luis M. Botana²³²,
Juan Botas²³³, Mathieu Bourdenx²³⁴, Benjamin Bourgeois²³⁵, Nollaig M. Bourke²³⁶, Patricia Boya²³⁷, Peter V. Bozhkov²³⁸,
Luiz H. M. Bozi²³⁹, Tolga O Bozkurt²⁴⁰, Doug E Brackney²⁴¹, Beate Brand-Saberi²⁴², Christian Brandts²⁴³, Ralf Braun²⁴⁴,
Gerhard H. Braus²⁴⁵, Roberto Bravo-Sagua²⁴⁶, Patrick Brest²⁴⁷, Marie-Agnès Bringer²⁴⁸, Alfredo Briones-Herrera²⁴⁹,
50 V. Courtney Broadbudd²⁵⁰, Peter Brodersen²⁵¹, Jeffrey L Brodsky²⁵², Steven L Brody²⁵³, Paola G Bronson²⁵⁴, Jeff Bronstein²⁵⁵,
Carolyn N. Brown²⁵⁶, Rhoderick E Brown²⁵⁷, Patricia C. Brum²⁵⁸, John H Brumell²⁵⁹, Nicola Brunetti-Pierri²⁶⁰

- Daniele Bruno¹⁹⁵², Robert James Bryson-Richardson²²⁴, Cecilia Bucci²²⁵, Shilpa Buch²²⁶, J Ross Buchan²²⁷,
 Carmen Buchrieser²²⁸, Erin M Buckingham²²⁹, Hikmet Budak²³⁰, Mauricio Budini²³¹, Marta Bueno²³², Laura Elisa Buitrago-
 Molina²³³, Geert Bultynck²³⁴, Florin Burada²³⁵, Simone Buraschi²³⁶, Joseph Burgoyne²³⁷, M. Isabel Burón²³⁸, Victor Bustos²³⁹,
 55 Sabrina Büttner²⁴⁰, Elena Butturini²⁴¹, Aaron Byrd²⁴², Isabel Cabas²⁴³, Sandra Cabrera-Benitez²⁴⁴, Ken Cadwell²⁴⁵,
 Jose Calbet²⁴⁶, Ilaria Campesi²⁴⁷, Barbara Canonico²⁴⁸, Jingjing Cai²⁴⁹, Lu Cai²⁵⁰, Qian Cai²⁵¹, Montserrat Cairó²⁵²,
 Guy Caldwell²⁵³, Kim A. Caldwell²⁵⁴, Jarrod A. Call²⁵⁵, Riccardo Calvani²⁵⁶, Ana C. Calvo²⁵⁷, Miguel Calvo-Rubio Barrera²⁵⁸,
 Niels Camara²⁵⁹, Jacques H Camonis²⁶⁰, Nadine Camougrand²⁶¹, Michelangelo Campanella²⁶², Edward M Campbell²⁶³,
 Francois-Xavier Campbell-Valois²⁶⁴, Silvia Campello²⁶⁵, Juliane C. Campos²⁶⁶, Olivier Camuzard²⁶⁷, Jorge Cancino²⁶⁸,
 60 Danilo Candido de Almeida²⁶⁹, Laura Canesi²⁷⁰, Isabella Caniggia²⁷¹, Carles Canti²⁷², Bin Cao²⁷³, Beatriz Caramés²⁷⁴,
 Evie H Carchman²⁷⁵, Elena Cardenal-Muñoz²⁷⁶, Cesar Cardenas²⁷⁷, Luis Cardenas²⁷⁸, Sandra M. Cardoso²⁷⁹,
 Jennifer S. Carew²⁸⁰, Michele Caraglia²⁸¹, Georges F. Carle²⁸², Gillian Carleton²⁸³, Silvia Carloni²⁸⁴, Didac Carmona-
 Gutierrez²⁸⁵, Julian M. Carosi²⁸⁶, Oliana Carnevali²⁸⁷, Leticia A. Carneiro²⁸⁸, Serena Carra²⁸⁹, Alice Carrier²⁹⁰,
 Lucie Carrier²⁹¹, Bernadette Carroll²⁹², A Brent Carter²⁹³, Andreia Neves Carvalho²⁹⁴, Caty Casas²⁹⁵, Josefina Casas²⁹⁶,
 65 Magali Casanova²⁹⁷, Chiara Cassioli²⁹⁸, Eliseo F Castillo²⁹⁹, Karen Castillo³⁰⁰, Sonia Castillo-Lluva³⁰¹, Francesca Castoldi³⁰²,
 Ariel F Castro³⁰³, Margarida Castro-Caldas³⁰⁴, Javier Castro-Hernandez³⁰⁵, Susana Castro-Obregon³⁰⁶, Marco Castori³⁰⁷,
 Sergio D Catz³⁰⁸, Claudia Cavadas³⁰⁹, Federica Cavaliere³¹⁰, Gabriella Cavallini³¹¹, Maria Cavinato³¹², Maria L. Cayuela³¹³,
 Paula Cebollada Rica³¹⁴, Valentina Cecarini³¹⁵, Francesco Cecconi³¹⁶, Marzanna Cechowska-Pasko³¹⁷, Simone Cenci³¹⁸,
 Victòria Ceperuelo-Mallafre³¹⁹, Joao Jose Cerqueira³²⁰, Janete Maria Cerutti³²¹, Davide Cervia³²², Vildan Cetintas³²³,
 70 Silvia Cetrullo³²⁴, Han-Jung Chae³²⁵, Andrei S Chagin³²⁶, Chee-Yin Chai³²⁷, Gopal Chakrabarti³²⁸, Oishee Chakrabarti³²⁹,
 Tapas Chakraborty³³⁰, Trinad Chakraborty³³¹, Mounia Chami³³², Georgios Chamilos³³³, Tracey Chapman³³⁴,
 David W Chan³³⁵, Edmond Y. W. Chan³³⁶, Edward D. Chan³³⁷, Helen H. Chan³³⁸, Ho Yin Edwin Chan³³⁹, Hung Chan³⁴⁰,
 Matthew T V Chan³⁴¹, Partha K Chandra³⁴², Chih-Peng Chang³⁴³, Chunmei Chang³⁴⁴, Hao-Chun Chang³⁴⁵, Kai Chang³⁴⁶,
 Jie Chao³⁴⁷, Nicolas Charlet-Berguerand³⁴⁸, Samrat Chatterjee³⁴⁹, Shail K Chaube³⁵⁰, Anu Chaudhary³⁵¹, Edward Chaum³⁵²,
 75 Santosh Chauhan³⁵³, Frédéric Checler³⁵⁴, Michael Cheetham³⁵⁵, Chang-Shi Chen³⁵⁶, Guang-Chao Chen³⁵⁷, Jianfu Chen³⁵⁸,
 Leilei Chen³⁵⁹, Liam Chen³⁶⁰, Lin Chen³⁶¹, Mingliang Chen³⁶², Mu-Kuan Chen³⁶³, Ning Chen³⁶⁴, Quan Chen³⁶⁵, Ruey-
 Hwa Chen³⁶⁶, Shi Chen³⁶⁷, Wei Chen³⁶⁸, Weiqiang Chen³⁶⁹, Xin-Ming Chen³⁷⁰, Xiong-Wen Chen³⁷¹, Xu Chen³⁷², Yan Chen³⁷³,
 Ye-Guang Chen³⁷⁴, Yingyu Chen³⁷⁵, Yongqiang Chen³⁷⁶, Yu-Jen Chen³⁷⁷, Yue-Qin Chen³⁷⁸, Z. Stephen Chen³⁷⁹, Zhi Chen³⁸⁰,
 Zhi-Hua Chen³⁸¹, Zhijian J Chen³⁸², Zhixiang Chen³⁸³, Zhong Chen³⁸⁴, Hanhua Cheng³⁸⁵, Jun Cheng³⁸⁶, Shi-Yuan Cheng³⁸⁷,
 80 Wei Cheng³⁸⁸, Xiaodong Cheng³⁸⁹, Xiu-Tang Cheng³⁹⁰, Yiyun Cheng³⁹¹, Zhiyong Cheng³⁹², Heesun Cheong³⁹³,
 Jit K. Cheong³⁹⁴, Boris V Chernyak³⁹⁵, Sara Cherry³⁹⁶, Chun Hei Antonio Cheung³⁹⁷, Chi Fai Randy Cheung³⁹⁸, King-
 Ho Cheung³⁹⁹, Eric Chevet⁴⁰⁰, Richard Chi⁴⁰¹, Alan K S Chiang⁴⁰², Ferdinando Chiaradonna⁴⁰³, Roberto Chiarelli⁴⁰⁴,
 Mario Chiariello⁴⁰⁵, Nathalia Chica⁴⁰⁶, Susanna Chiocca⁴⁰⁷, Mario Chiong⁴⁰⁸, Shih-Hwa Chiou⁴⁰⁹, Abhilash I Chiramel⁴¹⁰,
 Valerio Chiurchiù⁴¹¹, Dong-Hyung Cho⁴¹², Seong-Kyu Choe⁴¹³, Augustine M. K. Choi⁴¹⁴, Mary E Choi⁴¹⁵,
 85 Kamalika Roy Choudhury⁴¹⁶, NORMAN STEVEN CHOW⁴¹⁷, Charleen Chu⁴¹⁸, Jason P Chua⁴¹⁹, John J.E. Chua⁴²⁰,
 Hyewon Chung⁴²¹, Kin Pan Chung⁴²², Seockhoon Chung⁴²³, So-Hyang Chung⁴²⁴, Yuen-Li Chung⁴²⁵,
 Valentina Cianfanelli⁴²⁶, Iwona Anna Ciechomska⁴²⁷, Mariana Cifuentes⁴²⁸, Laura Cinque⁴²⁹, Sebahattin Cirak⁴³⁰,
 Mara Cirone⁴³¹, Michael J Clague⁴³², Robert Clarke⁴³³, Emilio Clementi⁴³⁴, Eliana Coccia⁴³⁵, Patrice Codogno⁴³⁶,
 Ehud Cohen⁴³⁷, Mickael M. Cohen⁴³⁸, Tania Colasanti⁴³⁹, Fiorella Colasuonno⁴⁴⁰, Robert A. Colbert⁴⁴¹, Anna Colell⁴⁴²,
 90 Nuria Coll⁴⁴³, Lucy M Collins⁴⁴⁴, Mark O Collins⁴⁴⁵, Miodrag Colic⁴⁴⁶, Maria Isabel Colombo⁴⁴⁷, Daniel Colon-Ramos⁴⁴⁸,
 Lydie Combaret⁴⁴⁹, Sergio Comincini⁴⁵⁰, Marcia Regina Cominetti⁴⁵¹, Antonella Consiglio⁴⁵², Andrea Conte⁴⁵³,
 Fabrizio Conti⁴⁵⁴, Viorica Raluca Contu⁴⁵⁵, Kevin M Coombs⁴⁵⁶, Mark R Cookson⁴⁵⁷, Isabelle Coppens⁴⁵⁸,
 Maria Tiziana Corasaniti⁴⁵⁹, Nils Cordes⁴⁶⁰, Dale P. Corkery⁴⁶¹, Katia Cortese⁴⁶², Maria do Carmo Costa⁴⁶³,
 Sarah Costantino⁴⁶⁴, Paola Costelli⁴⁶⁵, Ana Coto-Montes⁴⁶⁶, Peter Crack⁴⁶⁷, Jose L Crespo⁴⁶⁸, Valeria Crippa⁴⁶⁹,
 95 Alfredo Criollo⁴⁷⁰, Riccardo Cristofani⁴⁷¹, Tamas Csizmadia⁴⁷², Antonio Cuadrado⁴⁷³, Bing Cui⁴⁷⁴, Jun Cui⁴⁷⁵,
 Yixian Cui⁴⁷⁶, Yong Cui⁴⁷⁷, Emmanuel Culetto⁴⁷⁸, Andrea C Cumino⁴⁷⁹, Andrey V. Cybulsky⁴⁸⁰, Mark J Czaja⁴⁸¹,
 Stanislaw J Czuczwar⁴⁸², Stefania D'Adamo⁴⁸³, Marcello D'Amelio⁴⁸⁴, Daniela D Arcangelo⁴⁸⁵, Andrew C. D Lugos⁴⁸⁶,
 Gabriella D'Orazi⁴⁸⁷, James A. da Silva⁴⁸⁸, Hormos Dafsari⁴⁸⁹, Ruben K. Dagda⁴⁹⁰, Yasin Dagdas⁴⁹¹, Maria Daglia⁴⁹²,
 Xiaoxia Dai⁴⁹³, Yun Dai⁴⁹⁴, Yuyuan Dai⁴⁹⁵, Jessica Dal Col⁴⁹⁶, Paul Dalhaimer⁴⁹⁷, Luisa Dalla Valle⁴⁹⁸, Tobias Dallenga⁴⁹⁹,
 100 Guillaume Dalmasso⁵⁰⁰, Markus Damme⁵⁰¹, Ilaria Dando⁵⁰², Nico Dantuma⁵⁰³, April Darling⁵⁰⁴, Hiranmoy Das⁵⁰⁵,
 Srinivasan Dasarathy⁵⁰⁶, Santosh K. Dasari⁵⁰⁷, Srikanta Dash⁵⁰⁸, Oliver Daumke⁵⁰⁹, Adrian N Dauphinee⁵¹⁰,
 Jeffery S Davies⁵¹¹, Valeria A. Dávila⁵¹², Roger J Davis⁵¹³, Tanja Davis⁵¹⁴, Sharadha Dayalan Naidu⁵¹⁵,
 Francesca De Amicis⁵¹⁶, Brian J DeBosch⁵¹⁷, Karolien De Bosscher⁵¹⁸, Francesca De Felice⁵¹⁹, Lucia De Franceschi⁵²⁰,
 Chiara De Leonibus⁵²¹, Mayara G. de Mattos Barbosa⁵²², Guido R.Y. De Meyer⁵²³, Angelo De Milito⁵²⁴,
 105 Cosimo De Nunzio⁵²⁵, Clara De Palma⁵²⁶, Mauro De Santi⁵²⁷, Claudio De Virgilio⁵²⁸, Daniela De Zio⁵²⁹, Jean-
 Paul Decuypere⁵³⁰, Jayanta Debnath⁵³¹, Mark A. Deehan⁵³², Gianluca Deflorian⁵³³, James DeGregori⁵³⁴,
 Benjamin Dehay⁵³⁵, Gabriel Del Rio⁵³⁶, Joe Ryan Delaney⁵³⁷, Lea M. D. Delbridge⁵³⁸, Elizabeth Delorme-Axford⁵³⁹,
 M Victoria Delpino⁵⁴⁰, Francesca Demarchi⁵⁴¹, Vilma Dembitz⁵⁴², Nicholas D. Demers⁵⁴³, Hongbin Deng⁵⁴⁴,
 Zhiqiang Deng⁵⁴⁵, Jorn Dengjel⁵⁴⁶, Paul Dent⁵⁴⁷, Donna Denton⁵⁴⁸, Melvin L DePamphilis⁵⁴⁹, Channing J Der⁵⁵⁰,

- 110 Vojo Deretic⁴⁷⁵, Laura Devis¹¹⁹⁴, Sushil Devkota⁴⁷⁶, Albert Descoteaux⁴⁷⁷, Olivier Devuyst⁴⁷⁸, Grant Dewson⁴⁷⁹, Mahendiran Dharmasivam¹⁶⁵⁸, Rohan Dhiman¹⁶⁸, Diego di Bernardo^{618 2362}, Manlio Di Cristina⁴⁸⁰, Fabio Di Domenico⁴⁸¹, Pietro Di Fazio⁴⁸², Alessio Di Fonzo⁴⁸³, Giovanni Di Guardo⁴⁸⁴, Gianni M. Di Guglielmo⁴⁸⁵, Luca Di Leo⁴⁵⁹, Chiara Di Malta^{618 2363}, Alessia Di Nardo⁴⁸⁶, Martina Di Rienzo^{602 2364}, Federica Di Sano²⁵⁵, George Diallinas⁴⁸⁷, Jiajie Diao⁴⁸⁸, Guillermo Diaz-Araya⁴⁸⁹, Inés Díaz-Laviada¹⁶⁷¹, Jared M. Dickinson⁴⁹⁰, Marc Diederich⁴⁹¹, Mélanie Dieudé⁴⁹², Jelena Dinic⁴⁹³, Miroslav Dinic⁴⁹⁴, Ivan Dikic⁴⁹⁵, Albena T. Dinkova-Kostova⁴⁹⁶, Shiping Ding⁴⁹⁷, Wen-Xing Ding⁴⁹⁸, Luciana Dini⁴⁹⁹, Marc S Dionne⁵⁰⁰, Jorg HW Distler⁵⁰¹, Abhinav Diwan⁵⁰², Ian M C Dixon⁵⁰³, Mojgan Djavaheri-Mergny⁵⁰⁴, Ina Dobrinski⁵⁰⁵, Oxana Dobrovinskaya⁵⁰⁶, Radek Dobrowolski⁵⁰⁷, Renwick Cj Dobson⁵⁰⁸, Jelena Đokic⁵⁰⁹, Serap Dokmeci Emre⁵¹⁰, Massimo Donadelli¹²⁷³, Bo Dong⁵¹¹, Charlie Dong⁵¹², Xiaonan Dong^{1108 2365}, Zhiwu Dong⁵¹³, Gerald W 2nd Dorn⁵¹⁴, Volker Dotsch⁵¹⁵, Huan Dou⁵¹⁶, Juan Dou⁵¹⁷, Moataz Dowaidar⁵¹⁸, Sami Dridi⁵¹⁹, Liat Drucker⁵²⁰, Ailian Du⁵²¹, Caigan Du⁵²², Guangwei Du⁵²³, Hai-Ning Du⁵²⁴, Li-Lin Du⁵²⁵, André du Toit⁵⁵⁷, Shao-Bin Duan⁵²⁶, Xiaoqiong Duan⁵²⁷, Sónia P. Duarte^{266 2393}, Anna Dubrovskaya⁵²⁸, Elaine A. Dunlop⁵²⁹, Nicolas Dupont⁵³⁰, Raul V Duran⁵³¹, Bilikere S Dwarakanath⁵³², Sergey A Dyshlovoy⁵³³, Darius Ebrahimi-Fakhari⁵³⁴, Leopold Eckhart⁷¹², Charles Edelstein⁵³⁵, Thomas Efferth⁵³⁶, Eftekhar Eftekharpour⁵³⁷, Ludwig Eichinger⁵³⁸, Nabil Eid⁵³⁹, Tobias Eisenberg⁵⁴⁰, Sanaa Eissa⁵⁴¹, Tony Eissa⁵⁴², Miriam Ejarque⁵⁴³, Abdeljabar El Andaloussi⁸⁴⁷, Nazira El-Hage⁵⁴⁴, Eman S. El-Shafey⁵⁴⁵, Shahenda El-Naggar⁵⁴⁶, Eman S. El-Shafey⁵⁴⁷, Mohamed Elgendy⁵⁴⁸, Aristides G Eliopoulos⁴⁸⁷, Phil Elks⁵⁴⁹, Anna Maria Eleuteri⁵⁵⁰, Mercedes Elizalde⁵⁵¹, Hans-Peter Elsasser⁵⁵², Eslam S. Elsherbiny⁵⁴⁵, Brooke M Emerling⁵⁵³, Tolga Emre⁵⁵⁴, Christina H Eng⁵⁵⁵, Nikolai Engedal⁵⁵⁶, Anna-Mart Engelbrecht⁵⁵⁷, Agnete Engelsen⁵⁵⁸, Jorrit M Enserink⁵⁵⁹, Ricardo Escalante⁵⁶⁰, Audrey Esclatine⁵⁶¹, Mafalda Escobar-Henriques⁵⁶², Eva-Liisa Eskelinen⁵⁶³, Lucile Espert⁵⁶⁴, Makandjou-Ola Eusebio⁵⁶⁵, Gemma Fabrias⁵⁶⁶, Cinzia Fabrizi⁵⁶⁷, Antonio Facchiano⁵⁶⁸, Francesco Facchiano⁵⁶⁹, Bengt Fadeel⁸⁹⁵, Claudio Marcelo Fader⁵⁷⁰, Alex Faesen⁵⁷¹, W Douglas Fairlie⁵⁷², Alberto Falcó⁵⁷³, Bjorn H Falkenburger⁵⁷⁴, Daping Fan⁵⁷⁵, Jie Fan⁵⁷⁶, Yanbo Fan⁵⁷⁷, Evandro F. Fang⁵⁷⁸, Yanshan Fang⁵⁷⁹, Yognqi Fang⁵⁸⁰, Manolis Fanto⁵⁸¹, Tamar Farfel-Becker¹⁸²², Mathias Faure⁵⁸², Gholamreza Fazeli⁵⁸³, Anthony Fedele⁵⁸⁴, Arthur M Feldman⁵⁸⁵, Du Feng⁵⁸⁶, Jiachun Feng⁵⁸⁷, Lifeng Feng⁵⁸⁸, Wei Feng⁵⁸⁹, Yibin Feng⁵⁹⁰, Yuchen Feng⁵⁹¹, Thais Fenz Araujo⁵⁹², Thomas Ferguson⁵⁹³, Álvaro Fernández¹¹⁰⁸, Jose C Fernandez-Checa⁵⁹⁴, Sonia Fernandez-Veledo⁵⁹⁵, Alisdair R. Fernie⁵⁹⁶, Anthony W Jr Ferrante⁵⁹⁷, Alessandra Ferraresi⁸⁴⁶, Merari F R Ferrari⁵⁹⁸, Julio C. B. Ferreira⁵⁹⁹, Susan Ferro-Novick⁶⁰⁰, Antonio Figueras⁶⁰¹, Riccardo Filadi¹⁵⁸³, Gian Maria Fimia⁶⁰², Vittorio Fineschi⁶⁰³, Francesca Finetti¹⁰², Steven Finkbeiner⁶⁰⁴, Nicoletta Filigheddu⁶⁰⁵, Eduardo Filippi-Chiela⁶⁰⁶, Paul B Fisher⁶⁰⁷, Edward A Fisher⁶⁰⁸, Flavio Flamigni¹⁸⁰⁴, Steven Fliesler⁶⁰⁹, Trude Helen Flo⁶¹⁰, Ida Florance¹⁶³⁶, Oliver Florey⁶¹¹, Tullio Florio⁶¹², Erika Fodor²⁰²⁷, Carlo Follo²¹⁴, Edward A Fon⁶¹³, Antonella Forlino⁶¹⁴, Francesco Fornai⁶¹⁵, Paola Fortini⁶¹⁶, Anna Fracassi⁶¹⁷, Alessandro Fraldi⁶¹⁸, Brunella Franco⁶¹⁸, Rodrigo Franco⁶¹⁹, Flavia Franconi⁶²⁰, Lisa B Frankel⁶²¹, Scott L Friedman⁶²², Leopold F Fröhlich⁶²³, Gema Frühbeck¹⁶⁶⁹, Jose Manuel Fuentes Rodriguez^{690 2366}, Yukio Fujiki⁶²⁴, Naonobu Fujita⁶²⁵, Yuuki Fujiwara⁹¹⁰, Mitsunori Fukuda⁶²⁶, Simone Fulda⁶²⁷, Luc Furic⁶²⁸, Norihiko Furuya⁶²⁹, Carmela Fusco⁶³⁰, Michaela U Gack⁶³¹, Lidia Gaffke²¹¹⁰, Sehamuddin Galadari⁶³², Alessia Galasso⁶³³, Maria F Galindo⁸⁹⁴, Sachith Gallolu Kankanamalage⁶³⁴, Lorenzo Galluzzi⁶³⁵, Vincent Galy⁶³⁶, Noor Gammoh⁶³⁷, Boyi Gan⁶³⁸, Ian Ganley⁶³⁹, Feng Gao⁶⁴⁰, Hui Gao¹¹²⁶, Minghui Gao⁶⁴¹, Ping Gao⁶⁴², Shou-Jiang Gao⁶⁴³, Wentao Gao⁶⁴⁴, Xiaobo Gao²²⁷⁶, Ana Garcera⁶⁴⁵, Maria Noé Garcia⁶⁴⁶, Veronica Edith Garcia⁶⁴⁷, Francisco Garcia-Del Portillo⁶⁴⁸, Vega Garcia-Escudero⁶⁴⁹, ARACELY GARCIA-GARCIA¹⁶⁷², Marina Garcia-Macia⁶⁵⁰, Diana García-Moreno⁶⁵¹, Carmen Garcia-Ruiz^{594 2367}, Patricia García-Sanz⁶⁵², Abishek Garg⁶⁵³, Ricardo Gargini⁶⁵⁴, Tina Garofalo¹⁹²², Robert F Garry⁶⁵⁵, Nils C. Gassen⁶⁵⁶, Damian Gatica⁹⁸⁷, Liang Ge⁶⁵⁷, Wanzhong Ge⁶⁵⁸, Ruth Geiss-Friedlander⁶⁵⁹, Cecilia Gelfi⁶⁶⁰, Pascal Genschik⁶⁶¹, Ian E. Gentle⁶⁶², Valeria Gerbino⁶⁶³, Christoph Gerhardt⁶⁶⁴, Kyla R. Germain⁹⁶⁷, Marc Germain⁶⁶⁵, David A Gewirtz⁶⁶⁶, Elham Ghasemipour Afshar⁶⁶⁷, Saeid Ghavami⁶⁶⁸, Alessandra Ghigo⁶⁶⁹, Manosij Ghosh⁷⁸⁸, Georgios Giamas⁶⁷⁰, Claudia Giampietri⁶⁷¹, Alexandra Giatromanolaki⁶⁷², Gary E Gibson⁶⁷³, Spencer B Gibson⁶⁷⁴, Vanessa Ginet¹⁶¹⁰, Edward Giniger⁶⁷⁵, Carlotta Giorgi¹⁵⁸¹, Henrique Girao⁶⁷⁶, Stephen E Girardin⁶⁷⁷, Mridhula Giridharan¹²⁶², Sandy Giuliano^{1509 2368}, Cecilia Giulivi⁶⁷⁸, Sylvie Giuriato⁶⁷⁹, Julien Giustiniani⁶⁸⁰, Alexander Gluschko⁷⁶⁹, Veit Goder¹⁰⁹⁹, Alexander Goginashvili⁶⁸¹, Jakub Golab⁶⁸², David Goldstone⁶⁸³, Anna Golebiewska⁶⁸⁴, Luciana R Gomes¹⁵⁸, Rodrigo Gomez¹⁶⁴¹, Rubén Gómez Sánchez⁶⁸⁸, Maria Catalina Gomez-Puerto⁶⁸⁵, Raquel Gomez-Sintes⁹³⁷, Qingqiu Gong⁶⁸⁶, Felix M. Goni⁶⁸⁷, Javier Gonzalez-Gallego⁶⁸⁸, Tomas Gonzalez-Hernandez⁶⁸⁹, Rosa A Gonzalez-Polo⁶⁹⁰, Jose A Gonzalez-Reyes⁶⁹¹, Patricia Gonzalez Rodriguez⁸⁹⁵, Ing Swie Goping⁶⁹², Marina Gorbatyuk⁶⁹³, Nikolai V Gorbunov⁶⁹⁴, Kivanç Görgülü⁶⁹⁵, Roxana M. Gorojod⁶⁹⁶, Sharon M Gorski⁶⁹⁷, Sandro Goruppi⁶⁹⁸, Cecilia Gotor⁶⁹⁹, Roberta Gottlieb⁷⁰⁰, Illana Gozes⁷⁰¹, Devrim Gozuacik⁷⁰², Martin Graef⁷⁰³, Markus Gräler⁷⁰⁴, Veronica Granatiero⁷⁰⁵, Daniel Grasso¹⁵²⁷, Joshua P. Gray¹³⁴⁶, Douglas R Green⁷⁰⁶, Alexander Greenhough⁷⁰⁷, Stephen Gregory⁷⁰⁸, Edward F. Griffin⁷⁰⁹, Mark W. Grinstaff⁷¹⁰, Frederic Gros⁷¹¹, Charles Grose⁷¹², Angelina S. Gross^{703 2369}, Florian Gruber⁷¹², Paolo Grumati⁷¹³, Tilman Grune⁷¹⁴, Xueyan Gu⁷¹⁵, Jun-Lin Guan⁷¹⁶, Carlos Guardia¹⁹¹, Kishore Guda⁷¹⁷, Flora Guerra⁷¹⁸, Consuelo Guerri⁷¹⁹, Prasun Guha⁷²⁰, Carlos Guillén⁷²¹, Shashi Gujar⁷²², Anna Gukovskaya⁷²³, Ilya Gukovsky⁷²³, Jan Gunst²⁰¹⁶, Andreas Günther⁷²⁴, Anyonya R. Guntur⁷²⁵, Chuanyong Guo⁷²⁶, Chun Guo⁷²⁷, Hongqing Guo²²¹⁹, Lian-Wang Guo⁷²⁸, Ming Guo⁷²⁹, Pawan Gupta⁷³⁰, Shashi Kumar Gupta⁷³¹, Swapnil Gupta⁷³², Veer Bala Gupta⁷³³, Vivek Gupta⁷³⁴, Asa B Gustafsson⁷³⁵, David Gutterman⁷³⁶, Ranjitha H.B.⁷³⁷, Annakaisa Haapasalo⁷³⁸, James E Haber⁷³⁹, Aleksandra Hac⁷⁷¹, Shinji Hadano⁷⁴⁰, Anders Hafrén⁷⁴¹, Mansour Haidar⁷⁴², Belinda S. Hall¹⁸⁴², Anne Hamacher-Brady⁷⁴³, Gunnel Halldén⁷⁴⁴, Andrea Hamann¹⁴⁹⁸, Maho Hamasaki²²²⁷, Weidong Han⁷⁴⁵

- Malene Hansen⁷⁴⁶, Phyllis Hanson⁷⁴⁷, Zijian Hao²²⁷⁶, Masaru Harada⁷⁴⁸, Ljubica Harhaji-Trajkovic⁷⁴⁹, Nirmala Hariharan⁷⁵⁰,
 170 Nigil Haroon⁷⁵¹, James Harris⁷⁵², Takafumi Hasegawa⁷⁵³, Noor Hasima Nagoor⁷⁵⁴, Jeffrey A Haspel⁷⁵⁵, Volker Haucke⁷⁵⁶,
 Wayne D. Hawkins⁹⁸⁷, Bruce A Hay⁷⁵⁷, Cole Haynes⁷⁵⁸, Soren Hayrabydyan⁷⁵⁹, Thomas S Hays⁷⁶⁰, Congcong He⁷⁶¹,
 Qin He⁷⁶², Rong-Rong He⁷⁶³, You-Wen He⁷⁶⁴, Yu-Ying He⁷⁶⁵, Yasser Heakal⁷⁶⁶, Alexander M. Heberle^{1954 2370},
 J. Fielding Hejtmancik⁷⁶⁷, G Vignir Helgason⁷⁶⁸, Vanessa Henkel¹⁴⁹⁸, Marc Herb⁷⁶⁹, Alexander Hergovich⁷⁷⁰, Anna Herman-
 Antosiewicz⁷⁷¹, Agustín Hernández⁷⁷², Carlos Hernandez⁷⁷³, Sergio Hernandez-Diaz¹⁸⁷⁶, Virginia Hernandez-Gea⁷⁷⁴,
 175 Amaury Herpin⁷⁷⁵, Judit Herreros⁷⁷⁶, Javier H. Hervás⁷⁷⁷, Daniel Hesselson⁷⁷⁸, Claudio Hetz⁷⁷⁹, Volker Heussler⁷⁸⁰,
 Yujiro Higuchi⁷⁸¹, Joseph A Hill⁷⁸², William S Hlavacek⁷⁸³, Emmanuel A Ho⁷⁸⁴, Idy H.T. Ho²²⁷², Philip Wing-Lok Ho⁷⁸⁵, Shu-
 Leong Ho⁷⁸⁵, Wan Yun Ho¹¹⁶², G. Aaron Hobbs⁷⁸⁶, Mark Hochstrasser⁷⁸⁷, Peter H.M. Hoet⁷⁸⁸, Paul Hofman⁷⁸⁹,
 Daniel Hofius⁷⁹⁰, Annika Höhn⁷⁹¹, Carina I. Holmberg⁷⁹², Jose Romero Hombrebueno⁷⁹³, Chang-Won Hong⁷⁹⁴, Yi-
 Ren Hong⁷⁹⁵, Thorsten Hoppe⁷⁹⁶, Rastislav Horos⁷⁹⁷, Yujin Hoshida⁷⁹⁸, I-Lun Hsin⁹⁹⁴, Hsin-Yun Hsu⁷⁹⁹, Bing Hu⁸⁰⁰,
 180 Dong Hu⁸⁰¹, Li-Fang Hu⁸⁰², Ming Chang Hu⁸⁰³, Ronggui Cory Hu²²⁷⁶, Wei Hu⁸⁰⁴, Yu-Chen Hu⁸⁰⁵, Zhuo-Wei Hu⁸⁰⁶,
 Fang Hua⁸⁰⁶, Jinlian Hua⁸⁰⁷, Yingqi Hua⁸⁰⁸, Canhua Huang⁸⁰⁹, Chongmin Huan⁸¹⁰, Chuanshu Huang⁸¹¹, Chuanxin Huang⁸¹²,
 Chunling Huang⁸¹³, Haishan Huang⁸¹⁴, Kun Huang⁸¹⁵, Michael L.H. Huang¹⁶⁵⁸, Rui Huang⁸¹⁶, Shan Huang⁸¹⁷,
 Tianzhi Huang³⁵², Xing Huang⁸¹⁸, Yuxiang Jack Huang⁸¹⁹, Tobias Huber⁸²⁰, Virginie Hubert⁸²¹, Christian A Hubner⁸²¹,
 Stephanie M Hughes⁸²², William E. Hughes⁷³⁶, Magali Humbert⁸²³, Gerhard Hummer⁸²⁴, James H. Hurley⁸²⁵,
 185 Sabah N. A. Hussain⁸²⁶, Salik Hussain⁸²⁷, Patrick J Hussey⁸²⁸, Martina Hutabarat⁸²⁹, Hui-Yun Hwang¹⁰⁴¹,
 Seungmin Hwang⁸³⁰, Antonio Ieni⁸³¹, Fumiyo Ikeda⁸³², Yusuke Imagawa⁸³³, Yuzuru Imai⁸³⁴, Carol Imbriano⁸³⁵,
 Masaya Imoto⁸³⁶, Denise M Inman⁸³⁷, Ken Inoki⁸³⁸, Juan Iovanna⁸³⁹, Renato V Iozzo⁸⁴⁰, Giuseppe Ippolito⁸⁴¹,
 Javier Irazoqui⁸⁴², Pablo Iribarren, Mohd Ishaq⁸⁴³, Makoto Ishikawa⁸⁴⁴, Nestor Ishimwe⁸⁴⁵, Ciro Isidoro⁸⁴⁶, Nahed Ismail⁸⁴⁷,
 Shohreh Issazaded-Navikas⁸⁴⁸, Eisuke Itakura⁸⁴⁹, Daisuke Ito⁸⁵⁰, Davor Ivankovic⁹⁸⁴, Saka Ivanova^{2341 2371},
 190 Anand Krishnan V Iyer⁸⁵¹, José M Izquierdo⁸⁵², Masanori Izumi⁸⁵³, Marja Jaattela⁸⁵⁴, Majid Sakhi Jabir⁸⁵⁵,
 William T. Jackson⁸⁵⁶, Nadia J Jacobo-Herrera⁸⁵⁷, Anne-Claire Jacomin¹⁴⁴⁷, Elise Jacquin⁵⁵, Pooja Jadiya¹⁹⁶⁸,
 Hartmut Jaeschke⁸⁵⁸, Chinnaswamy Jagannath⁸⁵⁹, Arjen Jakobi⁸⁶⁰, Johan Jakobsson⁸⁶¹, Bassam Janji⁸⁶²,
 Alagie Jassey^{1153 2372}, Andreas Jenny⁸⁶³, Pidder Jansen-Dürr⁸⁶⁴, Patric Jansson⁸⁶⁵, Jonathan Jantsch⁸⁶⁶,
 Slawomir Januszewski¹⁵⁸⁸, Steve Jean⁸⁶⁷, Hélène Jeltsch-David⁸⁶⁸, Thomas Elbenhardt Jensen⁸⁶⁹, Pavla Jendelova⁸⁷⁰,
 195 Niels Jessen⁸⁷¹, Jenna L Jewell⁸⁷², Jing Ji⁸⁷³, Lijun Jia⁸⁷⁴, Rui Jia¹⁹¹, Liwen Jiang⁸⁷⁵, Qing Jiang⁸⁷⁶, Richeng Jiang^{1457 2373},
 Teng Jiang⁸⁷⁷, Yu Jiang⁸⁷⁸, Maria Jimenez-Sanchez⁸⁷⁹, Eun-Jung Jin⁸⁸⁰, Fengyan Jin⁸⁸¹, Hongchuan Jin⁸⁸², Li Jin⁸⁸³,
 Luqi Jin⁸⁸⁴, Meiyang Jin⁸⁸⁵, Si Jin⁸⁸⁶, Eun-Kyeong Jo⁸⁸⁷, Carine Joffre⁸⁸⁸, Terje Johansen¹⁰⁵³, Gail V W Johnson⁸⁸⁹,
 Simon Johnston⁸⁹⁰, Eija Jokitalo⁸⁹¹, Mohit Kumar Jolly⁸⁹², Leo A B Joosten⁸⁹³, Joaquin Jordan⁸⁹⁴, Bertrand Joseph⁸⁹⁵,
 Dianwen Ju⁸⁹⁶, Jeong-Sun Ju⁸⁹⁷, Jingfang Ju⁸⁹⁸, Esmeralda Juárez⁸⁹⁹, Delphine Judith¹⁵⁷, Gábor Juhász⁹⁰⁰,
 200 Youngsoo Jun⁹⁰¹, Chang Hwa Jung⁹⁰², Sung-Chul Jung⁹⁰³, Yong-Keun Jung⁹⁰⁴, Heinz Jungbluth⁹⁰⁵,
 Johannes Jungverdorben⁹⁰⁶, Steffen Just⁹⁰⁷, Kai Kaarniranta⁹⁰⁸, Allen Kaasik⁹⁰⁹, Tomohiro Kabuta⁹¹⁰, Daniel Kaganovich⁹¹¹,
 Alon Kahana⁹¹², Renate Kain⁹¹³, Shinjo Kajimura⁹¹⁴, Maria Kalamvoki⁹¹⁵, Manjula Kalia⁹¹⁶, Danuta S. Kalinowski¹⁶⁵⁸,
 Nina Kaludercic⁹¹⁷, Ioanna Kalvari⁹¹⁸, Joanna Kaminska²³³⁸, Vitaliy O Kaminsky⁹¹⁹, Hiromitsu Kanamori⁹²⁰,
 Keizo Kanasaki⁹²¹, Chanhee Kang⁹²², Rui Kang¹⁹³⁴, Sang Sun Kang⁹²³, Senthilvelrajan Kaniyappan^{1259 2374},
 205 Tomotake Kanki⁹²⁴, Thirumala-Devi Kanneganti⁹²⁵, Anumantha G Kanthasamy⁹²⁶, Arthi Kanthasamy⁹²⁶, Marc Kantorow⁹²⁷,
 Orsolya Kapuy⁹²⁸, Michalis V. Karamouzis⁹²⁹, Md. Razaul Karim⁹³⁰, Parimal Karmakar⁹³¹, Rajesh Katore⁹³², Masaru Kato⁹³³,
 Stefan H E Kaufmann⁹³⁴, Anu Kauppinen⁹³⁵, Gur P Kaushal⁹³⁶, Susmita Kaushik⁹³⁷, Kiyoshi Kawasaki⁹³⁸, Kemal Kazan⁹³⁹, Po-
 Yuan Ke⁹⁴⁰, Damien Keating⁹⁴¹, Ursula Keber⁹⁴², John Kehrl⁹⁴³, Christian W. Keller¹²¹⁷, Kate Keller⁹⁴⁴,
 Jongsook Kim Kemper⁹⁴⁵, Chandra Shekar Kenchappa⁹⁴⁶, Candia Kenific⁹⁴⁷, Oliver Kepp⁹⁴⁸, Stephanie Kermorgant⁹⁴⁹,
 210 Andreas Kern⁹⁵⁰, Tom G. Keulers¹⁶⁹⁰, Robin Ketteler⁹⁵¹, Boris Khalfin^{1433 2375}, Hany Khalil⁹⁵², Bilon Khambu⁹⁵³,
 Shahid Y. Khan¹⁶⁵⁴, Vinoth Khandelwal⁹⁵⁴, Rekha Khandia¹⁴¹⁰, Widuri Kho²⁰⁵⁵, Noopur V. Khobreakar²⁰⁰⁹,
 Sataree Khuansuwan²¹⁹, Mukhran Khundadze⁹⁵⁵, Samuel A. Killackey⁶⁷⁷, Dasol Kim¹⁰⁴¹, Deok Ryong Kim⁹⁵⁶, Do-
 Hyung Kim⁹⁵⁷, Dong-Eun Kim⁹⁵⁸, Eun Young Kim¹⁰⁸⁰, Eun-Kyoung Kim⁹⁵⁹, Hak Rim Kim⁹⁶⁰, Hee-Sik Kim⁹⁶¹, Hyung-
 Ryong Kim⁹⁶², Jeong Hun Kim⁹⁶³, Jin Kyung Kim⁸⁸⁷, Jin-Hoi Kim⁹⁶⁴, Joungmok Kim⁹⁶⁵, Ju Hwan Kim⁹⁶⁰, Keun Il Kim⁹⁶⁶,
 215 Peter Kijun Kim⁹⁶⁷, Seong-Jun Kim⁹⁶⁸, Scot R Kimball⁹⁶⁹, Adi Kimchi⁹⁷⁰, Alec Kimmelman⁹⁷¹, Tomonori Kimura⁹⁷²,
 Matthew A King⁹⁷³, Kerri J Kinghorn⁹⁷⁴, Conan Kinsey⁹⁷⁵, Vladimir Kirkin⁹⁷⁶, Lorrie A Kirshenbaum⁹⁷⁷, Sergey L Kiselev⁹⁷⁸,
 Shuji Kishi⁹⁷⁹, Katsuhiko Kitamoto⁹⁸⁰, Yasushi Kitaoka⁹⁸¹, Kaio Kitazato⁹⁸², Richard Kitsis⁹⁸³, Josef Kittler⁹⁸⁴, Ole Kjaerulff⁹⁸⁵,
 Peter S Klein⁹⁸⁶, Daniel J. Klionsky⁹⁸⁷, Thomas Klopstock⁹⁸⁸, Jochen Klucken⁹⁸⁹, Helene Knävelsrud⁹⁹⁰, Roland L Knorr⁹⁹¹,
 Ben C B Ko⁹⁹², Fred Ko⁹⁹³, Jiunn-Liang Ko⁹⁹⁴, Hotaka Kobayashi⁹⁹⁵, Satoru Kobayashi⁹⁹⁶, Nur M. Kocaturk³⁸⁷, Ina Koch⁹⁹⁷,
 220 Jan Christoph Koch⁹⁹⁸, Ulrich Koenig⁹⁹⁹, Donat Kögel¹⁰⁰⁰, Young Ho Koh¹⁰⁰¹, Sepp D. Kohlwein¹⁰⁰², Masato Koike¹⁰⁰³,
 Masaaki Komatsu¹⁰⁰⁴, Jeannette Konig¹⁰⁰⁵, Toru Kono¹⁰⁰⁶, Benjamin T Kopp¹⁰⁰⁷, Tamas Korcsmaros¹⁰⁰⁸, Gozde Korkmaz¹⁰⁰⁹,
 Viktor I Korolchuk¹⁰¹⁰, Monica Suarez Korsnes¹⁰¹¹, Ali Koskela¹⁰¹², Janaiah Kota¹⁰¹³, Yaichiro Kotake¹⁰¹⁴,
 Monica Lidia Kotler⁶⁹⁶, Yanjun Kou¹⁰¹⁵, Michael I Koukourakis¹⁰¹⁶, Evangelos Koustas⁹²⁹, Attila Kovacs^{900 2376},
 Tibor Kovács²⁰²⁷, Daisuke Koya¹⁰¹⁷, Tomohiro Kozako¹⁰¹⁸, Claudine Kraft¹⁰¹⁹, Dimitri Krainc¹⁰²⁰, Helmut Krämer¹⁰²¹,
 225 Anna Krasnodembskaya¹⁰²², Carole Kretz-Remy¹⁰²³, Guido Kroemer¹⁰²⁴, Nicholas Ktistakis¹⁰²⁵, Kazuyuki Kuchitsu¹⁰²⁶,
 Sabine Kuenen²⁰⁴¹, Lars Kuerschner¹⁰²⁷, Thomas Kukar¹⁰²⁸, Ajay Kumar¹⁰²⁹, Ashok Kumar¹⁰³⁰, Deepak Kumar¹⁰³¹,

- Dhiraj Kumar¹⁰³², Sharad Kumar¹⁰³³, Shinji Kume¹⁰³⁴, Caroline Kumsta⁷⁴⁶, Chanakya Nath Kundu¹⁰³⁵, Mondira Kundu¹⁰³⁶,
 Ajaikumar Kunnumakkara¹⁰³⁷, Lukasz Kurgan¹⁰³⁸, Tatiana G Kutateladze²²⁸⁷, Ozlem Kutlu¹⁰³⁹, SeongAe Kwak¹⁰⁴⁰,
 Ho Jeong Kwon¹⁰⁴¹, Taeg Kyu Kwon¹⁰⁴², Yong Tae Kwon¹⁰⁴³, Irene Kyrnizi³⁰⁶, Albert La Spada¹⁰⁴⁴, Patrick Labonté¹⁰⁴⁵,
 230 Sylvain Ladoire¹⁰⁴⁶, Ilaria Laface¹⁰⁴⁷, Frank Lafont¹⁰⁴⁸, Diane Lagace¹⁰⁴⁹, Vikramjit Lahiri⁹⁸⁷, Zhibing Lai¹⁰⁵⁰, Angela Laird¹⁰⁵¹,
 Aparna Lakkaraju¹⁰⁵², Trond Lamark¹⁰⁵³, Sheng-Hui Lan¹⁰⁵⁴, Ane Landajuela¹⁰⁵⁵, Darius J. R. Lane¹⁰⁵⁶, Jon D Lane¹⁰⁵⁷,
 Charles H Lang¹⁰⁵⁸, Carsten Lange¹⁰⁵⁹, Ülo Langel¹⁰⁶⁰, Rupert Langer¹⁰⁶¹, Pierre Lapaquette¹⁰⁶², Jocelyn Laporte¹⁰⁶³,
 Nicholass F LaRusso¹⁰⁶⁴, Isabel Lastres-Becker¹⁰⁶⁵, Wilson Chun Yu Lau⁸⁷⁵, Gordon W Laurie¹⁰⁶⁶, Sergio Lavandero³⁶⁸,
 Betty Yuen Kwan Law¹⁰⁶⁷, Helen Ka Wai Law¹⁹²⁸, Robert Layfield¹⁰⁶⁸, Weidong Le¹⁰⁶⁹, Herve Le Stunff¹⁰⁷⁰,
 235 Alexandre Y. Leary²⁰⁷, Jean-Jacques Lebrun¹⁰⁷¹, Lionel Y.W. Leck⁸⁶⁵, Jean-Philippe Leduc-Gaudet¹⁰⁷², Changwook Lee¹⁰⁷³,
 Chung-Pei Lee¹⁰⁷⁴, Da-Hye Lee⁹⁵⁷, Edward Lee¹⁰⁷⁵, Erinna F Lee⁵⁷², Gyun Min Lee¹⁰⁷⁶, He-Jin Lee¹⁰⁷⁷, Heung Kyu Lee¹⁰⁷⁸,
 Jason S Lee¹⁰⁷⁹, Jae Man Lee¹⁰⁸⁰, Jin-A Lee¹⁰⁸¹, Joo-Yong Lee¹⁰⁸², Jun Hee Lee¹⁰⁸³, Michael Lee¹⁰⁸⁴, Min Goo Lee¹⁰⁸⁵,
 Min Jae Lee¹⁰⁸⁶, Myung-Shik Lee¹⁰⁸⁷, Sang Yoon Lee¹⁰⁸⁸, Seung-Jae Lee¹⁰⁸⁹, Stella Y Lee¹⁰⁹⁰, Sung Bae Lee¹⁰⁹¹,
 Won Hee Lee¹⁰⁹², Ying-Ray Lee¹⁰⁹³, Yong-Ho Lee¹⁰⁹⁴, Youngil Lee¹⁰⁹⁵, Christophe Lefebvre¹⁰⁹⁸, Yu Lei¹⁰⁹⁶, Yuchen Lei⁹⁸⁷,
 240 Sergey Leikin¹⁰⁹⁷, Gerd Leitinger^{1167 2377}, Renaud Legouis¹⁰⁹⁸, Leticia Lemus¹⁰⁹⁹, Shuilong Leng¹¹⁰⁰, Olivia Lenoir^{1953 2378},
 Guido Lenz¹¹⁰¹, Heinz-Josef Lenz¹¹⁰², Paola Lenzi¹¹⁰³, Andreia Machado Leopoldino¹¹⁰⁴, Christoph Leschczyk¹⁷⁵⁶,
 Stina Leskelä⁷³⁸, Elisabeth Letellier¹¹⁰⁵, Chi-Ting Leung⁷⁸⁵, Po Sing Leung¹¹⁰⁶, Jeremy S Leventhal¹¹⁰⁷, Beth Levine¹¹⁰⁸,
 Patrick A Lewis¹¹⁰⁹, Klaus Ley¹¹¹⁰, Bin Li¹¹¹¹, Da-Qiang Li¹¹¹², Jian-Ming Li¹¹¹³, Jing Li⁷²⁸, Jiong Li¹¹¹⁴, Ke Li¹¹¹⁵, Liwu Li¹¹¹⁶,
 Mei Li¹¹¹⁷, Min Li¹¹¹⁸, Min Li¹¹¹⁹, Ming Li¹¹²⁰, Ming-Qing Li¹¹²¹, Mingchuan Li¹¹²², Pin-Lan Li¹¹²³, Qing Li²²⁷², Sheng Li¹¹²⁴,
 245 Tiangang Li¹¹²⁵, Wei Li¹¹²⁶, Wenming Li¹¹²⁷, Xue Li¹¹²⁸, Yi-Ping Li¹¹²⁹, Yuan Li¹¹²⁹, Zhiqiang Li¹¹⁸², Zhiyong Li¹¹³⁰, Zhiyuan Li²²⁸²,
 Zuguo Li¹¹³¹, Jiqin Lian¹¹³², Chengyu Liang¹¹³³, Qiangrong Liang¹¹³⁴, Weicheng Liang¹¹³⁵, YongTian Liang¹¹³⁶,
 Yongheng Liang¹¹³⁷, Guanghong Liao²²⁷⁶, Lujian Liao¹¹³⁸, Mingzhi Liao¹¹³⁹, Yung-Feng Liao¹¹⁴⁰, Mariangela Librizzi¹²²¹,
 Pearl P Y Lie¹¹⁴¹, Mary A Lilly¹¹⁴², Hyunjung Jade Lim¹¹⁴³, Thania R.R. Lima¹¹⁴⁴, Federica Limana¹¹⁴⁵, Chao Lin¹¹⁴⁶, Chih-
 Wen Lin¹¹⁴⁷, Dar-Shong Lin¹¹⁴⁸, Fu-Cheng Lin¹¹⁴⁹, Jiandie Lin¹¹⁵⁰, Kurt Ming-Chao Lin¹¹⁵¹, Kwang-Huei Lin¹¹⁵², Liang-
 250 Tzung Lin¹¹⁵³, Pei-Hui Lin¹¹⁵⁴, Qiong Lin¹¹⁵⁵, Shaofeng Lin²¹⁸⁵, Su-Ju Lin, Wenyu Lin¹¹⁵⁶, Xueying Lin¹¹⁵⁷, Yao-Xin Lin¹¹⁵⁸, Yee-
 Shin Lin¹¹⁵⁹, Yong Lin¹¹⁶⁰, Rafael Linden¹¹⁶¹, Paula Lindner⁵⁵⁶, Shuo-Chien Ling¹¹⁶², Paul Lingor¹¹⁶³, Amelia K Linnemann¹¹⁶⁴,
 Yih-Cherng Liou¹¹⁶⁵, Marta M Lipinski¹¹⁶⁶, Saka Lipovek¹¹⁶⁷, Vitor Lira¹¹⁶⁸, Natalia Lisiak¹¹⁶⁹, Paloma B Liton¹¹⁷⁰, Chao Liu¹¹⁷⁴,
 Cui Hua Liu¹¹⁷¹, Ching-Hsuan Liu^{1153 2372}, Chun-Feng Liu¹¹⁷², Fang Liu¹¹⁷³, Hao Liu⁵⁸⁶, Hsiao-Sheng Liu³¹³, Hua Feng Liu¹¹⁷⁴,
 Huifang Liu⁷⁸⁵, Jia Liu¹¹⁷⁵, Jing Liu¹¹⁷⁶, Leyuan Liu¹¹⁷⁷, Longhua Liu¹¹⁷⁸, Meilian Liu¹¹⁷⁹, Qin Liu¹¹⁸⁰, Wei Liu¹¹⁸¹, Wende Liu¹¹⁸²,
 255 Xiao-Hong Liu¹¹⁴⁹, Xiaodong Liu²²⁷², Xingguo Liu¹¹⁸³, Xu Liu¹¹⁸⁴, Xuedong Liu¹¹⁸⁵, Yang Liu¹¹⁸⁶, Yang Liu²⁰⁸¹, Yanfen Liu¹¹⁸⁷,
 Yueyang Liu¹¹⁸⁸, Yule Liu¹¹⁸⁹, J. Andrew Livingston¹¹⁹⁰, Gerard Lizard¹¹⁹¹, Jose M. Lizcano¹¹⁹², Senka Ljubojevic-Holzer¹⁷⁸⁸,
 Matilde E LLeonart¹¹⁹³, David Llobet-Navàs¹¹⁹⁴, Alicia Llorente¹¹⁹⁵, Chih Hung Lo¹¹⁹⁶, Damián Lobato-Márquez¹⁴⁰⁰,
 Qi Long¹¹⁹⁷, Yun Chau Long¹¹⁹⁸, Ben Loos⁵⁵⁷, Julia A. Loos⁴²², Manuela G. López¹¹⁹⁹, Guillermo López-Doménech⁹⁸⁴,
 José Antonio López-Guerrero¹²⁰⁰, Ana T. López-Jiménez¹⁴⁰⁰, Óscar López-Pérez¹²⁰¹, Israel López-Valero¹²⁰³,
 260 Magdalena J Lorenowicz¹²⁰², Mar Lorente¹²⁰³, Peter Lorincz^{900 2373}, Laura Lossi¹³³¹, Sophie Lotersztajn¹²⁰⁴, Penny E Lovat¹²⁰⁵,
 Jonathan Lovell¹²⁰⁶, Alenka Lovy¹²⁰⁷, Peter Low⁹⁰⁰, Guang Lu²⁰⁸⁴, Haocheng Lu, Jia-Hong Lu¹²⁰⁸, Jinjian Lu¹²⁰⁸, Mengji Lu⁵⁵⁶,
 Shuyan Lu¹²⁰⁹, Alessandro Luciani¹²¹⁰, John Milton Lucocq¹²¹¹, Paula Ludovico¹²¹², Micah A Luftig¹²¹³, Morten Luhr¹²¹⁷,
 Diego Luis-Ravelo¹²¹⁴, Julian J. Lum¹²¹⁵, Liany Luna-Dulcey⁴⁰⁶, Anders H Lund¹²¹⁶, Viktor K. Lund⁹⁸⁵, Jan Lunemann¹²²¹,
 Patrick Lüningschrör¹⁷⁹⁷, Honglin Luo¹²¹⁸, Rongcan Luo²²¹³, Shouqing Luo¹²¹⁹, Zhi Luo¹²²⁰, Claudio Luparello¹²²¹,
 265 Bernhard Lüscher¹²²², Luan Luu, Alex Lyakhovich¹²²³, Konstantin G. Lyamzaev³⁵⁹, Alf Håkon Lystad¹²²⁴,
 Lyubomyr Lytvynchuk¹²²⁵, Alvin CH Ma¹²²⁶, Changle Ma¹²²⁷, Mengxiao Ma¹²²⁸, Ning-Fang Ma¹²²⁹, Quan-Hong Ma¹²³⁰, Xin-
 Liang Ma¹²³¹, Yueyun Ma¹²³², Zhenyi Ma¹²³³, Ormond A MacDougald¹²³⁴, Fernando Macian¹²³⁵, Jeffrey P MacKeigan¹²⁷⁸,
 Kay F Macleod¹²³⁶, Gustavo C. MacIntosh¹²³⁷, Sandra Maday¹²³⁸, Frank Madeo¹²³⁹, Muniswamy Madesh¹²⁴⁰, Tobias Madl¹²⁴¹,
 Julio Madrigal-Matute¹²⁴², Yasuhiro Maejima¹²⁴³, Marta Magarinos¹²⁴⁴, Poornima Mahavadi⁷²⁴, Emiliano Maiani¹²⁴⁵,
 270 Kenneth Maiese¹²⁴⁶, Panchanan Maiti¹²⁴⁷, Chiara Maria Maiuri¹²⁴⁸, Barbara Majello¹²⁴⁹, Elena Makareeva¹⁰⁹⁷, Fayaz Malik¹²⁵⁰,
 Walter Malorni¹²⁵¹, Alina Maloyan¹²⁵², Joseph D Mancias¹²⁵³, Akiko Maeda¹²⁵⁴, Michael B Major¹²⁵⁵,
 Karthik Babu Mallilankaraman¹²⁵⁶, Najiba Mammadova¹²⁵⁷, Gene Chi Wai Man¹²⁵⁸, Federico Manai⁴⁰⁵, Eva-
 Maria Mandelkow¹²⁵⁹, Michael A Mandell^{475 2380}, Angelo A Manfredi¹²⁶⁰, Masoud H Manjili¹²⁶¹, Ravi Manjithaya¹²⁶²,
 Patricio A Manque¹²⁶³, Bella B Manshian¹⁸⁶⁸, Raquel Manzano¹⁹⁶⁷, Claudia Manzoni¹²⁶⁴, Kai Mao¹²⁶⁵, Cinzia Marchese¹²⁶⁶,
 275 Sandrine Marchetti¹⁶⁵⁶, Anna Maria Marconi¹²⁶⁷, fabrizio marcucci¹²⁶⁸, Stefania Mardente¹²⁶⁹, Olga A. Mareninova⁷²³,
 Marta Margeta¹²⁷⁰, Muriel Mari¹⁶⁴¹, Oliviero Marinelli¹⁴²², Sara Marinelli¹²⁷¹, Guillermo Mariño¹²⁷², Sofia Mariotto¹²⁷³,
 Richard Marshall¹²⁷⁴, Mark R. Marten¹²⁷⁵, Sascha Martens¹²⁷⁶, Alexandre PJ Martin¹²⁷⁷, Katie R. Martin¹²⁷⁸, Sara Martin¹⁷³⁷,
 Shaun Martin¹²⁷⁹, Miguel Martín-Acebes¹²⁸⁰, Inmaculada Martin-Burriel^{1967 2381}, Marcos Martin-Rincon¹²⁸¹, Paloma Martin-
 Sanz¹²⁸², Adrian Martin-Segura¹²⁸³, Wim Martinet¹²⁸⁴, Ana Martinez²⁰⁵, Jennifer Martinez¹²⁸⁵, Moises Martinez Velazquez¹²⁸⁶,
 280 Nuria Martinez-Lopez¹²⁸⁷, Marta Martinez-Vicente¹²⁸⁸, Daniel O. Martins¹²⁸⁹, Joilson O. Martins¹²⁹⁰, Waleska K. Martins¹²⁹¹,
 Tania Martins-Marques⁶⁷⁶, Emanuele Marzetti^{248 2382}, Shashank Masaldan¹⁰⁵⁶, Celine Masclaux-Daubresse¹²⁹²,
 Douglas G Mashek¹²⁹³, Valentina Massa¹²⁹⁴, Lourdes Massieu¹²⁹⁵, Glenn R. Masson¹⁴⁸³, Laura Masuelli¹²⁹⁶,
 Anatoliy I Masyuk¹⁰⁶⁴, Tetyana V. Masyuk¹⁰⁶⁴, Paola Matarrese¹²⁵¹, Ander Matheu¹²⁹⁷, Satoaki Matoba¹²⁹⁸,
 Sachiko Matsuzaki¹²⁹⁹, Pamela Mattar³⁸⁶, Alessandro Matte⁴⁵³, Domenico Mattoscio¹³⁰⁰, Jose Mauriz^{774 2383},

- 285 Caroline Mauvezin^{32 2384}, Emanuel Maverakis¹³⁰¹, Paola Maycotte¹³⁰², Johanna Mayer¹⁴⁵⁷, Gianluigi Mazzoccoli¹³⁰³,
Cristina Mazzoni¹³⁰⁴, Joseph R Mazzulli¹³⁰⁵, Nami McCarty¹³⁰⁶, Christine McDonald¹³⁰⁷, Mitchell McGill¹³⁰⁸,
Sharon McKenna¹³⁰⁹, BethAnn McLaughlin¹³¹⁰, Fionn McLoughlin¹²⁷⁴, Mark A McNiven¹³¹¹, Thomas McWilliams¹³¹²,
Fatima Mechta-Grigoriou¹³¹³, Tania Catarina Medeiros^{703 2369}, Diego L Medina¹³¹⁴, Lynn A Megeney¹³¹⁵, Klara Megyeri¹³¹⁶,
Maryam Mehrpour¹³¹⁷, Jawahar L. Mehta¹³¹⁸, Alfred J. Meijer¹³¹⁹, Annemarie H Meijer¹³²⁰, Jakob Mejlvang¹³²¹,
290 Alicia Melendez¹³²², Anette Melk¹³²³, Gonen Memisoglu¹³²⁴, Alexandrina F. Mendes²⁸⁹, Delong Meng⁸⁷², Fei Meng¹³²⁵,
Tian Meng⁵⁸⁶, Rubem Menna-Barreto¹³²⁶, Manoj B Menon¹³²⁷, Carol Mercer¹³²⁸, Anne E. Mercier¹³²⁹, Jean-Louis Mergny¹³³⁰,
Adalberto Merighi¹³³¹, Seth D. Merkley¹³³², Giuseppe Merla²⁸⁷, Volker Meske¹³³³, Ana Cecilia Mestre¹³³⁴,
Shree Padma Metur⁹⁸⁷, Christian Meyer¹³³⁵, Hemmo Meyer¹³³⁶, Wenyi Mi¹³³⁷, Jeanne Mialet-Perez¹³³⁸, Junying Miao¹³³⁹,
Lucia Micale⁶³⁰, Yasuo Miki¹³⁴⁰, Enrico Milan¹³⁴¹, Malgorzata Milczarek¹³⁴², Dana Miller¹³⁴³, Samuel I Miller¹³⁴⁴, Silke Miller¹³⁴⁵,
295 Steven W. Millward¹³⁴⁶, Ira Milosevic¹³⁴⁷, Elena A Minina¹³⁴⁸, Hamed Mirzaei¹³⁴⁹, Hamid Reza Mirzaei¹³⁵⁰, Mehdi Mirzaei¹³⁵¹,
Roberta Misasi¹⁹²², Amit Mishra¹³⁵², Nandita Mishra¹³⁵³, Paras Kumar Mishra¹³⁵⁴, Maja Misirkic Marjanovic⁷⁴⁹, Amit Misra¹³⁵⁵,
Gabriella Misso^{268 2385}, Claire Mitchell¹⁸⁴, Geraldine Mitou¹³⁵⁶, Tetsuji Miura¹³⁵⁷, makoto Miyazaki¹³⁵⁸, Mitsunori Miyazaki¹³⁵⁹,
Taiga Miyazaki¹³⁶⁰, Keisuke Miyazawa¹³⁶¹, Shigeki Miyamoto¹³⁶², Noboru Mizushima¹³⁶³, Trine Mogensen¹³⁶⁴,
Baharia Mograbi¹⁵⁰⁹, Reza Mohamadinejad¹³⁶⁵, Yasir Mohamud¹²¹⁸, Abhishek Mohanty¹³⁶⁶, Sipra Mohapatra¹³⁶⁷,
300 Torsten Möhlmann¹³⁶⁸, Asif Mohammed¹³⁶⁹, Anna Moles¹³⁷⁰, Kelle H. Moley¹³⁷¹, Maurizio Molinari¹³⁷²,
Vincenzo Mollace¹³⁷³, Andreas Buch Møller¹³⁷⁴, Bertrand Mollereau¹³⁷⁵, Faustino Mollinedo¹³⁷⁶, Costanza Montagna¹³⁷⁷,
Mervyn J. Monteiro¹³⁷⁸, Andrea Montella¹³⁷⁹, L. Ruth Montes¹³⁸⁰, Barbara Montico¹³⁸¹, Vinod K. Mony¹⁴⁷⁰,
Giacomo Monzio Compagnoni⁴⁸³, Michael Moore¹³⁸², Mohammad Amin Moosavi¹³⁸³, Ana Mora¹³⁸⁴, Marina Mora¹³⁸⁵,
David Morales-Alamo^{241 2386}, Paula I Moreira¹³⁸⁶, Elena Morelli^{1737 2387}, Sandra Moreno¹³⁸⁷, Daniel Moreno-Blas¹³⁸⁸,
305 Viviana Moresi¹³⁸⁹, Benjamin Morga¹³⁹⁰, Alwena Morgan¹³⁹¹, Fabrice Morin¹³⁹², Hideaki Morishita¹³⁹³, Orson L Moritz¹³⁹⁴,
Mariko Moriyama¹³⁹⁵, Yuji Moriyasu¹³⁹⁶, Manuela Morleo⁶¹⁸, Eugenia Morselli¹³⁹⁷, Rosario Mortalla⁶⁵², Jose F. Moruno-
Manchon¹³⁹⁸, Jorge Moscat¹³⁹⁹, Serge Mostowy¹⁴⁰⁰, Elisa Motori¹⁴⁰¹, Andrea Felinto Moura¹⁴⁰², Naima Moustaid-Moussa¹⁴⁰³,
Maria Mrakovcic¹⁴⁰⁴, Gabriel Muciño-Hernández²⁸⁶, Anupam Mukherjee¹⁴⁰⁵, Subhadip Mukhopadhyay¹⁴⁰⁶,
Jean Mulcahy Levy¹⁴⁰⁷, Victoriano Mulero¹⁴⁰⁸, Sylviane Muller¹⁴⁰⁹, Christian Münch⁴⁹⁵, Ashok Munjal¹⁴¹⁰, Pura Munoz-
310 Canoves¹⁴¹¹, Teresa Muñoz-Galdeano¹⁴¹², Christian Munz¹⁴¹³, Tomokazu Murakawa¹⁵⁰², Claudia Muratori¹⁴¹⁴,
Brona M. Murphy¹⁴¹⁵, J. Patrick Murphy¹⁴¹⁶, Aditya Murthy¹⁴¹⁷, Timo T Myöhänen¹⁴¹⁸, Indira U Mysorekar¹⁴¹⁹,
Jennifer Mytych¹⁴²⁰, Seyed Mohammad Nabavi¹⁴²¹, Massimo Nabissi¹⁴²², Péter Nagy¹⁴²³, Jihoon Nah¹⁴²⁴,
Aimable Nahimana¹⁴²⁵, Ichiro Nakagawa¹⁴²⁶, Ken Nakamura¹⁴²⁷, Hitoshi Nakatogawa¹⁴²⁸, Shyam Sundar Nandi¹⁴²⁹,
Meera Nanjundan¹⁴³⁰, Monica Nanni¹⁴³¹, Gennaro Napolitano^{618 2388}, Roberta Nardacci^{602 2389}, Masashi Narita¹⁴³²,
315 Melissa Nassif¹²⁶³, Ilana Nathan¹⁴³³, manabu Natsumeda¹⁴³⁴, Ryno Naude¹⁴³⁵, Christin Naumann¹⁴³⁶, Olaia Naveiras¹⁴³⁷,
Fatemeh Navid³⁹⁶, Steffan T. Nawrocki¹⁴³⁸, Taras Y Nazarko¹⁴³⁹, Francesca Nazio¹⁴⁴⁰, Florentina Negoita⁸⁶¹, Thomas Neill⁸⁴⁰,
Amanda L. Neisch⁷⁶⁰, Luca M Neri¹⁴⁴¹, Mihai G. Netea¹⁴⁴², Phillip T Newton¹⁴⁴³, Patrick Neubert⁸⁶⁶, Thomas P Neufeld¹⁴⁴⁴,
Dietbert Neumann¹⁴⁴⁵, Albert Neutzner¹⁴⁴⁶, Paul Ney, Ioannis P Nezis¹⁴⁴⁷, Charlene Ng¹⁴⁴⁸, Tzi B Ng¹⁴⁴⁹,
Hang Thi Thu Nguyen¹⁴⁵⁰, Long The Nguyen¹⁴⁵¹, Hong-Min Ni¹⁴⁵², Zhenhong Ni¹⁴⁵³, Cliona Ní Cheallaigh¹⁴⁵⁴,
320 M. Celeste Nicolao⁴²², Francesco Nicoli¹⁴⁵⁵, Manuel Nieto-Diaz¹⁴⁵⁶, Per Nilsson¹⁴⁵⁷, Shunbin Ning¹⁴⁵⁸, Rituraj Niranjana¹⁴⁵⁹,
Mireia Niso-Santano^{690 2390}, Hiroshi Nishimune¹⁴⁶⁰, Ralph A Nixon¹⁴⁶¹, Annalisa Nobili¹⁴⁶², Clevio Nobrega¹⁴⁶³,
Takeshi Noda¹⁴⁶⁴, Uxía Nogueira-Recalde, Trevor M. Nolan¹⁴⁶⁵, Ivan Nombela¹⁴⁹⁶, Ivana Novak¹⁴⁶⁶, Beatriz Novoa⁶⁰¹,
Takashi Nozawa¹⁴²⁶, Nobuyuki Nukina¹⁴⁶⁷, Carmen Nussbaum-Krammer¹⁴⁶⁸, Jesper Nylandsted¹⁴⁶⁹,
Tracey R. O Donovan¹³⁰⁹, Seónadh M. O Leary¹⁴⁷¹, Eyleen J. O'Rourke¹⁴⁷⁰, Mary P O'Sullivan¹⁴⁷¹, Timothy O Sullivan¹⁴⁷²,
325 Salvatore Oddo¹⁴⁷³, Ina Oehme¹⁴⁷⁴, Michinaga Ogawa¹⁴⁷⁵, M. H. Ögmundsdóttir¹⁴⁷⁶, Besim Ogretmen¹⁴⁷⁷, Eric Ogier-
Denis¹⁴⁷⁸, Goo Taeg Oh¹⁴⁷⁹, Seon-Hee Oh¹⁴⁸⁰, Young Oh¹⁴⁸¹, Takashi Ohama¹⁴⁸², Yohei Ohashi¹⁴⁸³, Masaki Ohmuraya¹⁴⁸⁴,
Vasileios Oikonomou²¹³⁴, Rani Ojha¹⁴⁸⁵, Koji Okamoto¹⁴⁸⁶, Hitoshi Okazawa¹⁴⁸⁷, Masahide Oku¹⁴⁸⁸, Jorge M A Oliveira¹⁴⁸⁹,
Michael M Ollmann¹⁴⁹⁰, James A Olzmann¹⁴⁹¹, Shakib Omari¹⁰⁹⁷, M Bishr Omary¹⁴⁹², Gizem Önal⁵¹⁰, Martin Ondrej¹⁹⁶², Sang-
Bing Ong¹⁴⁹³, Sang-Ging Ong¹⁴⁹⁴, Anna Onnis¹⁰², Juan Orellana¹⁴⁹⁵, Sara Orellana-Muñoz^{559 2355}, Maria Del Mar Ortega-
330 Villaizan¹⁴⁹⁶, Xilma R Ortiz-Gonzalez¹⁴⁹⁷, Elena Ortona¹²⁵¹, Heinz D Osiewacz¹⁴⁹⁸, Shigeru Oshima¹⁴⁹⁹, Abdel-
Hamid K Osman¹⁵⁰⁰, Rosario Osta²²⁵⁴, Marisa S Otegui¹⁵⁰¹, Kinya Otsu¹⁵⁰², Christiane Ott¹⁵⁰³, Luisa Ottobriani¹⁵⁰⁴, J-
H James Ou¹⁵⁰⁵, Tiago Fleming Outeiro¹⁵⁰⁶, Inger Oynebraten¹⁵⁰⁷, Melek Ozturk¹⁵⁰⁸, Gilles Pagès¹⁵⁰⁹, Susanta Pahari¹⁵¹⁰,
Marta Pajares^{690 2358 2391}, Utpal B. Pajvani¹⁵¹¹, Rituraj Pal¹⁵¹², Simona Paladino¹⁵¹³, Nicholas Pallet¹⁵¹⁴, Michela Palmieri¹⁵¹⁵,
Guiseppe Palmisano¹⁵¹⁶, Camilla Palumbo¹⁵¹⁷, Francesco Pampaloni¹⁵¹⁸, Lifeng Pan¹⁵¹⁹, Qingjun Pan¹⁵²⁰, Wenliang Pan⁴¹⁴,
335 Xin Pan¹⁵²¹, Ganna Panasyuk¹⁵²², Rahul Pandey¹⁵²³, Udai B Pandey¹⁵²⁴, Vrajesh Pandya¹⁵²⁵, Francesco Paneni¹⁵²⁶,
Shirley Y. Pang⁷⁸⁵, Elisa Panzarini¹⁵²⁷, Daniela Laura Papademetrio¹⁵²⁸, Elena Papaleo¹⁵²⁹, Daniel Papinski¹⁵³⁰,
Diana Papp¹⁵³¹, Eun Chan Park¹⁵³², Hwan Tae Park¹⁵³³, Ji-Man Park⁹⁵⁷, Jong-In Park¹⁵³⁴, Joon Tae Park¹⁵³⁵, Junsoo Park¹⁵³⁶,
Sang Chul Park¹⁵³⁷, Sang-Youel Park¹⁵³⁸, Abraham H. Parola¹⁵³⁹, Jan B Parys^{618 2388}, Adrien Pasquier¹⁵⁴⁰, Benoit Pasquier¹⁵⁴¹,
João F Passos¹⁵⁴², Nunzia Pastore¹⁵⁴³, Hemal H Patel¹⁵⁴⁴, Daniel Patschan¹⁵⁴⁵, Sophie Pattingre¹⁵⁴⁶, Gustavo Pedraza-
340 Alva¹⁵⁴⁷, Jose Pedraza-Chaverri¹⁵⁴⁸, Zully Pedrozo¹⁵⁴⁹, Jianming Pei¹⁵⁵⁰, Hadas Peled-Zehavi¹⁵⁵¹, Joaquín M. Pellegrini¹⁵⁵²,
Joffrey Pelletier^{32 2384}, Miguel A Penalva¹⁵⁵³, Di Peng²¹⁸⁵, Ying Peng¹⁵⁵⁴, Francesca Pentimalli¹⁵⁵⁵, Fabio Penna⁴¹⁵,
Maria Pennuto¹⁶⁷⁷, Cláudia MF Pereira¹⁵⁵⁶, Gustavo J.S. Pereira¹⁸⁶⁰, Lilian Cristina Pereira¹⁵⁵⁷, Luis Pereira de Almeida¹⁵⁵⁸,
Nirma D. Perera¹⁵⁵⁹, Angel Perez-Lara¹⁵⁶⁰, Ana B. Perez-Oliva¹⁵⁶¹, María Esther Pérez-Pérez⁴¹⁸, Palsamy Periyasamy¹⁵⁶²

- Andras Perl¹⁵⁶⁰, Cristiana Perrotta¹⁵⁶¹, Ida Perrotta¹⁵⁶², Richard G. Pestell¹⁵⁶³, Morten Petersen¹⁵⁶⁴, Irina Petrache¹⁵⁶⁵,
 345 Goran Petrovski¹⁵⁶⁶, Thorsten Pfirrmann¹⁵⁶⁷, Astrid Pfister¹⁵⁶⁸, Markus Plomann¹⁵⁶⁹, Jennifer A Philips¹⁵⁷⁰, Huifeng pi¹⁵⁷¹,
 Anna Picca¹⁵⁷², Alicia Pickrell¹⁵⁷³, Sandy Picot¹⁵⁷⁴, Giovanna Maria Pierantoni¹⁵⁷⁵, Marina Pierdominici¹⁵⁷⁶, Philippe Pierre¹⁵⁷⁷,
 Valerie Pierrefite-Carle¹⁵⁷⁸, Karolina Pierzynowska¹⁵⁷⁹, Federico Pietrocola¹⁵⁸⁰, Mirosława Pietruczuk¹⁵⁸¹,
 Claudio Pignata¹⁵⁸², Felipe X Pimentel-Muinos¹⁵⁸³, Mario Pinar¹⁵⁸⁴, Roberta Olmo Pinheiro¹⁵⁸⁵, Ronit Pinkas-Kramarski¹⁵⁸⁶,
 Paolo Pinton¹⁵⁸⁷, Karolina Pircs¹⁵⁸⁸, Sujan Piya¹⁵⁸⁹, Paola Pizzo¹⁵⁹⁰, Theo S Plantinga¹⁵⁹¹, Harald W Platta¹⁵⁹², Ainhoa Plaza-
 350 Zabala¹⁵⁹³, Egor Y Plotnikov¹⁵⁹⁴, Helene Plun-Favreau¹⁵⁹⁵, Ryszard Pluta¹⁵⁹⁶, Roger Pocock¹⁵⁹⁷, Stefanie Pöggeler¹⁵⁹⁸,
 Christian Pohl¹⁵⁹⁹, Marc Poirot¹⁶⁰⁰, Angelo Poletti¹⁶⁰¹, Marisa Ponpuak¹⁶⁰², Hana Popelka¹⁶⁰³, Blagovesta Popova¹⁶⁰⁴,
 Helena Porta¹⁶⁰⁵, Soledad Porte Alcon¹⁶⁰⁶, Eliana Portilla-Fernandez¹⁶⁰⁷, Martin Post¹⁶⁰⁸, Malia Potts, Joanna Poulton¹⁶⁰⁹,
 Ted Powers¹⁶¹⁰, Veena Prahlad¹⁶¹¹, Tomasz Prajsnar, Domenico Praticò¹⁶¹², Rosaria Prencipe¹⁶¹³, Muriel Priault¹⁶¹⁴,
 Tassula Proikas-Cezanne¹⁶¹⁵, Vasilis Promponas¹⁶¹⁶, Christopher G Proud¹⁶¹⁷, Rosa Puertollano¹⁶¹⁸, Luigi Puglielli¹⁶¹⁹,
 355 Thomas Pulinilkunnil¹⁶²⁰, Deepika Puri¹⁶²¹, Rajat Puri¹⁶²², Julien Puyal¹⁶²³, Xiaopeng Qi¹⁶²⁴, Yongmei Qi¹⁶²⁵, Wenbin Qian¹⁶²⁶,
 Lei Qiang¹⁶²⁷, Yu Qiu¹⁶²⁸, Joe Quadrilatero¹⁶²⁹, Jorge Quarieri¹⁶³⁰, Nina Raben¹⁶³¹, Hannah Rabinowich¹⁶³²,
 Debora Ragona¹⁶³³, Michael J Ragusa¹⁶³⁴, Nader Rahimi¹⁶³⁵, Marveh Rahmati¹⁶³⁶, Valeria Raia¹⁶³⁷, Nuno Raimundo¹⁶³⁸,
 Namakkal S Rajasekaran¹⁶³⁹, Sriganesh Ramachandra Rao¹⁶⁴⁰, Abdelhaq Rami¹⁶⁴¹, Ignacio Ramírez-Pardo¹⁶⁴²,
 David B. Ramsden¹⁶⁴³, Felix Randow¹⁶⁴⁴, Pundi N Rangarajan¹⁶⁴⁵, Danilo Ranieri¹⁶⁴⁶, Hai Rao¹⁶⁴⁷, Lang Rao¹⁶⁴⁸, Rekha Rao¹⁶⁴⁹,
 360 Sumit Rathore¹⁶⁵⁰, J Arjuna Ratnayaka¹⁶⁵¹, Edward Ratovitski¹⁶⁵², Palaniyandi Ramanan¹⁶⁵³, Gloria Ravegnini¹⁶⁵⁴,
 Swapan K Ray¹⁶⁵⁵, Babak Razani¹⁶⁵⁶, Vito Rebecca¹⁶⁵⁷, Fulvio Reggiori¹⁶⁵⁸, Anne Régnier-Vigouroux¹⁶⁵⁹,
 Andreas S Reichert¹⁶⁶⁰, David Reigada¹⁶⁶¹, Jan H Reiling¹⁶⁶², Rokeya Sultana Rekha¹⁶⁶³, Theo Rein¹⁶⁶⁴, Siegfried Reipert¹⁶⁶⁵,
 Hongmei Ren¹⁶⁶⁶, Jun Ren¹⁶⁶⁷, Weichao Ren¹⁶⁶⁸, Tristan Renault¹⁶⁶⁹, Giorgia Renga¹⁶⁷⁰, Karen Reue¹⁶⁷¹, Kim Rewitz¹⁶⁷²,
 S Amer Riazuddin¹⁶⁷³, Bruna Ribeiro de Andrade Ramos¹⁶⁷⁴, Teresa M. Ribeiro-Rodrigues¹⁶⁷⁵, Jean-Ehrland Ricci¹⁶⁷⁶,
 365 Romeo Ricci¹⁶⁷⁷, Victoria Riccio¹⁶⁷⁸, Des R Richardson¹⁶⁷⁹, Yasuko Rikihisa¹⁶⁸⁰, Makarand V Risbud¹⁶⁸¹,
 Ruth Muñoz Risueño¹⁶⁸², Konstantinos Ritis¹⁶⁸³, Salvatore Rizza, Rosario Rizzuto¹⁶⁸⁴, Helen C. Roberts¹⁶⁸⁵,
 Luke D. Roberts¹⁶⁸⁶, Katherine J Robinson¹⁶⁸⁷, Maria Carmela Roccheri¹⁶⁸⁸, Stephane Rocchi¹⁶⁸⁹, George G. Rodney¹⁶⁹⁰,
 Tiago Rodrigues¹⁶⁹¹, Vagner Ramon Rodrigues Silva¹⁶⁹², Amaia Rodriguez¹⁶⁹³, Ruth Rodriguez-Barrueco¹⁶⁹⁴,
 Nieves Rodriguez-Henche¹⁶⁹⁵, Humberto Rodriguez-Rocha¹⁶⁹⁶, Jeroen Roelofs¹⁶⁹⁷, Robert S. Rogers¹⁶⁹⁸, Vladimir Rogov¹⁶⁹⁹,
 370 Ana I Rojo¹⁷⁰⁰, Krzysztof Rolka¹⁷⁰¹, Vanina Romanello¹⁷⁰², Luigina Romani¹⁷⁰³, Alessandra Romano¹⁷⁰⁴,
 Patricia Silvia Romano¹⁷⁰⁵, David Romeo-Guitart¹⁷⁰⁶, Luis C. Romero¹⁷⁰⁷, Montserrat Romero¹⁷⁰⁸, Joseph Roney¹⁷⁰⁹,
 Yueguang Rong¹⁷¹⁰, Christopher Rongo¹⁷¹¹, Sante Roperto¹⁷¹², Mathias Rosenfeldt¹⁷¹³, Philip Rosenstiel¹⁷¹⁴,
 Anne Rosenwald¹⁷¹⁵, Kevin A Roth¹⁷¹⁶, Lynn Roth¹⁷¹⁷, Steven Roth¹⁷¹⁸, Kasper M A Rouschop¹⁷¹⁹, Benoit Roussel¹⁷²⁰,
 Sophie Roux¹⁷²¹, Patrizia Rovere-Querini¹⁷²², Ajit Roy¹⁷²³, Aureore Rozieres¹⁷²⁴, Diego Ruano¹⁷²⁵, David C Rubinsztein¹⁷²⁶,
 375 Maria P. Rubtsova¹⁷²⁷, Klaus Ruckdeschel¹⁷²⁸, Christoph Ruckenstein¹⁷²⁹, Emil Rudolf¹⁷³⁰, Ruediger Rudolf¹⁷³¹,
 Alessandra Ruggieri¹⁷³², Avnika Ruparelia¹⁷³³, Ryan R. Russell¹⁷³⁴, Gian Luigi Russo¹⁷³⁵, Maria Russo¹⁷³⁶, Rossella Russo¹⁷³⁷,
 Oxana O Ryabaya¹⁷³⁸, Kevin M. Ryan¹⁷³⁹, Kwon-Yul Ryu¹⁷⁴⁰, Maria Sabater-Arcis¹⁷⁴¹, Ulka Sachdev¹⁷⁴², Michael Sacher¹⁷⁴³,
 Carsten Sachse¹⁷⁴⁴, Abhishek Sadhu¹⁷⁴⁵, Junichi Sadoshima¹⁷⁴⁶, Nathaniel Safren¹⁷⁴⁷, Paul Saftig¹⁷⁴⁸,
 Amirhossein Sahebkar¹⁷⁴⁹, Gaurav Sahay¹⁷⁵⁰, Mustafa Sahin¹⁷⁵¹, Ozgur Sahin¹⁷⁵², Sumit Sahni¹⁷⁵³, Nayuta Saito¹⁷⁵⁴,
 380 Shigeru Saito¹⁷⁵⁵, Tsunenori Saito¹⁷⁵⁶, Ryohei Sakai¹⁷⁵⁷, Yasuyoshi Sakai¹⁷⁵⁸, Jun-Ichi Sakamaki¹⁷⁵⁹, Kalle Saksela¹⁷⁶⁰,
 Gloria Salazar¹⁷⁶¹, Anna Salazar-Degracia¹⁷⁶², Ghasem Hosseini Salekdeh¹⁷⁶³, Ashok Saluja¹⁷⁶⁴, Belém Sampaio-
 Marques¹⁷⁶⁵, Maria Cecilia Sanchez¹⁷⁶⁶, Jose A. Sanchez-Alcazar¹⁷⁶⁷, Victoria Sanchez-Vera¹⁷⁶⁸, Vanessa Sancho-
 Shimizu¹⁷⁶⁹, J. Thomas Sanderson¹⁷⁷⁰, Marco Sandri¹⁷⁷¹, Stefano Santaguida¹⁷⁷², Laura Santambrogio¹⁷⁷³,
 Magda Matos Santana¹⁷⁷⁴, Giorgio Santoni¹⁷⁷⁵, Alberto Sanz¹⁷⁷⁶, Pascual Sanz¹⁷⁷⁷, Shweta Saran¹⁷⁷⁸, Marco Sardiello¹⁷⁷⁹,
 385 Timothy J Sargeant¹⁷⁸⁰, Apurva Sarin¹⁷⁸¹, Chinmoy Sarkar¹⁷⁸², Sovan Sarkar¹⁷⁸³, Surajit Sarkar¹⁷⁸⁴, Dipanka Tanu Sarmah¹⁷⁸⁵,
 Jaakko Sarparanta¹⁷⁸⁶, Maria-Rosa Sarrias¹⁷⁸⁷, Aishwarya Sathyanarayan¹⁷⁸⁸, Ranganayaki Sathyanarayanan¹⁷⁸⁹,
 Kenneth Matthew Scaglione¹⁷⁹⁰, Francesca Scatozza¹⁷⁹¹, Liliana Schaefer¹⁷⁹², Zachary T. Schafer¹⁷⁹³, Ulrich E. Schaible¹⁷⁹⁴,
 Anthony H V Schapira¹⁷⁹⁵, Michael Scharl¹⁷⁹⁶, Hermann Schatzl¹⁷⁹⁷, Catherine H Schein¹⁷⁹⁸, Wiep Scheper¹⁷⁹⁹,
 David Scheuring¹⁸⁰⁰, Maria Vittoria Schiaffino¹⁸⁰¹, Monica Schiappacassi¹⁸⁰², Rainer Schindl¹⁸⁰³, Oliver Schmidt¹⁸⁰⁴,
 390 Stephen D Schmidt¹⁸⁰⁵, Roland Schmitt¹⁸⁰⁶, Ingo Schmitz¹⁸⁰⁷, Uwe Schlattner¹⁸⁰⁸, Eran Schmukler¹⁸⁰⁹, Anja Schneider¹⁸¹⁰,
 Bianca Schneider¹⁸¹¹, Romana Schober¹⁸¹², Alejandra C. Schoijet¹⁸¹³, Micah B. Schott¹⁸¹⁴, Michael Schramm¹⁸¹⁵,
 Bernd Schroder¹⁸¹⁶, Kai Schuh¹⁸¹⁷, Christoph Schüller¹⁸¹⁸, Ryan J Schulze¹⁸¹⁹, Lea Schürmanns¹⁸²⁰, Jens C Schwamborn¹⁸²¹,
 Melanie Schwarten¹⁸²², Filippo Scialo¹⁸²³, Sebastiano Sciarretta¹⁸²⁴, Andrea Scrima¹⁸²⁵, Melanie J Scott¹⁸²⁶,
 Kathleen W Scotto¹⁸²⁷, A Ivana Scovassi¹⁸²⁸, Aurora Scrivo¹⁸²⁹, David Sebastian¹⁸³⁰, Salwa Sebti¹⁸³¹, Simon Sedej¹⁸³²,
 395 Laura Segatori¹⁸³³, Nava Segev¹⁸³⁴, Per O Seglen¹⁸³⁵, Ekihiro Seki¹⁸³⁶, Iban Seiliez¹⁸³⁷, Scott B Selleck¹⁸³⁸, Frank W Sellke¹⁸³⁹,
 Joshua T. Selsby¹⁸⁴⁰, Michael Sendtner¹⁸⁴¹, Serif Senturk¹⁸⁴², Consolato Sergi¹⁸⁴³, Elena Seranova¹⁸⁴⁴, Ruth Serra-Moreno¹⁸⁴⁵,
 Hiromi Sesaki¹⁸⁴⁶, Carmine Settembre¹⁸⁴⁷, Subba Rao Gangi Setty¹⁸⁴⁸, Gianluca Sgarbi¹⁸⁴⁹, Ou Sha¹⁸⁵⁰, John J. Shacka¹⁸⁵¹,
 Javeed A. Shah¹⁸⁵², Dantong Shang¹⁸⁵³, Changshun Shao¹⁸⁵⁴, Feng Shao¹⁸⁵⁵, Soroush Sharbati¹⁸⁵⁶, Lisa Sharkey¹⁸⁵⁷,
 Dipali Sharma¹⁸⁵⁸, Gaurav Sharma, Kulbhushan Sharma¹⁸⁵⁹, Pawan Sharma¹⁸⁶⁰, Surendra Sharma¹⁸⁶¹, Han-Ming Shen¹⁸⁶²,
 400 Hangtao Shen¹⁸⁶³, Jiangang Shen¹⁸⁶⁴, Ming Shen¹⁸⁶⁵, Weili Shen, Zheni Shen¹⁸⁶⁶, Rui Sheng¹⁸⁶⁷, Zhi Sheng¹⁸⁶⁸, Zu-
 Hang Sheng¹⁸⁶⁹, Jianjian Shi¹⁸⁷⁰, Xiaobing Shi¹⁸⁷¹, Ying-Hong Shi¹⁸⁷², Kahori Shiba-Fukushima¹⁸⁷³, Jeng-Jer Shieh¹⁸⁷⁴,

- Yohta Shimada¹⁸²⁷, Shigeomi Shimizu¹⁸²⁸, Makoto Shimozaawa¹⁴⁵⁷, Takahiro Shintani¹⁸²⁹, Christopher J Shoemaker¹⁸³⁰,
 Shahla Shojaei⁶⁶⁸, Ikuo Shoji¹⁸³¹, Bhupendra V Shrivage¹⁸³², Viji Shridhar¹⁸³³, Chih-Wen Shu¹⁸³⁴, Hong-Bing Shu¹⁸³⁵,
 Ke Shui²²⁷⁵, Arvind K Shukla⁶⁷⁵, Tim E. Shutt¹⁸³⁶, Valentina Sica¹⁸³⁷, Aleem Siddiqui¹⁸³⁸, Amanda Sierra¹⁸³⁹, Virginia Sierra-
 405 Torre¹⁸³⁸, Santiago Signorelli¹⁸³⁹, Payel Sil¹⁸⁴⁰, Bruno J. de Andrade Silva¹⁸⁴¹, Johnatas D. Silva¹⁰²², Eduardo Silva-
 Pavez^{264 2347}, Sandrine Silvente-Poirot¹⁵⁹², Rachel E. Simmonds¹⁸⁴², Anna Katharina Simon¹⁸⁴³, Hans-Uwe Simon¹⁸⁴⁴,
 Matias Simons¹⁸⁴⁵, Anurag Singh¹⁸⁴⁶, Lalit Pukhrambam Singh¹⁸⁴⁷, Rajat Singh¹⁸⁴⁸, Shivendra Singh¹⁸⁴⁹,
 Shrawan K. Singh¹⁸⁵⁰, Sudha B. Singh¹⁸⁵¹, Sunaina Singh¹²⁶², Surinder P Singh¹⁸⁵², Debasish Sinha¹⁸⁵³, Rohit A Sinha¹⁸⁵⁴,
 Sangita C Sinha¹⁸⁵⁵, Agnieszka Sirko²³³⁸, Kapil Sirohi¹⁸⁵⁶, Efthimios Sivridis⁶⁷², Panagiotis Skendros¹⁸⁵⁷,
 410 Aleksandra Skirycz^{596 2395}, Iva Slaninová¹⁸⁵⁸, Judith Sluimer¹⁸⁵⁹, Soraya S Smaili¹⁸⁶⁰, Andrei Smertenko¹⁸⁶¹,
 Matthew Smith¹⁸⁶², Eun Jung Sohn¹⁸⁶³, Sophia P. M. Sok⁷⁵⁴, Giancarlo Solaini¹⁸⁰⁴, Thierry Soldati¹⁸⁶⁴,
 Scott Soleimanpour¹⁸⁶⁵, Rosa M Soler⁶⁴⁵, Alexei Solovchenko¹⁸⁶⁶, Jason A Somarelli¹⁸⁶⁷, Stefaan Soenen¹⁸⁶⁸,
 Avinash Sonawane¹⁸⁶⁹, Fuyong Song¹⁸⁷⁰, Hyun Kyu Song¹⁸⁷¹, Ju-Xian Song¹⁸⁷², Kunhua Song¹⁸⁷³, Zhiyin Song¹⁸⁷⁴,
 Leandro R. Soria⁷¹³, Maurizio Sorice¹⁹²², Alexander A Soukas¹⁸⁷⁵, Sandra-Fausia Soukup¹⁸⁷⁶, Diana Sousa^{2022 2396},
 415 Nadia Sousa¹⁶⁴², Paul A Spagnuolo¹⁸⁷⁷, Stephen A Spector¹⁸⁷⁸, M.M. Srinivas Bharath¹⁸⁷⁹, Daret K St. Clair¹⁸⁸⁰,
 Venturina Stagni¹⁸⁸¹, Leopoldo Staiano¹⁸⁸², Christina L Stallings¹⁸⁸³, Clint A. Stalneck⁴⁷⁴, Metodii Stankov¹⁸⁸⁴,
 Peter B Stathopoulos¹⁸⁸⁵, Katja Stefan^{1658 2397}, Sven Marcel Stefan^{1658 2397}, Leonidas Stefanis¹⁸⁸⁶, Joan Steffan¹⁸⁸⁷,
 Alexander Steinkasserer¹⁸⁸⁸, Harald Stenmark¹⁸⁸⁹, Jared Sternecker¹⁸⁹⁰, Craig Stevens¹⁸⁹¹, Stephan Storch¹⁸⁹²,
 Veronika Stoka¹⁸⁹³, Bjorn Stork¹⁸⁹⁴, Flavie Strappazzon¹⁸⁹⁵, Anne Marie Strohecker¹⁸⁹⁶, Dwayne G. Stupack¹⁸⁹⁷, Huan-
 420 Xing Su¹²⁰⁸, Ling-Yan Su²²¹³, Longxiang Su¹⁸⁹⁶, Ana M. Suarez-Fontes²⁰¹⁷, Carlos Subauste¹⁸⁹⁷, Selvakumar Subbian¹⁸⁹⁸,
 Paula V. Subirada¹⁷³¹, Ganapasam Sudhandiran¹⁸⁹⁹, Carolyn M Sue¹⁹⁰⁰, Xinbing Sui¹⁹⁰¹, Corey M Summers¹⁹⁰²,
 Guangchao Sun¹⁹⁰³, Jun Sun¹⁹⁰⁴, Kang Sun¹⁹⁰⁵, Meng-xiang Sun¹⁹⁰⁶, Qiming Sun¹⁹⁰⁷, Yi Sun¹⁹⁰⁸, Zhongjie Sun¹⁹⁰⁹,
 Karen KS Sunahara¹⁹¹⁰, Eva Sundberg¹⁹¹¹, Katalin Susztak¹⁹¹², Peter Sutovsky¹⁹¹³, Hidekazu Suzuki¹⁹¹⁴, Gary Sweeney¹⁹¹⁵,
 J. David Symons¹⁹¹⁶, Stephen Cho Wing Sze¹⁹¹⁷, Nathaniel J Szewczyk¹⁹¹⁸, Anna Tabecka-Lonczynska¹⁹¹⁹,
 425 Claudio Tabolacci^{569 2398}, Frank Tacke¹⁹²⁰, Heinrich Taegtmeier¹⁹²¹, Marco Tafani¹⁹²², Mitsuo Tagaya¹⁹²³, Haoran Tai¹⁹²⁴,
 Stephen W G Tait¹⁹²⁵, Yoshinori Takahashi¹⁹²⁶, Szabolcs Takats¹⁹²⁷, Priti Talwar¹⁶³⁶, Chit Tam^{1449 2399}, Shing Yau Tam¹⁹²⁸,
 Davide Tampellini¹⁹²⁹, Atsushi Tamura¹⁹³⁰, Chong Teik Tan²²³⁵, Eng-King Tan¹⁹³¹, Ya-Qin Tan^{2312 2400}, Masaki Tanaka¹⁹³²,
 Motomasa Tanaka¹⁹³³, Daolin Tang¹⁹³⁴, Jingfeng Tang¹⁹³⁵, Tie-Shan Tang¹⁹³⁶, Isei Tanida¹⁹³⁷, Zhipeng Tao¹⁹³⁸,
 Mohammed Taouis¹⁹³⁹, Lars Tatenhorst¹⁹⁴⁰, Nektarios Tavernarakis¹⁹⁴¹, allen taylor¹³⁸, Gregory Taylor¹⁹⁴²,
 430 Joan M. Taylor¹⁹⁴³, Elena Tchetina¹⁹⁴⁴, Andrew R Tee¹⁹⁴⁵, Irmgard Tegeder¹⁹⁴⁶, David Teis¹⁷⁶⁶, Natercia Teixeira²⁰⁰⁷,
 Fatima Teixeira-Clerc¹⁹⁴⁷, Kumsal Ayse Tekirdag⁹³⁷, Tegin Tencomnao¹⁹⁴⁸, Sandra Tenreiro¹⁹⁴⁹, Alexei Tepikin¹⁹⁵⁰,
 Pilar S Testillano¹⁹⁵¹, Gianluca Tettamanti¹⁹⁵², Pierre-Louis Tharaux¹⁹⁵³, Kathrin Thedieck¹⁹⁵⁴, Arvind A Thekkinghat¹⁶²⁹,
 Stefano Thellung^{612 2401}, Josephine W. Thinwa¹¹⁰⁸, Venkatesh P. Thirumalaikumar^{596 2395}, Sufi Mary Thomas¹⁹⁵⁵,
 Paul G Thomes¹⁹⁵⁶, Andrew Thorburn¹⁹⁵⁷, Lipi Thukral¹⁹⁵⁸, Thomas Thum¹⁹⁵⁹, Michael Thumm¹⁹⁶⁰, Ling Tian¹⁹⁶¹,
 435 Ales Tichy¹⁹⁶², Andreas Till¹⁹⁶³, Vincent Timmerman¹⁹⁶⁴, Vladimir I Titorenko¹⁹⁶⁵, Sokol V. Todi¹⁹⁶⁶, Krassimira Todorova⁷⁵⁹,
 Janne M. Toivonen¹⁹⁶⁷, Luana Tomaipitina⁶⁷¹, Dhanendra Tomar¹⁹⁶⁸, Cristina Tomas-Zapico¹⁹⁶⁹, Sergej Tomic¹⁹⁷⁰,
 Chao Tong¹⁹⁷¹, Chun-Kit Tong^{1119 2402}, Xin Tong¹⁹⁷², Sharon A Tooze¹⁹⁷³, Maria Torgersen¹⁹⁷⁴, Satoru Torii¹⁸²⁸, Liliana Torres-
 López⁵⁰⁶, Alicia Torriglia¹⁹⁷⁵, Christina Towers²²⁸⁷, Roberto Towns¹⁹⁷⁶, Shinya Toyokuni¹⁹⁷⁷, Vladimir Trajkovic¹⁹⁷⁸,
 Donatella Tramontano¹⁹⁷⁹, Quynh-Giao Tran⁹⁶¹, Leonardo Travassos¹⁹⁸⁰, Charles B Trelford⁴⁸⁵, Shirley Tremel²¹³³,
 440 Ioannis P Trougakos¹⁹⁸¹, Mario P Tschan¹⁹⁸², Betty P Tsao¹⁹⁸³, Hung-Fat Tse¹⁹⁸⁴, Tak F. Tse¹⁴⁴⁹, Hitoshi Tsugawa¹⁹¹⁴,
 Andrey S Tsvetkov¹⁹⁸⁵, David Tumbarello¹⁹⁸⁶, Yasin Tumtas²⁰⁷, María J. Tuñón⁶⁸⁸, Sandra Turcotte¹⁹⁸⁷, Boris Turk¹⁹⁸⁸,
 Vito Turk¹⁹⁸⁸, Bradley Turner¹⁹⁸⁹, Richard I Tuxworth¹⁹⁹⁰, Jess Tyler¹⁹⁹¹, Elena V. Tyutereva¹⁹⁹², Yasuo Uchiyama¹⁹⁹³,
 Aslihan Ugun-Klusek¹⁹⁹³, Holm H Uhlig¹⁹⁹⁴, Marzena Ulamek-Kozioł¹⁹⁹⁵, Ilya Ulasov¹⁹⁹⁶, Midori Umekawa¹⁹⁹⁷,
 Christian Ungermann¹⁹⁹⁸, Rei Unno²²¹⁵, Sylvie Urbe¹⁹⁹⁹, Elisabet Uribe-Carretero^{690 2366}, Suayib Ustun²⁰⁰⁰,
 445 Vladimir N Uversky²⁰⁰¹, Thomas Vaccari²⁰⁰², Maria I Vaccaro²⁰⁰³, Björn F. Vahsen²⁰⁰⁴, Helin Vakifahmetoglu-Norberg²⁰⁰⁵,
 Rut Valdor²⁰⁰⁶, Maria Joao Valente²⁰⁰⁷, Ayelén Valko²⁰⁰⁸, Richard B. Vallee²⁰⁰⁹, Angela M Valverde²⁰¹⁰, Stijn van der Veen²⁰¹¹,
 Greet Van den Berghe²⁰¹⁶, Luc Van Kaer²⁰¹², Jorg van Loosdregt²⁰¹³, Sjoerd J. L. van Wijk²⁰¹⁴, Wim Vandenbergh²⁰¹⁵,
 Ilse Vanhorebeek²⁰¹⁶, Marcos Andre Vannier-Santos²⁰¹⁷, Nicola Vannini²⁰¹⁸, M. Cristina Vanrell¹⁶⁸⁰, Chiara Vantaggiato²⁰¹⁹,
 Gabriele Varano²⁰²⁰, Isabel Varela-Nieto²⁰²¹, Máté Varga²⁰²², Helena Vasconcelos²⁰²³, Somya Vats¹²⁶², Demetrios Vavvas²⁰²³,
 450 Ignacio Vega-Naredo²⁰²⁴, Silvia Vega-Rubin-de-Celis²⁰²⁵, Anne Vehlow²⁰²⁶, Guillermo Velasco¹²⁰³,
 Ariadna P. Velázquez^{703 2369}, Tibor Vellai²⁰²⁷, Edo Vellenga²⁰²⁸, Francesca Velotti²⁰²⁹, Mireille Verdier²⁰³⁰,
 Panayotis Verginis²⁰³¹, Isabelle Vergne²⁰³², Paul Verkade²⁰³³, Manish Verma²⁰³⁴, Patrik Verstreken²⁰⁴¹, Tim Vervliet²³⁴,
 Jörg Vervoorts²⁰³⁵, Alexandre T Vessoni²⁰³⁶, Victor M. Victor²⁰³⁷, Michel Vidal²⁰³⁸, Chiara Vidoni⁸⁴⁶, Otilia V. Vieira²⁰³⁹,
 Richard D. Vierstra¹²⁷⁴, Sonia Viganó^{1737 2387}, Helena Vihinen²⁰⁴⁰, Vinoy Vijayan²⁰⁴¹, Miquel Vila²⁰⁴², Marçal Vilar²⁰⁴³,
 455 José M. Villalba⁶⁹¹, Antonio Villalobo²⁰⁴⁴, Beatriz Villarejo-Zori²⁰⁵, Francesc Villarroya²⁰⁴⁵, Joan Villarroya²⁰⁴⁶,
 Olivier Vincent²⁰⁴⁷, Cecile Vindis²⁰⁴⁸, Christophe Viret⁵⁸², Maria Teresa Viscomi²⁰⁴⁹, Dora Visnjic²⁰⁵⁰, Ilio Vitale²⁹,
 David J Vocadlo²⁰⁵¹, Olga Voitsekhovskaja²⁰⁵², Cinzia Volonte²⁰⁵³, Mattia Volta²⁰⁵⁴, Marta Vomero²⁰⁵⁵,
 Clarissa Von Haefen²⁰⁵⁶, Marc Vooijs²⁰⁵⁷, Wolfgang Voos²⁰⁵⁸, Ljubica Vucicevic²⁰⁵⁹, Richard Wade-Martins²⁰⁶⁰,
 Satoshi Waguri²⁰⁶⁰, Kenrick A. Waite¹⁶⁷³, Shuji Wakatsuki²⁰⁶¹, David Walker²⁰⁶², Mark Walker²⁰⁶³, Simon Walker²⁰⁶⁴,

- 460 Jochen Walter²⁰⁶⁵, Francisco Wandosell²⁰⁶⁶, Bo Wang²⁰⁶⁷, Chao-Yung Wang²⁰⁶⁸, Chen Wang²⁰⁶⁹, Chenran Wang⁷¹⁶,
Chenwei Wang²¹⁸⁵, Cun-Yu Wang²⁰⁷⁰, Dennis Qing Wang²⁰⁷¹, Dong Wang²⁰⁷², Fangyang Wang²⁰⁷³, Feng Wang²⁰⁷⁴, Feng-
Ming Wang²⁰⁷⁵, Guansong Wang²⁰⁷⁶, Han Wang²⁰⁷⁷, Hao Wang²⁰⁷⁸, Hexiang Wang²⁰⁷⁹, Hong-Gang Wang¹⁹²⁶,
Jianrong Wang²⁰⁸⁰, Jiou Wang²⁰⁸¹, Kui Wang²²⁹⁰, Jigang Wang²⁰⁸², Jundong Wang²⁰⁸³, Lianrong Wang³³⁴, Liming Wang²⁰⁸⁴,
Maggie Haitian Wang²⁰⁸⁵, Meiqing Wang²⁰⁸⁶, Nanbu Wang²⁰⁸⁷, Peipei Wang²⁰⁸⁸, Pengwei Wang²⁰⁸⁹, Ping Wang²²¹⁹,
465 Ping Wang²⁰⁹⁰, Qing Kenneth Wang²⁰⁹¹, Qiong Wang²⁰⁹², Qing Jun Wang²⁰⁹³, Wen-Tao Wang³⁴⁵, Wuyang Wang²⁰⁹⁴,
Xinnan Wang²⁰⁹⁵, Xuejun Wang²⁰⁹⁶, Yan Wang²⁰⁹⁷, Yanchang Wang²⁰⁹⁸, Yanzhuang Wang^{987 2403}, Yen-Yun Wang²⁰⁹⁹,
Yihua Wang²¹⁰⁰, Yipeng Wang^{1259 2404}, Yu Wang²¹⁰¹, Yuqi Wang²¹⁰², Zhe Wang²¹⁰³, Zhenyu Wang²¹⁰⁴, Zhouguang Wang²¹⁰⁵,
Gary Warnes²¹⁰⁶, Verena Warnsmann¹⁴⁹⁸, Hirotaka Watada²¹⁰⁷, Eizo Watanabe²¹⁰⁸, Maxinne Watchon¹⁰⁵¹,
Anna Wawrzynska²³³⁸, Timothy Weaver²¹⁰⁹, Grzegorz Wegrzyn²¹¹⁰, Ann Marie Wehman²¹¹¹, Huafeng Wei²¹¹², Lei Wei²¹¹³,
470 Taotao Wei²¹¹⁴, Yongjie Wei²¹¹⁵, Oliver H. Weiergräber²¹¹⁶, Conrad Wehl²¹¹⁷, Günther Weindl²¹¹⁸, Ralf Weiskirchen²¹¹⁹,
Alan Wells²¹²⁰, Runxia H. Wen²¹²¹, Xin Wen⁹⁸⁷, Antonia Werner²¹²², Beatrice Weykopf²¹²³, Sally Wheatley²¹²⁴,
J. Lindsay Whitton²¹²⁵, Alexander Whitworth²¹²⁶, Dieter Willbold²¹²⁷, Manon E Wildenberg²¹²⁸, Thomas Wileman²¹²⁹,
Simon Wilkinson²¹³⁰, Brett Williams²¹³¹, Robin S B Williams²¹³², Roger L Williams²¹³³, Peter Williamson²¹³⁴,
Richard A Wilson²¹³⁵, Beate Winner²¹³⁶, Nathaniel Winsor²¹³⁷, Steven S Witkin²¹³⁸, Katarzyna Wiktorska²¹³⁹,
475 Harald Wodrich²¹⁴⁰, Ute Woehlbier¹²⁶³, Thomas Wollert²¹⁴¹, Esther Wong²¹⁴², Jack H Wong²¹⁴³, Richard Wong,
Vincent Kam Wai Wong¹⁰⁶⁷, W. Wei-Lynn Wong²¹⁴⁴, An-Guo Wu²¹⁴⁵, Chengbiao Wu²¹⁴⁶, Jian Wu²¹⁴⁷, Junfang Wu²¹⁴⁸,
Kenneth K. Wu²¹⁴⁹, Min Wu²¹⁵⁰, Shan-Ying Wu³¹³, Shengzhou Wu²¹⁵¹, Shu-Yan Wu²¹⁵², Shufang Wu²¹⁵³, William K K Wu²²⁷²,
Xiaohong Wu²¹⁵⁴, Xiaoqing Wu²¹⁸², Yaowen Wu²¹⁵⁵, Yihua Wu²¹⁵⁶, Ramnik J Xavier²¹⁵⁷, Hongguang Xia²¹⁵⁸, Lixin Xia²¹⁵⁹,
Zhengyuan Xia²¹⁶⁰, Ge Xiang¹¹⁸³, Jin Xiang²¹⁶¹, Mingliang Xiang²¹⁶², Wei Xiang²¹⁶³, Bin Xiao²¹⁶⁴, Guozhi Xiao²¹⁶⁵,
480 Hengyi Xiao²¹⁶⁶, Hong-Tao Xiao²¹⁶⁷, Jian Xiao²¹⁶⁸, Lan Xiao²¹⁷⁰, Shi Xiao²¹⁶⁹, Yin Xiao²¹⁷⁰, Baoming Xie²¹⁷¹, Chuan-Ming Xie²¹⁷²,
Min Xie²¹⁷³, Yuxiang Xie¹⁸²², Zhiping Xie²¹⁷⁴, Zhonglin Xie²¹⁷⁵, Maria Xilouri²¹⁷⁶, Congfeng Xu²¹⁷⁷, En Xu²¹⁷⁸, Haoxing Xu²¹⁷⁹,
Jin-Rong Xu²¹⁸⁰, Jing Xu²¹⁸¹, Liang Xu²¹⁸², Wen Wen Xu²¹⁸³, Xiulong Xu²¹⁸⁴, Yu Xue²¹⁸⁵, Sokhna M.S Yakhine-Diop⁶⁹⁰,
Masamitsu Yamaguchi²¹⁸⁶, Osamu Yamaguchi²¹⁸⁷, Ai Yamamoto²¹⁸⁸, Shunhei Yamashina²¹⁸⁹, Shengmin Yan²²¹⁸, Shian-
Jang Yan²¹⁹⁰, Zhen Yan²¹⁹¹, Yasuo Yanagi²¹⁹², Chuanbin Yang²¹⁹³, Dun-Sheng Yang²¹⁹⁴, Huan Yang²¹⁹⁵, Huang-Tian Yang²¹⁹⁶,
485 Hui Yang²¹⁹⁷, Jin-Ming Yang²¹⁹⁸, Jing Yang²¹⁹⁹, Jingyu Yang²²⁰⁰, Ling Yang²²⁰¹, Liu Yang²²⁰², Ming Yang²²⁰³, Pei-
Ming Yang²²⁰⁴, Qian Yang²²⁰⁵, Seungwon Yang⁷⁶⁵, Shu Yang¹⁹¹, Shun-Fa Yang²²⁰⁶, Wannian Yang²²⁰⁷, Wei Yuan Yang³²⁵,
Xiaoyong Yang²²⁰⁸, Xuesong Yang²²⁰⁹, Yi Yang⁹⁸⁷, Ying Yang²²¹⁰, Honghong Yao²²¹¹, Shenggen Yao²²¹², Xiaoqiang Yao²²¹³,
Yong-Gang Yao²²¹⁴, Yong-Ming Yao²²¹⁵, Takahiro Yasui¹⁸⁵³, Meysam Yazdankhah²²¹⁶, Paul M Yen²²¹⁷, Cong Yi²²¹⁸, Xiao-
Ming Yin²²¹⁹, Yanhai Yin²²²⁰, Zhangyuan Yin⁹⁸⁷, Ziyi Yin²²⁹², Meidan Ying²²²⁰, Zheng Ying²²²¹, Calvin K. Yip²²²²,
490 Stephanie Pei Tung Yiu²²²³, Young Hyun Yoo²²²⁴, Kiyotsugu Yoshida²²²⁵, Saori Yoshii²²²⁶, Tamotsu Yoshimori²²²⁷,
Bahman Yousefi²²²⁸, Boxuan Yu²²²⁹, Haiyang Yu²²³⁰, Jun Yu²²³¹, Jun Yu²²³², Li Yu²²³³, Ming-Lung Yu²²³⁴, Seong-Woon Yu⁹⁵⁹,
Victor Yu²²³⁵, Wai Haung Yu²²³⁶, Zhengping Yu²²³⁷, Zhou Yu²²³⁸, Junying Yuan²²³⁹, Ling-Qing Yuan²²⁴⁰, Shilin Yuan²²⁷⁶,
Shyng-Shiou F Yuan²²⁴¹, Yanggang Yuan²²⁴², Zengqiang Yuan²²⁴³, Jianbo Yue²²⁴⁴, Zhenyu Yue²²⁴⁵, Jeanho Yun²²⁴⁶,
Raymond Yung²²⁴⁷, David Zacks²²⁴⁸, Gabriele Zaffagnini²²⁴⁹, Vanessa O. Zambelli²²⁵⁰, Isabella Zanella²²⁵¹, Sara Zanivan²²⁵²,
495 Qun S Zang²²⁵³, Silvia Zappavigna^{268 2385}, Pilar Zaragoza²²⁵⁴, Aitor Martinez Zarate²²⁵⁵, Konstantinos S. Zarbali²²⁵⁶,
Amir Zarebkohan²²⁵⁷, Amira Zarrouk²²⁵⁸, Scott O. Zeitlin²²⁵⁹, Jialiu Zeng^{709 2405}, Ju-deng Zeng²²⁷², Eva¹⁹⁸⁸,
Lixuan Zhan²¹⁷⁸, Bin Zhang²²⁶⁰, Donna D. Zhang²²⁶¹, Hanlin Zhang²²⁶², Hong Zhang²³²¹, Hong Zhang²²⁶³, Honghe Zhang²²⁶⁴,
Huafeng Zhang²²⁶⁵, Huaye Zhang²²⁶⁶, Hui Zhang²²⁶⁷, Hui-Ling Zhang²²⁶⁸, Jianbin Zhang²²⁶⁹, Jianhua Zhang²²⁷⁰, Jing-
Pu Zhang¹¹¹⁵, Kalin Y.B. Zhang⁵⁹⁰, Leshuai W Zhang²²⁷¹, Lin Zhang²²⁷², Lisheng Zhang²²⁷³, Lu Zhang²²⁷⁴, Luoying Zhang²²⁷⁵,
500 Menghuan Zhang²²⁷⁶, Peng Zhang²²⁷⁷, Sheng Zhang²²⁷⁸, Wei Zhang²²⁷⁹, Xiangnan Zhang²²⁸⁰, Xiao-Wei Zhang⁸⁰⁶,
Xiaolei Zhang²²⁸¹, Xiaoyan Zhang^{987 2406}, Xin Zhang²²⁸², Xinxin Zhang²²⁸³, Xu Dong Zhang²²⁸⁴, Yang Zhang²²⁸⁵,
Yanjin Zhang²²⁸⁶, Yi Zhang²²⁸⁷, Ying-Dong Zhang²²⁸⁸, Yingmei Zhang²²⁸⁹, Yuan-Yuan Zhang²²⁹⁰, Yuchen Zhang²²⁷²,
Zhe Zhang²²⁹¹, Zhengguang Zhang²²⁹², Zhibing Zhang²²⁹³, Zhihai Zhang⁹⁸⁷, Zhiyong Zhang²²⁹⁴, Zili Zhang²²⁹⁵,
Haobin Zhao²²⁹⁵, Lei Zhao^{1548 2407}, Shuang Zhao²²⁹⁶, Tongbiao Zhao²²⁹⁷, Xiao-Fan Zhao²²⁹⁸, Ying Zhao²²⁹⁹,
505 Yongchao Zhao²³⁰⁰, Yongliang Zhao²³⁰¹, Yuting Zhao¹¹⁰⁸, Guoping Zheng²³⁰², Kai Zheng²³⁰³, Ling Zheng²³⁰⁴,
Shizhong Zheng²²⁹⁴, Xi-Long Zheng²³⁰⁵, Yi Zheng²³⁰⁶, Zuguang Zheng²³⁰⁷, Boris Zhivotovsky²³⁰⁸, Qing Zhong²³⁰⁹, Ao Zhou²³¹⁰,
Ben Zhou²³¹¹, Cefan Zhou¹⁹³⁵, Gang Zhou²³¹², Hao Zhou²³¹³, Hong Zhou²³¹⁴, Hongbo Zhou²³¹⁵, Jie Zhou²³¹⁶, Jing Zhou²³¹⁷,
Jiyong Zhou²³¹⁸, Kailiang Zhou²³¹⁹, Rongjia Zhou²³²⁰, Xu-Jie Zhou²³²¹, Yanshuang Zhou²³²²,
Yinghong Zhou²³²³, Yubin Zhou²³²⁴, Zheng-Yu Zhou²³²⁵, Zhou Zhou²³²⁶, Binglin Zhu²³²⁷, Changlian Zhu²³²⁸, Guo-
510 Qing Zhu²³²⁹, Haining Zhu²³³⁰, Hongxin Zhu²³³¹, Hua Zhu²³³², Wei-Guo Zhu²³³³, Yanping Zhu²⁰⁵¹, Yushan Zhu²³³⁴,
Haixia Zhuang⁵⁸⁶, Xiaohong Zhuang⁸⁷⁵, Katarzyna Zientara-Rytter²³³⁵, Christine Zimmermann²³³⁶, Elena Ziviani²³³⁷,
Teresa Zoladek²³³⁸, Wei-Xing Zong²³³⁹, Dmitry Zorov²³⁴⁰, Antonio Zorzano²³⁴¹, Weiping Zou²³⁴², Zhen Zou²³⁴³,
Zhengzhi Zou, Steven Zuryn²³⁴⁴, and Werner Zwerschke²³⁴⁵

¹Life Sciences Institute, University of Michigan, Ann Arbor, MI, USA; ²Department of Molecular, Cellular and Developmental Biology University of Michigan, Ann Arbor, MI USA; ³Department of Molecular Signal Processing, Leibniz Institute of Plant Biochemistry, Halle (Saale), Germany; ⁴Hebrew University of Jerusalem, Department of Biochemistry and Food Science, Rehovot, Israel; ⁵Hospital Universitario de Canarias, Research Unit; CIBERNED and Universidad de La Laguna, ITB, Santa Cruz de Tenerife, Spain; ⁶University of California, Davis, Division of Rheumatology, Allergy and Clinical Immunology, School of Medicine, Sacramento, CA, USA; ⁷University of Toronto, Department of Biochemistry, Toronto, Ontario, Canada;

⁸Medical University Innsbruck, Department of Medicine I, Innsbruck, Austria; ⁹University of Calabria, Department of Pharmacy, Health and Nutritional Sciences, Arcavacata di Rende (CS), Italy; ¹⁰National Institutes of Health, National Eye Institute, Protein Structure and Function Section, Bethesda, MD, USA; ¹¹Ben-Gurion University of the Negev, Faculty of Health Sciences, Beer-Sheva, Israel; ¹²University of Alabama at Birmingham, Division of Nephrology and Birmingham VA Medical Center, Birmingham, AL, USA; ¹³The University of Texas M. D. Anderson Cancer Center, Houston, Texas, USA; ¹⁴University of Palermo, Dipartimento di Scienze e Tecnologie Biologiche, Chimiche e Farmaceutiche (STEBICEF), Palermo, Italy; ¹⁵Cell Death Research & Therapy (CDRT) Lab, Department of Cellular & Molecular Medicine, Center for Cancer Biology, VIB-KU Leuven, Leuven, Belgium; ¹⁶Indian Institute of Technology, Ropar, India; ¹⁷University of Dundee, School of Life Sciences, MRC Protein Phosphorylation and Ubiquitylation Unit, Dundee, UK; ¹⁸University of Texas Medical Branch, Department of Pathology, Galveston, TX, USA; ¹⁹Colby College, Department of Biology, Waterville, ME, USA; ²⁰University of Maryland School of Medicine, Departments of Otorhinolaryngology Head & Neck Surgery, Ophthalmology and Visual Science, Baltimore, MD, USA; ²¹Lund University, Department of Experimental Medical Science, Cell Death and Lysosomes Group, Lund, Sweden; ²²Nihon University, College of Bioresource Sciences, Fujisawa, Kanagawa, Japan; ²³The Institute of Cancer Research, Cancer Therapeutics Unit, Sutton, UK; ²⁴Pharmaceutical Sciences Department, College of Pharmacy, Gulf Medical University, Ajman, United Arab Emirates; ²⁵Insight Institute of Neurosurgery & Neuroscience, Department of Research, Flint, MI, USA; ²⁶McGill University, Departments of Medicine and Oncology and Segal Cancer Centre, Montreal, Quebec, Canada; ²⁷Technical University Dresden, Center for Molecular and Cellular Bioengineering (CMCB), Biotechnology Center (BIOTEC), Department of Cellular Biochemistry, Dresden, Germany; ²⁸Universidad de Sevilla, Departamento de Psicología Experimental, Facultad de Psicología, Sevilla, Spain; ²⁹Sapienza University of Rome, Department of Internal Medicine and Medical Specialties, Rome, Italy; ³⁰University of Rajshahi, Department of Pharmacy, Rajshahi, Bangladesh; ³¹Islamic University of Gaza, Faculty of science, Department of Biology and Biotechnology, Gaza, Palestine; ³²University of Barcelona, Faculty of Pharmacy, Department of Biochemistry and Physiology, Barcelona, Spain; Metabolism and Cancer Laboratory, Molecular Mechanisms and Experimental Therapy in Oncology Program (Oncobell), Institut d'Investigació Biomèdica de Bellvitge - IDIBELL, L'Hospitalet de Llobregat, Barcelona, Spain; ³³Cleveland Clinic, Department of Cancer Biology, Cleveland, OH, USA; ³⁴University of the Basque Country, Instituto Biofisika (UPV/EHU, CSIC), and Department of Biochemistry, Leioa, Spain; ³⁵Instituto de Investigaciones en Ingeniería Genética y Biología Molecular Dr. Héctor N. Torres, Laboratorio de señalización y mecanismos adaptativos en Tripanosomátidos, Buenos Aires, Argentina; Universidad de Buenos Aires, Departamento de Fisiología, Biología Molecular y Celular, Facultad de Ciencias Exactas y Naturales, Buenos Aires, Argentina; ³⁶Laboratory of Host-Pathogen Dynamics, National Heart Lung and Blood Institute, National Institutes of Health, Bethesda, MD 20892, USA; ³⁷The Wistar Institute, Philadelphia, PA, USA; ³⁸Buenos Aires University, Biochemistry and Pharmacy School, Department of Microbiology Immunology Biotechnology and Genetic, IDEHU, CABA, Argentina; ³⁹Islamic University of Gaza, Department of Medical Laboratory Sciences, Faculty of Health Sciences, Gaza, Palestine; ⁴⁰University of Pavia, Department of Drug Sciences, Pharmacology Unit, Pavia, Italy; ⁴¹University of Camerino, School of Biosciences and Veterinary Medicine, Camerino, Italy; ⁴²Ohio State University, Department of Microbial Infection and Immunity, and the Infectious Disease Research Institute, Columbus, OH, USA; ⁴³Save as Ravi Manjithaya; ⁴⁴University of California, San Francisco, San Francisco, CA, USA; ⁴⁵Aarhus University, Department of Molecular Biology and Genetics, Aarhus C, Denmark; ⁴⁶University of Bologna, Department of Pharmacy and Biotechnology, Bologna, Italy; ⁴⁷Departments of Pharmacology and Toxicology, and Neurology, The University of Alabama at Birmingham, Birmingham, AL, USA; ⁴⁸Cedars-Sinai Medical Center, Smidt Heart Institute, Los Angeles CA, USA; ⁴⁹City of Hope Comprehensive Cancer Center, Beckman Research Institute, Department of Diabetes Complications and Metabolism, Duarte, CA, USA; ⁵⁰University of Tennessee, Department of Chemical and Biomolecular Engineering, Knoxville, TN, USA; ⁵¹Northeast Ohio Medical University, Department of Anatomy & Neurobiology, Rootstown, OH, USA; ⁵²Max Planck Institute for Biology of Ageing and CECADE, University of Cologne, Germany; ⁵³University of Bristol, School of Biochemistry, Bristol, UK; ⁵⁴University of Helsinki, Molecular and Integrative Biosciences Research Programme, Helsinki, Finland; ⁵⁵Université de Bourgogne Franche Comté, INSERM, UMR1231, Dijon, France; ⁵⁶University of Valencia, Faculty of Medicine, Department of Pharmacology, Valencia, Spain; ⁵⁷Tokyo University of Pharmacy and Life Sciences, School of Life Sciences, Hachioji, Hachioji, Tokyo, Japan; ⁵⁸Universidade Federal de Viçosa, Departamento de Biologia Vegetal, Viçosa, MG, Brazil; ⁵⁹Jikei University school of Medicine, Division of Respiratory Disease, Department of Internal Medicine, Tokyo, Japan; ⁶⁰Newcastle University, Institute of Cellular Medicine, Newcastle Upon Tyne, UK; ⁶¹Albert Einstein College of Medicine, Department of Medicine, Bronx, NY, USA; ⁶²Tohoku University, Graduate School of Life Sciences, Sendai, Miyagi, Japan; ⁶³Instituto Cajal, Consejo Superior de Investigaciones Científicas (CSIC), Madrid, Spain; ⁶⁴University of Seville, Faculty of Pharmacy, Department of Physiology, Seville, Spain; ⁶⁵Howard University College of Medicine, Department of Anatomy, Washington D.C., USA; ⁶⁶Imperial College London, MRC Centre for Molecular Bacteriology and Infection, Department of Microbiology, London, UK; ⁶⁷Toulouse University, CNRS, UPS, Center for Integrative Biology (CBI), Research Center on Animal Cognition (CRCA), Toulouse, France; ⁶⁸Iowa State University, Department of Genetics, Development and Cell Biology, Roy J. Carver Co-Laboratory, Ames, IA, USA; ⁶⁹Universidad Nacional de Córdoba, Laboratorio de Oncohematología, Hospital Nacional de Clínicas, CONICET, Córdoba, Argentina; ⁷⁰York College/The City University of New York, Department of Biology, Jamaica, NY, USA; ⁷¹Translational Genomics Group, Incliva Health Research Institute, Burjassot, Valencia, Spain; Interdisciplinary Research Structure for Biotechnology and Biomedicine (ERI BIOTECMED), University of Valencia, Burjassot, Valencia, Spain; ⁷²Albert Einstein College of Medicine, Department of Molecular Pharmacology, Bronx, NY, USA; ⁷³University of Tabriz, Department of Basic Science, Faculty of Veterinary Medicine, Tabriz, Iran; ⁷⁴Meir Medical Center, Translational Hemato-Oncology Laboratory, Kfar-Saba, Israel; Tel Aviv University, Department of Human Molecular Genetics and Biochemistry, Sackler School of Medicine, Tel Aviv, Israel; ⁷⁵The Institute of Genetics and Animal Breeding, Polish Academy of Sciences, Magdalenka, Poland; Institute of Neurobiology, Bulgarian Academy of Sciences, Sofia, Bulgaria; Department of Pharmacognosy, University of Vienna, Vienna, Austria; ⁷⁶University of Pittsburgh Medical Center, Department of Critical Care Medicine, Department of Pediatrics, Safar Center for Resuscitation Research and the Children's Hospital of Pittsburgh, Pittsburgh, PA, USA; ⁷⁷University of Nice, Mediterranean Center for Molecular Medicine, Inserm U1065, Nice, France; ⁷⁸Imperial College London, Faculty of Medicine, London, UK; ⁷⁹Departments of Pharmacology and Microbiology, University of Maryland School of Medicine, Baltimore, MD, USA; Stanford University School of Medicine Stanford, CA, USA; ⁸⁰University of Turin, Department of Clinical and Biological Sciences, Turin, Italy; ⁸¹University of Milan, Department of Health Sciences, Milano, Italy; ⁸²Universidad de Santiago de Chile, Faculty of Chemistry and Biology, Department of Biology, Santiago, Chile; ⁸³Fondazione Istituto di Ricerca Pediatrica Città della Speranza, Neuroblastoma Laboratory, Padua, Italy; ⁸⁴The Hebrew University of Jerusalem, Alexander Silberman Institute of Life Sciences, Department of Plant and Environmental Sciences, Edmond Safra Campus, Jerusalem, Israel; ⁸⁵Tulane Health Sciences Center, Department of Pathology and Laboratory Sciences, New Orleans, LA, USA; ⁸⁶University of Arkansas for Medical Sciences, Department of Geriatrics, Little Rock, AR, USA; ⁸⁷Kogakuin University, Research Institute for Science and Technology, Hachioji, Tokyo, Japan; ⁸⁸Albert Einstein College of Medicine, Departments of Molecular Pharmacology and Biochemistry, Bronx, NY, USA; ⁸⁹Eastern Michigan University, Department of Chemistry, Ypsilanti, MI, USA; ⁹⁰Hanyang University, College of Pharmacy, Ansan, Gyeonggi-do, Korea; ⁹¹Yonsei University College of Medicine, Severance Biomedical Science Institute, Seoul, Korea; ⁹²University of Massachusetts Medical School, Department of Molecular, Cell and Cancer Biology, Worcester, MA, USA; ⁹³Ajou University, College of Pharmacy and Research Institute of Pharmaceutical Science and Technology (RIPST), Suwon, Korea; ⁹⁴Seoul National University, Department of Biological Sciences, Seoul, South Korea; ⁹⁵University of Calabria, Department of Pharmacy, Health Science and Nutrition, Section of Preclinical and Translational Pharmacology, Cosenza, Italy; ⁹⁶Adam Mickiewicz University/Faculty of Biology, Institute of Experimental Biology, Department of General Botany, Poznan, Poland; ⁹⁷Iowa State University, Department of Genetics,

Development, and Cell Biology, Ames, IA, USA; ⁹⁸Kunming University of Science and Technology, Medical School, Kunming, Yunnan, China; ⁹⁹University of Texas Health Science Center at San Antonio, Department of Cell Systems and Anatomy, San Antonio, TX, USA; ¹⁰⁰Jadavpur University, Department of Mathematics, Centre for Mathematical Biology and Ecology, Kolkata, India; ¹⁰¹Karolinska Institute, Department of Cell and Molecular Biology, Stockholm, Sweden; ¹⁰²University of Siena, Department of Life Sciences, Siena, Italy; ¹⁰³University of Urbino Carlo Bo, Department of Biomolecular Sciences, Urbino, Italy; ¹⁰⁴Telethon Institute of Genetics and Medicine (TIGEM), Federico II University, Naples, Italy; Baylor College of Medicine, Houston, TX, USA; ¹⁰⁵Institute for Research and Technology in Food and Agriculture (IRTA), Animal Breeding and Genetics Programme, Caldes de Montbui, Spain; ¹⁰⁶Max Planck Institute of Molecular Plant Physiology, Potsdam-Golm, Germany; ¹⁰⁷University of Malta, Department of Physiology & Biochemistry, Msida, Malta; ¹⁰⁸UCL Queen Square Institute of Neurology, Reta Lila Weston Institute, London, UK; ¹⁰⁹Middle East Technical University, Department of Biological Sciences, Ankara, Turkey; ¹¹⁰Michigan State University, Department of Biochemistry and Molecular Biology, East Lansing, MI, USA; ¹¹¹Université Côte D'Azur, CNRS, Inserm, Institut de Biologie Valrose, Nice, France; ¹¹²Universidade de São Paulo, Department of Biochemistry, Institute of Chemistry, Sao Paulo, Brazil; ¹¹³University of Bologna, Department of Biomedical and Neuromotor Sciences, Bologna, Italy; ¹¹⁴University of Rome Tor Vergata, Department of Biology, Rome, Italy; Istituto di Ricovero e Cura a Carattere Scientifico (IRCCS) Fondazione Santa Lucia, Laboratory of Cell Signaling, Rome, Italy; ¹¹⁵Edinburgh Napier University, School of Applied Sciences, Edinburgh, UK; ¹¹⁶University of Michigan, Department of Neurology, Ann Arbor, MI, USA; ¹¹⁷Pulmonology Department, Hospital del Mar-IMIM, Pompeu Fabra University, CIBERES, Barcelona, Spain; ¹¹⁸University of Limerick, Department of Biological Sciences, Limerick, Ireland; University of Limerick, Health Research Institute, Limerick, Ireland; ¹¹⁹Danish Cancer Society Research Center, Copenhagen, Denmark; ¹²⁰Rice University, Department of Biosciences, Houston, TX, USA; ¹²¹Columbia University, Department of Medicine, New York, NY, USA; ¹²²ICAR-Indian Veterinary Research Institute, FMD Vaccine Research Laboratory, Bengaluru, India; ¹²³Iowa State University, Department of Genetics, Development and Cell Biology, Ames, IA, USA; ¹²⁴The University of Texas M.D. Anderson Cancer Center, Department of Experimental Therapeutics, Houston, TX, USA; ¹²⁵University of North Texas Health Science Center, Department of Microbiology, Immunology & Genetics, Fort Worth, TX, USA; ¹²⁶University of Louvain, Louvain Institute of Biomolecular Science and Technology (LIBST), Louvain-la-Neuve, Belgium; ¹²⁷University of South Carolina Upstate, Spartanburg, SC, USA; ¹²⁸Institut National de la Santé et de la Recherche Médicale (INSERM) Unité 1138, Sorbonne University, Centre de Recherche des Cordeliers, Paris, France; ¹²⁹Francis Crick Institute, London, UK; UCL, Royal Free Hospital, London, UK; ¹³⁰NUMEA, INRA, University Pau & Pays Adour/E2S UPPA, Saint-Pée-sur-Nivelle, France; ¹³¹Emory University School of Medicine, Division of Endocrinology, Metabolism and Lipids, Atlanta, GA, USA; ¹³²University of Pennsylvania, Perelman School of Medicine, PENN Center for Pulmonary Biology, Lung Epithelial Biology Laboratories, Philadelphia, PA, USA; ¹³³Mater Research Institute, University of Queensland, Brisbane Australia; ¹³⁴Hannover Medical School, Department for Clinical Immunology and Rheumatology, Hannover, Germany; ¹³⁵Ludwig-Maximilians-Universität München, Munich Cluster for Systems Neurology, München, Germany; ¹³⁶University Medical Center of the Johannes Gutenberg University, Institute of Pathobiochemistry, Mainz, Germany; ¹³⁷University of Rome "Tor Vergata", Department of Clinical Sciences and Translational Medicine, Rome, Italy; ¹³⁸Tufts University, USDA Human Nutrition Research Center on Aging, Laboratory for Nutrition and Vision Research, Boston, MA, USA; ¹³⁹Bar-Ilan University, Azrieli Faculty of Medicine, Safed, Israel; ¹⁴⁰Boston University, Metcalf Science Center, Boston, MA, USA; ¹⁴¹Sorbonne Université, CNRS UMR8226, Institut de Biologie Physico-Chimique, Laboratoire de Biologie Moléculaire et Cellulaire des Eucaryotes, Paris, France; ¹⁴²Fondazione Italiana Fegato, Trieste, Italia OR Italian Liver Foundation, Trieste, Italy; ¹⁴³University of Rome "Sapienza", Department of Clinical and Molecular Medicine, Laboratory affiliated to Istituto Pasteur Italia Fondazione Cenci Bolognetti, Rome, Italy; ¹⁴⁴Centro Nacional de Biotecnología-CNB-CSIC, Madrid, Spain; ¹⁴⁵Universidad Autónoma de Madrid, Departamento de Biología Molecular, Madrid, Spain; ¹⁴⁶University of São Paulo, Faculty of Pharmaceutical Sciences, Department of Pathophysiology, Sao Paulo, Brazil; ¹⁴⁷University of Oklahoma Health Sciences Center/Stephenson Cancer Center, Department of Obstetrics and Gynecology, Section of Gynecologic Oncology, Oklahoma City, OK, USA; ¹⁴⁸UMR 7242 "Biotechnology and cellular signaling", CNRS, Illkirch, France; ¹⁴⁹Washington University in Saint Louis, School of Medicine, Department of Psychiatry, Saint Louis MO, USA; ¹⁵⁰Universidad Francisco de Vitoria, Madrid, Spain; ¹⁵¹University of Copenhagen, Department of Biology, Copenhagen, Denmark; ¹⁵²Lausanne University Hospital and Lausanne University, Institute of Pathology, Department of Laboratory Medicine and Pathology, Lausanne, Switzerland; ¹⁵³University of Cologne and University Hospital Cologne, Cologne Excellence Cluster on Cellular Stress Responses in Aging-Associated Diseases (CECAD), Cologne, Germany; Center for Molecular Medicine, Cologne, Germany; ¹⁵⁴Queen Mary University of London, Blizard Institute, Centre for Cell Biology and Cutaneous Research, London, UK; ¹⁵⁵University of Massachusetts Medical School, Department of Molecular, Cell and Cancer Biology (MCCB), Worcester, MA, USA; ¹⁵⁶Magna Graecia University, Department of Health Sciences, Catanzaro, Italy; ¹⁵⁷Université Paris Descartes, Institut Cochin, INSERM U1016, CNRS UMR8104, Paris, France; ¹⁵⁸CNRS, Université de Bordeaux, Laboratoire de Biogenèse Membranaire UMR5200, 33140 Villenave d'Ornon, Bordeaux, France; Université de Bordeaux, CNRS, Laboratoire de Biogenèse Membranaire UMR5200, Villenave d'Ornon, Bordeaux, France; ¹⁵⁹University of Michigan, Department of Ophthalmology and Visual Sciences, Ann Arbor, MI, USA; ¹⁶⁰University of Montpellier, CNRS/UMR5235 LPHI, Montpellier, France; ¹⁶¹Ghent University, VIB Center for Inflammation Research, Ghent, Belgium; ¹⁶²University of Oxford, Kennedy Institute of Rheumatology, Oxford, UK; ¹⁶³University of New Mexico, Department of Molecular Genetics and Microbiology, Department of Neurology, Albuquerque, NM, USA; ¹⁶⁴Comenius University, Department of Biochemistry, Bratislava, Slovakia; ¹⁶⁵University of Oklahoma Health Sciences Center, Department of Obstetrics and Gynecology, Oklahoma City, OK, USA; ¹⁶⁶Department of Biophysics, Post Graduate Institute of Medical Education and Research, Chandigarh, India; ¹⁶⁷Louisiana State University Health Sciences Center-Shreveport, Department of Pathology and Translational Pathobiology, Shreveport, LA, USA; ¹⁶⁸National Institute of Technology, Department of Life Science, Laboratory of Mycobacterial Immunology, Rourkela, Odisha, India; ¹⁶⁹Michigan Technological University, Department of Chemistry, Houghton, MI, USA; ¹⁷⁰Dalian Medical University, College of Basic Medical Sciences, Dalian, China; ¹⁷¹Garvan Institute of Medical Research, St Vincent's Medical School, Faculty of Medicine, UNSW, Sydney, Australia; ¹⁷²McGill University, Departments of Medicine and Oncology and Segal Cancer Centre, Montreal, Quebec, Canada; ¹⁷³Université Paris-Saclay, Inserm U1185, Le Kremlin-Bicêtre, France; ¹⁷⁴Federal University of São Paulo, Department of Pharmacology, Paulista School of Medicine, São Paulo, Brazil; ¹⁷⁵University Hospital of North Norway, The Heart and Lung Clinic; University of Tromsø-The Arctic University of Norway, Department of Clinical Medicine, Tromsø, Norway; ¹⁷⁶Norwegian University of Science and Technology, Department of Biomedical Laboratory Science, Trondheim, Norway; ¹⁷⁷University of York, Department of Biology, Heslington, UK; ¹⁷⁸University of Valencia, Faculty of Medicine, Department of Physiology, Valencia, Spain; CIBERehd, Valencia, Spain; ¹⁷⁹University of Lodz, Faculty of Biology and Environmental Protection, Lodz, Poland; ¹⁸⁰Linköping University, Department of Clinical and Experimental Medicine, Faculty of Medicine and Health Sciences, Linköping, Sweden; ¹⁸¹Karolinska Institutet, Department of Women's and Children's Health, Stockholm, Sweden AND Karolinska University Hospital, Pediatric Oncology, Stockholm, Sweden; ¹⁸²Indiana University School of Medicine, Department of Microbiology and Immunology, Indianapolis, IN, USA; ¹⁸³University of Zagreb, School of Medicine, Croatian Institute for Brain Research, Zagreb, Croatia; ¹⁸⁴University of Pennsylvania, Department of Basic and Translational research, School of Dental Medicine, Philadelphia, PA, USA; ¹⁸⁵Burnet Institute, Melbourne, Australia; ¹⁸⁶University College Cork, Department of Pharmacology and Therapeutics, County Cork, Ireland; ¹⁸⁷INSERM, University of Montpellier, Montpellier, France; ¹⁸⁸University of Padova, Department of Molecular Medicine, Padova, Italy; ¹⁸⁹Institut National de la Santé et de la Recherche Médicale, Centre de Recherche des Cordeliers, Sorbonne Université, Université de Paris, Paris, France; ¹⁹⁰University of Camerino, School of Biosciences and Veterinary Medicine, Camerino, Italy; ¹⁹¹National Institutes of Health, Eunice

Kennedy Shriver National Institute of Child Health and Human Development, Cell Biology and Neurobiology Branch, Bethesda, MD, USA; ¹⁹²West Virginia University, Department of Surgery, Morgantown, WV, USA; ¹⁹³The Open University, School of Life, Health and Chemical Sciences, Faculty of Science, Technology, Engineering and Mathematics, Milton Keynes, UK; ¹⁹⁴Albert Ludwigs University of Freiburg, Faculty of Medicine, Institute of Molecular Medicine and Cell Research, Freiburg, Germany; ¹⁹⁵University Children's Hospital Zurich, Children's Research Center and Department of Oncology, Zurich, Switzerland; ¹⁹⁶University of Texas M.D. Anderson Cancer Center, Department of Leukemia, Houston, TX, USA; ¹⁹⁷Case Western Reserve University School of Medicine, Department of Pediatrics, Cleveland, OH, USA; ¹⁹⁸InterRayBio, LLC, Baltimore, MD, USA; ¹⁹⁹Washington State University, Department of Veterinary Microbiology and Pathology, College of Veterinary Medicine, Pullman, WA, USA; ²⁰⁰Université de Paris, PARCC, INSERM, Paris, France; ²⁰¹University of Alabama at Birmingham, Department of Ophthalmology and Visual Sciences, Birmingham, AL, USA; ²⁰²University Paris 13, UMR_S942 Inserm; University of Paris, Bobigny, France; ²⁰³University Santiago de Compostela, Department of Pharmacology, Veterinary Faculty, Lugo, Spain; ²⁰⁴Baylor College of Medicine, Jan and Dan Duncan Neurological Research Institute and Department of Molecular and Human Genetics, Houston, TX, USA; ²⁰⁵Trinity College Dublin, School of Medicine, Trinity Translational Medicine Institute, Dublin, Ireland; ²⁰⁶Centro de Investigaciones Biológicas, CIB-CSIC, Madrid, Spain; ²⁰⁷Swedish University of Agricultural Sciences and Linnean Center for Plant Biology, Uppsala BioCenter, Department of Molecular Sciences, Uppsala, Sweden; ²⁰⁸Imperial College London, Department of Life Sciences, London, UK; ²⁰⁹The Connecticut Agricultural Experiment Station, Center for Vector Biology and Zoonotic Diseases, Department of Environmental Sciences, New Haven, CT, USA; ²¹⁰Inserm U1138, Centre de Recherche des Cordeliers, Sorbonne Université, Université de Paris, Paris, FRANCE; ²¹¹Goethe University, University Hospital, University Cancer Center Frankfurt (UCT), Department of Medicine, Hematology/Oncology, Frankfurt, Germany; ²¹²Danube Private University, Department of Medicine/Dental Medicine, Krems/Donau, Austria; ²¹³Universidad de Chile, Instituto de Nutrición y Tecnología de los Alimentos (INTA), Santiago, Chile; ²¹⁴Centre des Sciences du Goût et de l'Alimentation, AgroSup Dijon, CNRS, INRA, University of Bourgogne Franche-Comté, Eye and Nutrition Research Group, Dijon, France; ²¹⁵University of California San Francisco, Department of Medicine, Zuckerberg San Francisco General Hospital and TraumaCenter, San Francisco, CA, USA; ²¹⁶University of Copenhagen, Department of Biology, Denmark; ²¹⁷University of Pittsburgh, Department of Biological Sciences, Pittsburgh, PA, USA; ²¹⁸Washington University School of Medicine, Department of Medicine, Saint Louis, MO, USA; ²¹⁹Genentech, Research & Early Development; ²²⁰David Geffen School of Medicine at UCLA, Department of Neurology, Los Angeles, CA, USA; ²²¹University of Colorado, AMC, Department of Pharmacology, Aurora, CO, USA; ²²²University of Minnesota, Hormel Institute, Austin MN, USA; ²²³University of Sao Paulo, School of Physical Education and Sport, Cellular and Molecular Exercise Physiology Laboratory, Sao Paulo, SP, Brazil; ²²⁴Hospital for Sick Children, Cell Biology Program, Toronto, ON, Canada; ²²⁵Monash University, School of Biological Sciences, Melbourne, Victoria, Australia; ²²⁶University of Salento, Dept of Biological and Environmental Sciences and Technologies, Lecce, Italy; ²²⁷Department of Pharmacology and Experimental Neuroscience, University of Nebraska Medical Center, Omaha, NE, USA; ²²⁸University of Arizona, Department of Molecular and Cellular Biology, Tucson, AZ, USA; ²²⁹Institut Pasteur, Biologie des Bactéries Intracellulaires and CNRS UMR 3525, Paris, France; ²³⁰University of Iowa, Iowa City, IA, USA; ²³¹Montana BioAg. Inc. Missoula, MT, USA; ²³²Autophagy Research Center (ARC), Santiago, Chile; ²³³University of Pittsburgh, Aging Institute, Department of Medicine, Pittsburgh, PA, USA; ²³⁴University Duisburg-Essen, Essen University Hospital, Department of Gastroenterology and Hepatology, Essen, Germany; ²³⁵KU Leuven, Department of Cellular & Molecular Medicine, Campus Gasthuisberg, Leuven, Belgium; ²³⁶University of Medicine and Pharmacy of Craiova, Department of Medical Genetics, Craiova, Romania; ²³⁷King's College London, School of Cardiovascular Medicine & Sciences, The Rayne Institute, St Thomas' Hospital, London, UK; ²³⁸The Rockefeller University, Laboratory of Cellular and Molecular Neuroscience, New York, NY, USA; ²³⁹Stockholm University, The Wenner-Gren Institute, Department of Molecular Biosciences, Stockholm, Sweden; ²⁴⁰Universidad Nacional Autónoma de México, Faculty of Sciences, Department of Cell Biology, Fibrosis Lab, Mexico City, Mexico; ²⁴¹New York University School of Medicine, Skirball Institute and Department of Microbiology, New York, NY, USA; ²⁴²University of Las Palmas de Gran Canaria, Department of Physical Education and Research Institute of Biomedical and Health Sciences (IUIBS), Las Palmas de Gran Canaria, Spain; ²⁴³Norwegian School of Sport Sciences, Department of Physical Performance, Oslo, Norway; ²⁴⁴Università di Sassari, Dipartimento di Scienze Biomediche, Sassari, Italy; ²⁴⁵University of Urbino Carlo Bo, Department of Biomolecular Sciences, Urbino (PU), Italy; ²⁴⁶University of Louisville, Pediatric Research Institute, Department of Pediatrics, Louisville, KY, USA; ²⁴⁷Rutgers University, The State University of New Jersey, Department of Cell Biology and Neuroscience, Piscataway, NJ, USA; ²⁴⁸University of Alabama, Department of Biological Sciences, Tuscaloosa, AL, USA; ²⁴⁹University of Georgia, Department of Kinesiology, Athens, GA, USA; ²⁵⁰Fondazione Policlinico Universitario "Agostino Gemelli" IRCCS, Rome, Italy; ²⁵¹Università Cattolica del Sacro Cuore, Rome, Italy; ²⁵²University of São Paulo, Department of Immunology, Laboratory of Transplantation Immunobiology, São Paulo, SP, Brazil; ²⁵³CNRS, Institut Curie, Paris, France; ²⁵⁴IBGC, CNRS and University of Bordeaux, Bordeaux, France; ²⁵⁵University of London, The Royal Veterinary College, Department of Comparative Biomedical Sciences, UCL Consortium for Mitochondrial Research, London, UK; ²⁵⁶Loyola University, Stritch School of Medicine, Department of Microbiology and Immunology, Chicago, IL, USA; ²⁵⁷University of Ottawa, Department of Chemistry and Biomolecular Sciences and Department of Biochemistry, Microbiology and Immunology, Host-Microbe Interactions Laboratory, Ottawa, ON, Canada; ²⁵⁸University of Rome "Tor Vergata", Department of Biology, Rome, Italy; ²⁵⁹Universidad San Sebastián, Centro de Biología Celular y Biomedicina (CEBICEM), Facultad de Medicina y Ciencia, Santiago, Chile; ²⁶⁰Federal University of São Paulo, Department of Medicine, Nephrology Division, Laboratory of Clinical and Experimental Immunology, São Paulo, SP, Brazil; ²⁶¹University of Genoa, Department of Earth, Environment and Life Sciences, Genoa, Italy; ²⁶²University of Toronto, Sinai Health System, Lunenfeld-Tanenbaum Research Institute, Toronto, Ontario, Canada; ²⁶³IRBLleida-University of Lleida, Department of Experimental Medicine, Lleida, Spain; ²⁶⁴Xiamen University School of Medicine, Fujian Provincial Key Laboratory of Reproductive Health Research, Xiang'an, Xiamen, China; ²⁶⁵Instituto de Investigación Biomédica de A Coruña (INIBIC), Complejo Hospitalario Universitario de A Coruña (CHUAC), Sergas, Universidade da Coruña (UDC), A Coruña, Spain; ²⁶⁶University of Wisconsin, Department of Surgery, Madison, WI, USA; ²⁶⁷Universidad Mayor, Center of Integrative Biology, and Geroscience Center for Brain Health and Metabolism, Santiago, Chile; ²⁶⁸Universidad Nacional Autónoma de México, Institute of Biotechnology, Plant Molecular Biology Department, Cuernavaca, Morelos, México; ²⁶⁹University of Coimbra, Faculty of Medicine and CNC-Center for Neuroscience and Cell Biology, Coimbra, Portugal; ²⁷⁰University of Arizona Cancer Center, Tucson, AZ, USA; ²⁷¹University of Campania L. Vanvitelli, Department of Precision Medicine, Naples, Italy; ²⁷²Institute of Genetic Research, Biogen scarl, Laboratory of Molecular and Precision Oncology, Ariano Irpino (AV), Italy; ²⁷³Trev and Joyce Deeley Research Centre, BC Cancer, Victoria, British Columbia, Canada; ²⁷⁴Polytechnic University of Marche, Department of Life and Environmental Sciences, Ancona, Italy; ²⁷⁵Federal University of Rio de Janeiro, Institute of Microbiology, Department of Immunology, Rio de Janeiro, Brazil; ²⁷⁶University of Modena and Reggio Emilia, Department of Biomedical, Metabolic and Neural Sciences, Modena, Italy; ²⁷⁷Centre de Recherche en Cancerologie de Marseille (CRCM), INSERM U1068, CNRS UMR7258, Aix-Marseille Université U105, Institut Paoli-Calmettes, Parc Scientifique et Technologique de Luminy, Marseille, France; ²⁷⁸University Medical Center Hamburg-Eppendorf, Hamburg, Germany; ²⁷⁹DZHK (German Center for Cardiovascular Research), partner site Hamburg/Kiel/Lübeck, Hamburg, Germany; ²⁸⁰University of Bristol, School of Biochemistry, Bristol, UK; ²⁸¹University of Alabama at Birmingham, Department of Medicine, Pulmonary, Allergy, and Critical Care Medicine, Birmingham, AL, USA; ²⁸²Universitat Autònoma de Barcelona, Institute of Neuroscience, Barcelona, Spain; ²⁸³Aix Marseille Univ, IRD, AP-HM, SSA, VITROME, IHU-Mediterranée Infection, Marseille, France; ²⁸⁴University of Siena, Department of Life Sciences, Siena, Italy; ²⁸⁵University of New Mexico Health Sciences Center, Division of Gastroenterology and Hepatology, Department of Internal Medicine, Albuquerque, NM, USA; ²⁸⁶Universidad de

Valparaíso, Centro Interdisciplinario de Neurociencia de Valparaíso, Laboratory of Molecular Sensors, Valparaíso, Chile; ²⁸²Université de Paris, Sorbonne Université, Centre de Recherche des Cordeliers, INSERM U1138, Team "Metabolism, Cancer & Immunity", Paris, France; Gustave Roussy Cancer Campus, Metabolomics and Cell Biology Platforms, Villejuif, France; ²⁸³Universidad de Concepción, Department of Biochemistry and Molecular Biology, Concepción, Chile; ²⁸⁴Universidade de Lisboa, Faculty of Pharmacy, Research Institute for Medicines (iMed.Ulisboa), Lisboa, Portugal; Universidade NOVA de Lisboa, Faculdade de Ciências e Tecnologia, Departamento Ciências da Vida, UCIBIO, Caparica, Portugal; ²⁸⁵Universidad de La Laguna, Departamento de Ciencias Médicas Básicas, Tenerife, Spain; ²⁸⁶Universidad Nacional Autónoma de México (UNAM), Instituto de Fisiología Celular, Ciudad Universitaria, Ciudad de México, México; ²⁸⁷Division of Medical Genetics, Fondazione IRCCS-Casa Sollevo della Sofferenza, San Giovanni Rotondo, Italy; ²⁸⁸The Scripps Research Institute, Department of Molecular Medicine, La Jolla, CA, USA; ²⁸⁹University of Coimbra, CNC - Center for Neuroscience and Cell Biology, Coimbra & Faculty of Pharmacy, Coimbra, Portugal; ²⁹⁰University of Pisa, Interdepartmental Research Centre on Biology and Pathology of Aging, Pisa, Italy; ²⁹¹Biomedical Research Institute of Murcia, IMIB-Arrixaca, Telomerase, Cancer and Aging Group, Surgical Department, Murcia, Spain; ²⁹²Danish Cancer Society Research Center, Center for Autophagy, Recycling and Disease (CARD), Cell Stress and Survival Unit, Copenhagen, Denmark; IRCCS Bambino Gesù Children's Hospital, Department of Pediatric Hemato-Oncology and Cell and Gene therapy, Rome, Italy; University of Rome Tor Vergata, Department of Biology, Rome, Italy; ²⁹³Medical University of Białystok, Department of Pharmaceutical Biochemistry, Białystok, Poland; ²⁹⁴Ospedale San Raffaele and Vita-Salute San Raffaele University, Division of Genetics and Cell Biology, Milano, Italy; ²⁹⁵University of Minho, School of Medicine, Life and Health Sciences Research Institute (ICVS), Braga, Portugal; ²⁹⁶Universidade Federal de São Paulo, Department of Morphology and Genetics, São Paulo, SP, Brazil; ²⁹⁷University of Tuscia, Department for Innovation in Biological, Agro-food, and Forest systems (DIBAF), Viterbo, Italy; ²⁹⁸Ege University, Faculty of Medicine, Department of Medical Biology, Izmir, Turkey; ²⁹⁹Chonbuk National University, Jeonju, Chonbuk, Korea; ³⁰⁰Karolinska Institutet, Department of Physiology and Pharmacology, Stockholm, Sweden; ³⁰¹Kaohsiung Medical University, Department of Pathology, Kaohsiung City, Taiwan; ³⁰²University of Calcutta, Department of Biotechnology and Dr. B.C. Guha Centre for Genetic Engineering and Biotechnology, Kolkata, India; ³⁰³Saha Institute of Nuclear Physics, Biophysics & Structural Genomics Division, HBNI, Kolkata, India; ³⁰⁴Justus-Liebig-University Giessen, Institute of Medical Microbiology, Giessen, Germany; ³⁰⁵Université Côte d'Azur, CNRS, IPMC, Sophia Antipolis, France; ³⁰⁶University of Crete, School of Medicine, Laboratory of Clinical Microbiology and Microbial Pathogenesis, Voutes, Heraklion, Crete, Greece; Foundation for Research and Technology, Institute of Molecular Biology and Biotechnology (IMBB), Heraklion, Crete, Greece; ³⁰⁷University of East Anglia, School of Biological Sciences, Norwich Research Park, UK; ³⁰⁸The University of Hong Kong, LKS Faculty of Medicine, Department of Obstetrics & Gynaecology, Hong Kong, China; ³⁰⁹Queen's University, Department of Biomedical and Molecular Sciences, Kingston, Ontario, Canada; ³¹⁰National Jewish Health, Department of Academic Affairs, Denver, CO, USA; ³¹¹The Chinese University of Hong Kong, School of Life Sciences, Shatin N.T., Hong Kong, China; ³¹²Tulane University School of Medicine, Department of Pathology, New Orleans, LA, USA; ³¹³National Cheng Kung University, College of Medicine, Department of Microbiology and Immunology, Tainan, Taiwan; ³¹⁴University of California, Berkeley, Department of Molecular Biology and Cell Biology, Berkeley, CA, USA; University of California, Berkeley, California Institute for Quantitative Biosciences, Berkeley, CA, USA; ³¹⁵Southeast University, School of Medicine, Department of Physiology, Nanjing, Jiangsu, China; ³¹⁶Institut de Génétique et de Biologie Moléculaire et Cellulaire (IGBMC), INSERM U964, CNRS UMR7104, University of Strasbourg, Illkirch, France; ³¹⁷NCR Biotech Science Cluster, Translational Health Science and Technology Institute, Complex Analysis Group, Faridabad, India; ³¹⁸Banaras Hindu University, Institute of Science, Department of Zoology, Lanka, Varanasi, Uttar Pradesh, India; ³¹⁹University of Washington, Department of Laboratory Medicine, Seattle, WA, USA; ³²⁰Vanderbilt University Medical Center, Vanderbilt Eye Institute, Nashville, TN, USA; ³²¹Institute of Life Sciences, Bhubaneswar, Odisha, India; ³²²Université Côte d'Azur, INSERM, CNRS, IPMC, team labeled Laboratory of Excellence (LABEX) Distal, Valbonne, France; ³²³UCL Institute of Ophthalmology, London, UK; ³²⁴National Cheng Kung University, Department of Biochemistry and Molecular Biology, Tainan, Taiwan; ³²⁵Academia Sinica, Institute of Biological Chemistry, Taipei, Taiwan; ³²⁶University of Southern California, Center for Craniofacial Molecular Biology, Los Angeles, CA, USA; ³²⁷Qingdao University, Institute of Brain Science and Disease, Qingdao, Shandong, China; ³²⁸Johns Hopkins University School of Medicine, Department of Pathology, Baltimore, MD, USA; ³²⁹Army Medical University (Third Military Medical University), Daping Hospital, Center of Bone Metabolism and Repair, State Key Laboratory of Trauma, Burns and Combined Injury, Trauma Center, Research Institute of Surgery, Laboratory for the Prevention and Rehabilitation of Training Related Injuries, Chongqing, China; ³³⁰Third Military Medical University, Southwest Hospital, Institute of Pathology and Southwest Cancer Centre, Chongqing, China; ³³¹Changhua Christian Hospital, Department of Otorhinolaryngology-Head and Neck Surgery, Changhua, Taiwan; ³³²Wuhan Sports University, College of Health Science, Tianjiu Research and Development Center for Exercise Nutrition and Foods, Hubei Key Laboratory of Exercise Training and Monitoring, Wuhan, Hubei, China; ³³³College of Life Sciences, Nankai University, Tianjin, China; ³³⁴Wuhan University, School of Pharmaceutical Sciences, Zhongnan Hospital, Wuhan, China; ³³⁵Duke University, Department of Medicine, Durham, NC, USA; ³³⁶Chinese Academy of Sciences, Institute of Modern Physics, Lanzhou, China; ³³⁷University of Sydney, Sydney Medical School, Renal Medicine, St Leonards, NSW, Australia; ³³⁸Temple University, Lewis Katz School of Medicine, Cardiovascular Research Center and Department of Physiology, Philadelphia, PA, USA; ³³⁹Chinese Academy of Medical Sciences and Peking Union Medical College, Institute of Dermatology, Jiangsu Key Laboratory of Molecular Biology for Skin Diseases and STIs, Nanjing, Jiangsu, China; ³⁴⁰Institute of Nutrition and Health Shanghai Institutes for Biological Sciences (SIBS), Chinese Academy of Sciences, Shanghai, China; ³⁴¹Tsinghua University, School of Life Sciences, Beijing, C; ³⁴²Peking University School of Basic Medical Science, Department of Immunology, Beijing, China; ³⁴³Research Institute in Oncology and Hematology, CancerCare Manitoba, Winnipeg, Manitoba, Canada; ³⁴⁴Mackay Memorial Hospital, Department of Radiation Oncology, Taipei, Taiwan; ³⁴⁵Sun Yat-sen University, School of Life Science, Guangzhou, China; ³⁴⁶Wuhan University, School and Hospital of Stomatology, Key Lab of Oral Biomedicine of Ministry of Education (KLOBME), Wuhan, Hubei, China; ³⁴⁷2nd Affiliated Hospital of Zhejiang University School of Medicine, Department of Respiratory and Critical Care Medicine, Hangzhou, China; ³⁴⁸University of Texas Southwestern Medical Center, Department of Molecular Biology, Dallas, Texas, USA; ³⁴⁹Purdue University, Department of Botany and Plant Pathology, West Lafayette, IN, USA; ³⁵⁰Zhejiang University, College of Pharmaceutical Sciences, Institute of Pharmacology and Toxicology, Hangzhou, Zhejiang, China; ³⁵¹Capital Medical University, Beijing Ditan Hospital, Liver Disease Center, Beijing, China; ³⁵²Northwestern University Feinberg School of Medicine, Department of Neurology & Lou & Jean Malnati Brain Tumor Institute, Chicago, IL, USA; ³⁵³Albert Einstein College of Medicine, Department of Genetics, Bronx, NY, USA; ³⁵⁴Department of Integrative Biology and Pharmacology, The University of Texas Health Science Center, Houston, USA; ³⁵⁵East China Normal University, School of Life Sciences, Shanghai, China; ³⁵⁶University of Florida, Food Science and Human Nutrition Department, Gainesville, FL, USA; ³⁵⁷National Cancer Center Korea, Goyang, Gyeonggi, Korea; ³⁵⁸National University of Singapore, Yong Loo Lin School of Medicine, Department of Biochemistry, Singapore; ³⁵⁹Lomonosov Moscow State University, A.N. Belozersky Institute of Physico-Chemical Biology, Moscow, Russia; ³⁶⁰University of Pennsylvania, Department of Pathology and Laboratory Medicine, Philadelphia, PA, USA; ³⁶¹National Cheng Kung University, College of Medicine, Department of Pharmacology, Tainan, Taiwan; ³⁶²INSERM U1242, University of Rennes, Rennes, France; Centre de Lutte Contre le Cancer Eugène Marquis, Rennes, France; ³⁶³University of North Carolina at Charlotte, Department of Biological Sciences, Charlotte, NC, USA; ³⁶⁴University of Milano-Bicocca, Department of Biotechnology and Biosciences, Milan, Italy; ³⁶⁵University of Palermo, Dipartimento di Scienze e Tecnologie Biologiche, Chimiche e Farmaceutiche (STEBICEF), Palermo, Italy; ³⁶⁶Istituto di Fisiologia Clinica, Consiglio Nazionale delle Ricerche, Siena, Italy; Core Research Laboratory, Istituto per lo Studio, la Prevenzione

e la Rete Oncologica, Siena, Italy; ³⁶⁷IEO, European Institute of Oncology IRCCS, IFOM-IEO Campus, Department of Experimental Oncology, Milan, Italy; ³⁶⁸University of Chile, Faculty of Chemical and Pharmaceutical Sciences, Advanced Center for Chronic Diseases (ACCDiS), Santiago, Chile; ³⁶⁹Taipei Veterans General Hospital, Department of Medical Research, Taipei, Taiwan. ; ³⁷⁰National Institutes of Health (NIH), National Institute of Allergy and Infectious Diseases (NIAID), Rocky Mountain Laboratories (RML), Laboratory of Virology, Innate Immunity and Pathogenesis Section, Hamilton, MT, USA; ³⁷¹University Campus Bio-Medico, Department of Medicine and Department of Science and Technology for Humans and Environment, Rome, Italy; IRCCS Santa Lucia Foundation, Department of Experimental Neurosciences, Rome, Italy; ³⁷²Kyungpook National University, Department of Life Science, Daegu, Korea; ³⁷³Wonkwang University School of Medicine, Department of Microbiology, Iksan, Jeonbuk, Korea; ³⁷⁴Weill Cornell Medicine, Department of Medicine, New York, NY, USA; ³⁷⁵Weill Cornell Medicine, Division of Nephrology and Hypertension, Joan and Sanford I. Weill Department of Medicine, New York, NY, USA; ³⁷⁶CSIR-Indian Institute of Chemical Biology, Kolkata, India; ³⁷⁷BC Cancer Research Centre, Department of Experimental Therapeutics, Vancouver, BC, Canada; ³⁷⁸University of Pittsburgh School of Medicine, Department of Pathology, Pittsburgh, PA, USA; ³⁷⁹National University of Singapore, Yong Loo Lin School of Medicine, Department of Physiology; National University of Singapore, LSI Neurobiology Programme; National University of Singapore, Institute for Health Innovation and Technology; National University Hospital Singapore, Centre for Healthy Longevity; Institute of Molecular and Cell Biology, Agency for Science, Technology and Research (A*STAR), Singapore; ³⁸⁰Konkuk University School of Medicine, Department of Ophthalmology, Seoul, Korea; ³⁸¹Max-Planck-Institut für Molekulare Pflanzenphysiologie, Potsdam, Germany; ³⁸²University of Ulsan College of Medicine, Asan Medical Center, Department of Psychiatry, Seoul, Korea; ³⁸³The Catholic University of Korea, Seoul St. Mary's Hospital, Department of Ophthalmology and Visual Science, Seoul, Korea; ³⁸⁴Institute of Cancer Research, Cancer Research UK Cancer Imaging Centre, Division of Radiotherapy and Imaging, London, UK; ³⁸⁵Nencki Institute of Experimental Biology of Polish Academy of Science, Neurobiology Center, Laboratory of Molecular Neurobiology, Warsaw, Poland; ³⁸⁶University of Chile, Institute of Nutrition and Food Technology (INTA), Advanced Center for Chronic Diseases (ACCDiS), Santiago, Chile; ³⁸⁷University of Cologne, Faculty of Medicine and University Hospital Cologne, Department of Pediatrics, Cologne, Germany; University of Cologne, Faculty of Medicine and University Hospital Cologne, Center for Molecular Medicine (CMMC), Cologne, Germany; ³⁸⁸University of Rome "La Sapienza", Rome, Italy; ³⁸⁹University of Liverpool, Institute of Translational Research, Cellular and Molecular Physiology, Liverpool, UK; ³⁹⁰Georgetown University Medical Center, Department of Oncology, Washington, DC, USA; ³⁹¹L. Sacco, Università di Milano, Department of Biomedical and Clinical Sciences, Milan, Italy; ³⁹²Istituto Superiore di Sanità, Department of Infectious Diseases, Rome, Italy; ³⁹³Université Paris Descartes-Sorbonne Paris Cité, Institut Necker Enfants-Malades (INEM), INSERM U1151-CNRS UMR 8253, Paris, France; ³⁹⁴The Hebrew University of Jerusalem, The Institute for Medical Research Israel-Canada, Department of Biochemistry and Molecular Biology, Ein Karem, Jerusalem, Israel; ³⁹⁵Sorbonne Université, CNRS UMR8226, Institut de Biologie Physico-Chimique, Laboratoire de Biologie Moléculaire et Cellulaire des Eucaryotes, Paris, France; ³⁹⁶National Institutes of Health, National Institute of Arthritis and Musculoskeletal and Skin Diseases, Pediatric Translational Research Branch, Bethesda, MD, USA; ³⁹⁷Institut d'Investigacions Biomèdiques de Barcelona (CSIC, IDIBAPS), and Centro de Investigación Biomédica en Red sobre Enfermedades Neurodegenerativas (CIBERNED), Barcelona, Spain; ³⁹⁸Centre for Research in Agricultural Genomics (CRAG), CSIC-IRTA-UAB-UB, Campus UAB, Bellaterra, Barcelona, Spain; ³⁹⁹AstraZeneca, Melbourne, Royston, UK; ⁴⁰⁰University of Sheffield, Department of Biomedical Science, Firth Court, Western Bank, Sheffield, UK; ⁴⁰¹University of Belgrade, Institute for the Application of Nuclear Energy, Belgrade, Serbia; ⁴⁰²Instituto de Histología y Embriología (IHEM)-Universidad Nacional de Cuyo-CONICET, Mendoza, Argentina; ⁴⁰³Yale University School of Medicine, Department of Neuroscience and Department of Cell Biology, New Haven, CT, USA; ⁴⁰⁴Clermont-Auvergne University, INRA, Human Nutrition Unit, F-63000, Clermont-Ferrand, France; ⁴⁰⁵University of Pavia, Department of Biology and Biotechnology "L. Spallanzani", Pavia, Italy; ⁴⁰⁶Federal University of São Carlos, Department of Gerontology, São Carlos, SP, Brazil; ⁴⁰⁷Department of Pathology and Experimental Therapeutics and Institute of Biomedicine of the University of Barcelona (IBUB), Bellvitge University Hospital-IDIBELL, Hospitalet de Llobregat; University of Brescia, Department of Molecular and Translational Medicine, Brescia BS, Italy; ⁴⁰⁸National Institutes of Health, NIAMS, Lymphocyte Nuclear Biology, Bethesda, MD, USA; ⁴⁰⁹University of Manitoba, Department of Medical Microbiology & Infectious Diseases, Winnipeg, MB, Canada; ⁴¹⁰National Institutes of Health, National Institute on Aging, Laboratory of Neurogenetics, Bethesda, MD, USA; ⁴¹¹Johns Hopkins University, Department of Molecular Microbiology and Immunology, Baltimore, MD, USA; ⁴¹²University Magna Graecia of Catanzaro, Department of Health Sciences, Catanzaro, Italy; ⁴¹³University of Genoa, DIMES Department of Experimental Medicine, Human Anatomy, Genoa, Italy; ⁴¹⁴University of Zürich, Center for Molecular Cardiology, Zurich, Switzerland; ⁴¹⁵University of Turin, Department of Clinical and Biological Sciences, Turin, Italy; ⁴¹⁶University of Oviedo, Department of Morphology and Cell Biology, Oviedo, Spain; ⁴¹⁷University of Melbourne, Department of Pharmacology and Therapeutics, Melbourne, Victoria, Australia; ⁴¹⁸CSIC-Universidad de Sevilla, Instituto de Bioquímica Vegetal y Fotosíntesis, Sevilla, Spain; ⁴¹⁹Universidad de Chile, Facultad de Odontología, Advanced Center for Chronic Diseases, Santiago, Chile; ⁴²⁰Sun Yat-sen University, School of Life Sciences, MOE Key Laboratory of Gene Function and Regulation, Guangzhou, Guangdong, China; ⁴²¹University of California, San Diego, Department of Cellular and Molecular Medicine, La Jolla, CA, USA; ⁴²²University of Mar del Plata, Department of Biology and Chemistry, Mar del Plata, BA, Argentina; ⁴²³Emory University School of Medicine, Department of Medicine, Atlanta, GA, USA; ⁴²⁴Medical University of Lublin, Department of Pathophysiology, Lublin, Poland; ⁴²⁵University of Bologna, Department of Medical and Surgical Sciences; Rizzoli Orthopaedics Institute, Laboratory of Immunorheumatology and Tissue Regeneration, Bologna, Italy; ⁴²⁶University Campus Bio-Medico, Department of Medicine, Rome, Italy; ⁴²⁷University of Florida, Department of Physical Therapy, Gainesville, FL, USA; ⁴²⁸University "G. D'Annunzio", Department of Medical Sciences DSMOB, Chieti, Italy; Regina Elena National Cancer Institute, Department of Research, Rome, Italy; ⁴²⁹Federal University of Sergipe, Department of Pharmacy, São José, SE, Brazil; ⁴³⁰University of Cologne, Faculty of Medicine and University Hospital Cologne, Department of Pediatrics, Cologne, Germany; ⁴³¹University of Nevada, Reno School of Medicine, Department of Pharmacology, Reno, NV, USA; ⁴³²Gregor Mendel Institute, Vienna Biocenter, Vienna, Austria; ⁴³³University of Naples Federico II, Department of Pharmacy, Naples, Italy; ⁴³⁴Xi'an Jiaotong University, Department of Public Health, Xi'an, Shaanxi, China; ⁴³⁵The First Hospital of Jilin University, Laboratory of Cancer Precision Medicine, Changchun, Jilin, China; ⁴³⁶Model Animal Research Center of Nanjing University, Nanjing, Jiangsu, China; ⁴³⁷University of Salerno, Department of Medicine, Surgery and Dentistry "Scuola Medica Salernitana", Baronissi, SA, Italy; ⁴³⁸University of Padova, Department of Biology, Padova, Italy; ⁴³⁹Research Center Borstel, Cellular Microbiology, Borstel, Germany; ⁴⁴⁰University of Clermont Auvergne, M2iSH (Microbes, Intestine, Inflammation and Susceptibility of the Host), UMR 1071 Inserm, INRA USC 2018, CRNH, Clermont-Ferrand, France; ⁴⁴¹Karolinska Institutet, Biomedicum, Department of Cell and Molecular Biology, Stockholm, Sweden; ⁴⁴²Texas Tech University Health Sciences Center, Department of Pharmaceutical Sciences, Amarillo, TX, USA; ⁴⁴³Cleveland Clinic, Department of Gastroenterology, Hepatology and Nutrition, Cleveland, OH, USA; ⁴⁴⁴MD Anderson Cancer Center, Department of Gynecologic Oncology and Reproductive Medicine, Houston, TX, USA; ⁴⁴⁵Tulane University Health Sciences Center, Department of Pathology and Laboratory Medicine, New Orleans, LA, USA; ⁴⁴⁶Max-Delbrück-Center for Molecular Medicine, Department of Crystallography, Berlin, Germany; ⁴⁴⁷Institute of Life Sciences, School of Medicine, Swansea University, Swansea, Wales, UK; ⁴⁴⁸University of Massachusetts Medical School, Program in Molecular Medicine, Worcester, MA, USA; ⁴⁴⁹University of Calabria, Department of Pharmacy Health and Nutritional Sciences, Rende, Italy; ⁴⁵⁰Washington University School of Medicine, Departments of Pediatrics and Cell Biology & Physiology, St. Louis, MO, USA; ⁴⁵¹Ghent University, Translational Nuclear Receptor Research, VIB Center for Medical Biotechnology, Department of Biomolecular Medicine, Ghent, Belgium; ⁴⁵²"Sapienza" University of Rome, Department of Radiotherapy, Policlinico Umberto I, Rome, Italy;

- 865 ⁴⁵³University of Verona, Azienda Ospedaliera Universitaria Integrata-Verona, Department of Medicine, Verona, Italy; ⁴⁵⁴Department of Oncology-
Pathology, Cancer Center Karolinska, Karolinska Institute, Stockholm, Sweden.; ⁴⁵⁵Sapienza University of Rome, Ospedale Sant Andrea, Rome, Italy;
⁴⁵⁶Università degli Studi di Milano, Department of Medical Biotechnology and Translational Medicine, Milano, Italy; ⁴⁵⁷University of Urbino Carlo Bo,
Department of Biomolecular Sciences, Unit of Pharmacology and Public Health, Urbino, Italy; ⁴⁵⁸University of Fribourg, Department of Biology,
Fribourg, Switzerland; ⁴⁵⁹Danish Cancer Society Research Center, Cell Stress and Survival Unit, Center for Autophagy, Recycling and Disease (CARD),
870 Copenhagen, Denmark; ⁴⁶⁰KU Leuven, Department of Development and Regeneration, Laboratory of Pediatrics, PKD Research Group, Leuven,
Belgium; ⁴⁶¹University of California, San Francisco, Department of Pathology, San Francisco, CA, USA; ⁴⁶²Boston University, Department of Biology,
Boston, MA, USA; ⁴⁶³IFOM, The FIRC Institute of Molecular Oncology, Milan, Italy; ⁴⁶⁴University of Colorado Anschutz Medical Campus, Department
of Biochemistry and Molecular Genetics, Aurora, CO, USA; ⁴⁶⁵University de Bordeaux, Institut des Maladies Neurodegeneratives, UMR 5293,
Bordeaux, France; CNRS, Institut des Maladies Neurodegeneratives, UMR 5293, Bordeaux, France; ⁴⁶⁶Instituto de Fisiologia Celular, UNAM,
875 Department of Biochemistry and Structural Biology, Mexico City, Mexico; ⁴⁶⁷University of Melbourne, School of Biomedical Sciences, Melbourne,
Victoria, Australia; ⁴⁶⁸University of Buenos Aires. Faculty of Pharmacy and Biochemistry. Institute of Immunology, Genetics and Metabolism
(INIGEM), CONICET. Buenos Aires, Argentina; ⁴⁶⁹L.N.C.I.B. Laboratorio Nazionale Consorzio Interuniversitario Biotecnologie, AREA Science Park,
Trieste, Italy; ⁴⁷⁰Wuhan University, School of Pharmaceutical Sciences, Zhongnan Hospital, Wuhan, China; ⁴⁷¹University of Fribourg, Department of
Biology, Fribourg, Switzerland; ⁴⁷²Virginia Commonwealth University, Department of Biochemistry and Molecular Biology, Richmond, VA, USA;
880 ⁴⁷³Division of Developmental Biology, National Institute of Child Health & Human Development, National Institutes of Health, Bethesda, MD, USA;
⁴⁷⁴University of North Carolina at Chapel Hill, Lineberger Comprehensive Cancer Center, Chapel Hill, NC, USA; ⁴⁷⁵University of New Mexico Health
Sciences Center, Autophagy, Inflammation and Metabolism (AIM) Center, Albuquerque, NM, USA; ⁴⁷⁶University of California, San Diego; Section of
Cell and Developmental Biology, La Jolla, CA, USA; ⁴⁷⁷Institut National de la Recherche Scientifique, Centre Armand-Frappier Santé Biotechnologie,
Laval, QC, Canada; ⁴⁷⁸University of Zurich, Department of Physiology, Zurich, Switzerland; ⁴⁷⁹Walter and Eliza Hall Institute of Medical Research,
885 Ubiquitin Signalling Division, Melbourne, Australia; University of Melbourne, Department of Medical Biology, Melbourne, Australia; ⁴⁸⁰University of
Perugia, Department of Chemistry, Biology and Biotechnology, Perugia, Italy; ⁴⁸¹Sapienza University of Rome, Department of Biochemical Sciences
A. Rossi Fanelli, Rome, Italy; ⁴⁸²Philipps University of Marburg, Department of Visceral, Thoracic and Vascular Surgery, Marburg, Germany; ⁴⁸³IRCCS
Foundation Ca' Granda Ospedale Maggiore Policlinico, Dino Ferrari Center, Neuroscience Section, University of Milan, Department of
Pathophysiology and Transplantation, Milan, Italy; ⁴⁸⁴University of Teramo, Faculty of Veterinary Medicine, Teramo, Italy; ⁴⁸⁵Western University,
890 Department of Physiology and Pharmacology, London, ON, Canada; ⁴⁸⁶Harvard Medical School, Boston Children's Hospital, F.M. Kirby Neurobiology
Center, Translational Neuroscience Center, Department of Neurology, Boston, MA, USA; ⁴⁸⁷National and Kapodistrian University of Athens,
Department of Biology, Panepistimioupolis, Athens, Greece; ⁴⁸⁸University of Cincinnati College of Medicine, Department of Cancer Biology,
Cincinnati, OH, USA; ⁴⁸⁹University of Chile, Faculty of Chemical and Pharmaceutical Sciences, Department of Chemical Pharmacology and
Toxicology, Santiago de Chile, Chile; ⁴⁹⁰Arizona State University, Phoenix, AZ; ⁴⁹¹Seoul National University, College of Pharmacy, Seoul, Korea;
895 ⁴⁹²University of Montreal, Faculty of Medicine, Microbiology, Infectious diseases and Immunology Department, CRCHUM, Montréal, QC, Canada;
⁴⁹³University of Belgrade, Institute for Biological Research "Sinia Stankovic", Department of Neurobiology, Bulevar Despota Stefana 142, 11060
Belgrade, Serbia; ⁴⁹⁴University of Belgrade, Institute of Molecular Genetics and Genetic Engineering, Belgrade, Serbia; ⁴⁹⁵Goethe University, Institute
of Biochemistry II, Faculty of Medicine, Frankfurt am Main, Germany; ⁴⁹⁶University of Dundee School of Medicine, Division of Cellular Medicine,
Dundee, Scotland, UK; Johns Hopkins University School of Medicine, Department of Pharmacology and Molecular Sciences and Department of
900 Medicine, Baltimore, MD, USA; ⁴⁹⁷Zhejiang University, School of Medicine, Department of Cell Biology, Hangzhou, Zhejiang Province, China;
⁴⁹⁸University of Kansas Medical Center, Department of Pharmacology, Toxicology and Therapeutics, Kansas City, KS, USA; ⁴⁹⁹University of Rome La
Sapienza, Department of Biology and Biotechnology C. Darwin, Rome, Italy; ⁵⁰⁰Imperial College London, Department of Life Sciences and MRC
Centre for Molecular Bacteriology and Infection, London, UK; ⁵⁰¹Friedrich-Alexander University (FAU) Erlangen-Nürnberg and Universitätsklinikum
Erlangen, Department of Internal Medicine 3 - Rheumatology and Immunology, Erlangen, Germany; ⁵⁰²Washington University School of Medicine
905 and John Cochran VA Medical Center, Department of Medicine, St. Louis, MO, USA; ⁵⁰³University of Manitoba, Institute of Cardiovascular Sciences,
Department of Physiology and Pathophysiology, Winnipeg, Manitoba, Canada; ⁵⁰⁴Equipe labellisée par la Ligue contre le cancer, Université Paris
Descartes, Université Sorbonne Paris Cité, Université Paris Diderot, Sorbonne Université, INSERM U1138, Centre de Recherche des Cordeliers, Paris
France. Metabolomics and Cell Biology Platforms, Institut Gustave Roussy, Villejuif, France; ⁵⁰⁵University of Calgary, Department of Comparative
Biology and Experimental Medicine, Calgary, AB, Canada; ⁵⁰⁶University of Colima, University Center for Biomedical Research, Colima, Mexico;
910 ⁵⁰⁷Rutgers University, Department of Biological Sciences, Newark, NJ, USA; ⁵⁰⁸University of Canterbury, Biomolecular Interaction Centre, School of
Biological Sciences, Christchurch, New Zealand; ⁵⁰⁹University of Belgrade, Institute of Molecular Genetics and Genetic Engineering, Belgrade, Serbia;
⁵¹⁰Hacettepe University, Faculty of Medicine, Department of Medical Biology, Ankara, Turkey; ⁵¹¹University of Kentucky, College of Medicine, Markey
Cancer Center, Lexington, KY, USA; ⁵¹²Indiana University School of Medicine, Department of Biochemistry and Molecular Biology, Indianapolis, IN,
USA; ⁵¹³Jinshan Branch of Shanghai Sixth People's Hospital, Department of Laboratory Medicine, Shanghai, China; ⁵¹⁴Washington University in St
915 Louis School of Medicine, Department of Internal Medicine, St. Louis, MO, USA; ⁵¹⁵Goethe University, Institute of Biophysical Chemistry, Frankfurt,
Germany; ⁵¹⁶Nanjing University, Medical School, Division of Immunology, Nanjing, Jiangsu, China; ⁵¹⁷Emory University School of Medicine,
Department of Psychiatry and Behavioral Sciences, Atlanta, GA, USA; ⁵¹⁸Umeå University, Department of Chemistry, Umeå, Sweden; ⁵¹⁹University of
Arkansas, Center of Excellence for Poultry Science, Fayetteville, AR, USA; ⁵²⁰Tel Aviv University, Oncogenetic laboratory, Meir Medical Center, Kfar
Saba, and Sackler Faculty of Medicine, Tel Aviv, Israel; ⁵²¹Tongren Hospital, Shanghai Jiaotong University School of Medicine, Department of
920 Neurology, Shanghai, China; ⁵²²University of British Columbia, Department of Urologic Sciences, Vancouver, BC, Canada; ⁵²³The University of Texas
Health Science Center at Houston, Department of Integrative Biology and Pharmacology, Houston, TX, USA; ⁵²⁴Wuhan University, Hubei Key
Laboratory of Cell Homeostasis, College of Life Sciences, Wuhan, China; ⁵²⁵National Institute of Biological Sciences, Beijing, China; ⁵²⁶Central South
University, The Second Xiangya Hospital, Department of Nephrology, Changsha, Hunan, China; ⁵²⁷Chinese Academy of Medical Sciences and
Peking Union Medical College, Institute of Blood Transfusion, Chengdu, China; ⁵²⁸OncoRay National Center for Radiation Research in Oncology,
925 Faculty of Medicine and University Hospital Carl Gustav Carus, Technische Universität Dresden, Germany; Helmholtz-Zentrum Dresden - Rossendorf,
Institute of Radiooncology - OncoRay, Dresden, Germany; German Cancer Consortium (DKTK), Partner site Dresden, Germany; German Cancer
Research Center (DKFZ), Heidelberg, Germany; ⁵²⁹Cardiff University, Division of Cancer and Genetics, Heath Park, Cardiff, UK; ⁵³⁰Université Paris
Descartes-Sorbonne Paris Cité, Institut Necker Enfants-Malades (INEM), INSERM U1151-CNRS UMR 8253, Paris, France; ⁵³¹Centro Andaluz de Biología
Molecular y Medicina Regenerativa CABIMER, Consejo Superior de Investigaciones Científicas, Universidad de Sevilla, Universidad Pablo de Olavide,
930 Seville, Spain; ⁵³²Shanghai Proton and Heavy Ion Center, Department of Research & Development, Pudong, Shanghai, China; ⁵³³University Medical
Center Hamburg-Eppendorf, Department of Oncology, Hematology and Bone Marrow Transplantation with Section Pneumology, Hamburg,
Germany; Russian Academy of Sciences, A.V. Zhirmunski National Scientific Center of Marine Biology, Far Eastern Branch, Laboratory of
Pharmacology, Vladivostok, Russian Federation; Far Eastern Federal University, School of Natural Sciences, Vladivostok, Russian Federation;

- 935 ⁵³⁴Department of Neurology, Boston Children's Hospital, Boston, MA, USA; ⁵³⁵University of Colorado Anschutz Medical Campus, Division of Renal diseases, Aurora, CO, USA; ⁵³⁶Johannes Gutenberg University, Institute of Pharmacy and Biochemistry, Department of Pharmaceutical Biology, Mainz, Germany; ⁵³⁷University of Manitoba, Department of Physiology and Pathophysiology, Regenerative Medicine Program, Winnipeg, MB, Canada; ⁵³⁸University of Cologne, Centre for Biochemistry, Institute of Biochemistry I, Medical Faculty, Cologne, Germany; ⁵³⁹United Arab Emirates University, College of Medicine & Health Sciences, Department of Anatomy, Al Ain, UAE; ⁵⁴⁰University of Graz, NAWI Graz, Institute of Molecular Biosciences, Graz, Austria; BioTechMed Graz, Graz, Austria; NAWI Graz, NAWI Graz Central Lab Gracia, Graz, Austria; ⁵⁴¹Ain Shams University, Department of Medical Biochemistry and Molecular Biology, Cairo, Egypt; ⁵⁴²Long Beach VA and University of California, Irvine, Irvine, CA, USA; ⁵⁴³Hospital Universitari de Tarragona Joan XXIII, Institut d'Investigació Sanitària Pere Virgili, Tarragona, Spain; ⁵⁴⁴Florida International University, Department of Immunology and Nano-Medicine, Miami, Florida, USA; ⁵⁴⁵Damietta University, Faculty of Science, Biochemistry Department, Damietta, Egypt; ⁵⁴⁶Children's Cancer Hospital Egypt, Tumor Biology Research Program, Cairo, Egypt; ⁵⁴⁷Damietta University, Faculty of Science, Biochemistry Department, Damietta, Egypt; ⁵⁴⁸Technische Universität Dresden, Medical Clinic I, University Hospital Carl Gustav Carus, Dresden, Germany; Technische Universität Dresden, Faculty of Medicine, Institute for Clinical Chemistry and Laboratory Medicine, Dresden, Germany; Institute of Molecular Genetics of the ASCR, Department of Cancer Cell Biology, Prague, Czech Republic; ⁵⁴⁹University of Sheffield, The Bateson Centre, Department of Infection, Immunity and Cardiovascular Disease, Sheffield, South Yorkshire, UK; ⁵⁵⁰University of Camerino, Department of Biosciences and Biotechnology, Camerino, Italy; ⁵⁵¹Instituto de Investigaciones Biomédicas en Retrovirus y SIDA (INBIRS), Universidad de Buenos Aires-CONICET, Argentina; ⁵⁵²Philipps University of Marburg, Department of Cytobiology and Cytopathology, Marburg, Germany; ⁵⁵³Sanford Burnham Prebys Medical Discovery Research Institute, La Jolla, CA, USA; ⁵⁵⁴Bogazici University, Department of Molecular Biology and Genetics, Bebek, Istanbul, Turkey; ⁵⁵⁵Pfizer, Oncology Research & Development, Pearl River, NY, USA; ⁵⁵⁶Oslo University Hospital, Institute for Cancer Research, Department of Tumor Biology, Montebello, Oslo, Norway; ⁵⁵⁷Stellenbosch University, Department of Physiological Sciences, Stellenbosch, Western Cape, South Africa; ⁵⁵⁸University of Bergen, Department of Biomedicine/ Centre for Cancer Biomarkers (CCBio), Bergen, Norway; ⁵⁵⁹The Norwegian Radium Hospital, Institute for Cancer Research, Department of Molecular Cell Biology, Montebello, Oslo, Norway; University of Oslo, Faculty of Mathematics and Natural Sciences, The Department of Biosciences, Oslo, Norway; ⁵⁶⁰Instituto de Investigaciones Biomédicas Alberto Sols, C.S.I.C./U. A.M., Madrid, Spain; ⁵⁶¹Institute for Integrative Biology of the Cell (I2BC), CEA, CNRS, University of Paris-Sud, Université Paris-Saclay, Gif-sur-Yvette cedex, France; ⁵⁶²Universität zu Köln, CECAD Forschungszentrum, Institut für Genetik, Köln, Germany; ⁵⁶³University of Turku, Institute of Biomedicine, Turku, Finland; ⁵⁶⁴IRIM, University of Montpellier, CNRS, Montpellier, France; ⁵⁶⁵Medical University of Lodz, Department of Laboratory Diagnostics, Lodz, Poland; ⁵⁶⁶Institute for Advanced Chemistry of Catalonia (IQAC-CSIC), Department of Biological Chemistry; Networking Biomedical Research Centre on Hepatic and Digestive Diseases (CIBER-EHD), Barcelona, Spain; ⁵⁶⁷Sapienza University of Rome, DAHFM-Section of Anatomy, Rome, Italy; ⁵⁶⁸Istituto Dermatologico dell'Immacolata, IDI-IRCCS, Rome, Italy; ⁵⁶⁹Istituto Superiore di Sanità, Department of Oncology and Molecular Medicine, Rome, Italy; ⁵⁷⁰Universidad Nacional de Cuyo, Facultad de Ciencias Médicas, Laboratorio de Biología Celular y Molecular, IHM-CONICET, Mendoza, Argentina; ⁵⁷¹Max-Planck-Institute of Biophysical Chemistry, Biochemistry of Signal Dynamics, Göttingen, Germany; ⁵⁷²La Trobe Institute for Molecular Science, La Trobe University, Melbourne, Victoria, Australia; Olivia Newton-John Cancer Research Institute, Heidelberg, Victoria, Australia; School of Cancer Medicine, La Trobe University, Melbourne, Victoria, Australia; ⁵⁷³Miguel Hernández University (UMH), Instituto de Investigación, Desarrollo e Innovación en Biotecnología Sanitaria de Elche (IDIIBE), Elche, Spain; ⁵⁷⁴Dresden University Medical Center, Department of Neurology, Dresden, Germany; ⁵⁷⁵University of South Carolina School of Medicine, Department of Cell Biology and Anatomy, Columbia, SC, USA; ⁵⁷⁶University of Pittsburgh, Department of Surgery, Pittsburgh, PA, USA; ⁵⁷⁷University of Cincinnati, Department of Cancer Biology, Cincinnati, OH, USA; ⁵⁷⁸University of Oslo and Akershus University Hospital, Department of Clinical Molecular Biology, Lørenskog, Norway; ⁵⁷⁹The Norwegian Centre on Healthy Ageing (NO-Age), Oslo, Norway; ⁵⁸⁰Shanghai Institute of Organic Chemistry, Chinese Academy of Science, Interdisciplinary Research Center on Biology and Chemistry, Shanghai, China; University of Chinese Academy of Sciences, Beijing, China; ⁵⁸¹The First Affiliated Hospital of Guangzhou University of Chinese Medicine, Guangzhou, China; ⁵⁸²King's College London, Department of Basic and Clinical Neuroscience, London, United Kingdom; ⁵⁸³Institut du Cerveau et de la Moelle épinière (ICM), Paris, France; ⁵⁸⁴Centre International de Recherche en Infectiologie (CIRI), University Lyon, Inserm, U1111, Université Claude Bernard Lyon 1, CNRS, UMR5308, ENS Lyon, Lyon, France; ⁵⁸⁵Rudolf Virchow Center, University of Würzburg, Würzburg, Germany; ⁵⁸⁶South Australian Health and Medical Research Institute, Hopwood Centre for Neurobiology, Lifelong Health Theme, Adelaide, South Australia, Australia; ⁵⁸⁷Lewis Katz School of Medicine at Temple University, Philadelphia, PA, USA; ⁵⁸⁸Guangzhou Medical University, School of Basic Medical Sciences, State Key Laboratory of Respiratory Disease, Guangzhou, China; ⁵⁸⁹The First Hospital of Jilin University, Department of Neurology, Changchun, China; ⁵⁹⁰Medical School of Zhejiang University, Sir Run Run Shaw Hospital, Key lab of Biotherapy in Zhejiang, Laboratory of Cancer Biology, Hangzhou, China; ⁵⁹¹Chinese Academy of Sciences, Institute of Biophysics, Beijing, China; ⁵⁹²The University of Hong Kong, School of Chinese Medicine, Li Ka Shing Faculty of Medicine, Hong Kong, China; ⁵⁹³Baylor College of Medicine, Department of Biochemistry and Molecular Biology, Houston TX, USA; ⁵⁹⁴University of São Paulo (USP), Ribeirão Preto Medical School, Department of Genetics, Ribeirão Preto, SP, Brazil; ⁵⁹⁵Washington University in St. Louis, Department of Ophthalmology and Visual Sciences, St. Louis, MO, USA; ⁵⁹⁶Institute of Biomedical Research of Barcelona (IIBB)-CSIC, Barcelona, Spain; Liver Unit, Hospital Clinic i Provincial de Barcelona, IDIBAPS and CIBER-EHD, Barcelona, Spain; Research Center for ALPD, Keck School of Medicine, University of Southern California, Los Angeles, CA, USA; ⁵⁹⁷Universitari de Tarragona Joan XXIII, Institut d'Investigació Sanitària Pere Virgili, Unitat de Recerca, Hospital Tarragona, Spain; CIBER de Diabetes y Enfermedades Metabólicas Asociadas (CIBERDEM), Instituto de Salud Carlos III, Madrid, Spain; ⁵⁹⁸Max-Planck-Institute of Molecular Plant Physiology, Potsdam-Golm, Germany; ⁵⁹⁹Columbia University, New York, NY, USA; ⁶⁰⁰University of São Paulo, Institute of Biosciences, São Paulo, SP, Brazil; ⁶⁰¹University of São Paulo, Institute of Biomedical Sciences, São Paulo, SP, Brazil; Stanford University, Department of Chemical & Systems Biology, Stanford, CA, USA; ⁶⁰²University of California, San Diego, Department of Cellular and Molecular Medicine, La Jolla, CA, USA; ⁶⁰³Instituto de Investigaciones Marinas CSIC, Department of Biotechnology and Aquaculture, Immunology and Genomics, Vigo, Spain; ⁶⁰⁴National Institute for Infectious Diseases 'L. Spallanzani' IRCCS, Rome, Italy; Department of Molecular Medicine, Sapienza University of Rome, Rome, Italy; ⁶⁰⁵Università degli Studi Sapienza di Roma, SAIMLAL Department, Roma, Italy; ⁶⁰⁶Center for Systems and Therapeutics, Gladstone Institutes; Departments of Neurology and Physiology, University of California San Francisco, San Francisco, CA, USA; ⁶⁰⁷University of Piemonte Orientale, Department of Translational Medicine, Novara, Italy; ⁶⁰⁸Universidade Federal do Rio Grande do Sul (UFRGS), Morphological Sciences Department, Porto Alegre, RS, Brazil; ⁶⁰⁹Virginia Commonwealth University, School of Medicine, Department of Human and Molecular Genetics, Richmond, VA, USA; Virginia Commonwealth University, VCU Institute of Molecular Medicine, Richmond, VA, USA; Columbia University, College of Physicians and Surgeons, Departments of Pathology, Neurosurgery and Urology, New York, NY, USA; ⁶¹⁰NYU School of Medicine, Department of Medicine, NY, NY, USA; ⁶¹¹State University of New York, University at Buffalo, Jacobs School of Medicine and Biomedical Sciences, Departments of Ophthalmology/ Biochemistry and Neuroscience Program, Buffalo, NY, USA; ⁶¹²Norwegian University of Science and Technology, Department of Clinical and Molecular Medicine, Centre for Molecular Inflammation Research, Trondheim, Norway; ⁶¹³Babraham Institute, Signalling ISP, Cambridge, UK; ⁶¹⁴University of Genova, Department of Internal Medicine and IRCCS Policlinico San Martino, Genova, Italy; ⁶¹⁵Montreal Neurological Institute, Department of Neurology and Neurosurgery, McGill University, Montreal, Quebec, Canada; ⁶¹⁶University of Pavia, Department of Molecular

- Medicine, Biochemistry Unit, Pavia, Italy; ⁶¹⁵University of Pisa, Department of Translational Medicine and New Technologies in Medicine and Surgery, Pisa, Italy; I.R.C.C.S. Neuromed Pozzilli, Pozzilli, Italy; ⁶¹⁶Istituto Superiore di Sanità, Department of Environment and Health, Section of Mechanisms, Biomarkers and Models, Rome, Italy; ⁶¹⁷University of Texas Medical Branch, Mitchell Center for Neurodegenerative Diseases, Department of Neurology, Galveston, TX, USA; ⁶¹⁸Telethon Institute of Genetics and Medicine (TIGEM), Pozzuoli, Naples, Italy; University of Naples "Federico II", Department of Translational Medicine, Naples, Italy; ⁶¹⁹University of Nebraska-Lincoln, Redox Biology Center, Lincoln, NE, USA; ⁶²⁰Laboratory of Sex-gender Medicine, National Institute of Biostructures and Biosystems, Sassari, Italy; ⁶²¹Danish Cancer Society Research Center, RNA and Autophagy group, Copenhagen, Denmark; Biotech Research and Innovation Centre, University of Copenhagen, Copenhagen, Denmark; ⁶²²Icahn School of Medicine at Mount Sinai, Department of Medicine, Division of Liver Diseases, New York, NY, USA; ⁶²³Institute of Science and Technology Austria (IST), Klosterneuburg, Austria; ⁶²⁴Kyushu University, Medical Institute of Bioregulation, Fukuoka, Japan; ⁶²⁵Tokyo Institute of Technology, Institute of Innovative Research, Cell Biology Center, Yokohama, Japan; ⁶²⁶Tohoku University, Graduate School of Life Sciences, Department of Integrative Life Sciences, Sendai, Miyagi, Japan; ⁶²⁷Goethe-University Frankfurt, Institute for Experimental Cancer Research in Pediatrics, Frankfurt, Germany; ⁶²⁸Monash University, Cancer Program, Biomedicine Discovery Institute and Department of Anatomy & Developmental Biology, VIC, Australia; Peter MacCallum Cancer Centre, Prostate Cancer Translational Research Laboratory, Melbourne, VIC, Australia; University of Melbourne, Sir Peter MacCallum Department of Oncology, Parkville, VIC, Australia; ⁶²⁹Juntendo University Graduate School of Medicine, Department of Neurology, Bunkyo-ku, Tokyo Japan; ⁶³⁰Fondazione IRCCS Casa Sollievo della Sofferenza, Poliambulatorio Giovanni Paolo II, Division of Medical Genetics, San Giovanni Rotondo (FG), Italy; ⁶³¹The University of Chicago, Department of Microbiology, Chicago, IL, USA; ⁶³²New York University - Abu Dhabi, Saadiyat Island Campus, Division of Science (Biology), Cell Death Signaling Laboratory, Abu Dhabi, UAE ; ⁶³³University of Oxford, Sir William Dunn School of Pathology, Oxford, UK; ⁶³⁴Beckman Research Institute at City of Hope, Department of Systems Biology, Monrovia, CA, USA; ⁶³⁵Weill Cornell Medical College, Department of Radiation Oncology, New York, NY, USA; Sandra and Edward Meyer Cancer Center, New York, NY, USA; Yale School of Medicine, Department of Dermatology, New Haven, CT, USA; Université Paris Descartes/Paris V, Paris, France; ⁶³⁶Sorbonne Université, Developmental Biology Laboratory, CNRS, Institut de Biologie Paris Seine, IBPS, UMR7622, Paris, France; ⁶³⁷University of Edinburgh, Cancer Research UK Edinburgh Centre, Institute of Genetics and Molecular Medicine, Edinburgh, UK; ⁶³⁸University of Texas MD Anderson Cancer Center, Department of Experimental Radiation Oncology, Houston, TX, USA; ⁶³⁹MRC Protein Phosphorylation and Ubiquitylation Unit, School of Life Sciences, University of Dundee, UK; ⁶⁴⁰Fourth Military Medical University, School of Aerospace Medicine, Xi'an, China; ⁶⁴¹Harbin Institute of Technology, the HIT Center for Life Sciences, School of Life Sciences and Technology, Harbin, China; ⁶⁴²South China University of Technology, School of Medicine and Institute for Life Sciences, Guangzhou, China; ⁶⁴³University of Pittsburgh School of Medicine, Hillman Cancer Center and Department of Microbiology and Molecular Genetics, Pittsburgh, PA, USA; ⁶⁴⁴University of Pittsburgh School of Medicine, Department of Surgery, Pittsburgh, PA, USA; ⁶⁴⁵Universitat de Lleida, Department of Experimental Medicine, IRBLleida, Lleida, Spain; ⁶⁴⁶Universidad de Buenos Aires, Facultad de Farmacia y Bioquímica, Departamento de Microbiología, Inmunología y Biotecnología, Cátedra de Inmunología, Buenos Aires, Argentina; Universidad de Buenos Aires, CONICET, Instituto de Estudios de la Inmunidad Humoral (IDEHU), Buenos Aires, Argentina; ⁶⁴⁷Universidad de Buenos Aires, Consejo Nacional de Investigaciones Científicas y Técnicas (CONICET), Instituto de Química Biológica de la Facultad de Ciencias Exactas y Naturales (IQUIBICEN), Ciudad Universitaria, Buenos Aires, Argentina; ⁶⁴⁸National Center for Biotechnology (CNB)-CSIC, Laboratory of Intracellular Bacterial Pathogens, Madrid, Spain; ⁶⁴⁹Universidad Autónoma de Madrid, Facultad de Medicina, Departamento de Anatomía, Histología y Neurociencia, Madrid, Spain; ⁶⁵⁰Universidad de Salamanca, Institute of Functional Biology and Genomics (IBFG), Instituto de Investigación Biomédica de Salamanca (IBSAL), Salamanca, Spain; ⁶⁵¹Department of Cell Biology and Histology, Faculty of Biology, University of Murcia, IMIB-Arixaca, Murcia, Spain; ⁶⁵²Cajal Institute/CSIC and CIBERNED, ISCIII, Madrid, Spain; ⁶⁵³KU Leuven, Department of Cellular and Molecular Medicine, Leuven, Belgium; ⁶⁵⁴Centro de Biología Molecular Severo Ochoa (CSIC-UAM), Madrid, Spain; ⁶⁵⁵Tulane University, Department of Microbiology and Immunology, New Orleans, LA, USA; ⁶⁵⁶University of Bonn, Clinical Centre, Department of Psychiatry, Neurohomeostasis Group, Bonn, Germany; ⁶⁵⁷Tsinghua University, School of Life Sciences, Beijing, China; ⁶⁵⁸Zhejiang University School of Medicine, Women's Hospital, Hangzhou, Zhejiang, China; ⁶⁵⁹University Medical Center Goettingen, Department of Molecular Biology, Goettingen, Germany; ⁶⁶⁰University of Milano, Department of Biomedical Sciences for Health, Milan, Italy; ⁶⁶¹Institut de Biologie Moléculaire des Plantes, Centre National de la Recherche Scientifique, Unité Propre de Recherche 2357, Conventioonné avec l'Université de Strasbourg, Strasbourg, France; ⁶⁶²University Clinic Freiburg, Institute for Microbiology and Hygiene, Freiburg, Germany; ⁶⁶³Mortimer B. Zuckerman Mind Brain and Behavior Institute, Columbia University, New York, NY, USA; ⁶⁶⁴Institute for Animal Developmental and Molecular Biology, Heinrich-Heine University Düsseldorf, Düsseldorf, Germany; ⁶⁶⁵Université du Québec à Trois-Rivières, Département de Biologie Médicale, Trois-Rivières, Québec, Canada; ⁶⁶⁶Virginia Commonwealth University, Departments of Pharmacology, Toxicology and Medicine and Massey Cancer Center, Richmond, VA, USA; ⁶⁶⁷Kerman University of Medical Sciences, Institute of Neuropharmacology, Neuroscience Research Center, Kerman, Iran; ⁶⁶⁸Department of Human Anatomy and Cell Science, Max Rady College of Medicine, Rady Faculty of Health Sciences, University of Manitoba, Winnipeg, Canada; ⁶⁶⁹University of Torino, Department of Molecular Biotechnology and Health Sciences, Torino, Italy; ⁶⁷⁰University of Sussex, School of Life Sciences, Department of Biochemistry and Biomedicine, Brighton, UK; ⁶⁷¹Sapienza University of Rome, Department of Anatomy, Histology, Forensic Medicine and Orthopedics, Rome, Italy; ⁶⁷²Democritus University of Thrace, Medical School, Department of Pathology, Alexandroupolis, Greece; ⁶⁷³Weill Cornell Medicine, Brain and Mind Research Institute, Burke Neurological Institute, White Plains, NY, USA; ⁶⁷⁴University of Manitoba, Departments of Biochemistry and Medical Genetics, Winnipeg, Canada; ⁶⁷⁵National Institutes of Health, National Institutes of Neurological Disorders and Stroke (NINDS), Bethesda, MD, USA; ⁶⁷⁶University of Coimbra, Coimbra Institute for Clinical and Biomedical Research (iCBER), Faculty of Medicine, Coimbra, Portugal; University of Coimbra, Center for Innovative Biomedicine and Biotechnology, Coimbra, Portugal; ⁶⁷⁷University of Toronto, Department of Laboratory Medicine and Pathobiology, Toronto, Ontario, Canada; ⁶⁷⁸University of California, Davis and MIND Institute, School of Veterinary Medicine, Dept. Molecular Biosciences, Davis, CA; ⁶⁷⁹INSERM, UMR1037 CRCT, Toulouse, France; Université Toulouse III-Paul Sabatier, UMR1037 CRCT, Toulouse, France; CNRS, ERL5294 CRCT, Toulouse, France; ⁶⁸⁰INSERM UMR1195, Université Paris-Saclay, Hôpital Le Kremlin Bicêtre, Le Kremlin Bicêtre, France; ⁶⁸¹Ludwig Institute for Cancer Research; University of California San Diego, Department of Cellular and Molecular Medicine, La Jolla, CA, USA; ⁶⁸²University of Auckland, School of Biological Sciences, Auckland, New Zealand; ⁶⁸³Luxembourg Institute of Health, Department of Oncology, NorLux Neuro-Oncology Laboratory, Luxembourg, Luxembourg; ⁶⁸⁴Center of Toxins, Immune-response and Cell Signaling (CeTICS) and Laboratório Especial de Ciclo Celular (LECC), Instituto Butantan, São Paulo, Brazil; ⁶⁸⁵Leiden University Medical Center, Department of Cell and Chemical Biology and Oncode Institute, Leiden, The Netherlands; ⁶⁸⁶Shanghai Jiao Tong University, School of Life Sciences and Biotechnology, Shanghai, China; ⁶⁸⁷University of the Basque Country, Instituto Biofisika (UPV/EHU, CSIC), and Department of Biochemistry, Leioa, Spain; ⁶⁸⁸University of León, Institute of Biomedicine (IBIOMED) and Centro de Investigación Biomédica en Red de Enfermedades Hepáticas y Digestivas (CIBERehd), León, Spain; ⁶⁸⁹University of La Laguna, Institute of Biomedical Technologies, Department of Basic Medical Sciences, La Laguna, Tenerife, Spain; ⁶⁹⁰Universidad de Extremadura, Centro de Investigación Biomédica en Red sobre Enfermedades Neurodegenerativas (CIBERNED), Instituto de Investigación INUBE, Departamento de Bioquímica y Biología Molecular y Genética, Facultad de Enfermería y Terapia Ocupacional, Cáceres, Spain; ⁶⁹¹University of Cordoba, Department of Cell Biology, Physiology and Immunology, Córdoba, Spain; ⁶⁹²University of Alberta,

Department of Biochemistry, Edmonton, AB, Canada; ⁶⁹³University of Alabama at Birmingham, Department of Optometry and Vision Science, Birmingham, AL, USA; ⁶⁹⁴The Henry M. Jackson Foundation, Inc. Bethesda, MD, USA; ⁶⁹⁵Technische Universität München, Klinikum rechts der Isar, Comprehensive Cancer Center München, München, Germany; ⁶⁹⁶Instituto de Química Biológica Ciencias Exactas y Naturales (IQUIBICEN-CONICET), Universidad de Buenos Aires, Facultad de Ciencias Exactas y Naturales, Departamento de Química Biológica, Buenos Aires, Argentina; ⁶⁹⁷BC Cancer, Michael Smith Genome Sciences Centre, Vancouver, BC, Canada; ⁶⁹⁸Harvard Medical School, Department of Dermatology, Cutaneous Biology Research Center Massachusetts General Hospital, Boston MA, USA; ⁶⁹⁹Consejo Superior de Investigaciones Científicas, Instituto de Bioquímica Vegetal y Fotosíntesis (CSIC-IBVF), Sevilla, Spain; ⁷⁰⁰Smidt Heart Institute, Cedars-Sinai Medical Center, Los Angeles, CA, USA; ⁷⁰¹Tel Aviv University, Sackler Faculty of Medicine and Sagol School of Neuroscience, Department of Human Molecular Biology and Biochemistry, Tel Aviv, Israel; ⁷⁰²Sabancı University, Molecular Biology, Genetics and Bioengineering Program, Istanbul, Turkey; ⁷⁰³Max Planck Institute for Biology of Ageing, Cologne, Germany; University of Cologne, Cologne Excellence Cluster on Cellular Stress Responses in Aging-Associated Diseases (CECAD), Cologne, Germany; ⁷⁰⁴Jena University Hospital, Department of Anesthesiology and Intensive Care Medicine, Center for Molecular Biomedicine (CMB) and Center for Sepsis Control and Care (CSCC), Jena, Germany; ⁷⁰⁵Weill Cornell Medicine, Feil Family Brain and Mind Research Institute, New York, NY, USA; ⁷⁰⁶St. Jude Children's Research Hospital, Department of Immunology, Memphis, TN, USA; ⁷⁰⁷University of Adelaide, School of Biological Sciences, Adelaide, S.A., Australia; ⁷⁰⁸University of Alabama at Birmingham, Center for Neurodegeneration and Experimental Therapeutics, Department of Neurology, Birmingham, AL, USA; ⁷⁰⁹Boston University, Departments of Biomedical Engineering, Chemistry, and Medicine, Boston, MA, USA; ⁷¹⁰Université de Strasbourg/CNRS UPR 3572 Institut de Biologie Moléculaire et Cellulaire, Strasbourg, France; ⁷¹¹University of Iowa, Departments of Pediatrics and Microbiology, Iowa City, IA, USA; ⁷¹²Medical University of Vienna, Department of Dermatology, Division for Biology and Pathobiology of the Skin, Vienna, Austria; ⁷¹³Telethon Institute of Genetics and Medicine (TIGEM), Pozzuoli, Naples, Italy; ⁷¹⁴German Institute of Human Nutrition, Department of Molecular Toxicology, Nuthetal, Germany; ⁷¹⁵Lanzhou University, School of Public Health, Lanzhou, Gansu, China; ⁷¹⁶University of Cincinnati College of Medicine, Department of Cancer Biology, Cincinnati, OH, USA; ⁷¹⁷Case Western Reserve University, Comprehensive Cancer Center, Cleveland, OH, USA; ⁷¹⁸University of Salento, Department of Biological and Environmental Sciences and Technologies, Lecce, Italy; ⁷¹⁹Research Center Principe Felipe, Cellular Pathology Laboratory, Valencia, Spain; ⁷²⁰Johns Hopkins University School of Medicine, Department of Neuroscience, Baltimore, MD, USA; ⁷²¹School of Pharmacy, Complutense University, Madrid, Spain; Centro de Investigación Biomédica en Red (CIBER) de Diabetes y Enfermedades Metabólicas Asociadas (CIBERDEM), Madrid, Spain; ⁷²²Dalhousie University, Faculty of Medicine, Departments of pathology, Biology, and Microbiology & Immunology, Halifax, NS, Canada; ⁷²³David Geffen School of Medicine at UCLA, Department of Medicine, Los Angeles, CA, USA; ⁷²⁴Justus-Liebig University, Department of Internal Medicine, Giessen, Germany; ⁷²⁵Center for Molecular Medicine, Maine Medical Center Research Institute, Scarborough, ME, USA; ⁷²⁶Tongji University School of Medicine, Shanghai Tenth People's Hospital, Department of Gastroenterology, Shanghai, China; ⁷²⁷The University of Sheffield, Department of Biomedical Science, Firth Court, Western Bank, Sheffield, UK; ⁷²⁸University of Virginia, School of Medicine, Department of Surgery, Charlottesville, VA, USA; ⁷²⁹University of California, Los Angeles, Department of Neurology, Molecular and Medical Pharmacology, David Geffen School of Medicine, Los Angeles, CA, USA; ⁷³⁰Institute of Microbial Technology, Department of Molecular Biology, Chandigarh, India; ⁷³¹CSIR-Central Drug Research Institute, Lucknow, India; ⁷³²University of Oslo, Institute of Basic Medical Sciences, Oslo, Norway; ⁷³³Deakin University, School of Medicine, Faculty of Health, Victoria, Australia; ⁷³⁴Macquarie University, Faculty of Medicine and Health Sciences, NSW, Australia; ⁷³⁵University of California, San Diego, Skaggs School of Pharmacy and Pharmaceutical Sciences, La Jolla, CA, USA; ⁷³⁶Medical College of Wisconsin, Department of Medicine and Cardiovascular Center, Milwaukee, WI, USA; ⁷³⁷ICAR-Indian Veterinary Research Institute, Bareilly, Uttar Pradesh, India; ⁷³⁸University of Eastern Finland, A. I. Virtanen Institute for Molecular Sciences, Kuopio, Finland; ⁷³⁹Brandeis University, Department of Biology and Rosenstiel Basic Medical Sciences Research Center, Waltham, MA, USA; ⁷⁴⁰Tokai University School of Medicine, Department of Molecular Life Sciences, Isehara, Kanagawa, Japan; ⁷⁴¹Swedish Agricultural University (SLU), Department of Plant Biology, Uppsala, Sweden; ⁷⁴²Hasselt University, Biomedical Research Institute, Diepenbeek, Belgium; ⁷⁴³Johns Hopkins University Bloomberg School of Public Health, W. Harry Feinstein Department of Molecular Microbiology and Immunology, Baltimore, MD, USA; ⁷⁴⁴Barts Cancer Institute, Queen Mary University of London, Centre for Biotherapeutics and Biomarkers, London, UK; ⁷⁴⁵Zhejiang University, Sir Run Run Shaw Hospital, College of Medicine, Department of Medical Oncology, Zhejiang, Hangzhou, China; ⁷⁴⁶Sanford Burnham Medical Discovery Institute, Program of Development, Aging and Regeneration, La Jolla, CA, USA; ⁷⁴⁷University of Michigan, Department of Biological Chemistry, Ann Arbor, MI, USA; ⁷⁴⁸Third Department of Internal Medicine, University of Occupational and Environmental Health, Kitakyushu, Japan; ⁷⁴⁹University of Belgrade, Institute for Biological Research, "Sinisa Stankovic", Belgrade, Serbia; ⁷⁵⁰University of California, Davis, School of Medicine, Department of Pharmacology, Davis, CA, USA; ⁷⁵¹University of Toronto, Department of Medicine, Toronto, Ontario, Canada; ⁷⁵²Monash University, School of Clinical Sciences at Monash Health, Centre for Inflammatory Diseases, Rheumatology Group, Clayton, Victoria, Australia; ⁷⁵³Tohoku University Graduate School of Medicine, Division of Neurology, Department of Neuroscience & Sensory Organs, Sendai, Japan; ⁷⁵⁴University of Malaya, Institute of Biological Sciences (Genetics), Kuala Lumpur, Malaysia; ⁷⁵⁵Washington University School of Medicine, Division of Pulmonary and Critical Care Medicine, St. Louis, MO, USA; ⁷⁵⁶Leibniz Forschungsinstitut für Molekulare Pharmakologie (FMP), Department of Molecular Pharmacology and Cell Biology, Berlin, Germany; ⁷⁵⁷California Institute of Technology, Division of Biology and Biological Engineering, Pasadena, CA, USA; ⁷⁵⁸University of Massachusetts Medical School, Molecular, Cell and Cancer Biology, Worcester, MA, USA; ⁷⁵⁹Bulgarian Academy of Sciences, Institute of Biology and Immunology of Reproduction Acad. Kiril Bratanov, Sofia, Bulgaria; ⁷⁶⁰University of Minnesota, Department of Genetics, Cell Biology and Development, Minneapolis, MN, USA; ⁷⁶¹Northwestern University, Feinberg School of Medicine, Department of Cell and Developmental Biology, Chicago, IL, USA; ⁷⁶²Sichuan University, West China School of Pharmacy, Key Laboratory of Drug-Targeting and Drug Delivery System of the Education Ministry, Chengdu, China; ⁷⁶³Jinan University, College of Pharmacy, Guangzhou, China; ⁷⁶⁴Department of Immunology, Duke University Medical Center, Durham, NC, USA; ⁷⁶⁵University of Chicago, Department of Medicine, Section of Dermatology, Chicago, IL, USA; ⁷⁶⁶D Youville College, School of Pharmacy, Department of Pharmaceutical, Social and Administrative Sciences, Buffalo, NY, USA; ⁷⁶⁷National Institutes of Health, National Eye Institute, Ophthalmic Genetics and Visual Function Branch, Ophthalmic Molecular Genetics Section, Bethesda, MD, USA; ⁷⁶⁸University of Glasgow, Wolfson Wohl Cancer Research Centre, Institute of Cancer Sciences, Glasgow, UK; ⁷⁶⁹University of Cologne, Faculty of Medicine and University Hospital Cologne, Institute for Medical Microbiology, Immunology and Hygiene, Cologne, Germany; ⁷⁷⁰University College London, Cancer Institute, London, UK; ⁷⁷¹University of Gdansk, Department of Medical Biology and Genetics, Gdansk, Poland; ⁷⁷²Universidade Federal de São Carlos, Department of Genetics and Evolution, São Carlos (SP), Brazil; ⁷⁷³Instituto de Investigación Sanitaria de Navarra (IdISNA), Fundación Miguel Servet, Biomedical Research Center of Navarre-Navarrabiomed, Immunomodulation Group, Pamplona, Spain; ⁷⁷⁴University of Barcelona, Barcelona Hepatic Hemodynamic Unit, Liver Unit, Hospital Clinic, Hospital Clínic-Institut d'Investigacions Biomèdiques (IDIBAPS), Centro de Investigación Biomédica Red de enfermedades Hepáticas y Digestivas (CIBERehd), Barcelona, Spain; ⁷⁷⁵INRA, UR1037 Laboratory of Fish Physiology and Genomics, Campus de Beaulieu, Rennes, France; Hunan Normal University, College of Life Sciences, State Key Laboratory of Developmental Biology of Freshwater Fish, Changsha, Hunan, China; ⁷⁷⁶University of Lleida, Department of Basic Medical Sciences, IRBLleida, Lleida, Spain; ⁷⁷⁷The Francis Crick Institute, Molecular Cell Biology of Autophagy, London, UK; Universidad del País Vasco, Instituto Biofisika (CSIC, UPV/EHU) and Departamento de Bioquímica y Biología Molecular, Bilbao, Spain; ⁷⁷⁸Garvan Institute of Medical

- Research, Diabetes and Metabolism Division, Sydney, Australia; St Vincent's Clinical School, UNSW Sydney, Australia; ⁷⁷⁹University of Chile, Biomedical Neuroscience Institute, Faculty of Medicine, Santiago, Chile; FONDAP Center for Geroscience Brain Health and Metabolism, Santiago, Chile; University of Chile, Institute of Biomedical Science, Program of Cellular and Molecular Biology, Santiago, Chile; Buck Institute for Research on Aging, Novato, CA, USA; ⁷⁸⁰University of Bern, Institute of Cell Biology, Bern, Switzerland; ⁷⁸¹Kyushu University, Department of Bioscience and Biotechnology, Nishi-ku, Fukuoka, Japan; ⁷⁸²UT Southwestern Medical Center, Department of Molecular Biology, Dallas, TX, USA; ⁷⁸³Theoretical Division, Los Alamos National Laboratory, Los Alamos, NM, USA; ⁷⁸⁴University of Waterloo, School of Pharmacy, Kitchener, ON, Canada; ⁷⁸⁵University of Hong Kong, Department of Medicine, Division of Neurology, Pokfulam, Hong Kong, China; ⁷⁸⁶University of North Carolina at Chapel Hill, Department of Pharmacology, Chapel Hill, NC, USA; ⁷⁸⁷Yale University, Department of Molecular Biophysics and Biochemistry, New Haven, CT, USA; ⁷⁸⁸KU Leuven, Department of Public Health and Primary Care, Centre Environment & Health, Leuven, Belgium; ⁷⁸⁹University Côte d'Azur, FHU OncoAge, Department of Pathology, Nice, France; ⁷⁹⁰Swedish University of Agricultural Sciences (SLU) and Linnean Center for Plant Biology, Uppsala BioCenter, Department of Plant Biology, Uppsala, Sweden; ⁷⁹¹German Institute of Human Nutrition Potsdam-Rehbruecke (DIfE), Department of Molecular Toxicology, Nuthetal, Germany; ⁷⁹²University of Helsinki, Medicum, Biochemistry and Developmental Biology, Helsinki, Finland; ⁷⁹³University of Birmingham, College of Medical and Dental Sciences, Institute of Inflammation and Ageing, Birmingham, UK; ⁷⁹⁴Kyungpook National University, School of Medicine, Department of Physiology, Daegu, Korea; ⁷⁹⁵Kaohsiung Medical University, Graduate Institute of Medicine & Department of Biochemistry, Faculty of Medicine, College of Medicine, Kaohsiung, Taiwan; ⁷⁹⁶University of Cologne, Institute for Genetics and CECAD Research Center, Cologne, Germany; ⁷⁹⁷European Molecular Biology Laboratory, Heidelberg, Germany; ⁷⁹⁸University of Texas Southwestern Medical Center, Department of Internal Medicine, Dallas, TX, USA; ⁷⁹⁹National Chiao-Tung University, Department of Applied Chemistry and Institute of Molecular Science, Hsinchu, Taiwan; ⁸⁰⁰University of Plymouth, Faculty of Health: Medicine, Dentistry and Human Sciences, Peninsula Dental School, Plymouth, Devon, UK; ⁸⁰¹Anhui University of Science and Technology, Department of Medical Immunology, Huainan, China; ⁸⁰²Soochow University, Institute of Neuroscience, Suzhou, Jiangsu Province, China; ⁸⁰³University of Texas Southwestern Medical Center, Department of Internal Medicine, Charles and Jane Center for Mineral Metabolism and Clinical Research, Dallas, Texas, USA; ⁸⁰⁴Southern Medical University, Shenzhen Hospital, Department of Gastroenterology, Shenzhen, Guangdong, China; ⁸⁰⁵National Tsing Hua University, Department of Chemical Engineering, and Frontier Research Center on Fundamental and Applied Sciences of Matters, Hsinchu, Taiwan; ⁸⁰⁶Chinese Academy of Medical Sciences & Peking Union Medical College, Institute of Materia Medica, State Key Laboratory of Bioactive Substance and Function of Natural Medicines, Molecular Immunology and Cancer Pharmacology Group, Beijing, China; ⁸⁰⁷Northwest A&F University, College of Veterinary Medicine, Shaanxi Centre of Stem Cells Engineering & Technology, Yangling, Shaanxi, China; ⁸⁰⁸Shanghai Jiao Tong University School of Medicine, Shanghai General Hospital, Department of Orthopedics, Shanghai, China; Shanghai Bone Tumor Institution, Shanghai, China; ⁸⁰⁹Sichuan University, and Collaborative Innovation Center for Biotherapy, West China Hospital, West China School of Basic Medical Sciences & Forensic Medicine, and State Key Laboratory of Biotherapy and Cancer Center, Chengdu, China; ⁸¹⁰State University of New York, Downstate Health Sciences University, Department of Surgery and Cell Biology, Brooklyn, NY, USA; ⁸¹¹New York University School of Medicine, Department of Environmental Medicine, Urology, Biochemistry and Molecular Pharmacology, New York, NY, USA; ⁸¹²Shanghai Jiao Tong University School of Medicine, Shanghai Institute of Immunology & Department of Immunology and Microbiology, Shanghai, China; ⁸¹³University of Sydney, Kolling Institute, Renal Research Lab, Sydney, New South Wales, Australia; ⁸¹⁴Wenzhou Medical University, School of Laboratory Medicine and Life Sciences, Wenzhou, Zhejiang Province, China; ⁸¹⁵Huazhong University of Science and Technology, Tongji Medical College, School of Pharmacy, Wuhan, Hubei, China; ⁸¹⁶Chongqing University, School of Medicine, Center for Neurointelligence, Chongqing, China; ⁸¹⁷The Second Affiliated Hospital of Xi'an Jiaotong University, Department of Radiation Oncology, Xi'an, Shaanxi, China; ⁸¹⁸Zhejiang University, The First Affiliated Hospital, School of Medicine, Zhejiang Provincial Key Laboratory of Pancreatic Disease, Hangzhou, Zhejiang, China; ⁸¹⁹III. Department of Medicine, University Medical Center Hamburg-Eppendorf, Hamburg, Germany; ⁸²⁰Medical University of Vienna, Clinical Institute of Pathology, Vienna, Austria; ⁸²¹University Hospital Jena, Institute of Human Genetics, Jena, Thuringia, Germany; ⁸²²University of Otago, School of Biomedical Sciences and Brain Health Research Centre, Department of Biochemistry, Dunedin, New Zealand; ⁸²³University of Bern, Institute of Pathology, Bern, Switzerland; TRANSAUTOPHAGY: European network for multidisciplinary research and translation of autophagy knowledge, COST Action CA15138; ⁸²⁴Max Planck Institute of Biophysics, Department of Theoretical Biophysics, Frankfurt am Main, Germany; ⁸²⁵University of California, Berkeley, Department of Molecular and Cell Biology, Berkeley, CA, USA; ⁸²⁶McGill University Health Centre, Montréal, QC, Canada; ⁸²⁷West Virginia University, School of Medicine, Department of Physiology and Pharmacology, Morgantown, WV, USA; ⁸²⁸Durham University, Department of Biosciences, Durham, UK; ⁸²⁹University of Indonesia, Faculty of Medicine, Department of Obstetric and Gynecology, Jakarta, Indonesia; ⁸³⁰VIR Biotechnology, San Francisco, CA, USA; ⁸³¹University of Messina, Department of Human Pathology in Adult and Developmental Age "Gaetano Barresi", Section of Pathology, Messina, Italy; ⁸³²Kyushu University, Medical Institute of Bioregulation (MIB), Fukuoka, Japan; ⁸³³Osaka International Cancer Institute, Department of Molecular and Cellular Biology, Osaka, Japan; ⁸³⁴Juntendo University Graduate School of Medicine, Department of Research for Parkinson's Disease, Tokyo, Japan; ⁸³⁵University of Modena and Reggio Emilia, Department of Life Sciences, Modena, Italy; ⁸³⁶Juntendo University, Juntendo University Graduate School of Medicine, Division for Development of Autophagy Modulating Drugs, Tokyo, Japan; ⁸³⁷University of North Texas Health Science Center, North Texas Eye Research Institute and Department of Pharmaceutical Sciences, Fort Worth, TX, USA; ⁸³⁸University of Michigan, Life Sciences Institute, Department of Molecular and Integrative Physiology, Ann Arbor, MI, USA; ⁸³⁹Centre de Recherche en Cancérologie de Marseille (CRCM), INSERM U1068, CNRS UMR 7258, Aix-Marseille Université and Institut Paoli-Calmettes, Parc Scientifique et Technologique de Luminy, Marseille, France; ⁸⁴⁰Thomas Jefferson University, Department of Pathology, Anatomy, and Cell Biology, Philadelphia, PA, USA; ⁸⁴¹National Institute for Infectious Diseases L. Spallanzani, I.R.C.C.S., Rome, Italy; ⁸⁴²University of Massachusetts Medical School, Department of Microbiology and Physiological Systems, Worcester, MA, USA; ⁸⁴³Stanford University School of Medicine, Department of Pathology, Stanford, CA, USA; ⁸⁴⁴Akita University Graduate School of Medicine, Department of Ophthalmology, Akita, Japan; ⁸⁴⁵University of Science and Technology of China, School of Life Sciences, Hefei, Anhui, China; South China University of Technology, Guangzhou First People's Hospital, School of Medicine and Institutes for Life Sciences, Guangzhou, Guangdong, China; ⁸⁴⁶Università del Piemonte Orientale, Department of Health Sciences, Laboratory of Molecular Pathology, Novara, Italy; ⁸⁴⁷University of Illinois at Chicago, Department of Pathology, College of Medicine, Chicago, IL, USA; ⁸⁴⁸University of Copenhagen, Copenhagen Biocentre, Faculty of Health and Medical Sciences, Biotech Research & Innovation Centre (BRIC), Neuroinflammation Unit, Copenhagen N, Denmark; ⁸⁴⁹Chiba University, Department of Biology, Chiba, Japan; ⁸⁵⁰Keio University School of Medicine, Department of Neurology, Tokyo, Japan; ⁸⁵¹Hampton University, School of Pharmacy, Department of Pharmaceutical Sciences, Hampton, VA, USA; ⁸⁵²Centro de Biología Molecular Severo Ochoa, Consejo Superior de Investigaciones Científicas, Universidad Autónoma de Madrid, Madrid, Spain; Department of Cell Biology and Immunology, Campus de Cantoblanco, Madrid, Spain; ⁸⁵³RIKEN, Center for Sustainable Resource Science, Wako, Saitama, Japan; ⁸⁵⁴Danish Cancer Society Research Center, Copenhagen, Denmark; University of Copenhagen, Department of Cellular and Molecular Medicine, Copenhagen, Denmark; ⁸⁵⁵University of Technology, Department of applied science, Division of Biotechnology, Baghdad, Iraq; ⁸⁵⁶University of Maryland School of Medicine, Department of Microbiology and Immunology, Baltimore, MD, USA; ⁸⁵⁷Instituto Nacional de Ciencias Médicas y Nutrición Salvador Zubiran, Unidad de Bioquímica, Mexico City, Mexico; ⁸⁵⁸University of Kansas Medical Center, Department of Pharmacology, Toxicology and

- 1210 Therapeutics, Kansas City, KS, USA; ⁸⁵⁹Houston Methodist Research Institute, Weill-Cornell Medicine, Houston, TX, USA; ⁸⁶⁰Delft University of Technology, Kavli Institute of Nanoscience, Department of Bionanoscience, Delft, The Netherlands; ⁸⁶¹Lund University, Department of Experimental Medical Science, Laboratory of Molecular Neurogenetics, Wallenberg Neuroscience Center and Lund Stem Cell Center, Lund, Sweden; ⁸⁶²Luxembourg Institute of Health, Tumor Immunotherapy and Microenvironment (TIME) group, Department of Oncology, Luxembourg City, Luxembourg; ⁸⁶³Albert Einstein College of Medicine, Department of Developmental and Molecular Biology and Department of Genetics, New York, NY, USA; ⁸⁶⁴University of Innsbruck, Institute for Biomedical Aging Research, Department of Molecular Biology, Innsbruck, Austria; ⁸⁶⁵Cancer Drug Resistance and Stem Cell Program, University of Sydney, NSW, Australia; ⁸⁶⁶University Hospital of Regensburg, Institute of Clinical Microbiology and Hygiene, Regensburg, Germany; ⁸⁶⁷Université de Sherbrooke, Département d'immunologie et de biologie cellulaire, Sherbrooke, Québec, Canada; ⁸⁶⁸UMR7242, CNRS, Université de Strasbourg, Strasbourg, France; ⁸⁶⁹University of Copenhagen, Department of Nutrition, Exercise and Sports, Section of Molecular Physiology, Copenhagen, Denmark; ⁸⁷⁰Institute of Experimental Medicine CAS, Department of Neuroregeneration, Prague, Czech Republic; ⁸⁷¹Aarhus University Hospital, Steno Diabetes Center Aarhus, Aarhus, Denmark; ⁸⁷²University of Texas Southwestern Medical Center, Department of Molecular Biology, Dallas, TX, USA; ⁸⁷³The First Affiliated Hospital of Nanjing Medical University, Department of Neurosurgery, Nanjing, Jiangsu, China; ⁸⁷⁴Shanghai University of Traditional Chinese Medicine, Longhua Hospital, Cancer Institute, Shanghai, China; ⁸⁷⁵The Chinese University of Hong Kong, School of Life Sciences, Centre for Cell & Developmental Biology and State Key Laboratory of Agrobiotechnology, Shatin, New Territories, Hong Kong, China; ⁸⁷⁶Purdue University, Department of Nutrition Science, West Lafayette, IN, USA; ⁸⁷⁷Nanjing Medical University, Nanjing First Hospital, Department of Neurology, Nanjing, China; ⁸⁷⁸University of Pittsburgh, Department of Pharmacology and Chemical Biology, Pittsburgh, PA, USA; ⁸⁷⁹King's College London, Institute of Psychiatry, Psychology & Neuroscience, Department of Basic and Clinical Neuroscience, Maurice Wohl Clinical Neuroscience Institute, London, UK; ⁸⁸⁰Wonkwang University, Department of Biological Sciences, Iksan, Chunbuk, Korea; ⁸⁸¹The First Hospital of Jilin University, Cancer Center, Department of Hematology, Changchun, Jilin, China; ⁸⁸²Zhejiang University, Sir Run Run Shaw Hospital, School of Medicine, Key Lab of Biotherapy in Zhejiang Province, Hangzhou, China; ⁸⁸³Xi'an Jiaotong University, Kidney Hospital, the First Affiliated Hospital, School of Medicine, Department of Nephrology, Xi'an City, Shaanxi Province, China; ⁸⁸⁴Zhejiang University School of Medicine, Department of Cell Biology, Hangzhou, Zhejiang Province, China; ⁸⁸⁵University of California, Berkeley, Department of Molecular and Cell Biology, Berkeley, CA, USA; ⁸⁸⁶Huazhong University of Science and Technology, Liyuan hospital of Tongji Medical College, Department of Endocrinology, Wuhan, Hubei, China; ⁸⁸⁷Chungnam National University School of Medicine, Infection Control Convergence Research Center, Daejeon, Korea; ⁸⁸⁸Cancer Research Center of Toulouse (CRCT), INSERM U1037, CNRS ERL5294, University of Toulouse, Toulouse, France; ⁸⁸⁹University of Rochester, Department of Anesthesiology and Perioperative Medicine, Rochester, NY, USA; ⁸⁹⁰University of Sheffield, Department of Infection, Immunity and Cardiovascular Disease and the Bateson Centre, Sheffield, UK; ⁸⁹¹University of Helsinki, Institute of Biotechnology, Cell and Tissue Dynamics Programme and Electron Microscopy Unit, Helsinki, Finland; ⁸⁹²Indian Institute of Science, Centre for BioSystems Science and Engineering, Bangalore, India; ⁸⁹³Radboud University Medical Centre, Department of Internal Medicine, Nijmegen, The Netherlands; ⁸⁹⁴Universidad Castilla La Mancha, Departamento Ciencias Medicas, Albacete, Spain; ⁸⁹⁵Karolinska Institutet, Institute of Environmental Medicine, Stockholm, Sweden; ⁸⁹⁶Fudan University School of Pharmacy, Department of Biological Medicines, Shanghai, China; ⁸⁹⁷The University of Suwon, Department of Health Science, Hwaseong, Gyeonggi, Korea; ⁸⁹⁸Stony Brook University, Department of Pathology, Stony Brook, NY, USA; ⁸⁹⁹Instituto Nacional de Enfermedades Respiratorias Isamel Cosío Villegas, Departamento de Investigación en Microbiología, Ciudad de México, México; ⁹⁰⁰Hungarian Academy of Sciences, Institute of Genetics, Biological Research Centre, Szeged, Hungary; ⁹⁰¹Eötvös Loránd University, Department of Anatomy, Cell and Developmental Biology, Budapest, Hungary; ⁹⁰²Gwangju Institute of Science and Technology, School of Life Sciences, Gwangju, South Korea; ⁹⁰³Korea Food Research Institute, Research Group of Natural Material and Metabolism, Jeollabuk-do, Korea; ⁹⁰⁴Ewha Womans University, Department of Biochemistry, College of Medicine, Seoul, Korea; ⁹⁰⁵Seoul National University, School of Biological Science, Seoul, Korea; ⁹⁰⁶Evelina Children's Hospital, Guy's & St Thomas' NHS Foundation Trust, Children's Neuroscience Centre, London, UK; ⁹⁰⁷King's College London, Muscle Signalling Section, Randall Division of Cell and Molecular Biophysics, London, UK; ⁹⁰⁸King's College London, Institute of Psychiatry, Psychology and Neuroscience (IoPPN), Department of Basic and Clinical Neuroscience, London, UK; ⁹⁰⁹Memorial Sloan Kettering Cancer Center, New York, NY, USA; ⁹¹⁰University of Ulm, Department of Internal Medicine II, Molecular Cardiology, Ulm, Germany; ⁹¹¹University of Eastern Finland and Kuopio University Hospital, Department of Ophthalmology, Kuopio, Finland; ⁹¹²University Tartu, Department of Pharmacology, Tartu, Estonia; ⁹¹³National Institute of Neuroscience, National Center of Neurology and Psychiatry, Department of Degenerative Neurological Diseases, Kodaira, Tokyo, Japan; ⁹¹⁴University Medical Center Gottingen, Department of Experimental Neurodegeneration, Gottingen, Germany; ⁹¹⁵University of Michigan, Kellogg Eye Center, Department of Ophthalmology and Visual Sciences, Ann Arbor, MI, USA; ⁹¹⁶Medical University of Vienna, Department of Pathology, Vienna, Austria; ⁹¹⁷University of California, San Francisco UCSF Diabetes Center, Department of Cell and Tissue Biology, San Francisco, CA, USA; ⁹¹⁸University of Kansas Medical Center, Department of Microbiology, Molecular Genetics and Immunology, Kansas City, KS, USA; ⁹¹⁹Regional Centre for Biotechnology, NCR Biotech Science Cluster, Faridabad, India; ⁹²⁰National Research Council of Italy (CNR), Neuroscience Institute, Padua, Italy; ⁹²¹European Molecular Biology Laboratory, European Bioinformatics Institute (EMBL-EBI), Wellcome Genome Campus, Hinxton, Cambridge, UK; ⁹²²Karolinska institutet, Department of Oncology/Pathology, Stockholm, Sweden; ⁹²³Gifu University Graduate School of Medicine, Department of Cardiology, Gifu, Japan; ⁹²⁴Shimane University Faculty of Medicine, Internal Medicine 1, Izumo, Shimane, Japan; ⁹²⁵Seoul National University, School of Biological Sciences, Seoul, Korea; ⁹²⁶Chungbuk National University, Department of Biology Education, Seowon-Gu, Cheongju, Chungbuk, Korea; ⁹²⁷Niigata University Graduate School of Medical and Dental Sciences, Department of Cellular Physiology, Niigata, Japan; ⁹²⁸St. Jude Children's Research Hospital, Department of Immunology, Memphis, TN, US; ⁹²⁹Iowa State University, Iowa Center for Advanced Neurotoxicology, Department of Biomedical Sciences, Ames, IA, USA; ⁹³⁰Florida Atlantic University, Charles E. Schmidt College of Medicine, Department of Biomedical Science, Boca Raton, FL, USA; ⁹³¹Semmelweis University, Budapest, Hungary; ⁹³²National and Kapodistrian University of Athens, Medical School, Division of Molecular Oncology, Department of Biological Chemistry, Athens, Greece; ⁹³³University of Minnesota, Institute for Translational Neuroscience, Department of Neuroscience, Minneapolis, MN, USA; ⁹³⁴Jadavpur University, Department of Life Science and Biotechnology, Kolkata, India; ⁹³⁵University of Otago, Department of Physiology-HeartOtago, Dunedin, Otago, New Zealand; ⁹³⁶Hokkaido University, Department of Rheumatology, Endocrinology and Nephrology, Sapporo, Japan; ⁹³⁷Max Planck Institute for Infection Biology, Berlin, Germany; ⁹³⁸University of Eastern Finland, Faculty of Health Sciences, School of Pharmacy, Kuopio, Finland; ⁹³⁹University of Arkansas for Medical Sciences, Little Rock, Arkansas, USA; ⁹⁴⁰Albert Einstein College of Medicine, Department of Developmental and Molecular Biology, Bronx, NY, USA; ⁹⁴¹Doshisha Women's College of Liberal Arts, Faculty of Pharmaceutical Sciences, Kyotanabe, Kyoto, Japan; ⁹⁴²Commonwealth Scientific and Industrial Research Organization (CSIRO), Agriculture and Food, Brisbane, Queensland, Australia; ⁹⁴³Chang Gung University, Department of Biochemistry and Molecular Biology, Taoyuan, Taiwan, China; ⁹⁴⁴Flinders University, Flinders Health and Medical Research Institute, Adelaide, Australia; ⁹⁴⁵Philipps University and University Hospital of Marburg, Department of Neuropathology, Marburg, Germany; ⁹⁴⁶National Institutes of Health, National Institute of Allergy and Infectious Diseases, Laboratory of Immunoregulation, Bethesda, MD, USA; ⁹⁴⁷Oregon Health & Science University, Casey Eye Institute, Portland, OR, USA; ⁹⁴⁸University of Illinois at Urbana-Champaign, Department of Molecular and Integrative Physiology, Urbana, IL, USA; ⁹⁴⁹Swedish University of Agricultural Sciences, Department of Forest Mycology and Plant Pathology, Uppsala, Sweden; ⁹⁵⁰Weill Cornell Medicine, Departments

of Pediatrics and Cell and Developmental Biology, New York, NY, USA; ⁹⁴⁸Metabolomics and Cell Biology Platforms, Gustave Roussy Comprehensive Cancer Institute, Villejuif, France; Equipe 11 labellisée Ligue contre le Cancer, Centre de Recherche des Cordeliers, INSERM U 1138, Paris, France; ⁹⁴⁹Queen Mary University of London, Barts Cancer Institute, London, UK; ⁹⁵⁰University Medical Center of the Johannes Gutenberg University, Institute of Pathobiochemistry, Mainz, Germany; ⁹⁵¹University College London, MRC Laboratory for Molecular Cell Biology, London, UK; ⁹⁵²University of Sadat City, Department of Molecular Biology, Genetic Engineering and Biotechnology Research Institute, Sadat City, Egypt; ⁹⁵³Indiana University-Purdue University (IUPUI), Department of Pathology and Laboratory Medicine, Indianapolis, IN, USA; ⁹⁵⁴University of Eastern Finland, School of Pharmacy, Kuopio, Finland; ⁹⁵⁵Friedrich-Schiller-University Jena, University Hospital Jena, Institute of Human Genetics, Jena, Germany. ; ⁹⁵⁶Gyeongsang National University School of Medicine, Department of Biochemistry and Convergence Medical Sciences and Institute of Health Sciences, Jinju, Republic of Korea; ⁹⁵⁷University of Minnesota, Department of Biochemistry, Molecular Biology, and Biophysics, Minneapolis, MN, USA; ⁹⁵⁸Konkuk University, Department of Bioscience and Biotechnology, Seoul, Korea; ⁹⁵⁹Daegu Gyeongbuk Institute of Science and Technology (DGIST), Department of Brain and Cognitive Sciences, Daegu, Korea; ⁹⁶⁰Dankook University, College of Medicine, Department of Pharmacology, Cheonan, Chungnam, Korea; ⁹⁶¹Korea Research Institute of Bioscience and Biotechnology (KRIBB), Cell Factory Research Center, Daejeon, Korea; ⁹⁶²Dankook University, College of Dentistry, Cheonan, Korea; ⁹⁶³Seoul National University College of Medicine, Department of Biomedical Sciences, and Ophthalmology, Seoul, Korea; ⁹⁶⁴Konkuk University, Department of Stem Cell and Regenerative Biotechnology, Seoul, Korea; ⁹⁶⁵Kyung Hee University, Department of Oral Biochemistry and Molecular Biology, School of Dentistry, Seoul, Korea; ⁹⁶⁶Sookmyung Women's University, Department of Biological Sciences, Seoul, Korea; ⁹⁶⁷Hospital for Sick Children, Program in Cell Biology Department, Toronto, Canada; ⁹⁶⁸University of Toronto, Department of Biochemistry, Toronto, Canada; ⁹⁶⁹Korea Research Institute of Chemical Technology, Center for Convergent Research of Emerging Virus Infection, Daejeon, Korea; ⁹⁷⁰Penn State College of Medicine, Department of Cellular and Molecular Physiology, Hershey, PA, USA; ⁹⁷¹Weizmann Institute of Science, Department of Molecular Genetics, Rehovot, Israel; ⁹⁷²New York University School of Medicine, Department of Radiation Oncology, Perlmutter Cancer Center, New York, NY, USA; ⁹⁷³National Institute of Biomedical Innovation, Health and Nutrition (NIBIOHN), Center for Rare Disease Research, Ibaraki, Osaka, Japan; ⁹⁷⁴AstraZeneca, Bioscience, Oncology R&D, Cambridge, UK; ⁹⁷⁵University College London, Institute of Healthy Ageing, Department of Genetics, Evolution & Environment, London, UK; ⁹⁷⁶University of Utah, Huntsman Cancer Institute, Salt Lake City, UT, USA; ⁹⁷⁷University of Utah School of Medicine, Division of Oncology, Department of Internal Medicine, Salt Lake City, UT, USA; ⁹⁷⁸Cancer Research UK Cancer Therapeutics Unit, The Institute of Cancer Research London, Sutton, UK; ⁹⁷⁹St. Boniface Hospital Albrechtsen Research Centre, Departments of Physiology and Pathophysiology, and Pharmacology and Therapeutics, Max Rady College of Medicine; Rady Faculty of Health Sciences, University of Manitoba, Winnipeg, Manitoba, Canada; ⁹⁸⁰Vavilov Institute of General Genetics RAS, Department of Epigenetics, Moscow, Russia; ⁹⁸¹S&J Kishi Research Corporation, Jupiter, FL, USA; ⁹⁸²Nihon Pharmaceutical University, Department of Pharmaceutical and Medical Business Sciences, Bunkyo-ku, Tokyo, Japan; ⁹⁸³St. Marianna University Graduate School of Medicine, Department of Molecular Neuroscience, Kanagawa, Japan; ⁹⁸⁴Nagasaki University, Institute of Biomedical Sciences, Department of Clinical Research Pharmacy, Nagasaki, Japan; ⁹⁸⁵Albert Einstein College of Medicine, Departments of Medicine and Cell Biology and Wilf Family Cardiovascular Research Institute, Bronx, NY, USA; ⁹⁸⁶University College London, Department of Neuroscience, Physiology and Pharmacology, London, UK; ⁹⁸⁷University of Copenhagen, Department of Neuroscience, Copenhagen, Denmark; ⁹⁸⁸Perelman School of Medicine at the University of Pennsylvania, Department of Medicine (Hematology-Oncology), Philadelphia, PA, USA; ⁹⁸⁹Life Sciences Institute and Department of Molecular, Cellular and Developmental Biology, University of Michigan, Ann Arbor, MI, USA; ⁹⁹⁰Friedrich-Baur-Institute, Department of Neurology, University of Munich, Munich, Germany; ⁹⁹¹University Hospital Erlangen, Department of Molecular Neurology, Erlangen, Germany; ⁹⁹²University of Oslo, Centre for Cancer Cell Reprogramming, Institute of Clinical Medicine, Faculty of Medicine, Montebello, Norway; ⁹⁹³Oslo University Hospital, Department of Molecular Cell Biology, Institute for Cancer Research, Montebello, Norway; ⁹⁹⁴Max Planck Institute of Colloids and Interfaces, Department of Theory and Bio-Systems, Potsdam, Germany; ⁹⁹⁵The University of Tokyo, Graduate School and Faculty of Medicine, Tokyo, Japan; ⁹⁹⁶The Hong Kong Polytechnic University, Department of Applied Biology and Chemical Technology, Hong Kong, China; ⁹⁹⁷Icahn School of Medicine at Mount Sinai, Department of Geriatrics and Palliative Medicine, New York, NY, USA; ⁹⁹⁸Chung Shan Medical University, Institute of Medicine, Taiwan; ⁹⁹⁹The University of Tokyo, Institute for Quantitative Biosciences, Laboratory of RNA Function, Tokyo, Japan; ¹⁰⁰⁰Albert Einstein College of Medicine, Department of Anatomy and Structural Biology, Bronx, NY, USA; ¹⁰⁰¹New York Institute of Technology, College of Osteopathic Medicine, Department of Biomedical Sciences, Old Westbury, NY, USA; ¹⁰⁰²Johann Wolfgang Goethe-University Frankfurt am Main, Faculty of Computer Science and Mathematics, Institute of Computer Science, Frankfurt am Main, Germany; ¹⁰⁰³University Medicine Göttingen, Clinic for Neurology, Göttingen, Germany; ¹⁰⁰⁴University Hospital Münster (UKM), Institute of Musculoskeletal Medicine, Münster, Germany; ¹⁰⁰⁵Goethe University Hospital Frankfurt, Neuroscience Center, Experimental Neurosurgery, Main, Germany; ¹⁰⁰⁶Korea National Institute of Health, Division of Brain Diseases, Cheongju-si, Korea; ¹⁰⁰⁷University of Graz, Institute of Molecular Biosciences, BioTechMed-Graz, Graz, Austria; ¹⁰⁰⁸Juntendo University Graduate School of Medicine, Department of Cell Biology and Neuroscience, Hongo, Bunkyo-ku, Tokyo, Japan; ¹⁰⁰⁹Juntendo University School of Medicine, Department of Physiology, Bunkyo-ku, Tokyo, Japan; ¹⁰¹⁰German Institute of Human Nutrition Potsdam-Rehbruecke (Dife), Department of Molecular Toxicology, Nuthetal, Germany; ¹⁰¹¹Sapporo Higashi Tokushukai Hospital, Advanced Surgery Center, Sapporo, Hokkaido, Japan; ¹⁰¹²The Abigail Wexner Research Institute at Nationwide Children's Hospital, Center for Microbial Pathogenesis, Columbus, OH, USA; ¹⁰¹³Earlham Institute, Norwich, UK; ¹⁰¹⁴Koç University, School of Medicine, Istanbul, Turkey; ¹⁰¹⁵Newcastle University, Ageing Research Laboratories, Institute for Cell and Molecular Biosciences, Newcastle upon Tyne, UK; ¹⁰¹⁶Norwegian University of Science and Technology (NTNU), Department of Biotechnology and Food Science, Trondheim, Norway; ¹⁰¹⁷Korsnes Biocomputing (KoBio), Trondheim, Norway; ¹⁰¹⁸University of Eastern Finland, Department of Ophthalmology, Kuopio, Finland; ¹⁰¹⁹Indiana University School of Medicine, Indianapolis, IN, USA; ¹⁰²⁰Hiroshima University, Graduate School of Biomedical and Health Sciences, Hiroshima, Japan; ¹⁰²¹China National Rice Research Institute, State Key Laboratory of Rice Biology, Hangzhou, China; ¹⁰²²Democritus University of Thrace, Department of Radiotherapy/Oncology, Alexandroupolis, Greece; ¹⁰²³Kanazawa Medical University, Department of Diabetology & Endocrinology, Uchinadacho, Ishikawa, Japan; ¹⁰²⁴Fukuoka University, Faculty of Pharmaceutical Sciences, Department of Biochemistry, Fukuoka, Japan; ¹⁰²⁵University of Freiburg, Institute of Biochemistry and Molecular Biology, ZBMZ, Faculty of Medicine, Freiburg, Germany; ¹⁰²⁶University of Freiburg, CIBSS - Centre for Integrative Biological Signalling Studies, Freiburg, Germany; ¹⁰²⁷Northwestern University Feinberg School of Medicine, Department of Neurology, Chicago, IL, USA; ¹⁰²⁸University of Texas, Southwestern Medical Center, Dallas, TX, USA; ¹⁰²⁹Queen's University of Belfast, Wellcome-Wolfson Institute for Experimental Medicine, Belfast, UK; ¹⁰³⁰Université Lyon, Université Claude Bernard Lyon 1, CNRS UMR 5310, INSERM U1217, Institut NeuroMyoGène, Lyon, France; ¹⁰³¹Université de Paris, Sorbonne Université, INSERM U1138, Centre de Recherche des Cordeliers, Equipe labellisée par la Ligue contre le cancer, Paris, France; Institut Gustave Roussy, Metabolomics and Cell Biology Platforms, Villejuif, France; Hôpital Européen Georges Pompidou, AP-HP, Pôle de Biologie, Paris, France; Chinese Academy of Medical Sciences, Suzhou Institute for Systems Medicine, Suzhou, China; Karolinska Institute, Karolinska University Hospital, Department of Women's and Children's Health, Stockholm, Sweden ; ¹⁰³²Babraham Institute, Babraham, Cambridge, UK; ¹⁰³³Tokyo University of Science, Department of Applied Biological Science, Noda, Chiba, Japan; ¹⁰³⁴University of Bonn, LIMES Institute, Bonn, Germany; ¹⁰³⁵Emory University, Department of Pharmacology and Chemical Biology, School of Medicine, Atlanta, GA, USA; ¹⁰³⁶PK-PD-Toxicology

and Formulation Division, CSIR-Indian Institute of Integrative Medicine, Jammu, India; ¹⁰³⁰University of Houston, Department of Pharmacological and Pharmaceutical Sciences, Houston, TX, USA; ¹⁰³¹Julius L. Chambers Biomedical/Biotechnology Research Institute (BBRI) and North Carolina Central University, Department of Pharmaceutical Sciences, Durham, NC; ¹⁰³²International Centre for Genetic Engineering and Biotechnology, Cellular Immunology Group, Aruna Asaf Ali Marg, New Delhi, India; ¹⁰³³Centre for Cancer Biology, University of South Australia, Adelaide, Australia; ¹⁰³⁴Shiga University of Medical Science, Department of Medicine, Otsu, Shiga, Japan; ¹⁰³⁵Kalinga Institute of Industrial Technology (KIIT-DU), School of Biotechnology, Campus 11, Patia, Bhubaneswar, Odisha, India; ¹⁰³⁶St. Jude Children's Research Hospital, Department of Pathology, Memphis, TN, USA; ¹⁰³⁷Indian Institute of Technology (IIT) Guwahati, Department of Biosciences and Bioengineering, Guwahati, Assam, India; ¹⁰³⁸Virginia Commonwealth University, Department of Computer Science, Richmond, VA, USA; ¹⁰³⁹Sabanci University Nanotechnology Research and Application Center (SUNUM), Tuzla, Istanbul, Turkey; ¹⁰⁴⁰Wonkwang University School of Medicine, Zoonosis Research Center, Iksan, Jeonbuk, Korea; ¹⁰⁴¹Yonsei University, Department of Biotechnology, Seodaemun-gu, Seoul, Korea; ¹⁰⁴²Keimyung University, School of Medicine, Department of Immunology, Daegu, Korea; ¹⁰⁴³Protein Metabolism Medical Research Center and Department of Biomedical Sciences, Seoul National University School of Medicine, Seoul, Korea; ¹⁰⁴⁴Duke University School of Medicine, Durham, NC, USA; ¹⁰⁴⁵INRS, INRS-Institut Armand-Frappier, Montréal, QC, Canada; ¹⁰⁴⁶University of Burgundy, Centre Georges François Leclerc, Department of Medical Oncology, Dijon, France; ¹⁰⁴⁷Icahn School of Medicine at Mount Sinai, Department Hematology and Medical Oncology, New York, NY, USA; ¹⁰⁴⁸Cellular Microbiology and Physics of Infection Group, Center for Infection and Immunity of Lille, Institut Pasteur de Lille, CNRS, INSERM, CHU Lille, University of Lille, Lille Cedex, France; ¹⁰⁴⁹University of Ottawa, Department of Cellular & Molecular Medicine, Ottawa, Ontario, Canada; ¹⁰⁵⁰Huazhong Agricultural University, National Key Laboratory of Crop Genetic Improvement, Wuhan, China; ¹⁰⁵¹Macquarie University, Faculty of Medicine, Health and Human Sciences, Department of Biomedical Science, Centre for Motor Neuron Disease Research, Sydney, NSW, Australia; ¹⁰⁵²University of California, San Francisco Department of Ophthalmology, San Francisco, CA, USA; ¹⁰⁵³University of Tromsø - The Arctic University of Norway, Department of Medical Biology, Tromsø, Norway; ¹⁰⁵⁴National Yang-Ming University, Department of Life Sciences and Institute of Genome Sciences, Taipei, Taiwan; ¹⁰⁵⁵Yale University, Department of Cellular and Molecular Physiology, New Haven, CT, USA; ¹⁰⁵⁶Melbourne Dementia Research Centre, The Florey Institute of Neuroscience & Mental Health, The University of Melbourne, Parkville, VIC, Australia; ¹⁰⁵⁷School of Biochemistry, University of Bristol, Bristol, UK; ¹⁰⁵⁸Penn State College Medicine, Department of Cellular and Molecular Physiology, Hershey, PA, USA; ¹⁰⁵⁹University of Greifswald, Institute of Pharmacy, Greifswald, Germany; ¹⁰⁶⁰Stockholm University, Department of Biochemistry and Biophysics, Stockholm, Sweden; ¹⁰⁶¹Johannes Kepler University Linz, Kepler University Hospital GmbH, Institute of Pathology and Molecular Pathology, Linz, Austria; ¹⁰⁶²University Bourgogne Franche-Comté, AgroSup Dijon, PAM UMR A 02.102, Dijon, France; ¹⁰⁶³IGBMC, Inserm U1258, Cnrs UMR7104, Strasbourg University, Illkirch, France; ¹⁰⁶⁴Mayo Clinic, Department of Medicine, Division of Gastroenterology and Hepatology, Rochester, MN, USA; ¹⁰⁶⁵Centro de Investigación Biomédica en Red sobre Enfermedades Neurodegenerativas (CIBERNED), Instituto de Investigación Sanitaria La Paz (IdiPaz), Instituto de Investigaciones Biomédicas Alberto Sols UAM-CSIC, Madrid, Spain; ¹⁰⁶⁶Universidad Autónoma de Madrid, School of Medicine, Department of Biochemistry, Madrid, Spain; ¹⁰⁶⁷University of Virginia, Department of Cell Biology, Charlottesville, VA, USA; ¹⁰⁶⁸Macau University of Science and Technology, State Key Laboratory of Quality Research in Chinese Medicine, Taipa, Macau, China; ¹⁰⁶⁹University of Nottingham, School of Life Sciences, Nottingham, UK; ¹⁰⁷⁰Shanghai Jiao-Tong University School of Medicine, Institute of Neurology, Shanghai, China; ¹⁰⁷¹Université Paris-Sud, Institut des Neurosciences Paris-Saclay (Neuro-PSI)- CNRS UMR 9197, Orsay cedex, France; ¹⁰⁷²McGill University Health Center, Department of Medicine, Cancer Research Program, Montreal, QC, Canada; ¹⁰⁷³Research Institute of the McGill University Health Centre, Meakins-Christie Laboratories and Translational Research in Respiratory Diseases Program, Montréal, Québec, Canada; ¹⁰⁷⁴McGill University, Department of Critical Care and Division of Experimental Medicine, Montréal, Québec, Canada; ¹⁰⁷⁵UQAM, Faculté des Sciences, Département des Sciences de l'activité physique, Montréal, Canada; ¹⁰⁷⁶Ulsan National Institute of Science and Technology, Department of Biological Sciences, Ulsan, Korea; ¹⁰⁷⁷National Taipei University of Nursing and Health Sciences, School of Nursing, Taipei, Taiwan; ¹⁰⁷⁸University of Pennsylvania, Department of Pathology and Laboratory Medicine, Philadelphia, PA, USA; ¹⁰⁷⁹KAIST, Department of Biological Sciences, Daejeon, Korea; ¹⁰⁸⁰Konkuk University, School of Medicine, Department of Anatomy, Seoul, Korea; ¹⁰⁸¹Korea Advanced Institute of Science and Technology, Graduate School of Medical Science and Engineering, Daejeon, Korea; ¹⁰⁸²QIMR Berghofer Medical Research Institute, Herston, Queensland, Australia; ¹⁰⁸³Kyungpook National University, School of Medicine, Department of Biochemistry and Cell Biology, Daegu, Korea; ¹⁰⁸⁴Hannam University, Department of Biological Sciences and Biotechnology, Daejeon, South Korea; ¹⁰⁸⁵Chungnam National University, Graduate School of Analytical Science and Technology (GRAST), Daejeon 305-764, Republic of Korea; ¹⁰⁸⁶University of Michigan, Department of Molecular & Integrative Physiology, Ann Arbor, MI, USA; ¹⁰⁸⁷Incheon National University, College of Life Sciences and Bioengineering, Division of Life Sciences, Incheon, Korea; ¹⁰⁸⁸Yonsei University College of Medicine, Department of Pharmacology, Seoul, Korea; ¹⁰⁸⁹Seoul National University College of Medicine, Department of Biochemistry and Molecular Biology, Seoul, Korea; ¹⁰⁹⁰Yonsei University College of Medicine, Severance Biomedical Science Institute and Department of Internal Medicine, Seoul, Korea; ¹⁰⁹¹Ajou University Graduate School of Medicine, Department of Biomedical Sciences, Suwon, Gyeonggi, Korea; ¹⁰⁹²Seoul National University College of Medicine, Department of Biomedical Sciences, Neuroscience Research Institute, Seoul, Korea; ¹⁰⁹³University of Kansas Medical Center, Department of Biochemistry and Molecular Biology, Kansas City, KS, USA; ¹⁰⁹⁴DGIST, Department of Brain & Cognitive Sciences, Daegu, Korea; ¹⁰⁹⁵University of Arizona College of Medicine, Department of Basic Medical Sciences, Phoenix, AZ, USA; ¹⁰⁹⁶Ditmanson Medical Foundation Chia-Yi Christian Hospital, Translational Medicine Research Center, Chiayi City, Taiwan; ¹⁰⁹⁷Yonsei University College of Medicine, Department of Internal Medicine, Seoul, Korea; ¹⁰⁹⁸University of West Florida, Department of Movement Sciences and Health, Pensacola, FL, USA; ¹⁰⁹⁹University of Michigan, Rogel Cancer Center, Department of Periodontics and Oral Medicine, Department of Otolaryngology - Head and Neck Surgery, Ann Arbor, MI, USA; ¹¹⁰⁰National Institutes of Health, Eunice Kennedy Shriver National Institute of Child Health and Human Development, Bethesda, MD, USA; ¹¹⁰¹Institute for Integrative Biology of the Cell (I2BC), CEA, CNRS, Université Paris-Sud, Université Paris-Saclay, Gif-sur-Yvette cedex, France; ¹¹⁰²University of Seville, Department of Genetics, Seville, Spain; ¹¹⁰³Guangzhou Medical University, School of Basic Medical Sciences, Guangzhou, China; ¹¹⁰⁴Universidade Federal do Rio Grande do Sul (UFRGS), Center of Biotechnology and Department of Biophysics, Porto Alegre, RS, Brazil; ¹¹⁰⁵USC Norris Comprehensive Cancer Center, Los Angeles, CA, USA; ¹¹⁰⁶University of Pisa, Department of Translational Research and New Technologies in Medicine and Surgery, Pisa, Italy; ¹¹⁰⁷University of São Paulo, Department of Clinical Analyses, Toxicology and Food Sciences, Ribeirão Preto, SP, Brazil; ¹¹⁰⁸University of Luxembourg, Life Sciences Research Unit, Molecular Disease Mechanisms Group, Belval, Luxembourg; ¹¹⁰⁹The Chinese University of Hong Kong, Faculty of Medicine, School of Biomedical Sciences, Shatin, New Territories, Hong Kong; ¹¹¹⁰Icahn School of Medicine at Mount Sinai, Department of Medicine, New York, NY, USA; ¹¹¹¹University of Texas Southwestern Medical Center, Center for Autophagy Research, Department of Internal Medicine and Howard Hughes Medical Institute, Dallas, TX, USA; ¹¹¹²Royal Veterinary College, London, UK; ¹¹¹³UCL Queen Square Institute of Neurology, Department of Neurodegenerative Disease, London, UK; ¹¹¹⁴La Jolla Institute for Immunology and University of California San Diego, Division of Inflammation Biology, La Jolla, CA, USA; ¹¹¹⁵College of Life Science and Technology, Jinan University, Guangzhou, China; ¹¹¹⁶Fudan University, Shanghai Cancer Center and Institutes of Biomedical Sciences, Shanghai, China; ¹¹¹⁷Sun Yat-sen University, Sun Yat-sen Memorial Hospital, Department of Pathology, Guangzhou, Guangdong Province, China; ¹¹¹⁸Sichuan University, West China Hospital, State key laboratory of biotherapy, Chengdu, Sichuan, China; ¹¹¹⁹Chinese Academy of Medical Sciences & Peking Union Medical College, Institute of Medicinal

Biotechnology, Beijing, China; ¹¹¹⁶Virginia Polytechnic Institute, Department of Biological Sciences, Blacksburg, VA, USA; ¹¹¹⁷Children's Hospital of Soochow University, Institute of Pediatric Research, Suzhou, China; ¹¹¹⁸Sun Yat-Sen University, School of Pharmaceutical Sciences, Guangzhou, China; ¹¹¹⁹Hong Kong Baptist University, School of Chinese Medicine, Hong Kong, China; ¹¹²⁰Department of Molecular, Cellular and Developmental Biology, University of Michigan, Ann Arbor, MI, USA; ¹¹²¹Fudan University, Hospital of Obstetrics and Gynecology, Institute of Obstetrics and Gynecology, Laboratory for Reproductive Immunology, Shanghai, China; ¹¹²²Jinan University, College of Life Science and Technology, Department of Biology, Guangzhou, China; ¹¹²³Virginia Commonwealth University, Department of Pharmacology and Toxicology, Richmond, VA, USA; ¹¹²⁴South China Normal University, School of Life Sciences, Institute of Insect Science and Technology, Guangdong Provincial Key Laboratory of Insect Developmental Biology and Applied Technology, Guangzhou, China; ¹¹²⁵University of Kansas Medical Center, Department of Pharmacology, Toxicology and Therapeutics, Kansas City, KS, USA; ¹¹²⁶Chinese Academy of Sciences, Institute of Zoology, State Key Laboratory of Stem cell and Reproductive Biology, Beijing, China; ¹¹²⁷Emory University School of Medicine, Department of Pharmacology and Chemical Biology, Atlanta, GA, USA; ¹¹²⁸Boston Children's Hospital, Harvard Medical School, Departments of Urology and Surgery, Boston, MA, USA; ¹¹²⁹Stanford University, Department of Gastroenterology & Hepatology, Stanford, CA, USA; ¹¹³⁰Chinese Academy of Agriculture Sciences, Lanzhou Veterinary Research Institute, State Key Laboratory of Veterinary Etiological Biology, Lanzhou, Gansu, China; ¹¹³¹Southern Medical University, Shenzhen Hospital, Department of Pathology, Bao'an District, Shenzhen, Guangdong, China; ¹¹³²Army Medical University, Department of Biochemistry and Molecular Biology, Chongqing, Chongqing, China; ¹¹³³The Wistar Institute, Molecular and Cellular Oncogenesis Program, Philadelphia, PA, USA; ¹¹³⁴New York Institute of Technology, College of Osteopathic Medicine, Department of Biomedical Sciences, Old Westbury, NY, USA; ¹¹³⁵Sun Yat-sen University, The 3rd Affiliated Hospital of Sun Yat-sen University, Vaccine Research Institute, Guangzhou, China; ¹¹³⁶Free University of Berlin, Department of Biology, Chemistry and Pharmacy, Berlin, Germany; ¹¹³⁷Nanjing Agricultural University, College of Life Sciences, Key Laboratory of Agricultural Environmental Microbiology of Ministry of Agriculture and Rural Affairs, Nanjing, China; ¹¹³⁸East China Normal University, School of Life Sciences, Shanghai, China; ¹¹³⁹Northwest A&F University, College of Life Sciences, Yangling, Shaanxi, China; ¹¹⁴⁰Academia Sinica, Institute of Cellular and Organismic Biology, Taipei, Taiwan; ¹¹⁴¹Nathan S. Kline Institute, Center for Dementia Research, Orangeburg, NY, USA; ¹¹⁴²National Institute of Child Health and Human Development, National Institutes of Health, Cell Biology and Neurobiology Branch, Bethesda, MD, USA; ¹¹⁴³Konkuk University, Department of Veterinary Medicine, Seoul, Korea; ¹¹⁴⁴São Paulo State University, Botucatu Medical School, Department of Pathology, Botucatu, SP, Brazil; ¹¹⁴⁵San Raffaele Open University and IRCCS San Raffaele Pisana, Laboratorio di Patologia Cellulare e Molecolare, Rome, Italy; ¹¹⁴⁶First Affiliated Hospital of Nanjing Medical University, Department of Neurosurgery, Nanjing, China; Jiangsu Province Hospital, Department of Neurosurgery, Nanjing, China; ¹¹⁴⁷Division of Gastroenterology and Hepatology, Department of Internal Medicine, E-Da Hospital, Kaohsiung, Taiwan; I-Shou University, College of Medicine, School of Medicine, Kaohsiung, Taiwan; ¹¹⁴⁸Mackay Memorial Hospital, Department of Pediatrics, Taipei, Taiwan; Mackay Medical College, Department of Medicine, New Taipei, Taiwan; ¹¹⁴⁹Zhejiang University, Biotechnology Institute, State Key Laboratory for Rice Biology, Hangzhou, China; ¹¹⁵⁰Life Sciences Institute and Department of Cell & Developmental Biology, University of Michigan, Ann Arbor, MI, USA; ¹¹⁵¹National Health Research Institutes, Institute of Biomedical Engineering and Nanomedicine, Zhunan, Miaoli, Taiwan; ¹¹⁵²Chang Gung Memorial Hospital, Liver Research Center, Linkou, Taoyuan, Taiwan; Chang Gung University, College of Medicine, Graduate Institute of Biomedical Sciences, Taoyuan, Taiwan; Chang Gung University of Science and Technology, College of Human Ecology, Research Center for Chinese Herbal Medicine, Taoyuan, Taiwan; ¹¹⁵³Taipei Medical University, College of Medicine, Graduate Institute of Medical Sciences, Taipei, Taiwan; Taipei Medical University, School of Medicine, College of Medicine, Department of Microbiology and Immunology, Taipei, Taiwan; ¹¹⁵⁴The Ohio State University, Wexner Medical Center, Department of Surgery, Columbus, OH, USA; ¹¹⁵⁵School of Medicine, Jiangsu University, 301 Xuefu Road, Zhenjiang, Jiangsu, China; ¹¹⁵⁶Harvard Medical School, Massachusetts General Hospital, Gastrointestinal Unit/Medicine, Boston, MA, USA; ¹¹⁵⁷Mayo Clinic, Department of Biochemistry and Molecular Biology, Rochester, MN, USA; ¹¹⁵⁸Brigham and Women's Hospital, Harvard Medical School, Center for Nanomedicine and Department of Anesthesiology, Boston, MA, USA; ¹¹⁵⁹National Cheng Kung University, College of Medicine, Department of Microbiology and Immunology, Tainan, Taiwan; ¹¹⁶⁰Lovelace Respiratory Research Institute, Molecular Biology and Lung Cancer Program, Albuquerque, NM, USA; ¹¹⁶¹Instituto de Biofísica da UFRJ, Rio de Janeiro, Brazil; ¹¹⁶²National University of Singapore, Department of Physiology, Singapore; ¹¹⁶³Technical University of Munich, School of Medicine, Klinikum rechts der Isar, Department of Neurology, Munich, Germany; ¹¹⁶⁴Indiana University School of Medicine, Department of Pediatrics and Center for Diabetes and Metabolic Diseases, Indianapolis, IN, USA; ¹¹⁶⁵University of Singapore, Department of Biological Sciences, Singapore; ¹¹⁶⁶University of Maryland School of Medicine, Department of Anesthesiology, Baltimore, MD, USA; ¹¹⁶⁷University of Maribor, Faculty of Medicine, Maribor, Slovenia; University of Maribor, Faculty of Natural Sciences and Mathematics, Department of Biology, Maribor, Slovenia; University of Maribor, Faculty of Chemistry and Chemical Engineering, Maribor, Slovenia; Medical University of Graz, Division of Cell Biology, Histology and Embryology, Gottfried Schatz Research Center, Graz, Austria; ¹¹⁶⁸University of Iowa, Fraternal Order of Eagles Diabetes Research Center, Obesity Research and Education Initiative, Department of Health and Human Physiology, Iowa City, IA, USA; ¹¹⁶⁹Poznan University of Medical Sciences, Department of Clinical Chemistry and Molecular Diagnostics, Poznan, Poland; ¹¹⁷⁰Duke University, Department of Ophthalmology, Durham, NC, USA; ¹¹⁷¹Chinese Academy of Sciences, Center for Biosafety Mega-Science, Institute of Microbiology, CAS Key Laboratory of Pathogenic Microbiology and Immunology, Chaoyang District, Beijing, China; ¹¹⁷²Institute of Neuroscience of Soochow University, Suzhou, China; ¹¹⁷³Nankai University, Department of Microbiology, Tianjin, China; ¹¹⁷⁴Guangdong Medical University, Institute of Nephrology, and Zhanjiang Key Laboratory of Prevention and Management of Chronic Kidney Disease, Zhanjiang, Guangdong, China; ¹¹⁷⁵Capital Medical University, Beijing Institute for Brain Disorders, Beijing, China; ¹¹⁷⁶Central South University, School of Life Sciences, Molecular Biology Research Center, Changsha, Hunan, China; ¹¹⁷⁷Texas A&M University, The Institute of Biosciences and Technology, Houston, TX, USA; ¹¹⁷⁸Columbia University, Naomi Berrie Diabetes Center, Department of Pathology and Cell Biology, College of Physicians and Surgeons, New York, NY, USA; ¹¹⁷⁹University of New Mexico Health Sciences Center, Department of Biochemistry and Molecular Biology, Albuquerque, NM, USA; ¹¹⁸⁰Henan Academy of Agricultural Sciences, Institute of Plant Nutrition, Agricultural Resources and Environmental Science, Jinshui District, Zhengzhou, Henan, China; ¹¹⁸¹Zhejiang University School of Medicine, Department of Biochemistry and Department of Cardiology of the Second Affiliated Hospital, Hangzhou, Zhejiang, China; ¹¹⁸²Chinese Academy of Agricultural Sciences, Institute of Plant Protection, State Key Laboratory for Biology of Plant Diseases and Insect Pests, Beijing, China; ¹¹⁸³CAS Key Laboratory of Regenerative Biology, Guangzhou Institutes of Biomedicine and Health, Chinese Academy of Sciences, Guangzhou, China; ¹¹⁸⁴Harvard Medical School, Department of Microbiology; Brigham and Women's Hospital, Division of Infectious Diseases, Boston, MA, USA; ¹¹⁸⁵University of Colorado at Boulder, Department of Biochemistry, Boulder, CO, USA; ¹¹⁸⁶Saarland University, Department of Neurology, Homburg, Germany; ¹¹⁸⁷ShanghaiTech University, School of Life Science and Technology, Shanghai, China; ¹¹⁸⁸Shenyang Pharmaceutical University, Department of Pharmacology, Shenyang, China; ¹¹⁸⁹Tsinghua University, School of Life Sciences, Beijing, China; ¹¹⁹⁰University of Texas MD Anderson Cancer Center, Department of Sarcoma Medical Oncology, Houston, TX, USA; ¹¹⁹¹University of Bourgogne Franche-Comté, Team 'Biochemistry of the Peroxisome, Inflammation and Lipid Metabolism (EA7270), Faculty of Sciences Gabriel, Dijon, France; ¹¹⁹²Universitat Autònoma de Barcelona, Departament de Bioquímica and Institut Neurociències, Faculty of Medicine, Bellaterra, Barcelona, Spain; ¹¹⁹³Vall d'Hebron Research Institute, Barcelona, Spain; ¹¹⁹⁴Bellvitge Biomedical Research Institute-IDIBELL, Oncobell Program. L'Hospitalet de Llobregat, Barcelona, Spain; ¹¹⁹⁵Oslo University Hospital, Institute for

Cancer Research, Department of Molecular Cell Biology, Oslo, Norway; ¹¹⁹⁶Harvard Medical School, Brigham and Women's Hospital, Department of Neurology, Boston, MA, USA; ¹¹⁹⁷CAS Key Laboratory of Regenerative Biology, Guangzhou Institutes of Biomedicine and Health, Chinese Academy of Sciences, Guangzhou, China; ¹¹⁹⁸National University of Singapore, Yong Loo Lin School of Medicine, Department of Biochemistry, Singapore; ¹¹⁹⁹Universidad Autonoma de Madrid, School of Medicine, Department of Pharmacology, Madrid, Spain; ¹²⁰⁰Universidad Autónoma de Madrid, Departamento de Biología Molecular, Madrid, Spain and Centro de Biología Molecular Severo Ochoa (CSIC-UAM), Madrid, Spain; ¹²⁰¹Universidad de Zaragoza, IA2, IIS, Laboratorio de Genética Bioquímica (LAGENBIO), Zaragoza, Spain; Universidad de Zaragoza, IA2, IIS, Centro de Encefalopatías y Enfermedades Transmisibles Emergentes, Zaragoza, Spain; ¹²⁰²University Medical Center Utrecht, Center for Molecular Medicine, UUtrecht, The Netherlands; Regenerative Medicine Center, Utrecht, The Netherlands; ¹²⁰³Complutense University, Instituto de Investigaciones Sanitarias San Carlos (IdISSC), Department of Biochemistry and Molecular Biology, School of Biology, Madrid, Spain; ¹²⁰⁴Université de Paris, Centre de Recherche sur l'Inflammation (CRI), Inserm-UMR1149, Paris, France; ¹²⁰⁵Newcastle University, Institute of Translation and Clinical Studies, Precision Medicine, The Medical School, Newcastle upon Tyne, UK; ¹²⁰⁶State University of New York at Buffalo, Buffalo, NY, USA; ¹²⁰⁷Universidad Mayor, Center for Integrative Biology and Geroscience for Brain, Health and Metabolism, Santiago, Chile; ¹²⁰⁸University of Macau, Institute of Chinese Medical Sciences, State Key Laboratory of Quality Research in Chinese Medicine, Taipa, Macao, China; ¹²⁰⁹Pfizer Inc, DSRD, La Jolla, CA, USA; ¹²¹⁰University of Zurich, Institute of Physiology, Zurich, Switzerland; ¹²¹¹University of St Andrews, Department of Medicine, North Haugh, St Andrews, UK; ¹²¹²Life and Health Sciences Research Institute (ICVS), School of Medicine, University of Minho, Braga, Portugal and ICVS/3B - PT Government Associate Laboratory, Braga/Guimarães, Portugal; ¹²¹³Duke University, School of Medicine, Duke Center for Virology, Department of Molecular Genetics and Microbiology, Durham, NC, USA; ¹²¹⁴Universidad de La Laguna, Facultad de Medicina, Departamento de Ciencias Médicas Básicas, Tenerife, Spain; Universidad de La Laguna, Instituto de Tecnologías Biomédicas (ITB), Tenerife, Spain; ¹²¹⁵BC Cancer, Trev and Joyce Deeley Research Centre, Victoria, BC, Canada; University of Victoria, Department of Biochemistry, Victoria, BC, Canada; ¹²¹⁶University of Copenhagen, Biotech Research and Innovation Centre, Copenhagen, Denmark; ¹²¹⁷University of Münster, University Hospital, Department of Neurology, Münster, Germany; ¹²¹⁸University of British Columbia, Centre for Heart Lung Innovation/Department of Pathology and Laboratory Medicine, Vancouver, BC, Canada; ¹²¹⁹Plymouth University, Peninsula School of Medicine and Dentistry, Plymouth, UK; ¹²²⁰Huazhong Agricultural University, Laboratory of Molecular Nutrition for Aquatic Economic Animals, Fishery College, Wuhan, China; ¹²²¹University of Palermo, Department of Biological, Chemical and and Pharmaceutical Sciences and Technologies, Palermo, Italy; ¹²²²RWTH Aachen University, Institute of Biochemistry and Molecular Biology, Aachen, Germany; ¹²²³International Clinical Research Center, St'Anne University Hospital, Brno, Czech Republic; Institute of Molecular Biology and Biophysics, Federal Research Center of Fundamental and Translational Medicine, Novosibirsk, Siberia, Russia; ¹²²⁴University of Oslo, Faculty of Medicine, Institute of Basic Medical Sciences, Department of Molecular Medicine, Oslo, Norway; University of Oslo, Faculty of Medicine, Institute of Clinical Medicine, Centre for Cancer Cell Reprogramming, Oslo, Norway; ¹²²⁵Justus Liebig University, University Hospital Giessen and Marburg GmbH, Departement of Ophthalmology, Giessen, Germany; ¹²²⁶The Hong Kong Polytechnic University, Department of Health Technology and Informatics, Hong Kong, China; ¹²²⁷Shandong Normal University, Shandong Provincial Key Laboratory of Plant Stress, College of Life Sciences, Jinan, Shandong, China; ¹²²⁸Yale School of Medicine, Department of Cell Biology, New Haven, CT, USA; ¹²²⁹Guangzhou Medical University, Department of Histology and Embryology, Guangzhou, China; ¹²³⁰Soochow University, Institute of Neuroscience, Jiangsu Key Laboratory of Translational Research and Therapy for Neuro-Psycho-Diseases, Suzhou, Jiangsu, China; ¹²³¹Department of Emergency Medicine, Thomas Jefferson University, Philadelphia, PA, USA; ¹²³²Air Force Medical University, Xijing Hospital, Department of Clinical Laboratory, Xi'an, China; ¹²³³Tianjin Medical University, Department of Biochemistry and Molecular Biology; School of Basic Medical Sciences, Tianjin Key Laboratory of Medical Epigenetics, Tianjin, China; ¹²³⁴University of Michigan, Department of Molecular & Integrative Physiology, Ann Arbor, MI, USA; ¹²³⁵Albert Einstein College of Medicine, Department of Pathology, Bronx, NY, USA; ¹²³⁶Ben May Department for Cancer Research, University of Chicago, Chicago IL, USA; ¹²³⁷Iowa State University, Roy J. Carver Department of Biochemistry, Biophysics and Molecular Biology, Ames, IA, USA; ¹²³⁸Perelman School of Medicine at the University of Pennsylvania, Department of Neuroscience, Philadelphia, PA, USA; ¹²³⁹University of Graz, Institute of Molecular Biosciences, Graz, Austria; BioTechMed-Graz, Graz, Austria; ¹²⁴⁰University of Texas Health San Antonio, Department of Medicine, San Antonio, TX, USA; ¹²⁴¹Medical University of Graz, Gottfried Schatz Research Center for Cell Signaling, Metabolism and Aging, Molecular Biology and Biochemistry, Graz, Austria; ¹²⁴²Albert Einstein College of Medicine, Institute for Aging Studies, Department of Developmental and Molecular Biology, Bronx, NY, USA; ¹²⁴³Tokyo Medical and Dental University, Department of Cardiovascular Medicine, Tokyo, Japan; ¹²⁴⁴Universidad Autónoma de Madrid, Department of Biology, Madrid, Spain; ¹²⁴⁵Part overlaps with Costanza Montagna: Danish Cancer Society Research Center, Computational Biology Laboratory, Copenhagen, Denmark; UniCamillus, Saint Camillus International University of Health Sciences, Rome, Italy; ¹²⁴⁶Cellular and Molecular Signaling, New York, NY, USA; ¹²⁴⁷Central Michigan University, Department of Psychology and Neuroscience Program, Mt. Pleasant, MI, USA; ¹²⁴⁸Inserm U1138, Centre de Recherche des Cordeliers, Sorbonne Université, Université de Paris, Paris, France; ¹²⁴⁹University of Naples Federico II, Department of Biology, Naples, Italy; ¹²⁵⁰CSIR - Indian Institute of Integrative Medicine, Department of Cancer Pharmacology, Sanat Nagar, Srinagar, Jammu and Kashmir, India; ¹²⁵¹Center for gender-specific medicine, Italian National Health Institute, Rome, Italy; ¹²⁵²Oregon Health and Science University, Knight Cardiovascular Institute, Portland, OR, USA; ¹²⁵³Dana-Farber Cancer Institute, Division of Genomic Stability and DNA Repair, Department of Radiation Oncology, Boston, MA, USA; ¹²⁵⁴RIKEN, Laboratory for Retinal Regeneration, Kobe, Hyogo, Japan; ¹²⁵⁵Washington University in St. Louis, Department of Cell Biology and Physiology, St. Louis, MO, USA; ¹²⁵⁶National University of Singapore, Yong Loo Lin School of Medicine, Department of Physiology, Mitochondrial Physiology and Metabolism Lab, Singapore; National University of Singapore, NUHS Centre for Healthy Ageing, Singapore; ¹²⁵⁷Iowa State University, Department of Biomedical Sciences, Ames, IA, USA; ¹²⁵⁸The Chinese University of Hong Kong, The Prince of Wales Hospital, The Faculty of Medicine, Department of Orthopaedics and Traumatology, New Territories, Shatin, Hong Kong, China; ¹²⁵⁹German Center for Neurodegenerative Diseases (DZNE), Bonn, Germany; CAESAR Research Center, Bonn, Germany; ¹²⁶⁰Vita-Salute San Raffaele University & IRCCS San Raffaele Scientific Institute, Division of Immunology, Transplantation and Infectious Diseases, Milano, Italy; ¹²⁶¹Virginia Commonwealth University School of Medicine, VCU Institute of Molecular Medicine, Massey Cancer Center, Department of Microbiology and Immunology, Richmond, VA, USA; ¹²⁶²Jawaharlal Nehru Centre for Advanced Scientific Research, Molecular Biology and Genetics Unit, and Neuroscience Unit, Autophagy Laboratory, Jakkur, Bangalore, India; ¹²⁶³Universidad Mayor, Center for Integrative Biology, Santiago, Chile; ¹²⁶⁴UCL School of Pharmacy, Department of Pharmacology, Bloomsbury, London, United Kingdom; ¹²⁶⁵Massachusetts General Hospital, Department of Molecular Biology, Boston, MA, USA; ¹²⁶⁶Sapienza University of Rome, Department of Experimental Medicine, Rome, Italy; ¹²⁶⁷Presidio San Paolo Polo Universitario, Dipartimento di Scienze della Salute San Paolo, Milano, Italy; ¹²⁶⁸University of Milan, Department of Pharmacological and Biomolecular Sciences, Milan, Italy; ¹²⁶⁹Sapienza University of Rome, Department of Experimental Medicine, Rome, Italy; ¹²⁷⁰University of California San Francisco, Department of Pathology, San Francisco, CA, USA; ¹²⁷¹Consiglio Nazionale delle Ricerche, Istituto di Biochimica e Biologia Cellulare, Monterotondo scalo (RM), Italy; ¹²⁷²University of Oviedo, Principality of Asturias Institute for Biomedical Research,

- 1555 Department of Functional Biology, Oviedo, Spain; ¹²⁷³University of Verona, Department of Neuroscience, Biomedicine and Movement Sciences, Biological Chemistry Section, Verona, Italy; ¹²⁷⁴Washington University in St. Louis, Department of Biology, St. Louis, MO, USA; ¹²⁷⁵UMBC, Department of Chemical, Biochemical and Environmental Engineering, Baltimore, MD, USA; ¹²⁷⁶University of Vienna, Max Perutz Labs, Department of Biochemistry and Cell Biology, Vienna BioCenter, Vienna, Austria; ¹²⁷⁷Harvard Medical School, Department of Biological Chemistry and Molecular Pharmacology, Boston, MA, USA; ¹²⁷⁸Michigan State University, College of Human Medicine, Grand Rapids, MI, USA;
- 1560 ¹²⁷⁹KU Leuven, Department of cellular and Molecular Medicine, Laboratory of cellular transport systems, Leuven, Belgium; ¹²⁸⁰Instituto Nacional de Investigación y Tecnología Agraria y Alimentaria (INIA), Department of Biotechnology, Madrid, Spain; ¹²⁸¹University of Las Palmas de Gran Canaria, Department of Physical Education and Research Institute of Biomedical and Health Sciences (IUIBS), Las Palmas de Gran Canaria, Spain; ¹²⁸²Instituto de Investigaciones Biomédicas "Alberto Sols", CSIC-UAM, Madrid, Spain; ¹²⁸³Albert Einstein College of Medicine, Department of Developmental and Molecular Biology, Bronx, NY, USA; ¹²⁸⁴University of Antwerp, Laboratory of Physiopharmacology, Antwerp, Belgium; ¹²⁸⁵National Institutes of Health, National Institute of Environmental Health Sciences, Durham, NC, USA; ¹²⁸⁶Centro de Investigación y Asistencia en Tecnología y Diseño del Estado de Jalisco, AC, Unidad de Biotecnología Médica y Farmacéutica, Guadalajara, Jalisco, México; ¹²⁸⁷Albert Einstein College of Medicine, Radiation Oncology, Bronx, NY, USA; ¹²⁸⁸Vall d'Hebron research Institute-UAB/Neurodegenerative Diseases Group, Barcelona, Spain; ¹²⁸⁹University of São Paulo, Institute of Biomedical Sciences, Department of Anatomy, Laboratory of Functional Neuroanatomy of Pain, São Paulo, Brazil; ¹²⁹⁰Laboratory of Immunoendocrinology, Department of Clinical and Toxicological Analyses, University of São Paulo, São Paulo, Brazil; ¹²⁹¹Universidade Anhanguera de São Paulo, Programa de Pós-graduação Stricto sensu e Pesquisa, São Paulo, Brazil; ¹²⁹²INRA-AgroParisTech, Institut Jean-Pierre Bourgin, UMR1318, ERL CNRS 3559, Saclay Plant Sciences, Versailles, France; ¹²⁹³University of Minnesota, Department of Biochemistry, Molecular Biology and Biophysics and Department of Medicine, Minneapolis, MN, USA; ¹²⁹⁴Università degli Studi di Milano, Dipartimento di Scienze della Salute, Milano, Italy; ¹²⁹⁵Universidad Nacional Autónoma de México, Instituto de Fisiología Celular, División de Neurociencias, Departamento de Neuropatología Molecular, Mexico, DF, Mexico;
- 1575 ¹²⁹⁶University of Rome "Sapienza", Department of Experimental Medicine, Rome, Italy; ¹²⁹⁷Biodonostia Health Research Institute, group of Cellular Oncology; IKERBASQUE; CIBERfes, Spain; ¹²⁹⁸Kyoto Prefectural University of Medicine, Graduate School of Medical Science, Department of Cardiovascular Medicine, Kyoto, Japan; ¹²⁹⁹CHU Clermont-Ferrand, Chirurgie Gynécologique, Clermont-Ferrand, France; Université Clermont Auvergne, Institut Pascal, UMR6602, CNRS/UCR/SIGMA, Clermont-Ferrand, France; ¹³⁰⁰University of Chieti-Pescara, Department of Medical, Oral, and Biotechnological Science, Chieti, Italy; ¹³⁰¹University of California, Davis, Department of Dermatology, Sacramento, CA, USA;
- 1580 ¹³⁰²CONACYT - Centro de Investigación Biomédica de Oriente, Instituto Mexicano del Seguro Social, Puebla, Mexico; ¹³⁰³IRCCS "Casa Sollievo della Sofferenza", Opera di Padre Pio da Pietrelcina, Division of Internal Medicine and Chronobiology Unit, Department of Medical Sciences, San Giovanni Rotondo (FG), Italy; ¹³⁰⁴Sapienza University of Rome, Department of Biology and Biotechnology C. Darwin, Rome, Italy; ¹³⁰⁵Northwestern University Feinberg School of Medicine, Department of Neurology, Chicago, IL, USA; ¹³⁰⁶University of Texas Health Science Center at Houston, Center for Stem Cell and Regenerative Disease, Institute of Molecular Medicine (IMM), Houston, TX, USA; ¹³⁰⁷Cleveland Clinic, Lerner Research Institute, Department of Inflammation & Immunity, Cleveland, OH, USA; ¹³⁰⁸University of Arkansas for Medical Sciences, Fay W. Boozman College of Public Health, Department of Environmental and Occupational Health, Little Rock, AR, USA; ¹³⁰⁹University College Cork, Department of Cancer Research, Cork, Ireland; ¹³¹⁰Academic Decency, MeTooSTEM, Nashville, TN, USA; ¹³¹¹Mayo Clinic, Rochester, MN, USA; ¹³¹²University of Helsinki, Translational Stem Cell Biology & Metabolism Program, Research Programs Unit and Department of Anatomy, Faculty of Medicine, Helsinki, Finland; ¹³¹³PSL Research University, Equipe labellisée par la Ligue Contre le Cancer, Institut Curie, Inserm, U830, Stress and Cancer laboratory, Paris, France; ¹³¹⁴Telethon Institute of Genetics and Medicine (TIGEM), Pozzuoli, Naples, Italy; Medical Genetics Unit, Department of Medical and Translational Science, Federico II University, Naples, Italy; ¹³¹⁵Sprott Centre for Stem Cell Research, Ottawa Hospital Research Institute, and University of Ottawa, Department of Medicine, Ottawa, ON, Canada; ¹³¹⁶University of Szeged, Department of Medical Microbiology and Immunobiology, Szeged, Hungary; ¹³¹⁷Université Paris Descartes-Sorbonne Paris Cité, Institut Necker Enfants-Malades (INEM), INSERM U1151-CNRS UMR 8253, Paris, France; ¹³¹⁸University of Arkansas for Medical Sciences and Central Arkansas Veterans Healthcare System, Little Rock, AR, USA; ¹³¹⁹University of Amsterdam, Medical Biochemistry, Amsterdam UMC, Amsterdam, The Netherlands; ¹³²⁰Leiden University, Institute of Biology Leiden, Leiden, The Netherlands; ¹³²¹UIT The Arctic University of Norway, Department of Pharmacy, Pharmacology Research Group, Tromsø, Norway; ¹³²²The City University of New York, Queens College, The Graduate Center of the City University of New York, Department of Biology, Flushing, NY, USA; ¹³²³Childrens Hospital, Hannover Medical School, Hannover, Germany; ¹³²⁴Northwestern University, Feinberg School of Medicine, Department of Neurology, Chicago, IL, USA;
- 1600 ¹³²⁵Anhui Province Key Laboratory of Medical Physics and Technology, Center of Medical Physics and Technology, Hefei Institutes of Physical Science, Chinese Academy of Sciences, Hefei, Anhui, China; University of Science and Technology of China, Anhui, China; ¹³²⁶Laboratory of Cell Biology, Oswaldo Cruz Institute, Oswaldo Cruz Foundation, Rio de Janeiro, Brazil; ¹³²⁷Indian Institute of Technology Delhi, Kusuma School of Biological Sciences, New Delhi, India; ¹³²⁸University of Cincinnati, Division of Hematology/Oncology, Cincinnati, OH, USA; ¹³²⁹University of Pretoria, School of Medicine, Faculty of Health Sciences, Department of Physiology, Pretoria, South Africa; ¹³³⁰Institut Curie, CMIB laboratory, Université Paris-Saclay, CNRS, Inserm, Orsay, France; ¹³³¹University of Turin, Department of Veterinary Sciences, Grugliasco (TO), Italy; ¹³³²University of New Mexico, Clinical and Translational Sciences Center, Albuquerque, NM, USA; ¹³³³Carité-Universitätsmedizin Berlin, Campus Mitte, Institut für Integrative Neuroanatomie, Berlin, Germany; ¹³³⁴Ruprecht-Karls University of Heidelberg, Women's Hospital, Department of Gynecological Endocrinology and Fertility Disorders, Heidelberg, Germany; ¹³³⁵Institut Jean-Pierre Bourgin, INRA, AgroParisTech, CNRS, Université Paris-Saclay, Versailles, France; ¹³³⁶University of Duisburg-Essen, Centre for Medical Biotechnology, Faculty of Biology, Essen, Germany; ¹³³⁷Tianjin Medical University, Department of Immunology, School of Basic Medical Sciences, Tianjin, China; ¹³³⁸INSERM Institute of Metabolic and Cardiovascular Diseases (I2MC), Université de Toulouse, Toulouse, France; ¹³³⁹Shandong University, School of Life Science, Shandong Provincial Key Laboratory of Animal Cells and Developmental Biology, Qingdao, China; ¹³⁴⁰Hirosaki University Graduate School of Medicine, Institute of Brain Science, Department of Neuropathology, Hirosaki, Japan; UCL Queen Square Institute of Neurology, Queen Square Brain Bank for Neurological Disorders, London, UK; ¹³⁴¹University Vita-Salute San Raffaele, Age Related Diseases Laboratory, Milan, Italy; ¹³⁴²National Medicines Institute, Department of Drug Biotechnology and Bioinformatics, Warszawa, Poland; ¹³⁴³University of Washington School of Medicine, Department of Biochemistry, Seattle, WA, USA; ¹³⁴⁴University of Washington, Departments of Medicine, Microbiology and Genome Sciences, Seattle, WA, USA; ¹³⁴⁵Sage Therapeutics, Cambridge, MA, USA; ¹³⁴⁶University of Texas MD Anderson Cancer Center, Department of Cancer Systems Imaging, Houston, TX, USA; ¹³⁴⁷European Neuroscience Institute (ENI) - A Joint Initiative of the University Medical Center Göttingen and the Max Planck Society, Göttingen, Germany; ¹³⁴⁸Swedish University of Agricultural Sciences and Linnean Center for Plant Biology, Department of Molecular Sciences, Uppsala BioCenter, Uppsala, Sweden; Heidelberg University, Center for Organismal Studies, Neuenheimer Feld, Heidelberg, Germany; ¹³⁴⁹Kashan University of Medical Sciences, Research Center for Biochemistry and Nutrition in Metabolic Disease, Kashan, Iran; ¹³⁵⁰Tehran University of Medical Sciences, School of Medicine, Department of Medical Immunology, Tehran, Iran; ¹³⁵¹Macquarie University, Faculty of Medicine and Health Sciences, Sydney, NSW, Australia;

- ¹³⁵² Indian Institute of Technology Jodhpur, Cellular and Molecular Neurobiology Unit, Jodhpur, Rajasthan, India; ¹³⁵³Amrita Vishwa Vidyapeetham, School of Biotechnology, Kollam, Kerala, India; ¹³⁵⁴University of Nebraska Medical Center, Department of Cellular and Integrative Physiology, Omaha, NE, USA; ¹³⁵⁵CSIR-Central Drug Research Institute, Lucknow, India; ¹³⁵⁶Université Toulouse III, Toulouse, France; ¹³⁵⁷Sapporo Medical University, Department of Cardiovascular, Renal and Metabolic Medicine, Sapporo, Japan; ¹³⁵⁸University of Colorado Denver, Department of Medicine, Aurora, CO, USA; ¹³⁵⁹Health Sciences University of Hokkaido, College of Rehabilitation Sciences, Department of Physical Therapy, Ishikari-Tobetsu, Hokkaido, Japan; ¹³⁶⁰Nagasaki University Graduate School of Biomedical Sciences, Department of Infectious Diseases, Nagasaki, Japan; ¹³⁶¹Tokyo Medical University, Department of Biochemistry, Tokyo, Japan; ¹³⁶²University of California San Diego, Department of Pharmacology, La Jolla, CA, US; ¹³⁶³The University of Tokyo, Department of Biochemistry and Molecular Biology, Graduate School of Medicine, Tokyo, Japan; ¹³⁶⁴Aarhus University, Department of Biomedicine, Aarhus, Denmark; ¹³⁶⁵Kerman University of Medical Sciences, Institute of Neuropharmacology, Pharmaceutics Research Center, Kerman, Iran; ¹³⁶⁶MVR Cancer Hospital and Research Institute, Molecular Oncology, Cancer Genomics/Proteomics, Kerala, India; ¹³⁶⁷EHIME UNIVERSITY, DEPARTMENT OF AQUATIC LIFE SCIENCES, AINAN, EHIME, JAPAN; ¹³⁶⁸University of Kaiserslautern, Department of Biology, Plant Physiology, Kaiserslautern, Germany; ¹³⁶⁹International Centre for Genetic Engineering and Biotechnology, New Delhi, India; ¹³⁷⁰Institute of Biomedical Research of Barcelona, Spanish Research Council, Barcelona, Spain; ¹³⁷¹Washington University in St. Louis, Professor of Obstetrics and Gynecology, St. Louis, MO, USA; ¹³⁷²Università della Svizzera italiana (USI), Faculty of Biomedical Sciences, Institute for Research in Biomedicine, Bellinzona, Switzerland; School of Life Sciences, École Polytechnique Fédérale de Lausanne, Lausanne, Switzerland; ¹³⁷³University "Magna Graecia" of Catanzaro, Department of Health Sciences, Catanzaro, Italy; ¹³⁷⁴Aarhus University Hospital, Steno Diabetes Center Aarhus, Aarhus, Denmark; Aarhus University, Department of Clinical Medicine, Research Laboratory for Biochemical Pathology, Aarhus, Denmark; ¹³⁷⁵Université de Lyon, ENSL, UCBL, CNRS, LBMC, UMS 3444 Biosciences Lyon Gerland, Lyon, France; ¹³⁷⁶Centro de Investigaciones Biológicas, Consejo Superior de Investigaciones Científicas, Department of Molecular Biomedicine, Laboratory of Cell Death and Cancer Therapy, Madrid, Spain; ¹³⁷⁷Bispebjerg Hospital, Institute of Sports Medicine Copenhagen, Copenhagen, Denmark; ¹³⁷⁸Unicamillus, Saint Camillus International University of Health Sciences, Rome, Italy; ¹³⁷⁹University of Maryland School of Medicine, Center for Biomedical Engineering and Technology, Baltimore, MD, USA; ¹³⁸⁰Università degli Studi di Sassari, Dipartimento di Scienze Biomediche, Sassari, Italy; ¹³⁸¹University of the Basque Country (UPV/EHU), Department of Biochemistry and Molecular Biology, Leioa, Spain; ¹³⁸²Centro di Riferimento Oncologico di Aviano (CRO), IRCCS, Immunopathology and Cancer Biomarkers, Aviano, Italy; ¹³⁸³University of Exeter Medical School, European Centre for Environment & Human Health (ECEHH), Knowledge Spa, Royal Cornwall Hospital, Truro, Cornwall, UK; Plymouth Marine Laboratory (PML), Plymouth, UK; University of Plymouth, School of Biological & Marine Sciences, Plymouth, UK; ¹³⁸⁴National Institute of Genetic Engineering and Biotechnology, Institute of Medical Biotechnology, Molecular Medicine Department, Tehran, Iran; ¹³⁸⁵University of Pittsburgh, Department of Medicine, Aging Institute, Pittsburgh, PA, USA; ¹³⁸⁶Fondazione IRCCS Istituto Neurologico Carlo Besta, Neuromuscular Diseases and Neuroimmunology Unit, Milano, Italy; ¹³⁸⁷University of Coimbra, Institute of Physiology, Faculty of Medicine, Coimbra, Portugal and CNC - Center for Neuroscience and Cell Biology, Coimbra, Portugal; ¹³⁸⁸University Roma Tre, Department of Science, Rome, Italy; ¹³⁸⁹National Autonomous University of Mexico (UINAM), Department of Neurodevelopment and Physiology, Institute of Cellular Physiology, Mexico City, Mexico; ¹³⁹⁰Sapienza University of Rome, Department of Anatomy, Histology, Forensic Medicine & Orthopedics, Histology & Medical Embryology Section, Rome, Italy; ¹³⁹¹Ifremer, SG2M-LGPM, Laboratoire de Génétique et Pathologie des Mollusques Marins, La Tremblade, France; ¹³⁹²Swansea University Medical School, Molecular Neurobiology group, Swansea, United Kingdom; ¹³⁹³Normandie University, UNIROUEN, INSERM U1239, DC2N, Rouen, France; ¹³⁹⁴Institute for Research and Innovation in Biomedicine (IRIB), Rouen, France; ¹³⁹⁵Juntendo University Graduate School of Medicine, Department of Physiology, Tokyo, Japan; ¹³⁹⁶University of British Columbia, Department of Ophthalmology and Visual Sciences, Vancouver, British Columbia, Canada; ¹³⁹⁷Kindai University, Pharmaceutical Research and Technology Institute, Higashi-Osaka, Osaka, Japan; ¹³⁹⁸Saitama University, Department of Regulatory Biology, Saitama, Japan; ¹³⁹⁹Pontificia Universidad Católica de Chile, Faculty of Biological Sciences, Department of Physiology, Santiago de Chile, Chile; ¹⁴⁰⁰University of Texas Health Science Center at Houston, Department of Neurology, Houston, TX, USA; ¹⁴⁰¹Weill Cornell Medicine, Rockefeller University Campus, Department of Pathology and Laboratory Medicine, New York, NY, USA; ¹⁴⁰²London School of Hygiene & Tropical Medicine, Department of Infection Biology, London, UK; ¹⁴⁰³Max Planck Institute for the Biology of Ageing, Cologne, Germany; ¹⁴⁰⁴Federal University of Ceara, Drug Research and Development Center, Fortaleza, CE, Brazil; ¹⁴⁰⁵Texas Tech University, Department of Nutritional Sciences & Obesity Research Institute, Lubbock, TX, USA; ¹⁴⁰⁶University of Münster, Institute of Medical Microbiology, Münster, Germany; ¹⁴⁰⁷Indian Council of Medical Research - National AIDS Research Institute, Division of Molecular Virology, Pune, MH, India; ¹⁴⁰⁸New York University Medical School, Laura and Isaac Perlmutter Cancer Center, Department of Radiation Oncology, New York, NY, USA; ¹⁴⁰⁹University of Colorado Denver, Children's Hospital Colorado, Morgan Adams Foundation Pediatric Brain Tumor Research Program, Aurora, CO; ¹⁴¹⁰Departamento de Biología Celular e Histología, Facultad de Biología, Universidad de Murcia, Instituto Murciano de Investigación Biosanitaria (IMIB)-Arrixaca, Murcia, Spain; ¹⁴¹¹CNRS Biotechnology and cell signaling, Ecole Supérieure de Biotechnologie de Strasbourg, Strasbourg University/Laboratory of excellence Medalis; University of Strasbourg Institute for Advanced Study, Strasbourg, France; ¹⁴¹²Barkatullah University, Department of Biochemistry & Genetics, Bhopal, India; ¹⁴¹³ICREA, Pompeu Fabra University (UPF), Department of Experimental and Health Sciences, Ciberned, Barcelona, Spain; ¹⁴¹⁴Spanish National Cardiovascular Research Center (CNIC), Madrid, Spain; ¹⁴¹⁵Hospital Nacional de Paraplejicos (SESCAM), UDI-HNP, Laboratory of Molecular Neuroprotection, Toledo, Spain; ¹⁴¹⁶University of Zürich, Institute of Experimental Immunology, Viral Immunobiology, Zürich, Switzerland; ¹⁴¹⁷Old Dominion University, Frank Reidy Research Center for Bioelectrics, Norfolk, VA, USA; ¹⁴¹⁸Royal College of Surgeons in Ireland, Department of Physiology & Medical Physics, Dublin 2, Ireland; ¹⁴¹⁹University of Prince Edward Island, Charlottetown, Prince Edward Island, Canada; ¹⁴²⁰Genentech, Inc. Department of Cancer Immunology, South San Francisco, CA, USA; ¹⁴²¹University of Helsinki, Faculty of Pharmacy, Division of Pharmacology and Pharmacotherapy/Drug Research Program, Helsinki, Finland; ¹⁴²²Washington University School of Medicine, Department of Obstetrics and Gynecology, and Department of Pathology and Immunology, St. Louis, MO, USA; ¹⁴²³University of Rzeszow, Department of Animal Physiology and Reproduction, Rzeszow, Poland; ¹⁴²⁴Applied Biotechnology Research Center, Baqiyatallah University of Medical Sciences, Tehran, P.O. Box 19395-5487, Iran; ¹⁴²⁵University of Camerino, School of Pharmacy, Camerino, MC, Italy; ¹⁴²⁶Cornell University, Department of Entomology, Ithaca, NY, USA; ¹⁴²⁷Rutgers-New Jersey Medical School, Department of Cell Biology and Molecular Medicine, Newark, NJ, USA; ¹⁴²⁸University Hospital of Lausanne, Central Laboratory of Hematology, Lausanne, Switzerland; ¹⁴²⁹Kyoto University, Department of Microbiology, Graduate School of Medicine, Kyoto, Japan; ¹⁴³⁰Gladstone Institute of Neurological Disease and University of California, San Francisco, Department of Neurology, San Francisco, CA, USA; ¹⁴³¹Tokyo Institute of Technology, School of Life Science and Technology, Yokohama, Japan; ¹⁴³²University of Nebraska Medical Center, Department of Cellular and Integrative Physiology, Omaha, NE, USA; ¹⁴³³University of South Florida, Department of Cell Biology, Microbiology, and Molecular Biology, Tampa, FL, USA; ¹⁴³⁴"Sapienza" University of Rome, Department of Clinical and Molecular Medicine, Laboratory affiliated to Istituto Pasteur Italia Fondazione Cenci Bolognetti, Rome, Italy; ¹⁴³⁵University of Cambridge, Cancer Research UK Cambridge Institute, Cambridge, UK; ¹⁴³⁶Ben-Gurion University of the Negev, Faculty of Health Sciences, Department of

Clinical Biochemistry and Pharmacology, and Soroka University Medical Center, Beer Sheva, Israel; ElaPharma, Ltd, Tel Aviv, Israel; ¹⁴³⁴Niigata University, Brain Research Institute, Department of Neurosurgery, Niigata, Japan; ¹⁴³⁵Nelson Mandela University, Department of Biochemistry and Microbiology, Port Elizabeth, South Africa; ¹⁴³⁶Leibniz Institute of Plant Biochemistry, Department of Molecular Sensing, Halle, Germany; ¹⁴³⁷Ecole Polytechnique Fédérale de Lausanne (EPFL), Institute of Bioengineering (IBI) and Swiss Institute for Experimental Cancer Research (ISREC), Laboratory of Regenerative Hematopoiesis, Lausanne, Switzerland; Centre Hospitalier Universitaire Vaudois (CHUV), Departments of Oncology and Laboratory Medicine, Hematology Service, Lausanne, Switzerland; ¹⁴³⁸University of Arizona, Department of Medicine, Tucson, AZ, USA; ¹⁴³⁹Georgia State University, Department of Biology, Atlanta, GA, USA; ¹⁴⁴⁰IRCCS Bambino Gesù Children's Hospital, Department of Pediatric Hemato-Oncology and Cell and Gene Therapy, Rome, Italy; ¹⁴⁴¹University of Ferrara, Department of Morphology, Surgery and Experimental Medicine, Ferrara, Italy; ¹⁴⁴²Radboud University Medical Center, Department of Internal Medicine, Nijmegen, The Netherlands; ¹⁴⁴³Karolinska Institutet, Department of Physiology and Pharmacology, Stockholm, Sweden; Karolinska University Hospital, Karolinska Institutet and Pediatric Endocrinology Unit, Department of Women's and Children's Health, Stockholm, Sweden; ¹⁴⁴⁴University of Minnesota, Department of Genetics, Cell Biology and Development, Minneapolis, MN, USA; ¹⁴⁴⁵Maastricht University Medical Center, CARIM School for Cardiovascular Diseases, Department of Pathology, Maastricht, The Netherlands; ¹⁴⁴⁶University Hospital Basel, Department of Biomedicine, Ocular Pharmacology and Physiology, Basel, Switzerland; ¹⁴⁴⁷University of Warwick, School of Life Sciences, Coventry, UK; ¹⁴⁴⁸King's College London GKT School of Medical Education, London, UK; ¹⁴⁴⁹The Chinese University of Hong Kong, School of Biomedical Sciences, Hong Kong, China; ¹⁴⁵⁰University of Clermont Auvergne, M2iSH (Microbes, Intestine, Inflammation and Susceptibility of the Host), UMR 1071 Inserm, INRA USC 2018, CRNH, Clermont-Ferrand, France; ¹⁴⁵¹The University of Sydney, Kolling Institute, Renal Medicine, Sydney, New South Wales, Australia; ¹⁴⁵²University of Kansas Medical Center, Department of Pharmacology, Toxicology and Therapeutics, Kansas City, KS, USA; ¹⁴⁵³Army Medical University (Third Military Medical University), Daping Hospital, Center of Bone Metabolism and Repair, State Key Laboratory of Trauma, Burns and Combined Injury, Trauma Center, Research Institute of Surgery, Laboratory for the Prevention and Rehabilitation of Military Training Related Injuries, Chongqing, China; ¹⁴⁵⁴Trinity College Dublin, Department of Clinical Medicine, Trinity Centre for Health Sciences, Dublin, Ireland; ¹⁴⁵⁵University of Ferrara, Department of Pharmaceutical Sciences, Ferrara, Italy; ¹⁴⁵⁶National Hospital for Paraplegics (SESCAM), Research Unit, Molecular Neuroprotection Group, Toledo, Spain; ¹⁴⁵⁷Karolinska Institutet, Department of Neurobiology, Care Sciences and Society, Division of Neurogeriatrics, Solna, Stockholm, Sweden; ¹⁴⁵⁸East Tennessee State University, Quillen College of Medicine, Center of Excellence for Inflammation, Infectious Diseases, and Immunity, Department of Medicine, Johnson City, TN, USA; ¹⁴⁵⁹ICMR-Vector Control Research Center, Unit of Microbiology and Molecular Biology, Puducherry, India; ¹⁴⁶⁰University of Kansas School of Medicine, Department of Anatomy and Cell Biology, Kansas City, KS, USA; ¹⁴⁶¹New York University School of Medicine, Departments of Psychiatry and Cell Biology, and the Nathan Kline Institute, Orangeburg, NY, USA; ¹⁴⁶²Santa Lucia Foundation IRCCS, Rome, Italy; ¹⁴⁶³Universidade do Algarve, Campus de Gambelas, Department of Biomedical Sciences and Medicine & Centre for Biomedical Research, Faro, Portugal; ¹⁴⁶⁴Osaka University, Graduate School of Dentistry, Osaka, Japan; ¹⁴⁶⁵Duke University, Department of Biology and Howard Hughes Medical Institute, Durham, NC, USA; ¹⁴⁶⁶University of Split, School of Medicine, Split, Croatia; ¹⁴⁶⁷Doshisha University Graduate School of Brain Science, Laboratory of Structural Neuropathology, Kyoto, Japan; ¹⁴⁶⁸Center for Molecular Biology of Heidelberg University (ZMBH) and German Cancer Research Center (DKFZ), DKFZ-ZMBH Alliance, Heidelberg, Germany; ¹⁴⁶⁹Danish Cancer Society Research Center, Unit for Cell Death and Metabolism, Center for Autophagy, Recycling and Disease, Copenhagen, Denmark; University of Copenhagen, Department of Cellular and Molecular Medicine, Faculty of Health Sciences, Copenhagen N, Denmark; ¹⁴⁷⁰University of Virginia, Department of Biology, Charlottesville, VA, USA; ¹⁴⁷¹Trinity College Dublin, Trinity Translational Medicine Institute, Dublin, Ireland; ¹⁴⁷²David Geffen School of Medicine at UCLA, Department of Microbiology, Immunology, and Molecular Genetics, Los Angeles, CA, USA; ¹⁴⁷³Arizona State University, School of Life Sciences, Tempe, AZ, USA; ¹⁴⁷⁴Hopp Children's Cancer Center at NCT Heidelberg (KITZ), Preclinical Program, Heidelberg, Germany; German Cancer Research Center (DKFZ), and German Cancer Consortium (DKTK), Clinical Cooperation Unit Pediatric Oncology, Im Neuenheimer Feld, Heidelberg, Germany; ¹⁴⁷⁵National Institute of Infectious Diseases, Department of Bacteriology I, Toyama, Tokyo, Japan; ¹⁴⁷⁶University of Iceland, Faculty of Medicine, Biomedical center, Reykjavik, Iceland; ¹⁴⁷⁷Hollings Cancer Center, Department of Biochemistry and Molecular Biology, Charleston, SC, USA; ¹⁴⁷⁸Université de Paris, Centre de recherche sur l'inflammation, Team Gut Inflammation, Inserm, U1149, CNRS, ERL8252, Paris, France; ¹⁴⁷⁹Ewha Womans University, Department of Life Science, Immune and Vascular Cell Network Research Center, National Creative Initiatives, Seoul, Korea; ¹⁴⁸⁰Chosun University, School of Medicine, Gwangju, Korea; ¹⁴⁸¹Yonsei University, Wonju, Korea; ¹⁴⁸²Yamaguchi University, Joint Faculty of Veterinary Medicine, Laboratory of Veterinary Pharmacology, Yoshida, Yamaguchi, Japan; ¹⁴⁸³MRC Laboratory of Molecular Biology, Cambridge, UK; ¹⁴⁸⁴Hyogo College of Medicine, Department of Genetics, Hyogo, Japan; ¹⁴⁸⁵Stanford University, School of Medicine, Department of Pathology, CA, USA; ¹⁴⁸⁶Osaka University, Laboratory of Mitochondrial Dynamics, Graduate School of Frontier Biosciences, Osaka, Japan; ¹⁴⁸⁷Tokyo Medical and Dental University, Tokyo, Japan; ¹⁴⁸⁸Kyoto University of Advanced Science, Faculty of Bioenvironmental Science, Kameoka, Kyoto, Japan; ¹⁴⁸⁹University of Porto, REQUIMTE/LAQV, Faculty of Pharmacy, Porto, Portugal; ¹⁴⁹⁰Amgen Inc., South San Francisco, CA, USA; ¹⁴⁹¹University of California, Berkeley, Department of Nutritional Sciences and Toxicology, Berkeley, CA, USA; Chan Zuckerberg Biohub, San Francisco, CA, USA; ¹⁴⁹²Rutgers University, Center for Advanced Biotechnology and Medicine, Piscataway, NJ, USA; ¹⁴⁹³The Chinese University of Hong Kong, Lui Che Woo Institute of Innovative Medicine, Centre for Cardiovascular Genomics and Medicine (CCGM), Shatin, Hong Kong, China; The Chinese University of Hong Kong, Faculty of Medicine, Department of Medicine & Therapeutics, Shatin, Hong Kong, China; Xiamen University, Cardiovascular Hospital, Institute for Translational Medicine, Xiamen, China; ¹⁴⁹⁴The University of Illinois at Chicago College of Medicine, Department of Pharmacology, Chicago, IL, USA; ¹⁴⁹⁵Pontificia Universidad Católica de Chile, Escuela de Medicina and Centro Interdisciplinario de Neurociencias, Facultad de Medicina, Departamento de Neurología, Santiago, Chile; ¹⁴⁹⁶University Miguel Hernandez, Institute of Research, Development, and Innovation in Healthcare Biotechnology of Elche, Elche, Alicante, Spain; ¹⁴⁹⁷University of Pennsylvania Perelman School of Medicine and Division of Neurology, The Children's Hospital of Philadelphia, Department of Neurology, Philadelphia, PA, USA; ¹⁴⁹⁸Goethe University, Institute for Molecular Biosciences, Frankfurt/Main, Germany; ¹⁴⁹⁹Tokyo Medical and Dental University (TMDU), Medical Hospital, Department of Gastroenterology and Hepatology, Bunkyo-ku, Tokyo, Japan; ¹⁵⁰⁰Suez Canal University, Faculty of Veterinary Medicine, Ismailia, Egypt; ¹⁵⁰¹University of Wisconsin-Madison, Laboratory of Cell and Molecular Biology and Departments of Botany and Genetics, WI, USA; ¹⁵⁰²King's College London, School of Cardiovascular Medicine and Sciences, London, UK; ¹⁵⁰³German Institute of Human Nutrition Potsdam-Rehbruecke, Department of Molecular Toxicology, Nuthetal, Germany; ¹⁵⁰⁴Institute of Molecular Bioimaging and Physiology (IBFM), CNR, Milan, Italy; ¹⁵⁰⁵University of Southern California, Keck School of Medicine, Department of Molecular Microbiology and Immunology, Los Angeles, CA, USA; ¹⁵⁰⁶University Medical Center Göttingen, Center for Biostructural Imaging of Neurodegeneration, Department of Experimental Neurodegeneration, Göttingen, Germany; Max Planck Institute for Experimental Medicine, Göttingen, Germany; Newcastle University, The Medical School, Institute of Neuroscience, Newcastle upon Tyne, UK; ¹⁵⁰⁷Oslo University Hospital and University of Oslo, Department of Pathology, Tumor Immunology Lab, Oslo, Norway; ¹⁵⁰⁸Istanbul University, Cerrahpasa Faculty of Medicine, Medical Biology Department,

Cerrahpasa, Istanbul, Turkey; ¹⁵⁰⁹University Côte d Azur, Institute for research on cancer and aging of Nice CNRS UMR 7284/INSERM U 1081, Nice, France; Centre Scientifique de Monaco, Biomedical Department, Monaco Principality ; ¹⁵¹⁰Texas Biomedical Research Institute, Host-Pathogen Interactions Program, San Antonio, TX, USA; ¹⁵¹¹Columbia University, Department of Medicine, New York, NY, USA; ¹⁵¹²Baylor College of Medicine, Department of Molecular and Human Genetics, Houston, TX, USA; ¹⁵¹³Université de Paris, Centre de Recherche des Cordeliers, Paris, France; ¹⁵¹⁴IRCCS San Raffaele Scientific Institute, Division of Neuroscience, Milan, Italy; ¹⁵¹⁵University of São Paulo, Department of Parasitology, São Paulo, Brazil; ¹⁵¹⁶University of Rome Tor Vergata, Department of Clinical Sciences and Translational Medicine, Rome, Italy; ¹⁵¹⁷Goethe University Frankfurt, Buchmann Institute for Molecular Life Sciences (BMLS), Frankfurt am Main, Germany; ¹⁵¹⁸Shanghai Institute of Organic Chemistry, Chinese Academy of Sciences, Shanghai, China; ¹⁵¹⁹Affiliated Hospital of Guangdong Medical University, Key Laboratory of Prevention and Management of Chronic Kidney Disease of Zhanjiang City, Zhanjiang, Guangdong, China; ¹⁵²⁰Beth Israel Deaconess Medical Center, Harvard Medical School, Boston, MA, USA; ¹⁵²¹National Center of Biomedical Analysis, Beijing, China; ¹⁵²²Institut Necker Enfants Malades (INEM), INSERM U1151/CNRS UMR 8253, Paris, France; ¹⁵²³The Children's Hospital of Philadelphia, Center for Applied Genomics, Philadelphia, PA, USA; ¹⁵²⁴University of Pittsburgh Medical Center, Department of Pediatrics, Pittsburgh, PA, USA; ¹⁵²⁵University of Alberta, Department of Biochemistry, Edmonton, Canada; ¹⁵²⁶University of Salento, Department of Biological and Environmental Sciences and Technologies (Di.S.Te.B.A.), Lecce, Italy; ¹⁵²⁷Universidad de Buenos Aires. facultad de farmacia y Bioquímica. Departamento de Microbiología, Inmunología y Biotecnología, cátedra de inmunología, Buenos Aires, Argentina. Universidad de Buenos Aires, CONICET, Instituto de Estudios de la Inmunidad Humoral (IDEHU), Buenos Aires, Argentina; ¹⁵²⁸Danish Cancer Society Research Center, Computational Biology Laboratory, Copenhagen, Denmark; ¹⁵²⁹Max Perutz Labs, University of Vienna, Vienna Biocenter (VBC), Vienna, Austria; ¹⁵³⁰Quadram Institute Bioscience, Department of Gut, Microbes and Health, Norwich, UK; ¹⁵³¹Dong-A University Medical School, Department of Molecular Neuroscience, Busan, Korea; ¹⁵³²Medical College of Wisconsin, Department of Biochemistry, Milwaukee, WI, USA; ¹⁵³³Incheon National University, Division of Life Sciences, College of Life Sciences and Bioengineering, Incheon, Korea; ¹⁵³⁴Yonsei University, Division of Biological Science and Technology, Wonju, Korea; ¹⁵³⁵Chonnam National University, The Future Life & Society Research Center, Gwangju, Korea; ¹⁵³⁶Chonbuk National University, Department of Veterinary Medicine, Iksan, Korea; ¹⁵³⁷Ben Gurion University of the Negev, Department of Chemistry, Be'er Sheva, Israel; ¹⁵³⁸KU Leuven, Department of Cellular and Molecular Medicine & Leuven Kanker Instituut, Leuven, Belgium; ¹⁵³⁹Sanofi, Vitry Sur Seine, France; ¹⁵⁴⁰Mayo Clinic, Department of Physiology and Biomedical Engineering, Rochester, MN, USA; ¹⁵⁴¹Baylor College of Medicine, Department of Human and Molecular Genetics, Houston, TX, USA/ Telethon Institute of Genetics and Medicine (TIGEM), Pozzuoli (NA), Italy; ¹⁵⁴²VA San Diego Healthcare Systems and University of California, San Diego, Department of Anesthesiology, La Jolla, CA, USA; ¹⁵⁴³Internal Medicine 1, Brandenburg Hospital, Faculty of Health Sciences, Joint Faculty of the Brandenburg University of Technology Cottbus Senftenberg, the Brandenburg Medical School Theodor Fontane and the University of Potsdam, Brandenburg, Germany; ¹⁵⁴⁴IRCM, Institut de Recherche en Cancérologie de Montpellier, INSERM U1194, Université de Montpellier, Institut régional du Cancer de Montpellier, Montpellier, France; ¹⁵⁴⁵Universidad Nacional Autónoma de México, Instituto de Biotecnología, Departamento de Medicina Molecular y Bioprocesos, Laboratorio de Neuroinmunobiología, Cuernavaca, Morelos, México; ¹⁵⁴⁶National Autonomous University of Mexico, Faculty of Chemistry, Department of Biology, Mexico city, Mexico; ¹⁵⁴⁷Universidad de Chile, School of Medicine, Instituto de Ciencias Biomédicas, Santiago de Chile, Chile; ¹⁵⁴⁸The Fourth Military Medical University, National Key Discipline of Cell Biology, Department of Physiology and Pathophysiology, Xi'an, Shaanxi, China; ¹⁵⁴⁹Weizmann Institute of Science, Department of Plant and Environmental Sciences, Rehovot, Israel; ¹⁵⁵⁰University of Buenos Aires, School of Sciences, Department of Chemical Biology, C.A. Buenos Aires, Argentina; ¹⁵⁵¹Centro de Investigaciones CSIC, Department of Cellular and Molecular Biology, Madrid, Spain; ¹⁵⁵²Sun Yat-Sen University, Sun Yat-sen Memorial Hospital, Department of Neurology, Guangzhou City, Guangdong, China; ¹⁵⁵³Fondazione G. Pascale, Istituto Nazionale Tumori IRCCS, Cell Biology and Biotherapy Unit, Naples, Italy; ¹⁵⁵⁴University of Coimbra, Rua Larga, Faculty of Medicine, Center for Neuroscience and Cell Biology (CNC), Coimbra, Portugal; University of Coimbra, Rua Larga, Faculty of Medicine, bCIBB-Center for Innovative Biomedicine and Biotechnology, Coimbra, Portugal; ¹⁵⁵⁵São Paulo State University, College of Agronomy Sciences, Department of Bioprocesses and Biotechnology, Center for Evaluation of Environmental Impact on Human Health (TOXICAM), Botucatu, SP, Brazil; ¹⁵⁵⁶University of Coimbra, CNC - Center for Neuroscience and Cell Biology, Coimbra & Faculty of Pharmacy, Coimbra, Portugal; ¹⁵⁵⁷Florey Institute of Neuroscience and Mental Health, University of Melbourne, Melbourne, VIC, Australia; ¹⁵⁵⁸Max Planck Institute for Biophysical Chemistry, Department of Neurobiology, Göttingen, Germany; ¹⁵⁵⁹University of Nebraska Medical Center, Department of Pharmacology and Experimental Neuroscience, Omaha, NE, USA; ¹⁵⁶⁰State University of New York, Upstate Medical University, Departments of Medicine, Microbiology and Immunology, Biochemistry and Molecular Biology, Syracuse, NY, USA; ¹⁵⁶¹Università degli Studi di Milano, Department of Biomedical and Clinical Sciences "L. Sacco", Milan, Italy; ¹⁵⁶²University of Calabria, Department of Biology, Ecology and Earth Sciences, Centre for Microscopy and Microanalysis (CM2), Rende (CS), Calabria, Italy; ¹⁵⁶³Baruch S. Blumberg Institute, Pennsylvania Cancer and Regenerative Medicine Research Center, Wynnewood, PA, USA; Xavier University School of Medicine, Woodbury, NY, USA; ¹⁵⁶⁴University of Copenhagen, Department of Biology, Copenhagen, Denmark; ¹⁵⁶⁵National Jewish Health and the University of Colorado, Denver, CO, USA; ¹⁵⁶⁶University of Oslo, Oslo University Hospital and Institute for Clinical Medicine, Department of Ophthalmology, Center for Eye Research, Oslo, Norway; ¹⁵⁶⁷Martin-Luther University, Institute of Physiological Chemistry, Halle (Saale), Germany; ¹⁵⁶⁸Ulm University, Institute of Biochemistry and Molecular Biology, Faculty of Medicine, Ulm, Germany; ¹⁵⁶⁹University of Cologne, Center for Biochemistry, Cologne, Germany; ¹⁵⁷⁰Washington University, Division of Infectious Diseases, Department of Medicine and Molecular Microbiology, St. Louis, MO, USA; ¹⁵⁷¹Third Military Medical University, Department of Occupational Health, Chongqing, China; ¹⁵⁷²Virginia Polytechnic Institute and State University, School of Neuroscience, Blacksburg, VA, USA; ¹⁵⁷³University of Naples Federico II, Department of Molecular Medicine and Medical Biotechnology, Naples, Italy; ¹⁵⁷⁴Aix Marseille Université, CNRS, INSERM, CIML, Marseille, France; University of Aveiro, Institute for Research in Biomedicine (iBiMED) and Ilidio Pinho Foundation, Department of Medical Sciences, Aveiro, Portugal; ¹⁵⁷⁵Université Côte d Azur, Université Nice Sophia Antipolis, CEA/DRF/BIAM, Faculté de Médecine, UMR E-4320 TIRO-MATOs, Nice, France ; ¹⁵⁷⁶Karolinska Institutet, Department of Biosciences and Nutrition, SHuddinge, Sweden; ¹⁵⁷⁷Federico II University, Department of Translational Medical Sciences, Naples, Italy; ¹⁵⁷⁸Consejo Superior de Investigaciones Científicas (CSIC), Instituto de Biología Molecular y Celular del Cáncer (IBMCC), Centro de Investigación del Cáncer (CSIC-Universidad de Salamanca), Universidad de Salamanca, Campus Unamuno, Salamanca, Spain; ¹⁵⁷⁹Oswaldo Cruz Foundation, Oswaldo Cruz Institute, Leprosy Laboratory, Rio de Janeiro, Brazil; ¹⁵⁸⁰Tel Aviv University, School of Neurobiology, Biochemistry and Biophysics, Tel Aviv, Israel; ¹⁵⁸¹University of Ferrara, Department of Morphology, Surgery and Experimental Medicine, Ferrara, Italy; ¹⁵⁸²The University of Texas MD Anderson Cancer Center, Department of Leukemia, Houston, TX, USA; ¹⁵⁸³University of Padua, Department of Biomedical Sciences, Padua, Italy; Italian National Research Council (CNR), Neuroscience Institute, Padua, Italy; ¹⁵⁸⁴Radboud University Medical Center, Nijmegen, The Netherlands; ¹⁵⁸⁵Ruhr-Universität Bochum, Medizinische Fakultät, Biochemie Intrazellulärer Transportprozesse, Bochum, Germany; ¹⁵⁸⁶Moscow State University, A.N.Belozersky Institute of Physico-Chemical Biology, Laboratory of Structure and function of mitochondria, Moscow, Russia; ¹⁵⁸⁷UCL Queen Square Institute of Neurology, London, UK; ¹⁵⁸⁸Polish Academy of Sciences, Mossakowski Medical Research Centre, Laboratory of Ischemic and Neurodegenerative Brain Research, Warsaw, Poland;

- ¹⁵⁸⁹Monash Biomedicine Discovery Institute and Monash University, Department of Anatomy and Developmental Biology, Melbourne, Victoria, Australia; ¹⁵⁹⁰Georg-August University Göttingen, Institute of Microbiology and Genetics, Department of Genetics of Eukaryotic Microorganisms, Göttingen, Germany; ¹⁵⁹¹Buchmann Institute & Institute of Biochemistry II, Medical Faculty, Goethe University, Frankfurt, Germany; ¹⁵⁹²Cancer Research Center of Toulouse, UMR 1037 Inserm-university of Toulouse, Toulouse, France; ¹⁵⁹³Università degli Studi di Milano, Dipartimento di Scienze Farmacologiche e Biomolecolari, Centro di Eccellenza per lo studio delle Malattie Neurodegenerative, Milano, Italy; ¹⁵⁹⁴Mahidol University, Department of Microbiology, Faculty of Science, Ratchathewi, Bangkok, Thailand; ¹⁵⁹⁵Georg-August-Universität Göttingen, Institute for Microbiology and Genetics, Department of Molecular Microbiology and Genetics, Göttingen, Germany; ¹⁵⁹⁶Erasmus University Medical Center, Department of Epidemiology; Division of Pharmacology, Department of Internal Medicine, Rotterdam, The Netherlands; ¹⁵⁹⁷The Hospital for Sick Children, Translational Medicine Program, Toronto, Canada; ¹⁵⁹⁸University of Oxford, Nuffield Department of Women's and Reproductive Health, Oxford, UK; ¹⁵⁹⁹University of California, Davis, Department of Molecular and Cellular Biology, Davis, CA, USA; ¹⁶⁰⁰University of Iowa, Department of Biology, Aging Mind and Brain Initiative, Iowa City, IA, USA; ¹⁶⁰¹Temple University, Alzheimer's Center at Temple, Philadelphia, PA, USA; ¹⁶⁰²CNRS, IBGC, UMR5095, Bordeaux, France; ¹⁶⁰³Université de Bordeaux, IBGC, UMR5095, Bordeaux, France; ¹⁶⁰⁴Eberhard Karls University Tübingen, Interfaculty Institute of Cell Biology, Tübingen, Germany; ¹⁶⁰⁵University of Cyprus, Department of Biological Sciences, Bioinformatics Research Laboratory, Nicosia, Cyprus; ¹⁶⁰⁶Lifelong Health, South Australian Health & Medical Research Institute, North Terrace, Adelaide, Australia; ¹⁶⁰⁷Cell and Developmental Biology Center, National Heart, Lung, and Blood Institute, National Institutes of Health, Bethesda, MD, USA; ¹⁶⁰⁸University of Wisconsin-Madison, Department of Medicine and Neuroscience, Madison, WI, USA; ¹⁶⁰⁹Dalhousie University, Department of Biochemistry and Molecular Biology, Dalhousie Medicine New Brunswick, Saint John, NB, Canada; ¹⁶¹⁰National Center for Cell Science, Pune, India; ¹⁶¹¹University of Lausanne, Department of Fundamental Neurosciences, Lausanne, Switzerland; ¹⁶¹²Chinese Academy of Sciences, Kunming Institute of Zoology, Key Laboratory of Animal Models and Human Disease Mechanisms of Chinese Academy of Sciences, Kunming, Yunnan, China; ¹⁶¹³Lanzhou University, School of Life Sciences, Lanzhou, China; ¹⁶¹⁴Zhejiang University, College of Medicine, The First Affiliated Hospital, Malignant Lymphoma Diagnosis and Therapy Center, Hangzhou, Zhejiang, China; ¹⁶¹⁵China Pharmaceutical University, School of Basic Medicine and Clinical Pharmacy, State Key Laboratory of Natural Medicines, Jiangsu Key Laboratory of Carcinogenesis and Intervention, Nanjing, China; ¹⁶¹⁶Sanofi, Biologics Research, 49 New York Ave, Framingham, MA, USA; ¹⁶¹⁷University of Waterloo, Department of Kinesiology, Waterloo, Ontario, Canada; ¹⁶¹⁸Instituto de Investigaciones Biomedicas en Retrovirus y Sida, Universidad de Buenos Aires-CONICET, Argentina; ¹⁶¹⁹NIH, Cell Biology and Physiology Center, National Heart, Lung, and Blood Institute, Bethesda, MD, USA; ¹⁶²⁰University of Pittsburgh, Department of Pathology; University of Pittsburgh Cancer Institute, Pittsburgh, PA, USA; ¹⁶²¹Dartmouth College, Department of Chemistry, Hanover, NH, USA; ¹⁶²²Boston University, Department of Pathology and Laboratory Medicine, Boston, MA, USA; ¹⁶²³Tehran University of Medical Sciences, Cancer Biology Research Center, Tehran, Iran; ¹⁶²⁴University of Naples Federico II, Department of Translational Medical Sciences, Naples, Italy; ¹⁶²⁵University Medical Center Goettingen, Institute of Cellular Biochemistry, Göttingen, Germany; ¹⁶²⁶University of Alabama at Birmingham, Cardiac Aging & Redox Signaling Laboratory, Molecular and Cellular Pathology, Department of Pathology, Birmingham, AL, USA; ¹⁶²⁷Johann Wolfgang Goethe-University, Institute of Anatomy III- 'Cellular and Molecular Anatomy', Frankfurt, Germany; ¹⁶²⁸University of Birmingham, Institute of Metabolism and Systems Research, Birmingham, UK; ¹⁶²⁹MRC Laboratory of Molecular Biology, Division of Protein and Nucleic Acid Chemistry, Cambridge, UK; ¹⁶³⁰Indian Institute of Science, Department of Biochemistry, Bangalore, India; ¹⁶³¹University of Texas Health Science Center at San Antonio, Department of Molecular Medicine, San Antonio, TX, USA; ¹⁶³²Baylor College of Medicine, Department of Medicine, Houston, TX, USA; ¹⁶³³The University of Kansas Cancer Center, Division of Hematologic Malignancies and Cellular Therapeutics, Kansas City, KS, USA; ¹⁶³⁴All India Institute of Medical Sciences, Department of Biotechnology, New Delhi, India; ¹⁶³⁵University of Southampton, Clinical and Experimental Sciences, Faculty of Medicine, UK; ¹⁶³⁶Johns Hopkins University School of Medicine, Department of Otolaryngology/Head and Neck Surgery, Head and Neck Cancer Research Division, Baltimore, MD, USA; ¹⁶³⁷Central University of Tamil Nadu, Thiruvavur, Tamil Nadu, India; ¹⁶³⁸University of Bologna, Department of Pharmacy and Biotechnology, Bologna, Italy; ¹⁶³⁹University of South Carolina School of Medicine, Department of Pathology, Microbiology, and Immunology, Columbia, SC, USA; ¹⁶⁴⁰Washington University School of Medicine, Department of Medicine, Cardiovascular Division, and John Cochran VA Medical Center, St. Louis, MO, USA; ¹⁶⁴¹Johns Hopkins University, Bloomberg School of Public Health, Biochemistry and Molecular Biology Department, Baltimore, MD, USA; ¹⁶⁴²University of Groningen, University of Groningen Medical Center, Department of Biomedical Sciences of Cells and Systems, Groningen, The Netherlands; ¹⁶⁴³Johannes Gutenberg University-Mainz, Institute of Developmental Biology and Neurobiology, Mainz, Germany; ¹⁶⁴⁴Heinrich Heine University Düsseldorf, Medical faculty, Institute of Biochemistry and Molecular Biology I, Düsseldorf, Germany; ¹⁶⁴⁵Hospital Nacional de Paraplégicos, Neuroprotection Group, Toledo, Spain; ¹⁶⁴⁶The University of Texas MD Anderson Cancer Center, Institute for Applied Cancer Science (IACS), Translational Research to Advance Therapeutics and Innovation in Oncology (TRACION), Houston, TX, USA; ¹⁶⁴⁷Karolinska Institutet, Department of Laboratory Medicine, Division of Clinical Microbiology, Stockholm, Sweden; ¹⁶⁴⁸Max Planck Institute of Psychiatry, Translational Research in Psychiatry, Munich, Germany; ¹⁶⁴⁹University of Vienna, Cell Imaging and Ultrastructure Research (CIUS), Vienna, Austria; ¹⁶⁵⁰Wright State University, Department of Biochemistry & Molecular Biology, Dayton, OH, USA; ¹⁶⁵¹University of Wyoming, College of Health Sciences, Laramie, WY, USA; ¹⁶⁵²Qingdao Agricultural University, College of Plant Health and Medicine, Qingdao, Shandong, China; ¹⁶⁵³University of California, Los Angeles, David Geffen School of Medicine, Department of Human Genetics, Los Angeles, CA, USA; ¹⁶⁵⁴University of Copenhagen, Department of Biology, Copenhagen, Denmark; ¹⁶⁵⁵The Wilmer Eye Institute, Johns Hopkins University School of Medicine, Baltimore, MD, USA; ¹⁶⁵⁶Botucatu Medical School, São Paulo State University, Botucatu, SP, Brazil; ¹⁶⁵⁷Université Côte d'Azur, INSERM, C3M, Nice, France; ¹⁶⁵⁸Institut de Génétique et de Biologie Moléculaire et Cellulaire, Illkirch, France; ¹⁶⁵⁹University of Sydney, Department of Pathology and Bosch Institute, Sydney, NSW, Australia; ¹⁶⁶⁰The Ohio State University, College of Veterinary Medicine, Department of Veterinary Biosciences, Columbus, OH, USA; ¹⁶⁶¹Thomas Jefferson University, Department of Orthopaedic Surgery and Graduate Program in Cell Biology and Regenerative Medicine, Philadelphia, PA, USA; ¹⁶⁶²Josep Carreras Leukaemia Research Institute, Barcelona, Spain; ¹⁶⁶³University of Padua, Department of Biomedical Sciences, Padua, Italy; ¹⁶⁶⁴Middlesex University, Department of Natural Sciences, London, UK; ¹⁶⁶⁵University of Palermo, Dipartimento di Scienze e Tecnologie Biologiche, Chimiche e Farmaceutiche (STEBICEF), Palermo, Italy; ¹⁶⁶⁶INSERM U1065, Centre Méditerranéen de Médecine Moléculaire (C3M), Nice, France; ¹⁶⁶⁷Université de Nice Sophia Antipolis, UFR de Médecine, Nice, France; ¹⁶⁶⁸Baylor College of Medicine, Department of Molecular Physiology & Biophysics, Houston, TX, USA; ¹⁶⁶⁹Federal University of ABC (UFABC), Center for Natural and Human Sciences (CCNH), Santo André, SP, Brazil; ¹⁶⁷⁰University of Campinas (UNICAMP), School of Applied Science, Department of Sport Sciences, Limeira, Brazil; ¹⁶⁷¹Clínica Universidad de Navarra, Metabolic Research Laboratory, CIBEROBN, IdiSNA, Pamplona, Spain; ¹⁶⁷²University of Barcelona, School of Medicine, Unit of Anatomy, Department of Pathology and Experimental Therapeutics, Barcelona, Spain; ¹⁶⁷³L'Hospitalet de Llobregat, Institut d'Investigació Biomèdica de Bellvitge -IDIBELL, Molecular Mechanisms and Experimental Therapy in Oncology Program (oncobell), Barcelona, Spain; ¹⁶⁷⁴University of Alcalá, Department of Systems Biology, Biochemistry and Molecular Biology, Alcalá de Henares, Madrid, Spain; ¹⁶⁷⁵Universidad Autónoma de Nuevo Leon, School of Medicine, Department of Histology, Monterrey, Nuevo Leon, Mexico; ¹⁶⁷⁶University of Kansas Medical Center, Department of Biochemistry and Molecular Biology, Kansas City, KS, USA; ¹⁶⁷⁷Kansas City University of Medicine and Biosciences,

- Department of Basic Science, Kansas City, MO, USA; ¹⁶⁷⁵Goethe University Frankfurt, Institute of Biophysical Chemistry, Frankfurt am Main, Germany; ¹⁶⁷⁶University of Gdansk, Faculty of Chemistry, Gdansk, Poland; ¹⁶⁷⁷University of Padova, Department of Biomedical Science, Padova, Italy; ¹⁶⁷⁸University of Perugia, Department of Experimental Medicine, Perugia, Italy; ¹⁶⁷⁹Università degli Studi di Catania, Dipartimento di Chirurgia Generale e Specialità Medico-Chirurgiche, Catania, Italy; ¹⁶⁸⁰CONICET-Universidad Nacional de Cuyo, Instituto de Histología y Embriología de Mendoza, Mendoza, Argentina; ¹⁶⁸¹INSERM U1151, Institut Necker Enfants-Malades (INEM), Team 14, Université Paris Descartes-Sorbonne-Paris Cité, Paris, France; ¹⁶⁸²Huazhong University of Science and Technology, School of Basic Medicine, Wuhan, HuBei, China; ¹⁶⁸³Waksman Institute, Department of Genetics, Rutgers University, Piscataway, NJ, USA; ¹⁶⁸⁴Naples University, Department of Veterinary Medicine and Animal Productions, Naples, Italy; ¹⁶⁸⁵University of Würzburg, Institute of Pathology, Würzburg, Germany; ¹⁶⁸⁶Kiel University and University Hospital Schleswig-Holstein, Campus Kiel, Institute of Clinical Molecular Biology, Kiel, SH, Germany; ¹⁶⁸⁷Georgetown University, Department of Biology, Washington, DC, USA; ¹⁶⁸⁸Columbia University, Department of Pathology and Cell Biology, New York, NY, USA; ¹⁶⁸⁹University of Illinois, Department of Anesthesiology, Chicago, IL, USA; ¹⁶⁹⁰Maastricht University Medical Centre, GROW-School for Oncology and Developmental Biology, Maastricht Radiation Oncology (Maastro) lab, Maastricht, The Netherlands; ¹⁶⁹¹Normandy University, UNICAEN, INSERM, UMR-S U1237, Physiopathology and Imaging of Neurological Disorders (PhIND), Caen, France; ¹⁶⁹²University of Sherbrooke, Division of Rheumatology, Department of Medicine, Sherbrooke, QC, Canada; ¹⁶⁹³Section on Eukaryotic DNA Replication, National Institute of Child Health and Human Development, National Institutes of Health, Bethesda, MD, USA; ¹⁶⁹⁴University of Seville. School of Pharmacy, Instituto de Biomedicina de Sevilla. Sevilla, Spain; ¹⁶⁹⁵University of Cambridge, Cambridge Institute for Medical Research, UK Dementia Research Institute and Department of Medical Genetics, Cambridge, UK; ¹⁶⁹⁶Lomonosov Moscow State University, Chemistry Department, Moscow, Russia; ¹⁶⁹⁷University Medical Center Eppendorf, Institute for Medical Microbiology, Hamburg, Germany; ¹⁶⁹⁸University of Graz, Institute of Molecular Biosciences, NAWI Graz, Graz, Austria; ¹⁶⁹⁹Charles University, Faculty of Medicine in Hradec Kralove, Department of Medical Biology and Genetics, Hradec Kralove, Czech Republic; ¹⁷⁰⁰University of Heidelberg, Mannheim University of Applied Sciences & Interdisciplinary Center of Neurosciences (IZN), Faculty of Biotechnology, Mannheim, Germany; ¹⁷⁰¹Fondazione IRCCS Istituto Neurologico Carlo Besta, Neuromuscular Disease and Immunology Unit, Milan, Italy; University of Brescia, Unit of Biology and Genetics, Department of Molecular and Translation Medicine, Brescia, Italy; ¹⁷⁰²Monash University, Australian Regenerative Medicine Institute, Clayton, Victoria, Australia; ¹⁷⁰³University of Ottawa, Department of Cellular and Molecular Medicine, Ottawa, ON, Canada; ¹⁷⁰⁴National Research Council, Institute of Food Sciences, Avellino, Italy; ¹⁷⁰⁵National Research Council, Institute of Food Sciences, Avellino, Italy; ¹⁷⁰⁶University of Calabria, Department of Pharmacy, Health and Nutritional Sciences, Cosenza, Italy; ¹⁷⁰⁷N.N. Blokhin National medical research center of oncology, Department of biomarkers and mechanisms of tumor angiogenesis, Moscow, Russia; ¹⁷⁰⁸Cancer Research UK Beatson Institute, Glasgow, UK; ¹⁷⁰⁹University of Seoul, Department of Life Science, Seoul, Korea; ¹⁷¹⁰University of Pittsburgh Medical Center, Pittsburgh, PA, USA; ¹⁷¹¹Concordia University, Department of Biology, Montreal, Quebec, Canada; McGill University, Department of Anatomy and Cell Biology, Quebec, Canada; ¹⁷¹²Ernst-Ruska Centre for Microscopy and Spectroscopy with Electrons (ER-C-3/StructuralBiology), Forschungszentrum Jülich, Jülich, Germany; ¹⁷¹³Saitama University, Graduate School of Science and Engineering, Saitama, Japan; ¹⁷¹⁴Rutgers New Jersey Medical School, Department of Cell Biology and Molecular Medicine, Newark, NJ, USA; ¹⁷¹⁵Christian-Albrechts-University Kiel, Biochemical Institute, Kiel, Germany; ¹⁷¹⁶Mashhad University of Medical Sciences, Pharmaceutical Technology Institute, Biotechnology Research Center, Mashhad, Iran; ¹⁷¹⁷Oregon State University, College of Pharmacy, Department of Pharmaceutical Sciences, Portland, OR, USA; ¹⁷¹⁸Boston Children's Hospital and Harvard Medical School, Boston, MA, USA; ¹⁷¹⁹University of South Carolina, Department of Drug Discovery and Biomedical Sciences, Columbia, SC, USA; ¹⁷²⁰University of Sydney, Northern Clinical School, Kolling Institute of Medical Research, Sydney, NSW, Australia; ¹⁷²¹Institute for Research in Biomedicine (IRB Barcelona), Cellular Plasticity and Disease Group, Barcelona, Spain; ¹⁷²²University of Toyama, Sugitani, Toyama, Japan; ¹⁷²³Cedars-Sinai Medical Center, Smidt Heart Institution, West Hollywood, CA, USA; ¹⁷²⁴The University of Tokyo, Graduate School of Medicine, Department of Biochemistry and Molecular Biology, Tokyo, Japan; ¹⁷²⁵University of Helsinki and Helsinki University Hospital, Department of Virology, Helsinki, Finland; ¹⁷²⁶Florida State University, Department of Nutrition, Food and exercise Sciences, Tallahassee, FL, USA; ¹⁷²⁷Institut Hospital del Mar d'Investigacions Mèdiques (IMIM), Research Group in Critical Disorders (GREPAC), Barcelona, Spain; ¹⁷²⁸Agricultural Biotechnology Research Institute of Iran (ABRII), Department of Systems Biology, Karaj, Iran; ¹⁷²⁹University of Miami, Department of Surgery and Sylvester Comprehensive Cancer Center, Miami, FL, USA; ¹⁷³⁰University of Minho, School of Medicine, Life and Health Sciences Research Institute (ICVS), Braga, Portugal; ICVS/3B's - PT Government Associate Laboratory, Braga/Guimarães, Portugal; ¹⁷³¹National University of Córdoba, Clinical Biochemistry Department, Córdoba, Argentina; ¹⁷³²CABD/CSIC/Universidad Pablo de Olavide, Departamento de Fisiología, Anatomía y Biología Celular, Sevilla, Spain; ¹⁷³³University of Malaga, Department of Molecular Biology and Biochemistry, Malaga, Spain; ¹⁷³⁴Imperial College London, Section of Paediatric Infectious Disease, London, UK; ¹⁷³⁵INRS-Institut Armand-Frappier, Laval, QC, Canada; ¹⁷³⁶University of Padova, Department of Biomedical Science, Padova, Italy; ¹⁷³⁷European Institute of Oncology (IEO) IRCCS, Department of Experimental Oncology, Milan, Italy; University of Milano, Department of Oncology and Hemato-Oncology, Milan, Italy; ¹⁷³⁸Weill-Cornell, Englander Institute of Precision Medicine, Department of Radiation Oncology, New York, NY, USA; ¹⁷³⁹National Institutes of Health, National Institute of Allergy and Infectious Diseases, Vaccine Research Center, Bethesda, MD, USA; ¹⁷⁴⁰University of Glasgow, Institute of Molecular, Cell and Systems Biology, Glasgow, Scotland, United Kingdom; ¹⁷⁴¹Instituto de Biomedicina de Valencia, CSIC, Valencia, Spain; ¹⁷⁴²Jawaharlal Nehru University, School of Life Sciences, New Delhi, India; ¹⁷⁴³Baylor College of Medicine, Department of Molecular and Human Genetics, Houston, TX, USA; ¹⁷⁴⁴Hopwood Centre for Neurobiology, Lifelong Health Theme, South Australian Health and Medical Research Institute, Adelaide, Australia; ¹⁷⁴⁵Institute for Stem Cell Science & Regenerative Medicine (inStem), Bangalore, Karnataka, India; ¹⁷⁴⁶University of Maryland School of Medicine, Department of Anesthesiology, Shock, Trauma and Anesthesiology Research Center, Baltimore, MD, USA; ¹⁷⁴⁷University of Birmingham, Institute of Biomedical Research, Institute of Cancer and Genomic Sciences, College of Medical and Dental Sciences, Edgbaston, Birmingham, UK; ¹⁷⁴⁸University of Delhi South Campus, Department of Genetics, New Delhi, India; ¹⁷⁴⁹Folkhälsan Research Center, Helsinki, Finland; ¹⁷⁵⁰Health Research Institute Germans Trias i Pujol, Innate Immunity Group, Badalona, Barcelona, Spain; ¹⁷⁵¹Mayo Clinic, Department of Molecular Medicine, Rochester, MN, USA; ¹⁷⁵²National Institute of Mental Health and Neurosciences, Department of Neurochemistry, Bengaluru, Karnataka, India; ¹⁷⁵³Duke University, Department of Molecular Genetics and Microbiology, Durham, NC, USA; ¹⁷⁵⁴Goethe University, Institute of Pharmacology and Toxicology, Frankfurt, Germany; ¹⁷⁵⁵University of Notre Dame, Department of Biological Sciences, Notre Dame, IN, USA; ¹⁷⁵⁶Research Center Borstel - Leibniz Lung Center, Priority Area Infections, Division Cellular Microbiology, Borstel, Germany; ¹⁷⁵⁷UCL Queen Square Institute of Neurology, Department of Clinical and Movement Neurosciences, London, UK; ¹⁷⁵⁸University Hospital and University of Zürich, Department of Gastroenterology and Hepatology, Zürich, Switzerland; ¹⁷⁵⁹University of Calgary, Department of Comparative Biology & Experimental Medicine, Calgary, AB, Canada; ¹⁷⁶⁰University of Texas Medical Branch at Galveston, Institute for Human Infection and Immunity, Department of Biochemistry and Molecular Biology, Galveston, TX, USA; ¹⁷⁶¹Amsterdam University Medical Centers location VUmc, Department of Clinical Genetics, Amsterdam, The Netherlands; ¹⁷⁶²University of Kaiserslautern, Phytopathology, Kaiserslautern, Germany; ¹⁷⁶³IRCCS San Raffaele Scientific Institute, Division of Genetics and Cell Biology, Milan, Italy; ¹⁷⁶⁴Centro di Riferimento Oncologico, CRO-IRCCS, Molecular Oncology Unit, Aviano, Italy; ¹⁷⁶⁵Medical University of

- Graz, Gottfried Schatz research center, Graz, Austria; ¹⁷⁶⁶Medical University of Innsbruck, Institute for Cell Biology, Innsbruck, Austria; ¹⁷⁶⁷Vaccine Research Center, National Institutes of Health, Bethesda, MD, USA; ¹⁷⁶⁸Hannover Medical School, Department of Nephrology and Hypertension, Hannover, Germany; ¹⁷⁶⁹Ruhr-University Bochum, Department of Molecular Immunology, Bochum, Germany; ¹⁷⁷⁰University Grenoble Alpes and Inserm U1055, Laboratory of Fundamental and Applied Bioenergetics (LBFA), Grenoble, France; ¹⁷⁷¹German Center for Neurodegenerative Diseases, DZNE, Bonn, Germany and Department of Neurodegenerative Diseases and Geriatric Psychiatry, University Bonn, Bonn, Germany; ¹⁷⁷²Research Center Borstel, Leibniz Lung Center, Priority Research Area Infections, Junior Research Group Coinfection, Borstel, Germany; ¹⁷⁷³Johannes Kepler University Linz, Institute of Biophysics, Linz, Austria; ¹⁷⁷⁴Mayo Clinic, Department of Biochemistry and Molecular Biology, Division of Gastroenterology and Hepatology, Rochester, MN, USA; ¹⁷⁷⁵Technische Universität Dresden, Institute for Physiological Chemistry, Dresden, Germany; ¹⁷⁷⁶University of Wuerzburg, Department of Vegetative Physiology, Wuerzburg, Germany; ¹⁷⁷⁷University of Natural Resources and Life Sciences, Department of Applied Genetics and Cell Biology, Vienna, Austria; ¹⁷⁷⁸Mayo Clinic, Division of Gastroenterology and Hepatology, Rochester, MN, USA; ¹⁷⁷⁹University of Luxembourg, Luxembourg Centre for Systems Biomedicine (LCSB), Esch-sur-Alzette, Luxembourg; ¹⁷⁸⁰University of Campania L. Vanvitelli, Dipartimento di Scienze Mediche Traslazionali, Naples, Italy; ¹⁷⁸¹Department of Medical and Surgical Sciences and Biotechnologies, Sapienza University of Rome, Italy; IRCCS Neuromed, Pozzilli (IS), Italy; ¹⁷⁸²Helmholtz Centre for Infection Research, Braunschweig, Germany; ¹⁷⁸³University of Pittsburgh, Department of Surgery, Pittsburgh, PA, USA; ¹⁷⁸⁴Rutgers Biomedical and Health Sciences, Rutgers University, Robert Wood Johnson Medical School, Department of Pharmacology, New Brunswick, NJ, USA; ¹⁷⁸⁵National Research Council, Institute of Molecular Genetics, Pavia, Italy; ¹⁷⁸⁶Albert Einstein College of Medicine, Department of Developmental and Molecular Biology, Bronx, NY; Albert Einstein College of Medicine, Institute for Aging Studies, Bronx, NY, USA; ¹⁷⁸⁷The Barcelona Institute of Science and Technology, Institute for Research in Biomedicine (IRB Barcelona), Barcelona, Spain; Universitat de Barcelona, Departament de Bioquímica i Biomedicina Molecular, Barcelona, Spain; Instituto de Salud Carlos III, CIBER de Diabetes y Enfermedades Metabólicas Asociadas (CIBERDEM), Madrid, Spain; ¹⁷⁸⁸Medical University of Graz, Division of Cardiology, Graz, Austria; ¹⁷⁸⁹Rice University, Department of Bioengineering, Houston, TX, USA; ¹⁷⁹⁰University of Illinois at Chicago, College of Medicine, Department of Biochemistry and Molecular Genetics, Chicago, IL, USA; ¹⁷⁹¹University of Oslo, Centre for Molecular Medicine Norway (NCMM), Oslo, Norway; ¹⁷⁹²Cedars-Sinai Medical Center, Department of Medicine, Division of Digestive and Liver Diseases, Los Angeles, CA, USA; ¹⁷⁹³INRA-UPPA, UMR 1419 Nutrition, Métabolisme, Saint Pée-sur-Nivelle, France; ¹⁷⁹⁴Pennsylvania State University, Department of Biochemistry and Molecular Biology, University Park, PA, USA; ¹⁷⁹⁵Alpert Medical School of Brown University/Rhode Island Hospital, Division of Cardiothoracic Surgery, Providence, RI, USA; ¹⁷⁹⁶Iowa State University, Animal Science Department, Ames, IA, USA; ¹⁷⁹⁷University of Würzburg, Institute of Clinical Neurobiology, Würzburg, Germany; ¹⁷⁹⁸Dokuz Eylul University, Izmir International Biomedicine and Genome Institute, Izmir, Turkey; ¹⁷⁹⁹University of Alberta, Department of Laboratory Medicine and Pathology, Edmonton, AB, Canada; ¹⁸⁰⁰Texas Tech University, Department of Biological Sciences, Lubbock, TX, USA; ¹⁸⁰¹Johns Hopkins University School of Medicine, Department of Cell Biology, Baltimore, MD, USA; ¹⁸⁰²Telethon Institute of Genetics and Medicine (TIGEM), Naples, Italy; 3 Federico II University of Naples, Naples, Italy; ¹⁸⁰³Indian Institute of Science, Department of Microbiology and Cell Biology, Bangalore, KA, India; ¹⁸⁰⁴University of Bologna, Dipartimento di Scienze Biomediche e Neuromotorie, Bologna, Italy; ¹⁸⁰⁵Shenzhen University Health Science Center, School of Dentistry, Shenzhen, Guangdong Province, China; ¹⁸⁰⁶University of Alabama at Birmingham, Department of Pharmacology & Toxicology, Birmingham, AL, USA; ¹⁸⁰⁷University of Washington, Department of Medicine, Seattle, WA, USA; VA Puget Sound Health Care System, Seattle, WA, USA; ¹⁸⁰⁸Soochow University, Institutes for Translational Medicine, Suzhou, Jiangsu, China; ¹⁸⁰⁹National Institute of Biological Sciences, Beijing, China; ¹⁸¹⁰Freie Universität Berlin, Department of Veterinary Medicine, Institute of Veterinary Biochemistry, Berlin, Germany; ¹⁸¹¹University of Michigan Medical School, Department of Neurology, Ann Arbor, MI, USA; ¹⁸¹²Johns Hopkins University, Department of Oncology, Sidney Kimmel Comprehensive Cancer Center, Baltimore, MD, USA; ¹⁸¹³Division of Stem Cell and Gene Therapy Research, Institute of Nuclear Medicine & Allied Sciences (INMAS), Defence Research and Development Organization (DRDO), Timar Pur, New Delhi, India; ¹⁸¹⁴Thomas Jefferson University, Center for Translational Medicine, Philadelphia, PA, USA; ¹⁸¹⁵Women and Infants Hospital of Rhode Island-Warren Alpert Medical School of Brown University, Departments of Pediatrics, Providence, RI, USA; ¹⁸¹⁶University of Macau, Faculty of Health Sciences, Macau, China; ¹⁸¹⁷The University of Hong Kong, School of Chinese Medicine, Hong Kong, China; ¹⁸¹⁸Nanjing Agricultural University, College of Animal Science and Technology, Nanjing, Jiangsu, China; ¹⁸¹⁹Total Toxicology Labs, Southfield, MI, USA; ¹⁸²⁰Soochow University, College of Pharmaceutical Sciences, Department of Pharmacology and Laboratory of Aging and Nervous Diseases, Suzhou, China; ¹⁸²¹Fralin Biomedical Research Institute, Roanoke, VA, USA; ¹⁸²²National Institutes of Health, National Institute of Neurological Disorders and Stroke, Bethesda, MD, USA; ¹⁸²³Van Andel Institute, Center for Epigenetics, Grand Rapids, MI, USA; ¹⁸²⁴Fudan University, Zhongshan Hospital, Liver Cancer Institute, Department of Liver Surgery & Transplantation, Shanghai, China; ¹⁸²⁵Juntendo University Graduate School of Medicine, Department of Treatment and Research in Multiple Sclerosis and Neuro-intractable Disease, Bunkyo-ku, Tokyo, Japan; ¹⁸²⁶National Chung-Hsing University, Institute of Biomedical Sciences, Taichung City, Taiwan; ¹⁸²⁷Jikei University School of Medicine, Research Center for Medical Sciences, Division of Gene Therapy, Tokyo, Japan; ¹⁸²⁸Tokyo Medical and Dental University, Department of Pathological Cell Biology, Tokyo, Japan; ¹⁸²⁹Tohoku University, Graduate School of Agricultural Science, Sendai, Japan; ¹⁸³⁰Geisel School of Medicine at Dartmouth, Department of Biochemistry and Cell Biology, Hanover, NH, USA; ¹⁸³¹Kobe University Graduate School of Medicine, Center for Infectious Diseases, Division of Infectious Disease Control, Kobe, Japan; ¹⁸³²Agharkar Research Institute, Developmental Biology Group, Pune, India; Savitribai Phule Pune University, Ganeshkhind, Pune, Maharashtra, India; ¹⁸³³Mayo Clinic College of Medicine, Department of Experimental Pathology, Rochester, MN, USA; ¹⁸³⁴I-Shou University, School of Medicine for International Students, Kaohsiung, Taiwan; ¹⁸³⁵Wuhan University, Medical Research Institute, Wuhan, China; ¹⁸³⁶University of Calgary, Cumming School of Medicine, Departments of Medical Genetics and Biochemistry & Molecular Biology, Calgary, Alberta, Canada; ¹⁸³⁷Inserm U1138, Centre de Recherche des Cordeliers, Sorbonne Université, Université de Paris, Paris, France; ¹⁸³⁸Achucarro Basque Center for Neurosciences, University of the Basque Country, Leioa, Bizkaia, Spain; ¹⁸³⁹Universidad de la República, Facultad de Agronomía, Departamento de Biología Vegetal, Montevideo, Uruguay; ¹⁸⁴⁰National Institutes of Health, NIEHS, RTP, Durham, NC, USA; ¹⁸⁴¹David Geffen School of Medicine at University of California, Los Angeles, Department of Medicine, Division of Dermatology, Los Angeles, CA, USA; ¹⁸⁴²University of Surrey, School of Bioscience and Medicine, Department of Microbial Sciences, Stag Hill Campus, Guildford, Surrey, UK; ¹⁸⁴³University of Oxford, Kennedy Institute of Rheumatology, Oxford, UK; ¹⁸⁴⁴University of Bern, Institute of Pharmacology, Bern, Switzerland; ¹⁸⁴⁵INSERM UMR1163, Laboratory of Epithelial Biology and Disease, Imagine Institute, Paris Descartes University, Sorbonne Paris Cité, Hôpital Necker-Enfants Malades, Paris, France; ¹⁸⁴⁶Boston University School of Medicine, Division of Hematology & Medical Oncology, Department of Pharmacology & Experimental Therapeutics, Boston, MA, USA; ¹⁸⁴⁷Wayne State University School of Medicine, Department of ophthalmology, Visual and Anatomical Sciences, Detroit, MI, USA; ¹⁸⁴⁸Albert Einstein College of Medicine, Department of Medicine, Bronx, NY, USA; ¹⁸⁴⁹University of Pittsburgh, Department of Pharmacology & Chemical Biology, Pittsburgh, PA, USA; ¹⁸⁵⁰Post Graduate Institute of Medical Education and Research (PGIMER), Department of Urology, Chandigarh, India; ¹⁸⁵¹Biomedical Research Institute of New Mexico, VA Healthcare System, Albuquerque, NM, USA; ¹⁸⁵²CSIR-National Physical Laboratory, Dr. K. S. Krishnan Marg, New Delhi, India; ¹⁸⁵³University of Pittsburgh School of Medicine, Departments of Ophthalmology, Cell Biology, and Developmental Biology,

Pittsburgh, PA, USA; ¹⁸⁵⁴Sanjay Gandhi Postgraduate Institute of Medical Sciences, Department of Endocrinology, Lucknow, India; ¹⁸⁵⁵North Dakota State University, Department of Chemistry and Biochemistry, Fargo, ND, USA; ¹⁸⁵⁶National Jewish Health, Department of Medicine, Division of Allergy & Immunology, and Division of Pulmonary and Critical Care Medicine, Denver, CO, USA; ¹⁸⁵⁷Democritus University of Thrace, First Department of Internal Medicine & Laboratory of Molecular Hematology, Alexandroupolis, Greece; ¹⁸⁵⁸Masaryk University, Faculty of Medicine, Department of Biology, Brno, Czech Republic; ¹⁸⁵⁹Maastricht University Medical Center, School for Cardiovascular disease (CARIM), Department of Pathology, Maastricht, The Netherlands; University of Edinburgh, Centre for Cardiovascular Science, Edinburgh, UK; ¹⁸⁶⁰Universidade Federal de São Paulo, Paulista School of Medicine, Department of Pharmacology, São Paulo, Brazil; ¹⁸⁶¹Washington State University, Institute of Biological Chemistry, Pullman, WA, USA; ¹⁸⁶²Edinburgh Cancer Research UK Centre, MRC Institute of Genetics and Molecular Medicine, University of Edinburgh, Edinburgh, UK; ¹⁸⁶³Dong-A University, College of Medicine, Department of Molecular Neuroscience, Peripheral Neuropathy Research Center, Busan, Korea; ¹⁸⁶⁴University of Geneva, Department of Biochemistry, Faculty of Science, Switzerland; ¹⁸⁶⁵University of Michigan, Department of Internal Medicine, Ann Arbor, MI, USA; ¹⁸⁶⁶Lomonosov Moscow State University, Department of Biology, Moscow, Russia; ¹⁸⁶⁷Duke University, Department of Medicine, Durham, NC, USA; ¹⁸⁶⁸KU Leuven, Department of Imaging and Pathology, Leuven, Belgium; ¹⁸⁶⁹Indian Institute of Technology Indore, Discipline of Biosciences and Biomedical Engineering, Indore, Madhya Pradesh, India; ¹⁸⁷⁰Shandong University, School of public health, Department of Toxicology and nutrition. Jinan, Shandong, China; ¹⁸⁷¹Korea University, Department of Life Sciences, Seoul, Korea; ¹⁸⁷²Guangzhou University of Chinese Medicine, Medical College of Acupuncture-Moxibustion and Rehabilitation, Guangzhou, China; Hong Kong Baptist University, School of Chinese Medicine, Mr. and Mrs. Ko Chi Ming Centre for Parkinson's Disease Research, Hong Kong SAR, China; ¹⁸⁷³University of Colorado Anschutz Medical Campus, Division of Cardiology, Aurora, CO, USA; ¹⁸⁷⁴Hubei Key Laboratory of Cell Homeostasis, College of Life Sciences, Wuhan University, Wuhan, Hubei, China; ¹⁸⁷⁵Massachusetts General Hospital and Harvard Medical School, Department of Medicine, Endocrine Division, Boston, MA, USA; ¹⁸⁷⁶Université de Bordeaux, Institut des Maladies Neurodégénératives (IMN), CNRS UMR 5293, Bordeaux, France; ¹⁸⁷⁷University of Guelph, Department of Food Science, Guelph, Canada; ¹⁸⁷⁸University of California, San Diego, Department of Pediatrics, La Jolla, CA, USA; ¹⁸⁷⁹Department of Clinical Psychopharmacology and Neurotoxicology, National Institute of Mental Health and Neurosciences, Bengaluru-560029, Karnataka, India; ¹⁸⁸⁰University of Kentucky, Department of Toxicology and Cancer Biology, Lexington, KY, USA; ¹⁸⁸¹Institute of Molecular Biology and Pathology, National Research Council (CNR), Rome, Italy; Istituto di Ricovero e Cura a Carattere Scientifico (IRCCS) Fondazione Santa Lucia, Laboratory of Cell Signaling, Rome, Italy; ¹⁸⁸²Telethon Institute of Genetics and Medicine (TIGEM), Pozzuoli (NA), Italy; ¹⁸⁸³Department of Molecular Microbiology, Washington University School of Medicine, St. Louis, MO, USA; ¹⁸⁸⁴Hannover Medical School, Department for Clinical Immunology and Rheumatology, Hannover, Germany; ¹⁸⁸⁵University of Western Ontario, Department of Physiology and Pharmacology, London, Ontario, Canada; ¹⁸⁸⁶Biomedical Research Foundation of the Academy of Athens, Laboratory of Neurodegenerative Diseases, Athens, Greece; National and Kapodistrian University of Athens Medical School, First Department of Neurology, Athens, Greece; ¹⁸⁸⁷Friedrich-Alexander-Universität Erlangen-Nürnberg, Department of Immune Modulation, University Hospital Erlangen, Erlangen, Germany; ¹⁸⁸⁸Oslo University Hospital, Institute for Cancer Research, Department of Molecular Cell Biology, Montebello, Oslo, Norway; ¹⁸⁸⁹Technische Universität Dresden, Center for Regenerative Therapies Dresden, Dresden, Germany; ¹⁸⁹⁰Edinburgh Napier University, School of Applied Sciences, Edinburgh, UK; ¹⁸⁹¹University Medical Center Hamburg-Eppendorf, Children's Hospital, University Children's Research@Kinder-UK, Hamburg, Germany; ¹⁸⁹²Heinrich-Heine-University, Medical Faculty, Institute of Molecular Medicine I, Düsseldorf, Germany; ¹⁸⁹³IRCCS Fondazione Santa Lucia, Rome, Italy; ¹⁸⁹⁴The Ohio State University, Department of Cancer Biology and Genetics, Columbus, OH, USA; ¹⁸⁹⁵University of California San Diego, UCSD Moores Cancer Center, La Jolla, CA, USA; ¹⁸⁹⁶Peking Union Medical College and Chinese Academy of Medical Sciences, Peking Union Medical College Hospital, Department of Critical Care Medicine, Beijing, China; ¹⁸⁹⁷Case Western Reserve University School of Medicine, Departments of Medicine and Pathology, Cleveland, OH USA; ¹⁸⁹⁸Rutgers University, New Jersey Medical School and Public Health Research Institute, Newark, NJ, USA; ¹⁸⁹⁹University of Madras, Department of Biochemistry, Guindy Campus, Chennai, India; ¹⁹⁰⁰Kolling Institute, Department of Neurogenetics, University of Sydney and Royal North Shore Hospital, St Leonards NSW, Australia; ¹⁹⁰¹Hangzhou Normal University, Affiliated Hospital of Hangzhou Normal University, College of Medicine, Holistic Integrative Pharmacy Institutes and Comprehensive Cancer Diagnosis and Treatment Center, Hangzhou, Zhejiang, China; ¹⁹⁰²Iowa State University, Department of Kinesiology, Ames, IA, USA; ¹⁹⁰³University of Nebraska Lincoln, Department of Agronomy and Horticulture, Center for Plant Science Innovation, Lincoln, NE, USA; ¹⁹⁰⁴University of Illinois at Chicago, Department of Medicine, Chicago, IL, USA; ¹⁹⁰⁵Shanghai Jiao Tong University, School of Medicine, Ren Ji Hospital, Center for Reproductive Medicine, Shanghai, China; ¹⁹⁰⁶Wuhan University, College of Life Sciences, Wuhan, Hubei, China; ¹⁹⁰⁷Zhejiang University, School of Medicine, Department of Biochemistry, Hangzhou, Zhejiang, China; ¹⁹⁰⁸University of Michigan, Department of Radiation Oncology, Ann Arbor, MI, USA; ¹⁹⁰⁹University of Tennessee Health Science Center, Department of Physiology, Memphis, TN, USA; ¹⁹¹⁰Experimental Physiopathology, Department of Sciences/Experimental Physiopathology, Medical School, University of São Paulo, Brazil; ¹⁹¹¹Swedish University of Agricultural Sciences, The Linnean Centre of Plant Biology in Uppsala, Department of Plant Biology, Uppsala, Sweden; ¹⁹¹²University of Pennsylvania, Perelman School of Medicine, Department of Medicine, Philadelphia, PA, USA; ¹⁹¹³University of Missouri, Division of Animal Science and Department of Obstetrics, Gynecology & Women's Health, Columbia, MO, USA; ¹⁹¹⁴Tokai University School of Medicine, Department of Gastroenterology and Hepatology, Isehara, Kanagawa, Japan; ¹⁹¹⁵York University, Department of Biology, Toronto, Canada; ¹⁹¹⁶University of Utah, Department of Nutrition and Integrative Physiology; Division of Endocrinology, Metabolism, and Diabetes; Investigator, Molecular Medicine Program, Salt Lake City, UT, USA; ¹⁹¹⁷Hong Kong Baptist University, Faculty of Science, Department of Biology, Hong Kong, China; Hong Kong Baptist University, Golden Meditech Centre for NeuroRegeneration Sciences, Hong Kong, China; ¹⁹¹⁸University of Nottingham, School of Medicine, MRC/ARUK Centre for Musculoskeletal Ageing Research and NIHR Nottingham BRC, Derby, UK; ¹⁹¹⁹University of Rzeszow, Collegium Scientarium Naturalium, Institute of Biology and Biotechnology, Department of Animal Physiology and Reproduction, Kolbuszowa, Poland; ¹⁹²⁰Charité University Medicine Berlin, Department of Hepatology & Gastroenterology, Berlin, Germany; ¹⁹²¹University of Texas Health Science Center at Houston, McGovern Medical School, Department of Internal Medicine, Cardiology, Houston, TX, USA; ¹⁹²²Sapienza University of Rome, Department of Experimental Medicine, Rome, Italy; ¹⁹²³Tokyo University of Pharmacy and Life Sciences, School of Life Sciences, Hachioji, Horinouchi, Tokyo, Japan; ¹⁹²⁴Chengdu Medical College, Department of Anatomy and Histology and Embryology, Development and Regeneration Key Lab of Sichuan Province, Chengdu, China; ¹⁹²⁵University of Glasgow, Institute of Cancer Sciences, Glasgow, UK; ¹⁹²⁶Penn State University College of Medicine, Department of Pediatrics, Hershey, PA, USA; ¹⁹²⁷Oslo University Hospital, Institute for Cancer Research, Department of Molecular Cell Biology, Oslo, Norway; ¹⁹²⁸The Hong Kong Polytechnic University, Faculty of Health and Social Sciences, Department of Health Technology and Informatics, Hung Hom, Hong Kong; ¹⁹²⁹Inserm Unit 1195 - University of Paris Saclay/Paris Saclay, Le Kremlin-Bicêtre, France; ¹⁹³⁰Tokyo Medical and Dental University (TMDU), Institute of Biomaterials and Bioengineering, Tokyo, Japan; ¹⁹³¹National Neuroscience Institute, Duke NUS Medical School, Singapore; ¹⁹³²Kyoto Prefectural University of Medicine, Department of Anatomy and Neurobiology, Kyoto, Japan; ¹⁹³³RIKEN Center for Brain Science, Laboratory for Protein Conformation Diseases, Wako, Saitama, Japan; ¹⁹³⁴UT Southwestern Medical Center, Department of Surgery, Dallas, Texas, USA; ¹⁹³⁵Hubei University of Technology, National "111" Center for Cellular Regulation and Molecular Pharmaceuticals, Wuhan, China; ¹⁹³⁶University of Chinese Academy of

- Sciences, Institute of Zoology, Chinese Academy of Sciences, State Key Laboratory of Membrane Biology, Beijing, China; ¹⁹³⁷Juntendo University School of Medicine, Department of Cell Biology and Neuroscience, Tokyo, Japan; ¹⁹³⁸Harvard Medical School, Massachusetts General Hospital, Cutaneous Biology Research Center, Charlestown, MA, USA; ¹⁹³⁹Institute of Neurosciences Paris-Saclay (Neuro-PSI) UMR 9197 CNRS, University Paris-Sud/University Paris-Saclay, Orsay, France; ¹⁹⁴⁰University Medicine Goettingen, Neurology, Department of Translational Neurodegeneration, Center for Biostructural Imaging of Neurodegeneration (BIN), Goettingen, Germany; ¹⁹⁴¹Foundation for Research and Technology-Hellas, Institute of Molecular Biology and Biotechnology, Heraklion, Crete, Greece; University of Crete, Medical School, Heraklion, Crete, Greece; ¹⁹⁴²Duke University, Department of Medicine; Duke University, Department of Molecular Genetics and Microbiology; Duke University, Department of Immunology, Durham, NC, USA; Geriatric Research, Education, and Clinical Center, VA Health Care Center, Durham, NC, USA; ¹⁹⁴³University of North Carolina, Department of Pathology, Chapel Hill, NC, USA; ¹⁹⁴⁴Nasonova Research Institute of Rheumatology, Moscow, Russia; ¹⁹⁴⁵Cardiff University, Division of Cancer and Genetics, Heath Park Way, Cardiff, UK; ¹⁹⁴⁶Goethe-University, Faculty of Medicine, Department of Clinical Pharmacology, Frankfurt, Germany; ¹⁹⁴⁷INSERM U955, Team "Virus Hepatology Cancers", Cr teil, France; Universit  Paris-Est, UMR S955, UPEC, Cr teil, France; ¹⁹⁴⁸Chulalongkorn University, Faculty of Allied Health Sciences, Age-Related Inflammation and Degeneration Research Unit, Department of Clinical Chemistry, Bangkok, Thailand; ¹⁹⁴⁹Chronic Diseases Research Center (CEDOC), Faculdade de Ci ncias M dicas, Universidade Nova de Lisboa, Lisboa, Portugal; ¹⁹⁵⁰University of Liverpool, Department of Cellular and Molecular Physiology, Liverpool, UK; ¹⁹⁵¹Biological Research Center, CIB-CSIC, Madrid, Spain; ¹⁹⁵²University of Insubria, Department of Biotechnology and Life Sciences, Varese, Italy; ¹⁹⁵³Institut National de la Sant  et de la Recherche M dicale (Inserm), Universit  de Paris, Paris Cardiovascular Center - PARCC, Paris, France; ¹⁹⁵⁴University of Innsbruck, Institute of Biochemistry and Center for Molecular Biosciences Innsbruck, Innsbruck, Austria; University Medical Center Groningen, University of Groningen, Section Systems Medicine of Metabolism and Signaling, Laboratory of Pediatrics, Groningen, The Netherlands; Carl von Ossietzky University Oldenburg, School of Medicine and Health Sciences, Department for Neuroscience, Oldenburg, Germany; ¹⁹⁵⁵University of Kansas Medical Center, Department of Otolaryngology, Kansas City, KS, USA; ¹⁹⁵⁶University of Nebraska Medical Center, Departments of Internal Medicine and Biochemistry and Molecular Biology, Omaha, NE, USA; ¹⁹⁵⁷University of Colorado School of Medicine, Department of Pharmacology, Aurora, CO, USA ; ¹⁹⁵⁸CSIR-Institute of Genomics and Integrative Biology, South Campus, New Delhi, India; ¹⁹⁵⁹Hannover Medical School, Institute for Molecular and Therapeutic Strategies (IMTTS), Hannover, Germany; ¹⁹⁶⁰University Medical Center G ttingen, Institute of Cellular Biochemistry, G ttingen, Germany; ¹⁹⁶¹South China Agricultural University, Guangdong Provincial Key Laboratory of Agro-animal Genomics and Molecular Breeding/Guangdong Provincial Sericulture and Mulberry Engineering Research Center, College of Animal Science, Guangzhou, China; ¹⁹⁶²University of Defense, Faculty of Military Health Sciences, Department of Radiobiology, Hradec Kralove, Czech Republic; ¹⁹⁶³University Hospital of Bonn, Institute of Reconstructive Neurobiology, Bonn, Germany; ¹⁹⁶⁴University of Antwerp, Department of Biomedical Sciences, Peripheral Neuropathy Research Group, Antwerp, Belgium; ¹⁹⁶⁵Concordia University, Department of Biology, Montreal, Quebec, Canada; ¹⁹⁶⁶Wayne State University School of Medicine, Department of Pharmacology, Detroit, MI, USA; ¹⁹⁶⁷University of Zaragoza, Faculty of Veterinary-IIS Arag n, IA2-CITA, CIBERNED, Laboratory of Genetics and Biochemistry (LAGENBIO), Zaragoza, Spain; ¹⁹⁶⁸Lewis Katz School of Medicine at Temple University, Center for Translational Medicine, Philadelphia, PA, USA; ¹⁹⁶⁹University of Oviedo, Department of Functional Biology, Physiology, Oviedo, Asturias, Spain; ¹⁹⁷⁰University of Belgrade, Institute for the Application of Nuclear Energy (INEP), Belgrade, Serbia; ¹⁹⁷¹Zhejiang University, Life Sciences Institute and Innovation Center for Cell Signaling Network, Hangzhou, China; ¹⁹⁷²Northwestern University, Feinberg School of Medicine, Department of Pathology, Chicago, IL, USA; ¹⁹⁷³The Francis Crick Institute, Molecular Cell Biology of Autophagy, London, UK; ¹⁹⁷⁴Oslo University Hospital, Institute for Cancer Research, Department of Molecular Cell Biology, Oslo, Norway; ¹⁹⁷⁵Centre de Recherche des Cordeliers, INSERM, Universit  de Paris, Sorbonne Universit , Paris, France; ¹⁹⁷⁶University of Michigan, Department of Internal Medicine, Ann Arbor, MI, USA; ¹⁹⁷⁷Nagoya University Graduate School of Medicine, Department of Pathology and Biological Responses, Nagoya, Japan; ¹⁹⁷⁸University of Belgrade, Faculty of Medicine, Institute of Microbiology and Immunology, Belgrade, Serbia; ¹⁹⁷⁹University Federico II of Naples, Department of Molecular Medicine and Medical Biotechnology, Naples, Italy; ¹⁹⁸⁰Universidade Federal do Rio de Janeiro, Institute of Biophysics Carlos Chagas Filho, Immunobiology Program, Rio de Janeiro, RJ, Brazil; ¹⁹⁸¹National and Kapodistrian University of Athens, Faculty of Biology, Department of Cell Biology and Biophysics, Panepistimiopolis, Athens, Greece; ¹⁹⁸²University of Bern, Institute of Pathology, Division of Experimental Pathology, Bern, Switzerland; ¹⁹⁸³Medical University of South Carolina, Department of Medicine, Division of Rheumatology & Immunology, Charleston, SC, USA; ¹⁹⁸⁴University of Hong Kong, Cardiology Division, Department of Medicine, Hong Kong, China; ¹⁹⁸⁵The University of Texas McGovern Medical School at Houston, Department of Neurobiology and Anatomy, Houston, TX, USA; ¹⁹⁸⁶University of Southampton , Biological Sciences, Faculty of Environmental and Life Sciences, Highfield, Southampton, UK; ¹⁹⁸⁷Universit  de Moncton, Department of Chemistry and Biochemistry, Moncton, NB, Canada; ¹⁹⁸⁸Joef Stefan Institute, Department of Biochemistry and Molecular and Structural Biology, Ljubljana, Slovenia; ¹⁹⁸⁹University of Melbourne, Florey Institute of Neuroscience and Mental Health, Parkville, VIC, Australia; ¹⁹⁹⁰University of Birmingham, Institute of Cancer and Genomic Sciences, Birmingham, UK; ¹⁹⁹¹Weill Cornell Medicine, Department of Pathology and Laboratory Medicine, New York, NY, USA; ¹⁹⁹²Komarov Botanical Institute RAS, Laboratory of Molecular and Ecological Physiology, Saint Petersburg, Russian Federation; ¹⁹⁹³Nottingham Trent University, School of Science and Technology, Nottingham, UK; ¹⁹⁹⁴University of Oxford, John Radcliffe Hospital, Translational Gastroenterology Unit and Department of Paediatrics, Oxford, UK; ¹⁹⁹⁵Institute of Psychiatry and Neurology, First Department of Neurology, Warsaw, Poland; ¹⁹⁹⁶Sechenov First Moscow State Medical University, Institute for Regenerative Medicine, Moscow, Russia; ¹⁹⁹⁷Mie University, Graduate School of Bioresources, Tsu, Japan; ¹⁹⁹⁸University of Osnabr ck, Department of Biology/Chemistry, Osnabr ck, Germany; ¹⁹⁹⁹University of Liverpool, Department of Cellular and Molecular Physiology, Liverpool, UK; ²⁰⁰⁰University of T bingen, Center for Plant Molecular Biology (ZMBP), T bingen, Germany; ²⁰⁰¹University of South Florida, Morsani College of Medicine, Department of Molecular Medicine and USF Health Byrd Alzheimer's Research Institute, Tampa, FL, USA; Institute for Biological Instrumentation of Russian Academy of Sciences, Laboratory of New Methods in Biology, Pushchino, Moscow region, Russia; ²⁰⁰²University of Milan, Department of Biosciences, Milan, Italy; ²⁰⁰³University of Buenos Aires, Institute of Biochemistry and Molecular Medicine, Pathophysiology Department, School of Pharmacy and Biochemistry, CONICET, Buenos Aires, Argentina; ²⁰⁰⁴University of Oxford, Nuffield Department of Clinical Neurosciences, Oxford, UK; ²⁰⁰⁵Karolinska Institute, Department of Physiology and Pharmacology, Stockholm, Sweden; ²⁰⁰⁶University of Murcia, Internal Medicine Department; Biomedical Research Institute of Murcia IMIB-Virgen de la Arrixaca, Brain Regionalization and Development Gen Unit, Murcia, Spain; ²⁰⁰⁷University of Porto, Faculty of Pharmacy, UCIBIO, REQUIMTE, Porto, Portugal; ²⁰⁰⁸Fundaci n Instituto Leloir and IIBBA, CONICET, Buenos Aires, Argentina; Laboratorio de Glicobiolog a Celular y Gen tica Aplicada de Levaduras, Facultad de Ciencias Exactas y Naturales, Universidad de Buenos Aires, Argentina; ²⁰⁰⁹Columbia University, Vagelos College of Physicians and Surgeons, Department of Pathology and Cell Biology, New York, NY, USA; ²⁰¹⁰Instituto de Investigaciones Biom dicas Alberto Sols (CSIC-UAM), Madrid, Spain; Centro de Investigaci n Biom dica en Red de Diabetes y Enfermedades Metab licas Asociadas (CIBERdem), Instituto de Salud Carlos III, Madrid, Spain; ²⁰¹¹Zhejiang University, School of Medicine, Department of Microbiology and Parasitology, Hangzhou, China; ²⁰¹²Vanderbilt University School of Medicine, Department of Pathology, Microbiology and Immunology, Nashville, TN, USA; ²⁰¹³Center of Translational Immunology, University Medical Center Utrecht, Utrecht, The Netherlands; ²⁰¹⁴Goethe University, Institute for

Experimental Cancer Research in Pediatrics, Frankfurt am Main, Germany; ²⁰¹⁵University Hospitals Leuven, Department of Neurology, Leuven, Belgium; KU Leuven, Department of Neurosciences, Leuven, Belgium; ²⁰¹⁶KU Leuven, Clinical Division and Laboratory of Intensive Care Medicine, Department of Cellular and Molecular Medicine, Leuven, Belgium; ²⁰¹⁷Instituto Oswaldo Cruz, LITEB/IOC, Fundação Oswaldo Cruz, FIOCRUZ, Rio de Janeiro, Brazil; ²⁰¹⁸University of Lausanne, Ludwig Institute for Cancer Research Lausanne, Department of Oncology UNIL CHUV, Laboratory of Immunoscience and Stem Cell Metabolism, Epalinges, Switzerland; ²⁰¹⁹Scientific Institute, IRCCS E. Medea, Laboratory of Molecular Biology, Bosio Parini, Lecco, Italy; ²⁰²⁰Icahn School of Medicine at Mount Sinai, Department of Oncological Sciences, New York, NY, USA; ²⁰²¹CSIC-UAM & CIBERER, Instituto de Investigaciones Biomédicas “Alberto Sols”, Neurobiology of Hearing Group, Madrid, Spain; ²⁰²²Universidade do Porto, i3S-Instituto de Investigação e Inovação em Saúde, Porto, Portugal; IPATIMUP - Institute of Molecular Pathology and Immunology of the University of Porto, Cancer Drug Resistance Group, Porto, Portugal; FFUP - Faculty of Pharmacy of the University of Porto, Department of Biological Sciences, Porto, Portugal; ²⁰²³Harvard Medical School, Ophthalmology, Boston, MA, USA; ²⁰²⁴University of Oviedo, Department of Morphology and Cell Biology, Oviedo, Spain; ²⁰²⁵Universitätsklinikum Essen, Institute for Cell Biology (Cancer Research), Essen, Germany; ²⁰²⁶National Center for Tumor Diseases (NCT), Partner Site Dresden, Germany; German Cancer Research Center (DKFZ), Heidelberg, Germany; Faculty of Medicine and University Hospital Carl Gustav Carus, Technische Universität Dresden, Dresden, Germany; Helmholtz Association/Helmholtz-Zentrum Dresden - Rossendorf (HZDR), Dresden, Germany; ²⁰²⁷Eötvös Loránd University (ELTE), Department of Genetics, Budapest, Hungary; ²⁰²⁸University of Groningen, University Medical Center Groningen, Department of Hematology, Groningen, The Netherlands; ²⁰²⁹Tuscia University, Department of Ecological and Biological Sciences (DEB), Viterbo, Italy; ²⁰³⁰EA 3842, Limoges University, Faculty of Medicine, Limoges cedex, France; ²⁰³¹Biomedical Research Foundation, Academy of Athens, Center of Clinical, Experimental Surgery and Translational Research, Athens, Greece; ²⁰³²Institut de Pharmacologie et de Biologie Structurale, UMR 5089 CNRS - Université de Toulouse, Toulouse, France; ²⁰³³University of Bristol, School of Biochemistry, Bristol, UK; ²⁰³⁴University of Pittsburgh, Department of Pathology, Pittsburgh, PA, USA; ²⁰³⁵RWTH Aachen University, Medical School, Institute of Biochemistry and Molecular Biology, Aachen, Germany; ²⁰³⁶Washington University in St. Louis, Department of Medicine, St. Louis, MO, USA; ²⁰³⁷Service of Endocrinology, University Hospital Doctor Peset, Foundation for the Promotion of Health and Biomedical Research in the Valencian Region (FISABIO)-Department of Physiology, University of Valencia, Valencia, Spain; ²⁰³⁸University of Montpellier, UMR 5235, Montpellier, France; ²⁰³⁹Universidade NOVA de Lisboa, CEDOC, NOVA Medical School, Faculdade de Ciências Médicas, Lisboa, Portugal; ²⁰⁴⁰University of Helsinki, Institute of Biotechnology, Electron Microscopy Unit, Helsinki, Finland; ²⁰⁴¹VIB-KU Leuven Center for Brain & Disease Research, Leuven, Belgium; KU Leuven, Department of Neurosciences, Leuven Brain Institute, Leuven, Belgium; ²⁰⁴²Vall d'Hebron Research Institute (VHIR)-Network Center for Biomedical Research in Neurodegenerative Diseases (CIBERNED)-Catalan Institution for Research and Advanced Studies (ICREA), Barcelona, Spain; ²⁰⁴³Institute of Biomedicine of Valencia, Spanish Research Council (CSIC), Valencia, Spain; ²⁰⁴⁴University Hospital La Paz Research Institute (IdiPAZ), Cancer and Human Molecular Genetics Area - Oto-Neurosurgery Research Group, Madrid, Spain; ²⁰⁴⁵University of Barcelona, Department of Biochemistry and Molecular Biomedicine, Barcelona, Spain; ²⁰⁴⁶Instituto de Investigaciones Biomédicas Alberto Sols; C.S.I.C./U.A.M.; Madrid, Spain; ²⁰⁴⁷University of Toulouse, Institute of Metabolic and Cardiovascular Diseases, INSERM UMR 1048, Toulouse, France; ²⁰⁴⁸Università Cattolica del Sacro Cuore, Institute of Histology and Embryology, Rome, Italy; ²⁰⁴⁹University of Zagreb School of Medicine, Department of Physiology and Croatian Institute for Brain Research, Zagreb, Croatia; ²⁰⁵⁰Italian Institute for Genomic Medicine (IIGM), Candiolo (TO), Italy; Candiolo Cancer Institute, FPO-IRCCS, Candiolo (TO), Italy; ²⁰⁵¹Simon Fraser University, Department of Chemistry, Department of Molecular Biology and Biochemistry, Burnaby, British Columbia, Canada; ²⁰⁵²Komarov Botanical Institute RAS, Laboratory of Molecular and Ecological Physiology, Saint Petersburg, Russian Federation; ²⁰⁵³CNR/IRCCS Fondazione Santa Lucia, Institute for Systems Analysis and Computer Science, Rome, Italy; ²⁰⁵⁴Eurac Research, Institute for Biomedicine, Bolzano, Italy; ²⁰⁵⁵Charité - Universitätsmedizin Berlin, Department of Anesthesiology and Intensive Care Medicine, Campus Charité Mitte and Campus Virchow-Klinikum, Berlin, Germany; ²⁰⁵⁶Maastricht University Medical Center, GROW School for Oncology, Department of Radiotherapy, Maastricht, The Netherlands; ²⁰⁵⁷Rheinische Friedrich-Wilhelms-Universität, Institut für Biochemie und Molekularbiologie (IBMB), Bonn, Germany; ²⁰⁵⁸Institute for Biological Research “Sinisa Stankovic”, University of Belgrade, Belgrade, Serbia; ²⁰⁵⁹University of Oxford, Oxford Parkinson's Disease Centre, Department of Physiology, Anatomy and Genetics, Oxford, UK; ²⁰⁶⁰Fukushima Medical University, School of Medicine, Department of Anatomy and Histology, Fukushima, Japan; ²⁰⁶¹National Institute of Neuroscience, National Center of Neurology and Psychiatry, Department of Peripheral Nervous System Research, Kodaira, Tokyo, Japan; ²⁰⁶²University of California, Los Angeles, Department of Integrative Biology and Physiology, Los Angeles, CA, USA; ²⁰⁶³The University of Queensland, School of Chemistry and Molecular Biosciences and Australian Infectious Diseases Research Centre, St. Lucia, Brisbane, Queensland, Australia; ²⁰⁶⁴Babraham Institute, Cambridge, UK; ²⁰⁶⁵University of Bonn, Department of Neurology, Molecular Cell Biology Unit, Bonn, Germany; ²⁰⁶⁶Universidad Autónoma de Madrid, Centro de Biología Molecular Severo Ochoa (CSIC-UAM & CIBERNED), Madrid, Spain; ²⁰⁶⁷St Jude Children's Research Hospital, Department of Pathology, Memphis, TN, USA; ²⁰⁶⁸Chang Gung University College of Medicine and Chang Gung Memorial Hospital, Department of Cardiology, Taoyuan City, Taiwan; National Health Research Institutes, Institute of Cellular and System Medicine, Zhunan, Taiwan; ²⁰⁶⁹China Pharmaceutical University, School of Life Science and Technology, Nanjing, Jiangsu, China; ²⁰⁷⁰University of California Los Angeles, School of Dentistry, Division of Oral Biology and Medicine, Los Angeles, CA, USA; ²⁰⁷¹Zhujiang Hospital of Southern Medical University, Department of Neurology, Guangzhou, Guangdong Province, China; ²⁰⁷²Southern Medical University, School of Basic Medical Sciences, Department of Bioinformatics, Guangzhou, China; ²⁰⁷³University of Michigan, Department of Internal Medicine, Division of Hematology and Oncology, Ann Arbor, MI, USA; ²⁰⁷⁴Shanghai Ninth People's Hospital, National Clinical Research Center for Oral Disease, Shanghai Jiao Tong University, School of Medicine, Shanghai, China; ²⁰⁷⁵Texas A&M College of Dentistry, Department of Endodontics, Dallas, TX, USA; ²⁰⁷⁶Third Military Medical University of China, Xinqiao Hospital, Institute of Respiratory Diseases, Chongqing, China; ²⁰⁷⁷Soochow University, Center for Circadian Clocks; School of Biology & Basic Medical Sciences, Medical College, Suzhou, Jiangsu, China; ²⁰⁷⁸CAS Center for Excellence in Nanoscience, CAS Key Laboratory for Biomedical Effects of Nanomaterials and Nanosafety, National Center for Nanoscience and Technology (NCNST), Zhongguancun, Beijing, China; ²⁰⁷⁹China Agricultural University, College of Biological Sciences, State Key Laboratory of Agro-Biotechnology and MOA Key Laboratory of Soil Microbiology, Beijing, China; ²⁰⁸⁰Soochow University, Hematology Center of Cyrus Tang Hematology Institute, School of Medicine, Suzhou, China; ²⁰⁸¹Johns Hopkins University, Department of Biochemistry and Molecular Biology, Baltimore, MD, USA; ²⁰⁸²China Academy of Chinese Medical Sciences, Artemisinin Research Center and the Institute of Chinese Materia Medica, Beijing, China; ²⁰⁸³Shanxi Agricultural University, Shanxi Key Laboratory of Ecological Animal Science and Environmental Veterinary Medicine, Taigu, Shanxi, China; ²⁰⁸⁴National University of Singapore, Yong Loo Lin School of Medicine, Department of Physiology, Singapore; ²⁰⁸⁵The Chinese University of Hong Kong, School of Public Health and Primary Care, Hong Kong, China; ²⁰⁸⁶Fourth Military Medical University, College of Stomatology, Department of Oral Anatomy and Physiology and TMD, Xi'an, China; ²⁰⁸⁷The First Affiliated Hospital, Jinan University, Guangzhou, China; ²⁰⁸⁸National University of Singapore, Department of Medicine, Cardiovascular Research Institute, Singapore; ²⁰⁸⁹Huazhong Agricultural University, College of Horticulture and Forestry Science, Key Laboratory of Horticultural Plant Biology (Ministry of Education), Wuhan, China; ²⁰⁹⁰Feinstein Institutes for Medical Research, Center for Immunology and Inflammation, Manhasset, NY, USA; ²⁰⁹¹Cleveland Clinic, Department of Cardiovascular Medicine/Heart and Vascular Institute, Cleveland, OH, USA;

- ²⁰⁹²Diabetes and Metabolism Research Institute, Department of Molecular & Cellular Endocrinology; City of Hope Medical Center, Beckman Research Institute, Comprehensive Cancer Center, Duarte, CA, USA; ²⁰⁹³University of Kentucky, Department of Ophthalmology and Visual Sciences, Lexington, KY, USA; ²⁰⁹⁴Xuzhou Medical University, Department of Anesthesiology, Xuzhou, Jiangsu, China; ²⁰⁹⁵Stanford University School of Medicine, Department of Neurosurgery, Palo Alto, CA, USA; ²⁰⁹⁶University of South Dakota, Division of Basic Biomedical Sciences, Vermillion, SD, USA; ²⁰⁹⁷Tsinghua University, School of Life Sciences, Beijing, China; ²⁰⁹⁸Department of Biomedical Sciences, College of Medicine, Florida State University, Tallahassee, FL 32306-4300; ²⁰⁹⁹Kaohsiung Medical University, School of Dentistry, College of Dental Medicine, Kaohsiung, Taiwan; ²¹⁰⁰University of Southampton, Faculty of Environmental and Life Sciences, Biological Sciences, and the Institute for Life Sciences, Southampton, UK; ²¹⁰¹Nanjing Agricultural University, College of Horticulture, Weigang NO. 1, Nanjing, China; ²¹⁰²Saint Louis University, Department of Biology, Saint Louis, MO, USA; ²¹⁰³Air Force Medical University, Xijing Hospital and School of Basic Medicine, Department of Pathology, State Key Laboratory of Cancer Biology, Xi'an, China; ²¹⁰⁴Affiliated Union Hospital of Fujian Medical University, Fuzhou, Fujian, China; ²¹⁰⁵Wenzhou Medical University, Key Laboratory of Biotechnology and Pharmaceutical Engineering, School of Pharmaceutical Sciences, Wenzhou, China; ²¹⁰⁶Queen Mary University, Blizard Institute, Flow Cytometry Core Facility, London, UK; ²¹⁰⁷Juntendo University Graduate School of Medicine, Department of Metabolism & Endocrinology, Bunkyo-ku, Tokyo, Japan; ²¹⁰⁸Chiba University Graduate School of Medicine, Department of General Medical Science, Chiba, Japan; ²¹⁰⁹University of Cincinnati College of Medicine, Cincinnati Children's Research Foundation, Division of Pulmonary Biology, Department of Pediatrics, Cincinnati, OH, USA; ²¹¹⁰University of Gdansk, Department of Molecular Biology, Gdansk, Poland; ²¹¹¹Department of Biological Sciences, University of Denver, Denver, CO, USA; ²¹¹²University of Pennsylvania, Department of Anesthesiology, Philadelphia, PA, USA; ²¹¹³Indiana University School of Medicine, Department of Pediatrics, Indianapolis, IN, USA; ²¹¹⁴Chinese Academy of Sciences, Institute of Biophysics, Beijing, China; ²¹¹⁵Affiliated Cancer Hospital and Institute of Guangzhou Medical University, Guangzhou, China; ²¹¹⁶Institute of Complex Systems, ICS-6 (Structural Biochemistry), Forschungszentrum Jülich, Jülich, Germany; ²¹¹⁷Washington University School of Medicine, Department of Neurology, St. Louis, MO, USA; ²¹¹⁸University of Bonn, Pharmaceutical Institute, Section Pharmacology and Toxicology, Bonn, Germany; ²¹¹⁹University Hospital RWTH Aachen, Institute of Molecular Pathobiochemistry, Experimental Gene Therapy and Clinical Chemistry (IFMPEGKC), Aachen, Germany; ²¹²⁰Univ of Pittsburgh and Pittsburgh VA HealthSystem, Department of Pathology, Pittsburgh, PA, USA; ²¹²¹Stanford University, Department of Ophthalmology, Stanford, CA, USA; ²¹²²Georg August University Göttingen, Institute of Microbiology and Genetics, Department of Genetics of Eukaryotic Microorganisms, Göttingen, Germany; ²¹²³Harvard Medical School and Brigham & Women's Hospital, Precision Neurology Program & APDA Center for Advanced Parkinson Research, Boston, MA, USA; ²¹²⁴University of Nottingham, School of Life Sciences, Queen's Medical Centre, Nottingham, UK; ²¹²⁵Scripps Research Institute, La Jolla, CA, USA; ²¹²⁶University of Cambridge, MRC Mitochondrial Biology Unit, Cambridge, UK; ²¹²⁷Forschungszentrum Jülich, Institute of Complex Systems (ICS-6), Jülich, Germany; Heinrich-Heine-Universität Düsseldorf Institut für Physikalische Biologie, Düsseldorf, Germany; ²¹²⁸Amsterdam University Medical Centers, Location AMC, Tytgat Institute for Intestinal Research, Department of Gastroenterology and Hepatology, Amsterdam, The Netherlands; ²¹²⁹Quadram Institute Bioscience, Norwich Research Park, Norwich, Norfolk, UK; ²¹³⁰University of Edinburgh, MRC Institute of Genetics and Molecular Medicine, Scotland, UK; ²¹³¹Queensland University of Technology, Centre for Tropical Crops and Biocommodities, Science and Engineering Faculty, Brisbane, Queensland, Australia; ²¹³²Royal Holloway University of London, Centre for Biomedical Sciences, Egham, Surrey, UK; ²¹³³MRC Laboratory of Molecular Biology, Cambridge, UK; ²¹³⁴National Institutes of Health, Laboratory of Clinical Immunology and Microbiology, National Institute of Allergy and Infectious Diseases, Bethesda, MD, USA; ²¹³⁵University of Nebraska-Lincoln, Department of Plant Pathology, Lincoln, NE, USA; ²¹³⁶Friedrich-Alexander-Universität Erlangen-Nürnberg (FAU), Department of Stem Cell Biology, Erlangen, Germany; ²¹³⁷University of Toronto, Faculty of Medicine, Department of Immunology, Toronto, ON, Canada; ²¹³⁸Department of Obstetrics and Gynecology, Weill Cornell Medicine, 1300 York Avenue, Box 35, New York, NY, United States.; ²¹³⁹National Medicines Institute, Department of Drug Biotechnology and Bioinformatics, Warszawa, Poland; ²¹⁴⁰MFP CNRS UMR 5234, University of Bordeaux, Bordeaux, France; ²¹⁴¹Institut Pasteur, Membrane Biochemistry and Transport, Paris, France; ²¹⁴²National University of Singapore, Yong Loo Lin School of Medicine, Department of Physiology, Singapore; National University Health System, Centre for Healthy Ageing, Singapore; ²¹⁴³School of Medicine, Shenzhen University, Shenzhen, China; ²¹⁴⁴University of Zurich, Institute of Experimental Immunology, Switzerland, Zurich; ²¹⁴⁵Southwest Medical University, Luzhou Key Laboratory of Activity Screening and Druggability Evaluation for Chinese Materia Medica, Jiangyang District, Luzhou, China; ²¹⁴⁶University of California San Diego, Department of Neurosciences, La Jolla, CA, USA; ²¹⁴⁷Weizmann Institute of Science, Department of Plant and Environmental Sciences, Rehovot, Israel; ²¹⁴⁸University of Maryland School of Medicine, Center for Shock, Trauma and Anesthesiology Research (STAR), Departments of Anesthesiology, Anatomy & Neurobiology, Baltimore, MD, USA; ²¹⁴⁹NHRI, Institute of Cellular and System Medicine, Zhunan, Taiwan; ²¹⁵⁰University of North Dakota, Biochemistry and Molecular Biology School of Medicine and Health Sciences, Grand Forks, ND, USA; ²¹⁵¹Wenzhou Medical University, State Key Laboratory of Ophthalmology, Optometry and Visual Science, School of Optometry and Ophthalmology and the Eye Hospital, Wenzhou, China; ²¹⁵²Soochow University, Department of Pathogenic Biology, Suzhou, Jiangsu Province, China; ²¹⁵³First Affiliated Hospital of Xi'an Jiaotong University School of Medicine, Center for Translational Medicine, Xi'an, Shaanxi, China; ²¹⁵⁴Zhejiang Provincial People's Hospital, Department of Endocrinology, Hangzhou, China; ²¹⁵⁵Umeå University, Umeå Centre for Microbial Research (UCMR), Department of Chemistry, Umeå, Sweden; ²¹⁵⁶Zhejiang University School of Medicine, Department of Toxicology of School of Public Health, and Department of Gynecologic Oncology of Women's Hospital, Hangzhou, China; ²¹⁵⁷The Broad Institute of Harvard and MIT, Massachusetts General Hospital, Harvard Medical School, Department of Molecular Biology, Cambridge, MA, USA; ²¹⁵⁸Zhejiang University, Department of Biochemistry in School of Medicine, Hangzhou, Zhejiang Province, China; ²¹⁵⁹Shenzhen University, College of Medicine, Shenzhen, Guangdong, China; ²¹⁶⁰The University of Hong Kong, Department of Anesthesiology, Queen Mary Hospital, Hong Kong, China; ²¹⁶¹Wuhan University, Key Laboratory of Combinatorial Biosynthesis and Drug Discovery, Ministry of Education, School of Pharmaceutical Sciences, Wuhan, China; ²¹⁶²Shanghai Jiao Tong University School of Medicine, Ruijin Hospital, Department of Otolaryngology & Head and Neck Surgery, Shanghai, China; ²¹⁶³Friedrich-Alexander University Erlangen-Nürnberg, University Hospital Erlangen, Department of Molecular Neurology, Erlangen, Germany; ²¹⁶⁴Research Department, National Neuroscience Institute, Singapore; ²¹⁶⁵Southern University of Science and Technology, Department of Biology, Shenzhen, China; ²¹⁶⁶Sichuan University, West China Hospital, Centre of Geriatrics and Gerontology, Chengdu, China; ²¹⁶⁷University of Electronic Science and Technology of China, School of Medicine, Chengdu, China; Sichuan Cancer Hospital @ Institute, Department of Clinical Pharmacy, Sichuan Cancer Center; ²¹⁶⁸Wenzhou Medical University, School of Pharmaceutical Sciences, Wenzhou, China; ²¹⁶⁹Sun Yat-sen University, School of Life Sciences, Guangdong Provincial Key Laboratory of Plant Resources, State Key Laboratory of Biocontrol, Guangzhou, China; ²¹⁷⁰Queensland University of Technology, Institute of Health and Biomedical Innovation, Kelvin Grove, Brisbane, Queensland, Australia; ²¹⁷¹South China Agricultural University, College of Veterinary Medicine, Guangzhou, Guangdong, China; ²¹⁷²Southwest Hospital, Third Military Medical University (Army Medical University), Key Laboratory of Hepatobiliary and Pancreatic Surgery, Institute of Hepatobiliary Surgery, Chongqing, China; ²¹⁷³University of Alabama at Birmingham, Division of Cardiovascular Disease, Department of Medicine, Birmingham, AL, USA; ²¹⁷⁴Shanghai Jiao Tong University, School of Life Sciences and Biotechnology, Shanghai, China; ²¹⁷⁵Georgia State University, The Center for Molecular and Translation Medicine, Atlanta, GA, USA; ²¹⁷⁶Biomedical Research Foundation of the Academy of Athens (BRFAA), Center of

Clinical, Experimental Surgery, & Translational Research, Athens, Greece; ²¹⁷⁷Shanghai Sixth People's Hospital, Department of Cardiovascular Medicine, and Shanghai Jiaotong University School of Medicine, Shanghai Institute of Immunology, Shanghai, China; ²¹⁷⁸Institute of Neurosciences and Department of Neurology of the Second Affiliated Hospital of Guangzhou Medical University, Guangzhou, China; ²¹⁷⁹University of Michigan, Department of Molecular, Cellular and Developmental Biology, Ann Arbor, MI, USA; ²¹⁸⁰Purdue University, Department of Botany and Plant Pathology, West Lafayette, IN, USA; ²¹⁸¹Shanghai Jiao Tong University School of Medicine, Shanghai General Hospital, Department of Orthopedics, Shanghai, China; Shanghai Bone Tumor Institution, Shanghai, China; ²¹⁸²University of Kansas, Department of Molecular Biosciences, and University of Kansas Medical School, University of Kansas Cancer Center, Department of Radiation Oncology, Lawrence, KS, USA; ²¹⁸³Jinan University, College of Life Science and Technology, Guangzhou, China; ²¹⁸⁴Yangzhou University, College of Veterinary Medicine, Jiangsu Province, China; ²¹⁸⁵Huazhong University of Science and Technology, College of Life Science and Technology, Hubei Bioinformatics and Molecular Imaging Key Laboratory, Key Laboratory of Molecular Biophysics of Ministry of Education, Wuhan, Hubei, China; ²¹⁸⁶Kyoto Institute of Technology, Department of Applied Biology, Matsugasaki, Sakyo-ku, Kyoto, Japan; ²¹⁸⁷Ehime University Graduate School of Medicine, Department of Cardiology, Pulmonology, Hypertension & Nephrology, Shitsukawa, Toon, Ehime, Japan; ²¹⁸⁸Columbia University, Department of Neurology, and Pathology and Cell Biology, New York, NY, USA; ²¹⁸⁹Juntendo University School of Medicine, Department of Gastroenterology, Bunkyo-ku, Tokyo, Japan; ²¹⁹⁰National Cheng Kung University, College of Medicine, Department of Physiology, Tainan City, Taiwan; ²¹⁹¹University of Virginia, Departments of Medicine, Pharmacology, Molecular Physiology & Biological Physics, Center for Skeletal Muscle Research at Robert M. Berne Cardiovascular Research Center, University of Virginia School of Medicine, Charlottesville, VA, USA; ²¹⁹²Asahikawa Medical University, Department of Ophthalmology, Hokkaido, Japan; ²¹⁹³Hong Kong Baptist University, Mr. and Mrs. Ko Chi Ming Centre for Parkinson's Disease Research, School of Chinese Medicine, Hong Kong, China; ²¹⁹⁴Nathan Kline Institute for Psychiatric Research, Center for Dementia Research, Orangeburg, NY; New York University Langone Health, Department of Psychiatry, New York, NY, USA; ²¹⁹⁵University of Wisconsin-Madison, Department of Surgery, Madison, WI, USA; ²¹⁹⁶Chinese Academy of Sciences, Shanghai Institutes for Biological Sciences, Shanghai Institute of Nutrition and Health, Laboratory of Molecular Cardiology, Shanghai, China; ²¹⁹⁷Capital Medical University, School of Basic Medical Sciences, Department of Neurobiology, Beijing, China; ²¹⁹⁸University of Kentucky, Department of Cancer Biology & Toxicology, Lexington, KY, USA; ²¹⁹⁹University of Alabama at Birmingham, Department of Medicine, Division of Cardiovascular Disease, Birmingham, AL, USA; ²²⁰⁰Shenyang Pharmaceutical University, Department of Pharmacology, Shenyang, China; ²²⁰¹University of Iowa Carver College of Medicine, Fraternal Order of Eagles Diabetes Research Center, Department of Anatomy and Cell Biology, Iowa City, IA, USA; ²²⁰²The Fourth Military Medical University, Xijing Hospital, Department of Orthopaedics, Xi'an, China; ²²⁰³Shandong Cancer Hospital and Institute, Cancer Research Center, Jinan, Shandong Province, China; ²²⁰⁴Taipei Medical University, College of Medical Science and Technology, Graduate Institute of Cancer Biology and Drug Discovery, Taipei, Taiwan; ²²⁰⁵The Fourth Military Medical University, Tangdu Hospital, Department of Experimental Surgery, Xi'an, Shaanxi, China; ²²⁰⁶Chung Shan Medical University, Institute of Medicine, Taichung, Taiwan; ²²⁰⁷Jiangsu University, School of Medicine, Zhenjiang, Jiangsu, China; ²²⁰⁸Jinan University, Medical College, Key Laboratory for Regenerative Medicine of the Ministry of Education, Division of Histology and Embryology, Guangzhou, China; ²²⁰⁹Hangzhou Normal University, Department of Pharmacology, Hangzhou, Zhejiang, China; ²²¹⁰University of Southeast, School of Medicine, Department of Pharmacology, Nanjing, Jiangsu, China; ²²¹¹University of Melbourne, Bio21 Molecular Science and Biotechnology Institute, Parkville, Victoria, Australia; ²²¹²Chinese University of Hong Kong, School of Biomedical Sciences, Hong Kong, China; ²²¹³Kunming Institute of Zoology, Key Laboratory of Animal Models and Human Disease Mechanisms of the Chinese Academy of Sciences & Yunnan Province, Kunming, Yunnan, China; ²²¹⁴Fourth Medical Center of the Chinese PLA General Hospital, Trauma Research Center, Beijing, China; ²²¹⁵Nagoya City University Graduate School of Medical Sciences, Department of Nephro-urology, Nagoya, Aichi, Japan; ²²¹⁶Duke-NUS Medical School, Cardiovascular and Metabolic Disorders Program, Singapore, Singapore; ²²¹⁷Zhejiang University School of Medicine, Department of Biochemistry, and Department of Hepatobiliary and Pancreatic Surgery of the First Affiliated Hospital, Hangzhou, China; ²²¹⁸Indiana University School of Medicine, Department of Pathology and Laboratory Medicine, Indianapolis, IN, USA; ²²¹⁹Iowa State University, Department of Genetics, Development and Cell Biology, Ames, IA, USA; ²²²⁰Zhejiang University, College of Pharmaceutical Sciences, Hangzhou, China; ²²²¹Soochow University, College of Pharmaceutical Sciences, Department of Pharmacology, Suzhou, Jiangsu, China; ²²²²The University of British Columbia, Department of Biochemistry and Molecular Biology, Vancouver, BC, Canada; ²²²³The University of Hong Kong, Queen Mary Hospital, Department of Paediatrics and Adolescent Medicine, Pokfulam, Hong Kong, China; ²²²⁴Dong-A University College of Medicine, Department of Anatomy and Cell Biology, Busan, Korea; ²²²⁵The Jikei University School of Medicine, Department of Biochemistry, Minato-ku, Tokyo, Japan; ²²²⁶ETH Zürich, Institute of Biochemistry, Zürich, Switzerland; ²²²⁷Osaka University, Graduate School of Medicine, Department of Genetics, Suita, Osaka, Japan; ²²²⁸Tabriz University of Medical Sciences, Molecular Medicine Research Center, Tabriz, Iran; ²²²⁹Hwa Chong Institution, Singapore, Singapore; ²²³⁰Tianjin University of Traditional Chinese Medicine, Tianjin State Key Laboratory of Modern Chinese Medicine, Tianjin, China; ²²³¹Temple University, Center for Metabolic Disease Research and Department of Physiology, Philadelphia, PA, USA; ²²³²The Chinese University of Hong Kong, State Key Laboratory of Digestive Disease, Department of Medicine and Therapeutics, Hong Kong, China; ²²³³Tsinghua University, School of Life Sciences, Tsinghua University-Peking University Joint Center for Life Sciences, State Key Laboratory of Membrane Biology, Beijing, China; ²²³⁴Kaohsiung Medical University, Center for Cancer Research and School of Medicine, College of Medicine, Kaohsiung, Taiwan; ²²³⁵National University of Singapore, Faculty of Sciences, Department of Pharmacy, Singapore; ²²³⁶University of Toronto, Centre for Addiction and Mental Health, Toronto, Ontario, Canada; ²²³⁷Third Military Medical University, Department of Occupational Health, Chongqing, China; ²²³⁸Air Force Medical University, Xijing Hospital, Department of Plastic and Reconstructive Surgery, Xi'an, China; ²²³⁹Interdisciplinary Research Center on Biology and Chemistry, Shanghai Institute of Organic Chemistry, Chinese Academy of Sciences, 201203 Shanghai, China; Department of Cell Biology, Harvard Medical School, Boston, MA, USA; ²²⁴⁰Central South University, The Second Xiang-Ya Hospital, National Clinical Research Center for Metabolic Diseases, Department of Metabolism and Endocrinology, Changsha, Hunan, China; ²²⁴¹Kaohsiung Medical University, Graduate Institute of Medicine, Kaohsiung, Taiwan; ²²⁴²First Affiliated Hospital of Nanjing Medical University, Jiangsu Province Hospital, Nanjing, China; ²²⁴³Beijing Institute of Basic Medical Sciences, Beijing, China; ²²⁴⁴City University of Hong Kong, Department of Biomedical Sciences, Hong Kong, China; ²²⁴⁵Icahn School of Medicine at Mount Sinai, Departments of Neurology and Neuroscience, New York, NY, USA; ²²⁴⁶Dong-A University, College of Medicine, Department of Biochemistry, Busan, Korea; ²²⁴⁷University of Michigan, Department of Internal Medicine, Ann Arbor, MI, USA; ²²⁴⁸University of Michigan, Department of Ophthalmology and Visual Sciences, Ann Arbor, MI, USA; ²²⁴⁹Centre for Genomic Regulation (CRG), Department of Cell and Developmental Biology, Barcelona, España; ²²⁵⁰Laboratory of Pain and Signaling, Butantan Institute, Sao Paulo, SP, Brazil; Stanford University, Department of Anesthesiology, Perioperative and Pain Medicine, Stanford, CA, USA; ²²⁵¹University of Brescia, Department of Molecular and Translational Medicine, Brescia, Italy; ²²⁵²Cancer Research UK Beatson Institute, Glasgow, UK; University of Glasgow, Institute of Cancer Sciences, Glasgow, UK; ²²⁵³University of Texas Southwestern Medical Center, Department of Surgery, Dallas, TX, USA; ²²⁵⁴University of Zaragoza, CIBERNED, IA2-CITA, Faculty of Veterinary-IIS Aragón, Laboratory of Genetics and Biochemistry (LAGENBIO), Zaragoza, Spain; ²²⁵⁵University of Cambridge, Cambridge Biomedical Campus, MRC Mitochondrial Biology Unit, Cambridge, UK; ²²⁵⁶University of California, Davis, Department of Pathology and Laboratory Medicine, Shriners Hospitals for

Children, Institute for Pediatric Regenerative Medicine, Sacramento, CA, USA; ²²⁵⁷Tabriz University of Medical Sciences, Faculty of Advanced Medical Sciences, Department of Medical Nanotechnology, Tabriz, Iran; ²²⁵⁸University of Monastir, Faculty of Medicine, Biochemistry Laboratory, Monastir, Tunisia; ²²⁵⁹University of Virginia, Department of Neuroscience, Charlottesville, VA, USA; ²²⁶⁰Army Medical University (Third Military Medical University), Daping Hospital, Center of Bone Metabolism and Repair, State Key Laboratory of Trauma, Burns and Combined Injury, Trauma Center, Research Institute of Surgery, Laboratory for the Prevention and Rehabilitation of Military Training Related Injuries, Chongqing, China; ²²⁶¹University of Arizona, Department of Pharmacology and Toxicology, Tucson, AZ, USA; ²²⁶²University of Oxford, Kennedy Institute of Rheumatology, Oxford, UK; ²²⁶³Chinese Academy of Sciences, Institute of Biophysics, National Laboratory of Biomacromolecules, Beijing, China; ²²⁶⁴Zhejiang University School of Medicine, Department of Pathology, Hangzhou, China; ²²⁶⁵University of Science & Technology of China, School of Life Sciences, Hefei, Anhui, China; ²²⁶⁶Rutgers Robert Wood Johnson Medical School, Department of Neuroscience and Cell Biology, Piscataway, NJ, USA; ²²⁶⁷Thomas Jefferson University/Vickie & Jack Farber Institute for Neuroscience, Hospital for Neuroscience, Philadelphia, PA, USA; ²²⁶⁸Soochow University, Department of Pharmacology and Laboratory of Cerebrovascular Pharmacology, College of Pharmaceutical Science, Suzhou, Jiangsu, China; ²²⁶⁹People's Hospital of Hangzhou Medical College, Zhejiang Provincial People's Hospital, Department of Oncology, Hangzhou, China; Zhejiang Provincial People's Hospital, Clinical Research Institute, Key Laboratory of Tumor Molecular Diagnosis and Individualized Medicine of Zhejiang Province, Hangzhou, China; ²²⁷⁰University of Alabama at Birmingham, Department of Pathology, Birmingham, AL, USA; ²²⁷¹School of Radiation Medicine and Protection and State Key Laboratory of Radiation Medicine and Protection, Soochow University, Suzhou, China; ²²⁷²The Chinese University of Hong Kong, Department of Anaesthesia and Intensive Care, Hong Kong, China; ²²⁷³Huazhong Agricultural University, School of Veterinary Medicine/ Biomedical Center, Hongshan, Wuhan, China; ²²⁷⁴Henan University of Technology, College of Bioengineering, Zhengzhou, China; ²²⁷⁵Huazhong University of Science and Technology, College of Life Science and Technology, Key Laboratory of Molecular Biophysics of Ministry of Education, Wuhan, Hubei, China; ²²⁷⁶Chinese Academy of Sciences Center for Excellence in Molecular and Cellular Sciences, Shanghai Institute of Biochemistry and Cell Biology, Shanghai, China; ²²⁷⁷University of Utah, Huntsman Cancer Institute and Department of Oncological Sciences, Salt Lake City, UT, USA; ²²⁷⁸The University of Texas Health Science Center at Houston (UTHealth), McGovern Medical School, The Brown Foundation Institute of Molecular Medicine, Department of Neurobiology and Anatomy, Programs in Human and Molecular Genetics and Neuroscience of the MD Anderson UTHealth GSBS, Houston, TX, USA; ²²⁷⁹Wake Forest Baptist Comprehensive Cancer Center, Department of Cancer Biology, Winston-Salem, NC, USA; ²²⁸⁰Zhejiang University, College of Pharmaceutical Sciences, Institute of Pharmacology and Toxicology, Hangzhou, Zhejiang, China; ²²⁸¹The Second Affiliated Hospital and Yuying Children's Hospital of Wenzhou Medical University, Department of Orthopaedics, Wenzhou, Zhejiang Province, China; ²²⁸²Chinese Academy of Sciences, Hefei Institute of Physical Sciences, High Magnetic Field Laboratory, Hefei, Anhui Province, China; ²²⁸³Department of Pulmonary Medicine, Xijing Hospital, The Fourth Military Medical University, Xi'an, Shaanxi, China; ²²⁸⁴University of Newcastle, School of Biomedical Sciences and Pharmacy, NSW, Australia; ²²⁸⁵University of Houston, College of Pharmacy, Department of Pharmacological & Pharmaceutical Sciences, Houston, TX, USA; ²²⁸⁶University of Maryland, Molecular Virology Laboratory, VA-MD College of Veterinary Medicine, College Park, MD, USA; ²²⁸⁷University of Colorado Anschutz Medical Campus, Department of Pharmacology, Aurora, CO, USA; ²²⁸⁸Nanjing Medical University, Nanjing First Hospital, Department of Neurology, Nanjing, China; ²²⁸⁹Lanzhou University, School of Life Sciences, Lanzhou, China; ²²⁹⁰Sichuan University, West China School of Basic Medical Sciences & Forensic Medicine, Chengdu, China; ²²⁹¹East China Normal University, Key Laboratory of Adolescent Health Assessment and Exercise Intervention of Ministry of Education, Shanghai, China; ²²⁹²Nanjing Agricultural University, College of Plant Protection, Department of Plant Pathology, Nanjing, China; ²²⁹³Rutgers University, Department of Surgery, New Brunswick, NJ, USA; ²²⁹⁴Nanjing University of Chinese Medicine, Nanjing, China; ²²⁹⁵Central China Normal University, College of Life Sciences, Wuhan, Hubei Province, China; ²²⁹⁶Beijing Academy of Agriculture and Forestry Sciences, Institute of Plant and Environment Protection, Beijing, China; ²²⁹⁷Chinese Academy of Sciences, Institute of Zoology, State Key Laboratory of Stem Cell and Reproductive Biology, Beijing, China; ²²⁹⁸Shandong University, School of Life Sciences, Shandong Provincial Key Laboratory of Animal Cells and Developmental Biology, Qingdao, China; ²²⁹⁹Peking University Health Sciences Center, Department of Biochemistry and Molecular Biology, Beijing, China; ²³⁰⁰Zhejiang University, the First Affiliated Hospital, Hangzhou, Zhejiang, China; ²³⁰¹Beijing Institute of Genomics, Chinese Academy of Sciences, Beijing, China; ²³⁰²University of Sydney, Westmead Institute for Medical Research, Centre for Transplant and Renal Research, Sydney NSW, Australia; ²³⁰³Shenzhen University, Health Science Center, School of Pharmaceutical Sciences, Shenzhen, Guangdong, China; ²³⁰⁴Wuhan University, Department of Cell Biology, College of Life Sciences, Wuhan, Hubei, China; ²³⁰⁵University of Calgary, Cumming School of Medicine, Libin Cardiovascular Institute of Alberta, Departments of Biochemistry & Molecular Biology and Physiology & Pharmacology, Calgary, Alberta, Canada; ²³⁰⁶Children's Hospital Medical Center, Division of Experimental Hematology and Cancer Biology, Cincinnati, OH, USA; ²³⁰⁷China Pharmaceutical University, State Key Laboratory of Natural Medicines, Nanjing, Jiangsu, China; ²³⁰⁸Karolinska Institute, Division of Toxicology, Institute of Environmental Medicine, Stockholm, Sweden; Lomonosov Moscow State University, Faculty of Basic Medicine, Moscow, Russia; ²³⁰⁹Shanghai Jiaotong University School of Medicine, Shanghai, China; ²³¹⁰Southwest Medical University, Department of Medical Cellular Biology, Luzhou, Sichuan, China; ²³¹¹Massachusetts General Hospital, Department of Medicine, Diabetes Unit and Center for Genomic Medicine, Boston, MA, USA; Harvard Medical School, Department of Medicine, Boston, MA, USA; ²³¹²Wuhan University, School and Hospital of Stomatology, Department of Oral Medicine, Wuhan, Hubei, China; ²³¹³Chinese People's Liberation Army General Hospital, Department of Cardiology, Beijing, China; ²³¹⁴Third Military Medical University, College of Pharmacy, Department of Pharmacology, Chongqing, China; ²³¹⁵Huazhong Agricultural University, College of Veterinary Medicine, State Key Laboratory of Agricultural Microbiology, Wuhan, China; ²³¹⁶Zhejiang University, Department of Horticulture, Hangzhou, China; ²³¹⁷Guangxi Medical University, School of Preclinical Medicine, Department of Physiology, Nanning, China; ²³¹⁸Zhejiang University, MOA Key Laboratory of Animal Virology, Hangzhou, Zhejiang, China; ²³¹⁹The Second Affiliated Hospital and Yuying Children's Hospital of Wenzhou Medical University, Department of Orthopaedics, Wenzhou, Zhejiang, China; ²³²⁰Wuhan University, Hubei Key Laboratory of Cell Homeostasis, College of Life Sciences, Wuhan, China; ²³²¹Peking University First Hospital, Renal Division, Xi Cheng District, Beijing, China; ²³²²Chinese Academy of Sciences, Guangzhou Institutes of Biomedicine and Health, CAS Key Laboratory of Regenerative Biology, Guangzhou, China; ²³²³Queensland University of Technology, Institute of Health and Biomedical Innovation, Brisbane, QLD, Australia; ²³²⁴Texas A&M University, Institute of Biosciences and Technology, Houston, TX, USA; ²³²⁵Soochow University, Laboratory Animal Center, Suzhou, Jiangsu Province, China; ²³²⁶Zhejiang University School of Medicine, Department of Environmental Medicine, Hangzhou, Zhejiang Province, China; ²³²⁷University at Buffalo, The State University of New York, Department of Physiology and Biophysics, Buffalo, NY, USA; ²³²⁸Zhengzhou University, Third Affiliated Hospital and Institute of Neuroscience, Henan Key Laboratory of Child Brain Injury, Zhengzhou, China; Gothenburg University, Institute of Neuroscience and Physiology, Gothenburg, Sweden; ²³²⁹Nanjing Medical University, Department of Physiology, Nanjing, Jiangsu, China; ²³³⁰University of Kentucky, College of Medicine, Department of Molecular and Cellular Biochemistry, Lexington, KY, USA; ²³³¹Shanghai Jiao Tong University, Bio-X Institutes, Shanghai, China; ²³³²The Ohio State University, Department of Surgery, Columbus, OH, USA; ²³³³Shenzhen University Medical School, Department of Biochemistry and Molecular Biology, Shenzhen, China; ²³³⁴State Key Laboratory of Medicinal Chemical Biology, Tianjin

- 2460 Key Laboratory of Protein Science, College of Life Sciences, Nankai University, Tianjin, China; ²³³⁵University California, San Diego, Division of Biological Sciences, Section of Molecular Biology, CA, USA; ²³³⁶University Medical Center of Johannes Gutenberg-University, Institute for Virology, Mainz, Germany; ²³³⁷University of Padova, Biology Department, Padova, Italy; ²³³⁸Polish Academy of Sciences, Institute of Biochemistry and Biophysics, Warsaw, Poland; ²³³⁹Rutgers University, Department of Chemical Biology, Ernest Mario School of Pharmacy, Piscataway, NJ, USA; ²³⁴⁰Moscow State University, A.N.Belozersky Institute of Physico-Chemical Biology, Department of Functional Biochemistry of Biopolymers, Moscow, Russia; ²³⁴¹Institute for Research in Biomedicine (IRB Barcelona), Barcelona, Spain; ²³⁴²Universitat de Barcelona, Departament de Bioquímica i Biomedicina Molecular, Barcelona, Spain; CIBER de Diabetes y Enfermedades Metabólicas Asociadas (CIBERDEM), Instituto de Salud Carlos III, Madrid, Spain; ²³⁴³University of Michigan, Departments of Surgery and Pathology, Ann Arbor, MI, USA; ²³⁴⁴South China Normal University, College of Biophotonics, MOE Key Laboratory of Laser Life Science & Institute of Laser Life Science, Guangzhou, China; ²³⁴⁵South China Normal University, College of Biophotonics, Guangdong Provincial Key Laboratory of Laser Life Science, Guangzhou, China; ²³⁴⁶The University of Queensland, Queensland Brain Institute, Clem Jones Centre for Ageing Dementia Research, Brisbane, Australia; ²³⁴⁷University of Innsbruck, Division of Cell Metabolism and Differentiation Research, Research Institute for Biomedical Aging Research, Innsbruck, Austria; ²³⁴⁸Danish Cancer Society Research Center, RNA and Autophagy group, Copenhagen, Denmark; ²³⁴⁹Universidad Mayor, Center for Integrative Biology, Chile; ²³⁵⁰University of Crete, School of Medicine, Laboratory of Clinical Microbiology and Microbial Pathogenesis, Voutes, Heraklion, Crete, Greece; ²³⁵¹Federal University of São Paulo, Department of Medicine, Nephrology Division, Laboratory of Clinical and Experimental Immunology, São Paulo, SP, Brazil; ²³⁵²University Nove de Julho, Faculty of Pharmacy, São Paulo, SP, Brazil; ²³⁵³University of Michigan, Life Sciences Institute, Ann Arbor, MI USA; ²³⁵⁴University of Miami, Department of Surgery, Miami, FL, USA; ²³⁵⁵University of Sao Paulo, Institute of Biomedical Sciences, Sao Paulo, SP, Brazil; ²³⁵⁶University of Rome Tor Vergata, Department of Biology, Rome, Italy; ²³⁵⁷Universidade de Lisboa, Faculty of Pharmacy, Research Institute for Medicines (iMed.Ulisboa), Lisboa, Portugal; ²³⁵⁸The Norwegian Radium Hospital, Institute for Cancer Research, Department of Molecular Cell Biology, Montebello, Oslo, Norway; ²³⁵⁹University of Oslo, Faculty of Medicine, Institute of Clinical Medicine, Centre for Cancer Cell Reprogramming, Oslo, Norway; ²³⁶⁰Telethon Institute of Genetics and Medicine (TIGEM), Naples, Italy; ²³⁶¹OncoRay National Center for Radiation Research in Oncology, Faculty of Medicine, Technische Universität Dresden, Dresden, Germany; ²³⁶²Autonomous University of Madrid (UAM), Department of Biochemistry and Centro de Investigación Biomédica en Red sobre Enfermedades Neurodegenerativas (CIBERNED), Madrid, Spain; ²³⁶³University of South Florida, Morsani College of Medicine, Department of Molecular Medicine, Tampa, FL, USA; ²³⁶⁴University of Dundee School of Medicine, Division of Cellular Medicine, Dundee, Scotland, UK; ²³⁶⁵Department of Pharmacology and Toxicology, Faculty of Pharmacy, Ain Shams University, Cairo, Egypt; ²³⁶⁶Department of Experimental Oncology, European Institute of Oncology, Milan, Italy; ²³⁶⁷University of Naples Federico II, Department of Chemical, Materials and Industrial Production Engineering, Naples, Italy; ²³⁶⁸Telethon Institute of Genetics and Medicine (TIGEM), Naples, Italy; ²³⁶⁹Telethon Institute of Genetics and Medicine (TIGEM), Pozzuoli, Naples, Italy; ²³⁷⁰National Institute for Infectious Diseases 'L. Spallanzani' IRCCS, Rome, Italy; ²³⁷¹University of Texas Southwestern Medical Center, Center for Autophagy Research, Department of Internal Medicine, Dallas, TX, USA; ²³⁷²University of Extremadura, Centro de Investigación en Red de Enfermedades Neurodegenerativas (CIBERNED), Instituto de Investigación Biosanitaria de Extremadura (INUBE), Department of Biochemistry, Molecular Biology and Genetics, Faculty of Nursing and Therapy, Cáceres, Spain; ²³⁷³Department of Cell Death and Proliferation, Institute of Biomedical Research of Barcelona (IIBB- CSIC); Liver Unit, Hospital Clinic i Provincial de Barcelona, IDIBAPS, CIBEREHD, Barcelona, Spain; ²³⁷⁴University Côte d Azur (UCA), Institute for Research on Cancer and Aging of Nice (IRCAN), Centre National de la Recherche Scientifique (CNRS) UMR7284, Institut National de la Santé et de la Recherche Médicale (INSERM) U1081, Nice, France; ²³⁷⁵Max Planck Institute for Biology of Ageing, Cologne, Germany; ²³⁷⁶University of Innsbruck, Institute of Biochemistry and Center for Molecular Biosciences Innsbruck, Innsbruck, Austria; ²³⁷⁷University Medical Center Groningen, University of Groningen, Laboratory of Pediatrics, Section Systems Medicine of Metabolism and Signaling, Groningen, The Netherlands; ²³⁷⁸Barcelona Institute of Science and Technology (BIST), Institute for Research in Biomedicine (IRB Barcelona), Barcelona, Spain; ²³⁷⁹CIBER de Diabetes y Enfermedades Metabólicas Asociadas, Barcelona, Spain; ²³⁸⁰Universitat de Barcelona, Facultat de Biologia, Departament de Bioquímica i Biomedicina Molecular, Barcelona, Spain; ²³⁸¹Taipei Medical University, College of Medicine, Graduate Institute of Medical Sciences, Taipei, Taiwan; ²³⁸²Karolinska Institutet, Department of neurobiology, care sciences and society, Solna, Stockholm, Sweden; ²³⁸³The First Hospital of Jilin University, Department of ear, nose and throat, Changchun, Jilin, China; ²³⁸⁴German Center for Neurodegenerative Diseases (DZNE), Bonn, Germany; ²³⁸⁵Ben-Gurion University of the Negev, Faculty of Health Sciences, Department of Clinical Biochemistry and Pharmacology, Beer Sheva, Israel; ²³⁸⁶Eötvös Loránd University, Department of Anatomy, Cell and Developmental Biology, Budapest, Hungary; ²³⁸⁷Medical University of Graz, Division of Cell Biology, Histology and Embryology, Gottfried Schatz Research Center, Graz, Austria; ²³⁸⁸Université de Paris, Paris Cardiovascular Center - PARCC, Paris, France; ²³⁸⁹Hungarian Academy of Sciences, Budapest, Hungary; ²³⁹⁰Department of Anatomy, Cell and Developmental Biology, Eötvös Loránd University, Budapest, Hungary; ²³⁹¹University of New Mexico Health Sciences Center?, Autophagy, Inflammation, and Metabolism (AIM) center, Department of Molecular Genetics and Microbiology, Albuquerque, NM, USA; ²³⁹²Universidad de Zaragoza, IA2, IIS, Laboratorio de Genética Bioquímica (LAGENBIO), Zaragoza, Spain; ²³⁹³Universidad de Zaragoza, IA2, IIS, Centro de Encefalopatías y Enfermedades Transmisibles Emergentes, Zaragoza, Spain; ²³⁹⁴Fondazione Policlinico Universitario "Agostino Gemelli" IRCCS, Rome, Italy; ²³⁹⁵University of León, Institute of Biomedicine, León, Spain; ²³⁹⁶Centro de Investigación Biomédica en Red de Enfermedades Hepáticas y Digestivas (CIBERehd), Madrid, Spain; ²³⁹⁷Metabolism and Cancer Laboratory, Molecular Mechanisms and Experimental Therapy in Oncology Program (Oncobell), Institut d'Investigació Biomèdica de Bellvitge - IDIBELL, L Hospitalet de Llobregat, Barcelona, Spain; ²³⁹⁸University of Campania "Luigi Vanvitelli", Department of Precision Medicine, Naples, Italy; ²³⁹⁹University of Las Palmas de Gran Canaria, Department of Physical Education and Research Institute of Biomedical and Health Sciences (IUIBS), Las Palmas de Gran Canaria, Spain; ²⁴⁰⁰European Institute of Oncology (IEO) IRCCS, Department of Experimental Oncology, Milan, Italy; ²⁴⁰¹Telethon Institute of Genetics and Medicine (TIGEM), Pozzuoli, Naples, Italy; ²⁴⁰²National Institute for Infectious Diseases, IRCCS L. Spallanzani, Rome, Italy; ²⁴⁰³Universidad de Extremadura, Centro de Investigación Biomédica en Red sobre Enfermedades Neurodegenerativas (CIBERNED), Instituto de Investigación INUBE, Departamento de Bioquímica y Biología Molecular y Genética, Facultad de Enfermería y Terapia Ocupacional, Cáceres, Spain; ²⁴⁰⁴Autonomous University of Madrid, Faculty of Medicine, Department of Biochemistry, Madrid, Spain; ²⁴⁰⁵CONICET-Universidad de Buenos Aires, Instituto de Química Biológica Ciencias Exactas y Naturales (IQUIBICEN), Facultad de Ciencias Exactas y Naturales, Departamento de Química Biológica, Laboratorio de Disfunción Celular en Enfermedades Neurodegenerativas y Nanomedicina, Buenos Aires, Argentina; ²⁴⁰⁶CNC - Center for Neuroscience and Cell Biology, Coimbra & IIIUC - Instituto de Investigação Interdisciplinar, University of Coimbra, Coimbra, Portugal; ²⁴⁰⁷Instituto de Investigaciones en Ingeniería Genética y Biología Molecular Dr. Héctor N. Torres, Laboratorio de señalización y mecanismos adaptativos en Tripanosomátidos, Buenos Aires, Argentina; ²⁴⁰⁸Universidad de Buenos Aires, Departamento de Química Biológica, Facultad de Ciencias Exactas y Naturales, Buenos Aires, Argentina; ²⁴⁰⁹Max Planck Institute of Molecular Plant Physiology, Potsdam-Golm, Germany; ²⁴¹⁰Universidade do Porto, i3S-Instituto de Investigação e Inovação em Saúde, Porto, Portugal; ²⁴¹¹IPATIMUP - Institute of Molecular Pathology and Immunology of the University of Porto, Cancer Drug Resistance Group, Porto, Portugal; ²⁴¹²University of Sydney, Department

of Pathology and Bosch Institute, Sydney, NSW, Australia; University of Oslo, Department of Neuro-/Pathology, Oslo, Norway; ²³⁹⁸Istituto
 2530 Superiore di Sanità, Department of Oncology and Molecular Medicine, Rome, Italy; Fondazione Umberto Veronesi, Milan, Italy; ²³⁹⁹The Chinese
 University of Hong Kong, School of Biomedical Sciences, Hong Kong, China; The Chinese University of Hong Kong, Department of Obstetrics
 and Gynecology, Hong Kong, China; ²⁴⁰⁰The State Key Laboratory Breeding Base of Basic Science of Stomatology (Hubei-MOST) & Key
 Laboratory of Oral Biomedicine Ministry of Education; Wuhan University, School and Hospital of Stomatology, Department of Oral Medicine,
 2535 Wuhan, Hubei, China; ²⁴⁰¹University of Genova, Department of Internal Medicine, Genova, Italy; ²⁴⁰²Hong Kong Baptist University, School of
 Chinese Medicine, Hong Kong, China; ²⁴⁰³Department of Molecular, Cellular and Developmental Biology, University of Michigan, Ann Arbor,
 MI, USA; Department of Neurology, University of Michigan School of Medicine, Ann Arbor, MI, USA.; ²⁴⁰⁴German Center for Neurodegenerative
 Diseases (DZNE), Bonn, Germany; Max-Planck-Institute for Metabolism Research, Hamburg Outstation, Hamburg, Germany; Shanghai Qiangrui
 Biotech Co., Ltd., Fengxian District, Shanghai, China; ²⁴⁰⁵Boston University, Department of Biomedical Engineering, Boston, MA, USA;
 2540 ²⁴⁰⁶Department of Molecular, Cellular and Developmental Biology, University of Michigan, Ann Arbor, MI, USA; Department of Neurology,
 University of Michigan School of Medicine, Ann Arbor, MI, USA.; ²⁴⁰⁷The Fourth Military Medical University, Tangdu Hospital, Department of
 Neurosurgery, TXian, Shaanxi, China; The Fourth Military Medical University, National Key Discipline of Cell Biology, Department of Physiology
 and Pathophysiology, Xi an, Shaanxi, China; ²⁴⁰⁸Pasteur institute of Iran, Department of Hepatitis and HIV, Tehran, Iran.

ABSTRACT

2545 In 2008, we published the first set of guidelines for standardizing research in autophagy. Since
 then, this topic has received increasing attention, and many scientists have entered the field. Our
 knowledge base and relevant new technologies have also been expanding. Thus, it is important
 to formulate on a regular basis updated guidelines for monitoring autophagy in different organ-
 2550 isms. Despite numerous reviews, there continues to be confusion regarding acceptable methods
 to evaluate autophagy, especially in multicellular eukaryotes. Here, we present a set of guidelines
 for investigators to select and interpret methods to examine autophagy and related processes,
 and for reviewers to provide realistic and reasonable critiques of reports that are focused on
 these processes. These guidelines are not meant to be a dogmatic set of rules, because the
 2555 appropriateness of any assay largely depends on the question being asked and the system being
 used. Moreover, no individual assay is perfect for every situation, calling for the use of multiple
 techniques to properly monitor autophagy in each experimental setting. Finally, several core
 components of the autophagy machinery have been implicated in distinct autophagic processes
 (canonical and noncanonical autophagy), implying that genetic approaches to block autophagy
 2560 should rely on targeting two or more autophagy-related genes that ideally participate in distinct
 steps of the pathway. Along similar lines, because multiple proteins involved in autophagy also
 regulate other cellular pathways including apoptosis, not all of them can be used as a specific
 marker for *bona fide* autophagic responses. Here, we critically discuss current methods of asses-
 sing autophagy and the information they can, or cannot, provide. Our ultimate goal is to
 encourage intellectual and technical innovation in the field.

ARTICLE HISTORY

Received 14 July 2020
 Revised Vxx xxx xxx
 Accepted Axx xxx xxx

KEYWORDS

Autophagosome; cancer;
 flux; LC3; lysosome;
 macroautophagy;
 neurodegeneration;
 phagophore; stress; vacuole

Introduction

2565 Many researchers, especially those new to the field, need
 to determine which criteria are essential for demonstrat-
 ing autophagy, either for the purposes¹ of their own
 research, or in the capacity of a manuscript or grant
 review [1,2]. Acceptable standards are an important
 2570 issue, particularly considering that each of us may have
 her/his own opinion regarding the answer. Furthermore,
 as science progresses and the field evolves, the answer is
 in part a “moving target” [3]. This can be extremely
 frustrating for researchers who may think they have met
 2575 those criteria, only to find out that the reviewers of their
 work disagree. Conversely, as a reviewer, it is tiresome to
 raise the same objections repeatedly, wondering why
 researchers have not fulfilled some of the basic require-
 ments for establishing the occurrence of an autophagic
 2580 process. In addition, drugs that potentially modulate
 autophagy are increasingly being used in clinical trials,
 and screens are being carried out for new drugs that can
 modulate autophagy for therapeutic purposes. Clearly, it
 is important to determine whether these drugs are truly
 2585 affecting autophagy, and which step(s) of the process/es
 is/are affected, based on a set of accepted criteria. To this
 aim, we describe here a basic set of updated guidelines

that can be used by researchers to plan and interpret their
 experiments, by clinicians to evaluate the literature with
 regard to autophagy-modulating therapies, and by both
 2590 authors and reviewers to justify or criticize an experimen-
 tal approach.

Several fundamental points must be kept in mind as
 we establish guidelines for the selection of appropriate
 methods to monitor autophagy [2]. Importantly, there
 2595 are no absolute criteria for determining autophagic status
 that are applicable in every single biological or experi-
 mental context. This is because some assays are unsuita-
 ble, problematic or may not work at all in particular cells,
 tissues or organisms [1-4]. For example, autophagic
 2600 responses to drugs may be different in transformed versus
 nontransformed cells, in confluent versus nonconfluent
 cells, or in cells grown with or without glucose [5].
 These guidelines are likely to evolve as new methodolo-
 gies are developed and current assays are superseded.
 2605 Nonetheless, it is useful to establish a reference for accep-
 table assays that can reliably monitor autophagy in many
 experimental systems. It is important to note that in this
 set of guidelines the term “autophagy” generally refers to
 macroautophagy; other autophagy-related processes are
 2610 specifically designated when appropriate.

For the purposes of this review, the autophagic compartments (Figure 1) are referred to as the sequestering (pre-autophagosomal) phagophore (PG; previously called the isolation or sequestration membrane [6,7,8], the double-membrane autophagosome (AP; generated by scission of the phagophore membrane [9,10]), the single-membrane amphisome (AM; generated by the fusion of the outer autophagosomal membrane with endosomes) [11], the lysosome (LY), the autolysosome (AL; generated by fusion of the outer autophagosomal membrane or amphisome with a lysosome), and the autophagic body (AB; generated by fusion of the outer autophagosomal membrane with, typically, the vacuole in fungi and plants followed by the release of the internal autophagosomal compartment into the vacuole lumen). Except for cases of highly stimulated autophagic sequestration (Figure 2), autophagic bodies are not seen in animal cells, because lysosomes/autolysosomes are typically smaller than autophagosomes [11]. One critical point is that autophagy is a highly dynamic, multi-step process. Like other cellular pathways, it can be modulated at several steps, both positively and negatively. An accumulation of autophagosomes measured by transmission electron microscopy (TEM) image analysis [12], identified as green fluorescent protein (GFP)-MAP1LC3 (GFP-LC3) puncta under fluorescence microscopy, or as changes in the amount of lipidated LC3 (LC3-II) on a

western blot, could reflect a reduction in autophagosome turnover [13-15], or the inability of turnover to keep pace with increased autophagosome formation (Figure 1B) [16]. For example, inefficient fusion with endosomes and/or lysosomes, or perturbation of the transport machinery [17], would inhibit autophagosome maturation to amphisomes or autolysosomes (Figure 1C), whereas decreased flux could also be due to inefficient degradation of the cargo once fusion has occurred [18]. Moreover, GFP-LC3 puncta and LC3 lipidation can reflect the induction of a different/modified pathway such as LC3-associated phagocytosis (LAP) [19], or the noncanonical destruction pathway of paternal mitochondria after egg fertilization [20,21].

Thus, the use of autophagy markers such as LC3-II must be complemented by assays to estimate overall autophagic flux, or flow, to permit a correct interpretation of the results. That is, autophagic activity includes not just the increased synthesis or lipidation of Atg8/LC3/GABARAP (LC3 and GABARAP subfamilies constitute the mammalian homologs of yeast Atg8), or an increase in the formation of autophagosomes, but, most importantly, flux through the entire system, including lysosomes or the vacuole, and the subsequent release of the breakdown products. Therefore, autophagic substrates need to be monitored dynamically over time to verify that they have reached the lysosome/vacuole, and whether or not they are

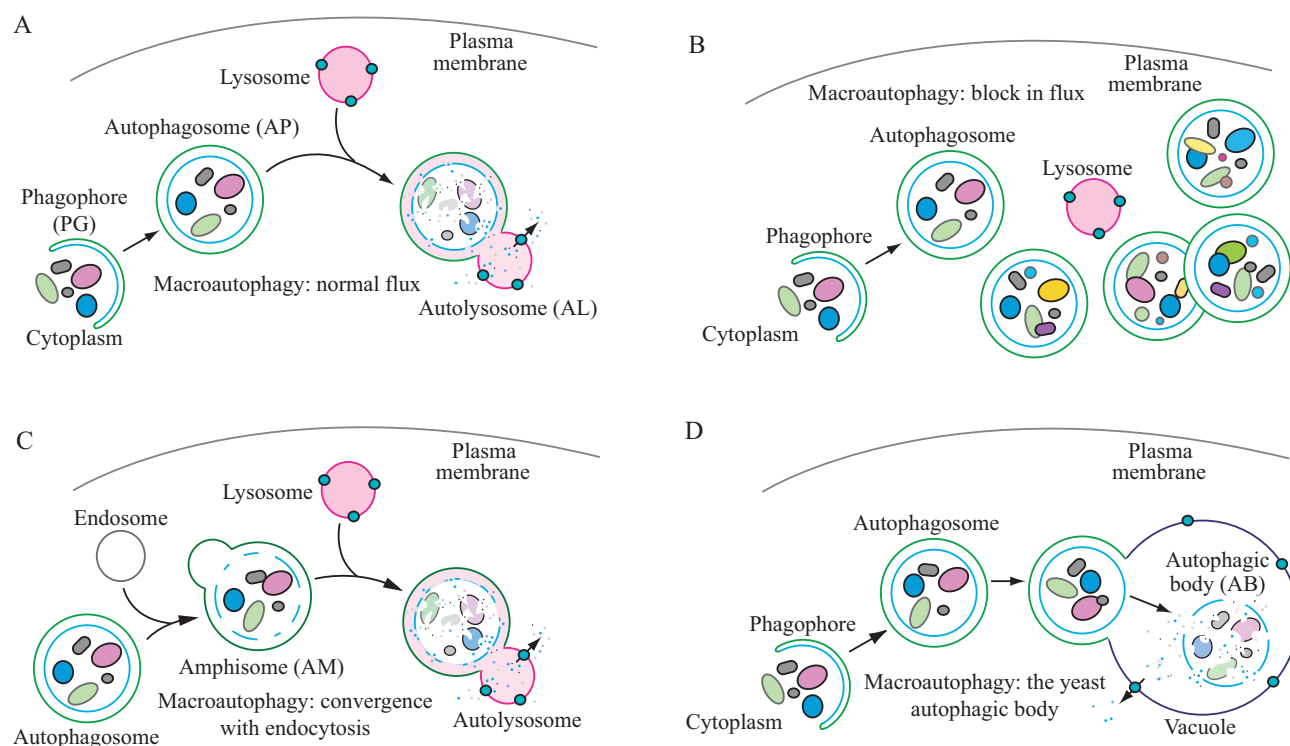


Figure 1. Schematic model demonstrating the induction of autophagosome formation when turnover is blocked versus normal autophagic flux, and illustrating the morphological intermediates of autophagy. (A) The initiation of autophagy includes the formation and expansion of the phagophore, the initial sequestering compartment, which expands into an autophagosome. Completion of the autophagosome requires an intraphagophore membrane scission step and is followed by fusion of the outer autophagosomal membrane with lysosomes and degradation of the contents, allowing complete flux, or flow, through the entire pathway. This is a different outcome than the situation shown in (B) where induction results in the initiation of autophagy, but a defect in autophagosome turnover due, for example, to a block in fusion with lysosomes or disruption of lysosomal functions will result in an increased number of autophagosomes. In this scenario, autophagy has been induced, but there is no or limited autophagic flux. (C) An autophagosome can fuse with an endosome to generate an amphisome, prior to fusion with the lysosome. (D) Schematic drawing showing the formation of an autophagic body in fungi. The large size of the fungal vacuole relative to autophagosomes allows the release of the single-membrane autophagic body within the vacuole lumen. In cells that lack vacuolar hydrolase activity, or in the presence of inhibitors that block hydrolase activity, intact autophagic bodies accumulate within the vacuole lumen and can be detected by light microscopy. The lysosome of most more complex eukaryotes is too small to accommodate an autophagic body.

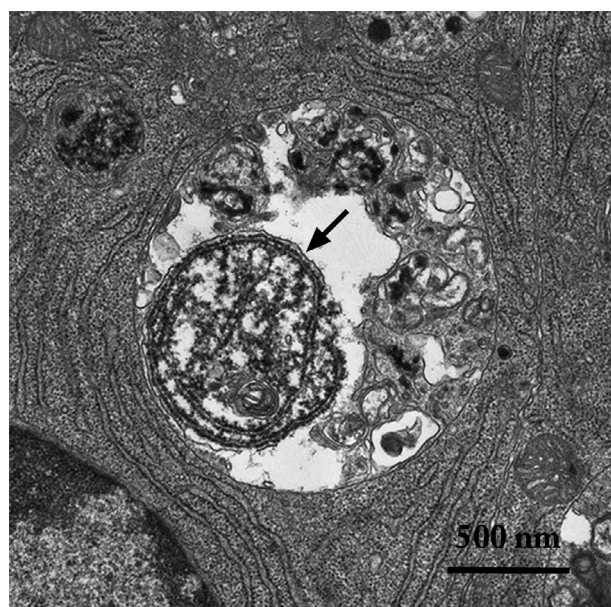


Figure 2. An autophagic body in a large lysosome of a mammalian epithelial cell in a mouse seminal vesicle *in vitro*. The arrow shows the single limiting membrane covering the sequestered rough ER. Image provided by A.L. Kovács.

indirect measurement for autophagic flux, the results may be difficult to interpret [30]. A general caution regarding the use of the term “steady state” is warranted at this point. It should not be assumed that an autophagic system is at steady state in the strict biochemical meaning of this term, as this implies that the level of autophagosomes does not change with time, and the flux through the system is constant. In these guidelines, we use “steady state” to refer to the baseline range of autophagic flux in a system that is not subjected to specific perturbations that increase or decrease that flux.

Autophagic flux refers to the entire process of autophagy over a period of time, which encompasses the selection of cargo and its inclusion within the autophagosome, the delivery of cargo to lysosomes (via fusion of the latter with autophagosomes or amphisomes) and its subsequent breakdown and release of the resulting macromolecules back into the cytosol, which may be referred to as productive or complete autophagy. Thus, increases in the level of phosphatidylethanolamine (PE)-modified Atg8-family proteins (Atg8-PE, or LC3/GABARAP-II), or even the appearance of autophagosomes, are not measures of autophagic flux *per se*, but can reflect the induction of autophagic sequestration and/or inhibition of autophagosome or amphisome clearance. Also, it is important to realize that while formation of Atg8-PE (or LC3/GABARAP-II) appears to correlate with the induction of autophagy, we do not know, at present, the actual mechanistic relationship between Atg8-PE (or LC3/GABARAP-II) formation and the rest of the autophagic process; indeed, some variants of autophagy proceed in the absence of LC3-II [31–35].

In addition, as the metabolic control of autophagy is becoming increasingly clear, highlighting a tight network between the autophagy machinery, energy sensing pathways and the cell’s metabolic circuits [36,37], mitochondrial parameters such as fission and fusion rate and the cell’s ATP demand should be monitored and correlated with autophagic flux data. In this regard, the use of mitochondria-localized mCherry-GFP tandem reporters (such as the *mito-QC* mouse [38]), may be important in understanding how deregulated mitophagy affects the progression of metabolic disorders, including diabetes [39]. These types of studies will provide a better understanding on the variability of autophagy and cell death susceptibility.

As a final note, we also recommend that researchers refrain from the use of the expression “percent autophagy” when describing experimental results, as in “The cells displayed a 25% increase in autophagy.” Instead, it is appropriate to indicate that the average number of GFP-Atg8-family protein puncta per cell is increased or a certain percentage of cells displayed punctate GFP-Atg8-family proteins that exceeds a particular threshold (and this threshold should be clearly defined in the Methods section), or that there is a specific increase or decrease in the rate of cargo sequestration or the degradation of long-lived proteins, when these are the actual measurements being quantified.

In previous versions of these guidelines [1,3], the methods were separated into two main sections—steady state and flux. In some instances, a lack of clear distinction between the actual methodologies and their potential uses made such a separation somewhat artificial. For example, fluorescence microscopy was

degraded. By responding to perturbations in the extracellular environment, cells tune the autophagic flux to meet intracellular metabolic demands and support repair mechanisms. The impact of autophagic flux on cell death and human pathologies, therefore, demands accurate tools to measure not only the current flux of the system, but also its capacity [22], and its response time, when exposed to a defined stress [23].

One approach to evaluate autophagic flux is to measure the rate of general protein breakdown by autophagy [6,24,25]. It is possible to arrest the autophagic flux at a given point, and then record the time-dependent accumulation of an organelle, an organelle marker, a cargo marker, or the entire cargo at the point of blockage; however, this approach assumes there is no feedback of the accumulating structure on its own rate of formation [26]. Thus, the chase period should be kept short, ideally with more than one time point. In an alternative approach, one can follow the time-dependent decrease of an autophagy-degradable marker following inhibition of protein synthesis (with the caveat that the potential contribution of other proteolytic systems needs to be experimentally addressed). A potential complication here is that inhibition of protein synthesis, for example, by cycloheximide (CHX), can activate MTORC1 signaling, which in turn impairs autophagy [27]. In theory, these nonautophagic processes can be assessed if degradation persists after blocking autophagic sequestration [13,15,28]. The key issue is to differentiate between the often transient accumulation of autophagosomes due to increased induction, and their accumulation due to inefficient clearance of sequestered cargos. This can be done by both measuring the levels of autophagosomes at static time points, and by measuring changes in the rates of autophagic degradation of cellular components, or, in neurons, by assaying autophagosome transport [18,29]. Multiple strategies have been used to estimate “autophagy,” but unless the experiments can relate changes in autophagosome quantity to a direct or

initially listed as a steady-state method, although this approach can clearly be used to monitor flux as described in this article, especially when considering the increasing availability of new technologies such as microfluidic chambers. Furthermore, the use of multiple time points and/or lysosomal fusion/degradation inhibitors can turn even a typically static method such as TEM into one that monitors flux. Therefore, although we maintain the importance of monitoring autophagic flux and not just induction, this revised set of guidelines does not separate the methods based on this criterion. Readers should be aware that this article is not meant to present protocols, but rather guidelines, including information that is typically not presented in protocol papers. For detailed information on experimental procedures we refer readers to various protocols that have been published elsewhere [25] [40-56]. Finally, throughout the guidelines we provide specific cautionary notes, and these are important to consider when planning experiments and interpreting data; however, these cautions are not meant to be a deterrent to undertaking any of these experiments or a hindrance to data interpretation.

Collectively, we propose the following guidelines for measuring various aspects of selective and nonselective autophagy in eukaryotes.

Nomenclature

To minimize confusion regarding nomenclature, we make the following notes: In general, we follow the conventions established by the nomenclature committees for each model organism whenever appropriate guidelines are available, and briefly summarize the information here using “ATG1” as an example for yeast and “ULK1” for mammals. The standard nomenclature of autophagy-related wild-type genes, mutants and proteins for yeast is *ATG1*, *atg1* (or *atg1Δ* in the case of deletions) and Atg1, respectively, according to the guidelines adopted by the *Saccharomyces* Genome Database (<https://www.yeastgenome.org/>). For mammals we follow the recommendations of the International Committee on Standardized Genetic Nomenclature for Mice (<http://www.informatics.jax.org/mgihome/nomen/>), which dictates the designations *Ulk1*, *ulk1* and ULK1 (for all rodents), respectively, and the guidelines for human genes established by the HUGO Nomenclature Committee (<http://www.genenames.org/guidelines.html>), which states that human gene symbols are in the form *ULK1* and recommends that proteins use the same designation without italics, as with ULK1; mutants are written for example as *ULK1*^{-/-} [57]. For simplicity unless referring to a specific species, the human gene/protein symbols and definitions will be used throughout the guidelines.

Methods for monitoring autophagy

Transmission electron microscopy

Autophagy was first detected by TEM in the 1950s (reviewed in ref [6]). This process was originally observed as focal degradation of cytoplasmic areas performed by lysosomes. Later analysis revealed that autophagy starts with the sequestration of portions of the cytoplasm by a special double-membrane structure (termed the phagophore), which matures into the autophagosome, also delimited by a double

membrane. Subsequent fusion events expose the cargo to the lysosome (or the vacuole in fungi or plants) for enzymatic breakdown.

The importance of TEM in autophagy research lies in several qualities. It is the only tool that reveals the morphology of autophagic structures at a resolution in the nm range; shows these structures in their natural environment and position among all other cellular components; allows their exact identification; and, in addition, can support quantitative studies if the rules of proper sampling are followed [12].

Autophagy can be both selective and nonselective, and TEM can be used to monitor both. In the case of selective autophagy, the cargo is the specific substrate being targeted for sequestration—bulk cytoplasm is essentially excluded. In contrast, during non-selective autophagy, disposable cytoplasmic constituents are sequestered. Sequestration of larger structures (such as big lipid droplets, extremely elongated or branching mitochondria or the entire Golgi complex) is rare, indicating an apparent upper size limit for individual autophagosomes. However, it has been observed that under special circumstances the potential exists for the formation of huge autophagosomes, which can even engulf a complete nucleus [28]. Cellular components that form large confluent areas excluding bulk cytoplasm, such as organized, functional myofibrillar structures, do not seem to be sequestered by autophagy. The situation is less clear with regard to glycogen [58-60].

Plant cell-specific structures called provacuoles have a striking similarity to a phagophore, but form in an autophagy-independent manner [61]. These structures have been detected in cells undergoing major changes in vacuolar morphology, such as meristematic cells [62]. Thus, using TEM to detect autophagosomes in plant cells must be done while comparing with an appropriate autophagy-deficient control sample.

After sequestration, the content of the autophagosome and its bordering double membrane remain morphologically unchanged, and recognizable for at least several minutes. During this period, the membranes of the sequestered organelles (for example the ER or mitochondria) remain intact, and the electron density of ribosomes is conserved at normal levels. Degradation of the sequestered material and the corresponding deterioration of ultrastructure commences and runs to completion within the amphisome and the autolysosome after fusion with a late endosome and lysosome (the vacuole in fungi and plants), respectively (Figure 1) [63]. The sequential morphological changes during the autophagic process can be followed by TEM [64]. The maturation from the phagophore through the autolysosome is a dynamic and continuous process [65], and, thus, the classification of compartments into discrete morphological subsets can be problematic; therefore, some basic guidelines for such classifications are offered below.

In the preceding sections the “autophagosome”, the “amphisome” and the “autolysosome” were terms used to describe or indicate three basic stages and compartments of autophagy. It is important to make it clear that for instances (which may be many) when we cannot or do not want to differentiate among the autophagosomal, amphisomal and autolysosomal stage we use the general term “autophagic vacuole”. In the yeast autophagy field, the term “autophagic vesicle” is used to avoid confusion with the primary vacuole, and by now the two terms are

used in parallel and can be considered synonyms. It is strongly recommended, however, to use only the term “autophagic vacuole” when referring to autophagy in more complex eukaryotic cells. Autophagosomes, also referred to as initial autophagic vacuoles (AVi), typically have a double membrane. This structure is usually distinctly visible by TEM as two parallel membrane layers (bilayers) separated by a relatively narrower or wider electron-translucent cleft, even when applying the simplest routine TEM fixation procedure (Figure 3A) [66,67]. This electron-translucent cleft, however, is less visible in freeze-fixed samples, suggesting it may be an artefact of sample preparation (see Fig. S3 in ref [68].). Amphisomes [69] can sometimes be identified by the presence of small intraluminal vesicles [70]. These intraluminal vesicles are delivered into the lumen by fusion of the autophagosome/autophagic vacuole (AV) limiting membrane with multivesicular endosomes, and care should, therefore, be taken in the identification of the organelles, especially in cells that produce large numbers of multivesicular body (MVB)-derived exosomes (such as tumor or stem cells) [71]. Late/degradative autophagic vacuoles/autolysosomes (AVd or AVI) typically have only one limiting membrane; frequently they contain electron-dense cytoplasmic material and/or organelles at various stages of degradation (Figure 3A and B) [63,72]; however, late in the digestion process they may contain only a few membrane fragments and be difficult to distinguish from lysosomes, endosomes, or tubular smooth ER cut in cross-section. It is not always easy to morphologically distinguish amphisomes, autolysosomes and lysosomes, even for an expert [6]. A simple solution to assess autophagy progression is to group all of these structures, which are typically stained dark in TEM samples, and define them as degradative compartments/vacuoles. As autophagy induction leads to an increase of autophagosomes, amphisomes and autolysosomes, an increase of degradative compartments per cell area provides a simple measurement to determine whether this degradative pathway is enhanced [73-75]. Unequivocal identification of these structures and of lysosomes devoid of visible content requires immuno-EM detection of a cathepsin or other lysosomal hydrolase (e.g., ACP2 [acid phosphatase 2, lysosomal] [76,77]) that is detected on the limiting membrane of the lysosome [78]. Smaller, often electron dense, lysosomes may predominate in some cells and exhibit hydrolase immunoreactivity within the lumen and on the limiting membrane [79].

In addition, structural proteins of the lysosome/late endosomes, such as LAMP1 and LAMP2 or SCARB2/LIMP-2, can be used for confirmation. No single protein marker, however, has been effective in discriminating autolysosomes from the compartments mentioned above, in part due to the dynamic fusion and “kiss-and-run” events that promote interchange of components that can occur between these organelle subtypes. Rigorous further discrimination of these compartments from each other and other vesicles ultimately requires demonstrating the colocalization of a second marker indicating the presence of an autophagic substrate (e.g., LC3 and CTSD [cathepsin D] colocalization) or the acidification of the compartment (e.g., mRFP/mCherry-GFP-LC3 probes or LysoTracker™ dyes; see *Tandem mRFP/mCherry-GFP fluorescence microscopy*), Keima probes, or BODIPY-pepstatin A that allows detection of CTSD in an activated form within an

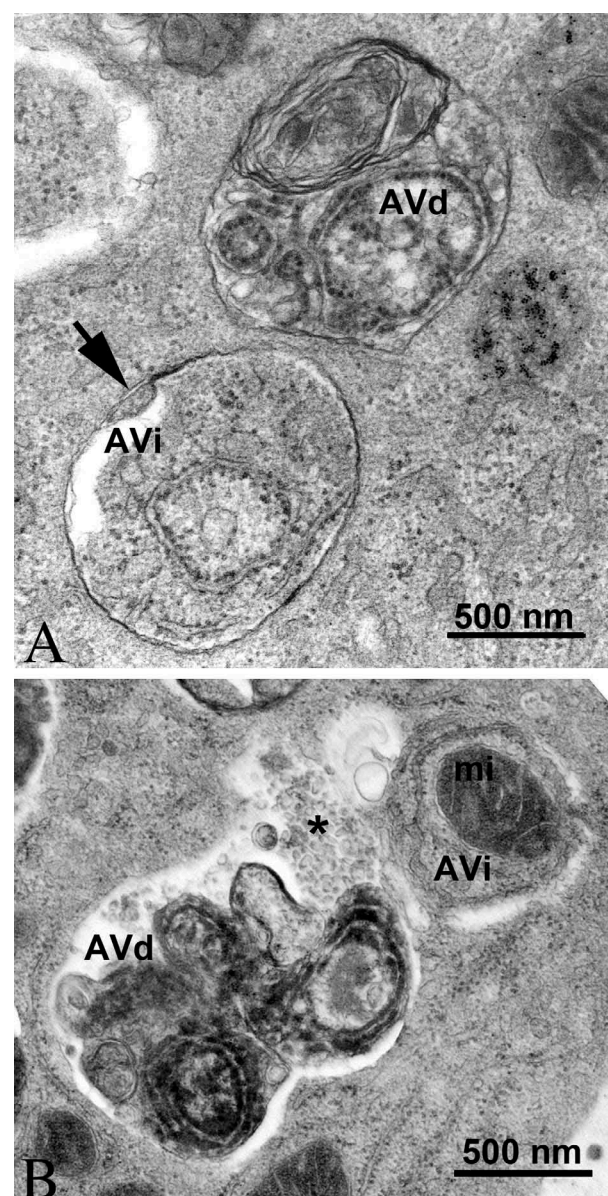


Figure 3. TEM images of autophagic vacuoles in isolated mouse hepatocytes. (A) One autophagosome or early autophagic vacuole (AVi) and one degradative autophagic vacuole (AVd) are shown. The AVi can be identified by its contents (morphologically intact cytoplasm, including ribosomes, and rough ER), and the limiting membrane that is partially visible as two bilayers separated by a narrow electron-lucent cleft, i. e., as a double membrane (arrow). The AVd can be identified by its contents, partially degraded, electron-dense rough ER. The vesicle next to the AVd is an endosomal/lysosomal structure containing 5-nm gold particles that were added to the culture medium to trace the endocytic pathway. (B) One AVi, containing rough ER and a mitochondrion, and one AVd, containing partially degraded rough ER, are shown. Note that the limiting membrane of the AVi is not clearly visible, possibly because it is tangentially sectioned. However, the electron-lucent cleft between the two limiting membranes is visible and helps in the identification of the AVi. The AVd contains a region filled by small internal vesicles (asterisk), indicating that the AVd has fused with a multivesicular endosome. mi, mitochondrion. Image provided by E.-L. Eskelinen.

acidic compartment), and, when appropriate, by excluding markers of other vesicular components [76,80,81].

The sequential deterioration of cytoplasmic structures being digested can be used for identifying autolysosomes by TEM. Even when the partially digested and destroyed structure of the cytoplasmic cargo cannot be recognized in itself, it can be traced back to earlier forms by identifying preceding stages of sequential morphological deterioration. Degradation

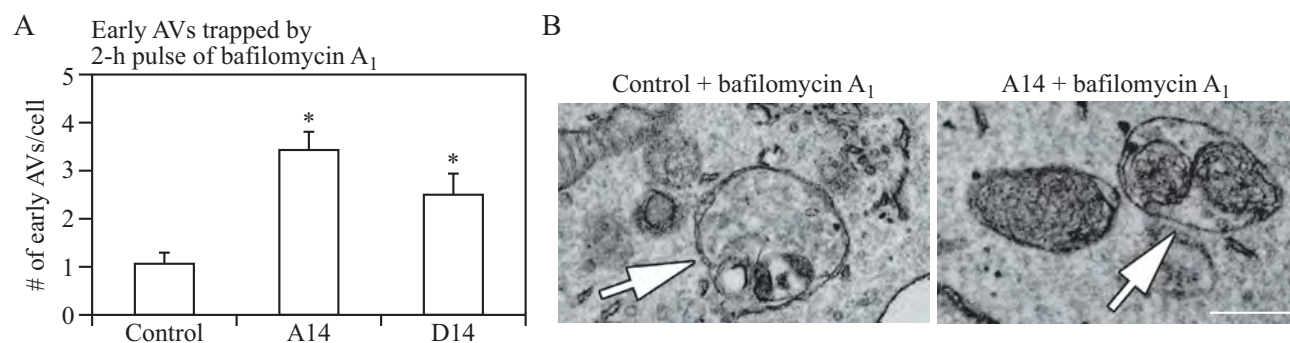


Figure 4. Autophagosomes with recognizable cargo are rare in cells. (A) To assess relative rates of autophagosome formation, the lysosomal inhibitor bafilomycin A₁ (10 nM) was applied for 2 h prior to fixation with 2% glutaraldehyde in order to trap newly formed autophagosomes (note that whereas short-term treatment with bafilomycin A₁ in most cases primarily blocks autolysosomal degradation, it can also inhibit autophagosome-lysosome fusion). Two different *PINK1* shRNA lines (A14 and D14) exhibit increased AV formation over 2 h compared to the control shRNA line. *, $p > 0.05$ vs. Control. (B) Autophagosomes in bafilomycin A₁-treated control cells contain a variety of cytoplasmic structures (left, arrow), whereas mitochondria comprise a prominent component of autophagosomes in bafilomycin A₁-treated (*PINK1* shRNA) cells (right, arrow). Scale bar: 500 nm. These data indicate induction of selective mitophagy in *PINK1*-deficient cells. This figure was modified from Figure 2 published in Chu CT. A pivotal role for *PINK1* and autophagy in mitochondrial quality control: implications for Parkinson disease. *Human Molecular Genetics* 2010; 19:R28-R37.

usually leads first to the increased electron density of still recognizable organelles, then to vacuoles with heterogeneous density, which become more homogeneous and amorphous, mostly electron dense, but sometimes light (i.e., electron translucent). It should be noted that, in pathological states, it is not uncommon that active autophagy of autolysosomes and damaged lysosomes (“lysophagy”) may yield populations of double-membrane limited autophagosomes containing partially digested amorphous substrate in the lumen. These structures, which are enriched in hydrolases, are seen in swollen dystrophic neurites in some neurodegenerative diseases, and in cerebellar slices cultured in vitro and infected with prions. Alternatively, it is possible to inhibit the fusion of autophagosomes and lysosomes using bafilomycin A₁ (a vacuolar-type H⁺-translocating ATPase [V-ATPase] inhibitor). It is then possible to both visualize the cargo(s) that are being actively sequestered within AVi structures during the chase period, as well as quantify their rates of formation provided the chase period is kept short [82] (Figure 4).

It must be emphasized that in addition to the autophagic input, other processes (e.g., endosomal, phagosomal, chaperone-mediated) also carry cargo to the lysosomes [64,65], in some cases through the intermediate step of direct endosome fusion with an autophagosome to form an amphisome. This process is exceptionally common in the axons of neurons [83,84]. Therefore, strictly speaking, we can only have a lytic compartment containing cargos arriving from several possible sources; however, we still may use the term “autolysosome” if the content appears to be overwhelmingly autophagic. Note that the engulfment of dying cells via phagocytosis also produces lysosomes that contain cytoplasmic structures, but in this case, it originates from the dying cell [85]; hence the possibility of an extracellular origin for such content must be considered when monitoring autophagy in settings where apoptotic cell death may be reasonably expected or anticipated.

For many physiological and pathological situations, the examination of both early and late autophagic vacuoles yields valuable data regarding the overall autophagy status in the cells [16,86]. Along these lines, it is possible to use

immunocytochemistry to follow particular cytosolic proteins such as SOD1/Cu,Zn-superoxide dismutase and CA (carbonic anhydrase) to determine the stage of autophagy; the former is much more resistant to lysosomal degradation [87].

In some autophagy-inducing conditions it is possible to observe multi-lamellar membrane structures in addition to the conventional double-membrane autophagosomes, although the nature of these structures is not fully understood. These multi-lamellar structures may indeed be multiple double layers of phagophores [88] and positive for LC3 [89], they could be autolysosomes [90], or they may form as an artefact of fixation. Depending on the cell type, it may be necessary to distinguish these from myelin or surfactant, both of which are also multi-lamellar. These multi-lamellar bodies are typical in lysosomal storage diseases, such as Niemann-Pick disease type I [91] and Parkinson disease (PD) [92–94]. In addition, cells treated with U18666A, an inhibitor of cholesterol transport [95,96], or chloroquine (CQ) that induces phospholipidosis [97], produce numerous large multi-lamellar bodies with concentric membrane stacks that represent dysfunctional lysosomes, containing undegraded phospholipids and cholesterol. Multi-lamellar bodies are formed through cellular autophagy, and the implication of various lysosomal enzymes in their formation suggests a lysosomal nature. Initially, single or multiple foci of lamella appear within an autophagic vacuole and then progress into multi-lamellar structures [90,93] as they are getting filled with lipids; these lipids are cholesterol-containing rafts in late endocytic/lysosomes organelles [94].

Special features of the autophagic process may be clarified by immuno-TEM with gold-labeling [98,99], using antibodies, for example, to cargo proteins of cytoplasmic origin and to LC3 to verify the autophagic nature of the compartment. LC3 immunogold labeling also enables the detection of novel degradative organelles within autophagy compartments. This is the case with the autophagoproteasome [100] that consists of single-, double-, or multiple-membrane LC3-positive autophagosomes costaining for specific components of the ubiquitin-proteasome system (UPS). It may be that a rich multi-enzymatic (both autophagic and UPS) activity takes place within these organelles instead of being segregated within different domains of the cell. Also in

plants, TEM immunogold labelling for ATG8 ultrastructural detection can be performed. This can be approached using either anti-GFP antibodies for GFP-ATG8 fusion proteins, or anti-ATG8 antibodies for direct labeling [101,102]. Freeze-substitution followed by cryo embedding in acrylic resins is the most convenient and feasible processing method for ATG8 immunogold labelling in plant cells.

Although labeling of LC3 can be difficult, an increasing number of commercial antibodies are becoming available, including reagents that enable visualization of the GFP moiety of GFP-LC3 reporter constructs [103]. It is important to keep in mind that LC3 can be associated with nonautophagic structures (see *Xenophagy*, and *Noncanonical use of autophagy-related proteins*), and that LC3 puncta can be observed in autophagy-deficient cells [104]. LC3 is involved in specialized forms of endocytosis such as LC3-associated phagocytosis. In addition, LC3 can decorate vesicles dedicated to exocytosis in nonconventional secretion systems (reviewed in ref [105,106]). Antibodies against an abundant cytosolic protein will result in high labeling all over the cytoplasm; however, organelle markers work well. Because there are very few characterized proteins that remain associated with the closed autophagosomes, the choices for confirmation of their autophagic nature are limited. Furthermore, autophagosome-associated proteins may be cell-, age-, sex- and/or condition-specific. Sex-specific expression of autophagic markers are observed both in humans and in rats [107-111]. At any rate, the success of this methodology depends on the quality of the antibodies and also on the TEM preparation and fixation procedures utilized. With immuno-TEM, authors should provide controls showing that labeling is specific. This may require a quantitative comparison of labeling over different cellular compartments not expected to contain antigen and those containing the antigen of interest.

It is difficult to clearly monitor autophagy in tissues of formalin-fixed and paraffin-embedded biopsy samples retrospectively, because (a) tissues fixed in formalin have low or no LC3 detectable by routine immunostaining, (b) because phospholipids melt together with paraffin during the sample preparation, and (c) immuno-EM of many tissues not optimally fixed for this purpose (e.g., using rapid fixation) produces low-quality images. Combining antigen retrieval with the avidin-biotin peroxidase complex (ABC) method may be quite useful for these situations. For example, immunohistochemistry can be performed using an antigen retrieval method, and then tissues are stained by the ABC technique using a labeled anti-human LC3 antibody. After imaging by light microscopy, the same prepared slides can be remade into sections for TEM examination, which can reveal peroxidase reaction deposits in vacuoles within the region that is LC3-immunopositive by light microscopy [112].

In addition, statistical information should be provided due to the necessity of showing only a selective number of sections in publications. Again, we note that for quantitative data it is necessary to use proper volumetric analysis rather than just counting numbers of sectioned objects. On the one hand, it must be kept in mind that even volumetric morphometry/stereology only shows either steady-state levels, or a snapshot in a changing dynamic process. Such data by themselves are not informative regarding autophagic flux, unless carried out

over multiple time points. Alternatively, investigation in the presence and absence of flux inhibitors can reveal the dynamic changes in various stages of the autophagic process [13,22,55,113,114]. On the other hand, if the turnover of autolysosomes is very rapid, a low number/volume in the experimental compared to the basal condition, will not necessarily be an accurate reflection of low autophagic activity; as with autophagosomes, a smaller number of autolysosomes can reflect increased degradation or decreased formation. However, quantitative analyses indicate that autophagosome volume in many cases does correlate with the rates of protein degradation [115-117]. One potential compromise is to perform whole cell quantification of autophagosomes using fluorescence methods, with qualitative verification by TEM [118], to show that the changes in fluorescent puncta reflect corresponding changes in autophagic structures.

One additional caveat with TEM, and to some extent with confocal fluorescence microscopy, is that the analysis of a single plane within a cell can be misleading and may make the identification of autophagic structures difficult. Confocal microscopy and fluorescence microscopy with deconvolution software (or with much more work, 3-dimensional TEM) can be used to generate multiple/serial sections of the same cell to reduce this concern; however, in many cases where there is sufficient structural resolution, analysis of a single plane in a relatively large cell population can suffice given practical limitations. EM technologies, such as focused ion beam scanning electron microscopy (SEM), Serial Block Face-SEM, and Automatic Tape-collecting Ultramicrotomy for SEM, should make it much easier to apply 3-dimensional analyses. An additional methodology to assess autophagosome accumulation is correlative light and electron microscopy (CLEM), which is helpful in confirming that fluorescent structures are autophagosomes [119-122]. Along these lines, it is important to note that even though GFP fluorescence will be quenched in the acidic environment of the autolysosome, some of the GFP puncta detected by fluorescence microscopy may correspond to early autolysosomes prior to GFP quenching. These numbers may increase substantially in pathological conditions where lysosomal/autolysosomal acidification is impaired. The mini Singlet Oxygen Generator (miniSOG) fluorescent flavoprotein, which is less than half the size of GFP, provides an additional means to genetically tag proteins for CLEM analysis under conditions that are particularly suited to subsequent TEM analysis [123], with the caveat that single oxygen targets aromatic amino acids, promoting artefactual protein damage as well as double bonds in lipids, promoting lipid peroxidation [124]. Combinatorial assays using tandem monomeric red fluorescent protein (mRFP)-GFP-LC3 (see *Tandem mRFP/mCherry-GFP fluorescence microscopy*) or other markers for acidic autophagic vacuoles (e.g., Keima) along with static TEM images should help in the analysis of flux and the visualization of cargo structures [125].

Another technique that has proven quite useful for analyzing the complex membrane structures that participate in autophagy is 3-dimensional electron tomography [126-128], and cryoelectron microscopy (cryo-EM; Figure 5) [129]. More sophisticated, cryo-soft X-ray tomography (cryo-SXT) is an emerging imaging technique used to visualize

3075

3080

Q4

3085

3090

3095

3100

3105

3110

3115

3120

3125

3130

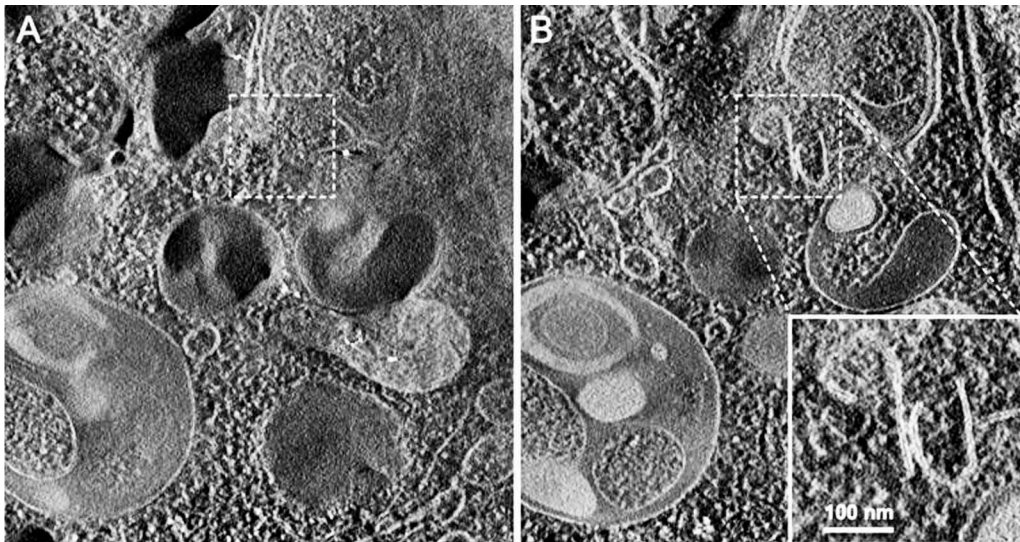


Figure 5. Cryoelectron microscopy can be used as a three-dimensional approach to monitor the autophagic process. Computed sections of an electron tomogram of the autophagic vacuole-rich cytoplasm in a hemophagocyte of a semi-thin section after high-pressure freezing preparation. The dashed area is membrane-free (A) but tomography reveals newly formed or degrading membranes with a parallel stretch (B). Image published previously [4082] and provided by M. Schneider and P. Walter.

autophagosomes [130]. Cryo-SXT extracts ultrastructural information from whole, unstained mammalian cells as close to the “near-native” fully-hydrated (living) state as possible. Correlative studies combining cryo-fluorescence and cryo-SXT workflow (cryo-CLXM) have been applied to capture early autophagosomes. In order to study the structural biology of purified autophagy components and complexes, high-resolution cryo-EM combined with 3-dimensional structure determination is also increasingly being used as an alternative to X-ray crystallography or nuclear magnetic resonance (NMR) spectroscopy [131,132].

Finally, although only as an indirect measurement, the comparison of the ratio of autophagosomes to autolysosomes by TEM can support alterations in autophagy identified by other procedures [133]. In this case, it is important to always compare samples to the control of the same cell type and in the same growth phase, and to acquire data at different time points, as the autophagosome:autolysosome ratio varies in time in a cell context-dependent fashion, depending on their clearance activity. An additional category of lysosomal compartments, especially common in disease states and aged postmitotic cells such as neurons, muscle cells and retinal pigment epithelium, is represented by residual bodies. This category includes ceroid and lipofuscin, lobulated vesicular compartments of varying size composed of highly indigestible complexes of protein and lipid, and abundant, mostly inactive, acid hydrolases. Reflecting end-stage unsuccessful incomplete autolysosomal digestion, lipofuscin is fairly easily distinguished from AVs and lysosomes by TEM but can be easily confused with autolysosomes in immunocytochemistry studies at the light microscopy level [76,134]; lipofuscin has broad spectral emission, and is the main cause of autofluorescence in tissues.

TEM observations of platinum-carbon replicas obtained by the freeze fracture technique can also supply useful ultrastructural information on the autophagic process. In quickly frozen and fractured cells the fracture runs preferentially along the

hydrophobic plane of the membranes, allowing characterization of the limiting membranes of the different types of autophagic vacuoles, and visualization of their limited protein intramembrane particles/integral membrane proteins (IMPs). Several studies have been carried out using this technique on yeast [135], as well as on mammalian cells or tissues including the mouse exocrine pancreas [136], the mouse and rat liver [137,138], mouse seminal vesicle epithelium [28,88], rat tumor and heart [139], and cancer cell lines (e.g., breast cancer MDA-MB-231) [140] to investigate the various phases of autophagosome maturation, and to reveal useful details about the origin and evolution of their limiting membranes [6,141-144].

The phagophore and the limiting membranes of autophagosomes contain few, or no detectable, IMPs (Figure 6A,B), when compared to other cellular membranes and to the membranes of lysosomes. In subsequent stages of the autophagic process the fusion of the autophagosome with an endosome and a lysosome results in increased density of IMPs in the membrane of the formed autophagic compartments (amphisomes, autolysosomes; Figure 6 C) [6, 28,135-138, 145, 146]. Autolysosomes are delimited by a single membrane because, in addition to the engulfed material, the inner membrane is also degraded by the lytic enzymes. Similarly, the limiting membrane of autophagic bodies in yeast (and presumably plants) is also quickly broken down under normal conditions. Autophagic bodies can be stabilized, however, by the addition of phenylmethylsulfonylfluoride (PMSF) or genetically by the deletion of the yeast *PEP4* gene (see *The Cvt pathway, mitophagy, pexophagy, piecemeal microautophagy of the nucleus and late nucleophagy in yeast and filamentous fungi*). Thus, another method to consider for monitoring autophagy in yeast (and potentially in plants) is to count autophagic bodies by TEM using at least two time points [147]. The advantage of this approach is that it can provide accurate information on flux even when the autophagosomes are abnormally small [148,149]. Thus, although a

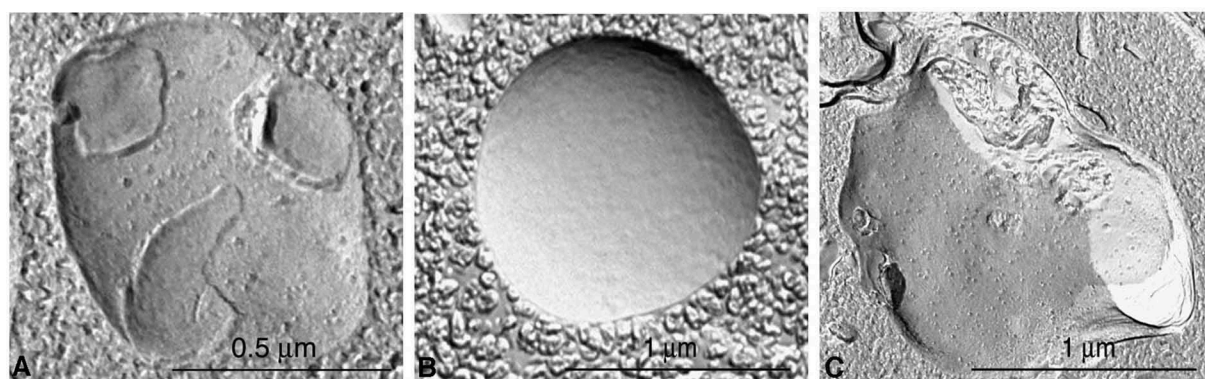


Figure 6. Different autophagic vacuoles observed after freeze fracturing in cultured osteosarcoma cells after treatment with the autophagy inducer voacamine [143]. (A) Early autophagosome delimited by a double membrane. (B) Inner monolayer of an autophagosome membrane deprived of protein particles. In the cross-fractured portion (on the right) the profile of the single membrane and the inner digested material are easily visible. Images provided by S. Meschini, M. Condello and A. Giuseppe.

high frequency of “abnormal” structures presents a challenge, TEM is still very helpful in analyzing autophagy.

Cautionary notes: Despite the introduction of many new methods, TEM maintains its special role in autophagy research. There are, however, difficulties in utilizing TEM. It is relatively time consuming and needs technical expertise to ensure proper handling of samples in all stages of preparation from fixation to sectioning and staining. It should be noted that some of the hurdles linked to ultrathin section preparation can be overcome by using focused ion beam scanning electron microscopy (FIB-SEM) technology, which enables the operator to selectively ablate in a nanometer scale a previously marked region of the sample by using a focused ion current from a gallium source. The milling process can be interrupted every few nanometers to take high-resolution images of cross sections by the SEM column [150]. Moreover, the prospects for application of cryopreparation techniques have been improved; the notoriously slow process of freeze substitution of frozen samples can be accelerated tremendously by sample agitation using either an experimental setup or agitation modules within automated freeze-substitution units [151,152].

After the criteria for sample preparation are met, an important problem is the proper identification of autophagic structures. This is crucial for both qualitative and quantitative characterization, and needs considerable experience, even in the case of one cell type. The difficulty lies in the fact that many subcellular components may be mistaken for autophagic structures. For example, some authors (or reviewers of manuscripts) assume that almost all cytoplasmic structures that, in the section plane, are surrounded by two (more or less) parallel membranes are autophagosomes. Structures appearing to be limited by a double membrane, however, may include swollen mitochondria, plastids in plant cells, cellular interdigitations, endocytosed apoptotic bodies, circular structures of lamellar smooth endoplasmic reticulum (ER), and even areas surrounded by rough ER. Endosomes, phagosomes and secretory vacuoles may have heterogeneous content that makes it possible to confuse them with autolysosomes. Additional identification problems may arise from damage caused by improper sample collection or fixation artefacts [66,67,153,154].

Whereas fixation of in vitro samples is relatively straightforward, fixation of excised tissues requires care to avoid sampling a nonrepresentative, uninformative, or damaged part of the tissue. For instance, if 95% of a tumor is necrotic, TEM analysis of the necrotic core may not be informative, and if the sampling is from the viable rim, this needs to be specified when reported. Clearly, this introduces the potential for subjectivity because reviewers of a paper cannot request multiple images with a careful statistical analysis with these types of samples. In addition, ex vivo samples are not typically randomized during processing, further complicating the possibility of valid statistical analyses. Ex vivo tissue should be fixed immediately and systematically across samples to avoid changes in autophagy that may occur simply due to the elapsed time ex vivo. It is recommended that for tissue samples, perfusion fixation should be used when possible. Rapid freezing techniques such as high-pressure freezing followed by freeze substitution (i.e., dehydration and chemical fixation at low temperature) have a widely accepted potential for improved sample preparation. Consequently, cryopreparation protocols have been established for many molecular biological model organisms and tissue culture [155]. Such cryopreparation techniques have already proven especially useful for elucidation of autophagy in yeast [156,157].

Quantification of autophagy by TEM morphometry can be very useful and accurate, but, unfortunately, unreliable procedures still continue to be used. For the principles of reliable quantification and to avoid misleading results, excellent reviews are available [12 [158-160]]. In line with the basic principles of morphometry we find it necessary to emphasize here some common problems with regard to quantification. Counting autophagic vacuole profiles in sections of cells (i.e., number of autophagic profiles per cell profile) may give unreliable results, partly because both cell areas and profile areas are variable and also because the frequency of section profiles depends on the size of the vacuoles. However, estimation of the number of autophagic profiles per cell area is more reliable and correlates well with the volume fraction mentioned below [161]. There are morphometric procedures to measure or estimate the size range and the number of spherical objects by profiles in sections [160]; however, such

methods have been used in autophagy research only a few times [42,149,162,163].

Proper morphometric procedures return data as μm^3 autophagic vacuole/ μm^3 cytoplasm for relative volume (also called volume fraction or volume density), or μm^2 autophagic vacuole surface/ μm^3 cytoplasm for relative surface (surface density). Examples of actual morphometric measurements for the characterization of autophagic processes can be found in several articles [22,154,160,164,165]. It is appropriate to note here that a change in the volume fraction of the autophagic compartment may come from two sources; from the real growth of its size in a given cytoplasmic volume, or from the decrease of the cytoplasmic volume itself. To avoid this so-called “reference trap,” the reference space volume can be determined by different methods [158,166]. If different magnifications are used for measuring the autophagic vacuoles and the cytoplasm (which may be practical when autophagy is less intense) correction factors should always be used.

In some cases, it may be prudent to employ tomographic reconstructions of TEM images to confirm that the autophagic compartments are spherical and are not being confused with interdigitations observed between neighboring cells, endomembrane cisternae or damaged mitochondria with similar appearance in thin-sections (e.g., see ref [167].), but this is obviously a time-consuming approach requiring sophisticated equipment. In addition, interpretation of tomographic images can be problematic. For example, starvation-induced autophagosomes should contain cytoplasm (i.e., cytosol and possibly organelles), but autophagosome-related structures involved in specific types of autophagy should show the selective cytoplasmic target, but may be relatively devoid of bulk cytoplasm. Such processes include selective peroxisome or mitochondria degradation (pexophagy or mitophagy, respectively) [168,169], targeted degradation of pathogenic microbes (xenophagy) [170-175], a combination of xenophagy and stress-induced mitophagy [176], as well as the yeast biosynthetic cytoplasm-to-vacuole targeting (Cvt) pathway [177]. Furthermore, some pathogenic microbes express membrane-disrupting factors during infection (e.g., phospholipases) that disrupt the normal double-membrane architecture of autophagosomes [178]. It is not even clear if the sequestering compartments used for specific organelle degradation or xenophagy should be termed autophagosomes or if alternate terms such as pexophagosome [179], mitophagosome and xenophagosome should be used, even though the membrane and mechanisms involved in their formation may be identical to those for starvation-induced autophagosomes. Indeed, the double-membrane vesicle of the Cvt pathway is referred to as a Cvt vesicle [180].

The confusion of heterophagic structures with autophagic ones is a major source of misinterpretation. A prominent example of this is related to cell death. Apoptotic bodies from neighboring cells can be readily phagocytosed by surviving cells of the same tissue [181,182]. Immediately after phagocytic uptake of apoptotic bodies, phagosomes may appear as double membraned. The inner one is the plasma membrane of the apoptotic body and the outer one is that of the phagocytizing cell. The early heterophagic vacuole formed in this way may appear similar to an autophagosome or, in a

later stage, an early autolysosome in that it contains recognizable or identifiable cytoplasmic material. A major difference, however, is that the surrounding membranes are the thicker plasma membrane type, rather than the thinner sequestration membrane type [153]. A good feature to distinguish between autophagosomes and double plasma membrane-bound structures is the lack of the distended empty space (characteristic for the sequestration membranes of autophagosomes) between the two membranes of the phagocytic vacuoles. In addition, engulfed apoptotic bodies usually have a larger average size than autophagosomes [183,184]. The problem of heterophagic elements interfering with the identification of autophagic ones is most prominent in cell types with particularly intense heterophagic activity (such as macrophages, and amoeboid or ciliate protists). Special attention has to be paid to this problem in cell cultures or in vivo treatments (e.g., with toxic or chemotherapeutic agents) causing extensive cell death.

The most common organelles confused with autophagic vacuoles are mitochondria, ER, endosomes, and also (depending on their structure) plastids in plants. Due to the cisternal structure of the ER, double membrane-like structures surrounding mitochondria or other organelles are often observed after sectioning [185], but these can also correspond to cisternae of the ER coming into and out of the section plane [66]. If there are ribosomes associated with these membranes they can help in distinguishing them from the ribosome-free double-membrane of the phagophore and autophagosome. Observation of a mixture of early and late autophagic vacuoles that is modulated by the time point of collection and/or brief pulses of bafilomycin A₁ to trap the cargo in a recognizable early state [55] increases the confidence that an autophagic process is being observed. In these cases, however, the possibility that feedback activation of sequestration gets involved in the autophagic process has to be carefully considered. To minimize the impact of errors, exact categorization of autophagic elements should be applied. Efforts should be made to clarify the nature of questionable structures by extensive preliminary comparison in many test areas. Elements that still remain questionable should be categorized into special groups and measured separately. Should their later identification become possible, they can be added to the proper category or, if not, kept separate.

For nonspecialists it can be particularly difficult to distinguish among amphisomes, autolysosomes and lysosomes, which are all single-membrane compartments containing material that has been more or less degraded. Therefore, we suggest in general to measure autophagosomes as a separate category for a start, and to compile another category of degradative compartments (including amphisomes, autolysosomes and lysosomes). All of the autophagic compartments increase in quantity upon true autophagy induction; however, in pathological states, it may be informative to discriminate among these different forms of degradative compartments, which may be differentially affected by disease factors. By applying both immuno-TEM and Airyscan confocal imaging, it is possible to obtain a comprehensive and quantitative analysis of LAMP1 distribution in various autophagic organelles in neurons [186,187]. A significant portion of LAMP1-labeled organelles lack major lysosomal hydrolases,

and LAMP1 intensity is not a sensitive readout to assess autophagic deficits in familial amyotrophic lateral sclerosis-linked motor neurons in vivo [188,189]. Thus, caution is warranted when interpreting LAMP1-labeled autolysosomes and labeling a set of active lysosomal hydrolases combined with various autophagic markers would be necessary to assess degradative autolysosomes under physiological and pathological conditions.

A new and fast developing technique is combining the temporal resolution of time-lapse fluorescence microscopy with the spatial resolution of super-resolution microscopy. HEK293 cells that express recombinant proteins of interest fused to fluorescent tags are imaged live to capture the formation of autophagosomes, fixed on stage to “snap-freeze” these structures, stained with appropriate antibodies, relocated, and imaged at super resolution by direct stochastic optical reconstruction microscopy [190].

Super-resolution microscopy techniques at ~ 20 nm spatial resolution via 3-color, 3-dimensional super-resolution fluorescence microscopy, makes it possible to image the structural organization of the ULK1 complex that scaffolds the formation of cup-like structures located at SEC12-enriched remodeled ER-exit sites prior to LC3 lipidation. This cup scaffold provides a structural asymmetry to enforce the directional recruitment of downstream components, including the ATG12–ATG5–ATG16L1 complex, WIPI2, and LC3, to the convex side of the cup [191].

In yeast, it is convenient to identify autophagic bodies that reside within the vacuole lumen, and to quantify them as an alternative to the direct examination of autophagosomes. However, it is important to keep in mind that it may not be possible to distinguish between autophagic bodies that are derived from the fusion of autophagosomes with the vacuole, and the single-membrane vesicles that are generated during microautophagy-like processes such as micropexophagy and micromitophagy.

Conclusion: EM is an extremely informative and powerful method for monitoring autophagy and is one of the few techniques that shows autophagy in its complex cellular environment with subcellular resolution. The cornerstone of successfully using TEM is the proper identification of autophagic structures, which is also the prerequisite to get reliable quantitative results by TEM morphometry. EM is best used in combination with other methods to ensure the complex and holistic approach that is becoming increasingly necessary for further progress in autophagy research.

Atg8-family protein detection and quantification

Atg8 and the Atg8-family proteins are the most widely monitored autophagy-related proteins. In this section we describe multiple assays that utilize these proteins.

Western blotting and ubiquitin-like protein conjugation systems. Atg8 is a ubiquitin-like protein that can be conjugated to PE (and possibly to phosphatidylserine [PS] [192]). In yeast and several other organisms, the conjugated form is referred to as Atg8–PE. The mammalian homologs of Atg8 constitute a family of proteins subdivided in two major subfamilies: MAP1LC3/LC3 and GABARAP. The former consists of LC3A (two splice variants), LC3B, LC3B2 and LC3C, whereas the latter family

includes GABARAP, GABARAPL1, and GABARAPL2/GATE-16 [193]. After cleavage of the precursor protein mostly by the cysteine protease ATG4B [194,195], the nonlipidated and lipidated forms are usually referred to respectively as LC3-I and LC3-II, or GABARAP and GABARAP–PE, etc. The PE-conjugated form of Atg8-family proteins, although larger in mass, shows faster electrophoretic mobility in SDS-PAGE gels, probably as a consequence of increased hydrophobicity. The positions of both the unconjugated (approximately 16–18 kDa) and lipid conjugated (approximately 14–16 kDa) forms of the Atg8-family proteins should be indicated on western blots whenever both are detectable. The differences among the LC3/GABARAP proteins with regard to function and tissue-specific expression are not well defined; however, new evidence suggests that LC3 proteins have distinct subcellular distributions and mediate different types of selective autophagy [196,197]. Therefore, it is important to indicate the isoform being analyzed just as it is for the GABARAP subfamily, and to specify which antibody is being used.

The mammalian Atg8 homologs share from 29% to 94% sequence identity with the yeast protein and have all been demonstrated to be involved in autophagosome biogenesis [198]. LC3 proteins are involved in autophagosome formation, with participation of GABARAP subfamily members in later stages of autophagosome formation [199]. Some evidence, however, suggests that, at least in certain cell types, the LC3 subfamily may be dispensable for bulk autophagic sequestration of cytosolic proteins, whereas the GABARAP subfamily is absolutely required [32]. Also, PINK1-PRKN-dependent mitophagy strongly requires the GABARAP subfamily, with little or no requirement for the LC3 subfamily [34,35]. Due to unique features in their molecular surface charge distribution [200], emerging evidence indicates that LC3 and GABARAP proteins may be involved in recognizing distinct sets of cargoes for selective autophagy [201–203]. Nevertheless, in most published studies, LC3 has been the primary Atg8-family homolog examined in mammalian cells and the one that is typically characterized as an autophagosome marker per se. Note that although this protein is referred to as “Atg8” in many other systems, we primarily refer to it in this section as LC3 to distinguish it from the yeast protein and from the GABARAP subfamily, whereas we generally refer to the “Atg8-family proteins” throughout the rest of these guidelines. LC3, like the other Atg8 homologs, is initially synthesized in an unprocessed form, proLC3, which is converted into a proteolytically processed form lacking amino acids from the C terminus, LC3-I, and is finally modified into the PE-conjugated form, LC3-II (Figure 7). Atg8–PE/LC3-II is the only protein marker that is reliably associated with completed autophagosomes, but is also localized to phagophores. In yeast, Atg8 protein levels increase at least 10-fold when autophagy is induced [204]. In mammalian cells, however, the total levels of LC3 do not necessarily change in a predictable manner, as there may be an increase in the conversion of LC3-I to LC3-II, or a decrease in LC3-II relative to LC3-I if degradation of LC3-II via lysosomal turnover is particularly rapid (this can also be a concern in yeast with regard to vacuolar turnover of Atg8–PE). Both of these events can be seen sequentially in several cell types as a response to total

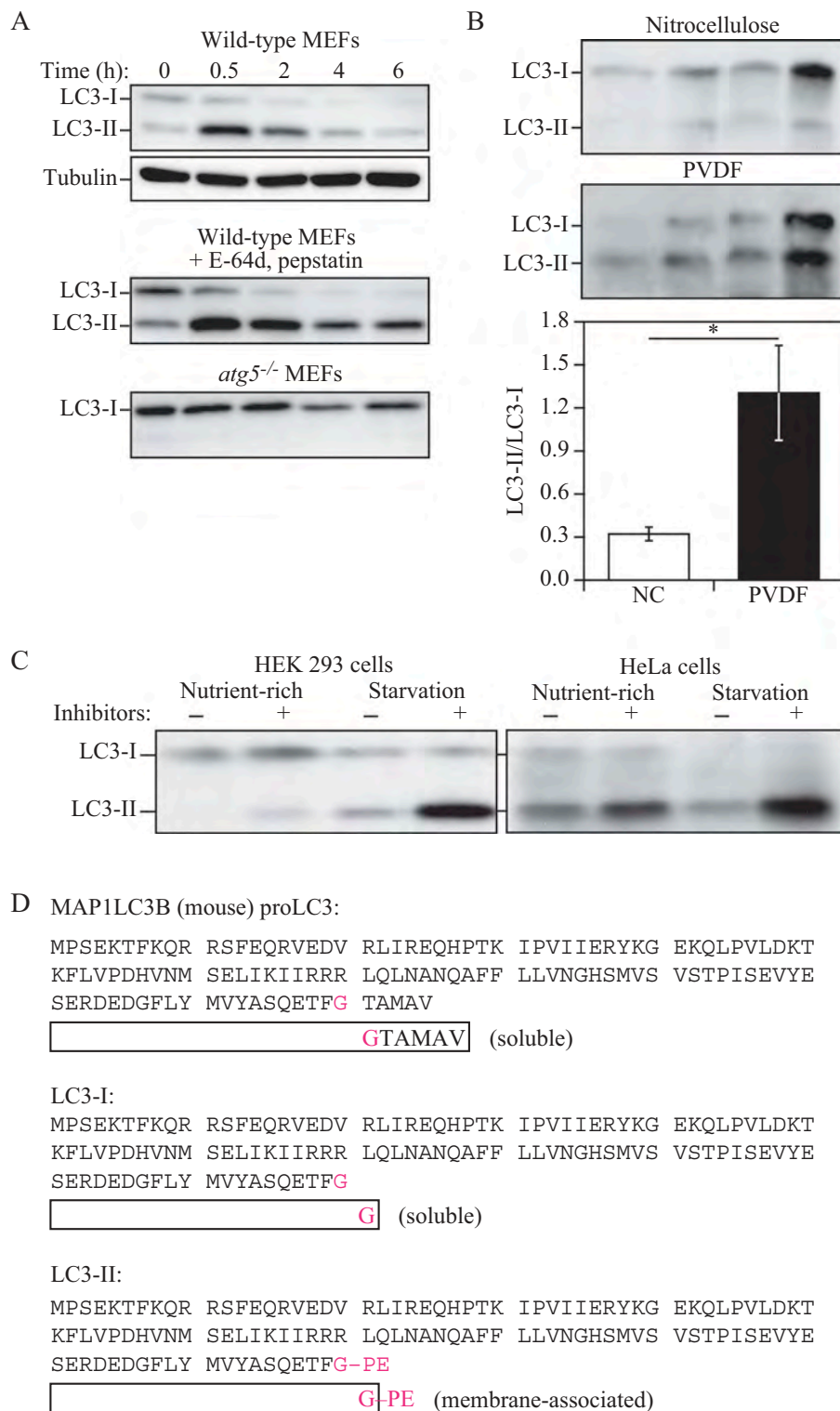


Figure 7. LC3-I conversion and LC3-II turnover. **(A)** Expression levels of LC3-I and LC3-II during starvation. *Atg5*^{+/+} (wild-type) and *atg5*^{-/-} MEFs were cultured in DMEM without amino acids and serum for the indicated times, and then subjected to immunoblot analysis using anti-LC3 antibody and anti-tubulin antibody. E-64d (10 μ g/ml) and pepstatin A (10 μ g/ml) were added to the medium where indicated. Positions of LC3-I and LC3-II are marked. The inclusion of lysosomal protease inhibitors reveals that the apparent decrease in LC3-II is due to lysosomal degradation as easily seen by comparing samples with and without inhibitors at the same time points (the overall decrease seen in the presence of inhibitors may reflect decreasing effectiveness of the inhibitors over time). Monitoring autophagy by following steady-state amounts of LC3-II without including inhibitors in the analysis can result in an incorrect interpretation that autophagy is not taking place (due to the apparent absence of LC3-II). Conversely, if there are high levels of LC3-II but there is no change in the presence of inhibitors this may indicate that induction has occurred but that the final steps of autophagy are blocked, resulting in stabilization of this protein. This figure was modified from data previously published in ref. [30], and is reproduced by permission of Landes Bioscience, copyright 2007. **(B)** Lysates of four human adipose tissue biopsies were resolved on two 12% polyacrylamide gels, as described previously [292]. Proteins were transferred in parallel to either a PVDF or a nitrocellulose membrane, and blotted with anti-LC3 antibody, and then identified by reacting the membranes with an HRP-conjugated anti-rabbit IgG antibody, followed by ECL. The LC3-II:LC3-I ratio was calculated based on densitometry analysis of both bands. *, $P < 0.05$. **(C)** HEK 293 and HeLa cells were cultured in nutrient-rich medium (DMEM containing 10% fetal calf serum) or incubated for 4 h in starvation conditions (Krebs-Ringer medium) in the absence (-) or presence (+) of E-64d and pepstatin at 10 μ g/ml each (Inhibitors). Cells were then lysed and the proteins resolved by SDS-PAGE. Endogenous LC3 was detected by immunoblotting. Positions of LC3-I and LC3-II are indicated. In the absence of

nutrient and serum starvation. It is also possible that following the induction of autophagy there is a decrease in both LC3-I and LC3-II due to rapid LC3-I conversion together with rapid LC3-II degradation [205]. In cells of neural lineage, a high ratio of LC3-I to LC3-II is a common finding [206]. For instance, SH-SY5Y neuroblastoma cell lines display only a slight increase of LC3-II after nutrient deprivation, whereas LC3-I is clearly reduced. This is likely related to a high basal autophagic flux, as suggested by the higher increase in LC3-II when cells are treated with NH_4Cl [207,208], although cell-specific differences in transcriptional regulation of LC3 may also play a role. In fact, stimuli or stress that inhibit transcription or translation of LC3 might actually be misinterpreted as inhibition of autophagy, and vice versa—stimuli or stress that increase transcription or translation of LC3 might be misinterpreted as activation of autophagy. The LC3-I:LC3-II ratio can vary across brain cancer cells depending on the basal level of autophagy, a phenomenon that can influence further analysis of autophagy activation upon stressful conditions such as hypoxia [209]. Importantly, in brain spinal cord and dorsal root ganglia tissue, LC3-I is much more abundant than LC3-II [210,211] and the latter form is most easily discernible in enriched fractions of autophagosomes, autolysosomes and ER, and may be more difficult to detect in crude homogenate or cytosol [212]. It is possible to readily detect both LC3-I and LC3-II in brain and spinal cord lysates with the use of a gel that allows sufficient separation of the LC3-I/LC3-II bands so the strong LC3-I band does not interfere with detection of the much weaker LC3-II band (e.g., a 4-20% gradient gel or a 4-12% Bis-Tris gel using MES buffer) [213,214]. In studies of the brain, immunoblot analysis of the membrane and cytosol fraction from a cell lysate, upon appropriate loading of samples to achieve quantifiable and comparative signals, can be useful to measure LC3 forms. For more accurate quantification of LC3-I and LC3-II levels, a correction factor for differential immunoreactivity of the two forms can be obtained through analyses of LC3-I and LC3-II protein levels upon ATG4-mediated delipidation [32].

The pattern of LC3-I to LC3-II conversion seems to be not only cell specific, but also related to the kind of stress to which cells are subjected. For example, SH-SY5Y cells display a strong increase of LC3-II when treated with the proton gradient uncoupler CCCP, a well-known disruptor of the mitochondrial membrane potential and inducer of mitophagy (although it has also been reported that CCCP may actually inhibit mitophagy [215]). Thus, neither assessment of LC3-I consumption nor the evaluation of LC3-II levels would necessarily reveal a slight induction of autophagy (e.g., by rapamycin). Also, there is not always a clear precursor/product relationship between LC3-I and LC3-II, because the conversion of the former to the latter is cell type-specific and dependent on the treatment used to induce autophagy. Accumulation of LC3-II, which is

generally proportional with time, can be obtained through the following: i) By interrupting the autophagosome-lysosome fusion step (e.g., by depolymerizing acetylated microtubules with vinblastine); ii) by inhibiting the $\text{ATP2A/SERCA Ca}^{2+}$ pump with thapsigargin [216]; iii) by specifically inhibiting the V-ATPase with bafilomycin A_1 [217-219]; iv) or by raising the lysosomal pH by the addition of CQ [220,221]. It should be noted that some of these treatments may increase autophagosome numbers by: i) Disrupting the lysosome-dependent activation of MTOR (mechanistic target of rapamycin kinase) complex 1 (MTORC1), a major suppressor of autophagy induction [222,223] (note that the original term “mTOR” was named to distinguish the “mammalian” target of rapamycin from the yeast proteins [224]); ii) by inhibiting lysosome-mediated proteolysis (e.g., with a cysteine protease inhibitor such as E-64d, the aspartic protease inhibitor pepstatin A, the cysteine, serine and threonine protease inhibitor leupeptin or treatment with bafilomycin A_1 , NH_4Cl or CQ [220, 225-227]); iii) by inhibiting autophagosome-lysosome fusion (by treatment with bafilomycin A_1 [218]). It should also be noted that low concentration treatment with lysosomal inhibitors increases lysosomal activity [228]. Western blotting can be used to monitor changes in LC3 amounts (Figure 7) [30,229]; however, even if the total amount of LC3 does increase, the magnitude of the response is generally less than that documented in yeast. It is worth noting that because the conjugated forms of the GABARAP subfamily members are usually undetectable without induction of autophagy in mammalian and other vertebrate cells [230,231], these proteins might be more suitable than LC3 to study and quantify subtle changes in autophagy induction.

As Atg8-family proteins are often synthesized with a C-terminal extension that is removed by Atg4, this processing event can be used to monitor Atg4 activity. For example, when GFP or tags such as HA, MYC or FLAG are fused at the C terminus of Atg8 (Atg8-GFP, etc.), the epitope is removed in the cytosol to generate free Atg8 and the corresponding tag. This processing can be easily monitored by western blot [232,233]. It is also possible to use assays with an artificial fluorogenic substrate, or a fusion of LC3B to PLA2 (phospholipase A2) that allows the release of the active phospholipase for a subsequent fluorogenic assay [234], and there is a Förster resonance energy transfer (FRET)-based assay utilizing CFP- and YFP-tagged versions of LC3B and GABARAPL2 that can be used for high-throughput screening [235]. Another method to monitor ATG4 activity in vivo uses the release of *Gaussia* luciferase from the C terminus of LC3 that is tethered to actin [236]. Note that there are 4 homologs of yeast Atg4 in mammals, and they have different activities with regard to the Atg8-family proteins [237]. ATG4A is able to cleave the GABARAP subfamily, but has very limited activity toward the LC3 subfamily, whereas ATG4B is apparently active against most or all of these proteins [194,195]. The ATG4C and

Figure 7. (Continued).

lysosomal protease inhibitors, starvation results in a modest increase (HEK 293 cells) or even a decrease (HeLa cells) in the amount of LC3-II. The use of inhibitors reveals that this apparent decrease is due to lysosome-dependent degradation. This figure was modified from data previously published in ref. [240], and is reproduced by permission of Landes Bioscience, copyright 2005. (D) Sequence and schematic representation of the different forms of LC3B. The sequence for the nascent (proLC3) from mouse is shown. The glycine at position 120 indicates the cleavage site for ATG4. After this cleavage, the truncated LC3 is referred to as LC3-I, which is still a soluble form of the protein. Conjugation to PE generates the membrane-associated LC3-II form (equivalent to Atg8-PE).

ATG4D isoforms have minimal activity for any of the Atg8-family protein homologs. In particular, because Atg4/ATG4 will cleave a C-terminal fusion immediately, researchers should be careful to specify whether they are using GFP-Atg8 (or GFP-LC3/GABARAP; an N-terminal fusion, which can be used to monitor various steps of autophagy) or Atg8-GFP (or LC3/GABARAP-GFP; a C-terminal fusion, which can only be used to monitor Atg4/ATG4 activity) [238].

Cautionary notes: There are several important caveats to using Atg8/LC3-II/GABARAP-II to visualize fluctuations in autophagy. First, changes in LC3-II amounts are tissue- and cell context-dependent [239,240]. Indeed, in some cases, autophagosome accumulation detected by TEM does not correlate well with the amount of LC3-II (Tallóczy Z, de Vries RLA, and Sulzer D, unpublished results; Eskelinen E-L, unpublished results). This is particularly evident in those cells that show low levels of LC3-II (based on western blotting) because of an intense autophagic flux that consumes this protein, or in cell lines having high levels of LC3-II that are tumor-derived, such as HeLa cells [240]. Conversely, the detectable formation of LC3-II is not sufficient evidence for autophagy. For example, homozygous deletion of *Becn1* does not prevent the formation of LC3-II in embryonic stem cells even though autophagy is substantially reduced, whereas deletion of *Atg5* results in the complete absence of LC3-II (see Fig. 6A and supplemental data in ref [241]). The same is true for the generation of Atg8-PE in yeast in the absence of *VPS30/ATG6* (see Fig. 7 in ref [242]). Thus, it is important to remember that not all of the autophagy-related proteins are required for Atg8-family protein processing, including lipidation [242]. Fluctuations in the detection and amounts of LC3-I versus LC3-II present technical problems. For example, LC3-I is very abundant in brain tissue, and the intensity of the LC3-I band may obscure detection of LC3-II, unless the polyacrylamide crosslinking density is optimized, or the membrane fraction of LC3 is first separated from the cytosolic fraction [41]. Conversely, some cell lines have much less visible LC3-I compared to LC3-II. In addition, tissues may have asynchronous and heterogeneous cell populations, and this variability may present challenges when analyzing LC3 by western blotting.

Second, LC3-II also associates with the membranes of nonautophagic structures. For example, some members of the γ -protocadherin family undergo clustering to form intracellular tubules that emanate from lysosomes [243]. LC3-II is recruited to these tubules, where it appears to promote or stabilize membrane expansion. Furthermore, LC3 can be recruited directly to apoptotic cell-containing phagosome membranes [244,245], macropinosomes [244], the parasitophorous vacuole of *Toxoplasma gondii* [246], and single-membrane entotic vacuoles [244], as well as to bacteria-containing phagosome membranes under certain immune activating conditions, for example, toll-like receptor (TLR)-mediated stimulation in LC3-associated phagocytosis [247,248]. Importantly, LC3 is involved in secretory trafficking as it has been associated with secretory granules in mast cells [249] and PC12 hormone-secreting cells [250]. LC3 is also detected on secretory lysosomes in osteoblasts [251] and in amphisome-like structures involved in mucin secretion by goblet cells [252]. Therefore, in studies of infection of

mammalian cells by bacterial pathogens, the identity of the LC3-II labelled compartment as an autophagosome should be confirmed by a second method, such as TEM. It is also worth noting that autophagy induced in response to bacterial infection is not directed solely against the bacteria but can also be a response to remnants of the phagocytic membrane [253]. Similar cautions apply with regard to viral infection. For example, coronaviruses induce autophagosomes during infection through the expression of nsp6; however, coronaviruses also induce the formation of double-membrane vesicles that are coated with LC3-I, and this plays an autophagy-independent role in viral replication [254,255]. Similarly, nonlipidated LC3 marks replication complexes in flavivirus (Japanese encephalitis virus)-infected cells and is essential for viral replication [256]. Along these lines, during herpes simplex virus type 1 (HSV-1) infection, an LC3⁺ autophagosome-like organelle that is derived from nuclear membranes and that contains viral proteins is observed [257], whereas influenza A virus directs LC3 to the plasma membrane via an LC3-interacting region (LIR) motif in its M2 protein [258]. In addition, shedding microvesicles isolated from HSV-1-infected cells are positive for LC3-II, suggesting a role for the autophagic pathway in microvesicle-mediated HSV-1 spread [259]. Moreover, in vivo studies have shown that coxsackievirus (an enterovirus) induces formation of autophagy-like vesicles in pancreatic acinar cells, together with extremely large autophagy-related compartments that have been termed megaphagosomes [260]; the absence of ATG5 disrupts viral replication and prevents the formation of these structures [261]. Of note, LC3 not only attaches to membrane lipids, but can also be covalently linked to other proteins [262], thus complicating interpretation of its distribution in cells.

Third, caution must be exercised in general when evaluating LC3 by western blotting, and appropriate standardization controls are necessary. For example, LC3-I may be less sensitive to detection by certain anti-LC3 antibodies; antibodies targeting the N-terminal region show lower binding efficiency of LC3-I compared to polyclonal antibodies against the entire protein, leading to a different interpretation of LC3 turnover (Figure 8) (C. Leschczyk, P. Cebollada Rica, U.E. Schaible, unpublished results) [263]. Moreover, LC3-I is more labile than LC3-II, being more sensitive to freezing-thawing and to degradation in SDS sample buffer. Therefore, fresh samples should be boiled and assessed as soon as possible and should not be subjected to repeated freeze-thaw cycles. Alternatively, trichloroacetic acid precipitation of protein from fresh cell homogenates can be used to protect against degradation of LC3 by proteases that may be present in the sample. A general point to consider when examining transfected cells concerns the efficiency of transfection. A western blot will detect LC3 in the entire cell population, including those that are not transfected. Thus, if transfection efficiency is too low, it may be necessary to use methods, such as fluorescence microscopy, that allow autophagy to be monitored in single cells. In summary, the analysis of the gel shift of transfected LC3 or GFP-LC3 can be employed to follow LC3 lipidation only in highly transfectable cells [264].

When dealing with animal tissues, western blotting of LC3 should be performed on frozen biopsy samples homogenized in

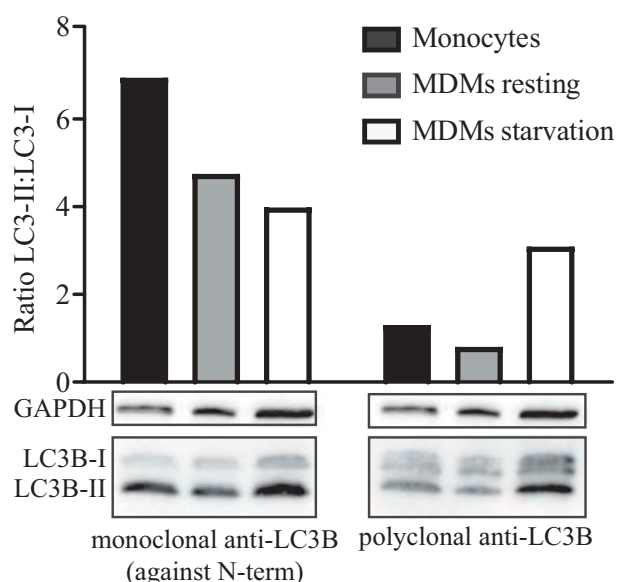


Figure 8. Different LC3B-I:LC3B-II ratios indicating turnover were assessed using a mono- as well as polyclonal anti-LC3B antibody. Monocytes were isolated from human whole blood and differentiated into monocyte-derived macrophages (MDMs) by incubation in human CSF1/M-CSF for 1 week. To induce autophagy, cells were starved by reducing the FCS concentration to 1% for one day. Monocytes, and resting and starved MDMs were lysed with Laemmli buffer; the proteins were separated by SDS-PAGE and analyzed by western blot. Membranes were labeled using a monoclonal antibody to the N terminus of LC3B (Novus, clone 1251D, NBP2-59800) or polyclonal antibodies (Sigma, L7543). Relative intensity of LC3B-I and LC3B-II was quantified with Image Lab™ to calculate LC3B-II:LC3B-I ratios.

the presence of general protease inhibitors (C. Isidoro, personal communication; see also *Human*) [265]. Caveats regarding detection of LC3 by western blotting have been covered in a dedicated review [30]. For example, PVDF membranes may result in a stronger LC3-II retention than nitrocellulose membranes, possibly due to a higher affinity for hydrophobic proteins (Figure 7B; J. Kovsan and A. Rudich, personal communication), and Triton X-100 may not efficiently solubilize LC3-II in some systems [266]. Heating in the presence of 1% SDS, or analysis of membrane fractions [41], may assist in the detection of the lipidated form of this protein. This observation is particularly relevant for cells with a high nucleocytoplasmic ratio, such as lymphocytes. Under these constraints, direct lysis in Laemmli loading buffer, containing SDS, just before heating, greatly improves LC3 detection on PVDF membranes, especially when working with a small number of cells (F. Gros, unpublished observations) [267]. Analysis of a membrane fraction is particularly useful for brain, where levels of soluble LC3-I greatly exceed the level of LC3-II.

One of the most important issues is the quantification of changes in LC3-II, because this assay is one of the most widely used in the field and is rather prone to misinterpretation. Levels of LC3-II should be compared not to LC3-I (see the caveat in the next paragraph), but ideally to more than one “housekeeping” protein (HKP) such as ACTB/β-actin. Actin and other HKPs, however, are usually abundant and can easily be overloaded on the gel [268] such that their density is saturated and, as such, they are not detected within a linear range. Moreover, actin levels may decrease when autophagy is induced in many organisms from yeast to mammals. Similar

considerations apply to GAPDH, at least in some cell types (L. Galluzzi, personal communication) [269]. For any proteins used as “loading controls” (including actin, tubulin, MAPK1 [270–272] and GAPDH) multiple exposures of the western blot are generally necessary to ensure that the signals are detected in the linear range when using film. Alternatively, the western blot signals can be detected using a gel imaging system compatible with secondary antibodies with infrared fluorescence, or an instrument that takes multiple chemiluminescence exposures and automatically selects the optimal exposure times. Another alternative approach is to stain for total cellular proteins with Coomassie Brilliant Blue or Ponceau Red [273] instead of using HKPs, but that approach is generally less sensitive and may not reveal small differences in protein loading. Stain-Free gels, which also stain for total cellular proteins, have been shown to be an excellent alternative to HKPs [274].

It is important to realize that ignoring the level of LC3-I in favor of LC3-II normalized to HKPs may not provide the full picture of the cellular autophagic response [239,275]. For example, in aging rat skeletal muscle, the increase in LC3-I is at least as important as that for LC3-II [276,277]. Yet in other settings, autophagy induction triggers a significant decrease in LC3-I levels, along with an increase in LC3-II levels, presumably due to its increased conversion into LC3-II [278]. Quantification of both isoforms is therefore informative, but requires adequate conditions of electrophoretic separation. This is particularly important for samples where the amount of LC3-I is high relative to LC3-II (as in brain tissues, where the LC3-I signal can be overwhelming). Under such a scenario, it may be helpful to use 15% or 16% polyacrylamide gels or gradient gels to increase the separation of LC3-I from LC3-II. Furthermore, because the dynamic range of LC3 immunoblots is generally quite limited, it is imperative that other assays be used in parallel in order to draw valid conclusions about changes in autophagy activity.

Fourth, in mammalian cells LC3 is expressed as multiple isoforms (LC3A, LC3B, LC3B2 and LC3C [279,280]), which exhibit different tissue distributions and whose functions are still poorly understood. A point of caution along these lines is that the increase in LC3A-II versus LC3B-II levels may not display equivalent changes in all organisms under autophagy-inducing conditions, and it should not be assumed that LC3B is the optimal protein to monitor [281]. A key technical consideration is that the isoforms may exhibit different specificities for antisera or antibodies. Thus, it is highly recommended that investigators report exactly the source and catalog number of the antibodies used to detect LC3 as this might help avoid discrepancies between studies (reporting company and catalog number is a requirement for publishing in the journal *Autophagy* [282]). The current commercialized anti-LC3B antibodies also recognize LC3A, but do not recognize LC3C, which shares less sequence homology. It is important to note that LC3C possesses in its primary amino acid sequence the DYKD motif that is recognized with a high affinity by anti-FLAG antibodies. Thus, the standard anti-FLAG M2 antibody can detect and immunoprecipitate overexpressed LC3C, and caution has to be taken in experiments using FLAG-tagged proteins (M. Biard-Piechaczyk and L.

Espert, personal communication). Note that according to Ensembl there is no *LC3C* in mouse or rat.

In addition, it is important to keep in mind the other subfamily of Atg8 proteins, the GABARAP subfamily (see above) [198,283]. Both starvation-induced autophagy and PINK1-PRKN-dependent mitophagy, as noted above, predominantly require the GABARAP subfamily over the LC3 subfamily [32,34,35]. Moreover, certain types of mitophagy induced by BNIP3L/NIX are highly dependent on GABARAP and less dependent on LC3 proteins [284,285]. Furthermore, commercial antibodies for GABARAPL1 also recognize GABARAP [32,193], which might lead to misinterpretation of experiments, in particular those using immunohistochemical techniques. Sometimes the problem with cross-reactivity of the anti-GABARAPL1 antibody can be overcome when analyzing these proteins by western blot because the isoforms can be resolved during SDS-PAGE using high concentration (15%) gels, as GABARAP migrates faster than GABARAPL1 (M. Boyer-Guittaut, personal communication; also see Fig. S4 in ref [32]). Because GABARAP and GABARAPL1 can both be proteolytically processed and lipidated, generating GABARAP-I or GABARAPL1-I and GABARAP-II or GABARAPL1-II, respectively, this may lead to a misassignment of the different bands. As soon as highly specific antibodies that are able to discriminate between GABARAP and GABARAPL1 become available, we strongly advise their use; until then, we recommend caution in interpreting results based on the detection of these proteins by western blot. Antibody specificity can be assessed after complete inhibition of GABARAP (or any other Atg8-family protein) expression by RNA interference [32,231]. In general, we advise caution in choosing antibodies for western blotting and immunofluorescence experiments and in interpreting results based on stated affinities of antibodies unless these have been clearly determined.

As with any western blot, proper methods of quantification must be used, which are, unfortunately, often not well disseminated; readers are referred to an excellent paper on this subject (see ref [286]). Unlike the other members of the GABARAP family, almost no information is available on GABARAPL3, perhaps because it is not yet possible to differentiate between GABARAPL1 and GABARAPL3 proteins, which have 94% identity. As stated by the laboratory that described the cloning of the human *GABARAPL1* and *GABARAPL3* genes [283], their expression patterns are apparently identical. It is worth noting that *GABARAPL3* is the only gene of the *GABARAP* subfamily that seems to lack an ortholog in mice [283]. *GABARAPL3* might therefore be considered as a pseudogene without an intron that is derived from *GABARAPL1*. Hence, until new data are published, *GABARAPL3* should not be considered as the fourth member of the *GABARAP* family. Another important consideration is that lipidated LC3/GABARAP isoforms (particularly GABARAP and GABARAPL1) can be unstable in non-denatured cell lysates due to ATG4B delipidation activity, even in the presence of a protease inhibitor cocktail. This can result in an underestimation of the true physiological levels of lipidated LC3/GABARAP detected by western blotting. To avoid this artefact, N-ethylmaleimide can be included in lysis buffer to irreversibly inhibit ATG4B, or lysis can be performed under reducing and denaturing conditions [287].

Fifth, in non-mammalian species, the discrimination of Atg8-PE from the nonlipidated form can be complicated by their nearly identical SDS-PAGE mobilities and the presence of multiple isoforms (e.g., there are nine in *Arabidopsis*). In yeast, it is possible to resolve Atg8 (the nonlipidated form) from Atg8-PE by including 6 M urea in the SDS-PAGE separating gel [288], or by using a 15% resolving gel without urea (F. Reggiori, personal communication). Similarly, urea combined with prior treatment of the samples with (or without) PLD (phospholipase D; that will remove the PE moiety) can often resolve the ATG8 species in plants [289,290]. It is also possible to label cells with radioactive ethanolamine, followed by autoradiography to identify Atg8-PE, and a C-terminal peptide can be analyzed by mass spectrometry (MS) to identify the lipid modification at the terminal glycine residue. Special treatments are not needed for the separation of mammalian LC3-I from LC3-II. However, in human cells, pro-LC3B and LC3B-II are indistinguishable by western blotting [291], and a PLD cleavage assay may be required to discriminate between the two isoforms [287], which is particularly important under conditions where ATG4 activity is reduced.

Sixth, it is important to keep in mind that *ATG8*, and to a lesser extent *LC3*, undergoes substantial transcriptional and posttranscriptional regulation. Accordingly, to obtain an accurate interpretation of Atg8-family protein levels it is also necessary to monitor the mRNA levels. Without analyzing the corresponding mRNA, it is not possible to discriminate between changes that are strictly reflected in altered amounts of protein versus those that are due to changes in transcription (e.g., the rate of transcription, or mRNA stability). For example, in cells treated with the calcium ionophore A23187 or the ER calcium pump blocker thapsigargin, an obvious correlation is found between the time-dependent increases in LC3B-I and LC3B-II protein levels, as well as with the observed increase in *LC3B* mRNA levels [216]. Clinically, in human adipose tissue, protein and mRNA levels of LC3 in omental fat are similarly elevated in obese compared to lean individuals [292]. Post-translational modifications, such as phosphorylation of LC3, may also affect its migration and/or the avidity of certain antibodies [293].

Seventh, LC3-I can be fully degraded by the 20S proteasome or, more problematically, processed to a form (LC3-T) appearing equal in size to LC3-II on a western blot; LC3-T was identified in HeLa cells and is devoid of the ubiquitin conjugation domain, thus lacking its adaptor function for autophagy [294].

Eighth, although it is usually possible to distinguish the nonlipidated (LC3-I) and lipidated (LC3-II) forms of LC3 using standard SDS-PAGE and western blotting (see above), some other protein separation systems fail to differentiate between them. For example, the widely used WES system, based on capillary electrophoresis and Simple Western™ technology (in which all assay steps, from protein separation, immunoprobng, detection and analysis of data are fully automated), can solve many problems found in traditional western blotting [295]; however, using this system it is not possible to distinguish LC3-I and LC3-II forms (see Figure 9 for comparison of separation of LC3 forms in traditional western blotting

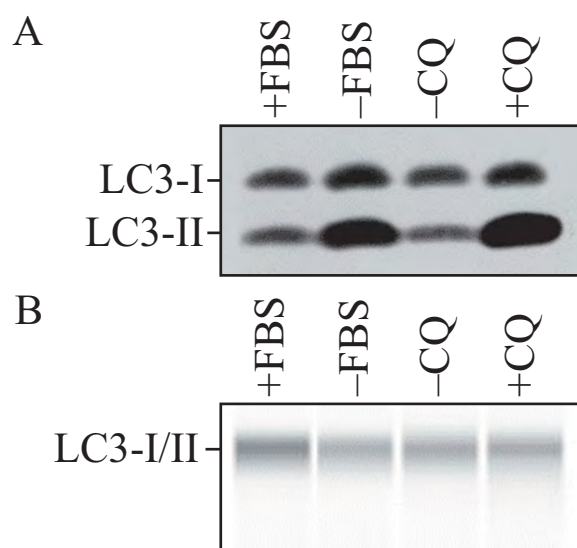


Figure 9. Detection of nonlipidated (LC3-I) and lipidated (LC3-II) forms of the LC3 protein using (A) traditional SDS-PAGE and western blotting or (B) the WES System (WES - Automated Western Blots with Simple Western; ProteinSimple, San Jose, CA, USA). HEK 293 cells were cultured in DMEM medium, containing 10% fetal bovine serum and a penicillin-streptomycin mixture, at 37°C in a humidified atmosphere with 5% CO₂. Cell cultures were treated with medium devoid of fetal bovine serum (-FBS) or with chloroquine (CQ; final concentration 10 μM) for 2 h. The forms of the LC3 protein were detected using anti-LC3 antibodies (MBL International, PM036). Materials from the same samples were used in experiments presented in panels A and B. The LC3-I and LC3-II forms can be effectively separated using traditional SDS-PAGE and western blotting, whereas these two forms of LC3 cannot be distinguished by using the WES system. Results provided by K. Pierzynowska, L. Gaffke and G. Wegrzyn.

and WES). Most likely, this is due to unusual (i.e., inconsistent with the actual molecular mass) migration of LC3-II in SDS-PAGE which does not take place during gel-free capillary electrophoresis [296]. Therefore, although the WES system is excellent for rapid and accurate detection of the vast majority of proteins, and makes it possible to avoid various technical problems met in traditional western blotting, including those met in studies on subjects related to autophagy (see for example [297,298]), it is not recommended for experiments where it is important to resolve LC3-I and LC3-II. This problem has been widely discussed with representatives of the WES system manufacturer who confirmed that it is technically not possible to separate these two forms of LC3 using Simple Western™ technology (K. Pierzynowska and G. Wegrzyn, personal communication). Nonetheless, the WES system can still be used to monitor changes in the total amount of LC3, and can thus provide useful information, especially in conjunction with other assays.

Conclusion: Atg8-family proteins are often excellent markers for autophagic structures; however, it must be kept in mind that there are multiple LC3 isoforms, there is a second family of mammalian Atg8-like proteins (GABARAPs), and antibody affinity (for LC3-I versus LC3-II) and specificity (for example, for LC3A versus LC3B) must be considered and/or determined. Moreover, LC3/GABARAP levels on their own do not address issues of autophagic flux. Finally, even when flux assays are carried out, there is a problem with the limited dynamic range of LC3/GABARAP immunoblots; accordingly, this method should not be used by itself to analyze changes in autophagy.

Turnover of LC3-II/Atg8-PE: Autophagic flux. Autophagic flux is often inferred on the basis of LC3-II turnover, measured by western blot (Figure 7C) [240] in both the presence and absence of lysosomal, or vacuolar degradation. However, it should be cautioned that such LC3 assays are merely indicative of autophagic “carrier flux”, not of actual autophagic cargo/substrate flux. It has, in fact, been observed that in rat hepatocytes, an autophagic-lysosomal flux of LC3-II can take place in the absence of an accompanying flux of cytosolic bulk cargo [299]. The relevant parameter in LC3 assays is the difference in the amount of LC3-II in both the presence and absence of saturating levels of inhibitors, which can be used to examine the transit of LC3-II through the autophagic pathway; if flux is occurring, the amount of LC3-II will be higher in the presence of the inhibitor [240]. Lysosomal degradation can be prevented through the use of protease inhibitors (e.g., pepstatin A, leupeptin and E-64d), compounds that neutralize the lysosomal pH such as bafilomycin A₁, CQ or NH₄Cl [17,206,220,226,300,301], or by treatment with agents that block the fusion of autophagosomes with lysosomes (note that CQ blocks autophagy predominantly by inhibiting autophagosome-lysosome fusion [302] and that bafilomycin A₁ will ultimately cause a fusion block as well as neutralize the pH [218], but the inhibition of fusion may be due to a block in ATP2A/SERCA activity [303]) [217-219], 304]. Alternatively, knocking down or knocking out LAMP2 (lysosomal associated membrane protein 2) represents a genetic approach to block the fusion of autophagosomes and lysosomes (for example, inhibiting LAMP2 in leukemic cells results in a marked increase of GFP-LC3 puncta and endogenous LC3-II protein compared to control cells upon autophagy induction during myeloid differentiation [M.P. Tschan, unpublished data], whereas in prostate cancer LNCaP cells, knocking down LAMP2 prevents autophagy [305]) [306]. This approach, however, is only valid when the knockdown of LAMP2 is directed against the mRNA region specific for the *LAMP2B* spliced variant, as targeting the region common to the three variants would also inhibit chaperone-mediated autophagy (CMA), which may result in the compensatory upregulation of autophagy [133,307,308].

Increased levels of LC3-II in the presence of lysosomal inhibition or interfering with autophagosome-lysosome fusion alone (e.g., with bafilomycin A₁), may be indicative of greater induction and cargo sequestration, but to assess whether a particular treatment alters complete autophagic flux through substrate digestion, the treatment plus bafilomycin A₁ must be compared with results obtained with treatment alone as well as with bafilomycin A₁ alone. An additive or supra-additive effect in LC3-II levels may indicate that the treatment enhances autophagic flux (Figure 7C). Moreover, higher LC3-II levels with treatment plus bafilomycin A₁ compared to bafilomycin A₁ alone may indicate that the treatment increases the synthesis of autophagy-related membranes. If the treatment by itself increases LC3-II levels, but the treatment plus bafilomycin A₁ does not increase LC3-II levels compared to bafilomycin A₁ alone, this may indicate that the treatment induced a partial block in autophagic flux. Thus, a treatment condition increasing LC3-II on its own that has no difference in LC3-II in the presence of bafilomycin A₁ compared to treatment alone may

suggest a complete block in autophagy at the terminal stages [309]. This procedure has been validated with several autophagy modulators [310]. With each of these techniques, it is essential to avoid assay saturation. The duration of the bafilomycin A₁ treatment (or any other inhibitor of autophagic flux such as CQ) needs to be relatively short (1-4 h) [311] to allow comparisons of the amount of LC3 that is lysosomally degraded over a given time frame under one treatment condition to another treatment condition. A concentration-curve and time-course standardization for the use of autophagic flux inhibitors is required for the initial optimization of the conditions to detect LC3-II accumulation and avoid nonspecific or secondary effects, and to exclude the possibility of a remaining residual flux, if inhibition is incomplete [312]. By using a rapid screening approach, such as a colorimetric based-platform method [313], it is possible to monitor a long time frame for autolysosome accumulation, which closely associates with autophagy activation [314-317]. Positive control experiments using treatment with known autophagy inducers, along with bafilomycin A₁ versus vehicle, are important to demonstrate the utility of this approach in each experimental context.

In some circumstances it may be important to evaluate alterations in autophagy flux once autophagy is induced by a particular agent or genetic manipulation. In that case, steady-state measurements are not adequate. This can be useful for example to evaluate if a gene modification by itself enhances or impairs autophagosome synthesis or degradation quantitatively (e.g., *Clec16a* [318-320]). With this aim, cells should be treated with an autophagy inducer in the presence and absence of a degradation inhibitor. As the LC3-II basal levels in the steady state may be different, it is necessary to establish a ratio to evaluate LC3-II synthesis and degradation flux. Therefore, the synthesis ratio can be considered as the rate of LC3-II levels in the presence of the inducer and the inhibitor divided by the LC3-II level in the presence of the inhibitor alone. Similarly, the degradation ratio would be the ratio of LC3-II levels in the cells treated with the inducer and the inhibitor divided by the LC3-II levels in the presence of the inducer alone. By comparing LC3-II synthesis and degradation ratios among different conditions, such as a gene modification, we can evaluate whether autophagy flux is modified by increasing or decreasing LC3-II synthesis or degradation phases [321,322]. Alternatively, the degradation can be determined by calculating LC3-II levels in the presence of inducer and the inhibitor minus the levels in the presence of inducer alone [323].

The same type of assay monitoring the turnover of Atg8-PE can be used to monitor flux in yeast, by comparing the amount of Atg8 present in a wild-type versus a *pep4Δ* strain following autophagy induction [324]; however, it is important to be aware that the *PEP4* knockout can influence yeast cell physiology (e.g., the inability to degrade and hence recycle autophagic cargo may trigger a starvation response). PMSF, which inhibits the activity of Prb1, can also be used to block Atg8-PE turnover.

Due to the advances in time-lapse fluorescence microscopy and the development of photoswitchable fluorescent proteins, autophagic flux can also be monitored by assessing the half-life of the LC3 protein [325,326] post-photoactivation, by

quantitatively measuring the autophagosomal pool size and its transition time [327], or by quantifying the rate of autophagosome formation [328]. Here, single-cell fluorescence live-cell imaging-based approaches, in combination with micro-patterning, have shown accurate quantitative monitoring of autophagic flux that allows standardization of basal and induced flux in key cell types and model systems [312,329] (Figure 10). These approaches deliver invaluable information on the kinetics of the system and the time required to clear a complete autophagosomal pool. Nonetheless, care must be taken for this type of analysis as changes in transcriptional/translational regulation of LC3 might also affect the readout.

Finally, autophagic flux can be monitored based on the turnover of LC3-II, by utilizing a luminescence-based assay. For example, a reporter assay based on the degradation of *Renilla reniformis* luciferase (Rluc)-LC3 fusion proteins is well suited for screening compounds affecting autophagic flux [330]. In this assay, Rluc is fused N-terminally to either wild-type LC3 or a lipidation-deficient mutant of LC3 (G120A). Because WT Rluc-LC3, in contrast to Rluc-LC3^{G120A}, specifically associates with autophagosomal membranes, WT Rluc-LC3 is more sensitive to autophagic degradation. A change in autophagy-dependent LC3 turnover can thus be estimated by monitoring the change in the ratio of luciferase activities between the two cell populations expressing either WT Rluc-LC3 or Rluc-LC3^{G120A}. In its simplest form, the Rluc-LC3-assay can be used to estimate autophagic flux at a single time point by defining the luciferase activities in cell extracts. Moreover, the use of a live cell luciferase substrate makes it possible to monitor changes in autophagic activity in live cells in real time. This method has been successfully used to identify positive and negative regulators of autophagy from cells treated with microRNA, siRNA and small molecule libraries [330-336].

Cautionary notes: The use of a radioactive pulse-chase analysis, which assesses complete autophagic flux, provides an alternative to lysosomal protease inhibitors [204]. Although such inhibitors should still be used to verify that degradation is lysosome dependent. In addition, drugs must be used at concentrations and for time spans that are effective in inhibiting fusion or degradation, but that do not provoke cell death. Thus, these techniques may not be practical in all cell types or in tissues from whole organisms where the use of protease inhibitors is problematic, and where pulse labeling requires artificial short-term culture conditions that may induce autophagy. Another concern when monitoring flux via LC3-II turnover may be seen in the case of a partial autophagy block; in this situation, agents that disrupt autophagy (e.g., bafilomycin A₁) will still result in an increase in LC3-II. Thus, care is needed in interpretation. For characterizing new autophagy modulators, it is ideal to test autophagic flux at early (e.g., 4 h) and late (e.g., 24 h) time points, because in certain instances, such as with calcium phosphate precipitates, a compound may increase or decrease flux at these two time points, respectively [204]. Moreover, it is important to consider assaying autophagy modulators in a long-term response in order to further understand their effects. Finally, many of the chemicals used to inhibit autophagy, such as bafilomycin A₁, NH₄Cl or CQ (see *Autophagy inhibitors and inducers*), also directly inhibit the endocytosis/uncoating of viruses (D.R. Smith, personal communication), and other endocytic

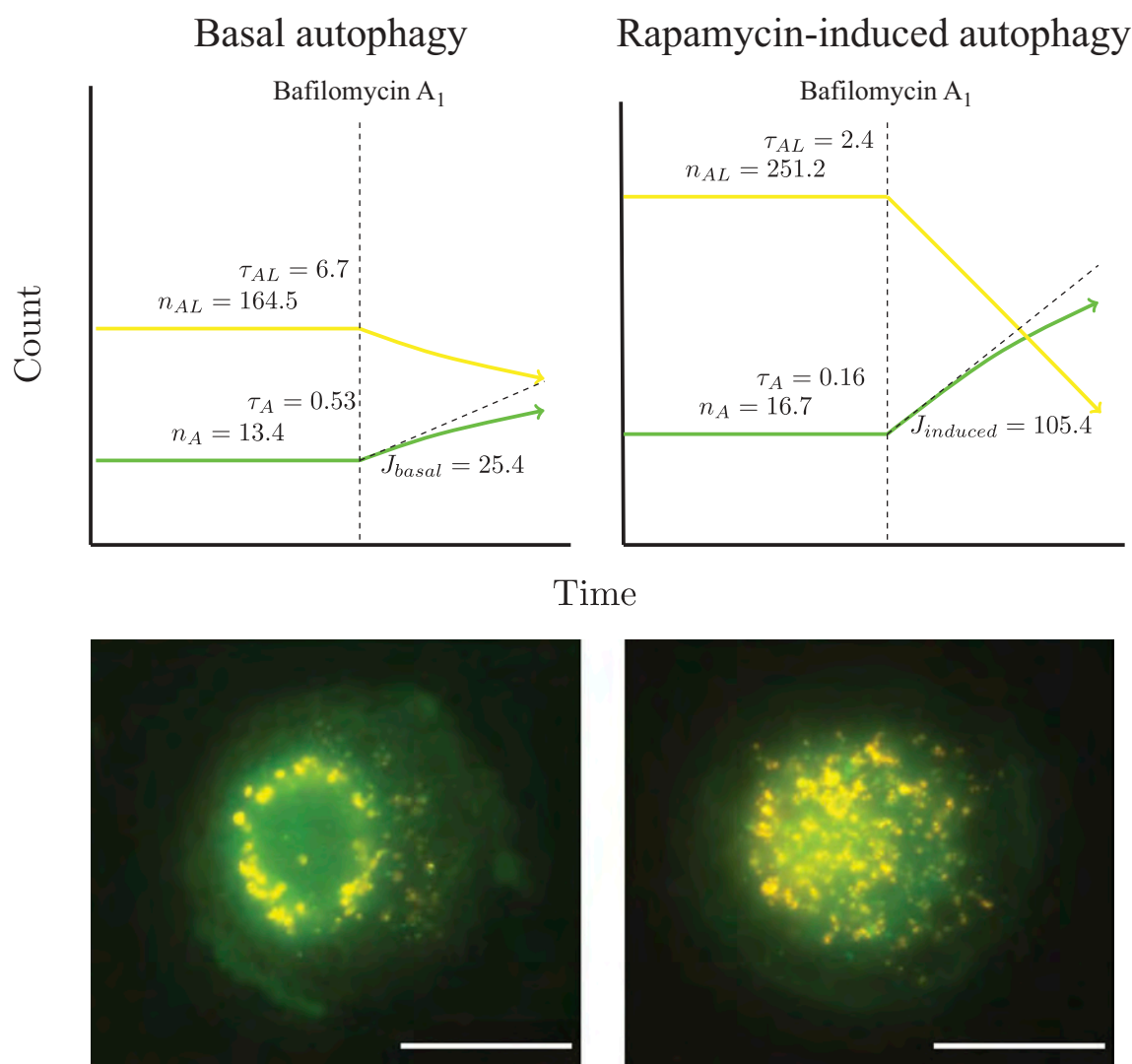


Figure 10. Measuring autophagic flux and pool size of pathway intermediates at the single-cell level: autophagosome, autolysosome and lysosome pool size and flux data, characterizing MEF cells with a basal flux of 25 autophagosomes/h/cell, which increases upon rapamycin treatment to 105 autophagosomes/h/cell. Scale bar: 20 μ m. This figure was previously published in ref. [312].

events requiring low pH, as well as exit from the Golgi (S. Tooze, personal communication). As such, agents that neutralize endosomal compartments should be used only with extreme caution in studies investigating autophagy-virus interactions. One means to address this is to carefully titrate the amounts of inhibitors to use, because, for example, low nanomolar amounts of bafilomycin A₁ can affect autophagy without apparently affecting acidification during influenza virus infections [337].

One additional consideration is that it may not be absolutely necessary to follow LC3-II turnover if other substrates are being monitored simultaneously. For example, an increase in LC3-II levels in combination with the lysosomal (or ideally autophagy-specific) removal of an autophagic substrate (such as an organelle [338,339]) that is not a good proteasomal substrate provides an independent assessment of autophagic flux. However, it is probably prudent to monitor both turnover of LC3-II and an autophagosome substrate in parallel, due to the fact that LC3 might be coupled to endosomal membranes and not just autophagosomes, and the levels of well-characterized autophagosome substrates such as SQSTM1/p62 can also be affected by proteasome inhibitors [340].

Another issue relates to the use of protease inhibitors (see *Autophagy inhibitors and inducers*). When using lysosomal protease inhibitors, it is of fundamental importance to assess proper conditions of inhibitor concentration and time of pre-incubation to ensure full inhibition of lysosomal cathepsins. In this respect, 1 h of pre-incubation with 10–20 μ M E-64d is sufficient in most cases, because this inhibitor is membrane permeable and rapidly accumulates within lysosomes, but another frequently used inhibitor, leupeptin, requires at least 6 h pre-incubation [78,341]. Moreover, pepstatin A is membrane impermeable (ethanol or preferably DMSO must be employed as a vehicle) and requires a prolonged incubation (> 8 h) and a relatively high concentration (>50–100 μ M) to fully inhibit lysosomal CTSD (Figure 11). An incubation of this duration, however, can be problematic due to indirect effects (see *GFP-Atg8-family protein lysosomal delivery and partial proteolysis*). At least in neurons, pepstatin A alone is a less effective lysosomal proteolytic block, and combining a lysosomal cysteine protease (i.e., cathepsin) inhibitor with it is most effective [78]. Also, note that the relative amount of lysosomal CTSB (cathepsin B) and CTSD is cell-specific and changes with culture conditions. A possible alternative to pepstatin A is the

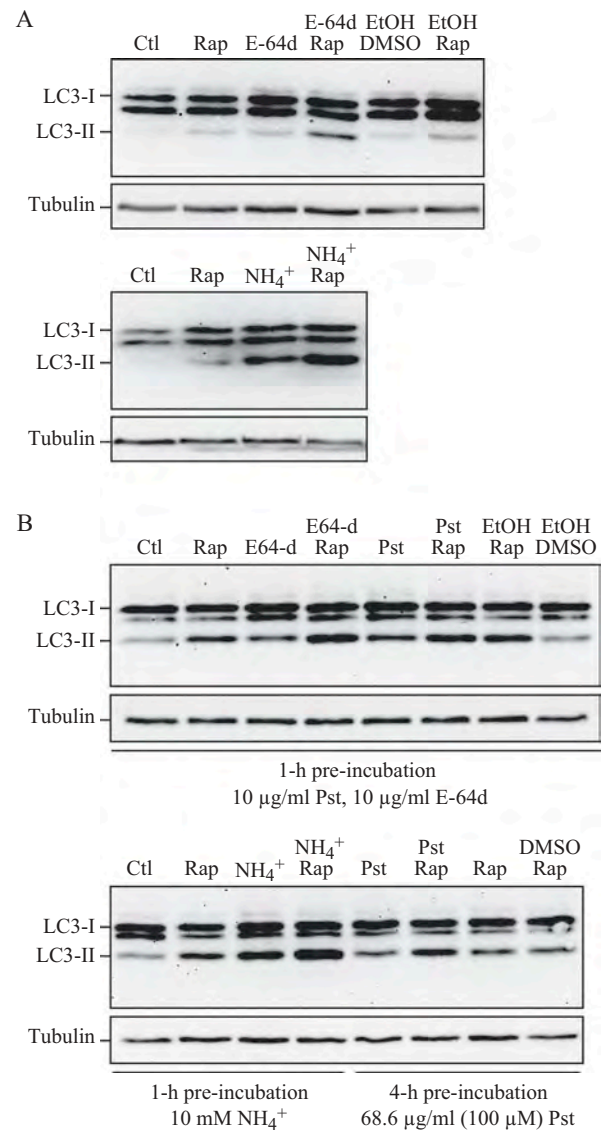


Figure 11. Effect of different inhibitors on LC3-II accumulation. SH-SY5Y human neuroblastoma cells were plated and allowed to adhere for a minimum of 24 h, then treated in fresh medium. Treatments were as follows: rapamycin (Rap), (A) 1 μ M, 4 h or (B) 10 μ M, 4 h; E-64d, final concentration 10 μ g/ml from a 1 mg/ml stock in ethanol (EtOH); NH_4Cl (NH_4^+), final concentration 10 mM from a 1 M stock in water; pepstatin A (Pst), final concentration 10 μ g/ml from a 1 mg/ml stock in ethanol, or 68.6 μ g/ml from a 6.86 mg/ml stock in DMSO; ethanol or DMSO, final concentration 1%. Pre-incubations in (B) were for 1 or 4 h as indicated. 10 mM NH_4Cl (or 30 μ M CQ, not shown) were the most effective compounds for demonstrating the accumulation of LC3-II. E-64d was also effective in preventing the degradation of LC3-II, with or without a preincubation, but ammonium chloride (or CQ) may be more effective. Pepstatin A at 10 μ g/ml with a 1-h pre-incubation was not effective at blocking degradation, whereas a 100 μ M concentration with 4-h pre-incubation had a partial effect. Thus, alkalinizing compounds are more effective in blocking LC3-II degradation, and pepstatin A must be used at saturating conditions to have any noticeable effect. Images provided by C. Isidoro. Note that the band running just below LC3-I at approximately 17.5 kDa may be a processing intermediate of LC3-I; it is detectable in freshly prepared homogenates, but is less visible after the sample is subjected to a freeze-thaw cycle.

pepstatin A BODIPY[®] FL conjugate [342,343], which is transported to lysosomes via endocytosis. In contrast to the protease inhibitors, CQ (10–40 μ M) or bafilomycin A₁ (1–100 nM) can be added to cells immediately prior to autophagy induction, although in some cases a pre-incubation with bafilomycin A₁ should be considered. bafilomycin A₁ requires ~30 min to

increase lysosomal pH [226,344]; therefore, a pre-incubation of 30 min is required in case of short autophagy induction times. Because cysteine protease inhibitors may upregulate CTSD and some such as E-64d and its derivatives have potential inhibitory activity toward calpains, whereas bafilomycin A₁ can have potential significant cytotoxicity, especially in cultured neurons and pathological states, the use of both methods may be important in some experiments to exclude off-target effects of a single method.

Conclusion: It is important to be aware of the difference between monitoring the steady-state level of Atg8-family proteins and autophagic flux. The latter may be assessed by following Atg8-family proteins in the absence and presence of autophagy flux inhibitors (such as lysosomal degradation inhibitors), and by examining the autophagy-dependent degradation of appropriate substrates. In particular, if there is any evidence of an increase in LC3-II (or autophagosomes), it is essential to determine whether this represents an induction of autophagy and increased synthesis of LC3, or decreased flux and the subsequent accumulation of LC3 due to a block in fusion or degradation, through the use of inhibitors such as CQ, bafilomycin A₁ or lysosomal protease inhibitors. In the case of a suspected impaired degradation, assessment of lysosomal function (i.e., pH or activity of lysosomal enzymes) is then required to validate the conclusion and to establish the basis.

GFP-Atg8-family protein lysosomal delivery and partial proteolysis. GFP-LC3B (hereafter referred to as GFP-LC3) has also been used to follow flux. It should be cautioned that, as with endogenous LC3, an assessment of autophagic GFP-LC3 flux is a carrier flux that cannot be equated with, and is not necessarily representative of, an autophagic cargo flux. When GFP-Atg8 or GFP-LC3 is delivered to a lysosome/vacuole, the Atg8-family protein part of the chimera is sensitive to degradation, whereas the GFP protein is relatively resistant to hydrolysis (note, however, that GFP fluorescence is quenched by low pH; see *GFP-Atg8-family protein fluorescence microscopy and Tandem mRFP/mCherry-GFP fluorescence microscopy*). Therefore, the appearance of free GFP on western blots can be used to monitor lysis of the inner autophagosome membrane and breakdown of the cargo in metazoans (Figure 12A) [324,345,346], or the delivery of autophagosomes to, and the breakdown of autophagic bodies within, the fungal [347–349] and plant vacuole [289,290,324,350]. Reports on *Dictyostelium discoideum* and mammalian cells highlight the importance of lysosomal pH as a critical factor in the detection of free GFP that results from the degradation of fused proteins. In these cell types, free GFP fragments are only detectable in the presence of nonsaturating levels of lysosomotropic compounds (NH_4Cl or CQ) or under conditions that attenuate lysosomal acidity; otherwise, the autophagic/degradative machinery appears to be too efficient to allow the accumulation of the proteolytic fragment (Figure 12B,C) [40,64,351]. Hence, a reduction in the intensity of the free GFP band may indicate reduced flux, but it may also be due to efficient turnover. Using a range of concentrations and treatment times of compounds that inhibit autophagy can be useful in distinguishing between these possibilities [352]. Because the pH in the yeast vacuole is higher than

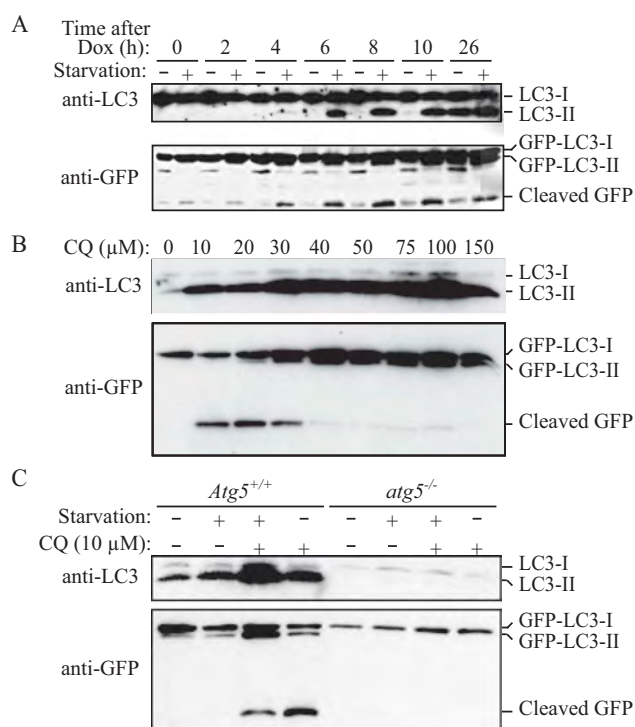


Figure 12. GFP-LC3 processing can be used to monitor delivery of autophagosomal membranes. **(A)** *atg5*^{-/-} MEFs engineered to express Atg5 under the control of the Tet-off promoter were grown in the presence of doxycycline (Dox; 10 ng/ml) for one week to suppress autophagy. Cells were then cultured in the absence of drug for the indicated times, with or without a final 2-h starvation. Protein lysates were analyzed by western blot using anti-LC3 and anti-GFP antibodies. The positions of untagged and GFP-tagged LC3-I and LC3-II, and free GFP are indicated. This figure was modified from data previously published in ref. [346], FEBS Letters, 580, Hosokawa N, Hara Y, Mizushima N, Generation of cell lines with tetracycline-regulated autophagy and a role for autophagy in controlling cell size, pp. 2623-2629, copyright 2006, with permission from Elsevier. **(B)** Differential role of unsaturating and saturating concentrations of lysosomal inhibitors on GFP-LC3 cleavage. HeLa cells stably transfected with GFP-LC3 were treated with various concentrations of CQ for 6 h. Total lysates were prepared and subjected to immunoblot analysis. **(C)** CQ-induced free GFP fragments require classical autophagy machinery. Wild-type and *atg5*^{-/-} MEFs were first infected with adenovirus GFP-LC3 (100 viral particles per cell) for 24 h. The cells were then either cultured in regular culture medium with or without CQ (10 μM), or subjected to starvation in EBSS buffer in the absence or presence of CQ for 6 h. Total lysates were prepared and subjected to immunoblot analysis. Panel B and C are modified from the data previously published in ref. [351].

new GFP-LC3 is continuously being synthesized. A potential solution to this problem is to follow the fluorescence of a photo-activatable version of the fluorescent protein [353], which allows this assay to be performed essentially as a pulse/chase analysis. Another alternative to follow flux is to monitor GFP-LC3 fluorescence by adding lysosomal protease or fusion inhibitors to cells expressing GFP-LC3 and monitoring changes in the number of puncta. In this case, the presence of lysosomal inhibitors should increase the number of GFP-LC3-positive structures, and the absence of an effect on the total number of GFP-LC3 puncta or on the percentage of cells displaying numerous puncta is indicative of a defect(s) in autophagic flux [64,354]. The combination of protease inhibitors (to prevent the degradation of GFP) or compounds that modify lysosomal pH and/or block fusion of autophagosomes such as NH₄Cl, bafilomycin A₁ or CQ, or compounds that block fusion of autophagosomes with lysosomes such as bafilomycin A₁ or others (e.g., vinblastine) may be most effective in preventing lysosome-dependent decreases in GFP-LC3 puncta. However, because the stability of GFP is affected by lysosomal pH, researchers may also consider the use of protease inhibitors whether or not lysosomotropic compounds or fusion inhibitors are included.

Cautionary notes: The GFP-Atg8 processing assay is used routinely to monitor autophagy in yeast. One caveat, however, is that this assay is not always carried out in a quantitative manner. For example, western blot exposures need to be in the linear range. Accordingly, an enzymatic assay such as the Pho8Δ60 assay may be preferred (see *Autophagic protein degradation*) [355,356], especially when the differences in autophagic activity need to be determined precisely (note that an equivalent assay has not been developed for more complex eukaryotic cells); however, as with any enzyme assay, appropriate caution must be used regarding, for example, substrate concentrations and linearity. The Pho8Δ60 assay also requires a control to verify equal Pho8Δ60 expression in the different genetic backgrounds or conditions to be tested [356]; differences in Pho8Δ60 expression potentially affect its activity and may thus cause misinterpretation of results. Another issue to keep in mind is that GFP-Atg8 processing correlates with the surface area of the inner sphere of the autophagosome, and thus provides a smaller signal than assays that measure the volume of the autophagosome. Pgk1 (3-phosphoglycerate kinase)-GFP processing [52] is another assay that can be used to monitor autophagy.

A thorough analysis of GFP proteolysis in plant roots reveals the importance of normalizing to tissue-specific reporter expression and autophagic activity range [102,357]. For instance, GFP-ATG8 expression in *Arabidopsis thaliana* is typically highest in the root apical meristem, but the response to the autophagy-inducing conditions in this root zone is much lower compared to the rest of the root. Thus, excluding this root zone from the samples for western blot provides a much more reliable readout of the GFP-ATG8 proteolysis.

As a note of caution, GFP-LC3 has been demonstrated to be present in protein aggregates in an autophagy-unrelated manner and this association is dependent on its interaction with SQSTM1. This interaction poses potential difficulties to distinguish LC3 bound to aggregates from those on autophagosomes [358]. The main limitation of the GFP-LC3

that in mammalian or *D. discoideum* lysosomes, the levels of free GFP fragments are detectable in yeast even in the absence of lysosomotropic compounds [52]. Additionally, in yeast the diffuse fluorescent haze from the released GFP moiety within the vacuole lumen can be observed by fluorescence microscopy.

The dynamic movement to lysosomes of GFP-LC3, or of its associated cargo, also can be monitored by time-lapse fluorescence microscopy, although, as mentioned above, the GFP fluorescent signal is more sensitive to acidic pH than other fluorophores (see *GFP-Atg8-family protein fluorescence microscopy*). A time-course evaluation of the cell population showing GFP-LC3 puncta can serve to monitor the autophagic flux, because a constant increase in the number of cells accumulating GFP-LC3 puncta is suggestive of defective fusion of autophagosomes with lysosomes. Conversely, a decline implies that GFP-LC3 is delivered to properly acidified lysosomes and may, in addition, reflect proteolytic elimination within them, although the latter needs to be independently established. In either case, it can be problematic to use GFP fluorescence to follow flux, as

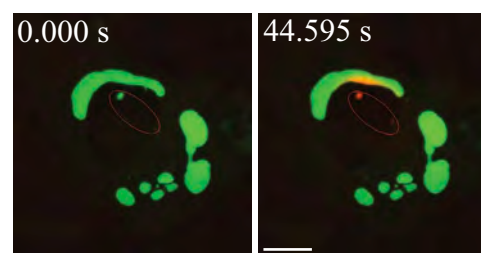


Figure 13. Movement of activated pDendra2-hp62 (SQSTM1; orange) from the nucleus (middle) to an aggregate in ARPE-19 cells, revealed by confocal microscopy. Cells were exposed to 5 μ M MG132 for 24 h to induce the formation of perinuclear aggregates [4083]. The cells were then exposed to a UV pulse (the UV-induced area is shown by red lines that are inside of the nucleus) that converts Dendra2 from green to red, and the time shown after the pulse is indicated. SQSTM1 is present in a small nuclear aggregate, and is shuttled from the nucleus to a perinuclear large protein aggregate (detected as red). Scale bar: 5 μ m. Image provided by K. Kaarniranta.

real-time tracking of LC3 and SQSTM1 (Figure 13 [359]);. A newer generation of photoswitchable proteins, EOS, are now available that are brighter than Dendra2 and display more efficient photoswitching (N.A. Castello and S. Finkbeiner, in press). Another alternative to mRFP or mCherry is to use the Venus variant of YFP, which is brighter than mRFP and less sensitive to pH than GFP [345].

The pH optimum of EGFP is important to consider when using GFP-LC3 constructs, as the original GFP-LC3 marker [346] uses the EGFP variant, which may result in a reduced signal upon the formation of amphisomes or autolysosomes. An additional caveat when using the photoactivatable construct PA-GFP [301] is that the process of activation by photons may induce DNA damage, which could, in turn, induce autophagy. Also, GFP is relatively resistant to denaturation, and boiling for 5 min may be needed to prevent the folded protein from being trapped in the stacking gel during SDS-PAGE.

As noted above (see *Western blotting and ubiquitin-like protein conjugation systems*), Atg4/ATG4 cleaves the residue (s) that follow the C-terminal glycine of Atg8-family proteins that will be conjugated to PE. Accordingly, it is critical that any chimeras should be constructed with the fluorescent tag at the amino terminus of Atg8-family proteins (unless the goal is to monitor Atg4/ATG4 activity).

Finally, lysosomal inhibition needs to be carefully controlled. Prolonged inhibition of lysosomal hydrolases (>6 h) is likely to induce a secondary autophagic response triggered by the accumulated undigested autophagy cargo. This secondary autophagic response can complicate the analysis of the autophagic flux, making it appear more vigorous than it would in the absence of the lysosomal inhibitors.

Conclusion: The GFP-Atg8 (or GFP-LC3/GABARAP) processing assay, which monitors free GFP generated within the vacuole/lysosome, is a convenient way to follow autophagy, but it does not work in all cell types, and is not as easy to quantify as enzyme-based assays. Furthermore, the assay measures the flux of an autophagic carrier, which may not necessarily be equivalent to autophagic cargo flux.

HaloTag-LC3 autophagosome completion assay. Upon phagophore closure, LC3-II on the convex side of the membrane is delipidated and recycled back into the cytosol, while that on the

processing assay in mammalian cells is that its usefulness seems to depend on cell type and culture conditions (N. Hosokawa and N. Mizushima, unpublished data). Apparently, GFP is more sensitive to mammalian lysosomal hydrolases than to the degradative milieu of the yeast vacuole or the lysosomes in *Drosophila*. Alternatively, the lower pH of mammalian lysosomes relative to that of the yeast vacuole may contribute to differences in detecting free GFP. Under certain conditions (such as Earle's balanced salt solution [EBSS]-induced starvation) in some cell lines, when the lysosomal pH becomes particularly low, free GFP is undetectable because both the LC3-II and free GFP fragments are quickly degraded [273]. Therefore, if this method is used it should be accompanied by immunoblotting and include controls to address the stability of nonlysosomal GFP such as GFP-LC3-I. It should also be noted that free GFP can be detected when cells are treated with nonsaturating doses of inhibitors such as CQ, E-64d and bafilomycin A₁. The saturating concentrations of these lysosomal inhibitors vary in different cell lines, and it would be better to use a saturating concentration of lysosomal inhibitors when performing an autophagic flux assay [273]. Therefore, caution must be exercised in interpreting the data using this assay; it would be helpful to combine an analysis of GFP-LC3 processing with other assays, such as the monitoring of endogenous LC3-II by western blot.

Along these lines, a caution concerning the use of the EGFP fluorescent protein for microscopy is that this fluorophore has a relatively neutral pH optimum for fluorescence [263], and its signal diminishes quickly during live cell imaging due to the acidic environment of the lysosome. It is possible to circumvent this latter problem by imaging paraformaldehyde-fixed cultures that are maintained in a neutral pH buffer, which retains EGFP fluorescence (M. Kleinman and J.J. Reiners, personal communication). Alternatively, it may be preferable to use a different fluorophore such as mRFP or mCherry, which retain fluorescence even at acidic pH [341]. On the one hand, a putative advantage of mCherry over mRFP is its enhanced photostability and intensity, which are an order of magnitude higher (and comparable to GFP), enabling acquisition of images at similar exposure settings as are used for GFP, thus minimizing potential bias in interpretation [342]. On the other hand, caution is required when evaluating the localization of mCherry fusion proteins during autophagy due to the persistence of the mCherry signal in acidic environments; all tagged proteins are prone to show enrichment in lysosomes during nonselective autophagy of the cytoplasm, especially at higher expression levels. In addition, red fluorescent proteins (even the monomeric forms) can be toxic due to oligomer formation [343]; the tendency to form abnormal accumulations may be a general feature of coral- and anemone-derived fluorescent proteins. Dendra2 is an improved version of the green-to-red photoswitchable fluorescent protein Dendra, which is derived from the octocoral *Dendronephthya* sp [344]. Dendra2 is capable of irreversible photoconversion from a green to a red fluorescent form, but can be used also as normal GFP or RFP vector. This modified version of the fluorophore has certain properties including a monomeric state, low phototoxic activation and efficient chromophore maturation, which make it suitable for

concave side is sequestered within the vacuole and delivered into the lysosome for degradation [240]. Exploiting the topological property of LC3, the HaloTag-LC3 (HT-LC3) assay is designed to analyze the process of phagophore closure (Figure 14A) [360]. The HaloTag is a modified haloalkane dehalogenase that covalently binds to synthetic HaloTag ligands [361]. The HT-LC3 assay employs the HaloTag-conjugated LC3 reporter in combination with membrane-permeable and -impermeable HaloTag ligands labelled with two different fluorescent dyes to distinguish membrane-unenclosed and -enclosed HT-LC3-II. By sequentially incubating plasma membrane-permeabilized HT-LC3-expressing cells with a saturating dose of membrane-impermeable ligands (MILs) followed by membrane-permeable ligands (MPLs), phagophores, nascent autophagosomes, and mature autophagosomes or

autolysosomes are visualized as MIL⁺ MPL⁻, MIL⁺ MPL⁺, and MIL⁻ MPL⁺ structures, respectively (Figure 14B). Because the cytosolic HT-LC3-I is released upon plasma membrane permeabilization, the assay provides a superior signal-to-noise ratio and the data can be semi-quantitatively analyzed by confocal or fluorescence microscopy. As MPL fluorescent signals are not retained in functional lysosomes, autophagic flux can also be measured by monitoring MPL signal accumulation upon exposure to a lysosomal inhibitor. Moreover, the assay has been successfully adapted to a fluorescence-activated cell sorting (FACS)-based high-throughput platform to screen genes required for phagophore closure [362].

Cautionary notes: Similar to fluorescent protein(s)-tagged LC3 assays, the HT-LC3 assay requires a system amenable to

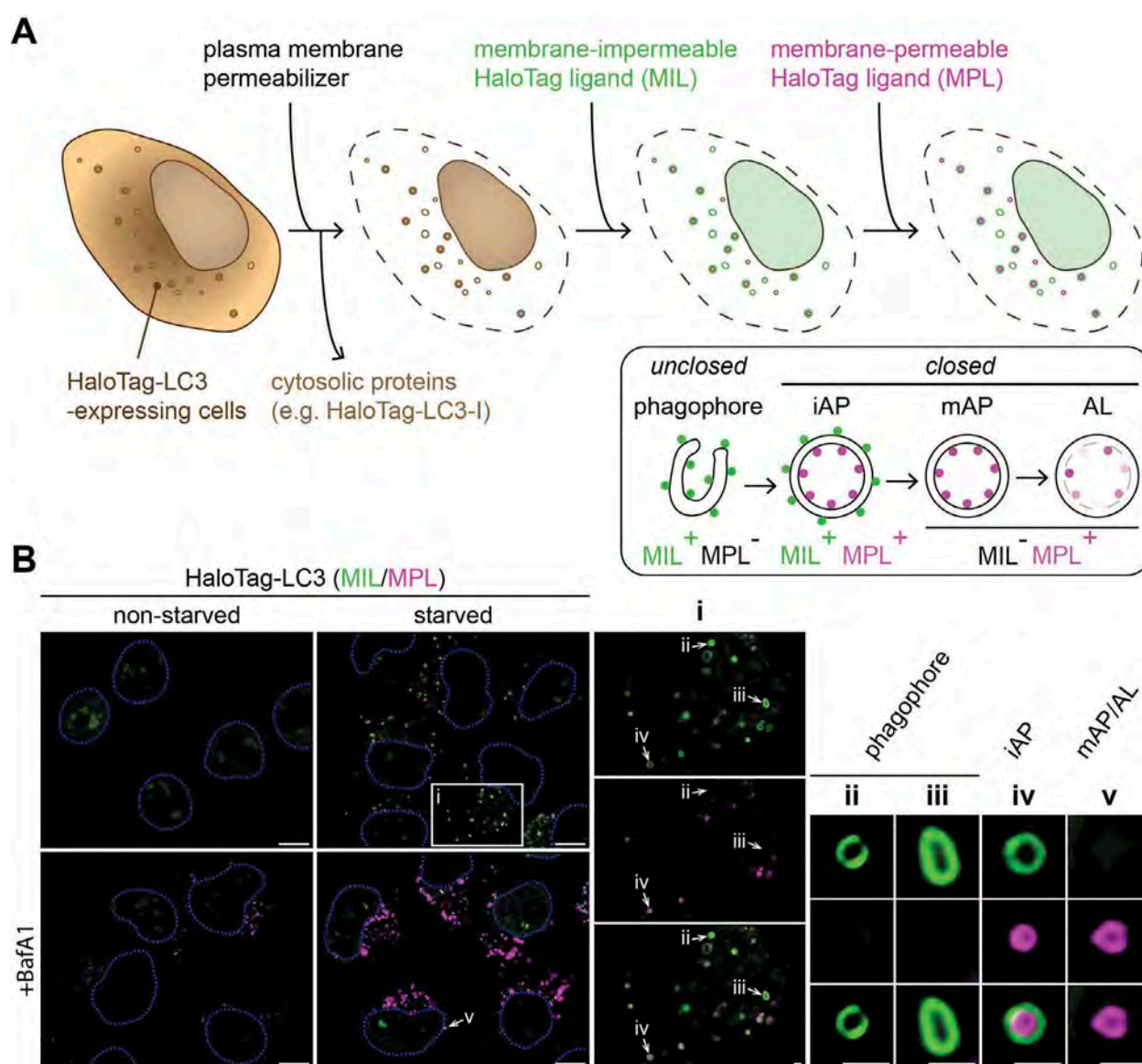


Figure 14. The HaloTag-LC3 assay distinguishes phagophores, immature autophagosomes, and mature autophagosomes and autolysosomes. **(A)** Schematic diagram of the HaloTag-LC3 (HT-LC3) assay. Cells expressing HT-LC3 are treated with a cholesterol-dependent plasma membrane permeabilizer to release cytosolic proteins including HT-LC3-I and sequentially labeled with a saturated dose of membrane-impermeable HaloTag ligands (MILs) conjugated with Alexa Fluor 488 (or 660) followed by membrane-permeable HaloTag ligands (MPLs) conjugated with tetramethylrhodamine to detect phagophores (MIL⁺ MPL⁻), immature autophagosomes (iAP; MIL⁺ MPL⁺), and mature autophagosomes and autolysosomes (AP and AL; MIL⁻ MPL⁺). **(B)** U-2 OS cells were stably transduced with HT-LC3-encoding lentiviruses, incubated in starvation medium or control complete medium in the presence or absence of 100 nM bafilomycin A₁ (BafA1) for 4 h, and subjected to the HT-LC3 assay followed by confocal microscopy. Magnified images of the boxed (i) and arrow-indicated (ii-v) areas are shown in the right panels. Scale bars: 10 μm (1 μm in the magnified images).

exogenous introduction. In addition, the assay requires plasma membrane permeabilization. Therefore, it would be challenging to use the assay in 3-dimensional-cultured cells, tissue samples, or live-cell imaging. Moreover, the current method employs cholesterol-dependent pore-forming agents such as recombinant perfringolysin O [363] and digitonin to permeabilize the plasma membrane. Therefore, it would also be challenging when a treatment or gene manipulation perturbs plasma membrane cholesterol distribution (e.g., prolonged treatment with a lysosomal inhibitor [Y. Takahashi and H.G. Wang, personal communication]). Along this line, because the plasma membrane cholesterol concentration is different among cell types, it is important to find an optimal permeabilization condition. If plasma membrane permeabilization fails or is incomplete, diffuse MPL signals, which represent cytosolic HT-LC3-I, will be detected in addition to cytoplasmic HT-LC3-II foci. In addition, it is critical to ensure the saturation of all available binding sites with each ligand. A secondary incubation with the same type of ligands conjugated with a different fluorophore (e.g., primary incubation with Alexa Fluor 488-conjugated MILs followed by secondary incubation with Alexa Fluor 600-conjugated MILs) make it possible to determine an appropriate staining condition. Another concern for the assay is that the detection of membrane-unenclosed HT-LC3-II relies on the accessibility of MILs. Therefore, if the pore size of the closure site is too small to pass through MILs, HT-LC3-II on the concave side of phagophores will be falsely negative for MILs; the structure will be detected as MIL⁺ MPL⁺ in this case.

Conclusion: Using two HaloTag ligands with different membrane permeability and fluorophores, the HT-LC3 assay can determine each step of autophagy by distinguishing membrane-unenclosed and -enclosed HT-LC3-II. However, unlike a fluorescent protein-tagged LC3 assay, the HT-LC3 assay requires several optimization steps to ensure the staining specificity. Once optimized, this assay provides a superior signal-to-noise ratio and is compatible with high-throughput screening platforms.

GFP-Atg8-family protein fluorescence microscopy. LC3B, or the protein tagged at its N terminus with a fluorescent protein such as GFP (GFP-LC3), has been used to monitor autophagy through indirect immunofluorescence or direct fluorescence

microscopy (Figure 15), measured as an increase in punctate LC3 or GFP-LC3 [364,365]. The detection of GFP-Atg8 (or GFP-LC3/GABARAP/LGG-1/2) is also useful for in vivo studies using transgenic organisms such as *Saccharomyces cerevisiae* [366], *Aspergillus nidulans* [348], *Caenorhabditis elegans* [367], *D. discoideum* [368], filamentous ascomycetes [369-373], *Ciona intestinalis* [374], *Drosophila melanogaster* [375-377], *A. thaliana* [378], *Zea mays* [379], *Trypanosoma brucei* [380-382], *Leishmania major* [383-385], *Trypanosoma cruzi* [386,387], zebrafish [328,388] and mice [239]. “Super-resolution” fluorescence images of GFP-LC3-positive phagophores have been shown in platelets prepared from GFP-LC3 mice by “super-resolution” microscopy (specifically, 3-dimensional structured illumination microscopy/3D-SIM) to be similar to what was observed by TEM [389,390]. It is also possible to use anti-Atg8-family protein antibodies for immunocytochemistry or immunohistochemistry (IHC) [265 [391-397],], procedures that have the advantages of detecting the endogenous protein, obviating the need for transfection and/or the generation of a transgenic organism, as well as avoiding potential artefacts resulting from overexpression. For example, high levels of overexpressed GFP-LC3 can result in its nuclear localization, although the protein can still relocate to the cytosol upon starvation. The use of imaging cytometry allows rapid and quantitative measures of the number of LC3 puncta and their relative number in individual or mixed cell types, using computerized assessment, enumeration, and data display (e.g., see refs. [41,398]). In this respect, the alternative use of an automated counting system may be helpful for obtaining an objective number of puncta per cell. For this purpose, the WatershedCounting3D plug-in for ImageJ may be useful [399,400]. Changes in the number of GFP-Atg8 puncta can also be monitored using flow cytometry (see *Autophagic flux* determination using flow and multispectral imaging cytometry) [382]. An alternative way to quantify LC3 immunofluorescence staining is to estimate the percentage of LC3 signals originating from puncta over total LC3 signals in the same cell [401]. This approach is useful if it is difficult to define the number of puncta per cell due to widely varying size or clustering of the puncta. A key control to perform when using these approaches is the use of a non-lipidatable mutant version of the Atg8-family protein that does not associate with autophagosomes.

LC3-positive autophagosomes can be quantified by confocal microscopy using a software program called Imaris (Oxford



Figure 15. Changes in the detection and localization of GFP-LC3 upon the induction of autophagy. U87 cells stably expressing GFP-LC3 were treated with PBS (Control), rapamycin (200 nM), or rapamycin in combination with 3-MA (2 mM) for 24 h. Representative fluorescence images of cells counterstained with DAPI (nuclei) are shown. Scale bar: 10 μ m. This figure was modified from Figure 6 published in ref. [364], Badr et al. Lanatoside C sensitizes glioblastoma cells to tumor necrosis factor-related apoptosis-inducing ligand and induces an alternative cell death pathway. *Neuro-Oncology*, 13(11):1213-24, 2011, by permission of Oxford University Press.

Instruments). Confocal Z-stacks of samples immunolabeled with an antibody to LC3 are reconstructed into 3-dimensional animations with the aid of Imaris software. The Spot function in Imaris automatically locates and enumerates autophagosomes within individual cells based on size and intensity thresholds [402,403].

Monitoring the endogenous Atg8-family proteins obviously depends on the ability to detect these proteins in the system of interest, which is not always possible. If the endogenous amount is below the level of detection, the use of an exogenous construct is warranted. In this case, it is important to consider the use of stable transformants versus transient transfections. On the one hand, stable transformants may have reduced background resulting from the lower gene expression, and artefacts resulting from recent exposure to transfection reagents (see below) are eliminated. Furthermore, with stable transformants more cells can be easily analyzed because nearly 100% of the population will express tagged LC3. On the other hand, a disadvantage of stable transfectants is that the integration sites cannot always be predicted, and expression levels may not be optimal. Therefore, it is worth considering the use of stable episomal plasmids that avoid the problem of unsuitable integration [344]. An important advantage of transient transfection is that this approach is better for examining the immediate effects of the transfected protein on autophagy; however, the transient transfection approach restricts the length of time that the analysis can be performed, and consideration must be given to the induction of autophagy resulting from exposure to the transfection reagents (see below). One word of caution is that optimizing the time of transient expression of GFP-LC3 is necessary, as some cell types (e.g., HeLa cells) may require 1 day for achieving optimal expression to visualize GFP-LC3 puncta, whereas neuronal cell lines such as SH-SY5Y cells typically need at least 48 h of expression prior to performing GFP-LC3 puncta analyses. In addition, a double transfection can be used (e.g., with GFP-LC3 and the protein of interest) to visually tag the cells that express the protein being examined.

A disadvantage of transfecting GFP-LC3 with liposomes is that frequently it leads to an unstable efficiency of transfection, causing a reduction in the number of cells effectively expressing GFP-LC3, and degradation of the plasmid, thus decreasing the numbers of GFP-LC3 puncta. Stable cell lines expressing GFP-LC3 can be generated using lentiviral systems and efficiently selected through antibiotic resistance leading to uniform and prolonged expression levels. These stable cell lines are sensitive to autophagy inducers as measured by the LC3-II:LC3-I ratio by western blot, and also show increased numbers of cytoplasmic GFP-LC3 puncta upon autophagic stimuli (unpublished results R. Muñoz-Moreno, R.I. Galindo, L. Barrado-Gil and C. Alonso).

In conclusion, there is no simple rule for the use of stable versus transient transfections. When stable transfections are utilized through a nonlentiviral system it is worthwhile screening for stable clones that give the best signal to noise ratio; when transient transfections are used, it is worthwhile optimizing the *GFP-LC3* DNA concentration to give the best signal-to-noise ratio (note potential problems with transfections under *Western blotting and ubiquitin-like protein*

conjugation systems). In clones, the uniformity of expression of GFP-LC3 facilitates “thresholding” when scoring puncta-positive cells (see below). However, there is also a need to be aware that a single cell clone may not be representative of the overall pool. Using a pool of multiple selected clones may reduce artefacts that can arise from the selection and propagation of individual clones from a single transfected cell (although the use of a pool is also problematic as its composition will change over time). Another possibility is to select a mixed stable population with uniform GFP-LC3 expression levels by the use of a fluorescence-activated cell sorter (FACS) [404]. Optimization, together with including the appropriate controls (e.g., transfecting GFP-LC3^{G120A} as a negative control), will help to overcome the effects of the inherent variability in these analyses. For accurate interpretations, it is also important to assess the level of overexpression of the GFP-LC3 constructs relative to endogenous LC3 by western blot. Finally, a recent advent of CRISPR-Cas9 gene-editing technologies provides a promising alternative to overcome potential pitfalls of GFP-LC3 overexpression—the generation of knockin cell lines, in which the coding sequence of GFP is added in frame with the 5′ sequence (encoding the N-terminal part) of endogenous *LC3* [120,405].

An additional use of GFP-LC3 is to monitor colocalization with a target during autophagy-related processes such as organelle degradation or the sequestration of pathogenic microbes [299–302]. Preincubation of cells stably expressing GFP-LC3 with leupeptin can help stabilize the GFP-LC3 signal during fluorescence microscopy, especially under conditions of induced autophagic flux. Leupeptin is an inhibitor of lysosomal cysteine and serine proteases and will therefore inhibit degradation of membrane-conjugated GFP-LC3 that is present within autolysosomes.

Cautionary notes: Quantification of autophagy by measuring GFP-LC3 puncta (or LC3 by immunofluorescence) can, depending on the method used, be more tedious than monitoring LC3-II by western blot; however, the former may be more sensitive and quantitative. Ideally, it is preferable to include both assays and to compare the two sets of results. In addition, if GFP-LC3 is being quantified, it is better to determine the number of puncta corresponding to GFP-LC3 on a per cell basis (or per cell area basis) rather than simply the total number (or percentage) of cells displaying puncta. This latter point is critical because, even in nutrient-rich conditions, cells display some basal level of GFP-LC3 puncta. There are, however, practical issues with counting puncta manually and reliably, especially if there are large numbers per cell. Nevertheless, manual scoring may be more accurate than relying on a software program, in which case it is important to ensure that only appropriate puncta are being counted (applicable programs include ImageJ, Imaris, and the open-source software CellProfiler [406]). Moreover, when autophagosome-lysosome fusion is blocked, larger autophagosomes are detected, possibly due to autophagosome-autophagosome fusion, or to an inability to resolve individual autophagosomes when they are present in large numbers. Although it is possible to detect changes in the size of GFP-Atg8-family protein puncta by fluorescence microscopy, it is not possible to correlate size with autophagy activity without

additional assay methods. Size determinations can be problematic by fluorescence microscopy unless careful standardization is carried out [407], and size estimation on its own without considering puncta number per cell is not recommended as a method for monitoring autophagy; however, it is possible to quantify the fluorescence intensity of GFP-Atg8-family proteins at specific puncta, which does provide a valid measure of protein recruitment [408].

In addition to autophagosome size, the number of puncta visible to the eye will also be influenced by both the level of expression of GFP-LC3 in a given cell (an issue that can be avoided by analyzing endogenous LC3 by immunofluorescence) and by the exposure time of the microscope, if using widefield microscopy. Another way to account for differential GFP-LC3 expression levels and/or exposure is to normalize the intensity of GFP-LC3 present in the puncta to the total GFP-LC3 intensity in the cell. This can be done either on the population level [306] or individual cell level [404]. The approach to measuring the proportion of total LC3 signals originating from puncta is also suitable for quantification of immunofluorescence staining of endogenous LC3. In many cell types it may be possible to establish a threshold value for the number of puncta per cell in conditions of “low” and “high” autophagy [409]. This can be tested empirically by exposing cells to autophagy-inducing and -blocking agents. Thus, cell populations showing significantly greater proportions of cells with autophagosome numbers higher than the threshold in perturbation conditions compared to the control cells could provide quantitative evidence of altered autophagy. It is then possible to score the population as the percentage of cells displaying numerous autophagosomes. This approach will only be feasible if the background number of puncta is relatively low. For this method, it is particularly important to count a large number of cells and multiple representative sections of the sample. Typically, it is appropriate to score on the order of 50 or more cells, preferably in at least three different fields, depending on the particular system and experiment, but the critical point is that this determination should be based on statistical power analysis. Accordingly, high-content imaging analysis methods enable quantification of GFP-LC3 puncta (or overall fluorescence intensity) in thousands of cells per sample (e.g., see refs. [334,352,410]). When using automated analysis methods, care must be taken to manually evaluate parameters used to establish background threshold values for different treatment conditions and cell types, particularly as many systems image at lower magnifications that may be insufficient to resolve individual puncta. Another note of caution is that treatments affecting cell morphology, leading to the “rounding-up” of cells for example, can result in apparent changes in the number of GFP-LC3 puncta per cell. To avoid misinterpretation of results due to such potential artefacts, manual review of cell images is highly recommended. If cells are rounding up due to apoptosis or mitosis, it is easy to automatically remove them from analysis based on nuclear morphology (using DAPI or Hoechst staining) or cell roundness. If levels of autophagy in the rounded-up cells are of particular interest, images can be acquired as z-stacks and either analyzed as a z-series or processed to generate maximum projection or extended depth-of-field images and then analyzed [411].

To allow comparisons by other researchers attempting to repeat these experiments, it is critical that the authors also

specify the baseline number of puncta that are used to define “normal” or “low” autophagy. Furthermore, the cells should be counted using unbiased procedures (e.g., using a random start point followed by inclusion of all cells at regular intervals), and statistical information should be provided for both baseline and altered conditions, as these assays can be highly variable. One possible method to obtain unbiased counting of GFP-LC3 puncta in a large number of cells is to perform multispectral imaging flow cytometry (see *Autophagic flux determination using flow and multispectral imaging cytometry*) [412,413]. Multispectral imaging flow cytometry allows characterization of single cells within a population by assessing a combination of morphology and immunofluorescence patterns, thereby providing statistically meaningful data [414]. This method can also be used for endogenous LC3, and, therefore, is useful for non-transfected primary cells [415]. For adherent cell cultures, one caution for flow cytometry is that the techniques necessary to produce single cell suspensions can cause significant injury to the cells, leading to secondary changes in autophagy. Therefore, staining for plasma membrane permeabilization (e.g., cell death) before versus after isolation is an important control, and allowing a period of recovery between harvesting the culture and staining is also advisable [416].

An important caveat in the use of GFP-LC3 is that this chimera can associate with aggregates, especially when expressed at high levels in the presence of aggregate-prone proteins, which can lead to a misinterpretation of the results [417]. Of note, GFP-LC3 can associate with ubiquitinated protein aggregates [418]; however, this does not occur if the GFP-LC3 is expressed at low levels (D.C. Rubinsztein, unpublished observations). These aggregates have been described in many systems and are also referred to as aggresome-like induced structures (ALIS) [418-420], dendritic cell ALIS/DCALIS [421], SQSTM1 bodies/sequestosomes [422,423] and inclusions. Indeed, many microbe-associated molecular patterns (MAMPs) described to induce the formation of autophagosomes in fact trigger massive formation of SQSTM1 bodies (L.H. Travassos, unpublished observations). Inhibition of autophagy in vitro and in vivo leads to the accumulation of these aggregates, suggesting a role for autophagy in mediating their clearance [418,420,422,424,425]. One way to control for background levels of puncta is to determine fluorescence from untagged GFP.

The receptor protein SQSTM1 is required for the formation of ubiquitinated protein aggregates in vitro (see *SQSTM1 and related LC3 binding protein turnover assays*) [423]. In this case, the interaction of SQSTM1 with both ubiquitinated proteins and LC3 is thought to mediate delivery of these aggregates to the autophagy system [426,427]. Many cellular stresses can induce the formation of aggregates, including transfection reagents [418], or foreign DNA (especially if the DNA is not extracted free of endotoxin). SQSTM1-positive aggregates are also formed by proteasome inhibition or puromycin treatment, and can be found in cells exposed to rapamycin for extended periods where the rates of autophagy are elevated [428]. Calcium phosphate transfection of COS7 cells or lipofectamine transfection of MEFs (R. Pinkas-Kramarski, personal communication), primary neurons (A.R. La Spada, personal communication) or neuronal cells (C.T. Chu, personal communication [429]); transiently increases basal levels of GFP-

LC3 puncta and/or the amount of LC3-II. One solution to this artefact is to examine GFP-LC3 puncta in cells stably expressing GFP-LC3; however, as transfection-induced increases in GFP-LC3 puncta and LC3-II are often transient, another approach is to use cells transfected with GFP, with cells subjected to a mock time-matched transfection as the background (negative) control. A lipidation-defective LC3 mutant where glycine 120 is mutated to alanine is targeted to these aggregates independently of autophagy (likely via its interaction with SQSTM1, see above); as a result, this mutant can serve as another specificity control [418]. When carrying out transfections it may be necessary to alter the protocol depending on the level of background fluorescence. For example, changing the medium and waiting 24 to 48 h after the transfection can help to reduce the background level of GFP-LC3 puncta that is due to the transfection reagent (M. I. Colombo, personal communication). Similarly, when using an mCherry-GFP-SQSTM1 double tag (see *Tandem mRFP/mCherry-GFP fluorescence microscopy*) in transient transfections it is best to wait 48 h after transfection to reduce the level of aggregate formation and potential inhibition of autophagy (T. Johansen, personal communication). An additional consideration is that, in addition to transfection, viral infection can activate stress pathways in some cells and possibly induce autophagy. Influenza virus induces autophagy and autophagy is required for subsequent viral-induced apoptosis [337]. Proteomic screens show that several viruses, including influenza virus [430] and Zika virus [431], can significantly alter the expression of numerous proteins involved in autophagy and other cell stress pathways. This again emphasizes the importance of appropriate controls, such as control viruses expressing GFP [432].

The formation and clearance of ubiquitinated protein aggregates appear to represent a cellular recycling process. Aggregate formation can occur when autophagy is either inhibited or when its capacity for degradation is exceeded by the formation of proteins delivered to the aggregates. In principle, formation of GFP-LC3-positive aggregates represents a component of the autophagy process. However, the formation of GFP-LC3-positive ubiquitinated protein aggregates does not directly reflect either the induction of autophagy (or autophagosome formation) or flux through the system. Indeed, formation of ubiquitinated protein aggregates that are GFP-LC3 positive can occur in autophagy-deficient cells [418]. Therefore, it should be remembered that GFP-LC3 puncta likely represent a mix of ubiquitinated protein aggregates in the cytosol, ubiquitinated protein aggregates within autophagosomes and/or more “conventional” phagophores and autophagosomes bearing other cytoplasmic cargo (this is one example where CLEM could help in resolving this question [119]). In *D. discoideum*, inhibition of autophagy leads to large ubiquitinated protein aggregates containing SQSTM1 and GFP-Atg8, when the latter is co-expressed [422]; the large size of the aggregates makes them easily distinguishable from autophagosomes. Saponin treatment has been used to reduce background fluorescence under conditions where no aggregation of GFP-LC3 is detected in hepatocytes, GFP-LC3 stably-transfected HEK 293 [432] and human osteosarcoma cells, and in nontransfected cells [433]; however, because treatment with saponin and other detergents can provoke artefactual GFP-LC3 puncta formation [434], specificity controls need to be included in such experiments. In general, it is preferable to include additional assays that measure autophagy rather than

relying solely on monitoring GFP-LC3. In addition, we recommend that researchers validate their assays by demonstrating the absence or reversal of GFP-LC3 puncta formation in cells treated with pharmacological or RNA interference-based autophagy inhibitors (Table 1). For example, 3-methyladenine (3-MA) is commonly used to inhibit starvation- or rapamycin-induced autophagy [435], but it has no effect on BECN1-independent forms of autophagy [118,208], and some data indicate that this compound can also have stimulatory effects on autophagy (see *Autophagy inhibitors and inducers*) [436,437], as well as induce cell death at progressively higher concentrations [438].

Another general limitation of the GFP-LC3 assay is that it requires a system amenable to the introduction of an exogenous gene. Accordingly, the use of GFP-LC3 in primary non-transgenic cells is more challenging. Here again, controls need to be included to verify that the transfection protocol itself does not artefactually induce GFP-LC3 puncta or cause LC3 aggregation. Furthermore, transfection should be performed with low levels of constructs, and the transfected cells should be followed to determine: i) when sufficient expression for detection is achieved, and ii) that, during the time frame of the assay, basal GFP-LC3 puncta remain appropriately low. In addition, the demonstration of a reduction in the number of induced GFP-LC3 puncta under conditions of autophagy inhibition is helpful. For some primary cells, delivering GFP-LC3 to precursor cells by infection with recombinant lentivirus, retrovirus or adenovirus [439], and subsequent differentiation into the cell type of interest, is a powerful alternative to transfection of the already differentiated cell type [103].

To implement the scoring of autophagy via fluorescence microscopy, one option is to measure pixel intensity. Because the expression of GFP-LC3 may not be the same in all cells—as discussed above—it is possible to use specific imaging software to calculate the standard deviation (SD) of pixel intensity within the fluorescence image and divide this by the mean intensity of the pixels within the area of analysis. This will provide a ratio useful for establishing differences in the degree of autophagy between cells. Cells with increased levels of autophagic activity, and hence a greater number of autophagosomes in their cytosol, are associated with a greater variability in pixel intensity (i.e., a high SD). Conversely, in cells where autophagy is not occurring, GFP-LC3 is uniformly distributed throughout the cytosol, and a variation in pixel intensity is not observed (i.e., a low SD; M. Campanella, personal communication).

Although LC3-II is primarily membrane-associated, it is not necessarily associated with autophagosomes as is often assumed; the protein is also found on phagophores, the precursors to autophagosomes, as well as on amphisomes and phagosomes (see *Western blotting and ubiquitin-like protein conjugation systems*) [247,440,441]. Along these lines, yeast Atg8 can associate with the vacuole membrane independent of lipidation, so that a punctate pattern does not necessarily correspond to autophagic compartments [442]. Thus, the use of additional markers is necessary to specify the identity of an LC3-positive structure; for example, ATG12-ATG5-ATG16L1 would be present on a phagophore, but not on an autophagosome, and thus colocalization of LC3 with any of these proteins would indicate the former structure. In addition, the site(s) of LC3 conjugation to PE is not definitively known, and levels

Table 1. Genetic and pharmacological regulation of autophagy.³

| Method | Comments |
|-------------------------------------|--|
| 1. 3-methyladenine | A PtdIns3K inhibitor that effectively blocks an early stage of autophagy by inhibiting the class III PtdIns3K, but it is important to note that it is not a specific autophagy inhibitor. 3-MA also inhibits the class I PI3K and can thus, at suboptimal concentrations in long-term experiments, promote autophagy in some systems [436,437], as well as affect cell survival through AKT and other kinases. 3-MA does not inhibit BECN1-independent autophagy. |
| 2. 10-NCP | 10-(4'-N-diethylamino)butyl)-2-chlorophenoxazine; an AKT inhibitor that induces autophagy in neurons [1950]. |
| 3. 17-AAG | An inhibitor of the HSP90-CDC37 chaperone complex; induces autophagy in certain systems (e.g., neurons), but impairs starvation-induced autophagy and mitophagy in others by promoting the turnover of ULK1 [647]. |
| 4. ABG33 | ABG33 (7-aminobenzo[cd]indol-2-(1 H)-one 33 is a small molecule inhibitor of ATG4B enzymatic activity in vitro. In cells, ABG33 results in a dose-dependent increase in LC3B-II levels [2576]. |
| 5. AC220/quizartinib | An FLT3 inhibitor that enhances the inhibitory activity of spautin-1. A70 is an improved derivative of AC220. Treatment sensitizes cancer cells to autophagy inhibition [5]. |
| 6. ACY-1215/ricolinostat | ACY-1215 is a selective HDAC6 inhibitor that inhibits the fusion of lysosomes with autophagosomes and abrogates the clearance of autophagosomes [2577]. |
| 7. AZD8055 | A catalytic MTOR inhibitor that acts as a potent autophagy inducer [2578]. |
| 8. Akti-1/2 | An allosteric inhibitor of AKT1 and AKT2 that promotes autophagy in B-cell lymphoma [2579]. |
| 9. AR-12 (OSU-03012) | A broad-specificity anti-viral celecoxib-derivative that stimulates autophagosome formation and viral protein degradation [2580]. |
| 10. AR7 | AR7 was developed as a highly potent and selective enhancer of CMA through antagonizing RARA/RAR α ; AR7 is the first small molecule developed to selectively stimulate CMA without affecting autophagy [2581]. |
| 11. ARN5187 | Lysosomotropic compound with a dual inhibitory activity against the circadian regulator NR1D2/REV-ERB β and autophagy [2582]. |
| 12. AS-605,240 | A selective PIK3CG/PI3Ky inhibitor that activates autophagy in the heart [2583]. |
| 13. ATG4 ^{C74A} | An active site mutant of ATG4 that is defective for autophagy [2584]. |
| 14. Autophinib | An autophagy inhibitor that targets the lipid kinase PIK3C3/VPS34 [2585]. |
| 15. Bafilomycin A ₁ | A V-ATPase inhibitor that causes an increase in lysosomal/vacuolar pH, and, ultimately, blocks fusion of autophagosomes with the vacuole; the latter may result from inhibition of ATP2A/SERCA [303]. |
| 16. Benzothiadiazole | A chemical analog of salicylic acid, which can be used to induce autophagy and autophagosome formation in plant cells including <i>A. thaliana</i> [128,2586]. |
| 17. Betulinic acid | A pentacyclic triterpenoid that promotes parallel damage in mitochondrial and lysosomal compartments, and, ultimately, jeopardizes lysosomal degradative capacity, which results in autophagy-associated cell death [314] or aging [315]. |
| 18. Butein | A plant-derived natural molecule that induces autophagy through the activation of AMPK [2587]. |
| 19. C12TPP | Dodecyltriphenylphosphonium is a penetrating cation that selectively accumulates in mitochondria, uncouples oxidative phosphorylation and stimulates autophagy and mitophagy without inhibition of autophagosome-lysosome fusion, in contrast to protonophores [2588]. |
| 20. Calcium | An intracellular signal that can promote autophagy at different steps. Calcium can be released from the ER upon physiological stimulation or from lysosomal stores under stress conditions, or can enter from the extracellular space [2001]. However, calcium has a complex effect as it can also inhibit autophagy, and the abrogation of calcium signaling can trigger autophagy [216,1990,1994,2589]. |
| 21. Carbamazepine | Induces autophagy by reducing inositol levels, and inhibits autophagy via neuronal voltage-gated sodium channels [1976,2590]. |
| 22. CB-5083 | A selective inhibitor of VCP/p97-mediated protein degradation that activates autophagy in human cancer cells [2591,2592]. |
| 23. CCCP | Carbonyl cyanide m-chlorophenylhydrazone is a prototype protonophore, uncoupler of oxidative phosphorylation that stimulates autophagy via the AMPK-ULK1 pathway [671,672] or alternative pathways [2593] and mitophagy [339], but inhibits autophagosome-lysosome fusion due to the increase of intralysosomal pH [215]. |
| 24. Chloroquine, NH ₄ Cl | Lysosomotropic compounds that elevate/neutralize the lysosomal/vacuolar pH [225]. |
| 25. Cinacalcet HCl | A calcimimetic that increases the sensitivity of CASR (calcium sensing receptor) to extracellular calcium. In some models, cinacalcet induces the formation of GFP-LC3 puncta [494] during starvation, whereas in others it causes an increase in LC3-II accumulation in basal [1563,2594,2595] and CQ conditions [2594]. In a diabetic nephropathy model, the proposed pathway through cinacalcet-induced autophagy is CAMKK2/CaMKK β -STK11/LKB1-AMPK-PPARGC1A/PGC1 α to decrease oxidative stress, which results in a decrease of apoptosis (increased BCL2:BAX ratio) and increased autophagy (increase of BECN1 and LC3-I to LC3-II conversion) [2595]. Cinacalcet may have a dual effect inducing autophagosome formation and inhibiting the late steps of autophagy. |
| 26. Clonidine | Activates the imidazoline receptor, which decrease cAMP in cells. An MTOR-independent inducer of autophagy [1951] |
| 27. Concanamycin A | A specific inhibitor of V-ATPases that reduces acidification of the lysosome or vacuole, and will block the degradation of autophagic bodies within the vacuole [128,2586]. |
| 28. DFMO | α -difluoromethylornithine is an irreversible inhibitor of ODC1 (ornithine decarboxylase 1) that blocks spermidine synthesis and ATG gene expression [2596]. |
| 29. DMMB | A photosensitizer derivative of methylene blue that promotes parallel damage in lysosomes and mitochondria after photoactivation with red light, leading to accumulation of non-functional autolysosomes and autophagy-associated cell death [316]. |
| 30. Docosahexaenoic | An omega-3 polyunsaturated fatty acid, that has been described as acid (DHA) an activator of autophagy, which could potentially be used in cancer therapy either alone or in combinatorial strategies, as well as in neurodegenerative, cardiovascular or infectious diseases [2597-2599]. |
| 31. E-64 c | A derivative of E-64, a cysteine protease inhibitor. |
| 32. E-64d | A membrane-permeable cysteine protease inhibitor that can block the activity of a subset of lysosomal hydrolases; should be used in combination with pepstatin A to inhibit lysosomal protein degradation. The ethyl ester of E-64 c. |
| 33. Eriocalyxin B | An autophagy inducer that exerts anti-tumor activity in breast cancer by inhibition of the AKT-MTOR-RPS6KB signaling pathway [2600]. |
| 34. ESC8 | A cationic estradiol derivative that induces autophagy and apoptosis simultaneously by downregulating the MTOR kinase pathway in breast cancer cells. |
| 35. Everolimus | An inhibitor of MTORC1 that induces both autophagy and apoptosis in B-cell lymphoma primary cultures [2579]. |

(Continued)

Table 1. (Continued).

| Method | Comments |
|------------------------------|--|
| 36. Ezetimibe | A cholesterol absorption inhibitor that acts by binding to NPC1L1, which induces autophagy via MTORC1-dependent [2601] and -independent [2602] pathways. Ezetimibe also activates TFEB and could potentially exert therapeutic effects on steatohepatitis and fibrosis [2601,2602]. |
| 37. Fasudil | An inhibitor of ROCK (Rho associated coiled-coil containing protein kinase) enhancing autophagy via phosphorylation of MAPK8/JNK1 and BCL2, and promoting BECN1-PIK3C3/VPS34 complex formation; shRNA-mediated approaches to inhibiting ROCK have similar results [2603-2605]. |
| 38. Flavonoids | A large class of polyphenols that have been described as autophagy modulators, which could potentially constitute useful adjuvant agents of conventional therapies for different human pathologies such as cancer, neurodegenerative, cardiovascular, hepatic or infectious diseases [2606]. |
| 39. Fumonisin B1 | An inhibitor of ceramide synthesis that interferes with autophagy. |
| 40. Gene deletion | This method provides the most direct evidence for the role of an autophagic component; however, more than one gene involved in autophagy should be targeted to avoid indirect effects. |
| 41. HBHA | Heparin-binding hemagglutinin of <i>M. tuberculosis</i> that inhibits autophagy. HBHA treatment inhibits LC3 expression and the maturation of autophagosomes, eventually inducing apoptosis [2607]. |
| 42. HMOX1 induction | Mitophagy and the formation of iron-containing cytoplasmic inclusions and corpora amylacea are accelerated in HMOX1-transfected rat astroglia and astrocytes of GFAP HMOX1 transgenic mice. Heme-derived ferrous iron and carbon monoxide, products of the HMOX1 reaction, promote autophagy in these cells [2608,2609]. |
| 43. Knockdown | This method (including miRNA, RNAi, shRNA and siRNA) can be used to inhibit gene expression and provides relatively direct evidence for the role of an autophagic component. However, the efficiency of knockdown varies, as does the stability of the targeted protein. In addition, more than one gene involved in autophagy should be targeted to avoid misinterpreting indirect effects. |
| 44. KU-0063794 | An MTOR inhibitor that binds the catalytic site and activates autophagy [453,2610]. |
| 45. Leupeptin | An inhibitor of cysteine, serine and threonine proteases that can be used in combination with pepstatin A and/or E-64d to block lysosomal protein degradation. Leupeptin is not membrane permeable, so its effect on cathepsins may depend on endocytic activity. |
| 46. LV-320 | A small molecule inhibitor of ATG4A and ATG4B enzymatic activity in vitro. In cells, LV-320 results in a dose-dependent increase in LC3B-II levels, reduces GABARAP levels and reduces autophagic flux [2611]. |
| 47. MB | A phenothiazine photosensitizer that promotes specific photodamage in lysosomes when used at low doses and photoactivated with red light. By targeting lysosomes to photodamage, MB can promptly switch autophagy to favor cell demise when parallel mitochondrial membrane damage by hydrogen peroxide or rotenone occurs [316]. |
| 48. Melatonin | N-acetyl-5-methoxy tryptamine is a sleep-wake cycle regulating and antioxidant hormone that inhibits autophagy in animal models of fibrosis [2612], cancer [2613] and acute organ failure [2614]. |
| 49. Metformin | Activates both AMPK-dependent and -independent autophagy [2615-2617]. |
| 50. microRNA | Can be used to reduce the levels of target mRNA(s) or block translation. |
| 51. MK2206 | A small molecule inhibitor of AKT that is able to induce Autophagy independently of MTORC1 activity [973,2618]. |
| 52. MLN4924 | A small molecule inhibitor of NAE (NEDD8 activating enzyme) [2619]; induces autophagy by blockage of MTOR activity via both DEPTOR and the HIF1A-DDIT4/REDD1-TSC1/2 axis as a result of inactivation of cullin-RING ligases [2620]. |
| 53. Mycolactone | A polyketide lactone and virulence exotoxin of <i>Mycobacterium ulcerans</i> that functions by blocking SEC61-dependent translocation of proteins into the ER [2022]. Mycolactone induces the integrated stress response [2021] and autophagy [2020,2021]. |
| 54. NAADP-AM | Activates the lysosomal TPCN/two-pore channel and induces autophagy [1996]. |
| 55. NED-19 | Inhibits the lysosomal TPCN and NAADP-induced autophagy [1996]. |
| 56. NeuroHeal | A combination of acamprosate and ribavirin that activates SIRT1 and autophagy, promoting neuroprotection [2015,2016]. |
| 57. NSC611216 | A small molecule inhibitor of ATG4B enzymatic activity in vitro [2576]. |
| 58. NVP-BEZ235 | A dual inhibitor of PIK3CA/p110 and the MTOR catalytic site that activates autophagy [2621,2622]. |
| 59. p140/Lupuzor™ | Small peptide that inhibits LAMP2A overexpression in lupus B cells and binds to the NBD domain of HSPA8 [2623,2624]. Furthermore, this drug has been described as a potent CMA inhibitor [2625]. |
| 60. Pathogen-derived factors | Virally-encoded autophagy inhibitors including HSV-1 ICP34.5, Kaposi sarcoma-associated herpesvirus vBCL2, γ -herpesvirus 68 M11, ASFV vBCL2, HIV-1 Nef and influenza A virus M2 [848,1418,1423,1424,1966]. |
| 61. Pepstatin A | An aspartyl protease inhibitor that can be used to partially block lysosomal degradation; should be used in combination with other inhibitors such as E-64d. Pepstatin A is not membrane permeable. |
| 62. PMI | SQSTM1/p62-mediated mitophagy inducer is a pharmacological activator of autophagic selection of mitochondria that operates without collapsing the mitochondrial membrane potential ($\Delta\Psi_m$) and hence by exploiting the autophagic component of the process [714]. |
| 63. Propolis | An inducer of autophagy that may be related with the classical autophagy pathway [2626]. |
| 64. Protease inhibitors | These chemicals inhibit the degradation of autophagic substrates within the lysosome/vacuole lumen. A combination of inhibitors (e.g., leupeptin, pepstatin A and E-64d) is needed for complete blockage of degradation. |
| 65. Rapamycin | Binds to FKBP1A/FKBP12 and inhibits MTORC1; the complex binds to the FRB domain of MTOR and limits its interaction with RPTOR, thus inducing autophagy, but only providing partial MTORC1 inhibition. Rapamycin also inhibits yeast TOR. |
| 66. Resveratrol | A natural polyphenol that affects many proteins [2627] and induces autophagy via activation of AMPK [2628, 2629]. |
| 67. RNAi | Can be used to inhibit gene expression. |
| 68. RSVAs | Synthetic small-molecule analogs of resveratrol that potently activate AMPK and induce autophagy [2630]. |
| 69. Saikosaponin-d | A natural small-molecule inhibitor of ATP2A/SERCA that induces autophagy and autophagy-dependent cell death in apoptosis-resistant cells [1909]. |
| 70. SAR405 | A low-molecular-mass kinase inhibitor of PIK3C3/VPS34 that interacts within the ATP binding cleft of human PIK3C3 and inhibits autophagy [1883]. |
| 71. SB02024 | Potent and selective PIK3C3/VPS34 inhibitor that binds in the active site of PIK3C3, thus inhibiting its catalytic function [2631]. |

(Continued)

Table 1. (Continued).

| Method | Comments |
|------------------------|---|
| 72. SBI-0206965 | A highly selective ULK1 kinase inhibitor <i>in vitro</i> that suppresses ULK1-mediated phosphorylation events in cells, regulating autophagy and cell survival [2632]. This compound is also an inhibitor of AMPK, competitively inhibiting ATP binding, and also inhibiting the binding of AMPK to its substrates [2633]. |
| 73. Sorafenib | An antitumoral inhibitor of tyrosine kinase receptors whose sustained administration induces a shift from early induction of survival autophagy to apoptosis [2634]. |
| 74. SMER28 | An MTOR-independent inducer of autophagy [2013]. |
| 75. Spautin-1 | An autophagy inhibitor that acts via suppression of USP10 and USP13, and degradation of the PIK3C3/VSP34-BECN1 complex [2635]. |
| 76. Spermidine | A chemical originally isolated from semen and enriched in many food products; it promotes autophagy flux by depleting cytosolic HDAC4 to enhance MAP1S-mediated autophagy [956]. Spermidine maintains basal autophagy in NIH 3T3 cells and B cells of mice or humans via hypusination of EIF5A and subsequent upregulation of TFEB [958]. |
| 77. Sulforaphane | A natural isothiocyanate, alone and in combination with cytostatics induces cell death via autophagy, and elevates the level of LC3-II [1905,2636,2637]. |
| 78. Tat-beclin 1 | A cell penetrating peptide that potently induces autophagy [2004,2638]. |
| 79. Thapsigargin | An inhibitor of ATP2A/SERCA that inhibits autophagic sequestration through the depletion of intracellular Ca^{2+} stores [216,2639]; however, thapsigargin may also block fusion of autophagosomes with endosomes by interfering with recruitment of RAB7, resulting in autophagosome accumulation [2640]. |
| 80. TMS | Trans-3,5,4-trimethoxystilbene upregulates the expression of TRPC4, resulting in MTOR inhibition [2641]. |
| 81. Torin1 | A catalytic MTOR inhibitor that induces autophagy and provides more complete inhibition than rapamycin (it inhibits all forms of MTOR) [802]. |
| 82. TPCK | An inducer of autophagic cell death. |
| 83. TPPS _{2a} | TPPS _{2a} photoexcitation promotes mainly lysosomal damage leading to autophagy-associated cell death [317]. |
| 84. Trehalose | A membrane-protective agent [2642] and inducer of autophagy that may be relevant for the treatment of different neurodegenerative diseases [973, 2036, 2643-2645]. |
| 85. Tunicamycin | A glycosylation inhibitor that induces autophagy due to ER stress [473,2646]. |
| 86. Vacuolin-1 | A RAB5A activator that reversibly blocks autophagosome-lysosome fusion [2647]. |
| 87. Verteporfin | An FDA-approved drug; used in photodynamic therapy, but it inhibits the formation of autophagosomes <i>in vivo</i> without light activation [2648]. |
| 88. Vinblastine | A depolymerizer of both normal and acetylated microtubules that interferes with autophagosome-lysosome fusion [304]. |
| 89. VP2.51 | A small molecule, ATP-competitive inhibitor of GSK3B enzymatic activity <i>in vitro</i> . <i>In vivo</i> , VP2.51 modulates autophagy and ameliorates motor neuron disease [2649]. |
| 90. VPS34-IN1 | A low-molecular-mass kinase inhibitor of PIK3C3/VPS34 similar to SAR-405 that interacts within the ATP binding cleft of human PIK3C3 and inhibits autophagy [2650]. |
| 91. Wortmannin | An inhibitor of PI3K and PtdIns3K that blocks autophagy, but is not a specific inhibitor (see 3-MA above). |
| 92. Yessotoxin (YTX) | A small molecule marine compound that can potentially induce autophagic-associated cell death [1515]. YTX can induce various cell death modalities [2651]; its molecular target and mode of action are not yet clarified. |

of Atg8-PE/LC3-II can increase even in autophagy mutants that cannot form autophagosomes [443]. One method that can be used to examine LC3-II membrane association is differential extraction in Triton X-114, which can be used with mammalian cells [439], or western blot analysis of total membrane fractions following solubilization with Triton X-100, which is helpful in plants [289,290]. Importantly, we stress again that numbers of GFP-LC3 puncta, similar to steady state LC3-II levels, reflect only a snapshot of the numbers of autophagy-related structures (e.g., autophagosomes) in a cell at one time, not autophagic flux. A potential solution to determine the effect of a given perturbation on flux, is to count GFP-LC3 puncta at various time points following the addition of 3-MA (to prevent formation of new puncta), with the rate of puncta disappearance essentially indicating the flux of disposal [444].

GFP-LC3 expression can perturb autophagy and cellular function, both in the basal state and disease models, as found in the exocrine pancreas of GFP-LC3 mice [445]. Compared to the wild type, the pancreatic ATG4B level is markedly decreased in GFP-LC3 mice, resulting in an increase of the endogenous LC3-II. These effects are organ specific (e.g., there are no effects on ATG4B and LC3 levels in lung and spleen). Autophagic flux analysis (using the lysosomal protease inhibitors E64d plus

pepstatin A) indicate that in GFP-LC3 pancreatic acinar cells the basal autophagosome formation is enhanced several-fold but is not fully counterbalanced by increased autophagic degradation. As a result, the exocrine pancreas of GFP-LC3 mice displays accumulation of enlarged autophagic vacuoles. GFP-LC3 expression affects functional parameters of acinar cells and worsens key pathological responses in mouse models of acute pancreatitis. The study referenced above demonstrates organ-specific effects of GFP-LC3 expression and indicates that application of GFP-LC3 mice in disease models should be done cautiously.

Finally, we offer a general note of caution with regard to GFP. First, the GFP tag is large, in particular relative to the size of LC3; therefore, it is possible that a chimera may behave differently from the native protein in some respects. Second, GFP is not native to most systems, and as such (i) it may be recognized as an aberrant protein and targeted for degradation, which has obvious implications when studying autophagy, and (ii) it may elicit immune responses targeting GFP-expressing cells *in vivo*. Third, some forms of GFP tend to oligomerize, which may interfere with protein function and/or localization. Fourth, EGFP inhibits polyubiquitination [446], and may cause defects in other cellular processes. Fifth, not all LC3 puncta represent LC3-II and correspond to autophagosomes [255,256,447,448]. Accordingly, it would be prudent to

4935

4940

4945

4950

4955

complement any assays that rely on GFP fusions (to Atg8-family proteins or any protein) with additional methods that avoid the use of this fluorophore. Similarly, with the emergence of “super-resolution” microscopy methods such as photoactivated localization microscopy (PALM), new tags are being used (e.g., the EosFP green-to-red photoconvertible fluorescent protein, or the Dronpa GFP-like protein) that will need to be tested and validated [449].

Conclusion: GFP-LC3 provides a marker that is relatively easy to use for monitoring autophagy induction (based on the appearance of puncta), or colocalization with cargo; however, monitoring this chimera does not determine flux unless utilized in conjunction with inhibitors of lysosomal fusion and/or degradation. In addition, it is recommended that results obtained by GFP-LC3 fluorescence microscopy are verified by additional assays.

Tandem mRFP/mCherry-GFP fluorescence microscopy. A fluorescence assay that is designed to monitor flux relies on the use of a tandem monomeric RFP-GFP-tagged LC3 (tfLC3; Figure 16) [344]. The GFP signal is sensitive to the acidic and/or proteolytic conditions of the lysosome lumen, whereas mRFP is more stable. Therefore, colocalization of both GFP and mRFP fluorescence indicates a compartment that has not fused with a lysosome, such as a phagophore, an amphisome or an autophagosome [450]. In a pathological state where acidification mechanisms are impaired, fusion may occur without GFP becoming quenched, and additional markers of fusion must be applied [451]. Although inhibiting lysosomal acidification may impede fusion in some cell types, fusion may proceed in other cell types under these conditions [218]. In contrast, an mRFP signal without GFP corresponds to an autolysosome. Other fluorophores such as mCherry are also suitable instead of mRFP [423], and an image-recognition algorithm has been developed to quantify flux of the reporter to acidified compartments [452–454]. One of the major advantages of the tandem mRFP/mCherry-GFP reporter method is that it enables simultaneous estimation of both the induction of autophagy and flux through autophagic compartments. However, determining the efficiency of the actual degradation of the substrate or carrier in the lysosome still requires the use of lysosomal protease inhibitors such as E64d and pepstatin. The competence of lysosomal digestion of the substrate requires additional analysis using methods described above. The use of more than one time point allows visualization of increased early autophagosomes followed by increases in late autophagosomes as an additional assurance that flux has been maintained [293]. In addition, this method can be used to monitor autophagy in high-throughput drug screening studies [453]. The quantification of “yellow” (where the yellow signal results from merging the red and green channels) and “red only” puncta in a stable tandem-fluorescent LC3-reporter cell line can be automated by a Celloomics microscope that can be used to assess a huge population of cells (1,000 or more) over a large number of random fields of view [311,455]. In the presence of a lysosomal acidification defect, additional markers of autophagosome-lysosome fusion need to be applied to assess autophagy flux alterations [451]. The use of late inhibitors of autophagy such as CQ or bafilomycin A₁, which prevent the formation of autolysosomes,

is recommended as a useful experimental control for the visualization of “yellow” puncta. Note that “green-only” dots may occur under certain conditions due to more rapid maturation of the GFP chromophore, allowing similar fusions to be used as timers [456,457]. Notably, organelle-specific variations of the tandem mRFP/mCherry-GFP reporter system have successfully been used to analyze selective types of autophagy, such as pexophagy [458,459], mitophagy [460–463] and reticulophagy [464,465] in mammalian cells. This tandem reporter is technically less challenging in plant cells due to accumulation of red fluorescent signal in the large relatively static plant vacuoles instead of small mobile dot-like lysosomes. Optimization of the tandem-tag assay for monitoring autophagic activity in plant roots has been described, providing a pipeline for automated high-throughput image analysis [357]. Importantly, *in vivo* systems to detect mitophagy have been generated employing *Drosophila* [466] and mouse models [38].

An alternative dual fluorescence assay involves the Rosella pH biosensor. This assay monitors the uptake of material to the lysosome/vacuole and complements the use of the tandem mRFP/mCherry-GFP reporter. The assay is based upon the genetically encoded dual color-emission biosensor Rosella, a fusion between a relatively pH-stable fast-maturing RFP variant, and a pH-sensitive GFP variant. When targeted to specific cellular compartments or fused to an individual protein, the Rosella biosensor provides information about the identity of the cellular component being delivered to the lysosome/vacuole for degradation. Importantly, the pH-sensitive dual color fluorescence emission provides information about the environment of the biosensor during autophagy of various cellular components. In yeast, Rosella has been successfully used to monitor autophagy of cytosol, mitochondria (mitophagy) and the nucleus (nucleophagy) [156,467,468]. Furthermore, the Rosella biosensor can be used as a reporter under various conditions including nitrogen depletion-dependent induction of autophagy [467,468]. The Rosella biosensor can also be expressed in mammalian cells to follow either nonselective autophagy (cytoplasmic turnover), or mitophagy [467,469]. A Rosella-based mitophagy reporter mouse line has been created to assess mitophagy activity in the heart [470].

Cautionary notes: The motion of puncta corresponding to Atg8-family proteins can complicate the use of tandem mRFP/mCherry-GFP-Atg-family protein reporters in live imaging experiments. As a consequence, conventional confocal microscopy may not allow visualization of colocalized mRFP/mCherry-GFP puncta. In this case, mRFP/mCherry-GFP colocalized puncta represent newly formed autophagic structures whereas mRFP/mCherry-only puncta are ambiguous. Spinning disk confocal microscopy or rapid acquisition times may be required for imaging tandem mRFP/mCherry-GFP proteins, although these techniques require a brighter fluorescent signal potentially associated with undesirably higher levels of transgene expression. Overexpression of these sensors can target the proteins to acidified lysosomes, which also results in mRFP/mCherry-only puncta. A good control is the non-lipidatable form of the sensor expressed at the same levels as the wild-type experimental sensor, to assess baseline targeting of the tandem proteins to lysosomes [471]. Another optimization is to use the mTagRFP-mWasabi-LC3 chimera [472,473], as mTagRFP is brighter

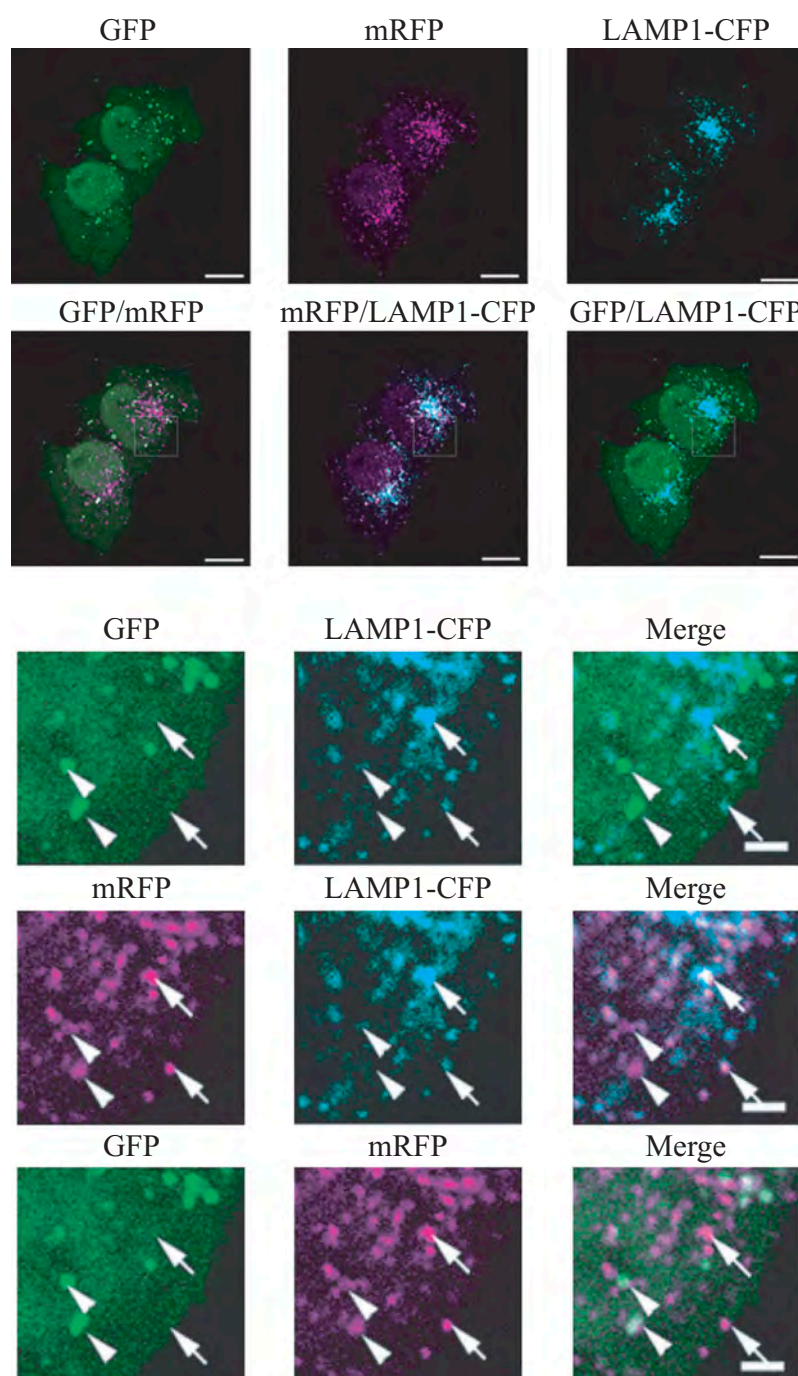


Figure 16. The GFP and mRFP signals of tandem fluorescent LC3 (tfLC3, mRFP-GFP-LC3) show different localization patterns. HeLa cells were cotransfected with plasmids expressing either tfLC3 or LAMP1-CFP. Twenty-four h after the transfection, the cells were starved in Hanks balanced salt solution for 2 h, fixed and analyzed by microscopy. The lower panels are a higher magnification of the upper panels. Bar: 10 μ m in the upper panels and 2 μ m in the lower panels. Arrows in the lower panels point to (or mark the location of) typical examples of colocalized signals of mRFP and LAMP1. Arrowheads point to (or mark the location of) typical examples of colocalized particles of GFP and mRFP signals. This figure was previously published in ref. [344], and is reproduced by permission of Landes Bioscience, copyright 2007.

than mRFP and mCherry, and mWasabi is brighter than EGFP [474]. An improved version of tfLC3 is pHluorin-mKate2-hLC3 reporter (PK-hLC3), because pHluorin is more sensitive to acidic pH (pKa 7.6, quenched at pH 6.5) than EGFP and mWasabi [450,475]. In the latter case, however, organelles that only achieve a lower level of acidification, such as amphisomes, may not be differentiated from fully acidified (i.e., mature) lysosomes [476]. A good quantitative technique for cells in suspension, which also require

identification by surface markers (such as immune cells), is the detection of LC3-II by flow cytometry. Here LC3-I is washed out after treatment with a mild detergent, and only membrane-bound LC3-II is retained for staining with an anti-LC3 antibody. Early fixation avoids the induction of artefacts due to centrifugation or mixing. This approach has been established for both cell lines [433] and primary cells [477].

Another possibility is to use fixed cells; however, this presents an additional concern: The use of tandem mRFP/mCherry-GFP

relies on the quenching of the GFP signal in the acidic autolysosome; however, fixation solutions are often neutral or weak bases, which will increase the pH of the entire cell. Accordingly, the GFP signal may be restored after fixation (Figure 17), which would cause an underestimation of the amount of signal that corresponds only to RFP (i.e., in the autolysosome). Thus, the tissue or cell samples must be properly processed to avoid losing the acidic environment of the autolysosomes. In addition, there may be weak fluorescence of EGFP even in an acidic environment (pH

between 4 and 5) [439,478]. Therefore, it may be desirable to choose a monomeric green fluorescent protein that is more acid sensitive than EGFP for assaying autophagic flux. For example, the pHluorin-based probe (PK-hLC3) referred to above can solve these problems [450]; in a PK-hLC3 transgenic mouse autophagic responses in the neurons are easily detectable, whereas such responses in the neurons of a GFP-LC3 transgenic mouse are hardly recognized [479]. pHluorin-LC3-mCherry is also an improved autophagic flux probe variant of GFP-LC3-RFP-

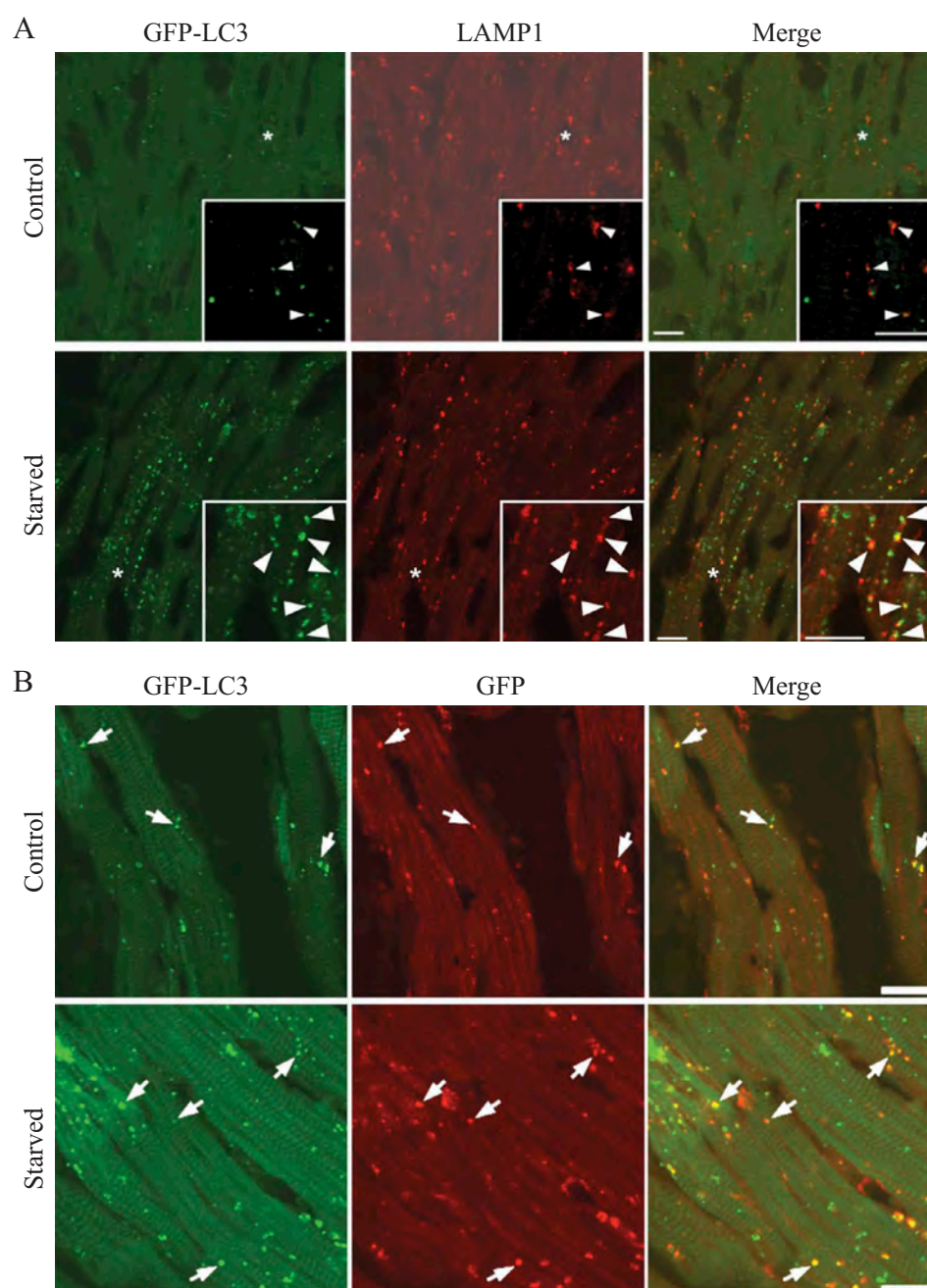


Figure 17. GFP fluorescence in the autolysosome can be recovered upon neutralization of the pH. **(A)** GFP-LC3 emits green fluorescence in the autolysosomes of post-mortem processed heart sections. Cryosections of 3.8% paraformaldehyde fixed ventricular myocardium from 3-week-old GFP-LC3 transgenic mice at the baseline (Control) or starved for 24 h (Starved) were processed for immunostaining using a standard protocol (buffered at pH 7.4). Most of the GFP-LC3 puncta are positive for LAMP1, suggesting that the autolysosomes had recovered GFP fluorescence. **(B)** Colocalization between GFP-LC3 direct fluorescence (green) and indirect immunostaining for GFP (red). Sections processed as in **(A)** were immunostained for GFP using a red fluorescence-tagged secondary antibody, and the colocalization with GFP fluorescence was examined by confocal microscopy. Almost all of the red puncta emit green fluorescence. Scale bar: 10 μ m. Image provided by Xuejun Wang.

LC3AG [480]. Finally, photobleaching, light-induced degradation of fluorophores, is a significant problem in live-cell imaging [481]. When examining live tissue, it is important to remember that marker fluorescence, particularly GFP fluorescence, can diminish rapidly with the decay of cell physiology. The use of the minimal possible exposure and light power level is therefore recommended. If sequential acquisition of fluorescence emissions is needed, they should be acquired in the order GFP then RFP, as RFP exhibits higher photostability. The experimenter can also take advantage of anti-fading media developed for live imaging [482]. In some tissues (e.g., *Drosophila* brain) it may be necessary to image each sample no more than 30-40 min after dissection of the individual sample.

Another caution in the interpretation of the tandem fluorescent marker is that an enhanced degree of colocalization of GFP and mRFP/mCherry might also be seen in the case of impaired proteolytic degradation within autolysosomes or altered lysosomal pH. This limitation may be overcome by incorporating two strategies in the experimental design: i) direct measurement of lysosomal pH in the *in vitro* model of interest, to discount lysosomal alkalinization as a cause for increased GFP⁺ RFP⁺ puncta [483-485], and ii) Immunohistochemical analysis against lysosomal markers such as CTSD and LAMP2. Whereas measuring lysosomal pH or proteolytic activity *in vivo* or in fixed tissue is not possible, colocalization of GFP⁺ RFP⁺ puncta, or target autophagic cargo with CTSD or LAMP2 may be indicative of lysosomal dysfunction [485].

RFP-GFP-LC3 and GFP-LC3 (or other Atg8-family proteins) methodology, which involves *in vitro* or *in vivo* overexpression of the fluorescent construct, requires careful microscopy by including a GFP-expressing control. A comparable *in vitro* or *in vivo* system overexpressing GFP is necessary to "titer" the minimum laser intensity, minimum gain, and offset parameters on the confocal microscope that are required to detect true GFP. Excessive laser intensity/gain often leads to an undesirable increase in signal:background ratio, may also contribute to increased false-positive counts, and often leads to rapid photobleaching as well. The same laser intensity/gain/offset setting to detect true GFP should strictly be applied to the RFP-GFP-LC3-expressing *in vitro* or *in vivo* system of interest. The other experimental positive control is CQ or bafilomycin A₁ treatment to induce lysosomal alkalinization. The intensity/gain settings (sufficient to detect true GFP) should be minimally sufficient to detect GFP⁺ RFP⁺ puncta in CQ-treated samples. Autophagosomes, typically, are 900 nm to 1.5 µm in diameter. Low magnification images (using 20X/40X objectives) do not provide enough resolution to obtain quantifiable data. Only higher magnification images should be used to monitor autophagy. Once the microscope "parameters" to detect GFP have been determined (using a GFP-overexpressing control), it is important that the user captures the fluorescence images in the green channel in experimental conditions, and the CQ treatment control, in a "blinded" manner; ImageJ, or other equivalent software, should be used for objective quantification of GFP/RFP puncta (S. Ramachandra Rao and S.J. Fliesler, unpublished results).

Finally, expression of tandem mRFP-GFP-LC3 is toxic to some cancer cell lines relative to GFP-LC3 or RFP-LC3 (K.S. Choi, personal communication). By contrast, transgenic expression of mRFP-GFP-LC3 in neurons, which generates strong

fluorescence signals at low levels of expression of the reporter construct, exhibit no evident toxicity or effects on baseline autophagy or lifespan [451]. The cytotoxicity of DsRed and its variants such as mRFP is associated with downregulation of BCL2L1/Bcl-X_L [486]. In contrast to mRFP-GFP-LC3, overexpression of mTagRFP-mWasabi-LC3 does not appear to be toxic to HeLa cells (J. Lin, personal communication) or LNCaP cells (N. Engedal, personal communication).

The Rosella assay has not been tested in a wide range of mammalian cell types. Accordingly, the sensitivity and the specificity of the assay must be verified independently until this method has been tested more extensively and used more widely.

Finally, it may be desirable to capture the dynamic behavior of autophagy in real time, to generate data revealing the rate of formation and clearance of autophagosomes over time, rather than single data points. For example, by acquiring signals from two fluorescent constructs in real time, the rate of change in colocalization signal as a measure of the fusion rate and recycling rate between autophagosomes and lysosomes can be assessed [487]. Importantly, due to the integral dynamic relationship of autophagic flux with the onset of apoptosis and necrosis, it is advantageous to monitor cell death and autophagic flux parameters concomitantly over time, which FRET-based reporter constructs make possible [488].

Tandem fluorescent markers show real-time changes in autophagosome fusion with lysosomes, due to entry into an acidic environment; however, fusion is not definitive evidence of substrate or carrier degradation. Lysosomes may be able to fuse, but be unable to degrade newly delivered cargo, as occurs in some lysosomal storage diseases and aging-related neurodegenerative diseases. Best practice would be to perform an autophagic flux assay in parallel with quantification of tandem fluorescent markers to confirm completion of carrier flux.

Conclusion: The use of tandem fluorescent constructs, which display different emission signals depending on the environment (in particular, GFP fluorescence is sensitive to an acidic pH), provides a convenient way to monitor autophagic flux in many cell types.

Autophagic flux determination using flow and multispectral imaging cytometry. Whereas fluorescence microscopy, in combination with novel autophagy probes, has permitted single-cell analysis of autophagic flux, automation for allowing medium- to high-throughput analysis has been challenging. A number of methods have been developed that allow the determination of autophagic flux using flow cytometry [300, 414, 433 [489-492], and commercial kits are now available for monitoring autophagy by flow cytometry. These approaches make it possible to capture data or, in specialized instruments, high-content, multiparametric images of cells in flow (at rates of up to 1,000 cells/s for imaging, and higher in nonimaging flow cytometers), and are particularly useful for cells that grow in suspension. This quantitative method is simple and can be used for high-content studies with simultaneous analysis of multiple parameters. This is especially useful for the study of complex mixtures of cell types, for example in the analysis of immune cells where it might require discrimination of the autophagic state of each cell

type or even subsets. The employment of a vital nuclear dye in combination with other markers makes it possible not only to exclude dead cells by detection of nuclear fragmentation, but also to analyze a cell population in a specific cell cycle phase. Notably, as living cells expressing fluorescence proteins are amenable to analysis by flow cytometry, this method may also be utilized to sort specific subpopulations for further characterization.

Optimization of image analysis permits the study of cells with heterogeneous LC3 puncta, thus making it possible to quantify autophagic flux accurately in situations that might perturb normal processes (e.g., microbial infection or drug treatment) [489,493]. Because EGFP-LC3 is a substrate for autophagic degradation, total fluorescence intensity of EGFP-LC3 can be used to indicate levels of autophagy in living mammalian cells [492]. When autophagy is induced, the decrease in total cellular fluorescence can be precisely quantified in large numbers of cells to obtain robust data; flux can also be directly associated with an increase of detectable puncta [413]. Moreover, current technology makes it possible to investigate the colocalization of EGFP-LC3 puncta and other specific proteins, identifying novel molecules degraded during autophagic flux. In another approach, soluble EGFP-LC3-I can be depleted from the cell by a brief saponin (or digitonin) extraction so that the total fluorescence of EGFP-LC3 then represents that of EGFP-LC3-II alone (Figure 18A) [432,433]. Because EGFP-LC3 transfection typically results in high relative levels of EGFP-LC3-I, this treatment significantly reduces the background fluorescence due to non-phagophore and non-autophagosome-associated reporter protein. By comparing treatments in the presence or absence of lysosomal degradation inhibitors, subtle changes in the flux rate of the GFP-LC3 reporter construct can be detected. If it is not

desirable to treat cells with lysosomal inhibitors to determine rates of autophagic flux, a tandem mRFP/mCherry-EGFP-LC3 (or similar) construct can also be used for autophagic flux measurements in flow cytometry experiments (see *Tandem mRFP/mCherry-GFP fluorescence microscopy*) [473,491].

These methods, however, require the cells of interest to be transfected with reporter constructs. Because the saponin extraction method can also be combined with intracellular staining for endogenous LC3 protein, subtle changes in autophagic flux can be measured without the need for reporter transfections (Figure 18B).

In addition to GFP-LC3, a novel probe has emerged in recent years: GFP-LC3-RFP-LC3 Δ G and GFP-LC3-RFP (without LC3 Δ G) that bypass the weaknesses of GFP-LC3 [494]. This probe is cleaved by endogenous ATG4 and releases an equal amount of GFP-LC3 and RFP-LC3 Δ G (or RFP) in the cells. While GFP-LC3 is lipidated and localizes to phagophores and autophagosomes (as described previously), the RFP-LC3 Δ G (or RFP) cannot be conjugated with PE and remains in the cytoplasm, acting as an internal control. The GFP-LC3:RFP-LC3 Δ G (or RFP) ratio (or GFP:RFP ratio) indicates the autophagic flux. The advantage of this probe compared to the “traditional” GFP-LC3 probe is that the release of the internal control makes it possible to discriminate the changes of overall GFP-LC3 levels caused by the autophagic flux to the ones resulting from variation of gene expression. The measurement of both GFP-LC3 and RFP-LC3 Δ G (or RFP) can be performed in a high-throughput manner using FACS for single-cell analysis or some plate readers. The most precise way to monitor autophagy with this probe is to use a single-cell derived colony of stable cell

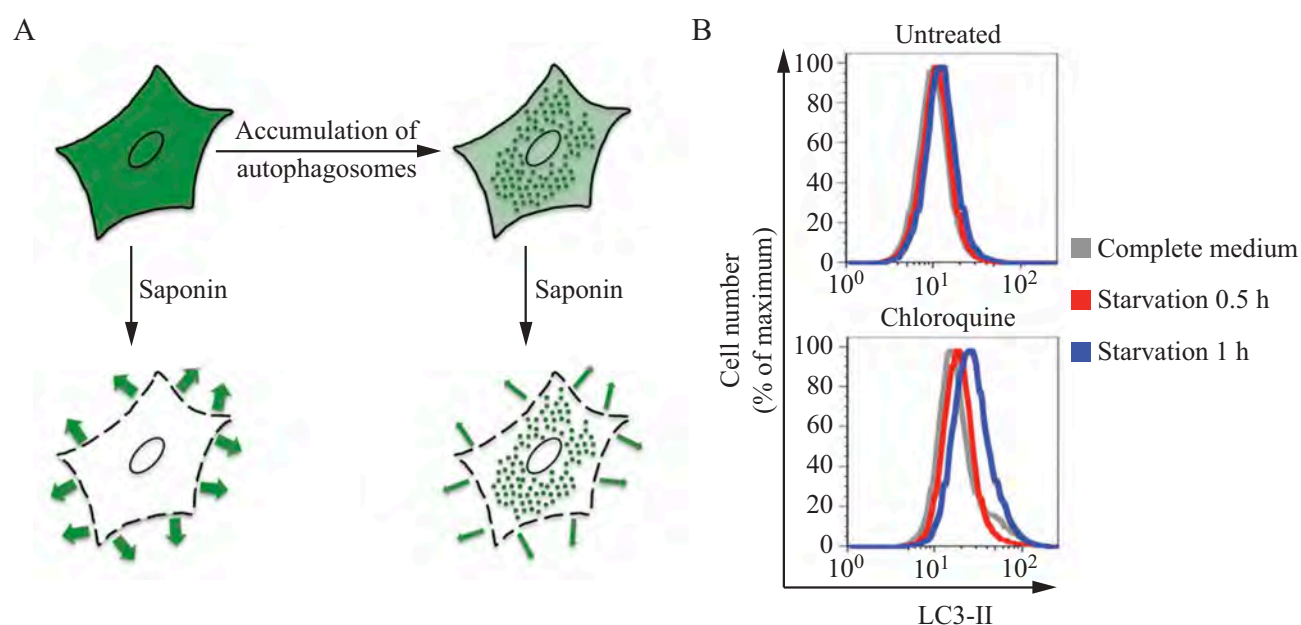


Figure 18. Saponin extraction allows quantification of LC3-II fluorescence by FACS. (A) Schematic diagram of the effects of the saponin wash. Due to the reorganization of the EGFP-LC3 reporter protein, induction of autophagosome formation does not change the total levels of fluorescence in EGFP-LC3-transfected cells. However, extraction of EGFP-LC3-I with saponin results in a higher level of fluorescence in cells with proportionally higher levels of EGFP-LC3-II-containing autophagosomes. This figure was previously published in ref. [433]. (B) Saponin extraction can also be used to measure flux of endogenous LC3 protein. Human osteosarcoma cells were starved of amino acids and serum by incubation in EBSS, for the indicated times in the presence or absence of a 1-h CQ (50 μ M) treatment. Cells were then washed with PBS containing 0.05% saponin and processed for FACS analysis for endogenous LC3. Image provided by K.E. Eng and G.M. McInerney.

lines, in order to have the most homogeneous population. This is also because the DNA sequence corresponding to GFP-LC3-RFP-LC3ΔG sometimes undergoes homologous recombination between the two LC3-encoding fragments during retrovirus infection (this does not occur with GFP-LC3-RFP).

Cautionary notes: Care must be taken when applying flow cytometry measurements to adherent cells, particularly neurons and other cells with interdigitated processes, as the preparation of single cell suspensions entails significant levels of plasma membrane disruption and injury that can secondarily induce autophagy.

Users of the saponin or digitonin extraction method should carefully titrate detergent concentrations and times of treatment to ensure specific extraction of LC3-I in their systems. Also, it has been observed in some cell types that saponin treatment can lead to nonautophagic aggregation of LC3 [434], which should be controlled for in these assays (see *GFP-Atg8-family protein fluorescence microscopy*). Similarly, for treatment with other detergents, such as Triton X-100, it is also important to carefully titrate the concentrations and times of treatment.

Cell membrane permeabilization with digitonin and extraction of the nonmembrane-bound form of LC3 allows combined staining of membrane-associated LC3-II protein and any markers for detection of autophagy in relation to other cellular events/processes. Based on this approach, a method for monitoring autophagy in different stages of the cell cycle was developed [495]. Thus, the presence of basal or starvation-induced autophagy is detected in G₁, S, and G₂/M phases of the cell cycle in MEFs with doxycycline-regulated ATG5 expression. In these experiments, cells were gated based on their DNA content and the relative intensity of GFP-LC3-II and LC3-II expression. This approach might also be used for the detection of autophagic flux in different stages of the cell cycle, or the subG₁ apoptotic cell population by measuring accumulation of LC3-II in the presence or absence of lysosomal inhibitors.

Although GFP-LC3 can be used as a reporter for flow cytometry, it is more stable (which is not necessarily ideal for flux measurements) than GFP-SQSTM1 or GFP-NBR1 (NBR1 is an autophagy receptor with structural similarity to SQSTM1 [496]). GFP-SQSTM1 displays the largest magnitude change following the induction of autophagy by amino acid deprivation or rapamycin treatment, and may thus be a better marker for following autophagic flux by this method (confirmed in SH-SY5Y neuronal cell lines stably expressing GFP-SQSTM1; E.M. Valente, personal communication) [497]. In addition, to reduce/eliminate potential effects on transcription or translation of the reporter, a doxycycline-inducible version of GFP-SQSTM1 can be used [497]. Flow cytometry for LC3, SQSTM1 or using commercial autophagy kits can also be used to measure autophagy in a specific cell sub-population isolated from tissue. For example, this approach can measure autophagy levels specifically in microglia and infiltrating macrophages in the mouse brain after traumatic brain injury (M. Lipinski, unpublished data).

Using purification of intracellular vesicles, flow cytometry can be adapted for a deeper understanding and better

characterization of individual autophagosomes. Single organelle fluorescence analysis can be applied for the analysis of endosomes [498], mitochondria [499], phagosomes [500], autophagosomes and lysosomes [501], using various fluorescent probes.

Finally, probes measuring the autophagic flux without requiring transfection or permeabilization have also been developed. Such methods are based on dyes that selectively label autophagic vesicles (autophagosomes and autolysosomes) but not lysosomes, and are used for both primary cells [502,503] and cell lines [504,505] from different species (including non-mammals). See also: <https://bio-protocol.org/e1090>.

Conclusion: Medium- to high-throughput analysis of autophagy is possible using flow and multispectral imaging cytometry (Figure 19). The advantage of this approach is that larger numbers of cells can be analyzed with regard to GFP-LC3 puncta, cell morphology and/or autophagic flux, and concomitant detection of surface markers can be included, potentially providing more robust data than is achieved with other methods. A major disadvantage, however, is that flow cytometry only measures changes in total GFP-LC3 levels, which can be subject to modification by changes in transcription or translation, or by pH, and this approach cannot accurately evaluate localization (e.g., to autophagosomes) or lipidation (generation of LC3-II) without further permeabilization of the cell.

Autophagosome-lytic compartment fusion. Technical limitations have prevented insight into the mechanism of autophagosome-lytic compartment fusion. Disrupting genes encoding components that play a role in membrane fusion in intact cells may not only affect autophagy directly but will affect general vesicular trafficking, which can cause indirect effects on autophagy. In addition, if a fusion component is involved in early steps of autophagosome formation, this requirement will mask its function in late stages of autophagy such as fusion with the lytic compartment. As a result, it is difficult to analyze the molecular mechanisms of autophagosome-lytic compartment fusion in intact cells.

In vitro reconstitutions of autophagosome-vacuole and autophagosome-lysosome fusion have partially overcome this problem and made it possible to identify relevant proteins and their functions in this specific step of autophagy. Both autophagosome-vacuole fusion in yeast and autophagosome-lysosome fusion in mammals has been recently reconstituted, using partially purified fractions of autophagosomes, vacuoles/lysosomes and cytosol [506-508].

Immunohistochemistry and immunofluorescent staining. Immunodetection of ATG and related proteins (particularly LC3 and BECN1) has been reported as a prognostic factor in various human carcinomas, including lymphoma [265,509], breast carcinoma [510,511], endometrial adenocarcinoma [512,513], head and neck squamous cell carcinoma [514-516], hepatocellular carcinoma [517,518], gliomas [519], non-small cell lung carcinomas [520], pancreatic [521] and colon adenocarcinomas [522-524], as well as in cutaneous and uveal melanomas [525,526]. Unfortunately, the reported changes often reflect overall diffuse staining intensity rather than appropriately compartmentalized puncta. Therefore, the observation of

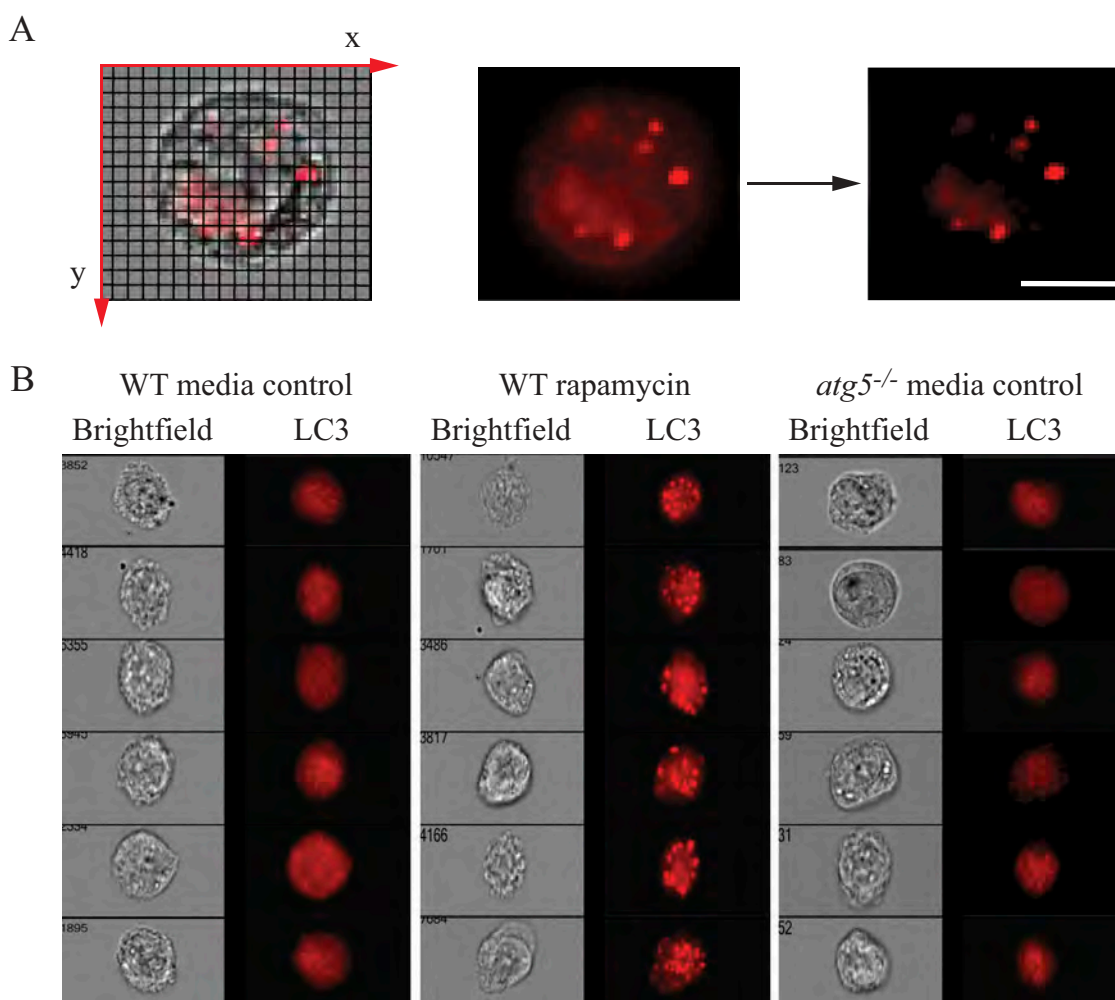


Figure 19. Assessing autophagy with multispectral imaging cytometry. **(A)** Bright Detail Intensity (BDI) measures the foreground intensity of bright puncta (that are 3 pixels or less) within the cell image. For each cell, the local background around the spots is removed before intensity calculation. Thus, autophagic cells with puncta have higher BDI values. **(B)** Media control (untreated wild type), rapamycin-treated wild-type and *atg5*^{-/-} MEFs were gated based on BDI. Representative images of cells with high or low BDI values. Scale bar: 10 μ m. Images provided by M.L. Albert.

increased levels of diffuse LC3 staining (which may reflect a decrease in autophagy) should not be used to draw conclusions that autophagy is increased in cancer or other tissue samples [527]. Assessing LC3 puncta fails to show prognostic significance in non-small cell lung cancer [528,529]. Importantly, this kind of assay should be performed as recommended by the Reporting Recommendations for Tumor Marker Prognostic Studies (REMARK) [530]. As we identify new drugs for modulating autophagy in clinical applications, this type of information may prove useful in the identification of subgroups of patients for targeted therapy [531-533].

In the brain of hypoxic-ischemic encephalopathy dead human newborns, LC3 immunostaining on paraffin sections has been used to quantify increased autophagosome presence in dying neurons as shown by increased LC3-positive dots [534,535]. In mouse and rat tissues, endogenous LC3, ATG4B, and ATG9A have been detected by immunohistochemical analyses using both paraffin sections and cryosections [85, 391 [536-539]]. When autophagosomes are absent, the localization pattern of LC3 in the cells of various tissues is diffuse and cytosolic. Moreover, intense fibrillary staining of LC3 is detectable along dendrites of intact neurons, whereas granular

staining for LC3 appears mainly in the perinuclear area of neurons in CTSD- or CTSB- and CTSL (cathepsin L)-deficient mouse brains [393]. LC3 puncta are also observed in mice in the peripheral nerves, specifically in Schwann cells after neurodegeneration [540], and Paneth cells of the small intestine from human Crohn disease patients and mouse models of intestinal inflammation driven by ER-stress and acute radiation injury exhibit strong LC3 puncta staining [541-543]. In various neurodegenerative states, LC3 puncta may be numerous in neurites, especially within dystrophic swellings and, in many cases, these vacuoles are amphisomes or autolysosomes, reflecting the delayed or inhibited degradation of LC3 despite the presence of abundant hydrolase activity [76,83]. In developing inner ear and retinal tissue in chicken, BECN1 is detected by immunofluorescence; in chick retina AMBRA1 is also detected [393-395]. IHC using ABC and 3,3'-diamino-benzidine (DAB) as chromogen has also been used to detect AMBRA1, thus accomplishing a complete map of AMBRA1 protein distribution in the mouse brain, and highlighting differential expression in neuronal/glial cell populations. Differences in AMBRA1 content have been related to specific neuronal features and properties,

particularly concerning susceptibility to neurodegeneration, during aging and amyloid pathology [544]. AMBRA1 and BECN1 IHC distribution have also been studied in rat brain, after anti-NGF administration, which results in increased levels of autophagic proteins in specific brain regions (olfactory bulb, neocortex and hippocampus), suggesting NGF-modulated autophagic pathways [545]. In mouse platelets, endogenous PtdIns3P, the product of the BECN1-PIK3C3/VPS34 protein complex-mediated enzymatic reaction, can be detected using recombinant GST-2×FYVE followed by anti-GST immunofluorescence [389]. Finally, in non-mammalian vertebrates, BECN1 is detected during follicular atresia in the ovary of three fish species using paraffin sections; a punctate immunofluorescent staining for BECN1 is scattered throughout the cytoplasm of the follicular cells when they are in intense phagocytic activity for yolk removal [546].

Cautionary notes: One problem with LC3 IHC is that in some tissues this protein can be localized in structures other than autophagosomes. For example, in murine hepatocytes and cardiomyocytes under starved conditions, endogenous LC3 is detected not only in autophagosomes but also on lipid droplets [547]. In neurons in ATG7-deficient mice, LC3 accumulates in ubiquitin- and SQSTM1-positive aggregates [548]. In neurons in aging or neurodegenerative disease states, LC3 is commonly present in autolysosomes and may be abundant in lipofuscin and other lysosomal residual bodies [76]. Similarly, accumulation of large LC3-positive puncta occurring during methamphetamine intoxication does not derive from stagnant autophagic vacuoles. In fact, the polarization of LC3 within granules is greatly reduced and LC3 IHC even monitored by confocal microscopy demonstrates cytosolic accumulation of the protein, which, despite being increased, loses its polarization within autophagic granules [549]. This is clearly demonstrated by counting stoichiometrically immunogold-stained LC3 particles within the cytosol compared with granules. Thus, immunodetection of LC3 in cytoplasmic granules is not sufficient to monitor autophagy in vivo. To evaluate autophagy by the methods of IHC, it is necessary to identify the autophagosomes directly using the ABC technique for TEM observation (see *Transmission electron microscopy*) [77]. Peroxidase depositions in the vacuoles indicate LC3 expression, detected by IHC, and therefore identify those structures as autophagic vacuoles [550].

Conclusion: It has not been clearly demonstrated that IHC of ATG proteins in tissues corresponds to autophagy activity, and this area of research needs to be further explored before we can make specific recommendations.

LC3-HiBiT reporter assay. The Autophagy LC3-HiBiT reporter assay system is a method that measures autophagic flux by monitoring total LC3-reporter levels [551]. A plasmid coding for a human LC3B is tagged to a HiBiT peptide through a linker. The approach is based on the high affinity of the HiBiT peptide to the inactive luciferase subunit LgBiT, that, upon binding, produces an active NanoBiT luciferase that generates luminescence proportional to the amount of autophagy. It is recommended to generate stable cell lines using G418 selection to avoid the variability due to

transfection efficiencies among different cell lines and experiments. The amount of LC3-reporter within the cell can be measured by the addition of lysis buffer mixed with the LgBiT protein and the substrate. After incubation at room temperature for 10 min, luminescence can be measured in a microplate reader (integration time of 0.5–2 s) and it is stable for up to three h. Induction of autophagy, such as through starvation, or MTORC1 inhibition via PP242 treatment or siRNA knockdown of RPTOR, decrease luminescence readings. Conversely, blockade of autophagy flux, for example by treatment with CQ, increases the luminescence readings (Figure 20A). A major advantage of this reporter system is that it allows for determination of autophagic flux upon exposure to a large number of conditions at the same time and, therefore, is suitable for large-scale screens using 96- or 386-well plate formats.

Cautionary notes: One caveat to the immunostaining validation of cells that stably express LC3-HiBiT is the inability of widely-used LC3 antibodies (such as the LC3B antibody from Cell Signaling Technology [2775] that targets the N terminus of LC3B) to recognize the amino terminal HiBiT-tagged LC3 resolved on protein blots. This limitation can be overcome by the use of the Nano-Glo® HiBiT blotting system (Promega, N2410) that detects the amino terminal HiBiT-tagged LC3B-I/II as proteins of approximately 55 kDa (Figure 20B,C). For conditions that might affect cell number/viability, it is recommended to prepare a separate culture plate(s) with an identical treatment condition(s) in parallel for cell number/viability measurement (e.g., using Hoechst staining of the nucleus followed by quantification). Alternatively, the Autophagy LC3-HiBiT reporter assay system could also be multiplexed with the CellTox™ Green Cytotoxicity Assay (Promega, G8741) for cell viability assessment within the same sample well.

In vitro enzymatic lipidation of human Atg8-family proteins: Preparation of fluorescent Atg8-PE conjugates. After activation by ATG4B, covalent attachment of an Atg8-family protein to PE is mediated by a ubiquitin-like chain of enzymatic steps involving the E1-like ATG7 and the E2-like ATG3. These reactions can be reconstituted in vitro, using recombinant purified proteins, liposomes and ATP. To study the role of these protein-lipid complexes in membrane tethering and fusion processes, the enzymatically driven lipidation reaction of the human Atg8-family proteins can be reconstituted. Reaction systems including ATG7, ATG3, ATP, and liposomes lead to the formation of a more rapidly migrating band that is readily visualized by Coomassie Brilliant Blue staining. To confirm the lipidation reaction, conjugation mixtures are prepared with liposomes containing 10% of the fluorescent phospholipid derivative NBD-PE. In each case, reactions lead to the formation of fluorescent, faster-migrating bands representing the lipidated products of Atg8-family proteins [552].

SQSTM1 and related LC3-binding protein turnover assays
In addition to LC3, SQSTM1, or other receptors such as NBR1, can also be used as protein markers, at least in certain settings [30,553]. For example, SQSTM1 can be detected as

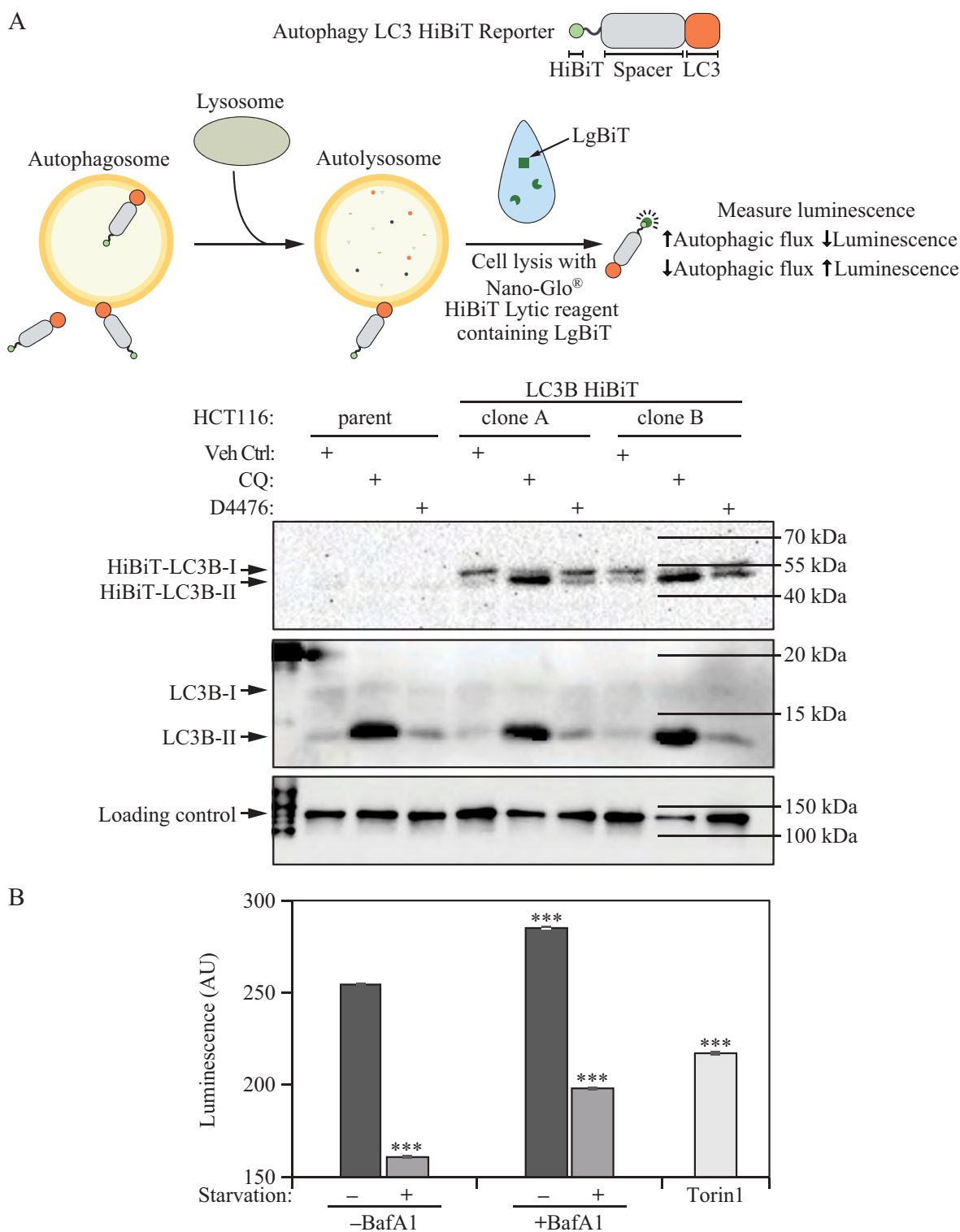


Figure 20. HiBiT-LC3B imitates endogenous LC3B response upon autophagy perturbation. **(A)** Principle of the Autophagy LC3-HiBiT reporter assay system. **(B)** HCT116 (parent) and stable HCT116-LC3 HiBiT cell lines were exposed to vehicle control (Veh Ctrl), chloroquine (CQ; 25 μ M) or the CSNK1A1/CK1 α (casein kinase 1 alpha 1) inhibitor D4476 (10 μ M) for 24 h, which increases LC3 abundance [4084]. Cell lysates (30 μ g) were resolved in 12% SDS-PAGE gels and transblotted to nitrocellulose membranes. Nano-Glo HiBiT Blotting System (Promega, N2410) was used to detect HiBiT-LC3B (expected molecular size of 55 kDa) using Tris-buffered saline supplemented with 0.1% Tween 20. The HiBiT-LC3B blot was imaged after 20 min incubation with the substrate. Loading control (KIF11/Eg5; Cell Signaling Technology, 4203) and endogenous LC3B (Cell Signaling Technology, 2775) were detected via standard immunoblotting (leftmost lane in immunoblots; protein ladder). Image provided by John J.E. Chua and Jit K. Cheong. **(C)** U2OS LC3 HiBiT cells treated with autophagy inducers or inhibitors. Effect on autophagic flux was measured in cells incubated in normal or starvation medium (HBSS) alone or containing bafilomycin A₁ (50 nM) or torin1 (25 nM) for 3 h using the HiBiT luminescence assay. Bars are mean \pm s.e.m. of triplicate samples. *** P < 0.001 vs. untreated normal media control; t -test. AU, arbitrary units. Image provided by Silvia Vega-Rubin-de-Celis.

puncta by IHC in cancer cells or primary neurons, similar to LC3 [515]; however, note that it is critical to freshly cut formalin fixed paraffin embedded/FFPE tissue before IHC for LC3 [554,555]. The SQSTM1 protein serves as a link between LC3 and ubiquitinated substrates [119]. SQSTM1 and SQSTM1-bound polyubiquitinated proteins become incorporated into the completed autophagosome and are degraded in autolysosomes, thus serving as an index of autophagic degradation (Figure 21). In addition, SQSTM1 can also bind RNA substrates, which controls RNA turnover via autolysosomes [556]. Inhibition of autophagy can correlate with increased levels of SQSTM1 in mammals, *C. elegans* and *Drosophila*, suggesting that steady state levels of this protein reflect the autophagic status [81, 536 [557-562]]. Deficiency of the LIR domain-containing, SQSTM1-interacting SPRED2 results in an accumulation of SQSTM1 in the heart in vivo, accompanied by an altered LC3 turnover and reduced autophagy [563]. Similarly, decreased SQSTM1 levels are associated with autophagy activation; however, similar to LC3-II, lysosomal inhibitors (such as CQ) can be used to assess increased autophagy flux based on an accumulation of SQSTM1 [86,564]. The phosphorylation of SQSTM1 at Ser403 appears to regulate its role in the autophagic clearance of ubiquitinated proteins, and anti-phospho-SQSTM1 antibodies can be used to detect the modified form of the protein [427].

Cautionary notes: SQSTM1 changes can be cell-type and context specific. In some cell types, there is no change in the overall amount of SQSTM1 despite strong levels of autophagy induction, verified by the tandem mRFP/mCherry-GFP-LC3 reporter as well as ATG7- and lysosome-dependent turnover of cargo proteins (C.T. Chu, personal observation). In other contexts, a robust loss of SQSTM1 does not correlate with increased autophagic flux as assessed by a luciferase-based measure of flux [336]; a decrease of SQSTM1 can even relate to a blockage of autophagy due to cleavage of the protein,

together with other autophagy proteins, by caspases or calpains [565].

In some systems, even transgenic constructs may not allow reliable detection of SQSTM1. For instance, although very informative to monitor autophagy levels in the *C. elegans* embryo, SQST-1::GFP (a tagged version of the *C. elegans* SQSTM1 homolog) is not detectable in most adult tissues unless it is stabilized with background mutations such as *rpl-43* (encoding the ribosomal protein RPL-43). Stabilization of SQST-1::GFP via *rpl-43* mutation does not affect the degradation of the autophagy substrates so far tested, and reduced SQST-1::GFP signal is observed in conditions of increased autophagic flux such as starvation [566]; however, animals show signs of generalized sickness, and altered lifespan, and RNAi against some autophagy genes (e.g., *vps-34*) leads to increased, instead of reduced, SQST-1::GFP signal (E.J. O'Rourke, personal communication). SQSTM1 changes can be treatment specific such that chemotherapy-induced autophagy increases LC3-II without changing SQSTM1, whereas radiation-induced autophagy increases LC3-II and decreases SQSTM1 in ERBB2/HER2-overexpressing mouse mammary carcinoma cells [567].

SQSTM1 may be transcriptionally upregulated under some conditions [419 [568-571]], as observed in several *C. elegans* longevity models [572,573], further complicating the interpretation of results. For example, SQSTM1 upregulation, and at least transient increases in the amount of SQSTM1, is seen in some situations where there is an increase in autophagic flux [574-576]. One such case is seen during retinoic acid-induced differentiation of acute myeloid leukemia (AML) cells where SQSTM1 is upregulated [569] with concomitant increased autophagic flux [577]. Synovial fibroblasts obtained from patients with rheumatoid arthritis also exhibit a significant upregulation of SQSTM1 with concomitant increased autophagy flux [578]. Activation of a signaling pathway, e.g., RAF1/Raf-MAP2K/MEK-MAPK/ERK, can also upregulate SQSTM1 transcription [579]. SQSTM1 mRNA is also upregulated following prolonged starvation, which can restore the SQSTM1 protein level to that before starvation [580,581]. In the same way, physical exercise, especially when performed during starvation, increases the SQSTM1 mRNA level in skeletal muscle, and can lead to an incorrect interpretation of autophagic flux if only the protein level is measured [582,583]. Another instance when both mRNA and protein levels of SQSTM1 are elevated, even though autophagic flux is not impaired, is observed in aneuploid human and murine cells that are generated by introduction of one or two extra chromosomes [584,585].

The SQSTM1 protein level also increases when autophagy needs to be triggered. SQSTM1 expression can be positively regulated post-transcriptionally by the ELAVL1/HuR protein which binds to the SQSTM1 transcript in ARPE19 cells exposed to 24-h MG132 treatment [359]. Two-h AICAR + MG132 pro-autophagic cotreatment similarly induces the binding of ELAVL1/HuR protein to SQSTM1 mRNA, its loading on polysomes and its translation into *de novo* protein, an effect that is required to trigger autophagy and is prevented by the protein synthesis inhibitor puromycin [586]. Moreover, SQSTM1 can be regulated by the integrated stress response,

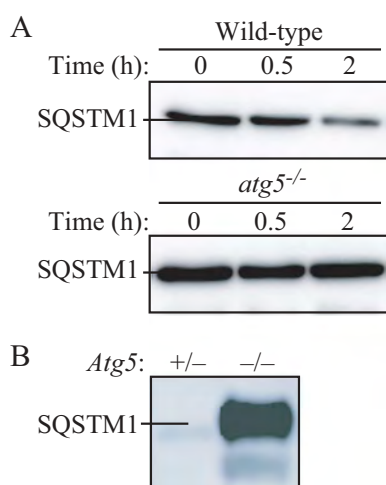


Figure 21. Regulation of the SQSTM1 protein during autophagy. (A) The level of SQSTM1 during starvation. *Atg5*^{+/+} and *atg5*^{-/-} MEFs were cultured in DMEM without amino acids and serum for the indicated times, and then subjected to immunoblot analysis using anti-SQSTM1 antibody (Progen Biotechnik, GP62). This figure was previously published in ref. [30], and is reproduced by permission of Landes Bioscience, copyright 2007. (B) The level of SQSTM1 in the brain of neural-cell specific *atg5* knockout mice. Image provided by T. Hara.

which can promote accumulation of protein in cells that is dependent on the EIF2S1/eIF2 α pathway of translational control (R.E. Simmonds, personal communication). Thus, appropriate positive and negative controls are needed prior to the use of SQSTM1 as a flux indicator in a particular cellular context, and we recommend monitoring the SQSTM1 mRNA level as part of a complete analysis, or determining the SQSTM1 protein level in the presence of the transcription inhibitor actinomycin D or the p-EIF2S1 antagonist ISRIB.

Of interest, SQSTM1 overexpression at both the gene and protein levels can be observed in muscle atrophy induced by cancer, though not by glucocorticoids, suggesting that the stimulus inducing autophagy may also be relevant to the differential regulation of autophagy-related proteins [587]. One solution to problems relating to variations in SQSTM1 expression levels is to use a HaloTag[®]-p62 (SQSTM1) chimera [588]. The chimeric protein can be covalently labeled with HaloTag[®] ligands, and the loss of signal can then be monitored without interference by subsequent changes in protein synthesis. Similarly, a stable cell line expressing EGFP-tagged SQSTM1 under the control of an inducible promoter can be used to assess the rates of SQSTM1 degradation, taking into account the limitations outlined above (see *Autophagic flux determination using flow and multispectral imaging cytometry*) [497]. A similar system exists in *Drosophila* in which a GFP-tagged ref(2)P/SQSTM1 can be expressed using the UAS-GAL4 system [589]. It is worth noting that tetracycline can reduce autophagy levels; therefore, the appropriate control of only tetracycline addition has to be included if using an inducible promoter that responds to this drug [590]. Furthermore, the toxicity of tetracycline antibiotics toward mitochondria is well known (these drugs induce a mitochondrial unfolded protein response) [591], such that their use may trigger mitophagy, or other mitochondrial signaling events that interface with the autophagic machinery, thus complicating the interpretation of any results. Yet another solution is to employ a radioactive pulse-chase assay to measure the rates of SQSTM1 degradation [592].

SQSTM1 contains a LIR as well as a ubiquitin binding domain and appears to act by linking ubiquitinated substrates with the autophagic machinery. Nonetheless, it would be prudent to keep in mind that SQSTM1 contains domains that interact with several signaling molecules [593], and SQSTM1 may be part of MTORC1 [594]. Thus, SQSTM1 may have additional functions that need to be considered with regard to its role in autophagy. In the context of autophagy as a stress response, the complexity of using SQSTM1 as an autophagy marker protein is underscored by its capacity to modulate the NFE2L2/NRF2 anti-oxidant response pathway through a KEAP1 binding domain [595,596]. In fact, SQSTM1 may, itself, be transcriptionally induced by NFE2L2 [597]. Furthermore, it is preferable to examine endogenous SQSTM1 because overexpression of this protein leads to the formation of protein inclusions. In fact, even endogenous SQSTM1 becomes Triton X-100-insoluble in the presence of protein aggregates and when autophagic degradation is inhibited; thus, results with this protein are often context-dependent.

Indeed, there is a reciprocal crosstalk between the UPS and autophagy, with SQSTM1 being a key link between them

[598,599]. First, SQSTM1 participates in proteasomal degradation, and its level may also increase when the proteasome is inhibited [600]. Accordingly, the SQSTM1 degradation rate should be analyzed in the presence of a proteasomal inhibitor such as epoxomicin or lactacystin to determine the contribution from the proteasome (see *Autophagy inhibitors and inducers* for potential problems with MG132) [601]. Second, the accumulation of SQSTM1 due to autophagy inhibition can impair UPS function by competitively binding ubiquitinated proteins, preventing their delivery to, and degradation by, the proteasome [602]. Inhibition of autophagy by treatment with 3-MA (5 mM, 4 h) increases the accumulation of MAPT/tau oligomers within neurites of primary transgenic (prepared from PS19 mouse embryos, expressing the frontotemporal dementia P301S mutant MAPT [603]) cultured neurons, reducing their access to the soma and lysosomes for degradation [604]. Furthermore, USP14, a major proteasomal deubiquitinase that regulates degradation through the proteasome, interacts with the UBA domain of SQSTM1 as well as LC3. In addition, levels as well as chromatin recruitment of USP14 are upregulated in autophagy-deficient cells upon DNA damage, and knockdown of SQSTM1 in autophagy-deficient cells decreases USP14 levels [605,606]. These data clearly indicate that autophagy regulates USP14 degradation in an SQSTM1-dependent manner. Accordingly, it may be advisable to measure the UPS flux by using Ub^{G76V}-GFP, a ubiquitin-proteasome activity reporter [607], when SQSTM1 accumulation is observed. Thus, it is very important to determine whether autophagy alone or in conjunction with the UPS accounts for substrate degradation induced by a particular biological change. A number of stressors that impair the UPS induce the aggregation/dimerization of SQSTM1, and this can be seen by the detection of a high molecular mass (~150 kDa) protein complex by western blot, which is recognized by SQSTM1 antibodies [564,608,609]. Although the accumulation of this protein complex can be related to the accumulation of ubiquitinated SQSTM1-bound proteins, or the dimerization/inactivation of SQSTM1 [564,610], evaluation of the ratio between SQSTM1 aggregates/dimers and SQSTM1 monomers is likely a better measurement of changes in SQSTM1 dynamics linked to autophagy or the UPS.

SQSTM1 is also a substrate for CASP6 (caspase 6) and CASP8 (as well as CAPN1 [calpain 1]), which may confound its use in examining cell death and autophagy [611]. This is one reason why SQSTM1 degradation should also be analyzed in the presence of a pan-caspase inhibitor such as Q-VD-OPh before concluding that autophagy is activated based on a decrease of this protein [565]. Another issue is that some phosphatidylinositol 3-kinase (PtdIns3K) inhibitors such as LY294002, and to a lesser extent wortmannin (but apparently not 3-MA) [435], can inhibit protein synthesis [612]; this might in turn affect the turnover of SQSTM1 and LC3, which could influence conclusions that are drawn from the status of these proteins regarding autophagic flux or ALIS formation. Accordingly, it may be advisable to measure protein synthesis and proteasome activity along with autophagy under inhibitory or activating conditions [613]. With regard to protein synthesis, it is worth noting that this can be monitored through a nonradioactive method [614].

Western blot analysis of cell lysates prepared using NP40- or Triton X-100-containing lysis buffers in autophagic conditions typically shows a reduction in SQSTM1 levels. However, this does not necessarily indicate that SQSTM1 is degraded, because SQSTM1 aggregates are insoluble in these detergent lysis conditions [419,615]. Moreover, in some instances SQSTM1 levels do not change in the soluble fractions despite autophagic degradation, a finding that might be explained by simultaneous transcriptional and translational induction of the gene encoding SQSTM1, because the soluble fraction accounts only for the diffuse or free form of SQSTM1. Accumulation of SQSTM1 in the Triton X-100-insoluble fraction can be observed when autophagy-mediated degradation is inhibited. Under conditions of higher autophagic flux, accumulation of SQSTM1 in Triton X-100-insoluble fractions may not be observed, and SQSTM1 levels may be reduced or maintained. The simplest approach to circumvent many of these problems is using lysis buffer that allows identification of the entire cellular pool of SQSTM1 (e.g., containing 1% SDS); however, additional assessment of both Triton X-100-soluble and -insoluble fractions will provide further information regarding the extent of SQSTM1 oligomerization [548]. Note, when performing a western blot using an SQSTM1 antibody, it is always a good idea to include a positive control in which SQSTM1 accumulates, such as an *atg8a* mutant (e.g., see Fig. S3 in ref [616]).

To conclusively establish SQSTM1 degradation by autophagy, SQSTM1 levels in both Triton X-100-soluble and -insoluble fractions need to be determined upon treatment with autophagy inducers in combination with autophagy inhibitors, such as those that inhibit the autolysosomal degradation steps (e.g., protease inhibitors, CQ or bafilomycin A₁). Additionally, an alteration in the level of SQSTM1 may not be immediately evident with changes observed in autophagic flux upon certain chemical perturbations (S. Sarkar, personal communication). Whereas LC3 changes may be rapid, clearance of autophagy substrates may require a longer time. Therefore, if LC3 changes are assessed at six h or 24 h after a drug treatment, SQSTM1 levels can be tested not only at the same time points, but also at later time points (24 h or 48 h) to determine the maximal impact on substrate clearance. An alternative method is immunostaining, with and without autophagy inhibitors, for SQSTM1, which will appear as either a diffuse or punctate pattern. Experiments with autophagy inducers and inhibitors, in combination with western blot and immunostaining analyses, best establish autophagic degradation based on SQSTM1 turnover. A final point, however, is that empirical evidence suggests that the species-specificity of antibodies for detecting SQSTM1 must be taken into account. For example, some commercial antibodies recognize both human and mouse SQSTM1, whereas others detect the human, but not the mouse protein [617]. Another issue with detecting SQSTM1 in the context of human diseases is that it can be mutated (e.g., in Paget disease of bone) [618]. Thus, care should be taken to ensure that potential mutations are not affecting the epitopes that are recognized by anti-SQSTM1 antibodies when using western blotting to detect this protein.

As an alternative, the SQSTM1:BECL1 protein level ratio can be used as a readout of autophagy [619]. Because both

decreased SQSTM1 levels and increased BECL1 levels correlate with enhanced autophagy, a decreased SQSTM1:BECL1 protein level ratio (when derived from the same protein extract) may, cautiously, be interpreted as augmented autophagy, keeping in mind that *SQSTM1* gene expression varies significantly under different conditions and may obscure the meaning of a change in the amount of SQSTM1 protein. Another substantial alternate is analysis of neomycinophosphotransferase II (NeoR) degradation. NeoR is an exclusive autophagic substrate [620,621]. NeoR-GFP degradation is completely blocked by autophagic inhibitors such as 3-MA, but does not respond to inhibitors of proteasomal degradation. Inhibition of autophagy leads to accumulation of NeoR-GFP, resulting in enhanced GFP fluorescence [621]. NeoR-GFP gene expression is not affected by most autophagy inducers including H₂O₂ (that transcriptionally upregulate SQSTM1), however, degradation can be evaluated by accumulation of NeoR-GFP puncta under confocal microscopy or by analyzing total protein level by western blot of GFP.

As a general note, using ratios of the levels of proteins changing in opposite directions, rather than the protein levels themselves, could be beneficial because it overcomes the loading normalization issue. The often-used alternative approach of housekeeping proteins to normalize for loading biases among samples is sometimes problematic as levels of the HKPs change under various physiological, pathological and pharmacological conditions [269 [622-626],].

Finally, a novel protein family of autophagy receptors, named CUET (from Cue5/TOLLIP), was identified, which in contrast to SQSTM1 and NBR1 has members that are present in all eukaryotes [627,628]. The CUET proteins also possess a ubiquitin-binding CUE-domain and an Atg8-family interacting motif (AIM)/LIR sequence that interacts with Atg8-family proteins. In their absence, cells are more vulnerable to the toxicity resulting from aggregation-prone proteins, showing that CUET proteins, and more generally autophagy, play a critical evolutionarily conserved role in the clearance of cytotoxic protein aggregates [627]. Experiments in yeast have shown that Cue5 and the cytoplasmic proteins that require this autophagy receptor for rapid degradation under starvation conditions could be potentially good marker proteins for measuring autophagic flux [629]. Studies with mammalian immune cells indicate that TOLLIP is primarily responsible for the final step of autophagy, and facilitates the fusion of lysosomes with autophagosomes, lipid droplets, or peroxisomes [630]. TOLLIP may fulfill its critical function of lysosome fusion through its interaction with phospholipid [631,632]. TOLLIP-deficient monocytes are defective in lysosome fusion and are programmed into an inflamed state with elevated CCR5 and enhanced expression of chemokines such as CCL2/MCP1 [631,633]. Pathologically, TOLLIP-deficient mice tend to develop more severe atherosclerosis as well as neurological defects [633,634].

Another recent study demonstrated a functional link between CLEC16A and disrupted mitophagy in murine splenic immune cells and showed that incomplete mitophagy predisposes *clec16a* knockout mice to a cascade of altered immune signaling functions resulting in pathogenic inflammation [319,320].

Special caution must be taken when evaluating SQSTM1 levels in models of protein aggregation. Small protoaggregates often stain positively for SQSTM1 and may be similar in size to autophagic puncta. Similarly, GFP-u/GFP-degron reporters (designed as an unstable variant that undergoes proteasome-dependent degradation) will mark SQSTM1-positive protein inclusions [635]. Finally, some types of aggregates and inclusions will release soluble SQSTM1 or GFP-u/GFP-degron under cell lysis or denaturing conditions, which can skew the interpretation of soluble SQSTM1 and/or proteasomal function, accordingly.

Conclusion: There is not always a clear correlation between increases in LC3-II and decreases in SQSTM1. Thus, although analysis of SQSTM1 can assist in assessing the impairment of autophagy or autophagic flux, we recommend using SQSTM1 only in combination with other methods detailed in these guidelines to monitor flux. See also the discussion in *Autophagic flux determination using flow and multispectral imaging cytometry*.

- (1) **TOR/MTOR, AMPK and Atg1/ULK1.** Atg1/ULK1 are central components in autophagy that likely act at more than one stage of the process. There are multiple ULK isoforms in mammalian cells including ULK1, ULK2, ULK3, ULK4 and STK36 [636]. ULK3 is a positive regulator of the Hedgehog signaling pathway [637], and its overexpression induces both autophagy and senescence [638]. Along these lines, ectopic ULK3 displays a punctate pattern upon starvation-induced autophagy induction [638]. ULK3, ULK4 and STK36, however, lack the domains present on ULK1 and ULK2 that bind ATG13 and RB1CC1/FIP200 [639]. Thus, ULK3 may play a role that is restricted to senescence and that is independent of the core autophagy machinery. ULK2 has a higher degree of identity with ULK1 than any of the other homologs, but they may have both similar and distinct functions that are tissue- or cell-type specific [640-644]. Specifically in relation to autophagy, pharmacological inhibition of ULK1 and ULK2, with the compound MRT68921, blocks the process, and expression of a drug-resistant ULK1 mutant is sufficient to rescue this block [457]. However, at least in some cell types, ULK2 can likely compensate for loss of ULK1. For instance, in LNCaP cells, combined knockdown of ULK1 and ULK2 provides a substantially stronger inhibition of basal and starvation-induced autophagic sequestration and degradation activity than knockdown of ULK1 alone (N. Engedal, personal communication). ULK1 activity can also be inhibited by the expression of a dominant-negative ULK1 mutant [645,646]. The stability and activation of ULK1, but not ULK2, is dependent on its interaction with the HSP90-CDC37 chaperone complex. Pharmacological or genetic inhibition of the chaperone complex increases proteasome-mediated turnover of ULK1, impairing its kinase activity and ability to promote both starvation-induced autophagy and mitophagy [647]. In addition, ULK1 is

ubiquitinated for its activation through TRAF6-dependent K63-linked ubiquitination [501], or for degradation through CUL3-KLHL20-dependent K48-linked ubiquitination [648]. GCA (grancalcin) inhibits K48-linked ubiquitination and activates TRAF6-dependent K63-linked ubiquitination of ULK1 to induce autophagy [649].

AMPK (AMP-activated protein kinase) is a multimeric serine/threonine protein kinase comprised of PRKAA1/AMPK α 1 or PRKAA2/AMPK α 2 (α , catalytic), the PRKAB1/AMPK β 1 or PRKAB2/AMPK β 2 (β , scaffold), and the PRKAG1/AMPK γ 1, PRKAG2/AMPK γ 2 or PRKAG3/AMPK γ 3 (γ , regulatory) subunits. The enzyme activity of AMPK is dependent on phosphorylation of the PRKAA2/ α 2-subunit on Thr172 (corresponds to Thr183 in α 1) [459,460], and, therefore, can be conveniently monitored by western blotting with a phosphospecific antibody against this site. Depending on the stimulus and cell type, Thr172 is phosphorylated either by CAMKK2/CaMKK β , STK11/LKB1 or MAP3K7/TAK1. Inhibition of AMPK activity is mediated primarily by Thr172-dephosphorylating protein phosphatases such as PPP1/PP1 (protein phosphatase 1) and PPP2/PP2A (protein phosphatase 2) [650]. Thr172 dephosphorylation is modulated by adenine nucleotides that bind competitively to regulatory sites in the PRKAG/ γ -subunit. AMP and ADP promote phosphorylation and AMPK activity, whereas Mg²⁺-ATP has the opposite effect [651]. Moreover, Thr172 phosphorylation and AMPK activation can be enhanced by PRKDC (protein kinase, DNA-activated, catalytic subunit)-mediated phosphorylation of PRKAG1/AMPK γ 1, which promotes the lysosomal localization of the AMPK complex [652]. Thus, AMPK acts as a fine-tuned sensor of the overall cellular energy charge that regulates cellular metabolism to maintain energy homeostasis. Overexpression of a dominant negative mutant (R531G) of PRKAG2, the γ -subunit isoform 2 of AMPK that is unable to bind AMP, makes it possible to analyze the relationship between AMP modulation (or alteration of energetic metabolism) and AMPK activity [653,654]. Activation of AMPK is also associated with the phosphorylation of downstream enzymes involved in ATP-consuming processes, such as fatty acid (ACAC [acetyl-CoA carboxylase]) and cholesterol (HMGCR [3-hydroxy-3-methylglutaryl-CoA reductase]) biosynthesis.

The role of AMPK in autophagy is complex and highly dependent on both cell type and metabolic conditions. In yeast, the AMPK ortholog Snf1 shows autophagy inhibitory functions dependent on its ability to inhibit cytosolic Acc1 (acetyl-CoA carboxylase)-mediated lipogenesis, which is required for autophagy in stationary phase cells [655]. AMPK also exerts autophagy inhibitory effects through distinct ULK1-dependent effects on autophagosome formation and lysosomal acidification in cancer cell lines [656]. Furthermore, as noted above, there are two isoforms of the catalytic subunit, PRKAA1/AMPK α 1 and PRKAA2/AMPK α 2, and these may have distinct effects with regard to autophagy (C. Koumenis, personal communication) [657]. In liver cells, AMPK suppresses autophagy at the level of cargo sequestration, as indicated by the rapid sequestration-inhibitory effects

of a variety of AMPK activators, whereas it appears to stimulate autophagy in many other cell types, including fibroblasts, colon carcinoma cells and skeletal muscle [658-667], and there appears to be a completely AMPK-dependent type of autophagy [668]. Autophagy-promoting effects of AMPK are most evident in cells cultured in a complete medium with serum and amino acids, where cargo sequestration is otherwise largely suppressed [664]. Amino acids acutely activate AMPK, which sustains autophagy under nutrient sufficiency [669]. Presumably, AMPK antagonizes the autophagy-inhibitory effect of amino acids (at the level of phagophore assembly) by phosphorylating proteins involved in MTORC1 signaling, such as TSC2 [670] and RPTOR/raptor [670] as well as the MTORC1 target ULK1 (see below) [671-673].

Compound C is an effective and widely used inhibitor of activated (phosphorylated) AMPK [674,675]. However, being a nonspecific inhibitor of oxidative phosphorylation [676,677], this drug has been observed to *inhibit* autophagy under conditions where AMPK is already inactive or knocked out [678,679], and it has even been shown to *stimulate* autophagy by an AMP-independent mechanism [677,680]. Compound C thus cannot be used as a stand-alone indicator of AMPK involvement, but can be used along with shRNA-mediated inhibition of AMPK.

TORC1 is an autophagy-suppressive regulator that integrates growth factor, nutrient and energy signals. In most systems, inhibition of MTOR leads to induction of autophagy, and AMPK activity is generally antagonistic toward MTOR function. MTORC1 mediates the autophagy-inhibitory effect of amino acids, which stimulate the MTOR protein kinase through a RRA GTPase heterodimer. INS (insulin) and growth factors activate MTORC1 through upstream kinases including AKT/protein kinase B and MAPK1/ERK2-MAPK3/ERK1 when the energy supply is sufficient, whereas energy depletion may induce AMPK-mediated MTORC1 inhibition and autophagy stimulation, for example, during glucose starvation. In contrast, amino acid starvation can strongly induce autophagy even in cells completely lacking AMPK catalytic activity [681]. The impact of MTORC1 on autophagy is furthermore underlined in the pathological setting of a lysosomal storage disease based on insufficient MTORC1 activation and subsequent increased autophagosome formation due to hereditary TBCK (TBC1 domain containing kinase) deficiency [682,683].

MTORC1-mediated autophagy is negatively regulated by SHOC2, a scaffold protein that activates the RAS-RAF-MAPK signaling pathway [684,685]. Specifically, SHOC2 binds to RPTOR and dislodges it from MTORC1, leading to MTORC1 inactivation and autophagy induction [686,687]. Thus, MTORC1 signaling can be negatively regulated by MAPK signaling.

AMPK and MTORC1 regulate autophagy through coordinated phosphorylation of ULK1. Under glucose starvation, AMPK apparently promotes autophagy by directly activating ULK1 through phosphorylation, although the exact AMPK-mediated ULK1 phosphorylation site(s) remains controversial (Table 2) [667 [671-673]]. Under conditions of nutrient sufficiency, high MTORC1 activity prevents ULK1 activation by phosphorylating alternate ULK1 residues and disrupting the interaction between ULK1 and AMPK. There are commercially available phospho-specific antibodies that recognize different

forms of ULK1. For example, phosphorylation at Ser556 in human (corresponds to Ser555 in mouse), an AMPK site, is indicative of increased autophagy in response to nutrient stress, whereas Ser758 in human (corresponds to Ser757 in mouse) is targeted by MTOR to inhibit autophagy. Even the autophagy-suppressive effects of AMPK could, conceivably, be mediated through ULK1 phosphorylation, for example, at the inhibitory site Ser638 [688]. AMPK inhibits MTORC1 by phosphorylating and activating TSC2 [670], as well as by phosphorylating the MTOR binding partner RPTOR [689]. Therefore, AMPK is involved in processes that synergize to activate autophagy, by directly activating ULK1, and indirectly impairing MTOR-dependent inhibition of ULK1. In addition, IPMK (inositol polyphosphate multikinase) can act as a scaffold protein to influence AMPK-dependent ULK phosphorylation [690]. The identification of ULK1 as a direct target of MTORC1 and AMPK represents a significant step toward the definition of new tools to monitor the induction of autophagy. ULK1 and ATG13 are also phosphorylated by CCNB/cyclin B in mitosis to activate autophagy [691].

In addition to ULK1 regulation by AMPK and MTORC1 under conditions of glucose starvation, in skeletal muscle ULK1 is activated by MAPK11/p38 β in response to a tumor burden through phosphorylation of Ser555 in mice. Despite AMPK activation (phosphorylation on Thr172) by factors released from tumor cells, inhibition of AMPK with compound C does not alter ULK1 phosphorylation on Ser555 and activation of autophagy in these conditions. Conversely, MAPK11 gain- and loss-of-function assays indicate that MAPK11 is a key activator of ULK1 and autophagy in the cancer milieu [692].

Further studies directed at identifying physiological substrates of ULK1 will be essential to understand how ULK1 activation results in initiation of the autophagy program. So far, several ULK1 substrates have been reported, and these can be classified into 4 subgroups: 1) components of the ULK1 complex; 2) components of the class III PtdIns3K complex I; 3) other autophagy-related proteins; or 4) non-autophagy-related proteins. Numerous groups have shown that ULK1 autophosphorylates and transphosphorylates its binding partners ATG13, RB1CC1, and ATG101 [646, 647 [693-701]]. So far, only the ULK1 autophosphorylation at Thr180 and Ser1047, and the phosphorylation of ATG13 at Ser318 (human isoform 2) have been shown to be functionally relevant. ATG13 phosphorylation at Ser318 by ULK1 is required for efficient clearance of damaged mitochondria [647]. The functional relevance of ULK1-dependent phosphorylation of RB1CC1 and ATG101 awaits further clarification. With regard to the components of the class III PtdIns3K complex I, ULK1-dependent phospho-acceptor sites have been identified in PIK3C3/VPS34 (phosphatidylinositol 3-kinase catalytic subunit type 3), BECN1, ATG14, and AMBRA1 [695 [702-706]]. Following amino acid starvation or MTOR inhibition, the activated ULK1 phosphorylates ATG14 on Ser29 and BECN1 on Ser14 and Ser30, enhancing the activity of the complexes containing ATG14 and PIK3C3/VPS34. These ATG14 and BECN1 phosphorylations by ULK1 are required for full autophagic induction in response to amino acid starvation or MTOR inhibition [702,705]. ULK1-dependent phosphorylation of BECN1 at Ser30 also stimulates autophagosome formation in response to hypoxia [706]. Next to the two autophagy-initiating complexes, other ATG proteins have been identified as ULK1 substrates, notably ATG4B, ATG9A, and ATG16L1

Table 2. Phosphorylation targets of AKT, AMPK, GSK3B, MTORC1, PKA and Atg1/ULK1.

| Protein and phosphorylation site | Main kinase | Function | Ref |
|---|--|--|-----------------|
| Acc1 (S1157 in yeast) | Snf1 | Inhibits de novo lipogenesis required for stationary phase autophagy | [655] |
| AMBRA1 S52 | MTORC1 | Inhibits AMBRA1-dependent activation of ULK1 | [741] |
| Atg1 | TORC1 | Inhibits Atg1 kinase activity | [744] |
| Atg1 | PKA | Regulation of kinase activity | [2652] |
| ATG4B S316 | ULK1 | Inhibits ATG4B activity and LC3 processing | [708] |
| Atg9 | Atg1 | Recruitment of Atg protein to the PAS | [2653] |
| ATG9 S14 | ULK1 | Promotes ATG9 trafficking in response to starvation | [707] |
| ATG9 S761 | AMPK | Participates in the recruitment of lipids to the phagophore | [2654] |
| Atg13 | TORC1 | Interaction with Atg1, assembly of Atg1 kinase complex | [744, 2655] |
| Atg13 | PKA | Regulates localization to the PAS | [2656] |
| ATG13 S318 | ULK1 | Required for clearance of depolarized mitochondria | [647] |
| ATG14 S29 | ULK1 | Promotes autophagy by increasing PtdIns3K complex activity | [702, 2657] |
| BECN1 S14 | ULK1 | Increases the activity of the PtdIns3K | [705] |
| BECN1 S30 | ULK1 | Activates the ATG14-containing PtdIns3K complex and stimulates autophagosome formation in response to amino acid starvation, hypoxia, and MTORC1 inhibition. | [706] |
| BECN1 S90 | MAPKAPK2-MAPKAPK3 | Stimulates autophagy | [2658] |
| BECN1 S91, S94 (S93, S96 in human) | AMPK | Required for glucose starvation-induced autophagy | [868] |
| BECN1 Y229, Y233 | EGFR | Inhibits autophagy | [775] |
| BECN1 S234, S295 | AKT | Suppresses autophagy | [774] |
| BECN1 unknown site | ERBB2/HER2 | Inhibits autophagy | [2659, 2660] |
| CCNY (cyclin Y) S326 | AMPK | Stimulates interaction with CDK16 and promotes autophagy | [762] |
| FUNDC1 S17 | ULK1 | Promotes mitophagy by enhancing FUNDC1 binding to LC3 | [735] |
| HTT S421 | AKT | Activates HTT clearance | [2661] |
| LC3 S12 | PKA | Inhibits autophagy by reducing recruitment to phagophores | [293] |
| MTOR S2448 | AKT | Correlates with the activity of MTORC1 | [2662] |
| MTOR S2481 | Autophosphorylation | Necessary for MTORC1 formation and kinase activity | [2663] |
| NBR1 T586 | GSK3A/B | Modulates protein aggregation | [2664] |
| RPS6KB T389 | MTORC1 (apparently indirect, through reduction of dephosphorylation) | Necessary for protein activity | [2665] |
| RPS6KB S371 | GSK3B | Necessary for T389 phosphorylation and the activity of RPS6KB | [2666] |
| RPTOR S792 | AMPK | Suppresses MTORC1 | [689] |
| RUBCNL/Pacer S157 | MTORC1 | Repress RUBCNL interaction with STX17 and HOPS complex | [2667] |
| SQSTM1 S293 | AMPK (S293/S294 in rat and human sequence, respectively) | Promotes autophagic cell death | [657] |
| SQSTM1 S403 | ULK1 (also TBK1, CSNK, CDK1) | Promotes autophagic degradation of SQSTM1 and its substrates | [2668] |
| TFEB S122, S142, S211 | MTORC1 | Inhibits TFEB nuclear translocation | [970-972, 2669] |
| TFEB S467 | AKT1 | Inhibits TFEB nuclear translocation | [973] |
| TSC2 T1227, S1345 | AMPK | Negative regulator of MTORC1 | [670] |
| ULK1 S317, S555, S574, S673 | AMPK | Required for mitophagy, mitochondrial homeostasis, and cell survival | [672] |
| ULK1 S467, S777 (mouse) | AMPK | Increase the kinase activity of ULK1 and promote autophagy | [672, 673] |
| ULK1 S757/S758 (mouse/human) | MTORC1 | Facilitates ULK1 interaction with AMPK | [688] |
| ULK1 S757 | MTORC1 | Prevents ULK1 interaction with AMPK | [673] |
| ULK1 S637 | MTORC1, AMPK | Facilitates ULK1 interaction with AMPK | [688] |
| ULK1 (uncertain site between 278 and 351) | Autophosphorylation | Modulates the conformation of the C-terminal tail and prevents its interaction with ATG13 | [646, 699] |
| USP14 S432 | AKT | Overcomes negative regulation of DNA repair | [2670] |
| UVRAG S498 | MTORC1 | Negatively regulates autophagosome and endosome maturation | [2671] |
| UVRAG S550, S571 | MTORC1 | Activates the PtdIns3K-UVRAG complex to regulate autolysosomal tubulation | [2672] |

[707-709]. Finally, there are several ULK1 substrates that are not specifically ATG proteins. These proteins are involved in the execution of autophagy, or fulfill additional cellular functions.

These substrates include RPTOR, AMPK, SQSTM1, FUNDC1, DAPK3, MAPK14/p38alpha, FLCN, enzymes involved in glucose metabolic flux, DENND3, SMCR8, TBK1, PDPK1, SEC16A,

SEC23A, SEC23B, EXOC7, SDCBP, STING1/TMEM173, CDC37, MAD1L1, VCP/p97, DVL1, NR3C2, YAP1, WWTR1, and RIPK1 [710-735]. The ULK1-dependent phosphorylation of RPTOR leads to inhibition of MTORC1 [711,718], and the ULK1-dependent inhibitory phosphorylation of AMPK subunits appears to generate a negative feedback loop [710]. Note that caution should be taken to use appropriate inhibitors of phosphatases (e.g., sodium fluoride, and β -glycerophosphate) in cell lysis buffer before analyzing the phosphorylation of AMPK and ULK1 at serine and threonine sites.

MTORC1 activity can be monitored by following the phosphorylation of its substrates, such as EIF4EBP1/4E-BP1/PHAS-I and RPS6KB/p70S6 kinase or the latter's downstream target, RPS6/S6, for which good commercial antibodies are available [736-738]. In mammalian cells, the analysis should focus on the phosphorylation of S6K1 at Thr389, and EIF4EBP1 at Ser65, a serum-responsive and rapamycin-sensitive site; phosphorylation of EIF4EBP1 at Thr37 and Thr46 primes the protein for phosphorylation at Ser65, and although directly phosphorylated by MTORC1, the modifications at Thr37 and Thr46 are only partially sensitive to serum and rapamycin [739]. The MTORC1-dependent phosphorylation of EIF4EBP1 can be detected as a molecular mass shift by western blot [736]. Examining the phosphorylation status of RPS6KB and EIF4EBP1 may be a better method for monitoring MTORC1 activity than following the phosphorylation of proteins such as RPS6, because the latter is not a direct substrate of MTORC1 (although RPS6 phosphorylation is a good readout for RPS6KB1/2 activities, which are directly dependent on MTOR), and it can also be phosphorylated by other kinases such as RPS6KA/RSK. Whereas RPS6KB1/2 phosphorylates RPS6 at Ser235, Ser236, Ser240, and Ser244, RPS6KA/RSK exclusively phosphorylates RPS6 at Ser235 and Ser236 in vitro and in vivo in a manner independent of MTORC1 [740]. Thus, the use of RPS6 phospho-Ser240/244 antibody is necessary for monitoring cellular MTORC1-RPS6KB1/2 activity specifically in western blot or immunocytochemistry.

Furthermore, the mechanisms that determine the selectivity as well as the sensitivity of MTORC1 for its substrates seem to be dependent on the integrity and configuration of MTORC1. For example, rapamycin strongly reduces RPS6KB1 phosphorylation, whereas its effect on EIF4EBP1 is more variable. In the case of rapamycin treatment, EIF4EBP1 can be phosphorylated by MTORC1 until rapamycin disrupts MTORC1 dimerization and its integrity, whereas RPS6KB1 phosphorylation is quickly reduced when rapamycin simply interacts with MTOR in MTORC1 (see *Autophagy inhibitors and inducers* for information on catalytic MTOR inhibitors such as torin1) [739]. Because it is likely that other inhibitors, stress, and stimuli may also affect the integrity of MTORC1, a decrease or increase in the phosphorylation status of one MTORC1 substrate does not necessarily correlate with changes in others, including ULK1. Therefore, reliable anti-phospho-ULK1 antibodies should be used to directly examine the phosphorylation state of ULK1, along with additional experimental approaches to analyze the role of the MTOR complex in regulating autophagy. The MTORC1-mediated phosphorylation of AMBRA1 on Ser52 has also been described as relevant to ULK1 regulation and autophagy

induction [703,741]. In line with what is described for ULK1, the anti-phospho-AMBRA1 antibody, which is commercially available, could be used to indirectly measure MTORC1 activity [741].

Activation/assembly of the Atg1 complex in yeast (composed of at least Atg1-Atg13-Atg17-Atg31-Atg29) or the ULK1 complex in mammals (ULK1-RB1CC1-ATG13-ATG101) is one of the first steps of autophagy induction. Therefore, activation of this complex can be assessed to monitor autophagy induction. In yeast, dephosphorylation of Atg13 is associated with activation/assembly of the core complex that reflects the reduction of TORC1 and PKA activities. Therefore, assessing the phosphorylation levels of this protein by immunoprecipitation or western blotting [742-745] can be used not only to follow the early steps of autophagy but also to monitor the activity of some of the upstream nutrient-sensing kinases. Because this protein is not easily detected when cells are lysed using conventional procedures, a detailed protocol has been described [746]. In addition, the autophosphorylation of Atg1 at Thr226 is required for its kinase activity and for autophagy induction; this can be detected using phospho-specific antibodies, by immunoprecipitation or western blotting (Figure 22) [747,748]. In *Drosophila*, TORC1-dependent phosphorylation of Atg1 and Atg1-dependent phosphorylation of Atg13 can be indirectly determined by monitoring phosphorylation-induced electromobility retardation (gel shift) of protein bands in immunoblot images [423,509,510]. Nutritional starvation suppresses TORC1-mediated Atg1 phosphorylation [423,509] while stimulating Atg1-mediated Atg13 phosphorylation [589,749,750]. In mammalian cells, the phosphorylation status of ULK1 at the activating sites (Ser317, 777 [position in the murine sequence, not conserved in human], 467, 556, 638, or Thr575 in the human sequence) or dephosphorylation at inactivating sites (Ser638, 758 in the human sequence) can be determined by western blot using phospho-specific antibodies [672-674], 688, 751, 752]. In general, the core complex is stable in mammalian cells, although, as noted above, upstream inhibitors (MTOR) or activators (AMPK) may interact dynamically with it, thereby determining the status of autophagy.

Alternatively, the activation of the ULK1 complex can be monitored by assessing the localization pattern of ATG13 by immunofluorescence. In fact, following ULK1 complex activation, ATG13 relocates to the omegasome, which results in a punctate pattern [753,754]. In mesothelioma ex vivo 3-dimensional models, the percentage of tumor cells with ATG13 puncta correlates with the level of autophagy, and the analysis of ATG13

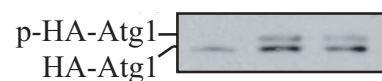


Figure 22. *S. cerevisiae* cells transformed with a plasmid encoding HA-Atg1 were cultured to mid-log phase and shifted to SD-N (minimal medium lacking nitrogen that induces a starvation response). Immunoblotting was done with anti-HA antibody. The upper band corresponds to autophosphorylation of Atg1. This figure was modified from data previously published in ref. [747], and is reproduced by permission of the American Society for Cell Biology, copyright 2011.

puncta has been proposed as an assay to monitor autophagy in mesothelioma formalin-fixed, paraffin-embedded and 3-dimensional models [755]. In the same model, the ULK1/2 inhibitor MRT68921 blocks both autophagy and the formation of ATG13 puncta [756]. As a cautionary note, ATG13 puncta do not reflect autophagy in traditional monolayer cultures of mesothelioma cells. Therefore, studies in 3-dimensional models of other tumors are needed to confirm the validity of ATG13 as a marker of autophagy.

One additional topic that bears on ULK1 concerns the process of LC3-associated phagocytosis (see *Noncanonical use of autophagy-related proteins*). LAP is a type of phagocytosis in macrophages that involves the conjugation of LC3 to single-membrane pathogen-containing phagosomes, a process that promotes phagosome maturation [247]. Although ULK1 is not required for the clearance of cell corpses by LAP, in mammals [245], and UNC-51 (the Atg1/ULK1 homolog in *C. elegans*) is not required for the clearance of neuroblast corpses in larval worms or released cell fragments in worm embryos [757,758], it is important to note that an increased number of apoptotic cell corpses persist during embryonic development in *unc-51* mutant worms [759], suggesting that UNC-51 could have a role in cell death or cell corpse clearance. A recent study shows that pancreatic acinar cells also have the ability to process post-exocytic organelles via LAP [760]. LAP-deficient tumor-associated macrophages also aid in promoting an anti-tumor response in T cells in a tumor microenvironment [761].

An additional substrate that is required for efficient AMPK-induced autophagy is CCNY (cyclin Y)-CDK16 [762]. AMPK phosphorylates CCNY, which promotes its interaction with CDK16, a PCTAIRE kinase family member. The loss of CCNY-CDK16 impairs AMPK-stimulated autophagy, whereas overexpression of CCNY-CDK16 is sufficient to induce autophagy. This outcome is dependent on the catalytic activity of CCNY-CDK16, albeit the substrates of this kinase have not been identified yet.

Cautionary notes: A decrease in TORC1 activity is a good measure for autophagy induction; however, TORC1 activity does not necessarily preclude autophagy induction because there are TOR-independent mechanisms that induce autophagy both in mammals and yeast [763-767]. Along these lines, the disassociation of the AMPK-MTORC1 axis is observed in some AML cells such as the KG-1 cell line, as well as in primary AML cells treated with the specific AMPK agonist GSK621 [768,769]. The co-activation of AMPK and MTORC1 in these cancer cells is associated with increased autophagy flux, with AMPK as the major regulator of autophagy in these conditions [768,769]. Whereas in most systems inhibition of MTOR leads to the induction of autophagy, there are instances in commonly used cancer cell lines and influenza A virus-infected cells in which MTOR appears to be a positive effector [770,771]. Also, MTOR suppression does not always induce autophagy, such as when BECN1 undergoes inhibitory phosphorylation by the growth factor signaling molecules EGFR and AKT, when microglia are activated by lipopolysaccharide (LPS), a TLR4 ligand [772], or during *Salmonella* infection [773-775]. Note that the effect of everolimus in EGFR-transgenic mice is not mainly attributable to autophagy although it suppresses MTOR and induces autophagy in EGFR-driven lung cancer cell lines [776]. In adult skeletal muscle, active MTORC1

phosphorylates ULK1 at Ser757 to inhibit the induction of autophagosome formation. Thus, induction of autophagy requires inhibition of MTORC1 and not of MTORC2 [777,778]. There is also evidence that inhibition of MTORC1 is not sufficient to maintain autophagic flux, but requires additional activation of FOXO transcription factors for the upregulation of autophagy gene expression [662]. In addition, MTORC1 is downstream of AKT; however, oxidative stress inhibits MTOR, thus allowing autophagy induction, despite the concomitant activation of AKT [207]. For neural cells, following administration of the class I phosphoinositide 3-kinase (PI3K) inhibitor LY294002, the phosphorylation levels of AKT and MTOR decrease, and the ratio of LC3-II:LC3-I is higher in the inhibitor-treated injury group than in the simple-injury group [779]. Also, persistent MTORC1 inhibition can cause downregulation of negative feedback loops on IRS-MTORC2-AKT that results in the reactivation of MTORC2 under conditions of ongoing starvation [581,780,781]. Along these lines, both TORC1 and autophagy can be active in specific cell subpopulations of yeast colonies [763]. Similarly, mature autophagosomes and MTOR accumulate in the TOR-autophagy spatial coupling compartment (TASCC) during RAS-induced senescence [782]. Thus, it is necessary to be cautious in deciding how to monitor the TOR/MTOR pathway, and to verify that the pathway being analyzed displays TOR/MTOR-dependent inhibition.

Another point is that the regulation of autophagy by MTOR can be ULK1-independent. During mycobacterial infection of macrophages, MTOR induces the expression of *MIR155* and *MIR31* to sustain the activation of the WNT5A and SHH/sonic hedgehog pathways. Together, these pathways contribute to the expression of lipoxigenases and downregulation of IFNG-induced autophagy [783]. Signaling pathways can be monitored by western blotting, and TaqMan miRNA assays are available to detect these miRNAs.

One problem in monitoring assembly of the ULK1 complex is the low abundance of endogenous ULK1 in many systems, which makes it difficult to detect phospho-ULK1 by western blot analysis. In addition, Atg1/ULK1 is phosphorylated by multiple kinases, and the amount of phosphorylation at different sites can increase or decrease during autophagy induction. Thus, although there is an increase in phosphorylation at the activating sites upon induction, the overall phosphorylation states of ULK1 and ATG13 are decreased under conditions that lead to induction of autophagy; therefore, monitoring changes in phosphorylation by following molecular mass shifts upon SDS-PAGE may not be informative. In addition, such phosphorylation/dephosphorylation events are expected to occur relatively early (1-2 h) in the signaling cascade of autophagy. Therefore, it is necessary to optimize treatment time conditions. Finally, in Arabidopsis and possibly other eukaryotes, the ATG1 and ATG13 proteins are targets of autophagy, which means that their levels may drop substantially under conditions that induce autophagic turnover [350].

At present, the use of Atg1/ULK1 kinase activity as a tool to monitor autophagy is limited because only a few physiological substrates have been identified, and the importance of Atg1/ULK1-dependent phosphorylation has not always been determined. Nonetheless, Atg1/ULK1 kinase activity appears to increase when autophagy is induced, irrespective of the pathway

leading to induction. As additional physiological substrates of Atg1/ULK1 are identified, it will be possible to follow their phosphorylation in vivo as is done with analyses for MTOR. Nonetheless, it must be kept in mind that monitoring changes in the activity of Atg1/ULK1 is not a direct assay for autophagy, although such changes may correlate with autophagy activity. Furthermore, the ULK1 substrates described above and additional ULK1-interacting proteins (e.g., PARP1) [784] already indicate that ULK1—next to its essential role for the induction of autophagy—participates in several additional physiological processes including axon guidance during brain development, type I interferon production, ER-Golgi trafficking, regulation of chaperone function, mitosis, stress granule dynamics, WNT-CTNNB1/ β -catenin signaling, NR3C2/mineralocorticoid receptor signaling, and non-autophagic regulation of cell death. In a *C. elegans* Parkinson disease model, RNAi knockdown of UNC-51/ULK1 results in the accumulation of a human SNCA-GFP fusion [785]. Accordingly, the ULK activity state may thus reflect its role in these processes [786-792]. Therefore, other methods as described throughout these guidelines should also be used to follow autophagy directly.

Finally, there is not a complete consensus on the specific residues of ULK1 that are targeted by AMPK or MTOR. Similarly, apparently contradictory data have been published regarding the association of AMPK and MTOR with the ULK1 kinase complex under different conditions. Therefore, caution should be used in monitoring ULK1 phosphorylation or the status of ULK1 association with AMPK until these issues are resolved.

Conclusion: Assays for Atg1/ULK1 can provide detailed insight into the induction of autophagy, but they are not a direct measurement of the process. Similarly, because MTOR substrates such as RPS6KB1 and EIF4EBP1 are not recommended readouts for autophagy, their analysis needs to be combined with other assays that directly monitor autophagy activity.

Estimation of PtdIns3K (PIK3C3/VPS34) activity

PIK3C3/VPS34 is highly conserved through evolution, and belongs to the class III PtdIns3K that phosphorylates the 3'-OH position of phosphatidylinositol (PtdIns) to synthesize PtdIns3P [793,794]. PtdIns3P is essential for the regulation of endocytic pathways and for the generation of various types of autophagosomes and phagosomes. However, PIK3C3/VPS34 cannot be found alone in the cell but mainly is present in two types of mutually exclusive complexes, complexes I and II. Complex I is composed of PIK3C3/VPS34, PIK3R4/VPS15/p150, BECN1, ATG14 and NRBF2 for mammals, or Vps34, Vps15, Vps30/Atg6, Atg14 and Atg38 for yeast. Complex II replaces ATG14/Atg14 with UVRAG, or Vps38 for mammals and yeast, respectively [795-799]. Complex I regulates autophagy, whereas complex II regulates endocytic pathways, LAP, and cytokinesis [800-802]. Both in yeast and mammals, PIK3C3/VPS34 shows higher activity in complexes than on its own. For example, yeast complexes I and II show higher activity than a Vps34-Vps15 heterodimer [800], and human PIK3C3 activity is increased by coexpressing it with PIK3R4/VPS15 [803]. Also, various post-translational modifications of the subunits of complexes I and II affect the kinase activity [804].

The most commonly used method to estimate PIK3C3/VPS34 activity is to immunoprecipitate the protein complex from cells, immobilize it on beads, mix with the substrate (PtdIns) and radioactive ATP, then measure the PtdIns3P production by autoradiography. Furthermore, two commercial kits are available; an ELISA-based kit from Echelon (K-3300), and a kit for measuring ADP generation from ATP from Promega (V6930). The PIK3C3/VPS34 activity is affected by enzyme concentration and substrate structure. First, for all methods it is important to estimate the concentration and purity of immobilized PIK3C3/VPS34 complex by Coomassie Brilliant Blue or silver staining. Second, the PtdIns structure and the environment where PtdIns is surrounded such as the length of acyl chain, and the size and composition of liposomes largely affect the activity. The PtdIns provided with the Echelon kit is water-soluble diC8-PtdIns. There are also PtdIns:phosphoserine mixture substrates at a 1:9 molar ratio (Thermo Fisher, PV5122), or at a 1:3 molar ratio (Promega, V1711). Although they are good substrates for drug screening, they are not physiological. If researchers are examining the kinase activity to reflect the intracellular conditions, it is recommended to make liposomes that mimic the lipid compositions of the organelle of interest. Therefore, it is necessary to describe the lipid compositions of liposomes, the catalog number for each lipid species, and procedures for making liposomes (just sonication, or whether the liposome size was adjusted by extruding) for publication.

For ADP-Glo assays, because it measures the ATP-ADP conversion, if the purified enzyme is contaminated with chaperones, the ATPase activities of the latter dominate the values. Therefore, it is important to check the purity of the purified enzyme in advance and additionally measure the luminescence values of the enzyme without substrate. Also, the measured luminescence values need to be subtracted by the background values, which can be the intercept value of the standard curve or the measured luminescence of a mixture of 0% ADP and 100% ATP (this should contain ATP in case of impurities). This means that the enzyme concentration needs to be adjusted high enough so that the luminescence values of enzyme plus substrate are higher than the background values (i.e., the measured luminescence values of enzyme without substrate or the mixture of 0% ADP and 100% ATP). The above points need to be considered not only for the PIK3C3/VPS34 assays, but also for all lipid kinase and phosphatase activity assays.

Additional autophagy-related protein markers

Although Atg8-family proteins have been the most extensively used proteins for monitoring autophagy, other proteins can also be used for this purpose. Here, we discuss some of the more commonly used or better-characterized possibilities.

Atg9/ATG9A. Atg9/ATG9A is the only integral membrane Atg protein that is essential for autophagosome formation in all eukaryotes. Mammalian ATG9A displays partial colocalization with GFP-LC3 [805], and ATG9A deficiency in the mouse brain causes axon-specific lesions including neuronal circuit dysgenesis [806]. Perhaps the most unique feature of

Atg9, however, is that it localizes to multiple discrete puncta, whereas most Atg proteins are detected primarily in a single punctum or diffusely within the cytosol. Yeast Atg9 may cycle between the phagophore assembly site (PAS) and peripheral reservoirs [807]; the latter correspond to tubulovesicular clusters that are precursors to the phagophore [808]. Anterograde movement to the PAS is dependent on Atg11, Atg23, Atg27 and actin. Retrograde movement requires Atg1-Atg13, Atg2-Atg18 and the PtdIns3K complex I [809]. Mutants such as *atg1Δ* accumulate Atg9 primarily at the PAS, and this phenotype forms the basis of the “transport of Atg9 after knocking out *ATG1*” (TAKA) assay [148]. In brief, this is an epistasis analysis in which a double-mutant strain is constructed (one of the mutations being *atg1Δ*) that expresses Atg9-GFP. If the second mutated gene encodes a protein that is needed for Atg9 anterograde transport, the double mutant will display multiple Atg9-GFP puncta. In contrast, if the protein acts along with or after Atg1, all of the Atg9-GFP will be confined to the PAS. One such example is a septin complex that regulates Atg9 retrograde transport. The temperature-sensitive point mutations in Cdc10 (P3S and G44D) show accumulation of Atg9 at the PAS at non-permissive temperatures [810]. Monitoring the localization of ATG9A has not been used as extensively in more complex eukaryotes, but this protein displays the same type of dependence on Atg1/ULK1 and PtdIns3P for cycling as seen in yeast [805,809], suggesting that it is possible to follow this ATG9A as an indication of ULK1 and ATG13 function [646,805,809].

There are two conserved classical adaptor protein sorting signals within the cytosolic N terminus of ATG9, which mediate trafficking of ATG9 from the plasma membrane and *trans*-Golgi network (TGN) via interaction with AP-1/2 [707,811]. SRC phosphorylates ATG9 at Tyr8 to maintain its endocytic and constitutive trafficking in unstressed conditions. In response to starvation, phosphorylation of ATG9 at Tyr8 by SRC, and at Ser14 by ULK1, functionally cooperate to promote interactions between ATG9 and the AP-1/2 complex, leading to redistribution of ATG9 from the plasma membrane and juxta-nuclear region to the peripheral pool for autophagy initiation [707]. Furthermore, the localization of mammalian

ATG9A is regulated by cellular sphingomyelin levels. In cells with excess sphingomyelin, ATG9A is trapped in juxtanuclear recycling endosomes, and its failure to be recruited to autophagic membranes results in defective phagophore closure [812]. In neurons ATG9 localizes to axons and presynaptic sites, and requires active transport by the kinesin motor KIF1A to direct its localization into distal neurites [29,537].

ATG9 is also conserved in plants including the model plant *A. thaliana*. A protease protection assay with microsomes isolated from *A. thaliana* cells shows that ATG9 has a similar membrane topology, with its N- and C-termini facing the cytosol [128]. Subcellular analysis indicates that *A. thaliana* ATG9 displays similar discrete puncta within the cytosol in close proximity to the *trans*-Golgi network and late endosomes, whereas ATG9-GFP fusion proteins show a transient association with the autophagosomal marker ATG8. However, in contrast to the yeast and mammalian *atg9* mutants, Arabidopsis *atg9* mutants accumulate numerous abnormal tubular autophagosomal structures, which are dynamically associated with the ER membranes. Using 3-dimensional electron tomography analysis, direct connections between these ATG8-positive tubular structures and the ER have been observed, implying that plant ATG9 plays an essential role in autophagosome progression from the ER, particularly under stress conditions [128]. Recently, the homotrimeric structure of *A. thaliana* ATG9 was resolved by cryo-EM at subnanometer resolution, which provides a structural basis for future studies of ATG9 function in eukaryotes [129].

Atg12–Atg5. ATG5, ATG12 and ATG16L1 associate with the phagophore and have been detected by fluorescence and immunofluorescence (Figure 23) [813,814]. The endogenous proteins form puncta that can be followed to monitor autophagy upregulation. Under non-stressed, nutrient-rich conditions, these proteins are predominantly diffusely distributed throughout the cytoplasm. Upon induction of autophagy, for example during starvation, there is a marked increase in the proportion of cells with punctate ATG5, ATG12 and ATG16L1. Furthermore, upstream inhibitors of autophagosome formation result in a block in this starvation-induced

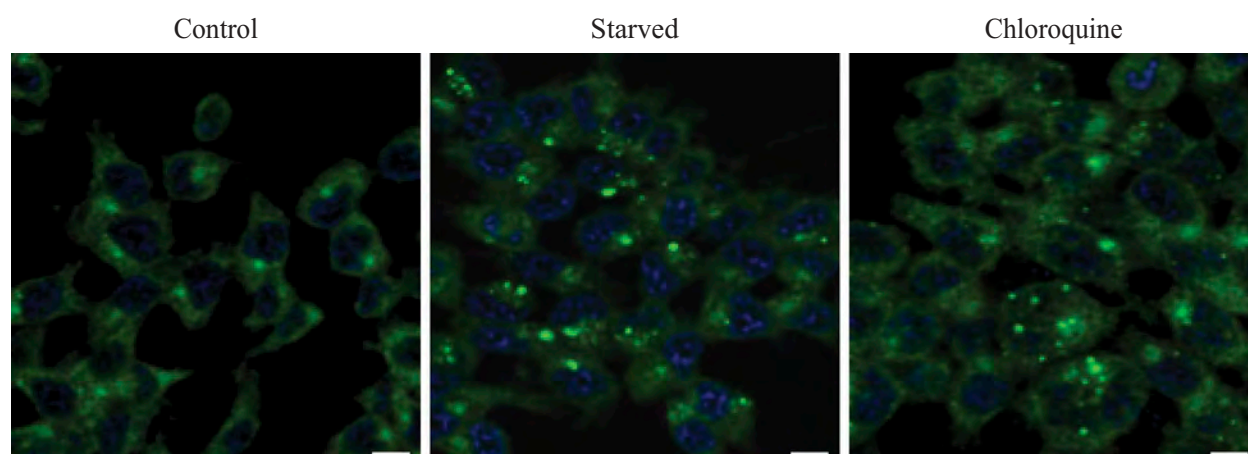


Figure 23. Confocal microscopy image of HCT116 cells immunostained with antibody specific to human ATG12. Cells were starved for 8 h or treated with CQ (50 μ M) for 3 h. Scale bar: 10 μ m. Image provided by M. Llanos Valero, M.A de la Cruz and R. Sanchez-Prieto.

puncta formation, and this assay is very robust in some mammalian cells. Conversely, downstream inhibition of autophagy at the level of phagophore expansion, such as with inhibition of LC3/GABARAP expression, results in an accumulation of the phagophore-associated ATG5, ATG12 and ATG16L1 immunofluorescent puncta [815]. Moreover, PLSCR1 (phospholipid scramblase 1) may play an inhibitory role in the autophagic process interfering with ATG12–ATG5–ATG16L1 complex formation and phagophore elongation as shown through co-immunoprecipitation experiments. Indeed, PLSCR1 binds the ATG12–ATG5 complex preventing ATG16L1 association [413]; therefore, the evaluation of active complexes by co-immunoprecipitation and subsequent immunoblotting analysis can be a further indirect way to evaluate autophagy activation.

ATG12–ATG5 conjugation has been used in some studies to measure autophagy. In *Arabidopsis* and some mammalian cells it appears that essentially all of the ATG5 and ATG12 proteins exist in the conjugated form, and the expression levels do not change, at least during short-term starvation [289,813,814,816]. Therefore, monitoring ATG12–ATG5 conjugation per se may not be a useful method for following the induction of autophagy. It is worth noting, however, that in some cell lines free ATG5 can be detected [817], suggesting that the amount of free ATG5 may be cell line-dependent; free ATG5 levels also vary in response to stress such as DNA damage [818]. Furthermore, free ATG12 can be detected in some cell lines and tissues and has ATG5-independent roles in cell signaling [819–821]. One final parameter that may be considered is that the total amount of the ATG12–ATG5 conjugate may increase following prolonged starvation as has been observed in hepatocytes and both mouse and human fibroblasts (A.M. Cuervo, personal communication; S. Sarkar, personal communication), even though in these conditions part of the ATG12–ATG5 population is secreted in association with exosomes [822].

ATG14. Yeast Atg14 is the autophagy-specific subunit of the Vps34 complex I [796], and a human homolog, named ATG14/ATG14 L/BARKOR, has been identified [795,798,799,823]. ATG14 localizes primarily to phagophores. The C-terminal fragment of the protein, named the BATS domain, is able to direct GFP and BECN1 to autophagosomes in the context of a chimeric protein [824]. ATG14-GFP or BATS-GFP detected by fluorescence microscopy or TEM can be used as a phagophore marker protein; however, ATG14 is not localized exclusively to phagophores, as it can also be detected on mature autophagosomes as well as the ER [824,825]. Accordingly, detection of ATG14 should be carried out in combination with other phagophore and autophagosome markers. A good antibody that can be used to detect endogenous ATG14 by immunostaining has been described [702].

ATG16L1. ATG16L1 has been used to monitor the movement of plasma membrane as a donor for autophagy, and thus an early step in the process. Indeed, ATG16L1 is located on phagophores, but not on completed autophagosomes [455,826]. ATG16L1 can be detected by immuno-TEM, by immunostaining of Flag epitope-tagged ATG16L1, and/or by

the use of GFP-tagged ATG16L1. ATG16L1 is phosphorylated on a serine residue at amino acid position 278 by ULK1 under autophagy-inducing conditions. Detection of endogenous phospho-ATG16L1 [827] has been demonstrated as a novel method to monitor autophagy induction. Because ATG16L1 is specifically located on phagophores but not complete autophagosomes, phospho-ATG16L1-based autophagy assays are unaffected by a late stage autophagy block, and thus able to circumvent a major caveat of LC3-based assays while serving as an alternative tool with unique advantages to monitor autophagy.

ATG16L1 is ubiquitinated by the GAN (gigaxonin) E3 ligase, through interaction with the WD40 domain [828]. GAN causes the clearance of ATG16L1 in cell lines, whereas its repression in primary neurons derived from the *gan*^{−/−} mouse induces an abnormal bundling of ATG16L1 within the soma. Action of GAN is dynamic, as restoration of its expression using lentiviral vector clears the aggregate and the endogenous ATG16L1, respectively, in GAN mutant and wild-type neurons. GAN mutant neurons exhibit a failure in producing autophagosomes over time upon autophagy induction, hence leading to a defective autophagic flux in subsequent steps. Thus, GAN is the first E3 ligase fine-tuning autophagosome production through ATG16L1.

Finally, the coding polymorphism of ATG16L1 (T300A, rs2241880), which is associated with Crohn disease, renders the protein sensitive to CASP3- and CASP7-mediated cleavage in the WD40 domain; this leads to decreased ATG16L1 function and can be detected by western blot [829,830].

Cautionary notes: The expression level of ATG16L1 does not always correlate with other components of the autophagic machinery, and in some cases may be altered in a manner that is independent of autophagy; for example, this can be seen in samples from patients with acute myeloid leukemia (P. Ludovico, unpublished results).

Atg18/WIP1 family. Yeast Atg18 [831,832] and Atg21 [443] (or the mammalian WIP1 homologs [833]) are required for both autophagy (i.e., nonselective sequestration of cytoplasm) and autophagy-related processes (e.g., the Cvt pathway [834,835], specific organelle degradation [168], and autophagic elimination of invasive microbes [171,172,174,175,836]). These proteins bind PtdIns3P that is present at the phagophore and autophagosome [837,838] and also PtdIns(3,5)P₂. Furthermore, fluorescence stopped-flow [839] and chemical cross-linking assays [840] show that Atg18 oligomerizes upon membrane binding, whereas it is mainly monomeric when unbound. Human WIP1 and WIP2 function downstream of the class III phosphatidylinositol 3-kinase complex I (PIK3C3/VPS34, BECN1, PIK3R4/VPS15, ATG14, NRBF2) and upstream of both the ATG12 and LC3 ubiquitin-like conjugation systems [837,841,842]. Upon the initiation of the autophagic pathway, WIP1 and WIP2 bind PtdIns3P and accumulate at limiting membranes, such as those of the ER, where they participate in the formation of omegasomes and/or autophagosomes [843,844]. On the basis of quantitative fluorescence microscopy, this specific WIP1 protein localization has been used as an assay to monitor autophagy in human cells [838].

Using either endogenous WIPI1 or WIPI2, detected by indirect fluorescence microscopy or EM, or transiently or stably expressed tagged fusions of GFP to WIPI1 or WIPI2, basal autophagy can be detected in cells that display WIPI puncta at autophagosomal membranes. In circumstances of increased autophagic activity, such as nutrient starvation or rapamycin administration, the induction of autophagy is reflected by the elevated number of cells that display WIPI puncta when compared to the control setting. Also, in circumstances of reduced autophagic activity such as upon wortmannin treatment, the reduced number of WIPI puncta-positive cells reflects the inhibition of autophagy. Basal, induced and inhibited formation of WIPI puncta closely correlates with both the protein level of LC3-II and the formation of GFP-LC3 puncta [838,842]. Accordingly, WIPI puncta can be assessed as an alternative to LC3. Automated imaging and analysis of fluorescent WIPI1 (Figure 24) or WIPI2 puncta represent an efficient and reliable opportunity to combine the detection of WIPI proteins with other parameters. It should be noted that there are two isoforms of WIPI2 (2B and 2D) [842], and in *C. elegans* EPG-6/WDR45/WIPI4 has been identified as the WIPI homolog required for autophagy [845]. Thus, these proteins, along with the currently uncharacterized WDR45B/WIPI3, provide additional possibilities for monitoring phagophore and autophagosome formation.

Cautionary notes: With regard to detection of the WIPI proteins, endogenous WIPI1 puncta cannot be detected in

many cell types [837], and the level of transiently expressed GFP-WIPI1 puncta is cell context-dependent [837,838]. However, this approach has been used in human and mouse cell systems [664,838] and mCherry-Atg18 also works well for monitoring autophagy in transgenic *Drosophila* [183], although one caution with regard to the latter is that GFP-Atg18 expression enhances Atg8 lipidation in the fat body of fed larvae. GFP-WIPI1 and GFP-WIPI2 have been detected on the completed (mature) autophagosome by freeze-fracture analysis [144], but endogenous WIPI2 has not been detected on mRFP-LC3- or LAMP2-positive autophagosomes or autolysosomes using immunolabeling [837]. Accordingly, it may be possible to follow the formation and subsequent disappearance of WIPI puncta to monitor autophagy induction and flux using specific techniques. As with GFP-LC3, overexpression of WIPI1 or WIPI2 can lead to the formation of aggregates, which are stable in the presence of PtdIns3K inhibitors.

BECN1/Vps30/Atg6. BECN1 (yeast Vps30/Atg6) and PIK3C3/VPS34 are essential partners in the autophagy interactome that signals the onset of autophagy [796,846,847], and many researchers use this protein as a way to monitor autophagy. Binding to the anti-apoptotic protein BCL2 inhibits BECN1 [848]. BECN1 also binds other anti-apoptotic BCL2-family members via its putative BH3 domain [849,850]. Autophagy is induced by the release of BECN1 from BCL2 by pro-apoptotic BH3 proteins, phosphorylation of BECN1 by DAPK1 and

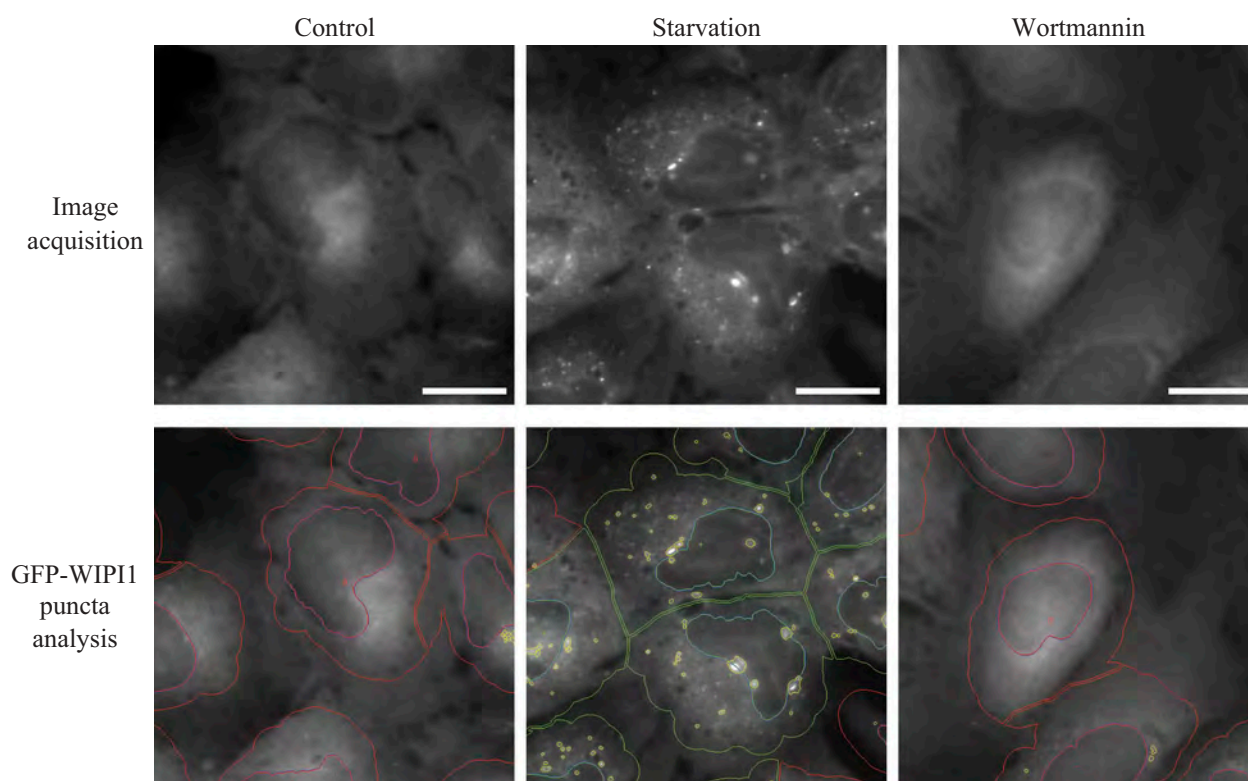


Figure 24. Automated WIPI1 puncta image acquisition and analysis monitors the induction and inhibition of autophagy. Stable U2OS clones expressing GFP-WIPI1 were selected using 0.6 $\mu\text{g}/\text{ml}$ G418 and then cultured in 96-well plates. Cells were treated for 3 h with nutrient-rich medium (Control), nutrient-free medium (EBSS), or with 233 nM wortmannin. Cells were fixed in 3.7% paraformaldehyde and stained with DAPI (5 $\mu\text{g}/\text{ml}$ in PBS). An automated imaging and analysis platform was used to determine the number of both GFP-WIPI1 puncta-positive cells and the number of GFP-WIPI1 puncta per individual cell [664]. Cells without GFP-WIPI1 puncta are highlighted in red (cell detection) and purple (nuclei detection), whereas GFP-WIPI1 puncta-positive cells are highlighted in yellow (GFP-WIPI1 puncta detection), green (cell detection) and blue (nuclei detection). Bars: 20 μm . Images provided by S. Pfisterer and T. Proikas-Cezanne.

DAPK2 (at Thr119, located in the BH3 domain) [851,852], or phosphorylation of BCL2 by MAPK8/JNK1 (at Thr69, Ser70 and Ser87) [853,854]. Release of BECN1 can also be achieved by the expression of the F121A mutant, which leads to enhanced basal autophagy in vivo [855]. The relationship between BECN1 and BCL2 is more complex in developing cerebellar neurons, as it appears that the cellular levels of BCL2 are, in turn, post-translationally regulated by an autophagic mechanism linked to a switch from immaturity to maturity [856,857]. It is important to be aware, however, that certain forms of autophagy are induced in a BECN1-independent manner and are not blocked by PtdIns3K inhibitors [118,858,859]. Interestingly, caspase-mediated cleavage of BECN1 inactivates BECN1-induced autophagy and enhances apoptosis in several cell types [860], emphasizing that the crosstalk between apoptosis and autophagy is complex.

Although a population of BECN1 may localize in proximity to the trans-Golgi network [861], it is also present at the ER and mitochondria [848]. In keeping with these observations, in cerebellar organotypic cultures BECN1 co-immunoprecipitates with BCL2 that is primarily localized at the mitochondria and ER; and in a mouse model of neurodegeneration, autophagic vacuoles in Purkinje neurons contain partially digested organelles that are immunoreactive for BCL2 [856,862]. In addition, as BECN1-PIK3C3/VPS34 are the major source of cellular PtdIns3P lipids and can be present in multiple complexes that act during endosome maturation in addition to autophagy [863], caution must be exercised when monitoring localization. On induction of autophagy by various stimuli, the presence of BECN1- and PIK3C3/VPS34-positive macroaggregates can be detected in the region of the Golgi complex by immunofluorescence [207,864]. Thus, BECN1-GFP puncta detected by fluorescence microscopy or TEM may serve as an additional marker for autophagy induction [865]; however, it should be noted that caspase cleavage of BECN1 can be detected in normal culture conditions (S. Luo, personal communication), and cleaved BECN1 is translocated into the nucleus [866]. Thus, care needs to be taken with these assays under stress conditions in which more pronounced BECN1 cleavage occurs. In addition, as with any GFP chimeras there is a concern that the GFP moiety interferes with correct localization of BECN1.

To demonstrate that BECN1 or PtdIns3K macroaggregates are an indirect indication of ongoing autophagy, it is mandatory to show their specific association with the process by including appropriate controls with inhibitors or preferably by autophagy gene silencing. When a BECN1-independent autophagy pathway is induced, such aggregates are not formed regardless of the fact that the cell expresses BECN1 (e.g., as assessed by western blotting; C. Isidoro, personal communication). As BECN1-associated PtdIns3K activity is crucial in autophagosome formation in BECN1-dependent autophagy, the measurement of PtdIns3K in vitro lipid kinase activity in BECN1 immunoprecipitates can be a useful technique to monitor the functional activity of this complex during autophagy modulation [774,775,867]. It is important to note that an in vitro lipid kinase assay with BECN1 immunoprecipitates represents the total PtdIns3K activity and does not make it possible to distinguish between the production of

PtdIns3P by PIK3C3/VPS34 in complex I versus that in complex II. Therefore, the most accurate measure of complex-specific activity of the class 3 PtdIns3K would be an in vitro lipid kinase assay using ATG14 and UVRAG immunoprecipitates [868,869].

STX17. STX17 is a SNARE protein implicated in autophagosome-endolysosome fusion in cooperation with SNAP29 and VAMP8 [795,870]. STX17 was initially reported to be recruited to completely sealed autophagosomes, but not to phagophores [871-875]. STX17 as a competence factor may be recruited just prior to fusion of autophagosomes with lysosomes, and not all autophagosomes are positive for this protein. However, later studies demonstrate that upon starvation STX17 colocalizes with the omegasome marker ZFYVE1/DFCP1 [876,877], consistent with the view that STX17 is also implicated in autophagosome formation in starvation-induced autophagy [872,873,877] and mitophagy [878,879]. In fed cells, STX17 principally localizes to the ER, mitochondria-associated ER membranes (MAMs), and mitochondria [871-873]. Some STX17 is phosphorylated by TBK1 at Ser202, and the phosphorylated form localizes to the Golgi apparatus [877]. STX17 also has a critical role in mediating the retrograde transport of autophagosomes upon their fusion with late endosome (LEs) in distal neuronal axons [880,881]. Neurons are highly polarized cells with long axons, and thus face special challenges to transport AVs toward the soma where mature lysosomes are relatively enriched. LE-loaded dynein-SNAPIN motor-adaptor complexes are recruited to AVs upon STX17-mediated LE-AV fusion. This motor sharing ride-on service enables neurons to maintain effective autophagic clearance in the soma, thus reducing autophagic stress in axons.

TECPR1. TECPR1 binds ATG5 through an AFIM (ATG5 [five] interacting motif). TECPR1 competes with ATG16L1 for binding to ATG5, suggesting that there is a transition from the ATG5-ATG16L1 complex that is involved in phagophore expansion to an ATG5-TECPR1 complex that plays a role in autophagosome-lysosome fusion [882]. TECPR1 thus marks lysosomes and autolysosomes [883].

ZFYVE1/DFCP1. ZFYVE1 binds PtdIns3P that localizes to the ER and Golgi. Starvation induces the translocation of ZFYVE1 to punctate structures on the ER; the ER population of ZFYVE1 marks the site of omegasome formation [884]. ZFYVE1 partially colocalizes with WIPI1 upon nutrient starvation [842] and also with WIPI2 [837].

Conclusion: Components of the autophagic machinery other than Atg8-family proteins can be monitored to follow autophagy, and these can be important tools to define specific steps of the process. For example, WIPI puncta formation can be used to monitor autophagy, but, similar to Atg8-family proteins, should be examined in the presence and absence of lysosomal inhibitors. Analysis of WIPI puncta should be combined with other assays because individual members of the WIPI family might also participate in additional, uncharacterized functions apart from their role in autophagy. At present, we caution against the use of changes in BECN1 localization as a marker of autophagy

induction, given its other cellular roles. It is also worth considering the use of different markers depending on the specific autophagic stimuli.

Sphingolipids

Sphingolipids are ubiquitous membrane lipids that can be produced in a de novo manner in the ER and Golgi apparatus or by cleavage involving phosphodiesterases (sphingomyelinases), hydrolases (glycosphingolipid glycosidases), sphingolipid ceramide N-deacylase (SCDase), phosphatases (acting on sphingosine-1-phosphate [S1P] and ceramide-1-phosphate) or lyases (e.g., SGPL1 [sphingosine-1-phosphate lyase 1]) [885-887]. For instance, SGPL1 is a ubiquitously expressed enzyme having a wide-range of functions in different cellular processes, including proliferation, motility and death. Moreover, SGPL1 is a critical determinant for the degradation of the sphingolipid S1P. The S1P pathway is a crucial mechanism for neuronal autophagy by providing PE for LC3 conjugation [888,889]. Ablation and deletion of *Sgpl1* result in reduced autophagic activity in mouse brain [888]. Likewise, mutations in SGPL1 and alterations in neuronal autophagy lead to severe neurodevelopmental phenotypes ranging from fetal hydrops to congenital brain malformations and neuropathies in humans [890]. The multiple different metabolites of the sphingolipid pathway, which are distinct by even a single double bond, carbon chain length of the fatty acid, or presence of a phosphate group, can have quite varied cellular functions. Sphingolipids were first recognized for their role in the architecture of membrane bilayers affecting parameters such as bilayer stiffness, neighboring lipid order parameter and microdomain/raft formation. They also act as second messengers in vital cellular signaling pathways and as key determinants of cellular homeostasis in what is called a sphingolipid rheostat [891]. Sphingolipids participate in the formation of different membrane structures and subcellular organelles, such as mitochondria and ER, and are also involved in the fusion and biophysical properties of cell membranes [892]. Moreover, they are constitutive components of MAMs, subdomains of the ER that interact with mitochondria [893].

Ceramides, positioned at the core of sphingolipid metabolism, play several roles that affect multiple steps of autophagy, by inhibition of nutrient transporters [894], by modulation of BCL2-BECN1 association at the level of AKT signaling [895], and by regulation of mitophagy [896]. The latter function is regulated by a particular ceramide species, stearyl (C18:0)-ceramide, a sphingolipid generated by CERS1 (ceramide synthase 1). C18-ceramide, in association with LC3-II, targets damaged mitochondria for phagophore sequestration in response to ceramide stress, leading to tumor suppression [896-900]. The binding of ceramide to LC3-II can be detected using anti-ceramide and anti-LC3 antibodies by immunofluorescence and confocal microscopy, co-immunoprecipitation using anti-LC3 antibody followed by liquid chromatography-tandem MS, using appropriate standards (targeted lipidomics), or labeling cells with biotin-sphingosine to generate biotin-ceramide, and immunoprecipitation using avidin columns followed by western blotting to detect LC3-II. It should be noted that inhibitors of ceramide generation, mutants of LC3 with altered ceramide binding (F52A or I35A), and/or that are conjugation defective (e.g., G120A),

should be used as negative controls [901]. The generation of C18-ceramide in the outer mitochondrial membrane, which recruits LC3-containing phagophores for mitophagy induction, is regulated through the trafficking of the metabolic enzyme CERS1 by RPL29P31/p17/PERMIT [901]. shRNA-mediated knockdown or deletion of this gene prevent mitophagy in response to cellular stress both in cultured cells and in knockout mice [901]. Thus, colocalization of CERS1 or RPL29P31/p17/PERMIT with TOMM20 using immunofluorescence can also be used to detect mitophagy signals in response to acute or chronic stress in situ and in vivo.

Other sphingolipids are also involved in autophagy. For example, accumulation of endogenous sphingosine-1-phosphate, a pro-survival downstream metabolite from ceramide triggers ER-stress associated autophagy, by activation of AKT [902], excess sphingomyelin inhibits phagophore closure by disturbing the trafficking of ATG9A [812], and SMPD1/acid sphingomyelinase inhibits autophagy through the activation of the MTOR pathway [903], whereas it is required for LC3-associated phagocytosis [904]. Likewise, dihydroceramides, the penultimate metabolite of ceramide biosynthesis have been implicated in the regulation of autophagy [905]. Specifically, changes in the levels of C16:0 and C18:0 dihydroceramides cause the destabilization of autolysosomal membranes thereby leading to the induction of autophagy-associated cell death [906]. In addition, gangliosides, have been implicated in autolysosome morphogenesis [907]. Moreover, a molecular interaction of the ganglioside GD3 with core-initiator proteins of autophagy, such as AMBRA1 and WIPI1, is revealed within lipid microdomains in MAMs, indicating that MAM raft-like microdomains can play a role in the initial organelle scrambling activity that finally leads to the formation of the autophagosome [908].

To analyze the role of gangliosides in autophagy, two main technical approaches can be used: co-immunoprecipitation and Förster resonance energy transfer. For the first method, lysates from untreated or autophagy-induced cells have to be immunoprecipitated with an anti-LC3 polyclonal antibody (a rabbit IgG isotypic antibody should be used as a negative control). The obtained immunoprecipitates are subjected to ganglioside extraction, and the extracts run on an HPTLC aluminum-backed silica gel and analyzed for the presence of specific gangliosides by using monoclonal antibodies. Alternatively, the use of FRET by flow cytometry appears to be highly sensitive to small changes in distance between two molecules, and is thus suitable to study molecular interactions, for example, between ganglioside and LC3. Furthermore, FRET requires ~10 times less biological material than immunoprecipitation.

Conclusion: Sphingolipids are bioactive molecules that play key roles in the regulation of autophagy at various stages, including upstream signal transduction pathways to regulate autophagy via transcriptional and/or translational mechanisms, autolysosome morphogenesis, and/or targeting phagophores to mitochondria for degradation via sphingolipid-LC3 association [276, 897, 899-901, 909].

Transcriptional and translational regulation

The induction of autophagy in certain scenarios is accompanied by an increase in the mRNA levels of certain autophagy-

related genes, such as *ATG1* [910], *ATG6* [911], *ATG7* [912,913], *ATG8/Lc3* [64, 473, 914-916], *GABARAPL1* [473,916], *ATG9* [917], *Atg12* [918], *ATG13* [473,916], *Atg14* [919], *ATG29* [910], *WIP1* [473,916], and *SQSTM1* [64], and an autophagy-dedicated microarray was developed as a high-throughput tool to simultaneously monitor the transcriptional regulation of all genes involved in, and related to, autophagy [920]. The mammalian gene that shows the greatest transcriptional regulation in the liver (in response to starvation and circadian signals) is *Ulk1*, but others also show more limited changes in mRNA levels including *Gabarapl1*, *Bnip3* and, to a minor extent, *Lc3b* [921]. In skin cancer and HeLa cells *ULK1* and *ULK2* expression is negatively regulated at the transcriptional level by the chromatin non-histone protein HMGAI (high mobility group AT-hook 1) [922]. In several mouse and human cancer cell lines, ER stress and hypoxia increase the transcription of *Lc3/LC3*, *GABARAPL1*, *Atg5/ATG5*, *Atg12/ATG12*, *ATG13*, and *WIP1* by a mechanism involving the unfolded protein response (UPR). Similarly, a stimulus-dependent increase in *LC3B* expression is detected in neural stem cells undergoing autophagy induction [923]. The *ATG9A* promoter, similar to those of *BNIP3* and *BNIP3L*, but in contrast to other *ATG* family members such as *ATG5* and *ATG7*, contains HIF1A-responsive elements and is transcriptionally activated in hypoxic glioblastoma cells [209]. Increased expression of *Atg5* in vivo after optic nerve axotomy in mice [924] and increased expression of *Atg7*, *Becn1* and *Lc3a* during neurogenesis at different embryonic stages in the mouse olfactory bulb are also seen [925]. *LC3* and *ATG5* are not required for the initiation of autophagy, but mediate phagophore expansion and autophagosome formation. In this regard, the transcriptional induction of *LC3* may be necessary to replenish the *LC3* protein that is turned over during extensive ER stress- and hypoxia-induced autophagy [918,926]. Of note, however, a recent study showed that although tunicamycin-induced ER stress activates autophagy and triggers a strong transcriptional increase in *LC3* mRNA and protein levels (via ATF4), depletion of *LC3* does not reduce ER stress-induced autophagy [473].

In the clinical setting, tissue expression of *ATG5*, *LC3A* and *LC3B* and their respective proteins accompanies elevated autophagy flux in human adipose tissue in obesity [292,927]. Thus, assessing the mRNA levels of *LC3* and other autophagy-related genes by northern blot or reverse transcriptase polymerase chain reaction (RT-PCR) may provide correlative data relating to the induction of autophagy; in addition, proteomic profiling of de novo protein synthesis in starvation-induced autophagy using bioorthogonal noncanonical amino acid tagging can further validate the function of the corresponding proteins in autophagy induction [928]. However, a time course may be necessary to obtain accurate information because mRNA levels are likely to change substantially over time. In addition, mRNA may be sequestered in P-bodies, resulting in suppression of protein translation and time-dependent loss of autophagy-related proteins, as was shown for *AMBRA1* and *BECN1* in cells exposed to the hypoxia mimetic *CoCl₂* [929]. Downregulation of autophagy-related mRNAs has been observed in human islets under conditions of lipotoxicity [571] that impair autophagic flux [930]. It is

not clear if these changes are sufficient to regulate autophagy, however, and therefore these are not direct measurements.

Several transcription factors of the nuclear receptor superfamily modulate expression of genes related to autophagy. For instance, *NR1D1/Rev-erba* modulates autophagy-associated genes in a tissue-specific manner. Whereas *NR1D1* represses *Ulk1*, *Bnip3*, *Atg5*, *Becn1* and *Prkn/park2/parkin* gene expression in mouse skeletal muscle [931] as well as *ulk1a* and *atp6v1d* in zebrafish larvae [932] by directly binding to regulatory regions in their DNA sequences, *STRA8* suppresses autophagy and at the same time transcriptionally represses *Nr1d1* and, thereby, inhibits the expression of *Ulk1* in mouse testis [933]. *NR1D1* upregulates *Ulk1* by direct engagement of distal RAR-related orphan receptor DNA elements as evaluated in *stra8^{-/-} nr1d1^{-/-}* double-knockout mice. Moreover, in human macrophages, *NR1D1* promotes lysosome biogenesis and autophagy, contributing to its antimicrobial properties against *M. tuberculosis* [934]. Whereas *NR1D1* represses autophagic flux in skeletal muscles, it upregulates the expression of autophagy- and lysosome-associated genes in mouse testis and human macrophages. Furthermore, *NR1D1* induces mitochondrial biogenesis in skeletal muscles, leads to improved oxidative capacity of cells, and induces lysosome biogenesis in human macrophages, augmenting antimicrobial properties.

The nuclear receptors *PPARA* and *NR1H4/FXR* also regulate hepatic autophagy in mice. Indeed, *PPARA* and *NR1H4* compete for the control of hepatic lipophagy in response to fasting and feeding nutritional cues, respectively [921]. In addition, activation of *PPARA*-mediated autophagy and the lysosomal pathway in the nervous system, contributes to A β clearance, and thus reduces Alzheimer disease (AD)-like pathology and cognitive decline in a mouse model [935]. *NR1H4* may also inhibit autophagy via inhibition of CREB-CRTC2 complex assembly [936]. Consistent with in vitro studies utilizing human cancer cell lines [937,938], in human adipose tissue explants, *E2F1* binds the *LC3B* promoter, in association with increased expression of several autophagy genes and elevated adipose tissue autophagic flux [292,927]. In this instance, classical promoter analysis studies, including chromatin immunoprecipitation and *ATG* promoter-luciferase constructs, provide insights into the putative transcriptional regulation of autophagy genes by demonstrating promoter binding in situ, and promoter activity in vitro [927].

Of note, large changes in *Atg* gene transcription just prior to *Drosophila* salivary gland cell death (that is accompanied by an increase in autophagy) are detected for *Atg2*, *Atg4*, *Atg5* and *Atg7*, whereas there is no significant change in *Atg8a* or *Atg8b* mRNA [939,940]. Autophagy is critical for *Drosophila* midgut cell death, which is accompanied by transcriptional upregulation of all of the *Atg* genes tested, including *Atg8a* (Figure 25) [375,941]. Similarly, in the silkworm (*Bombyx mori*) larval midgut [942], fat body [943] and silk gland [944] the occurrence of autophagy is accompanied by an upregulation of the mRNA levels of several *Atg* genes. Transcriptional upregulation of *Drosophila Atg8a* and *Atg8b* is also observed in the fat body following induction of autophagy at the end of larval development [945], and these genes as well as *Atg2*, *Atg9* and *Atg18* show a more than 10-fold induction during starvation [946]. *Atg5*, *Atg6*, *Atg8a* and *Atg18* are upregulated in the ovary of

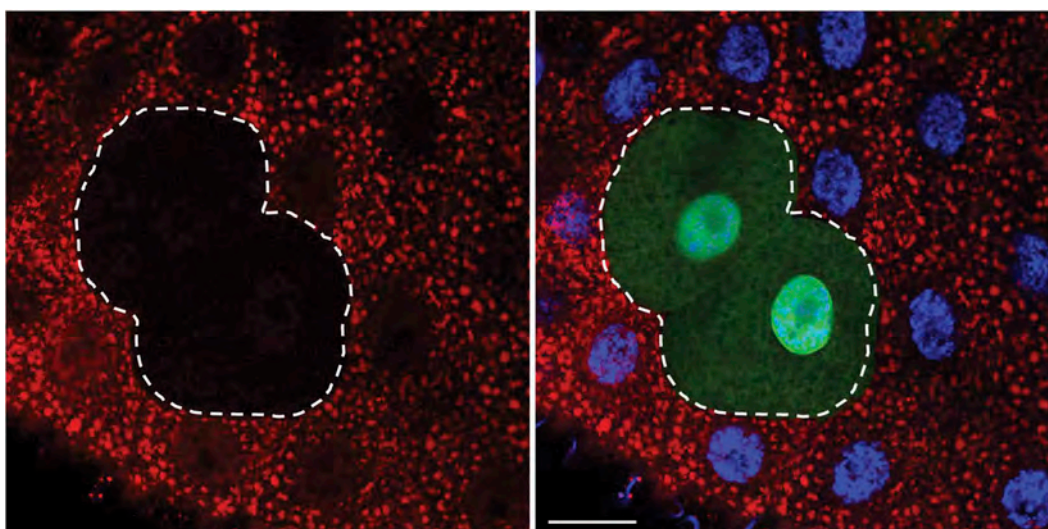


Figure 25. Clonal analysis of autophagy in the *Drosophila* larval midgut. Inhibition of autophagy in somatic clone cells marked by GFP (green, outlined) have decreased levels of mCherry-Atg8a puncta (red) compared to the control wild-type cells (non-GFP) with nuclei in blue (merged image, right panel). Bar: 20 μ m. Image provided by D. Denton and S. Kumar.

starved flies [947], and an increase in *Drosophila Atg8b* is observed in cultured *Drosophila l(2)mbn* cells following starvation (S. Gorski, personal communication). An upregulation of plant ATG8 may be needed during the adaptation to reproductive growth; a T-DNA inserted mutation of rice *ATG8b* blocked the change from vegetative growth to reproductive growth in both homozygous and heterozygous plant lines (M.-Y. Zhang, H. Budak, unpublished results).

Similarly, the upregulation of autophagy-related and -associated genes (*Atg4b*, *Atg12*, *Atg13*, *Bnip3*, *Gabarapl1*, *Lc3*, *WIP1*) has been documented at the transcriptional and translational level in several other species (e.g., *C. elegans* [948], mouse, rat, human [949], trout, Arabidopsis and maize) under conditions of ER stress [473,918], and diverse types of prolonged (several days) catabolic situations including cancer cachexia, diabetes mellitus, uremia and fasting [290, 662 [950-953],]. Along these lines, the mRNA levels of *atg1*, *atg8a/b* and *sqstm1* increase in *D. discoideum* upon infection with the fish and frog pathogen *Mycobacterium marinum* [64], a close relative of *M. tuberculosis*. Similarly, *ATG9* and *ATG16L1* are transcriptionally upregulated upon influenza virus infection (H. Khalil, personal communication), and in *C. elegans*, the FOXA transcription factor PHA-4 and the TFEB (transcription factor EB) ortholog HLH-30 regulate the expression of several autophagy-related genes (see *Methods and challenges of specialized topics/model systems. C. elegans*) [573,948]. Such prolonged induction of the expression of ATG genes has been thought to allow the replenishment of critical proteins (e.g., LC3 and GABARAP) that are destroyed during autophagosome fusion with the lysosome [954].

The polyamine spermidine increases life span and induces autophagy in cultured yeast and mammalian cells, as well as in nematodes, flies and mice. In aging yeast, spermidine treatment triggers epigenetic deacetylation of histone H3 through inhibition of histone acetyltransferases, leading to significant upregulation of various autophagy-related transcripts [955]. In mammalian cells, spermidine promotes autophagy flux by depleting cytosolic HDAC4 to enhance

the acetylation and stability of MAP1S (microtubule-associated protein 1S) to prolong mouse lifespan and prevent liver fibrosis and hepatocellular carcinomas [956]; however, the functional relevance of autophagy for liver fibrosis and cancer is highly dependent on the cell type. Whereas autophagy maintains cellular homeostasis in hepatocytes, Kupffer cells (macrophages), and liver sinusoidal endothelial cells, thereby counteracting fibrogenesis in the liver, it is the prime process of providing energy for the activation of hepatic stellate cells, which leads to collagen production and fibrogenesis [957]. Spermidine also drives the hypusination of the translation factor EIF5A, which in turn controls the translation of TFEB to rejuvenate B cell immunity [958]. In addition, spermidine stimulates mitophagy in cardiomyocytes and prevents typical age-related cardiac deterioration in an autophagy-dependent manner [959]. IPMK, can alter histone H4 acetylation and influence gene expression of *LC3B*, *BNIP3*, *BNIP3L*, *SQSTM1*, *GABARAP1* and *ATG12*; loss of IPMK in liver prevents lipophagy and liver regeneration [621,690].

In addition to spermidine, melatonin, a hormone present in both mammals and plants, plays a critical role in inducing the expression of ATG genes under heat stress in tomato [960]. Both foliar application of an optimal dose of melatonin and the overexpression of the *ASMT* (N-acetylserotonin O-methyltransferase) gene results in an upregulation of the expression of ATG genes and the formation of autophagosomes leading to the degradation of denatured proteins resulting from heat stress in tomato [960]. Under cadmium stress, HSF1A (heat shock factor 1A) promotes the accumulation of melatonin through directly activating the transcription of *COMT1* (caffeate O-methyltransferase 1), a key gene in melatonin biosynthesis [961], indicating that HSF1A might mediate autophagy in response to stress in plants. Indeed, silencing of *HSF1A* completely blocks drought stress-induced expression of *ATG10* and *ATG18F*, whereas the expression of these genes is increased in *HSF1A*-overexpressing plants [962]. An electrophoretic mobility shift assay and

ChIP-qPCR analysis show that HSFA1A binds to the promoters of these two *ATG* genes and directly regulates their expression to trigger autophagy under drought stress in tomato plants [962]. Furthermore, BZR1 (brassinazole-resistant 1), a phytohormone brassinosteroid-activated transcription factor, induces the expression of *ATG2* and *ATG6* to form autophagosomes, which mediate the response to nitrogen starvation in tomato [963].

In addition to the *ATG* genes, transcriptional upregulation of *VMP1* can be detected in mammalian cells subjected to rapamycin treatment or starvation, and in tissues undergoing disease-induced autophagy such as cancer [964]. *VMP1* is an essential autophagy gene that is conserved from *D. discoideum* to mammals [422,965], and the VMP1 protein regulates early steps of the autophagic pathway and is essential for correct functioning of membrane contact sites between the ER and other organelles including autophagosomes [841,966]. VMP1 is poorly expressed in mammalian cells under nutrient-normal conditions, but is highly upregulated in cells undergoing autophagy, and the expression of VMP1 induces autophagosome formation. The GLI3 transcription factor is an effector of KRAS that regulates the expression and promoter activity of *VMP1*, using the histone acetyltransferase EP300/p300 as a co-activator [967].

A gene regulatory network, named CLEAR (coordinated lysosomal expression and regulation) that controls both lysosome and autophagosome biogenesis was identified using a systems-biology approach [949,968,969,635,636]. The basic helix-loop-helix transcription factor TFEB acts as a master gene of the CLEAR network and positively regulates the expression of both lysosomal and autophagy genes, thus linking the biogenesis of two distinct types of cellular compartments (i.e., autophagosomes and lysosomes) that cooperate in the autophagic pathway. TFEB activity is regulated by starvation and is controlled by both MAPK1/ERK2-, MTOR-, and AKT-mediated phosphorylation at specific serine residues [949,970-973]; thus, it can serve as a new tool for monitoring transcriptional regulation connected with autophagy. TFEB is phosphorylated by MTORC1 on the lysosomal surface, preventing its nuclear translocation. A lysosome-to-nucleus signaling mechanism transcriptionally regulates autophagy and lysosomal biogenesis via MTOR and TFEB [971]. TFEB phosphorylation on specific residues also occurs in the nuclear compartment and enables TFEB nuclear export [974-976]. Thus, TFEB activity is tightly regulated by different phosphorylation events that control TFEB nuclear import and export rates. Therefore, a very useful readout of endogenous TFEB activity is the evaluation of TFEB subcellular localization, as activation of TFEB correlates with its relocation from the cytoplasm to the nucleus. This shift can be monitored by immunofluorescence using antibodies against TFEB. TFEB localization may also be studied to monitor MTOR activity, as in most cases TFEB nuclear localization correlates with inhibition of MTOR. However, due to the low expression levels of TFEB in most cells and tissues, it may be difficult to visualize the endogenous protein. Thus, a TFEB nuclear translocation assay was developed in a HeLa cell line stably transfected with TFEB-GFP. This fluorescence assay can be used to identify the conditions and factors that promote TFEB

activation [971]. TFE3 and MITF, two other members of the MiT/TFE family of transcription factors, in some cases can compensate for TFEB and are regulated in a similar manner [973,977,978]. In response to histone deacetylase inhibitors, TFEB acetylation exerts an important function in control of its transcriptional activity and lysosomal function [979]. Finally, an AMPK-SKP2-CARM1 signaling cascade has also been reported to play a role in transcriptional regulation of autophagy [980]; CARM1 exerts a transcriptional coactivator function on autophagy and lysosomal genes through TFEB.

Similar to TFEB, the erythroid transcription factor GATA1 and its coregulator ZFPM1/FOG1 as well as the myeloid master regulator SPI1/PU.1 induce the transcription of multiple genes encoding autophagy components. This developmentally regulated transcriptional response is coupled to increases in autophagosome number as well as the percent of cells that contain autophagosomes [981-983]. FOXO transcription factors, especially FOXO1 and FOXO3, also play critical roles in the regulation of autophagy gene expression [662,919,984]. A zinc finger family DNA-binding protein, ZKSCAN3, is a master transcriptional repressor of autophagy and lysosome biogenesis; starvation and MTOR inhibition with torin1 induce nucleus-to-cytoplasm translocation of ZKSCAN3 [985]. The expression of the transcription factor EGR1 (early growth response 1) is rapidly increased upon nutrient deprivation and can directly increase transcription of multiple components of the autophagy machinery. The EGR1 DNA-binding motif is significantly enriched in the promoters/enhancers of autophagy-associated genes; EGR1 positively regulates the transcription of these genes (including *ATG2A*, *ATG14*, *ATG3*, *ATG13*, *ATG101*, *LC3B*, *PIK3C3*, *PPM1D*, *ULK1*, and *ZFYVE1*), and thereby increases the autophagic flux [986]. Transcription factor NFE2L2/NRF2, considered as the master regulator of cellular homeostasis, modulates the expression of autophagy-related genes, including the already mentioned *Sqstm1* but also *Atg2b*, *Atg4d*, *Atg5*, *Atg7*, *Calcoco2/Ndp52*, *Gabarapl1* and *Ulk1* [987]. Moreover, NFE2L2/NRF2 is a regulator of *Lamp2a* transcription, and therefore, it controls CMA [988]. This transcription factor may have a relevant role upon stressful conditions, including proteotoxic or oxidative insults. Finally, CEBPB/C/EBP β is a transcription factor that regulates autophagy in response to the circadian cycle in mice [989] and zebrafish [932].

Although less work has been done on post-transcriptional regulation, several studies implicate microRNAs in controlling the expression of proteins associated with autophagy [332-334, 990-993]. In this context, an important player is represented by *MIR27A*. Autophagy implementation is linked to ATP and HMGB1 release and ecto-CALR (calreticulin) exposure in HCT116 colon cancer cells with knockdown of *MIR27A*. This pathway is active in basal conditions, as indicated by the presence of the mature LC3-II form and acquisition of autophagic morphological features (large bodies, multiple or multilobated nuclei, cytosolic vacuoles and granules) when compared to control and *MIR27A*-overexpressing HCT116 cells. Methotrexate treatment triggers autophagy in time-course experiments, as the mature LC3-II form rapidly increases following *MIR27A* knockdown, whereas the change is limited in control and *MIR27A*-overexpressing HCT116

cells. Treatment with the lysosomotropic agent CQ confirms that the higher LC3-II levels reveal an augmented autophagic flux leading to autophagosome development. The mature LC3-II form shows a remarkable dose-dependent increase upon *MIR27A* knockdown with respect to control and especially *MIR27A*-overexpressing HCT116 cells [994].

Cautionary notes: Most of the *ATG* genes do not show significant changes in mRNA levels when autophagy is induced. Even increases in *LC3* mRNA can be quite modest and are cell type- and organism-dependent [995]. In addition, it is generally better to follow protein levels, which, ultimately, are the significant parameter with regard to the initiation and completion of autophagy. However, *ATG* protein amounts do not always change significantly, and the extent of increase is again cell type- and tissue-dependent. Finally, changes in autophagy protein levels are not sufficient evidence of autophagy induction and must be accompanied by additional assays as described herein. Thus, monitoring changes in mRNA levels for either *ATG* genes or autophagy regulators may provide some evidence supporting upregulation of the potential to undergo autophagy, but should be used along with other methods.

Another general caution pertains to the fact that in any cell culture system mixed populations of cells (for example, those undergoing autophagy or not) exist simultaneously. Therefore, only an average level of protein or mRNA expression can be evaluated with most methods. This means that the results regarding specific changes in autophagic cells could be hidden due to the background of the average data. Along these lines, experiments using single-cell qPCR to examine gene expression in individual cardiomyocytes with and without signs of autophagy reveal that the transcription of *MTOR* markedly and significantly increases in autophagic cells in intact cultures (spontaneously undergoing autophagy) as well as in cultures treated with proteasome inhibitors to induce autophagy (V. Dosenko, personal communication). Finally, researchers need to realize that mammalian cell lines may have mutations that alter autophagy signaling or execution; this problem can be avoided by using primary cells.

Conclusion: Although there are changes in *ATG* gene expression that coincide with, and may be needed for, autophagy, in most cases this has not been carefully studied experimentally. Therefore, at the present time we do not recommend the monitoring of *ATG* gene transcription as a general readout for autophagy unless there is clear documentation that the change(s) correlates with autophagy activity.

Posttranslational modifications

Autophagy is controlled by posttranslational modification (PTM) of *ATG* proteins such as phosphorylation, ubiquitination, acetylation, O-GlcNAcylation, N6-methyladenosine modification, oxidation and cleavage, which can be monitored to analyze the status of the process [293, 611, 767, 775, 996-1000]. The global deacetylation of proteins, which often accompanies autophagy, can be conveniently measured by quantitative immunofluorescence and western blotting with antibodies specifically recognizing acetylated lysine residues [1001]. Indeed, depletion of the nutrient supply causes autophagy in yeast or mammalian cells by reducing the nucleo-cytosolic pool of acetyl-

coenzyme A, which provides acetyl groups to acetyltransferases, thus reducing the acetylation level of hundreds of cytoplasmic and nuclear proteins [1002]. A global deacetylation of cellular proteins is also observed in response to so-called “caloric restriction mimetics”, that is, a class of pharmacological agents that deplete the nucleo-cytosolic pool of acetyl-coenzyme A, inhibit acetyltransferases (such as EP300) or activate deacetylases (such as SIRT1). All these agents reduce protein acetylation levels in cells as they induce autophagy [1003]. One prominent *ATG* protein that is subjected to pro-autophagic deacetylation is *LC3* [1004,1005]. Moreover, SIRT1 inhibition by EX-527 decreases the lipidation of *LC3* [1006]. Recently, ULK1 O-GlcNAcylation was shown to be crucial for autophagy initiation [1007,1008]; this modification potentiates AMPK-dependent phosphorylation of ULK1 and allows binding to and phosphorylation of *ATG14*, and subsequent activation of *PIK3C3/VPS34*.

Another mechanism through which autophagy-related proteins are regulated is by means of S-nitrosylation, the covalent binding of nitric oxide (NO) to specific cysteine residues [1009]. High levels of free NO have been linked to an overall inhibitory effect on autophagic machinery [1010]. Conversely, the modulation of the amount of S-nitrosylated proteins triggered by changes in the activity or expression of the denitrosylase *ADH5/GSNOR* (alcohol dehydrogenase 5 [class III], chi polypeptide), seems to have no major effects on nonselective autophagy, whereas there is an effect on the recognition of damaged mitochondria to be targeted for selective mitophagy [1011,1012]. Persulfidation (S-sulphydration) plays an important role in mitophagy-related proteins such as *PRKN*, whose catalytic activity is stimulated by persulfidation, whereas nitrosylation inactivates it [1013]. Mitophagy is also promoted by persulfidation of *USP8* (ubiquitin specific peptidase 8), which enhances deubiquitination of *PRKN* [1014]. Other important autophagy-related proteins such as *ATG3*, *ATG5*, *ATG7* and *ATG18A* in plants are also targets for persulfidation, but the role of this modification needs further clarification [1015].

Phosphorylation of other autophagic proteins plays a critical role in the regulation of autophagy activity. For example, *CSNK2* (casein kinase 2) and *ULK1* induce phosphorylation of *SQSTM1* at serine 403 and serine 409, respectively, increasing the binding affinity of *SQSTM1* for ubiquitin, and enhancing the autophagic degradation of ubiquitinated proteins [427,714]. Also, *EGFR* signaling induces multi-site tyrosine phosphorylation of *BECN1* to inhibit core autophagy machinery activation [775].

Finally, N6-methyladenosine (m^6A) mRNA modification plays an important role in regulating autophagy. *ULK1* mRNA undergoes m^6A modification in the 3' UTR, and the m^6A -marked *ULK1* transcripts can further be targeted for degradation by *YTHDF2* (YTH N6-methyladenosine RNA binding protein 2). Moreover, *FTO* (*FTO* alpha-ketoglutarate dependent dioxygenase) reverses the m^6A mRNA modification of *ULK1* transcripts, thereby promoting the initiation of autophagy [1016].

Autophagic protein degradation

Protein degradation assays represent a well-established methodology for measuring autophagic flux, and they allow good

quantification. The general strategy is first to label cellular proteins by incorporation of a radioactive amino acid (e.g., [^{14}C]- or [^3H]-leucine, [^{14}C]-valine or [^{35}S]-methionine; although valine may be preferred over leucine due to the strong inhibitory effects of the latter on autophagy), preferably for a period sufficient to achieve labeling of the long-lived proteins that best represent autophagic substrates, and then to follow this with a long cold-chase so that the assay starts well after labeled short-lived proteins are degraded (which occurs predominantly via the proteasome). Next, the time-dependent release of acid-soluble radioactivity from the labeled protein in intact cells or perfused organs is measured [4,25,1017]. Note that the inclusion of the appropriate unlabeled amino acid (i.e., valine, leucine or methionine) in the starvation medium at a concentration equivalent to that of other amino acids in the chase medium is necessary; otherwise, the released [^{14}C]-amino acid is effectively re-incorporated into cellular proteins, which results in a significant underestimation of protein degradation. A newer method of quantifying autophagic protein degradation is based on L-azidohomoalanine (AHA) labeling [1018,1019]. When added to cultured cells, L-azidohomoalanine is incorporated into proteins during active protein synthesis. After a click reaction between an azide and an alkyne, the azide-containing proteins can be detected with an alkyne-tagged fluorescent dye, coupled with flow cytometry. The turnover of specific proteins can also be measured in a pulse-chase regimen using the Tet-ON/OFF or GeneSwitch systems and subsequent western blot analysis [1020-1022].

In this type of assay a considerable fraction of the measured degradation will be nonautophagic, and thus it is important to also measure, in parallel, cell samples treated with autophagy-suppressive concentrations of 3-MA, SAR-405, bafilomycin A₁, CQ, ammonia, or amino acids, or generated under conditions of amino acid depletion, or in samples obtained from mutants missing central ATG components; these values are then subtracted from the total readouts. The complementary approach of using compounds that block other degradative pathways, such as proteasome and ER-associated degradation (ERAD) inhibitors, can also provide valuable information [216]. However, these inhibitors may sometimes cause unexpected results and should be interpreted with caution due to potential nonspecific effects and crosstalk among the degradative systems. For example, blocking proteasome function may activate autophagy [613 [1023-1026]], although those studies did not assess long-lived protein degradation. Studies that have directly compared the effects of proteasomal and lysosomal degradation inhibitors—alone and in combination—on long-lived protein degradation have demonstrated that proteasomal and lysosomal inhibitors have near perfectly additive effects [216,1027], thus suggesting that the crosstalk between the proteasomal and autophagic systems does not appreciably affect the results obtained in the long-lived protein degradation assay (although this does not exclude the possibility that this may occur under other conditions, so this needs to be tested from case to case). Conversely, interference with the CMA pathway does seem to activate a compensatory form of autophagy that increases the overall degradation of long-lived proteins [133,307]. In general, when using inhibitors, it is critical to know whether the inhibitors being used alter

autophagy in the particular cell type and context being examined. In addition, because 3-MA could have some autophagy-independent effects in particular settings it is advisable to verify that the 3-MA-sensitive degradation is also sensitive to specific class III PtdIns3K inhibitors such as SAR-405, and to general lysosomal inhibitors (such as NH₄Cl or leupeptin) [25,216].

The use of stable isotopes, such as ^{13}C and ^{15}N , in quantitative MS-based proteomics allows the recording of degradation rates of thousands of proteins simultaneously. These assays may be applied to autophagy-related questions enabling researchers to investigate differential effects in global protein or even organelle degradation studies [1028,1029]. Stable isotope labeling with amino acids in cell culture (SILAC) can also provide comparative information between different treatment conditions, or between a wild type and mutant.

Another assay that could be considered relies on the limited proteolysis of a BHMT (betaine-homocysteine S-methyltransferase) fusion protein. The 44-kDa full-length BHMT protein is cleaved in hepatocyte amphisomes in the presence of leupeptin to generate 32-kDa and 10-kDa fragments [1030-1033]. Accumulation of these fragments is time dependent and is blocked by treatment with autophagy inhibitors. A modified version of this marker, GST-BHMT, can be expressed in other cell lines where it behaves similar to the wild-type protein [1034]. Additional substrates may be considered for similar types of assays. For example, the neomycin phosphotransferase II-GFP (NeoR-GFP) fusion protein is a target of autophagy [620]. Transfection of lymphoblastoid cells with a plasmid encoding NeoR-GFP followed by incubation in the presence of 3-MA leads to an accumulation of the NeoR-GFP protein as measured by flow cytometry [1035].

A similar western blot assay is based on the degradation of a cytosolic protein fused to GFP. This method has been used in yeast and *D. discoideum* cells using GFP-Pgk1 and GFP-Tkt-1 (phosphoglycerate kinase and transketolase, respectively). In this case the relative amount of free GFP and the complete fusion protein is the relevant parameter for quantification; although it may not be possible to detect clear changes in the amount of the full-length chimera, especially under conditions of limited flux [40,52]. As described above for the marker GFP-Atg8-family proteins, nonsaturating levels of lysosomal inhibitors are also needed in *D. discoideum* cells to slow down the autophagic degradation, allowing the accumulation and detection of free GFP. It should be noted that this method monitors bulk autophagy because it relies on the passive transit of a cytoplasmic marker to the lysosome. Consequently, it is important to determine that the marker is distributed homogeneously in the cytoplasm.

Recently, the fluorescent coral protein Keima, which is resistant to lysosomal degradation, and which can be used to measure autophagic cargo flux to acidic environments [1036] has been fused (through genetic engineering) to a variety of cellular proteins, for example ribosomal, proteasomal, mitochondrial, or cytosolic proteins [1037]. These fusion proteins are proteolytically cleaved off from Keima and degraded (whereas Keima is stable). The cleavage can be detected by western blotting for Keima, where an increase in non-fused Keima reflects delivery of the fusion proteins to lysosomes. Thus, this approach represents a very versatile method to determine delivery of various cargo for

lysosomal proteolysis and thereby monitor both nonselective and selective autophagy [1037]. Generation of stable cell lines with inducible expression of the Keima fusion proteins may provide a more reliable result under certain conditions. For example, during oxidative stress the expression of the Keima fusion proteins themselves seem to be increased, possibly due to stress-induced activation of the *CMV* promoter. More reliable data are produced, especially for the high-turnover probe Keima-LC3, by inducing expression of the Keima-probe prior to the stimulus of interest, and then following the generation of cleaved Keima during a chase period (M. Torgersen, unpublished results).

Of note, however, the assay only assesses proteolytic activity, and cannot be used to tell whether the cargo has reached fully active autolysosomes or whether the degraded cargo is recycled to the cytosol. This is as opposed to the long-lived protein degradation assay, which is a true end-point measurement of autophagy, because it (with the inclusion of proper controls) can measure the amount of degraded, free amino acids (and short peptides) that have been released from the autolysosomes.

One of the most useful methods for monitoring autophagy in *S. cerevisiae* is the Pho8 Δ 60 assay. *PHO8* encodes a vacuolar phosphatase, which is synthesized as a zymogen before finally being transported to and activated in the vacuole [1038]. A molecular genetic modification that eliminates the first 60 amino acids prevents the mutant (Pho8 Δ 60) from entering the ER, leaving the zymogen in the cytosol. When autophagy is induced, the mutant zymogen is delivered to the vacuole nonselectively inside autophagosomes along with other cytoplasmic material. The resulting activation of the zymogen can be easily measured by enzymatic assays for phosphatase activity [356]. To minimize background activity, it is preferable to have the gene encoding the cytosolic Pho13 phosphatase additionally deleted (although this is not necessary when assaying certain substrates).

Cautionary notes: Measuring the degradation of long-lived proteins requires prior radiolabeling of the cells, and subsequent separation of acid-soluble from acid-insoluble radioactivity. The labeling can be done with relative ease both in cultured cells and in live animals [4], and has recently been scaled down to minimize the amount of radioactivity needed in cell culture experiments [25]. In cells, it is also possible to measure the release of an unlabeled amino acid by chromatographic methods, thereby obviating the need for prelabeling [1039]; however, it is important to keep in mind that amino acid release is also regulated by protein synthesis, which in turn is modulated by many different factors. In either case, one potential problem is that the released amino acid may be further metabolized. For example, branched chain amino acids are good indicators of proteolysis in hepatocytes, but not in muscle cells where they are further oxidized (A.J. Meijer, personal communication). In addition, the amino acid can be reincorporated into protein; for this reason, such experiments can be carried out in the presence of CHX, but this raises additional concerns (see *Turnover of autophagic compartments*). In the case of labeled amino acids, a nonlabeled chase is added where the tracer amino acid is present in excess (being cautious to avoid using an amino acid that inhibits autophagy), or by use of single-pass perfused organs

or superfused cells [1040,1041]. The perfused organ system also allows for testing the reversibility of effects on proteolysis and the use of autophagy-specific inhibitors in the same experimental preparation, which are crucial controls for proper assessment.

If the autophagic protein degradation is low (as it will be in cells in replete medium), it may be difficult to measure it reliably above the relatively high background of nonautophagic degradation. It should also be noted that the usual practice of incubating the cells under “degradation conditions,” that is, in a saline buffer, indicates the potential autophagic *capacity* (maximal attainable activity) of the cells rather than the autophagic *activity* that prevails *in vivo* or under rich-culture conditions. Finally, inhibition of a particular degradative pathway is typically accompanied by an increase in a separate pathway as the cell attempts to compensate for the loss of degradative capacity [1025]. This compensation might interfere with control measurements under conditions that attempt to inhibit autophagy; however, as the latter is the major degradative pathway, the contributions of other types of degradation over the course of this type of experiment are most often negligible. Another issue of concern, however, is that most pharmacological protease inhibitors have “off target” effects that complicate the interpretation of the data.

The Pho8 Δ 60 assay requires standard positive and negative (such as an *atg1 Δ* strain) controls, and care must be taken to ensure the efficiency of cell lysis. Glass beads lysis works well in general, provided that the agitation speed of the instrument is adequate. Instruments designed for liquid mixing with lower speeds should be avoided. We also recommend against holding individual sample tubes on a vortex, as it is difficult to maintain reproducibility; devices or attachments are available to allow multiple tubes to be agitated simultaneously. Finally, it is also important to realize that the deletion of *PHO8* can affect yeast cell physiology, especially depending on the growth conditions, and this may in turn have consequences for the cell wall; cells under starvation stress generate thicker cell walls that can be difficult to degrade enzymatically.

Conclusion: Measuring the turnover of long-lived proteins is a standard method for determining autophagic flux. Newer proteomic techniques that compare protein levels in autophagy-deficient animals relative to wild-type animals are promising [1042,1043], but the current ratiometric methods are affected by both protein synthesis and degradation, and thus analyze protein turnover, rather than degradation.

Selective types of autophagy

Although autophagy can be nonselective, in particular during starvation, there are many examples of selective types of autophagy.

The Cvt pathway, mitophagy, pexophagy, piecemeal microautophagy of the nucleus and late nucleophagy in yeast and filamentous fungi. The precursor form of aminopeptidase I (prApe1) is the major cargo of the Cvt pathway in yeast, a biosynthetic autophagy-related pathway [177]. The propeptide of prApe1 is proteolytically cleaved upon vacuolar delivery, and the resulting shift in molecular mass can be monitored by western blot. Under starvation conditions, prApe1 can enter

the vacuole through nonselective autophagy, and thus has been used as a marker for both the Cvt pathway and autophagy.

The yeast Cvt pathway is unique in that it is a biosynthetic route that utilizes the autophagy-related protein machinery, whereas other types of selective autophagy are degradative. The latter include pexophagy, mitophagy, reticulophagy and xenophagy, and each process has its own marker proteins, although these are typically variations of other assays used to monitor the Cvt pathway or autophagy. One common type of assay involves the processing of a GFP chimera similar to the GFP-Atg8 processing assay (see *GFP-Atg8-family protein lysosomal delivery and partial proteolysis*). For example, yeast pexophagy utilizes the processing of Pex14-GFP and Pot1/Fox3/thiolase-GFP [1044,1045], whereas mitophagy can be monitored by the generation of free GFP from Om45-GFP, Idh1-GFP, Idp1-GFP or mito-DHFR-GFP [1046-1050]. Important differences, however, can be observed between GFP chimera of endogenous mitochondrial proteins and an artificial construct such as mito-DHFR-GFP [1051]. In filamentous fungi, NBR1-dependent pexophagy can be monitored by inducing peroxisome proliferation through growth in fatty acid-containing medium and shifting the mycelium back to complete medium to visualize DsRED-labeled peroxisome degradation in the vacuole [1052]. Localization of mitochondrially-targeted proteins (or specific MitoTracker® dyes) or similar organelle markers such as those for the peroxisome (e.g., GFP-SKL with Ser-Lys-Leu at the C terminus that acts as a peroxisomal targeting signal, Aox3 [acyl-CoA oxidase 3]-EYFP that allows simultaneous observation of peroxisome-vacuole dynamics with the single FITC filter set, or GFP-Cta1 [catalase A]) can also be followed by fluorescence microscopy [831, 1045 [1053-1055]]. In addition, yeast mitophagy requires both the Slt2 and Hog1 signaling pathways; the activation and phosphorylation of Slt2 and Hog1 can be monitored with commercially available phospho-specific antibodies (Figure 26) [747]. It is also possible to monitor pexophagy in yeasts by the disappearance of activities of specific peroxisome markers such as catalase, alcohol oxidase or amine oxidase in cell-free extracts [1056], or permeabilized cell suspensions. Catalase activity, however, is a useful marker only when peroxisomal catalases are the

only such enzymes present or when activities of different catalases can be distinguished. In *S. cerevisiae* there are two genes, *CTT1* and *CTA1*, encoding catalase activity, and only one of these gene products, Cta1, is localized in peroxisomes. Activities of both catalases can be distinguished using an in-gel activity assay after PAGE under nondenaturing conditions by staining with diaminobenzidine [1057,1058]. Plate assays for monitoring the activity of peroxisomal oxidases in yeast colonies are also available [1054]. The decrease in the level of endogenous proteins such as alcohol oxidase, Pex14 or Pot1 can be followed by western blotting [831 [1059-1062], TEM [1063], fluorescence microscopy [831,1064,1065] or laser confocal scanning microscopy of GFP-labeled peroxisomes [1066,1067].

In yeast, nonselective autophagy can be induced by nitrogen-starvation conditions, whereas degradative types of selective autophagy generally require a carbon source change or ER stress for efficient induction. For example, in *S. cerevisiae*, to induce a substantial level of mitophagy, cells need to be pre-cultured in a nonfermentable carbon source such as lactate or glycerol to stimulate the proliferation of mitochondria (although this is not the case in *Komagataella phaffii*/Pichia pastoris). After sufficient mitochondria proliferation, shifting the cells back to a fermentable carbon source such as glucose will cause the autophagic degradation of superfluous mitochondria [1047]. It should be noted that in addition to carbon source change, simultaneous nitrogen starvation is also required for efficient mitophagy induction. This is possibly because excessive mitochondria can be segregated into daughter cells by cell division if growth continues [1047]. A similar carbon source change from oleic acid or methanol to ethanol or glucose (with or without nitrogen starvation) can be used to assay for pexophagy [1068]; whereas a shift to glucose induces micropexophagy, a shift to ethanol induces macropexophagy [1061]. Mitophagy can apparently be induced in *Magnaporthe oryzae* by treatment with ROS to induce mitochondrial damage [1069]; however, ROS or mitochondrial oxidative phosphorylation uncouplers such as CCCP do not induce mitophagy in *S. cerevisiae* [1048,1070]. Mitophagy can be induced by culturing yeast cells in a nonfermentable carbon source to post-log phase or before nitrogen starvation [1070,1071]. In this case, mitophagy may be induced because the energy demand is lower at post-log phase and the mitochondrial mass exceeds the cell's needs [169,1072,1073]. It has been suggested that this type of mitophagy, also known as "stationary phase mitophagy," reflects a quality-control function that culls defective mitochondria that accumulate in nondividing, respiring cells [1074]. Furthermore, there is some evidence that mitophagy can be induced in cells cultured with a fermentable carbon source such as glucose by a shift from nutrient-rich to nitrogen-starvation conditions, which makes it possible to examine mitophagy even in respiratory-deficient cells, although the amount of mitochondrial turnover may be quite low [1075]. Similarly, pexophagy can be induced by culturing the cells in a peroxisome proliferation medium to post-log phase (J.-C. Farré, unpublished results). Along these lines, it should also be realized that some types of selective autophagy continuously occur at a low level under noninducing conditions. Thus, organelles such as peroxisomes have a finite life span and are turned over at a slow rate by autophagy-related pathways [1076].

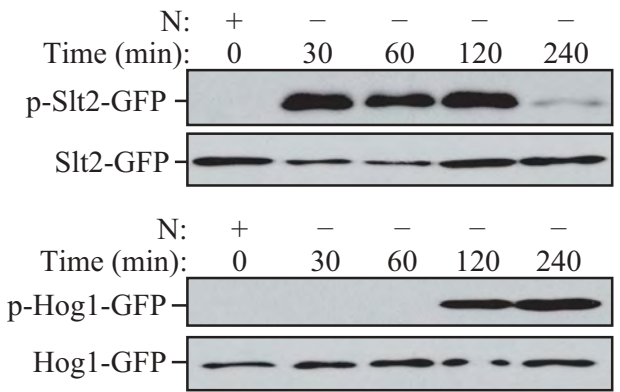


Figure 26. *S. cerevisiae* cells were cultured to mid-log phase and shifted to SD-N for the indicated times. Samples were taken before (+) and at the indicated times after (-) nitrogen starvation. Immunoblotting was done with anti-phospho-Slt2 and anti-phospho-Hog1 antibody. This figure was modified from data previously published in ref. [747], and is reproduced by permission of the American Society for Cell Biology, copyright 2011.

Piecemeal microautophagy of the nucleus (PMN, also termed micronucleophagy) is another selective autophagic subtype, which targets portions of the nucleus for degradation [157,1077,1078]. In *S. cerevisiae*, the nuclear outer membrane, which is continuous with the nuclear ER, forms contact sites with the vacuolar membrane. These nucleus-vacuole junctions (NVJs) are generated by interaction of the outer nuclear membrane protein Nvj1 with the vacuolar protein Vac8 [1079]. Nvj1 further recruits the ER-membrane protein Tsc13, which is involved in the synthesis of very-long-chain fatty acids (VLCFAs) and Swi1/Osh1, a member of a family of oxysterol-binding proteins. Upon starvation the NVJs bulge into the vacuole and subsequently a PMN-vesicle pinches off into the vacuole. PMN vesicles thus contain nuclear material and are limited by three membranes with the outermost derived from the vacuole, and the two inner ones from the nuclear ER. It is not clear which nuclear components are removed by PMN, but because PMN is not a cell death mechanism per se, it seems most likely that superfluous material is recycled. During PMN the NVJs are selectively incorporated into the PMN vesicles and degraded. Accordingly, PMN can be monitored using the proteins that are associated with the NVJs as markers. To quantitatively follow PMN, an assay analogous to the above-described GFP-Atg8 processing assay has been established using either GFP-Swi1/Osh1 or Nvj1-GFP. These GFP chimeras are, together with the PMN-vesicles, degraded in the vacuole. Thus, the formation of the relatively proteolysis-resistant GFP detected in western blots correlates with the PMN rate. In fluorescence microscopy, PMN can be visualized with the same constructs, and a chimera of mCherry fused to a nuclear localization signal (NLS-mCherry) can also be used. To assure that the measured PMN rate is indeed due to selective PMN/micro-nucleophagy, appropriate controls such as cells lacking Nvj1 or Vac8 should be included. Detailed protocols for the described assays are provided in ref [1080].

Late nucleophagy (LN) is another type of selective degradation of the nucleus, which specifically targets bulk nucleoplasm for degradation after prolonged periods (20-24 h) of nitrogen starvation [721]. LN induction occurs in the absence of the essential PMN proteins Nvj1 and Vac8 and, therefore, the formation of NVJs. Although, some components of the core Atg machinery are required for LN, Atg11 and the Vps34-containing PtdIns3K complex I are not needed. LN can be monitored by employing a nuclear-targeted version of the Rosella biosensor (n-Rosella) and following either its accumulation (by confocal microscopy), or degradation (by immunoblotting), within the vacuole [1081]. Dual labeling of cells with Nvj1-EYFP, a nuclear membrane reporter of PMN, and the nucleoplasm-targeted NAB35-DsRed.T3 (NAB35 is a target sequence for the Nab2 RNA-binding protein, and DsRed.T3 is the pH-stable, red fluorescent component of n-Rosella) allows detection of PMN soon after the commencement of nitrogen starvation, whereas delivery to the vacuole of the nucleoplasm reporter, indicative of LN, is observed only after prolonged periods of nitrogen starvation. Few cells show simultaneous accumulation of both reporters in the vacuole, indicating that PMN and LN are temporally and spatially separated [1081].

In contrast to unicellular yeasts, filamentous fungi form an interconnected mycelium of multinucleate hyphae containing up to 100 nuclei in a single hyphal compartment. A mycelial colony grows by tip extension with actively growing hyphae at the colony margin surrounded by an older, inner hyphal network that recycles nutrients to fuel the hyphal tips. By labeling organelle markers with GFP it is possible to show in *Aspergillus oryzae* that autophagy mediates degradation of basal hyphal organelles such as peroxisomes, mitochondria and entire nuclei [1082]. In contrast to yeast, PMN has not been observed in filamentous ascomycetes. In *M. oryzae*, germination of the conidiospore and formation of the appressorium is accompanied by nuclear degeneration in the spore [373]. The degradation of nuclei in spores requires the non-selective autophagy machinery, whereas conserved components of the PMN pathway such as Vac8 and Tsc13 are dispensable for nuclear breakdown during plant infection [1083]. Nuclei are proposed to function in storage of growth-limiting nutrients such as phosphate and nitrogen [1084,1085]. Similar to nuclei, mitochondria and peroxisomes are also preferentially degraded in the basal hyphae of filamentous ascomycetes [373 [1082-1086]].

Cautionary notes: The Cvt pathway has been demonstrated to occur only in yeast. In addition, the sequestration of prApe1 is specific, even under starvation conditions, as it involves the recognition of the propeptide by a receptor, Atg19, which in turn interacts with the scaffold protein Atg11 [1087,1088]. Thus, unless the propeptide is removed or the genes encoding Atg11 or Atg19 are deleted, prApe1 is recognized as a selective substrate. Overexpression of prApe1 saturates import by the Cvt pathway, and the precursor form accumulates, but is rapidly matured upon autophagy induction [408]. In addition, mutants such as *vac8Δ* and *tlg2Δ* accumulate prApe1 under nutrient-rich conditions, but not during autophagy [745,1089]. Accordingly, it is possible to monitor the processing of prApe1 when overexpressed, or in certain mutant strains to follow autophagy induction. However, under the latter conditions it must be kept in mind that the sequestering vesicles are substantially smaller than typical autophagosomes generated during nonselective autophagy; the Cvt complex (prApe1 bound to Atg19) is smaller than typical peroxisomes or mitochondrial fragments that are subject to autophagic degradation. Accordingly, particular mutants may display complete maturation of prApe1 under autophagy-inducing conditions, but may still have a defect in other types of selective autophagy, as well as being unable to induce a normal level of nonselective autophagy [148]. For this reason, it is good practice to evaluate autophagosome size and number by TEM. Actually, it is much simpler to monitor autophagic bodies (rather than autophagosomes) in yeast. First, the vacuole is easily identified, making the identification of autophagic bodies much simpler. Second, autophagic bodies can be accumulated within the vacuole, allowing for an increased sample size. It is best to use a strain background that is *pep4Δ vps4Δ* to prevent the breakdown of the autophagic bodies, and to eliminate confounding vesicles from the multivesicular body pathway. One caveat to the detection of autophagic bodies, however, is that they may coalesce in the vacuole lumen, making it difficult to obtain

an accurate quantification. Finally, it is important to account for biases in sample sectioning to obtain an accurate estimate of autophagic body number or size [147].

In general, when working with yeast it is preferable to use strains that have the marker proteins integrated into the chromosome rather than relying on plasmid-based expression, because plasmid numbers can vary from cell to cell. The GFP-Atg8, or a similar, processing assay is easy to perform and is suitable for analysis by microscopy as well as western blotting; however, particular care is needed to obtain quantitative data for GFP-Atg8, Pex14-GFP or Om45-GFP, etc. processing assays (see cautionary notes for *GFP-Atg8-family protein lysosomal delivery and partial proteolysis*).

A pHluorin-Atg8 chimera can be used to determine the breakdown of autophagic bodies in budding yeast by live cell fluorescence microscopy. In WT cells, fluorescence of pHluorin-Atg8 is detectable at neutral pH in the cytosol and at the PAS or on autophagosomes, but not at the lower pH within the vacuole upon starvation. In mutants that are either deficient in vacuolar peptidases (*atg42Δ*, *pep4Δ*, *prb1Δ*, *prc1Δ*) or vacuolar acidification (*vma4Δ*) pHluorin-Atg8 is not quenched and pHluorin-Atg8-positive vesicular structures are detected inside their vacuoles, suggesting that autophagic bodies are not efficiently lysed. Hence, pHluorin-Atg8 is a useful tool to detect defects in the breakdown of autophagic bodies inside vacuoles [1090].

An alternative method to monitor selective autophagy is to use an organelle-targeted Pho8Δ60 assay. For example, mitoPho8Δ60 can be used to quantitatively measure mitophagy [1048]. In addition, for the GFP-Atg8 processing assay, 2 h of starvation is generally sufficient to detect a significant level of free (i.e., vacuolar) GFP by western blotting as a measure of nonselective autophagy. For selective types of autophagy, the length of induction needed for a clearly detectable free GFP band will vary depending on the rate of cargo delivery/degradation. Usually 6 h of mitophagy induction is needed to be able to detect free GFP (e.g., from Om45-GFP) by western blot under starvation conditions, whereas stationary phase mitophagy typically requires 2 days before a free GFP band is observed. However, as with animal systems (see *Animal mitophagy and pexophagy*), it would be prudent to follow more than one GFP-tagged protein, as the kinetics, and even the occurrence of mitophagic trafficking, seems to be protein species-dependent, even within the mitochondrial matrix [1091]. The use of an artificial, non-mitochondrial protein as a chimeric mitophagy reporter (such as mtDHFR-GFP) can apparently be used as a reporter for “general” mitophagy as it does not appear to have any endogenous “selectivity” cues [1051].

Aggrephagy. Aggrephagy is the selective removal of aggregates by autophagy [1092]. This process can be followed in vitro (in cell culture) and in vivo (in mice) by monitoring the levels of an aggregate-prone protein such as an expanded polyglutamine (polyQ)-containing protein or mutant MAPT/tau or SNCA/α-synuclein (synuclein alpha). Levels are quantified by immunofluorescence, immunogold labeling, filter-trap assay or traditional immunoblot. In yeast, degradation of SNCA aggregates can be followed by promoter shut-off assays. Expression of the inducible *GAL1* promoter of GFP-

tagged SNCA is stopped by glucose repression. The removal of aggregates is thus monitored with fluorescence microscopy.

The relationship between SNCA clearance and autophagy has also been exploited in yeast studies during chronological aging with SNCA expressed under the control of a constitutive promoter [347,349,366,629]. In this model, SNCA toxicity is dependent on Atg11 [366] and promotes cell cycle re-entry, S-phase arrest, and DNA damage response activation, which is responsible for a dramatic increase in autophagy [349]. This selective pathway of autophagy has been termed genotoxin-induced targeted autophagy (GTA) and, in addition to Atg11, requires the involvement of the Mec1 and Rad53 kinases [1093].

The contribution of autophagy to SNCA aggregate clearance can be studied by the use of different autophagy mutants or by pharmacological treatment with the proteinase B inhibitor PMSF [1094-1096]. Similarly, fluorescently tagged aggregated proteins such as polyQ80-CFP can be monitored via immunoblot and immunofluorescence. In addition to fluorescence methods, aggregates formed by a splice variant of CCND2 (cyclin D2) can also be monitored in electron-dense lysosomes and autophagosomes by immunogold labeling and TEM techniques [1097]. A polyQ80-luciferase reporter, which forms aggregates, can also be used to follow aggrephagy [1098]. A nonaggregating polyQ19-luciferase or untagged full-length luciferase serves as a control. The ratio of luciferase activity from these two constructs can be calculated to determine autophagic flux.

Autophagic clearance of mutated human HTT (huntingtin) protein with a polyQ expansion (HTT103Q) can also be observed in budding yeast. After overnight induction from a galactose inducible promoter, HTT103Q proteins form inclusion bodies in yeast cells. When glucose is added into the cell culture to shut off HTT103Q expression, obvious vacuolar localization of the protein is detected within 1 h, and this localization depends on the core autophagy machinery. Moreover, the absence of the ubiquitin protein Dsk2 and some heat-shock proteins compromises the vacuolar localization of HTT103Q [1099,1100]. Therefore, mutated HTT protein can be used as a model substrate to study aggrephagy.

Autophagic degradation of endogenous aggregates such as lipofuscin can be monitored in some cell types by fluorescence microscopy, utilizing the autofluorescence of lipofuscin particles. Although under normal conditions almost 99% of the lipofuscin particles are located in autophagosomes or lysosomes, an impairment of autophagy leads to free lipofuscin in the cytosol [1101,1102]. The amount of lipofuscin in primary human adipocytes can be reduced by activation of autophagy, and the amount of lipofuscin is dramatically reduced in adipocytes from patients with type 2 diabetes and chronically enhanced autophagy [396]. Monitoring autophagy in tissues with lipofuscin accumulation is not possible using a mouse reporter model expressing GFP-LC3, because cytosolic lipofuscin appears as a hyperfluorescent punctum in the green channel [485]. A tandem tagged LC3 reporter model (CAG-mRFP-EGFP-LC3 [1103]) will be better suited to study pathologies involving lipofuscin accumulation. ImageJ, or other equivalent software, should be utilized to detect GFP-positive puncta that colocalize with RFP-positive structures.

Cytosolic lipofuscin will appear as an RFP-independent GFP (green) punctum.

Similarly, TFEB overexpression either in neurons or oligodendrocytes reduces neurodegeneration and the pathological burden of SNCA in many experimental models of synucleinopathies reported by independent investigators [1104-1106].

Cautionary notes: Caution must be used when performing immunoblots of aggregated proteins, as many protein aggregates fail to enter the resolving gel and are retained in the stacking gel. This drawback can be bypassed by performing a filter-trap assay in which protein extracts are forced by mild suction through a nitrocellulose membrane, and protein aggregates larger than the nitrocellulose pores are stuck on the membrane and can then be detected by traditional immunoblot [1107]. In addition, the polyQ80-luciferase in the aggregated state lacks luciferase activity, whereas soluble polyQ80-luciferase retains activity. Therefore, caution must be used when interpreting results with these vectors, as treatments that increase aggregate formation or enhance protein aggregation can lead to a decrease in luciferase activity [1108]. Finally, soluble polyQ reporters can be degraded by the proteasome; thus, changes in the ratio of polyQ19-luciferase:polyQ80-luciferase may also reflect proteasomal effects and not just changes in autophagic flux.

Allophagy. In *C. elegans*, mitochondria, and hence paternal mitochondrial DNA, from sperm are eliminated by an autophagic process. This process of allogeneic (nonself) organelle autophagy is termed “allophagy” [1109,1110]. During allophagy in *C. elegans*, both paternal mitochondria and membranous organelles (a sperm-specific membrane compartment) are eliminated by the 16-cell stage (100-120 min post-fertilization) [1111,1112]. The degradation process can be monitored in living embryos with GFP::ubiquitin, which appears in the vicinity of the sperm chromatin (labeled for example with mCherry-histone H2B) on the membranous organelles within 3 min after fertilization. GFP fusions and antibodies specific for LGG-1 and LGG-2 (Atg8-family protein homologs), which appear next to the sperm DNA, membranous organelles and mitochondria (labeled with CMXRos or mitochondria-targeted GFP) within 15 to 30 min post-fertilization, can be used to verify the autophagic nature of the degradation. TEM [1113-1115] can also be utilized to demonstrate the presence of mitochondria within autophagosomes in the early embryo. The respective functions of LGG-1 and LGG-2 have been addressed by RNAi depletion or through the use of genetic loss-of-function mutants *lgg-1(tm3489)* and *lgg-2(tm5755)*. LGG-1 is essential for autophagosome formation, whereas LGG-2 contributes to their efficient maturation [1114]. Ubiquitination of the substrates was first described for the membranous organelles and not for sperm-inherited mitochondria [1111,1112], but studies suggest that ubiquitination of sperm-mitochondria could be required for the initial step of allophagy [1116,1117]. The autophagy receptor ALLO-1 and its kinase IKKE-1 are required for the recruitment of LGG-1 around sperm-inherited organelles [1116]. This autophagy targeting requires both the ubiquitination of substrates and the loss of sperm mitochondrial membrane potential [1116,1118,1119].

Conclusion: There are many assays that can be used to monitor selective types of autophagy, but caution must be

used in choosing an appropriate marker(s). The potential role of other degradative pathways for any individual organelle or cargo marker should be considered, and it is advisable to use more than one marker or technique.

Animal mitophagy and pexophagy. There is no consensus at the present time with regard to the best method for monitoring mitophagy in animal cells. As with any organelle-specific form of autophagy, it is necessary to demonstrate: i) increased levels of phagophores interacting with, or autophagosomes containing, mitochondria; ii) maturation of these autophagosomes that culminates with mitochondrial degradation, which can be blocked by specific inhibitors of autophagy or of lysosomal degradation; and iii) whether the changes are due to selective mitophagy or increased mitochondrial degradation during nonselective autophagy. Techniques to address each of these points have been reviewed [55,1120]. Note that a common misconception is that mitophagy can be monitored *via* RT-qPCR of mRNA transcripts encoding mitophagy-associated factors (e.g., PINK1, PRKN, etc.); in fact, changes in mRNA levels of these factors do not necessarily reflect mitophagic activity and should not be used to infer changes in mitophagy in the absence of other assays.

The following methods can be used to follow all forms of mitophagy: Ultrastructural analysis by TEM at early time points can be used to establish selective mitophagy. It should be noted that a detailed handbook on how to specifically dissect the several phases of the mitophagic process by TEM is not available. This should ideally include an initial phase of mitochondrial fragmentation, followed by formation of a double-layered membrane that expands around the selected organelle to form a double-membrane mitophagosome that contains mitochondria-like structure. TEM can be used to demonstrate the presence of mitochondria within these vesicles, and this can be coupled with bafilomycin A₁ or CQ treatment to prevent fusion with the lysosome to trap early autophagosomes with recognizable cargo [55] (Figure 4). In the later phase, and in the absence of maturation inhibitors, it might become difficult to clearly identify mitochondria-like structures inside the mitophagosomes; however, these should be appropriate in size, retain a double-membrane structure, and contain remnants of mitochondrial cristae. Depending on the use of specific imaging techniques, dyes for living cells or antibodies for fixed cells have to be chosen. In any case, transfection of the phagophore and autophagosome marker GFP-LC3 to monitor the initiation of mitophagy, or RFP-LC3 to assess mitophagy progression, and visualization of mitochondria (independent of their mitochondrial membrane potential) makes it possible to determine the association of these two cellular compartments. Qualitatively, this may appear as fluorescence colocalization or as rings of GFP-LC3 surrounding mitochondria in higher-resolution images [201,1113,1121].

Care must be taken in interpreting these results, as some data indicate that autophagosomes form at ER-mitochondria contact sites [872]; hence, there will be some degree of colocalization between forming (non-mitophagic) autophagosomes and mitochondria. Fluorescence microscopy-based approaches for monitoring autophagosome or lysosome

colocalization with mitochondria in cells in which cytoplasm is almost fully occupied by mitochondria, such as brown adipocytes, may be particularly challenging. Background thresholds should be accurately set to avoid false positive results.

For live-cell imaging microscopy, mitochondria should be labeled by a matrix-targeted fluorescent protein through transfection or by the use of mitochondria-specific dyes. When using matrix-targeted fluorophores for certain cell lines (e.g., SH-SY5Y), it is important to allow at least 48 h of transient expression for sufficient targeting/import of mitochondrial GFP/RFP prior to analyzing mitophagy. Among the MitoTracker® probes are lipophilic cations that include a chloromethyl group and a fluorescent moiety. These probes concentrate in mitochondria due to their negative charge and react with the reduced thiols present in mitochondrial matrix proteins [1122–1124]. After this reaction, the probe can be fixed and remains in the mitochondria independent of subsequent alterations in mitochondrial function or mitochondrial membrane potential [1123,1125,1126]. This method can thus be used when cells remain healthy when the dye is applied, as the dye will remain in the mitochondria and is retained after fixation, although, as stated above, accumulation is dependent on the membrane potential. In addition, it is important to note that the various mitochondrial dyes are not identical in terms of their properties, and not all are suitable for use following fixation. For example, MitoTracker® Green FM is not retained well after aldehyde fixation, whereas MitoTracker® Red CMXRos works under these conditions. Although in some cases it is convenient to utilize the fixation step, it is possible to evaluate fresh, unfixed cells, and, consequently, with less manipulated mitochondria, obtain good results with both flow cytometry and confocal microscopy [1127]. Transfection with mitochondrially targeted fluorescent proteins can also be used with similar results to MitoTracker® Green FM [201]. Antibodies that specifically recognize mitochondrial proteins such as VDAC, TOMM20/TOM20 (translocase of outer mitochondrial membrane 20), SOD2 (superoxide dismutase 2), HSPD1/HSP60 (heat shock protein family D [Hsp60] member 1), HSPA9/mtHSP70 or COX4I1 (cytochrome c oxidase subunit 4I1) may be used to visualize mitochondria in immunohistochemical experimental procedures [1128–1132] or in human patient samples [1133].

Colocalization analyses of mitochondria and autophagosomes provide an indication of the degree of autophagy

sequestration. To quantify early mitophagy, the percentage of LC3 puncta (endogenous, RFP- or GFP-LC3 puncta) that colocalize with mitochondria and the number of colocalizing LC3 puncta per cell—as assessed by confocal microscopy—in response to mitophagic stimuli can be employed as well [1134]. Of note, PINK-PRKN-dependent mitophagy is independent of the LC3 subfamily, but strongly requires the GABARAPs [34,35]. Conversely, LC3 is involved in cardiolipin-mediated mitophagy [201]. Thus, monitoring of more than on Atg8 subfamily may be necessary. In addition, the percentage of lysosomes that colocalize with mitochondria can be used to quantify autophagy-mediated delivery of mitochondria. Furthermore, induction of mitophagy also promotes the formation of ring-shaped/spheroid mitochondria interacting with structures positive for LC3 and lysosomal proteins (based on immuno-EM). It is not clear whether these structures represent forming autophagosomes dedicated to the degradation of mitochondria, or whether they represent a distinct process of mitochondrial dynamics [1135,1136]. Overall, it is important to quantify mitophagy at various stages (initiation, progression, and late mitophagy) to identify stimuli that elicit this process [1137,1138].

The fusion process of mitophagosomes with hydrolase-containing lysosomes represents the next step in the degradation process. To monitor the amount of fused organelles via live cell imaging microscopy, MitoTracker® Green FM and LysoTracker™ Red DND-99 may be used to visualize the fusion process (Figure 27). Independent of the cell-type specific concentration used for both dyes, we recommend exchanging MitoTracker® Green FM medium with normal medium (preferably phenol red-free and CO₂ independent to reduce unwanted autofluorescence) after incubation with the dye, whereas it is best to maintain the LysoTracker™ Red stain in the incubation medium during the acquisition of images. Given that these fluorescent dyes are extremely sensitive to photobleaching, it is critical to perform live cell mitophagy experiments via confocal microscopy, preferably by using a spinning disc confocal microscope for long-term imaging experiments. For immunocytochemical experiments, antibodies specific for mitochondrial proteins and an antibody against LAMP1 (lysosomal associated membrane protein 1) can be used. Overlapping signals appear as a merged color and can be used as indicators for successful fusion of autophagosomes that contain mitochondria with lysosomal

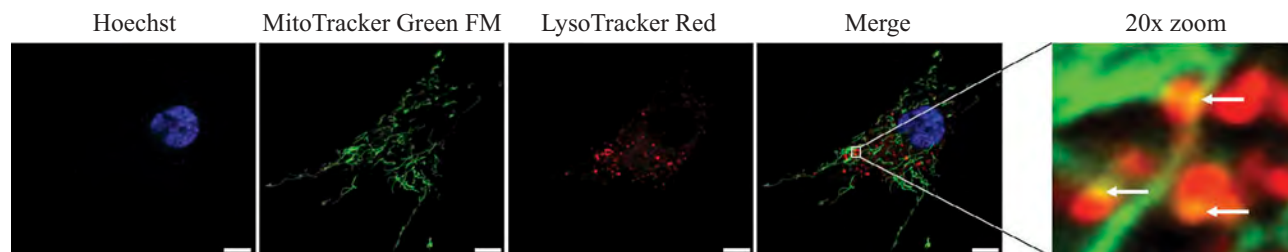


Figure 27. Human fibroblasts showing colocalization of mitochondria with lysosomes. The degree of colocalization of mitochondria with lysosomes in human fibroblasts was measured via live cell imaging microscopy at 37°C and 5% CO₂ atmosphere using the ApoTome® technique. LysoTracker™ Red DND-99 staining was applied to mark lysosomal structures (red), and MitoTracker™ Green FM to visualize mitochondria (green). Hoechst 33342 dye was used to stain nuclei (blue). A positive colocalization is indicated by yellow signals (Merge) due to the overlap of LysoTracker™ Red and MitoTracker™ Green staining (white arrows). Scale bar: 10 μm. Statistical evaluation is performed by calculating the Pearson's coefficient for colocalizing pixels. Image provided by L. Burbulla and R. Krüger.

structures [1139]. To measure the correlation between two variables by imaging techniques, such as the colocalization of two different fluorescent signals, we recommend some form of correlation analysis to assess the value correlating with the strength of the association. This may use, for example, ImageJ software or other colocalization scores that can be derived from consideration not only of pixel colocalization, but also from a determination that the structures have the appropriate shape. During live-cell imaging, the two structures (autophagosomes and mitochondria) should move together in more than one frame. Mitophagy can also be quantitatively monitored using a mitochondria-targeted version of the pH-dependent Keima protein [1036]. The peak of the excitation spectrum of the protein shifts from 440 nm to 586 nm when mitochondria are delivered to acidic lysosomes, which can provide a quantitative readout of mitophagy (Figure 28). However, it should be noted that long exposure time of the specimen to intense laser light leads to a similar spectral change. mt-Keima in combination with flow cytometry has been used to quantitatively monitor mitophagy flux [1130,1140,1141].

It is important to note that in a process distinct from mitophagy, mitochondria and lysosomes can also become dynamically tethered to one another in a RAB7A-GTP hydrolysis-dependent manner at inter-organelle mitochondria-lysosome contact sites, which are important for regulating mitochondrial dynamics [1142-1144]. Thus, high-resolution microscopy and preferably live cell imaging are strongly recommended to differentiate mitophagy (which results in mitochondria engulfed within the lysosomal membrane) from stably tethered mitochondria-lysosome contacts (mitochondria that are in contact [<10 nm] from a lysosome and can subsequently untether from one another without undergoing bulk mitochondrial degradation).

Finally, a mitochondria-targeted version of the tandem mCherry-GFP fluorescent reporter (see *Tandem mRFP/mCherry-GFP fluorescence microscopy*) using a targeting sequence from the mitochondrial membrane protein FIS1 [460,461] can be used to monitor mitophagic flux [460]. In addition, transgenic mice and *Drosophila* expressing mt-

Keima, mito-QC or mt-mCherry-GFP provide useful tools for analysis of mitophagy in vivo in many physiological and pathological conditions [38, 466, 1145-1148]. The tandem fluorescent and the mitochondrially-targeted Keima fluorescence microscopy approaches both assess delivery of mitochondria to acidic (endo-lysosomal) environments. To evaluate whether these acidic environments are proteolytically active, the cleavage of ectopically expressed TOMM20-Keima (or other mitochondria-targeted Keima fusion proteins) can be followed by western blotting [1037]. Whereas TOMM20 is sensitive to proteolytic enzymes, Keima is resistant, and thus the appearance of free Keima in the western blot indicates arrival of the mitochondria-targeted fusion protein to a proteolytic environment (lysosomes). The fold-change in TOMM20-Keima cleavage upon treatment with an autophagic stimulus can be compared with the fold change in the cleavage of a cytosolic Keima fusion protein (e.g., LDHB-Keima), to thereby assess the degree of selectivity of the autophagic response towards mitochondria over cytosolic proteins.

The third and last step of monitoring the degradation process is to examine the amount of remaining mitochondria by analyzing the mitochondrial mass. This final step provides the opportunity to determine the efficiency of degradation of dysfunctional, aged or impaired mitochondria. Mitochondrial mass can either be measured by a flow cytometry technique using MitoTracker® Green FM (or MitoTracker® Deep Red FM to monitor mitochondria with a polarized membrane) [1123] on a single-cell basis, by either live cell imaging or immunocytochemistry (using antibodies specifically raised against different mitochondrial proteins or, less specifically, by staining with acridine orange 10-nonyl bromide applied after chemical fixation [1149,1150]). Alternatively, mitochondrial content in response to mitophagic stimuli (in the presence and absence of autophagy inhibitors to assess the contribution of mitophagy) in live or fixed cells can be quantified at the single-cell level as the percentage of cytosol occupied by mitochondrial-specific fluorescent pixels using NIH ImageJ [1138,1151], specifically by using the MiNA plugin [1152]. One caveat of the latter is that mitochondrial mass may be overestimated when organelle swelling has occurred. Immunoblot analysis of the levels of

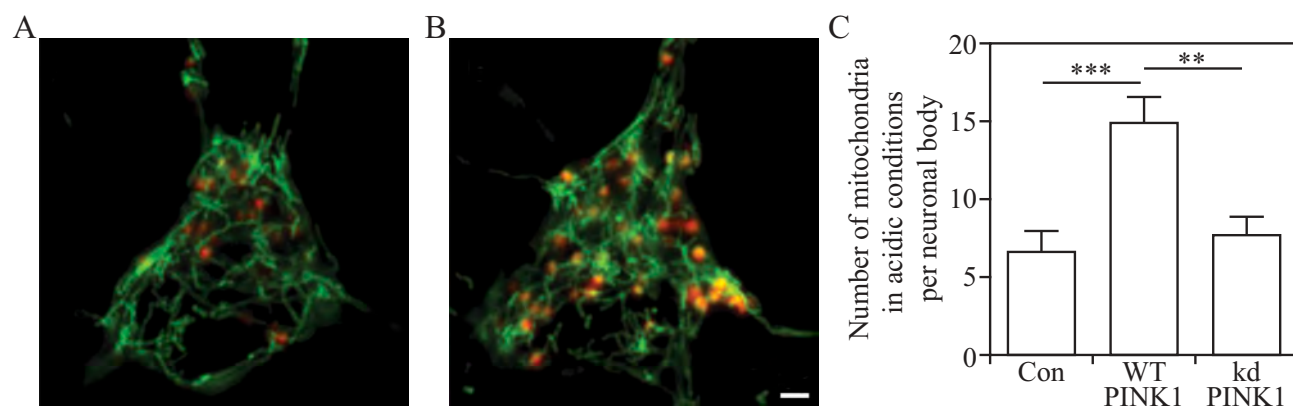


Figure 28. Detection of mitophagy in primary cortical neurons using mitochondria-targeted Keima. Neurons transfected with mito-Keima were visualized using 458-nm (green, mitochondria at neutral pH) and 561-nm (red, mitochondria in acidic pH) laser lines and 575-nm band pass filter. Compared with the control (A) wild-type PINK1 overexpression (B) increases the number of the mitochondria exposed to acidic conditions. Scale bar: 2 μ m. (C) Quantification of red puncta suggests increased mitophagy in wild-type PINK1 but not in the kinase dead (kd) PINK1^{K219M}-overexpressing neurons. Image provided by V. Choubey and A. Kaasik.

mitochondrial proteins from different mitochondrial subcompartments is valuable for validating the data from flow cytometry or microscopy studies, and it should be noted that OMM proteins, such as MFNs (mitofusins), TOMM complex proteins, and VDACs, but also PRKN, can be degraded by the proteasome, especially in the context of mitochondrial depolarization [1153-1155]. EM can also be used to verify loss of entire mitochondria, and qPCR (or fluorescence microscopy) to quantify mitochondrial DNA. A reliable estimation of mtDNA copy number per cell can be performed by qPCR of the *MT-ND1* (mitochondrially encoded NADH dehydrogenase 1) or *MT-ND2* gene expressed as a ratio of mtDNA:nuclear DNA by normalizing to that of the single nuclear-encoded PKM (pyruvate kinase M1/2) or *TERT* (telomerase reverse transcriptase) genomic DNA [764]. The spectrophotometric measurement of the activity of CS (citrate synthase) [1156], a mitochondrial matrix enzyme of the tricarboxylic acid cycle, which remains highly constant in these organelles and is considered a reliable marker of their intracellular content, has been used as a marker of mitochondrial mass in a variety of systems [1156-1159]. Mitophagy induction can also be examined by using mitochondrial fractionation followed by immunoblot to detect the levels of mitophagic or autophagosome-associated proteins (e.g., PRKN, LC3-II and SQSTM1) in the mitochondrial fraction. The levels of mitochondria-localized DNML/Drp1 (dynamin 1 like), which is involved in mitochondrial fission, could also be used to detect early events of mitophagy induction, because mitochondrial fission is required for mitophagy [1160], although mitochondrial DNML levels do not necessarily reflect a change in mitophagy.

Each of these techniques to monitor structures associated with the different steps of mitophagy—whether by single-cell analyses of Atg8-family protein mitochondrial colocalization or by immunoblotting for mitochondrial markers—can be combined with strategic use of inhibitors to determine whether mitophagy is impaired or activated in response to stimuli, and at which steps. Therefore, appropriate treatment (pharmacological inhibition and/or siRNA-mediated knockdown of *ATG* genes) may be applied to prevent mitochondrial degradation at distinct steps of the process. A recent method using flow cytometry in combination with autophagy and mitophagy inhibitors has been developed to determine mitophagic flux using MitoTracker® probes [1123]. Alternatively, mitophagic flux can be monitored by flow cytometry in cells from mito-Keima mice. In this case, it is important to remove dead cells on the basis of SYTOX Blue staining. As a positive control of the assay, carbonyl cyanide p-trifluoromethoxyphenyl-hydrazone (FCCP) is a potent mitochondrial uncoupler that stimulates mitophagic activity [1161].

Certain cellular models require stress conditions to measure the mitochondrial degradation capacity, as basal levels are too low to reliably assess organelle clearance. Exceptions include developmental clearance of large amounts of mitochondria as observed in erythrocyte maturation [1162], and during neuronal development where massive mitophagy is essential to promote a metabolic change towards glycolysis that is required for neurogenesis [1151]. Hence, it may be useful to treat cells with uncoupling agents, such as CCCP, that stimulate mitochondrial degradation and allow measurements of mitophagic activity. In this scenario, it has recently

been proposed that assessing the amount of mitochondrial proteins through western blot at basal level and after CCCP administration in human cells may be useful to assess the mitophagic flux [1163,1164]; however, it should be kept in mind that this treatment is not physiological and promotes the rapid degradation of outer membrane-localized mitochondrial proteins in addition to the loss of mitochondrially-derived ATP used for cellular work. In part for this reason a milder mitophagy stimulus has been developed that relies on a combination of antimycin A (AMA) and oligomycin, inhibitors of the electron transport chain and ATP synthase, respectively [1165]; this treatment is less toxic, and the resulting damage is time dependent. However, this treatment not only blocks ATP production by mitochondria but also substantially enhances mitochondrial ROS production inducing mitochondrial damage. The pharmacological compound PMI that pharmacologically induces mitophagy without disrupting mitochondrial respiration [1166] should provide further insight as it circumvents the acute, chemically induced, blockade of mitochondrial respiration. In addition, the molecule cloxyquin (not to be confused with chloroquine) also induces mitophagy via a mild uncoupling mechanism [444]. In certain conditions/cell types, mitophagy can be induced by NAD-boosting strategies [1167,1168]. Another method to induce mitophagy is by the treatment of cells with hypoxia-inducing and iron-deprivation agents. Mitochondria are the major site for oxygen consumption, and deprivation of oxygen induces receptor (FUNDC1, BNIP3, BNIP3L)-dependent mitophagy [1169-1171]. Treatment of animals including mice, *Drosophila* and *C. elegans* [1145,1148,1172] under hypoxic conditions or by exposure to iron-deprivation agents (deferiprone/DFP) induces mitochondrial degradation in different tissues, although the degrees of mitophagic activation are not the same in different organs. More specific induction of mitophagy can be achieved by expressing and activating a mitochondrially-localized fluorescent protein photosensitizer such as Killer Red [1173]. The excitation of Killer Red results in an acute increase of superoxide, due to phototoxicity, that causes mitochondrial damage resulting in mitophagy [462]. The advantage of using a genetically encoded photosensitizer is that it allows for both spatial and temporal control in inducing mitophagy. The forced targeting of AMBRA1 to the external mitochondrial membrane is sufficient to induce mitophagy [1174], and expression of constitutively active MAPK1 is sufficient to drive mitophagy in otherwise uninjured tumor cells [1138]. Finally, mitophagy can also be induced in vitro in different cell types by inhibiting the proteasome with the specific inhibitor IU1 [1175]. This type of mitophagy is induced following proteasome recruitment to mitochondria to expose the inner mitochondrial membrane mitophagy receptor PHB2 [1176], and is PINK1- and PRKN-independent [1175].

Mitochondrial turnover, mitochondrial oxidative stress and mitophagy can also be monitored through the use of MitoTimer, a time-sensitive fluorescent protein that targets to the mitochondrial matrix; the emission of MitoTimer shifts from green to red over time [1177-1179]. A lentiviral inducible system encoding MitoTimer is available allowing the controlled expression of this transgene in a wide range of cells

[1180]. A constitutively active plasmid DNA encoding MitoTimer as well as inducible transgenic flies and mice allow quantification of mitochondrial structure (fluorescent labeling of mitochondria), oxidative tension (red:green ratio) and mitophagy (pure red puncta that are positive for the mitochondrial protein COX4I1/Cox4 and the lysosomal marker LAMP1) in a variety of tissues, organs and whole animals [1177, 1179, 1181-1187]. Mitophagy can be monitored in mouse primary cells by exploiting the mitoQC mouse model, which ubiquitously expresses a GFP-mCherry tandem protein targeting the mitochondrial outer membrane [38], and the mt-Keima mouse model, which expresses a pH-sensitive protein targeting the mitochondrial matrix [1145].

It is important to keep in mind that there are multiple distinct or partially overlapping pathways of cargo recognition for selective mitophagy [1188]. These include PINK1-PRKN-dependent pathways utilizing p-S65-Ub, receptor-mediated mitophagy involving LIR-domain proteins, and the recognition of mitochondrial phospholipids such as cardiolipin by the LC3 phagophore system [201,1189,1190]; among others. Thus, it would be inappropriate to conclude that selective mitophagy is not occurring if markers of only one cargo recognition system are considered.

Antibodies against phosphorylated ubiquitin (p-S65-Ub) have been described as novel tools to detect PINK1-PRKN-mediated mitophagy [1191-1193]. p-S65-Ub is formed by the kinase PINK1 specifically upon mitochondrial stress, and is amplified in the presence of the E3 Ub ligase PRKN (reviewed in [1194]) [1195]. p-S65-Ub antibodies have

been used to demonstrate stress-induced activation of PINK1 in various cells including primary human fibroblasts (Figure 29) and dopaminergic neurons differentiated from iPS cells [1193]. Phosphorylated poly-ubiquitin chains specifically accumulate on damaged mitochondria, and staining with p-S65-Ub antibodies can be used, in addition to translocation of PRKN, to monitor the initiation of mitophagy. Given the complete conservation of the epitopes across species, mitochondrial p-S65-Ub can also be detected in mouse primary neurons upon mitochondrial depolarization and *park/PRKN*-deficient *Drosophila*. Furthermore, the p-S65-Ub signal partially colocalizes with mitochondrial, lysosomal, and total ubiquitin markers in cytoplasmic granules that appear to increase with age and disease in human postmortem brain samples [1191,1193]. Examination of the phosphorylation status of outer mitochondrial membrane (OMM) autophagy receptors such as FUNDC1 and BNIP3L is also useful for measuring mitophagy activity [1196,1197]. Note that care should be taken when choosing antibodies to assess the degree of mitochondrial protein removal by autophagy; the quality and clarity of the result may vary depending on the specifics of the antibody. In testing the efficiency of mitophagy, clearer results may be obtained by using antibodies against mitochondrial DNA (mtDNA)-encoded proteins. This experimental precaution may prove critical to uncover subtle differences that could be missed when evaluating the process with antibodies against nuclear encoded, mitochondrially imported proteins (M. Campanella, personal communication).

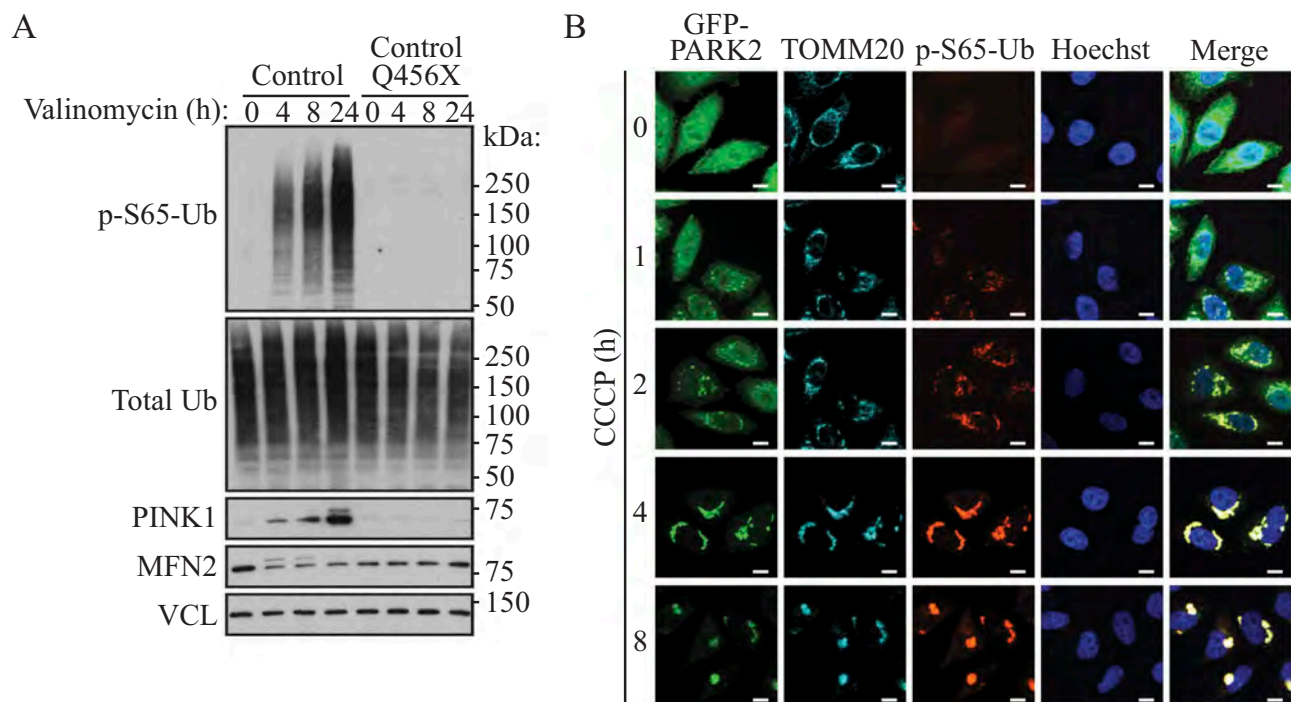


Figure 29. PINK1-dependent phosphorylation of ubiquitin (p-S65-Ub) upon mitophagic stress. **(A)** Human dermal fibroblasts from healthy controls or PD patients carrying a PINK1 loss-of-function mutation (Q456X) were treated with valinomycin for the indicated times, and lysates were analyzed by western blot. The p-S65-Ub signal is almost undetectable under nonstress conditions in controls, but is strongly induced in a PINK1 kinase-dependent manner during its stabilization on the outer mitochondrial membrane. MFN2 serves as a control substrate and VCL (vinculin) as a loading control. **(B)** HeLa cells stably expressing GFP-PRKN (wild type) were treated with CCCP for the indicated times, fixed and stained with p-S65-Ub (red) and GFP-PRKN (green) as well as mitochondrial (TOMM20, cyan) and nuclear (Hoechst, blue) markers. The p-S65-Ub staining is almost undetectable in nonstressed cells, but rapidly accumulates on damaged mitochondria where it functions to activate PRKN. On mitochondria, PINK1 and PRKN together amplify the p-S65-Ub signal. Scale bar: 10 μ m. Image provided by F.C. Fiesel and W. Springer.

Stabilized, unprocessed PINK1 that accumulates on the mitochondrial outer membrane in response to certain forms of acute mitochondrial damage can be used to differentiate between healthy mitochondria and those that have lost their membrane potential. However, caution should be taken with this approach in cells where mitochondria exhibit physiological uncoupling and lowered membrane potential, such as thermogenic brown adipocytes. Similarly, redistribution of cardiolipin to the OMM acts as an elimination signal to trigger mitophagy induction in mammalian cells, including primary neurons [201]. In addition, during CCCP-induced mitophagy, the hexameric protein NME4/NDPKD/NM23-H4 localizes to the mitochondrial inter-membrane space, binds cardiolipin and facilitates its redistribution to the OMM [1189], and the ANXA5 (annexin A5) binding assay for externalized cardiolipin can be used as a marker for damaged mitochondria and early mitophagy [201]. The charge of multiple anionic phospholipids present on the OMM can change in response to mild alterations in mitochondrial function. These signals are important to the regulation of protein signaling between mitochondria and the cytosol. Changes in surface charge can be estimated by detecting the binding of ANXA5. Mild metabolic insults (e.g., a 50% inhibition of the mitochondrial enzyme OGDH/ketoglutarate dehydrogenase) increase ANXA5 binding nearly three-fold, while stimulating translocation of DNMI1 and LC3 to mitochondria without altering cardiolipin translocation, ATP or the mitochondrial membrane potential [1198]; DNMI1 is a fundamental component of mitochondrial fission, which helps facilitate mitophagy. Finally, many of the LIR domain-containing mitophagy receptors undergo transcriptional upregulation during developmental stages when mitochondria are eliminated, or during hypoxia [1151,1188]. Changes in their expression can be used to gauge the potential for undergoing mitophagy, rather than as an estimate of mitophagy activity.

Previously, it was suggested that mitophagy can be divided into three types [1199]; however, this was based largely upon in vitro data. In vivo data from reporter animals suggests a simpler classification that has reached consensus in the field. In terms of mitophagy classifications in vitro: Type 1 mitophagy, involves the formation of a phagophore, and typically also requires mitochondrial fission; the PtdIns3K complex containing BECN1 mediates this process. In contrast, type 2 mitophagy is independent of BECN1 and takes place when mitochondria have been damaged [118], resulting in depolarization; sequestration involves the coalescence of GFP-LC3 membranes around the mitochondria rather than through fission and engulfment within a phagophore. Receptor-dependent mitophagy is found in the BECN1-independent pathway. In type 3 mitophagy, mitochondrial fragments or vesicles from damaged organelles are sequestered through a microautophagy-like process named micromitophagy that is independent of ATG5 and LC3, but requires PINK1 and PRKN; in mammals, this process occurs through the formation of mitochondria-derived vesicles/MDVs, small vesicles delivering damaged mitochondrial components to lysosomes for degradation.

Although the process of pexophagy is prominent and well described in yeast cells [1059,1200], relatively little work has been done in the area of selective mammalian peroxisome

degradation by autophagy (for a review see ref [1201]). Typically, peroxisomes are induced by treatment with hypolipidemic drugs such as clofibrate, ciprofibrate or dioctyl phthalate, which bind to a subfamily of nuclear receptors, referred to as PPARs (peroxisome proliferator activated receptors) [1202]. Of note, while inducing peroxisomal proliferation, PPARA/PPAR α may regulate neuronal autophagy, in physiological or pathological settings, such as AD models [921,1203]. Degradation of excess organelles is induced by drug withdrawal, although starvation without prior proliferation can also be used. EPAS1 activation in liver-specific *vhl*^{-/-} and *vhl*^{-/-} *hif1a*^{-/-} mice reduces peroxisome abundance by pexophagy, whereas ER and mitochondrial protein levels are not affected [774]. Pexophagy can also be induced by amino acid starvation, which induces the stabilization of the peroxisomal E3 ubiquitin ligase PEX2 [1204]. PEX2 is destabilized by MTORC1 such that the overexpression of PEX2 can induce pexophagy. PEX2 ubiquitinates PEX5 and ABCD3/PMP70 (ATP binding cassette subfamily D member 3), which then recruit NBR1 to target the peroxisome for pexophagy [1204]. The action of PEX2 is counteracted by the deubiquitinating enzyme USP30 [1205,1206]. Pexophagy can also be induced by the expression of a nondegradable active EPAS1 variant [1207]. Induction of pexophagy in response to endogenous and exogenous reactive oxygen species (ROS) and reactive nitrogen species has been observed in mammalian cells. In this setting, pexophagy is induced via ROS- or reactive nitrogen species-mediated activation of ATM/ataxia telangiectasia mutated (ATM serine/threonine kinase) [1208,1209], repression of MTORC1 and phosphorylation of PEX5 by ATM [1210,1211]; ATM phosphorylation of PEX5 at S141 triggers PEX5 ubiquitination and binding of SQSTM1 to peroxisomes targeted for pexophagy [1211].

Loss of peroxisomes can be followed enzymatically or by immunoblot, monitoring enzymes such as ACOX/fatty acyl-CoA oxidase (note that this enzyme is sometimes abbreviated “AOX,” but should not be confused with the enzyme alcohol oxidase that is frequently used in assays for yeast pexophagy) or CAT (catalase), and also by EM, cytochemistry or immunocytochemistry [1212-1215]. Finally, a HaloTag⁺-PTS1 marker that is targeted to peroxisomes has been used to fluorescently label the organelle [1216]. An alternative approach uses a peroxisome-specific tandem fluorochrome assay (RFP-EGFP localizing to peroxisomes by the C-terminal addition of the tripeptide SKL, or a peroxisomal membrane protein tagged with mCherry-mGFP), which has been used to demonstrate the involvement of ACBD5/Atg37, NBR1 and SQSTM1 in mammalian and fungal pexophagy [458,459,1052]. By showing that PEX14 directly interacts with LC3-II, which is competitively inhibited by PEX5, PEX14 is demonstrated to function in the dual processes of biogenesis and degradation of peroxisomes with the coordination of PEX5 in response to environmental changes [1217,1218]. Peroxisomal proteins are degraded preferentially over cytosolic proteins in CHO-K1 cells when starved and then cultured in a normal culture medium. Degradation of peroxisomes is dependent on LC3 and PEX14 [1219]. By making use of autophagy inhibitors or siRNA against NBR1, ubiquitin- and NBR1-mediated pexophagy is shown to be

induced by increased expression of PEX3 in mammalian cells, where ubiquitination of PEX3 is dispensable for pexophagy [1220,1221]. Another autophagic receptor protein, SQSTM1, is required only for the clustering of peroxisomes.

Cautionary notes: There are many assays that can be used to monitor specific types of autophagy, but caution must be used in choosing an appropriate marker(s). To follow mitophagy it is required to monitor more than one protein and to include an inner membrane and a matrix component (and preferably encoded by the mitochondrial DNA) in the analysis to evaluate mass, and not be biased by selective clearance of proteins located in different submitochondrial compartments. In this regard, it is not sufficient to follow a single mitochondrial outer membrane protein because it can be degraded independently of mitophagy through the UPS. Although the localization of PRKN to mitochondria as monitored by fluorescence microscopy is associated with the early stages of CCCP-driven mitochondria degradation [339], this by itself cannot be used as a marker for mitophagy, as these events can be dissociated [1222]. Even with PRKN translocation and ubiquitination, FCCP-induced donut mitochondria resist autophagy, by failing to recruit autophagy receptors CALCOCO2/NDP52 and OPTN [1223]. Moreover, mitophagy elicited in a number of disease models and by pharmacological means [1224]) does not involve mitochondrial PRKN translocation [201,460,1225]. Along these lines, recent studies implicate an essential role for TRAF2, an E3 ubiquitin ligase, as a mitophagy effector in concert with PRKN in cardiac myocytes; whereby mitochondrial proteins accumulate differentially with deficiency of either, indicating nonredundant roles for these E3 ubiquitin ligases in mitophagy [1226]. This finding necessitates an integrated approach to assess mitophagy based on a broad evaluation of multiple mitochondrial effectors and proteins. Because PINK1-PRKN-dependent mitophagy can only be detected under certain non-physiological conditions, it is a controversial matter of debate as to the role of PINK1-PRKN during mitophagy, and whether basal and stimulus (e.g., age)-induced mitophagy are regulated through the same pathways or employ distinct machineries [1227].

During canonical PRKN-mediated mitophagy, PRKN translocates to damaged mitochondria and ubiquitinates a wide range of outer membrane proteins including VDAC1, MFN1/2 and TOMM20 [1128,1153,1154,1228,1229]. This results in the preferential degradation of OMM proteins by the proteasome, while inner membrane proteins and mitochondrial DNA [1230] remain intact. Monitoring loss of a single protein such as TOMM20 by western blot or fluorescence microscopy to follow mitophagy may thus be misleading, as noted above [1228]. Similarly, following the level of DNM1L may provide some information with regard to mitophagy, but it must be kept in mind that alterations in mitochondrial dynamics and DNM1L recruitment to mitochondria mostly occur in response to conditions other than mitophagy, such as changing nutrient concentrations. MitoTracker® dyes are widely used to stain mitochondria and, when colocalized with GFP-LC3, they can function as markers for mitophagy. However, staining with MitoTracker® dyes depends on mitochondrial membrane potential (although MitoTracker® Green FM is less sensitive to loss of membrane potential), so that damaged, or sequestered

nonfunctional mitochondria may not be stained. In vitro this can be avoided by labeling the cells with MitoTracker® before the induction by the mitophagic stimuli [1123]. One additional point is that MitoTracker® dyes might influence mitochondrial motility in axons (D. Ebrahimi-Fakhari, personal communication).

Although it is widely assumed that autophagy is the major mechanism for degradation of entire organelles, there are multiple mitochondrial quality control mechanisms that may account for the disappearance of mitochondrial markers. These include proteasomal degradation of outer membrane proteins and/or proteins that fail to correctly translocate into the mitochondria, degradation due to proteases within the mitochondria, and reduced biosynthesis or import of mitochondrial proteins. PINK1 and PRKN are not essential for all types of mitophagy in vitro or in vivo [466,1188,1231]. Moreover, these two proteins also participate in an ATG gene-independent pathway for lysosomal degradation of small mitochondria-derived vesicles [791]. An unbiased proteomic study in vivo shows that PRKN ubiquitinates not only OMM proteins during mitophagy but also several proteins that a priori are unrelated to mitophagy [1229]. Furthermore, the PINK1-PRKN mitophagy pathway is also transcriptionally upregulated in response to starvation-triggered generalized autophagy, and is intertwined with the lipogenesis pathway [1232-1235]. In addition to mitophagy, mitochondria can be eliminated by extrusion from the cell (mitoptosis) [1112,1128,1139,1236]. Transcellular degradation of mitochondria, or transmitophagy, also occurs in the nervous system when astrocytes degrade axon-derived mitochondria [1237]. Thus, it is advisable to use a variety of complementary methods to monitor mitochondria loss including TEM, single-cell analysis of Atg-family protein fluorescent puncta that colocalize with mitochondria, and western blot, in conjunction with flux inhibitors and specific inhibitors of autophagy induction compared with inhibitors of the other major degradation systems (see cautions in *Autophagy inhibitors and inducers*).

To monitor and/or rule out changes in cellular capacity to undergo mitochondrial biogenesis, a process that is tightly coordinated with mitophagy and can dictate the outcome following mitophagy-inducing insults especially in primary neurons and other mitochondria-dependent cells, colocalization analysis after double staining for the mitochondrial marker TOMM20 and BrdU (for visualization of newly synthesized mtDNA) can be performed (Figure 30). Alternatively, direct assay for translation of mtDNA-encoded proteins is a straightforward assay for mitochondrial biogenesis, which can be combined with analysis of transcripts driven by mtDNA promoters [1238,1239].

Likewise, although the mechanism(s) of peroxisomal protein degradation in mammals awaits further elucidation, it can occur by both autophagic and proteasome-dependent mechanisms [1219]. Thus, controls are needed to determine the extent of degradation that is due to the proteasome. Moreover, two additional degradation mechanisms have been suggested: the action of the peroxisome-specific LONP2/Lon (lon peptidase 2, peroxisomal) protease and the membrane disruption effect of 15-lipoxygenase [1240].

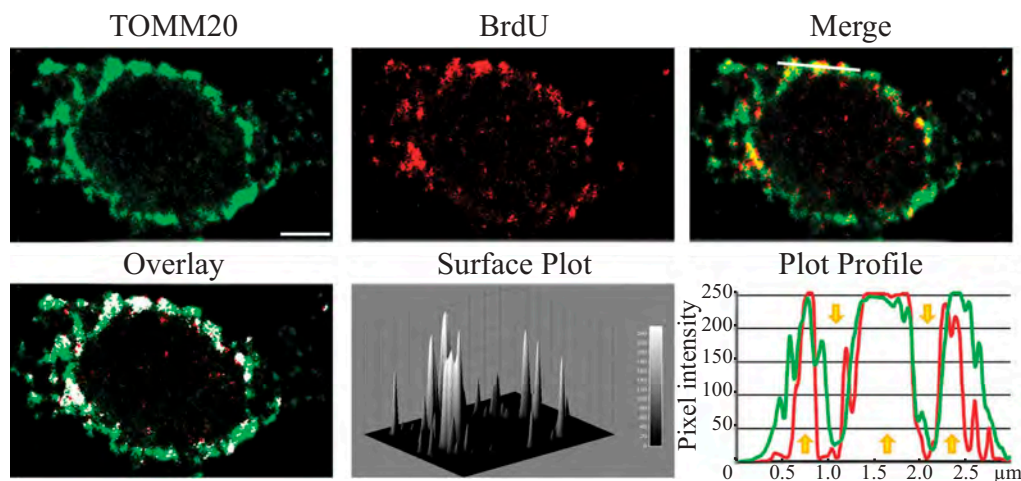


Figure 30. Confocal microscopy deconvolved (AutoQuant X3) images and colocalization image analysis (ImageJ 1.47; Imaris 7.6) through a local approach showing perinuclear mitochondrial biogenesis in hippocampal neuronal cultures. The upper channels show TOMM20 (green channel), BrdU (for visualization of newly synthesized mitochondrial DNA, red channel), and merged fluorescence channels. Overlay, corresponds to the spatial pattern of software thresholded colocalized structures (white spots) layered on the merged fluorescence channels. Surface Plot, or luminance intensity height, is proportional to the colocalization strength of the colocalized structures (white spots). Plot Profile, corresponds to the spatial intensity profiles of the fluorescence channels of the white line positioned in the Merge image. Yellow arrows indicate a qualitative evaluation of the spatial association trends for the fluorescence intensities. Arrows pointing up indicate an increase in the colocalization, whereas arrows pointing down show a decrease. Scale bar: 2 μ m. This figure was modified from previously published data [4085] and is provided by F. Florenzano.

Chlorophagy. Besides functioning as the primary energy suppliers for plants, chloroplasts represent a major source of fixed carbon and nitrogen to be remobilized from senescing leaves to storage organs and newly developing tissues. As such, the turnover of these organelles has long been considered to occur via an autophagy-type mechanism. However, while the detection of chloroplasts within autophagic body-like vesicles or within vacuole-like compartments has been observed for decades, only recently has a direct connection between chloroplast turnover and autophagy been made through the analysis of *atg* mutants combined with the use of fluorescent ATG8 reporters [1241-1244]. In fact, it is now clear that chlorophagy, the selective degradation of chloroplasts by autophagy, can occur via several routes, including the encapsulation of whole chloroplasts by the tonoplast via a microautophagy-type process [1244], or the budding of chloroplast material into small distinct autophagic vesicles called Rubisco-containing bodies (RCBs) and ATI1 (ATG8-interacting protein 1) plastid-associated (ATI-PS) bodies, which then transport chloroplast cargo to the vacuole [1241,1245]. Chloroplasts produce long tubes called stromules that project out from the organelle outer membrane. Recent studies suggest that stromules are part of the chlorophagy process, by which the stromule tips, presumably containing unwanted or damaged chloroplast material, are engulfed by autophagic membranes using ESCRT-II endocytic machinery that depends on ATG8 [1246]. Chloroplast morphology can easily be monitored by TEM, whereas chloroplast abundance and association with autophagic membranes can be studied by confocal fluorescence microscopy using chlorophyll autofluorescence in combination with appropriate fluorescent protein markers (e.g., stromally-targeted GFP, GFP-ATG8, or tonoplast markers such as GFP-TIP2/ δ TIP or VHP1-GFP). The appearance of RCBs is tightly linked with leaf carbon status, indicating that chlorophagy through RCBs represents an important route for recycling plant nutrients provided in plastid stores. As such,

it is critical to maintain consistent plant growth conditions, particularly with respect to light quality and intensity, and to take into account that different responses may be observed depending on the time of day experiments are performed.

Chromatophagy. Autophagy is best known for its pro-survival role in cells under metabolic stress and other conditions. However, excessively induced autophagy may be cytotoxic and may lead to cell death (Figure 31) [1247]. Chromatophagy (chromatin-specific autophagy) comes into view as one of the autophagic responses that can contribute to cell death [1248]. Chromatophagy can be seen in cells during nutrient depletion, such as arginine starvation, and its phenotype consists of giant-autophagosome formation, nucleus membrane rupture and histone-associated-chromatin/DNA leakage that is captured by phagophores. Arginine starvation can be achieved by adding purified arginine deiminase to remove arginine from the culture medium, or by using arginine-dropout medium. The degradation of leaked nuclear DNA/chromatin can be observed by fluorescence microscopy; with GFP-LC3 or anti-LC3 antibody, and LysoTracker™ Red or anti-LAMP1, multiple giant autophagosomes or autolysosomes containing leaked nuclear DNA can be detected. In addition, the chromatophagy-related autophagosomes also contain parts of the nuclear outer-membrane, including NUP98 (nucleoporin 98 and 96 precursor), indicating that the process involves a fusion event [1248].

Clockophagy. Clockophagy is the process of selective autophagic degradation of the key circadian clock protein ARNTL/BMAL1 (aryl hydrocarbon receptor nuclear translocator-like) during RSL3-induced ferroptosis in Calu-1 and HT1080 cells [1249]. SQSTM1 is a cargo receptor responsible for clockophagy-dependent ARNTL degradation during ferroptosis. Clockophagy-dependent ARNTL degradation dramatically

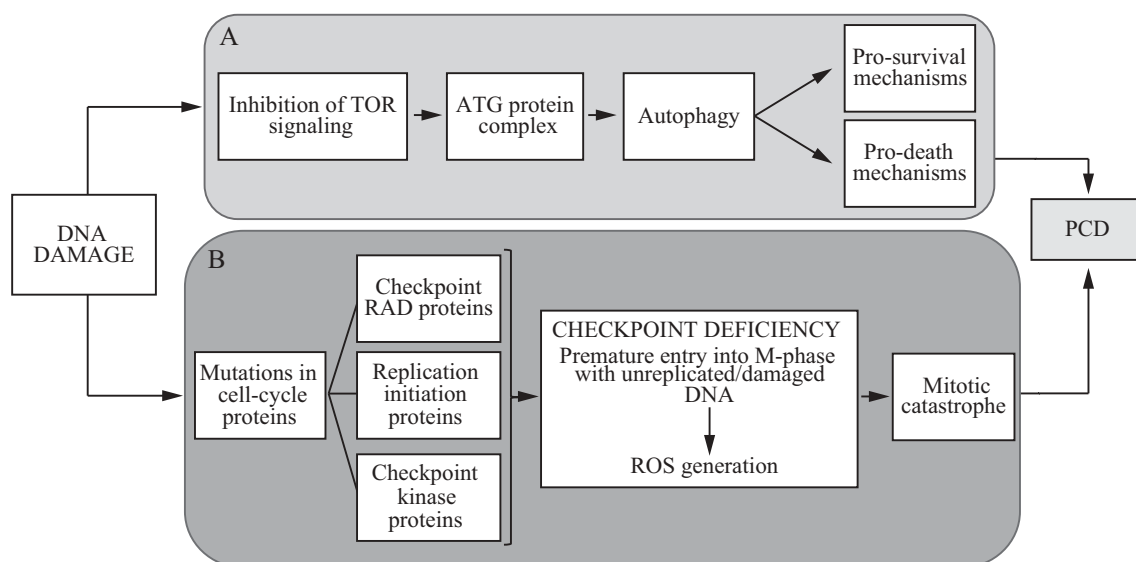


Figure 31. Pathways that follow DNA damage may result in PCD or cell survival through autophagy, or checkpoint deficiency. **(A)** DNA damage inhibits TOR signaling, which promotes the formation of an ATG protein complex, thereby bringing about autophagy. Autophagy may contribute to cell survival as well as to cell death by PCD. **(B)** DNA damage may cause mutations in genes encoding checkpoint RAD proteins and/or proteins involved in DNA replication initiation, as well as the simultaneous deletion of genes encoding checkpoint kinases. Such protein defects lead to deficient checkpoints, thereby causing cells to enter M-phase prematurely with damaged DNA or incompletely replicated DNA, resulting in ROS generation, mitotic catastrophe, and subsequently PCD. This figure was previously published in ref. [1247].

promotes ferroptotic cancer cell death through EGLN2/PHD1 (egl-9 family hypoxia-inducible factor 2)-mediated oxidative injury *in vitro* and *in vivo*. The interactome map of the *arntl/bmal1*^{-/-} mouse, an arrhythmic circadian rhythms model, reveals significant loss of genes encoding proteins such as COL6A/collagen VI and autophagy-related genes such as SQSTM1 [1250]. Given the importance of the accumulated data from both mice and human studies, deregulation of *Clock* genes might lead to enhanced autophagy through ATG14, whereas downregulated autophagy through the AKT pathway may be involved in the pathogenesis of COL6A myopathy and potentially contribute to other muscle-wasting diseases.

Crinophagy and the SINGD pathway. Distinct from cargo disposal that involves autophagosomes, crinophagy, the degradation of secretory granules via direct fusion with lysosomes, was discovered in the 1960s as a pituitary gland response to the inhibition of exocytosis [1251]. Crinophagy has been observed in different types of secretory cells including cells of the anterior pituitary gland, pancreatic α cells and β cells [1251-1254]. Traditionally, crinophagy was monitored using electron microscopy and immunoelectron microscopy. Newer molecular biology techniques have been employed to study crinophagy in the salivary gland of *Drosophila* [1255] and in mammalian pancreatic β cells [1256]. In *Drosophila*, reporter lines expressing granule and lysosomal markers with fluorescent tags have been used to assess crinophagic degradation of glue granules at different time points and elucidate the molecular mechanisms of this pathway [1255]. In β cells, short-term nutrient deprivation evokes rapid autophagy-independent lysosomal degradation of nascent INS (insulin) secretory granules, the pathway termed “stress-induced nascent granule degradation” (SINGD; pronounced 'sindi). SINGD

occurs via crinophagy and counters autophagy through localized activation of MTORC1; the depletion of secretory granules together with the inhibition of autophagy protect against unwanted INS release during fasting [120]. The major regulator of secretory granule biogenesis at the trans-Golgi network, PRKD (protein kinase D), controls SINGD, thus routing secretory granules to secretion or degradation depending on the nutrient availability. Furthermore, erroneous activation of the SINGD pathway contributes to β cell failure in type 2 diabetes [1256]. To further characterize the dynamics of the crinophagic SINGD pathway in β cells, the sequences coding fluorescent tags have been inserted directly into the endogenous loci of the secretory granule marker PTPRN2/Phogrin and the lysosomal protein CD63 using CRISPR-Cas9 gene-editing. This tool makes it possible to follow crinophagy in real time using several imaging techniques, including live-cell imaging combined with CLEM (live-CLEM). In addition, 3-dimensional reconstruction of large cellular volumes achieved by FIB-SEM is particularly helpful to detect crinophagic events in primary islets.

Doryphagy. Centriolar satellites (CSs) are protein complexes associated with microtubules and clustering around the centrosome. Whereas CSs have long been described as the structures regulating centrosome composition, the mechanisms controlling CS homeostasis and function are not yet understood in detail [1257]. A process targeting CSs for selective autophagy has been identified and termed “doryphagy”, from the Greek word “doryphoros” for satellites [1258]. Of note, the selective degradation of CSs is achieved by a LIR-mediated interaction between PCM1, a component of CSs, and GABARAPs. As a consequence of CS function in regulating centrosomes, disruption of doryphagy results in centrosome abnormalities and aberrant mitosis.

Ferritinophagy. Ferritinophagy is a selective form of autophagy that functions in intracellular iron processing [805]. Iron is recruited to ferritin for storage and to prevent the generation of oxygen free radicals through the Fenton and Haber-Weiss reactions [806,807]. Because ferritin is largely degraded by autophagy [1259,1260] the ferritin status can be used as a marker of the autophagic flux in a given cell. To release iron from ferritin, the iron-bound form is sequestered within an autophagosome [1261]. Fusion with a lysosome leads to breakdown of ferritin and release of iron. Furthermore, iron can be acidified in the lysosome, converting it from an inactive state of Fe^{3+} to Fe^{2+} [809,810]. Iron can be detected in the autolysosome via TEM [809]. Colocalization of iron with autolysosomes may also be determined utilizing calcein AM to tag iron [1262,1263]. NCOA4 is a cargo receptor that recruits ferritin to the autophagosome [1264]. NCOA4-dependent ferritinophagy promotes ferroptosis, an iron-dependent form of regulated cell death (RCD) [1265,1266], by the degradation of ferritin in multiple cells [1267] as discussed below. Note that ferritinophagy can be co-opted by pathogens for their own survival. For example, uropathogenic *E. coli* persist in host cells by taking advantage of ferritinophagy. Iron overload in urothelial cells induces ferritinophagy in a NCOA4-dependent manner causing increased iron availability for uropathogenic *E. coli* to overgrow, which can be reversed by inhibition of autophagy [1268].

Ferroptosis is currently defined as a form of programmed cell death initiated by oxidative perturbations of the intracellular microenvironment, that is under constitutive control by GPX4. This form of programmed cell death may be accompanied by excessive autophagy initiated after administration of erastin and glutamate, which results in inactivation of SLC7A11/cystine transporter/xCT. Uptake of cystine is essential for glutathione synthesis, and, therefore, a deficient SLC7A11 transporter will promote lipid peroxidation due to depletion of GPX4 (glutathione peroxidase 4) protein and activity [1269]. Cysteine deprivation also causes endoplasmic reticulum stress resulting in induction of DDIT4/REDD1 [1270]. DDIT4 acts as an inducer of autophagy by binding and inhibiting YWHA/14-3-3, which otherwise inhibits the TSC1-TSC2 complex, and ultimately leads to inhibition of MTOR. Increased autophagy induced by DDIT4 causes ferritin to be degraded and iron released to promote ferroptosis, whereas inhibition of autophagy protects against ferroptosis [1267]. Recent reports indicate that GPX4 depletion is facilitated by CMA involving HSP90. Inhibition of HSP90 using 2-amino-5-chloro-N,3-dimethylbenzamide (CDDO) can spare GPX4 depletion and rescue erastin-mediated cell death [1271]. Moreover, upregulation of the RNA-binding protein ELAVL1/HuR promotes BECN1 production via binding to the AU-rich elements (AREs) in the 3' UTR of *BECN1* mRNA, thus triggering autophagy activation, promoting autophagic ferritin degradation, and eventually leading to iron-dependent ferroptosis [1272]. Conversely, upregulation of the RNA-binding protein ZFP36 (ZFP36 ring finger protein) can result in *ATG16L1* mRNA decay via binding to the AREs in the 3' UTR, thus triggering autophagy inactivation, blocking autophagic ferritin degradation, and eventually conferring resistance to ferroptosis [1273].

Granulophagy. Granulophagy is a term generally applicable to the autophagic clearance of mRNA-protein granules in eukaryotic cells. First termed to describe the clearance of stress granules in *S. cerevisiae* and human cell lines [1274], other mRNP granules subject to autophagic clearance include P-bodies in mammalian cells [1275] and P-granules in *C. elegans* [1276]. Evidence that granulophagy is a selective autophagic process includes the identification of granule-specific autophagic receptor proteins, including SQSTM1 for stress granules in human cells, CALCOCO2 for P-bodies in human cells and SEPA-1 for P-granules in *C. elegans* [1275,1276]. In all cases, the receptor proteins colocalize in their respective mRNP granules while autophagic clearance occurs, and the absence of said receptor proteins leads to accumulation of the mRNP granule. SQSTM1- and LC3-adorned bodies resembling stress granules also localize in autophagosomes as revealed by electron microscopy [1277].

Granulophagy studies with stress granules suggest induction varies depending on cellular context. For example, yeast stress granules induced by transient nutrient deprivation or oxidative stress are not targeted by granulophagy, whereas diauxic shift and inhibition of mRNA decay do induce granulophagy [1274]. Additionally, studies involving various stress stimuli (e.g., heat shock, proteasome inhibition, or arsenite stress) in human cell lines reveal differing degrees of importance of autophagic versus chaperone-based mechanisms in the disassembly or degradation of stress granules [1274, 1275, 1277-1279]. Stress granule clearance following heat shock may involve migration via microtubules of stress granules to aggresomes, based on colocalization studies in the presence and absence of autophagic inhibitors [1279]. Thus, granulophagy and aggrephagy mechanisms may overlap in at least some cases. Moreover, stalled 48S translation pre-initiation complexes, forming stress granules upon accumulation and condensation, are found within exosomes secreted by cells submitted to prolonged serum starvation, a process enhanced by ATG5 depletion [822].

Granulophagy may affect the pathology of amyotrophic lateral sclerosis (ALS). Aberrant persistence or formation of stress granules has been hypothesized to facilitate formation of toxic cytoplasmic aggregates containing TARDBP or FUS RNA-binding proteins [1280]. Mutations in VCP that are associated with ALS onset also impair granulophagy and lead to persistence of TARDBP-containing stress granules in human cell models [1274]. ALS-mutant forms of FUS also induce aberrant stress granule assembly in neuronal cells, and lead to increased stress granule association with autophagosomes versus stress granules formed in control cells, suggesting granulophagy exerts selective clearance of potentially pathological stress granules [1281]. Finally, the most commonly mutated gene in ALS patients, *C9orf72*, may also function with SQSTM1 in autophagic clearance of FUS-containing stress granules. Supporting this, *C9orf72* physically interacts with SQSTM1 and localizes in stress granules, and its depletion impairs stress granule clearance following arsenite stress [1277].

Intrplastidial autophagy. Intrplastidial autophagy is a process whereby plastids of some cell types adopt autophagic functions, engulfing and digesting portions of the cytoplasm.

These plastids are characterized by formation of invaginations in their double-membrane envelopes that eventually generate a cytoplasmic compartment within the plastidial stroma, isolated from the outer cytoplasm. W. Nagl coined the term plastolysome to define this special plastid type [1282]. Initially, the engulfed cytoplasm is identical to the outer cytoplasm, containing ribosomes, vesicles and even larger organelles. Lytic activity was demonstrated in these plastids, in both the cytoplasmic compartment and the stroma. Therefore, it was suggested that plastolysomes digest themselves together with their cytoplasmic cargo, and transform into lytic vacuoles. Intraplastidial autophagy has been reported in plastids of suspensor cells of *Phaseolus coccineus* [1282] and *Phaseolus vulgaris* [1283], where plastids transformed into autophagic vacuoles during the senescence of the suspensor. This process was also demonstrated in petal cells of *Dendrobium* [1284], and in *Brassica napus* microspores experimentally induced towards embryogenesis [1285]. All these reports established a clear link between these plastid transformations and their engagement in autophagy. At present, descriptions of this process are limited to a few, specialized plant cell types. However, pictures of cytoplasm-containing plastids in other plant cell types have been occasionally published, although the authors did not make any mention of this special plastid type. For example, this has been seen in pictures of fertile and Ogu-INRA male sterile tetrads of *Brassica napus* [1286], and *Phaseolus vulgaris* root cells [1287]. Possibly, this process is not as rare as initially thought, but authors have only paid attention to it in those cell types where it is particularly frequent.

Lipophagy. The specific autophagic degradation of lipid droplets represents another type of selective autophagy [1288]. Lipophagy requires the core autophagic machinery and can be monitored by following triglyceride content, or total lipid levels using BODIPY 493/503 or HCS LipidTOX neutral lipid stains with fluorescence microscopy, cell staining with Oil Red O, the cholesterol dye filipin III [1289], or ideally label-free techniques such as coherent anti-stokes Raman scattering/CARS or spontaneous Raman scattering/SRS microscopy. BODIPY 493/503 should be used with caution, however, when performing costains (especially in the green and red spectra) because this commonly used fluorescent marker of neutral lipids is highly susceptible to bleed-through into the other fluorescence channels (hence often yielding false positives), unlike the LipidTOX stain that has a narrow emission spectrum [1290]. In addition, BODIPY 493/503 cannot be used to monitor lipophagy in *C. elegans* because it stains both lipid droplets and the lysosome [1291]. TEM can also be used to monitor lipid droplet size and number, as well as lipid droplet-associated double-membrane structures, which correspond to autophagosomes [1288,1292,1293].

The transcription factor TFEB positively regulates lipophagy [948], and promotes fatty acid β -oxidation [1294], thus providing a regulatory link between different lipid degradation pathways [1295]. Accordingly, TFEB overexpression rescues fat accumulation and metabolic syndrome in a diet-induced model of obesity [1294,1296] and in alcohol-induced fatty liver in mice [1297]. As a coactivator for TFEB and PPARG, CARM1

regulates lysosome biogenesis and lipid metabolism through processes that are partially dependent on lipophagy [980,1298]. Under conditions of nutrient starvation, CARM1-TFEB-mediated lipophagy is regulated by C9orf72 [1299,1300]. Genetic mutations in C9orf72 are linked to neurodegenerative diseases including ALS and frontotemporal dementia (FTD) [1301,1302]. Spermidine can also stimulate autophagy in adipose tissue, reducing visceral fat and obesity-associated alterations upon hypercaloric regimens [1303]. Expression of the *C. elegans* lysosomal lipases *lipl-1*, *lipl-3*, and *lipl-4* tightly correlates with activation of autophagy in the conditions so far tested [948,1304,1305], and this transcriptional activation is necessary for optimal lipid mobilization in conditions of autophagy activation such as fasting [948,1304].

The antioxidant enzyme PRDX1 (peroxiredoxin 1) is expressed most highly in macrophages, and plays an essential role in regulation of lipophagic flux and maintenance of cholesterol homeostasis against oxidative stress within atherosclerotic macrophages [1306]. The regulation of expression of lipid droplet regulators (such as the PLIN/perilipin family) and of autophagy adaptors (such as the TBC1D1 family) during starvation and disease deserves further exploration [1307-1309]. Members of the PNPLA (patatin like phospholipase domain containing) protein family, PNPLA1 [1310], PNPLA2 [1311,1312] and PNPLA3 [1313], as lipid droplet residents, play essential roles in lipophagy by regulating lipid droplet size and autophagic flux. Although a physiological receptor protein and specific induction signal for lipophagy are poorly understood, expression of a fusion protein of SQSTM1 and a lipid droplet-binding domain can induce forced lipophagy to promote the breakdown of lipid droplets [1314]. Coating PLINs (perilipins) can also be degraded through CMA, facilitating access of cytosolic lipases to the esterified lipids stored in the droplet [1315]. Lipophagy is often monitored in vitro using cell culture media supplemented with fatty acids to promote the formation of intracellular lipid droplets. Caution should be taken with the assessment and interpretation of lipophagy data in adipocytes. This cell type shows spontaneous physiological accumulation of lipid droplets, in contrast with cells in which lipid droplet accumulation is experimentally forced and is associated with lipotoxicity.

Cautionary notes: With regard to changes in the cellular neutral lipid content, the presence and potential activation of cytoplasmic lipases that are unrelated to lysosomal degradation must be considered. Caution should also be taken when interpreting lipophagy data using autophagy-related gene knockout mice. In response to fasting or diet-induced obesity, liver-specific *rb1cc1*, *atg7* or *atg5* knockout mice have decreased hepatic lipid accumulation, which is likely due to an adaptive response that includes increased FGF21 production and NFE2L2 activation in these knockout mice as a result of chronic impaired hepatic autophagy [1316-1318].

Lysophagy. Lysophagy is a selective autophagy process that participates in cellular quality control through lysosome turnover. By eliminating ruptured lysosomes, lysophagy prevents the subsequent activation of the inflammasome complex and innate response [1319-1321]. The conserved autophagy

machinery of *D. discoideum* also localizes at lysosomes damaged by lysosomotropic agents such as LLOMe (polymers of Leu-Leu-OMe). It has been proposed that autophagy, which also occurs at damaged compartments containing the bacterial pathogen *M. marinum*, plays a role in both the repair of the damaged compartment and its total engulfment for degradation [1322].

Myelinophagy. Myelinophagy or Schwann cell autophagy refers to selective autophagic degradation of myelin from Schwann cells in order to avoid or to reduce myelin debris and aggregates following peripheral nerve injury [1323]. An efficient Schwann cells myelin clearance, an early event in Wallerian degeneration, counteracts inflammatory processes facilitating recovery and nerve regeneration [1324,1325].

Schwann cells form autophagosomes in response to nerve injury. Inhibition of autophagy using both pharmacological inhibitors or genetic manipulation of autophagic genes (such as *Ambra1* and *Atg7*) leads to a severe neuropathy in response to injury, in vitro and in vivo [540,1326,1327]. A fundamental role of myelinophagy in peripheral neurodegeneration (i.e., demyelinating diseases) has been recognized [1328].

Nucleophagy. Nuclear autophagy is a mechanism by which cells maintain cellular homeostasis and ensure nuclear integrity, stability and correctness of gene expression. Targeted removal of nuclear material, part of or the entire nucleus, from a cell by autophagy (i.e., nucleophagy) has been reported as a selective mode occurring by autophagy as well as microautophagy [4]. The nuclear membrane may contribute to the phagophore membrane in addition to being an autophagic target. In autophagy, phagophores can sequester the nucleus-derived cargo, and autophagosomes subsequently merge with the vacuole or lysosomes, leading to the degradation of their contents [1329-1331]. In micronucleophagy, satellite nuclei are formed due to stress or genome instability and then engulfed directly [1077,1332,1333]. An alternative mechanism of nucleophagy has been reported in *Saccharomyces cerevisiae*, which is mediated by Atg39, a nuclear envelope receptor inducing autophagic sequestration of localized parts of the nucleus [1334].

The autophagy marker LC3 is expressed in the nucleus of human primary fibroblasts where it can directly interact with the nuclear lamina protein LMNB1 (lamin B1) [1335]; this process is associated with extensive DNA damage, and is triggered by oncogenic insult and senescence. The interaction of LC3 with LMNB1 does not downregulate LMNB1 during starvation, but can mediate its degradation upon oncogenic stress, providing a general mechanism to protect the cells from oncogene-induced senescence and tumorigenesis. Nucleophagy can thus be monitored through a quantification of the colocalization between LMNB1 and (GFP)-LC3 in puncta in the cytoplasm and in the nucleus, or through a dual fluorescent RFP-GFP-LMNB1 [1335].

Oxiapoptophagy. There are now several lines of evidence indicating that autophagy is an essential process in vascular and neurological functions. Autophagy can be considered as atheroprotective in the early stages of atherosclerosis, and

dysfunctional in advanced atherosclerotic plaques [1336]. A deregulated, amplified or attenuated autophagy process at different levels of the activation pathway appears to be associated with several neurodegenerative diseases [1337]. Currently, little is known about the molecules that promote autophagy on the cells of the vascular wall and on neural cells (glial and microglial cells, neurons). As increased levels of cholesterol oxidation products (named oxysterols) are found in atherosclerotic lesions [1338], and in the brain, cerebrospinal fluid and/or plasma of patients with neurodegenerative diseases [1339], the part taken by these molecules has been investigated, and several studies support the idea that some of them could contribute to the induction of autophagy [1339-1342]. There are several lines of evidence that oxysterols, especially 7-ketocholesterol and 7 β -hydroxycholesterol, which can be increased under various stress conditions in several age-related diseases including vascular and neurodegenerative diseases [1339], could trigger a particular type of autophagy termed oxiapoptophagy (OXIdation + APOPTosis + autoPHAGY) [1343] characterized by the simultaneous induction of oxidative stress associated with apoptosis, and autophagic criteria in different cell types from different species [1344-1346]. As oxiapoptophagy has also been observed with 7 β -hydroxycholesterol and 24(S)-hydroxycholesterol, which are potent inducers of cell death, it is suggested that oxiapoptophagy could characterize the effect of cytotoxic oxysterols [1344]. In addition, following treatment with 7 β -hydroxycholesterol, in 158 N murine oligodendrocytes, there is evidence of a link between 7 β -hydroxycholesterol-induced oxiapoptophagy and inflammation [1346,1347].

In any case, care must be taken in assigning an autophagy activating role to cholesterol-related compounds. Most of these studies usually consider such compounds as autophagy inducers because of their ability to convert LC3-I to LC3-II. However, the conversion of LC3 and/or the accumulation of LC3-labeled autophagosomes might be due to the blockade of this pathway at a later stage, as happens for some autophagy blockers such as CQ [302,1348,1349]. Furthermore, an increase in ROS generation is also commonly reported in these studies, which other authors have associated with lysosomal pH increases that ultimately prevent the fusion of lysosomes with autophagosomes [1348]. In this context, it is notable that the imbalance of membrane cholesterol has already been described to induce the generation of ROS [1350,1351].

Proteaphagy. The autophagic degradation of 26S proteasome complexes has been reported in plants [1352-1354], yeast [1355,1356], and humans [1357]. Two pathways for degradation have been reported: an ATG1-dependent pathway triggered by nutrient starvation, and an ATG1-independent pathway stimulated by chemical or genetic inhibition [1352,1353]. Starvation-induced proteaphagy occurs in response to nitrogen but not carbon starvation in Arabidopsis and yeast [1355], as carbon starvation instead triggers relocation of proteasomes into cytoplasmic proteasome storage granules that offer protection against autophagy [1358]. However, if proteasome storage granule formation is blocked, proteaphagy also becomes the default response to

carbon starvation. While little is currently known about the selectivity of starvation-induced proteaphagy in plants and yeast, in humans it appears to involve subunit ubiquitination and the autophagy receptor SQSTM1 [1357].

Inhibitor-induced proteaphagy also involves extensive ubiquitination of proteasome subunits to facilitate binding of autophagy receptors. In yeast, proteasomes first aggregate in the cytosol in an Hsp42-dependent manner, before the receptor Cue5 tethers the ubiquitinated, aggregated proteasomes to the expanding phagophore [1353]. In Arabidopsis, RPN10 instead acts as the receptor [1352]. RPN10 is a ubiquitin receptor within the proteasome regulatory particle, but is an unusual proteasome subunit as it also exists as a free form in the cytosol. The free form can bind ubiquitinated proteasome subunits via a standard ubiquitin-interacting motif (UIM), and also binds ATG8 via a related UIM-like sequence, rather than a canonical AIM/LIR [1359]. This casts RPN10 as the founding member of a new class of UIM-containing autophagy adaptors and receptors that are conserved across kingdoms. The exact subunits and residues to be ubiquitinated during proteaphagy, and the E3 ligases involved, are currently unknown.

As with other types of selective autophagy, proteaphagy can easily be monitored using fluorescently tagged proteasome subunits. Numerous core protease and regulatory particle subunits have been successfully tagged [1360], although care should be taken to ensure that the tag does not interfere with incorporation of the subunit into the proteasome particle. Once tagged, proteasome delivery to the vacuole can be studied by both confocal fluorescence microscopy, and by monitoring the release of free fluorescent protein by immunoblot. It is important to note that proteasome subunit levels do not necessarily correlate with levels of proteaphagy, particularly when studying the inhibitor-induced pathway. This is because synthesis of proteasome subunits is strongly induced upon proteasome inhibition by transcriptional feedback loops involving Rpn4 in yeast, NRF1 in humans and AT5G04410/NAC78 and AT3G10500/NAC53 in Arabidopsis [1360].

When yeast are grown under very low levels of glucose, proteasomes are also taken up directly into vacuoles by microautophagy [1361]. Microautophagy appears biased toward aberrant or inactive proteasomes, with functional proteasomes accumulating in proteasome storage granules. AMPK and ESCRT factors are required for proteasome microautophagy and also affect proteasome storage granule dissipation and nuclear reimport of proteasomes upon glucose refeeding.

Reticulophagy. Starvation in yeast induces a type of selective autophagy of the ER [1362], which depends on the autophagy receptors Atg39 and Atg40 [1334]. ER stress also triggers an autophagic response [1363], which includes the formation of multi-lamellar ER whorls and their degradation by a microautophagic mechanism [1364]. ER-selective autophagy has been termed reticulophagy/ER-phagy [1365]. Selective autophagy of the ER has also been observed in mammalian cells [1366], where multiple receptors have been recently characterized [1367–1369]. Reticulophagy receptors are selective not only for the ER itself, but they can also lead to the degradation of specific ER subdomains [1370]. RETREG1/FAM134B was

the first ER protein identified as an ER-specific autophagy receptor specific for ER sheets [74]. RTN3 and ATL3 have been described as reticulophagy receptors committed to the degradation of ER tubules ([1371,1372]; whereas TEX264 is mainly located in the ER 3-way junctions [464,1373]. SEC62 and CCPG1 are two other reticulophagy receptors with a broader ER distribution. SEC62 is involved in a particular form of reticulophagy (recoVER reticulophagy), which reduces the ER size to a normal level after an ER stress is resolved via ESCRT-III driven microreticulophagy [1374,1375]. In contrast, CCPG1 is activated directly under ER stress conditions [1376]. Because reticulophagy is selective, it is able to act in ER quality control [1370,1377,1378], and eliminate protein aggregates that cannot be removed in other ways. In the clearance of specific protein aggregates, the reticulophagy receptors cooperate with other ER proteins such as specific chaperones or elements of the COPII complex [1379–1382]. Moreover, reticulophagy functions to sequester parts of the ER that are damaged by the presence of pathogens such as viruses and bacteria [1383,1384]. The acetylation of ATG9A within the ER lumen seems to regulate its ability to interact with RETREG1/FAM134B and SEC62, and induce reticulophagy [1385,1386], a process that might be involved in the maintenance of proteostasis within the ER [1386,1387]. Reticulophagy can be monitored using reticulophagy reporters such as eGFP-mCherry-SERP1/RAMP4 [465], mCherry-GFP-REEP5 [1372], and ssRFP-GFP-KDEL [464]. These tandem fluorescent protein reporters are detected as yellow signals in the ER, but when they are delivered to lysosomes by autophagy, they become red, as the GFP signal is quenched. Cleavage of these reporters in lysosomes can also be monitored by immunoblotting.

The COPII complex has also been associated with an additional, less understood pathway involving noncanonical, microautophagy-like degradation of ER exit sites (ERES) containing misfolded procollagen [1388]. This pathway is characterized by cargo colocalization with COPII proteins and lysosomal markers without ER membrane or lumen markers; the colocalization is further enhanced by lysosomal hydrolase inhibitors. Cargo selectivity and activation mechanisms for this recently identified pathway have not yet been established.

Ribophagy. Autophagy has been reported for the selective removal of ribosomes in yeast, particularly upon nitrogen starvation [1389]; however, it remains unclear whether yeast has a dedicated ribophagy pathway that is activated under conditions of nitrogen starvation. Published papers monitor this process by western blot, following the generation of free GFP from Rpl5-GFP or Rpl25-GFP [1390], or the disappearance of ribosomal subunits such as Rps3. Vacuolar localization of Rpl5-GFP or Rpl25-GFP can also be seen by fluorescence microscopy. The Rkr1/Ltn1 ubiquitin ligase is reported to act as an inhibitor of 60S ribosomal subunit ribophagy via, at least, Rpl25 as a target, and is antagonized by the deubiquitinating Ubp3-Bre5 complex [1389,1390]. Rkr1/Ltn1 and Ubp3-Bre5 are proposed to contribute to adapt ribophagy activity to both nutrient supply and protein translation. Ribophagy has also been observed in animal cells, for instance in arsenite-treated mammalian cells, as was

demonstrated with Ribo-Keima flux assays alongside a variety of other Keima-based flux assays [1037].

RNA-silencing components. Several components of the RNA-silencing machinery are selectively degraded by autophagy in different organisms. This was first shown for the plant AGO1/ARGONAUTE1 protein, a key component of the Arabidopsis RNA-induced silencing complex (RISC) that, after ubiquitination by a virus encoded F-box protein, is targeted to the vacuole [1391]. AGO1 colocalizes with Arabidopsis ATG8a-positive bodies, and its degradation is impaired by various drugs such as 3-MA and E64d, or in Arabidopsis mutants in which autophagy is compromised such as the TOR-overexpressing mutant line G548 or the *atg7-2* mutant allele [1391]. Moreover, this pathway also degrades AGO1 in a nonviral context, especially when the production of miRNAs is impaired. Defects in miRNA biogenesis also cause autophagic degradation of *Drosophila* AGO1 [1392]. In mammalian cells, not only the main miRNA effector AGO2, but also the miRNA-processing enzyme DICER1, is degraded as a miRNA-free entity by selective autophagy [1393]. Chemical inhibitors of autophagy (bafilomycin A₁ and CQ) and, in HeLa cells, depletion of key autophagy components ATG5, BECN1/ATG6 or ATG7 using short interfering RNAs, blocks the degradation of both proteins. Electron microscopy shows that DICER1 is associated with membrane-bound structures having the hallmarks of autophagosomes. Moreover, the selectivity of DICER1 and AGO2 degradation might depend on the autophagy receptor CALCOCO2, at least in these cell types. Finally, in *C. elegans*, AIN-1, a homolog of mammalian TNRC6A/GW182 that interacts with AGO and mediates silencing, is also degraded by autophagy [1394]. AIN-1 colocalizes with the *C. elegans* SQSTM1 homolog SQST-1 that acts as a receptor for autophagic degradation of ubiquitinated protein aggregates, and also directly interacts with Atg8-family proteins contributing to cargo specificity.

RNautophagy and DNautophagy. RNautophagy and DNautophagy are non-macroautophagic pathways, where RNA and DNA, respectively, are taken up by lysosomes directly [1395-1398]. LAMP2C, one of the LAMP2 isoforms, can function as an RNA/DNA receptor in RNautophagy and DNautophagy. SIDT2 is another molecule that has been identified to mediate nucleic acid transport during RNautophagy and DNautophagy [1399-1401]. SIDT2 is a lysosomal multi-pass transmembrane protein, and a vertebrate ortholog of the *C. elegans* RNA transporter SID-1.

RNautophagy and DNautophagy were first discovered using *in vitro* assays with isolated lysosomes derived from mouse brains [1395,1397], and are also confirmed in isolated lysosomes from HeLa, Neuro2a cells, and MEFs. *In vitro* assays can be used to detect the activity of RNautophagy or DNautophagy in isolated lysosomes. The activity of RNautophagy at the cellular level can be detected in mammalian cells using a pulse-chase assay [1400]. For example, overexpression of SIDT2 in Neuro2a cells remarkably promotes lysosomal degradation of RNA at the cellular level [1401]. Knockdown of SIDT2 significantly inhibits lysosomal degradation of cellular RNA in MEFs [1400]. Currently, it remains unclear whether there is a SIDT2-independent pathway in

RNautophagy and DNautophagy. The activity of DNautophagy at the cellular level has not been reported to date. G/dG sequences in nucleic acids could be motifs that are recognized by RNautophagy and DNautophagy, because poly-G/dG are a substrate of RNautophagy and DNautophagy *in vitro*, but poly-C/dC, poly-A/dA, poly-U or poly-T are not [1398].

Conclusion: Currently, RNautophagy and DNautophagy activities can be significantly manipulated only by knockdown or overexpression of SIDT2. Identification of nucleic acid sequences that are recognized by RNautophagy or DNautophagy, or specific inhibitors of these pathways, would contribute to the development of novel methods that can monitor RNautophagy and DNautophagy more accurately.

Vacuole import and degradation pathway. In yeast, gluconeogenic enzymes such as Fbp1/FBPase (fructose-1,6-bisphosphatase), Mdh2 (malate dehydrogenase), Icl1(isocitrate lyase) and Pck1 (phosphoenolpyruvate carboxykinase) constitute the cargo of the vacuole import and degradation (Vid) pathway [1402]. These enzymes are induced when yeast cells are glucose starved (grown in a medium containing 0.5% glucose and potassium acetate). Upon replenishing these cells with fresh glucose (a medium containing 2% glucose), these enzymes are degraded in either the proteasome [1403-1405] or the vacuole [1402,1406] depending on the duration of starvation. Following glucose replenishment after 3 days of glucose starvation, the gluconeogenic enzymes are delivered to the vacuole for degradation [1407]. These enzymes are sequestered in specialized 30- to 50-nm Vid vesicles [1408]. Vid vesicles can be purified by fractionation and gradient centrifugation; western blotting analysis using antibodies against organelle markers and Fbp1, and the subsequent verification of fractions by EM facilitate their identification [1408]. Furthermore, the amount of marker proteins in the cytosol compared to the Vid vesicles can be examined by differential centrifugation. In this case, yeast cells are lysed and subjected to differential centrifugation. The Vid vesicle-enriched pellet fraction and the cytosolic supernatant fraction are examined with antibodies against Vid24, Vid30, Sec28 and Fbp1 [1409-1411].

The distribution of Vid vesicles containing cargo destined for endosomes, and finally for the vacuole, can be examined using FM 4-64, a lipophilic dye that primarily stains endocytic compartments and the vacuole limiting membrane [1412]. In these experiments, starved yeast cells are replenished with fresh glucose and FM 4-64, and cells are collected at appropriate time points for examination by fluorescence microscopy [1410]. The site of degradation of the cargo in the vacuole can be determined by studying the distribution of Fbp1-GFP, or other Vid cargo markers in wild-type and *pep4Δ* cells [1413]. Cells can also be examined for the distribution of Fbp1 at the ultrastructural level by immuno-TEM [1414].

As actin patch polymerization is required for the delivery of cargo to the vacuole in the Vid pathway, distribution of Vid vesicles containing cargo and actin patches can be examined by actin staining (with phalloidin conjugated to rhodamine) using fluorescence microscopy [1414]. The distribution of GFP-tagged protein and actin is examined by fluorescence microscopy. GFP-Vid24, Vid30-GFP and Sec28-GFP colocalize with actin during prolonged glucose starvation and for up

to 30 min following glucose replenishment in wild-type cells; however, colocalization is less obvious by the 60-min time point [1409,1414].

Virophagy. Virophagy is a type of xenophagy, and refers to the autophagic clearance of viruses. An important point when considering the convergence of autophagy and viral infection is that some viruses have evolved mechanisms to block autophagy or to subvert the process to promote viral replication. For example, infection of a cell by influenza and dengue viruses [1415,1416] or enforced expression of the hepatitis B virus X protein [1417] have profound consequences for autophagy, as viral proteins such as NS4A stimulate autophagy and protect the infected cell against apoptosis, thus extending the time in which the virus can replicate. Conversely, the HSV-1 ICP34.5 protein inhibits autophagy by targeting BECN1 [1418]. Whereas the impact of ICP34.5's targeting of BECN1 on viral replication in cultured permissive cells is minimal, it has a significant impact upon pathogenesis in vivo, most likely through interfering with activation of CD4⁺ T cells [1419,1420], and through cell-intrinsic antiviral effects in neurons [1421]. In addition, the ICP0 protein of HSV-1 downregulates major autophagy receptors such as SQSTM1 and OPTN during the early stages of HSV-1 infection. This could be a mechanism of HSV-1 to counteract the pleiotropic functions of these autophagy receptors, because in SQSTM1-overexpressing cells HSV-1 virus yields decrease [1422]. Also, viral BCL2 proteins, encoded by large DNA viruses, are able to inhibit autophagy by interacting with BECN1 [848] through their BH3 homology domain. Examples of these include γ -herpesvirus 68 [1423], Kaposi sarcoma-associated herpesvirus [848] and African swine fever virus (ASFV) vBCL2 homologs [1424]. ASFV encodes a protein homologous to HSV-1 ICP34.5, which, similar to its herpesvirus counterpart, inhibits the ER stress response activating PPP1/protein phosphatase 1; however, in contrast to HSV-1 ICP34.5 it does not interact with BECN1. ASFV vBCL2 strongly inhibits both autophagy (reviewed in ref [1425].) and apoptosis [1426]. The polyQ repeats in some viral proteins could also affect BECN1-mediated autophagy and play a role in virus survival [1427].

HIV has evolved to employ different strategies to finely regulate autophagy to favor its replication and dissemination. In particular, the HIV proteins TAT, NEF and ENV are involved in this regulation by either blocking or stimulating autophagy through direct interaction with autophagy proteins and/or modulation of the MTOR pathway [1428,1429].

Autophagy contributes to limiting viral pathogenesis in HIV-1 nonprogressor-infected patients by targeting viral components for degradation [1430]. Innate immune stimulation induces antiviral autophagy against Rift Valley fever virus from insects to humans [1431]. One of the Fanconi anemia (FA) genes, *Fancc*, is required for virophagy of two genetically distinct viruses, Sindbis virus and HSV-1 Δ ICP34.5BBD, but not for starvation-induced autophagy. Knockout of *Fancc* in mice increases susceptibility to lethal viral encephalitis [1432]

In the case of Epstein-Barr virus (EBV), several EBV proteins including EBNA1, EBNA3C, LMP1, LMP2A and Rta/Zta interact with the autophagy machinery in B cells. Autophagy

is involved in the processing and MHC-II presentation of EBNA1 [1433]. Conversely, EBNA3C, LMP1, LMP2A and Rta initiate and accelerate autophagy progression [1434-1437]. Moreover, autophagy inhibition by 3-MA or ATG5 knockdown diminishes EBV lytic protein expression and viral particle production in B cells [1438]. Autophagy also plays a key role in B-cell proliferation and survival early after infection [1439].

Adenoviruses rupture the endosomal membrane upon entry, thereby triggering antiviral autophagy mediated by LGALS8/galectin-8 (lectin, galactoside-binding, soluble, 8). Adenovirus subsequently limit the autophagic response by recruiting the cellular ubiquitin ligase NEDD4L/NEDD4.2 and escape from the endosome into the cytosol [1440]. In addition, autophagosomes may fuse with intermediate endosomes in response to certain specific viral infections, thus forming amphisomes [1441-1443].

Care must be taken in determining the role of autophagy in viral replication, as some viruses such as vaccinia virus use double-membrane structures that form independently of the autophagy machinery [1444]. Similarly, dengue virus replication, which appears to involve a double-membrane compartment, requires the ER rather than autophagosomes [1445,1446], whereas coronaviruses and Japanese encephalitis virus use a nonlipidated version of LC3 (see *Atg8-family protein detection and quantification*) [255,256]. Yet another type of variation is seen with hepatitis C virus, which requires BECN1, ATG4B, ATG5 and ATG12 for initiating replication, but does not require these proteins once an infection is established [1447].

Autophagy has been highlighted as a critical player in the process of Zika virus (ZIKV) infection and pathogenesis, particularly during pregnancy [1448]. In mammals, autophagy activation is triggered by ZIKV infection likely due to inhibition of the AKT-MTOR pathway, which is co-opted to facilitate viral entry, replication, and release [1448-1450]. Pharmacological blockade of autophagy activity, for example, treatment with lysosomotropic agents (especially hydroxychloroquine [HCQ]), is proposed as a promising therapeutic to counteract ZIKV infection and limit vertical transmission [1448].

After viral hemorrhagic septicemia virus (VHSV) entry into rainbow trout red blood cells, autophagy is induced as a mechanism for viral protein degradation. VHSV triggers an increase of LC3A/B protein levels and upregulation of autophagy-related genes such as *ULK1*, *BECN1*, and *ATG9A*, whereas SQSTM1 undergoes degradation early after VHSV exposure. Inhibition of autophagosome degradation with niclosamide results in intracellular VHSV and SQSTM1 accumulation [1451].

Xenophagy. Xenophagy refers to the autophagic pathway for the capture and lysosomal degradation of cytosolic pathogens, and pathogens in damaged intracellular vacuoles. Many *in vitro* and *in vivo* studies have demonstrated that genes encoding autophagy components are required for host defense against infection by bacteria, parasites and viruses. In a quest for survival, microbial pathogens have evolved strategies to overcome xenophagic clearance. The interactions of these pathogens with the host autophagy system are complex and

have been the subject of several excellent reviews [170-175,628,1452-1460]. There are a few key considerations when studying interactions of microbial pathogens with the autophagy system [1461]. Importantly, autophagy should no longer be considered as strictly antibacterial, and several studies have described the fact that autophagy may serve to either restrict or promote bacterial replication both in vivo [1462] and in vitro (reviewed in refs. [1463,1464]). Moreover, special care should be taken when evaluating bacterial-induced specific autophagy and autophagic flux, because an increased basal autophagy and flux perceived by western blot may be unlinked to the cellular compartment of the bacterial vacuole, which can be revealed by careful examination of the bacterial compartment using IHC and colocalization studies [1465]. For example, autophagy has been proposed to both support the survival of intraphagosomal *M. marinum*, by providing cytosolic material and/or membranes to the bacteria-containing compartment, and to restrict the proliferation of the cytosolic mycobacteria in *D. discoideum* [64,1322]. In addition to pathogenic bacteria, autophagy can be induced by beneficial bacteria, contributing to alleviation of the hepatotoxicity induced by acetaminophen, *in vitro* [1466].

LC3 is commonly used as a marker of autophagy. However, studies have established that LC3 can promote phagosome maturation independently of autophagy through LC3-associated phagocytosis (see cautionary notes in *Atg8-family protein detection and quantification*, and *Noncanonical use of autophagy-related proteins*). Other studies show that autophagy of *Salmonella enterica* serovar Typhimurium (*S. Typhimurium*) is dependent on ATG9, an essential autophagy protein, whereas LC3 recruitment to a bacteria-containing phagosome does not require ATG9 [1467]. In contrast, autophagy of these bacteria requires either glycan-dependent binding of LGALS8 to damaged membranes and subsequent recruitment of the cargo receptor CALCOCO2 [1468], or ubiquitination of target proteins (not yet identified) and recruitment of at least four different ubiquitin-binding receptor proteins, SQSTM1 [1469], CALCOCO2 [1470], TAX1BP1/CALCOCO3 [1471] and OPTN [1472]. In fibroblasts, *S. Typhimurium* triggers the formation of host endomembrane-containing aggregates that are further captured together with intravacuolar bacteria by phagophores harboring LC3 and SQSTM1, but devoid of CALCOCO2 and ubiquitin [1473]. Therefore, the available criteria to differentiate LAP from autophagy include: i) LAP involves LC3 recruitment to a bacteria-containing phagosome in a manner that requires ROS production by an NADPH oxidase. It should be noted that most cells express at least one member of the NADPH oxidase family. Targeting expression of the common CYBA/p22^{phox} subunit is an effective way to disrupt the NADPH oxidases. Scavenging of ROS by antioxidants such as NAC, resveratrol and alpha-tocopherol is also an effective way to inhibit LAP. ii) Autophagy of bacteria requires ATG9, whereas LAP apparently does not [1467]. iii) LAP involves single-membrane structures surrounding the bacterial cargo. CLEM is expected to show single-membrane structures that are LC3⁺ with LAP [247]. In contrast, autophagy is expected to generate double-membrane structures surrounding cargo (which may include single-membrane

phagosomes, giving rise to triple-membrane structures around the bacterial membrane(s), corresponding to an autophagolysosome [1467]). It is anticipated that more specific markers of LAP will be identified as these phagosomes are further characterized. *In vivo* xenophagy studies in mice show that *S. Typhimurium* reduces the level of basal autophagy in tissues such as intestine as seen by LC3-II levels at later times of infection [1474]. This suggests that pathogens have the ability to decrease host autophagy for their survival. Recently identified xenophagy-enhancing compounds show enhanced capture and degradation of *S. Typhimurium* in both cellular and in vivo models with enhanced LC3-II levels in tissues [1475].

Elegant mechanisms that differentiate autophagy from LAP have emerged that demonstrate that there are mechanistic differences between these processes. For example, ATG16L1 recruitment to the phagosome in *Salmonellae*-infected cells occurs through a carboxy-terminal WD40 domain that binds to the V-ATPase on the phagosome, which is dispensable for canonical autophagy [1476,1477]. This domain is also required in influenza infection [1478]. These studies illustrate that while LC3 targeting of a pathogen-containing vacuole uses components shared with canonical autophagy, it utilizes a distinct mechanism.

Nonmotile *Listeria monocytogenes* can be targeted to phagophores upon antibiotic treatment [883], which indicates that autophagy serves as a cellular defense against microbes in the cytosol. However, subsequent studies have revealed that autophagy can also target pathogens within phagosomes, damaged phagosomes or the cytosol, as illustrated by the various phases of infection of *M. marinum* in *D. discoideum* [1322,1459]. Therefore, when studying microbial interactions by EM, many structures can be visualized, with any number of membranes encompassing microbes, all of which may be LC3⁺ [1479,1480]. As discussed above, single-membrane structures that are LC3⁺ may arise through LAP, and we cannot rule out the possibility that both LAP and autophagy may operate at the same time to target the same phagosome. Indeed, autophagy may facilitate phagocytosis and subsequent bacterial clearance [1481]. Autophagy is not only induced by intracellular bacteria, but also can be activated by extracellular bacteria such as *Pseudomonas aeruginosa* and *Klebsiella pneumoniae*, which may involve complex mechanisms [1482-1484]. Furthermore, autophagy can be induced by Gram-negative bacteria via a common mechanism involving naturally-produced bacterial outer membrane vesicles [1485,1486]; these vesicles enter human epithelial cells, resulting in autophagosome formation and inflammatory responses mediated via the host pathogen recognition receptor NOD1 [1485,1487]. In addition, highly purified outer membrane proteins from bacteria and mitochondria can trigger autophagy [1488]. Upon specific stimulation, NOD1 binds to LC3 inducing an increased autophagy flux and autolysosome formation, and LC3-NLRP3 inflammasome interaction, in epithelial Sertoli cells [1489]. The ability of NOD1 to sense ER stress and cell damage and induce pro-inflammatory signaling is regulated by ATG16L1 [1490], implicating autophagy and inflammasomes in environmental stress responses. NOD2 also regulates autophagy upon stimulation by danger/damage-associated molecular patterns (DAMPs) such as the

bacterial NOD2 ligand sulfatide. NOD2 connects inflammation hypoxia and autophagy, as NOD2 is a direct transcriptional target of HIF1A, the main oxygen sensor in mammalian cells induced by reduced oxygen. Hypoxia-induced NOD2 functions upstream of CQ and directly binds to the V-ATPase complex, regulating vesicular pH [1491].

Viruses can also be targeted by autophagy, and in turn can act to inhibit autophagy (see *Virophagy*). Xenophagy has also been observed with intracellular parasites. Mice deficient in autophagy develop a more severe *Trypanosoma cruzi* infection, characterized by higher peaks of parasitemia, higher cardiac amastigote nests and premature death, compared to controls. Peritoneal macrophages from these mice display higher levels of infection that correlate with the minor recruitment of LC3 and other proteins, such as CALCOCO2 and SQSTM1, to amastigotes, observed in the cytoplasm of RAW cells in the presence of inhibitors of autophagy [1492].

Finally, it is important to realize that there may be other autophagy-like pathways that have yet to be characterized. For example, in response to cytotoxic stress (treatment with etoposide), autophagosomes are formed in an ATG5- and ATG7-independent manner (see *Noncanonical use of autophagy-related proteins*) [31]. While this does not rule out involvement of other autophagy regulators/components in the formation of these autophagosomes, it does establish that the canonical autophagy pathway involving LC3 conjugation is not involved. In contrast, RAB9 is required for this alternative pathway, potentially providing a useful marker for analysis of these structures. Returning to xenophagy, *M. marinum* can be targeted to phagophores in an ATG5-independent manner [1493]. Furthermore, up to 25% of intracellular *S. typhimurium* are observed in multi-lamellar membrane structures resembling autophagosomes in *atg5*^{-/-} MEFs [1469]. These findings indicate that an alternate autophagy pathway is relevant to host-pathogen interactions. Moreover, differences are observed that depend on the cell type being studied. *Yersinia pseudotuberculosis* is targeted to autophagosomes where it can replicate in bone marrow-derived macrophages [1494], whereas in RAW 264.7 and J774 cells, bacteria are targeted both to autophagosomes, and LC3-negative, single-membrane vacuoles (F. Lafont, personal communication).

One key consideration has recently emerged in studying xenophagy. Whereas the basal autophagic flux in most cells is essential for their survival, infecting pathogens can selectively modulate antibacterial autophagy (i.e., xenophagy) without influencing basal autophagy. This may help pathogens ensure prolonged cellular (i.e., host) survival. Thus, in the case of xenophagy it would be prudent to monitor substrate (pathogen)-specific autophagic flux to understand the true nature of the perturbation of infecting pathogens on autophagy [1495,1496]. Furthermore, this consideration particularly limits the sensitivity of LC3 western blots for use in monitoring autophagy regulation, and stresses that other techniques such as those enabling subcellular analysis of the pathogen-specific compartment/vacuole are additionally used. For instance, to verify that the effect of a total reduction in LC3-II during autophagy induction by western blot also extends to the subcellular compartment of the pathogen/bacterial vacuole by using LC3-based microscopy [1465].

Zymophagy. Zymophagy was originally defined as a specific mechanism that eliminates zymogen granules in the pancreatic acinar cells and, thus, prevents deleterious effects of prematurely activated and intracellularly released proteolytic enzymes, when impairment of secretory function occurs [1497]. Therefore, zymophagy is primarily considered to be a protective mechanism implemented to sustain secretory homeostasis and to mitigate pancreatitis. The presence of zymogen granules, however, is not only attributed to pancreatic acinar cells. Thus, zymophagy was also reported in activated secretory Paneth cells of the crypts of Lieberkühn in the small intestine [542]. Note that one of the major functions of Paneth cells is to prevent translocation of intestinal bacteria by secreting hydrolytic enzymes and antibacterial peptides to the crypt lumens. The similarity in mechanisms of degradation of secretory granules in these two different types of secretory cells sustains the concept of the protective role of autophagy when “self-inflicted” damage may occur due to overreaction and/or secretory malfunction in specialized cells.

Zymophagy can be monitored by TEM, identifying autophagosomes containing secretory granules, by following SQSTM1 degradation by western blot, and by examining the subcellular localization of VMP1-EGFP, which relocates to granular areas of the cell upon zymophagy induction. Colocalization of PRSS1/trypsinogen (which is packaged within zymogen granules) and LC3, or of GFP-ubiquitin (which is recruited to the activated granules) with RFP-LC3 can also be observed by indirect or direct immunofluorescence microscopy, respectively. Active trypsin is also detectable in zymophagosomes and participates in the early onset of acute pancreatitis (F. Fortunato et al., unpublished data). In addition, isolated zymogen granules from alcohol-fed mouse pancreas also contain LC3-II based on western blot analysis, which may also serve as another indirect quantitative marker for zymophagy [1498].

Of note, studies from the past decade have shown an essential role of autophagy in maintaining pancreatic acinar cell homeostasis and function, and strongly implicate impaired autophagy in initiation and development of pancreatitis (see *Large animals and rodents*). In particular, immunofluorescence data [1499] indicate autolysosomes as one compartment in which trypsinogen activation occurs in pancreatitis, as evidenced by colocalization of LC3-II and LAMP2 with trypsinogen activation peptide (an oligopeptide cleaved off trypsinogen in the process of its conversion to active trypsin). Impaired TFEB-mediated lysosomal biogenesis has also been shown to promote cerulein or alcohol-induced pancreatitis in mice. In addition to experimental pancreatitis, acinar cell nuclear TFEB staining markedly decreased in both human alcoholic and non-alcoholic pancreatitis, supporting a critical role of autophagy and lysosomal biogenesis in the pathogenesis of pancreatitis [1498,1500].

Autophagic sequestration assays

Although it is useful to employ autophagic markers such as LC3 in studies of autophagy, LC3-II levels or LC3 puncta cannot quantify actual autophagic activity, because LC3-II is not involved in all cargo sequestration events, and LC3-II can be found on phagophores and nonautophagosomal

membranes in addition to autophagosomes. Thus, quantification of autophagic markers such as LC3 does not tell how much cargo material has actually been sequestered inside autophagosomes. Moreover, LC3 and several other autophagic markers cannot be used to monitor noncanonical autophagy. Autophagic sequestration assays constitute marker-independent methods to measure the sequestration of autophagic cargo into autophagosomal compartments, and are among the few functional autophagy assays described to date.

Autophagic cargo sequestration activity can be monitored using either an (electro)injected, inert cytosolic marker such as [³H]-raffinose [1501] or an endogenous cytosolic protein such as LDH (lactate dehydrogenase) [1502], in the latter case along with treatment with a protease inhibitor (e.g., leupeptin) or other inhibitors of lysosomal activity or autophagosome-lysosome fusion (e.g., bafilomycin A₁, concanamycin A, or CQ) [216,302,1503] to prevent intralysosomal degradation of the protein marker. The assay simply measures the transfer of cargo from the soluble (cytosol) to the insoluble (sedimentable) cell fraction (which includes autophagic compartments), with no need for a sophisticated subcellular fractionation. Electrodissruption of the plasma membrane followed by centrifugation through a density cushion was originally used to separate cytosol from sedimentable cell fractions in primary hepatocytes [1504]. This method has also been used in various human cancer cell lines and mouse embryonic fibroblasts, where the LDH sequestration assay has been validated with pharmacological agents as well as genetic silencing or knockout of key factors of the autophagic machinery (N. Engedal, unpublished results) [32,56,216,473,1503,1505]. Moreover, a downscaling and simplification of the method that avoids the density cushion has been introduced and validated [56,473,1503,1506]. Homogenization and sonication techniques have also been successfully used for the LDH sequestration assay [1017,1507]. The endogenous LDH cargo marker can be quantified by an enzymatic assay, or by western blotting. In principle, any intracellular component can be used as a cargo marker, but cytosolic enzymes having low sedimentable backgrounds are preferable. Membrane-associated markers are less suitable, and proteins such as LC3, which are part of the sequestering system itself, will have a much more complex relationship to the autophagic flux than a pure cargo marker such as LDH.

In yeast, sequestration assays are typically done by monitoring protease protection of an autophagosome marker or a cargo protein. For example, prApe1, and GFP-Atg8 have been used to follow completion of the autophagosome [1508]. The relative resistance or sensitivity to an exogenous protease in the absence of detergent is an indication of whether the autophagosome (or other sequestering vesicle) is complete or incomplete, respectively. Thus, this method also distinguishes between a block in autophagosome formation versus fusion with the vacuole. The critical issues to keep in mind involve the use of appropriate control strains and/or proteins, and deciding on the correct reporter protein. In addition to protease protection assays, sequestration can be monitored by fluorescence microscopy during pexophagy of methanol-induced peroxisomes, using GFP-Atg8 as a pexophagosome marker and BFP-SKL to label the peroxisomes. The vacuolar

sequestration process during micropexophagy can also be monitored by formation of the vacuolar sequestering membrane stained with FM 4-64 [1053].

Sequestration assays can be designed to measure flux through individual steps of the autophagy pathway. For example, whereas electroinjected [³H]-raffinose or endogenous LDH can be used to measure the sequestration step, electroinjected [¹⁴C]-lactose can be used to monitor cargo flux to amphisomes and proteolytically active autolysosomes (as explained below). Whereas [³H]-raffinose is completely resistant to (auto)lysosomal degradation, the [¹⁴C]-lactose that reaches active autolysosomes is rapidly hydrolyzed into [¹⁴C]-glucose and galactose (by GLB1/beta-galactosidase), measurable by chromatography. [¹⁴C]-lactose thus marks prelysosomal compartments (autophagosomes and amphisomes), whereas [¹⁴C]-glucose marks the autolysosomal compartment. Experimental conditions or treatments that block autophagosome-lysosome fusion (e.g., asparagine or the microtubule inhibitor vinblastine) lead to an accumulation of lactose in prelysosomal compartments [11,1509]. By adding exogenous beta-galactosidase (that is endocytosed by the cells) in the presence of asparagine (which blocks autophagosome-lysosome fusion), the fusion of autophagosomes with endosomes (thus producing amphisomes) can be studied. In fact, this was the experimental approach that first identified the amphisome [11].

One caveat with using lysosome or autophagosome-lysosome inhibitors is that they may affect sequestration indirectly, for example, by modifying the uptake and metabolism (including protein synthesis) of autophagy-suppressive amino acids (see *Autophagy inhibitors and inducers*). Therefore, the time period of treatment with the inhibitor should be as short as possible (typically 2-3 h). Note that for measuring autophagic sequestration and degradation activity with electroinjected [³H]-raffinose or [¹⁴C]-lactose, respectively, no inhibitors are needed. Also note that the LDH sequestration assay, when used without addition of lysosomal degradation inhibitors, can be used to identify treatments or conditions that block autophagic flux at a post-sequestration step. For instance, autophagically sequestered LDH accumulates in cells depleted of RAB7A (but not RAB7B) [1505], thus confirming the role of RAB7A in autophagosome-lysosome fusion [344,1510,1511].

A variation of this approach applicable to mammalian cells includes live cell imaging. Autophagy induction is monitored as the movement of cargo, such as mitochondria, to GFP-LC3-colocalizing compartments, and then fusion/flux is measured by delivery of cargo to lysosomal compartments [439,1512]. In addition, sequestration of fluorescently tagged cytosolic proteins into membranous compartments can be measured, as fluorescent puncta become resistant to the detergent digitonin [1513]. Use of multiple time points and monitoring colocalization of a particular cargo with GFP-LC3 and lysosomes can also be used to assess sequestration of cargo with autophagosomes as well as delivery to lysosomes [1138]. Moreover, colocalization of cargo with endogenous LC3 puncta using immunofluorescent staining can be used [606].

Time-lapse microscopy allows direct visualization of vacuole transfer from mother cells to their daughters as seen for A549

lung cancer cells exposed to yessotoxin (YTX) [1514]. Such effects on downstream lineages may be significant for the interpretation of observations related to autophagy signaling especially for cells in environments where the stress varies. Autophagic activity caused by this toxin results in the sequestration and degradation, by an autophagic-like process, of ribosomes and lipid droplets associated with autophagic compartments and lamellar bodies in BC3H1 cells [1515].

In the *Drosophila* fat body, the localization of free cytosolic RFP-family proteins changes from a diffuse to a punctate pattern in an *Atg* gene-dependent manner, and these mCherry puncta colocalize with the lysosomal marker Lamp1-GFP during starvation [1516]. Thus, the redistribution of free cytosolic mCherry may be used to follow bulk, nonselective autophagy due to its stability and accumulation in autolysosomes.

Cautionary notes: The electro-injection of radiolabeled probes is technically demanding, but the use of an endogenous cytosolic protein probe is very simple and requires no pretreatment of the cells other than with a protease inhibitor. Another concern with electro-injection is that it can affect cellular physiology, so it is necessary to verify that the cells behave properly under control situations such as amino acid deprivation. An alternate approach for incorporating exogenous proteins into mammalian cell cytosol is to use “scrape-loading,” a method that works for cells that are adherent to tissue culture plates [1517]. Finally, these assays work well with hepatocytes but may be problematic with other cell types, and it can be difficult to load the cell while retaining the integrity of the compartments in the post-nuclear supernatant (S. Tooze, unpublished results). General points of caution to be addressed with regard to live cell imaging relate to photobleaching of the fluorophore, cell injury due to repetitive imaging, autofluorescence in tissues containing lipofuscin, and the pH sensitivity of the fluorophore.

There are several issues to keep in mind when monitoring sequestration by the protease protection assay in yeast [1508]. First, as discussed in *Selective types of autophagy*, prApe1 is not an accurate marker for nonselective autophagy; import of prApe1 utilizes a receptor (*Atg19*) and a scaffold (*Atg11*) that make the process specific. In addition, vesicles that are substantially smaller than autophagosomes can effectively sequester the Cvt complex. Another problem is that prApe1 cannot be used as an autophagy reporter for mutants that are not defective in the Cvt pathway, although this can be bypassed by using a *vac8Δ* background [1518]. At present, the prApe1 assay cannot be used in any system other than yeast. The GFP-*Atg8* protease protection assay avoids these problems, but the signal-to-noise ratio is typically substantially lower. In theory, it should be possible to use this assay in other cell types, and protease protection of GFP-LC3 and GFP-SQSTM1 has been analyzed in HeLa cells [1519]. Finally, tendencies of GFP-LC3 and particularly GFP-SQSTM1 to aggregate may make LC3 and SQSTM1 inaccessible to proteases.

Conclusion: Sequestration assays represent the most direct method for monitoring autophagy, and in particular for discriminating between conditions where the autophagosome is complete (but not fused with the lysosome/vacuole) or open (i.e., a phagophore). These assays can also be modified to measure autophagic flux.

Turnover of autophagic compartments

Inhibitors of autophagic sequestration (e.g., amino acids, 3-MA, wortmannin, SAR-405, BAPTA-AM, MRT67307, or thapsigargin) [32,56,216,299,1032,1503,1520] can be used to monitor the disappearance of autophagic elements (phagophores, autophagosomes, autolysosomes) to estimate their half-life by TEM morphometry/stereology. The turnover of the autophagosome or the autolysosome will be differentially affected if fusion or intralysosomal degradation is inhibited [13,15,28,1521]. The duration of such experiments is usually only a few hours; therefore, long-term side effects or declining effectiveness of the inhibitors can be avoided. It should be noted that fluorescence microscopy has also been used to monitor the half-life of autophagosomes, monitoring GFP-LC3 in the presence and absence of bafilomycin A₁ or following GFP-LC3 after starvation and recovery in amino acid-rich medium (see *Atg8-family protein detection and quantification*) [17,1522].

Cautionary notes: The inhibitory effect must be strong, and the efficiency of the inhibitor needs to be tested under the experimental conditions to be employed. Cycloheximide is sometimes used as an autophagy inhibitor, but its use in long-term experiments is problematic because of the many potential indirect effects. CHX inhibits translational elongation, and therefore protein synthesis. In addition, CHX decreases the efficiency of protein degradation in several cell types (A.M. Cuervo, personal communication) including hematopoietic cells (A. Edinger, personal communication). Treatment with CHX causes a potent increase in MTORC1 activity, which can decrease autophagy in part as a result of the increase in the amino acid pool resulting from suppressed protein synthesis (H.-M. Shen, personal communication; I. Topisirovic, personal communication) [27,1523]. In addition, at high concentrations (in the millimolar range) CHX inhibits complex I of the mitochondrial respiratory chain [1524,1525], but this is not a problem, at least in hepatocytes, at low concentrations (10–20 μM) that are sufficient to prevent protein synthesis (A.J. Meijer, personal communication).

Conclusion: The turnover of autophagic compartments is a valid method for monitoring autophagic-lysosomal flux, but CHX must be used with caution in long-term experiments.

Autophagosome-lysosome colocalization and dequenching assay

Another method to demonstrate the convergence of the autophagic pathway with a functional degradative compartment is to incubate cells with the bovine serum albumin derivative dequenched (DQ)-BSA that is labeled with the red-fluorescent BODIPY TR-X dye; this conjugate will accumulate in lysosomes. The labeling of DQ-BSA is so extensive that the fluorophore is self-quenched. Proteolysis of this compound results in dequenching and the release of brightly fluorescent fragments. Thus, DQ-BSA is useful for detecting intracellular proteolytic activity as a measure of a functional lysosome [1526].

Furthermore, DQ-BSA labeling can be combined with GFP-LC3 to monitor colocalization, and thus visualize the convergence, of amphisomes with a functional degradative compartment (DQ-BSA is internalized by endocytosis). This method can also be used to visualize fusion events in real-time

experiments by confocal microscopy (live cell imaging). Along similar lines, other approaches for monitoring convergence are to follow the colocalization of RFP-LC3 and LysoSensor Green (M. Bains and K.A. Heidenreich, personal communication), mCherry-LC3 and LysoSensor Blue [441], or tagged versions of LC3 and LAMP1 (K. Macleod, personal communication) or CD63 [439] as a measure of the fusion of autophagosomes with lysosomes. It is also possible to trace autophagic events by visualizing the pH-dependent excitation changes of the coral protein Keima [1036]. This quantitative technique is capable of monitoring the fusion of autophagosomes with lysosomes, that is, the formation of an autolysosome, and the assay does not depend on the analysis of LC3.

Cautionary notes: Some experiments require the use of inhibitors (e.g., 3-MA or wortmannin) or overexpression of proteins (e.g., RAB7 dominant negative mutants) that may also affect the endocytic pathway or the delivery of DQ-BSA to lysosomes (e.g., wortmannin causes the swelling of late endosomes [1527]). In this case, the lysosomal compartment can be labeled with DQ-BSA overnight before treating the cells with the drugs, or prior to the transfection.

Conclusion: DQ-BSA provides a relatively convenient means for monitoring lysosomal protease function and can also be used to follow the fusion of amphisomes with the lysosome. Colocalization of autophagosomes (fluorescently tagged LC3) with lysosomal proteins or dyes can also be monitored.

Tissue fractionation

The study of autophagy in the organs of larger animals, in large numbers of organisms with very similar characteristics, or in tissue culture cells provides an opportunity to use tissue fractionation techniques as has been possible with autophagy in rat liver [50,69,1528-1533]. Because of their sizes (smaller than nuclei but larger than membrane fragments [microsomes]), differential centrifugation can be used to obtain a subcellular fraction enriched in mitochondria and organelles of the autophagy-lysosomal system, which can then be subjected to density gradient centrifugation to enrich autophagosomes, amphisomes, autolysosomes and lysosomes [50, 69 [1533-1537],]. Please see previous versions of the guidelines [1,2] for a discussion of the uses and limitations of tissue fractionation.

In vitro determination of autophagosome formation

Mobilization of membranes from intracellular resources is required for autophagosome biogenesis. A cell-free assay was established to identify organelle membranes that form a precursor for autophagosome formation. The membrane from ATG5 mutant cells is defective in autophagosome formation in vivo during starvation [814]. In the cell-free assay, membranes from *atg5* knockout MEFs are mixed with cytosolic fractions from starved or untreated wild-type cells. These cytosolic fractions include a high amount of LC3-I and lack the lipidated form, LC3-II, which is sedimented with the membrane. The reaction is performed in the presence of GTP and an ATP regeneration system. The assay measures cell-free LC3 lipidation by the formation of LC3-II [1538]. The reaction thus identifies membranes responsible for LC3-

II generation. A three-step membrane fractionation is performed along with monitoring of lipidation enrichment with respect to different membrane markers. First, differential centrifugation is performed to obtain four membrane pellets with different markers. The 25 K fraction reveals the highest lipidation activity and includes peroxisomes (ABCD3/PMP70), late endosomes (LAMP2), cis-Golgi (GOLGA2/GM130) ER-Golgi intermediate compartment (ERGIC; SEC22B and LMAN1/ERGIC53), plasma membrane/early endosomes (TFRC), ER (RPN1), ER exit sites (ERES, active sites on the ER that generate COPII-coated vesicles; PREB/SEC12), lysosomes (CTSD), and ATG9 vesicles. The 25 K membrane is further fractionated using step-gradient ultracentrifugation, where the fraction with higher lipidation activity is determined to include ERGIC, cis-Golgi, ATG9 vesicles and plasma membrane/early endosomes.

This assay recapitulates the early cellular steps of autophagosome formation in different aspects. The cells are stimulated by starvation, and rapamycin or torin1 treatment and are inhibited in the absence of ULK1, which reflects the involvement of the MTORC1 pathway. PtdIns3K inhibitors abolish the LC3 lipidation, and LC3 lipidation is prohibited in the absence of ATG proteins such as ATG3, ATG5 or ATG7 [1539].

The contribution of different organelles to autophagosome biogenesis was tested using different fractionation and purification steps to obtain the ERGIC, which represents a primary membrane determinant that triggers LC3 lipidation. The ERGIC is a recycling compartment located in the ER and cis-Golgi compartments. PtdIns3K is activated upon starvation, and this enzyme facilitates the recruitment of COPII proteins to the ERGIC membrane. Subsequently, the ERGIC-derived COPII vesicles form a potential membrane source of the autophagosome and LC3 lipidation vesicles [1540].

A COPII vesicle-labelling system using the transmembrane cargo protein Axl2 was investigated by immuno-EM in yeast, showing that COPII acts as precursor for the formation of the autophagosome membrane [1541]. Another study employing super-resolution microscopy showed that starvation results in ER-exit site enlargement. COPII production served as positive control, and demonstrated contribution to autophagosome formation [1542].

Conclusion: The cell-free assay implicates the ERGIC as one of the primary cellular membrane determinants that facilitates LC3 lipidation. Further application of this method may reveal more with regard to functional forms of the cytosol and the triggering factors for autophagosome membrane formation.

Analyses in vivo

Monitoring autophagic flux in vivo or in organs is one of the least developed areas at present, and ideal methods relative to the techniques possible with cell culture may not exist. Importantly, the level of basal autophagy, time course of autophagic induction, and the bioavailability of autophagy-stimulating and -inhibiting drugs is likely tissue specific. Moreover, basal autophagy or sensitivity to autophagic induction may vary with animal age, sex or strain background. Therefore, methods may need to be optimized for the tissue

of interest. One method for in vivo studies is the analysis of GFP-Atg8-family proteins (see *GFP-Atg8-family protein fluorescence microscopy*). Autophagy can be monitored in tissue (e.g., skeletal muscle, heart, kidney, liver, brain, spinal cord, dorsal root ganglia, peripheral nerve, retina and platelets) in vivo in transgenic mice and zebrafish systemically expressing GFP-LC3 [109,210,214,239,388,390,540,561,924,1543,1544], or in other models by transfection with GFP-LC3-encoding plasmids or in transgenic strains that possess either mCherry- or GFP-Atg8-family proteins under the control of either inducible or Atg8-family protein gene promoter sequences [375,662]. All of these in vivo approaches require appropriate negative controls for Atg8-family protein localization to autophagosomes, through the use of point mutants that cannot be lipidated or associated with the autophagosomes [1545] or, in genetically tractable systems, mutations that predictably disrupt their association with autophagosomes [562].

It should be noted that tissues such as white adipose tissue, ovary, and testes, and some brain regions such as the hypothalamus, do not appear to express the *Actb* promoter-driven *GFP-Lc3* transgene strongly enough to allow detection of the fluorescent protein [239]. In addition, tissue-specific GFP-LC3 mice have been generated for monitoring cardiac myocytes [1546,1547]. In these settings, GFP fluorescent puncta are indicative of autophagic structures; however, the use of a lysosomal fusion or protease inhibitor would be needed to assess flux. Cleavage of GFP-LC3 to generate free GFP can be evaluated as one method to monitor the completion of autophagy. This has been successfully performed in mouse liver [351], suggesting the GFP-LC3 cleavage assay may also be applied to in vivo studies. Note that the accumulation of free GFP in the mouse brain is minimal after autophagy is induced with rapamycin (autophagy induction based on GFP-LC3 imaging and SQSTM1 IHC; M. Lipinski, personal communication), but significant when autophagic flux is partially blocked after traumatic brain injury [214]. Thus, caution needs to be taken when interpreting results of these assays in different tissues. We also recommend including a control under conditions known to induce autophagic flux such as starvation.

A simple methodology to measure autophagic flux in the brain was described [1548]. This strategy combines the generation of adeno-associated virus and the use of the dynamic fluorescent reporter mCherry-GFP-LC3 that allows an extended transduction and stable expression of mCherry-GFP-LC3 after intracerebroventricular injection in newborn animals. With this approach, a widespread transduction level is achieved along neurons at the central nervous system when newborn pups are injected, including pyramidal cortical and hippocampal neurons, Purkinje cells, and motor neurons in the spinal cord and also, to a lesser extent, in oligodendrocytes [1548]. The different serotypes of adeno-associated virus can be used to transduce other cell types at the CNS [1548-1550]. This methodology allows a reproducible and sensitive mCherry-GFP-LC3 detection, and a strong LC3 flux when animals are treated with autophagy inducers including rapamycin and trehalose [1550,1551]. Therefore, using these combined strategies can be applied to follow autophagy activity in mice or rats and can be particularly useful to evaluate it in

animal models of diseases affecting the nervous system [1548-1550]. A transgenic mouse with a low level neuron-specific expression of mCherry-RFP-GFP-LC3 was generated that has possible advantages over viral-expression models in achieving a relatively uniform expression reproducibly in a given mouse throughout its life or among different experimental groups of mice [451]. Alternatively, confocal laser scanning microscopy, which makes it possible to obtain numerous sections and substantial data about spatial localization features, can be a suitable system for studying autophagic structures (especially for whole mount embryo in vivo analysis) [1552]. In addition, this method can be used to obtain quantitative data through densitometric analysis of fluorescent signals [1553].

A number of transgenic autophagy mouse and *Drosophila* models have now been generated that rely on the expression of pH-sensitive fluorophores as mentioned above. In terms of monitoring general autophagy, mice stably expressing mRFP/mCherry-GFP-LC3, from the ubiquitous *ROSA26* locus, allow monitoring of autophagic flux in multiple organs [1103,1231]. When combined with immunohistochemical staining using cell-specific markers, autophagy can be quantified in distinct cell types within tissues. As with utilization of this marker in cell lines (see above), the same caveats apply, and care must be taken to maintain pH during fixation [1554].

Similar fluorescence methodology has been used to measure mitophagy in mouse and *Drosophila* tissue, either using mitochondrial matrix-localized mt-Keima [1145,1147] or OMM-localized mCherry-GFP in the case of the *mito-QC* mouse [38]. *mito-QC* is very similar to the mCherry-GFP-LC3 mouse (only differing in the fluorophore-targeting peptide), and thus allows an in vivo comparison between autophagy and mitophagy, which do not necessarily occur under the same conditions [1146,1231]. The *mito-QC* mouse has been used to monitor mitophagy in disease models, as shown with diabetes through the generation of *mito-QC* *Ins2^{Akita}* mice [39]. Analyses of tissues from both *mito-QC* and mt-Keima demonstrate the basal nature of mammalian mitophagy in vivo and its conservation to *Drosophila*. An important distinction between these mitophagy reporter mouse models is that tissues from the *mito-QC* mouse are compatible with fixation, whereas fluorescence in cells and tissues from the mt-Keima mouse is lost upon fixation [1554]. This difference has implications for applications where high throughput analyses of mitophagy in tissues and cells are required. Furthermore, because *mito-QC* is compatible with fixation, it is also possible to confirm the lysosomal localization of mCherry puncta using the *mito-QC* approach [38,1554]. Similarly, *Drosophila* harboring *GAL4/UAS* responsive transgenes for mt-mCherry-GFP (*mito-QC*) or mt-Keima have been developed, which allows spatiotemporal restricted expression analysis [466]. Utilizing such mitophagy reporters in *Drosophila* is particularly useful for rapidly and economically screening putative genetic or pharmacological regulators of mitophagy in vivo.

Another possibility is immunohistochemical staining, an important procedure that may be applicable to human studies as well, considering the role of autophagy in neurodegeneration, myopathies and cardiac disease where samples may be limited to biopsy/autopsy tissue. In this sense, special attention should be

taken in the sample extraction and preservation, as LC3B-II could undergo degradation. Immunodetection of LC3 as definite puncta is possible in paraffin-embedded tissue sections and fresh frozen tissue, by either IHC or immunofluorescence [265 [1555-1562],]. Immunostaining of LC3 puncta in peripheral nerve has been initially evaluated and compared to that obtained in GFP-LC3 mice (measured by means ImageJ RGB pixels analysis, which automatically converts pixels in brightness values) [540]. This method is, therefore, widely utilized in this kind of tissue [1327,1563,1564]; however, this methodology has not received extensive evaluation, and does not lend itself well to dynamic assays.

Other autophagic substrates can be evaluated via IHC and include SQSTM1, NBR1, ubiquitinated inclusions and protein aggregates [1562]. Similarly, autophagy can be evaluated by measuring levels of these autophagic substrates via traditional immunoblot; however, their presence or absence needs to be cautiously interpreted as some of these substrates can accumulate with either an increase or a decrease in autophagic flux (see *SQSTM1 and related LC3 binding protein turnover assays*). Bone marrow transfer has been used to document in vivo the role of autophagy in the reverse cholesterol transport pathway from peripheral tissues or cells (e.g., macrophages) to the liver for secretion in bile and for excretion [966], and a study shows that TGM2 (transglutaminase 2) protein levels decrease in mouse liver in vivo upon starvation in an autophagy-dependent manner (and in human cell lines in vitro in response to various stimuli; M. Piacentini, personal communication), presenting additional possible methods for following autophagy activity. In that respect, it is noteworthy to mention that TGM2 can also inhibit autophagic flux at the level of autophagosome-lysosome fusion by modifying ITPR1 (inositol 1,4,5-trisphosphate receptor, type 1) and suppressing its Ca^{2+} -release activity [1565].

It is also possible to analyze tissues ex vivo, and these studies can be particularly helpful in assessing autophagic flux as they avoid the risks of toxicity and bioavailability of compounds such as bafilomycin A₁ or other autophagy inhibitors. Along these lines, autophagic flux can be determined by western blot in retinas placed in culture for 4 h with protease inhibitors [968,969]. This method could be used in tissues that can remain “alive” for several hours in culture such as the retina [1566-1568], brain slices [214,1569] (particularly organotypic brain slices that can be cultured in vitro for weeks, allowing for treatments with autophagy stimulators or inhibitors for long periods [1570]), and spinal cord slices [1571]. Ex vivo tumors are relevant models of autophagy in mesothelioma. In these models, basal autophagy and its modulation can be measured by immunofluorescence to assess the presence of LC3 puncta when combined with lysosomal inhibitor treatment, or of ATG13 puncta without lysosomal inhibition [755,756,1572].

Several studies have demonstrated the feasibility of monitoring autophagic flux in vivo in skeletal muscle. Starvation is one of the easiest and most rapid methods for stimulating the autophagic machinery in skeletal muscles. Twelve h of fasting in mice may be sufficient to trigger autophagy in muscle [1573-1575], but the appropriate time should be determined empirically. It is also important to consider that the expression of autophagy-

related factors, as well as the autophagic response to various stimuli and disease states, can differ between muscles of different fiber type, metabolic, and contractile properties [239,1576-1579]. Thus, which muscle(s) or portion of muscle(s) used for analysis should be carefully considered and clearly outlined. Moreover, given that skeletal muscle properties can change during stress, exercise, and disease, attention should be given to the potential influence of these changes on the observed autophagic expression/signaling (J. Quadrilatero, personal communication). Although food deprivation does not induce detectable autophagy in the brain, it induces autophagy in the retina, and by the use of in vivo injection of leupeptin autophagic flux can be evaluated with LC3 lipidation by western blot [1567]. Although difficult to standardize and multifactorial, exercise may be a particularly appropriate stimulus to use for assessing autophagy in skeletal muscle [1543,1580]. Data about the autophagic flux can be obtained by treating mice or rats with, for example, CQ [86,1574], leupeptin [1567,1581] or colchicine [301] and then monitoring the change in accumulation of LC3 (see cautionary notes). It should be noted, however, that surgery itself profoundly affects intracellular signaling pathways such as those involving MTOR, MAPK/ERK, and autophagic flux itself (C.N. Brown and C.L. Edelman, personal communication). Thus, proper validation of such models should be carefully conducted before their use can be accepted. This type of flux analysis can also be done with liver, by comparing the LC3-II level in untreated liver (obtained by a partial hepatectomy) to that following subsequent exposure to CQ (V. Skop, Z. Papackova and M. Cahová, personal communication). Moreover, after peripheral nerve degeneration, to verify whether the increase in rapamycin-induced Schwann cell autophagy, can be attributed to increased autophagosome formation, the lysosomal inhibitor CQ can be injected both in vehicle- and rapamycin-treated mice, and 3 h after the injection, LC3 conversion is measured in sciatic nerves by western blot [540].

Additional reporter assays to monitor autophagic flux in vivo need to be developed, including tandem fluorescent-LC3 transgenic mice, expressing the construct in specific cell types beyond the existing neuron-specific model [451], or viral vectors to express this construct in vivo in localized areas. Moreover, LC3-independent approaches are also needed. The LDH sequestration assay is an LC3-independent method that may be useful to study autophagic sequestration activity in vivo, and which does not require any genetic modification of the experimental animals. Indeed, injection of leupeptin in rats results in accumulation of LDH within autophagic vacuoles in hepatocytes [1582]. One of the challenges of studying autophagic flux in intact animals is the demonstration of cargo clearance, but studies of fly intestines that combine sophisticated mosaic mutant cell genetics with imaging of mitochondrial clearance reveal that such analyses are possible [1162].

Another organ particularly amenable to ex vivo analysis is the heart, with rodent hearts easily subjected to perfusion by the methods of Langendorff established in 1895 (for review see [1583]). Autophagy has been monitored in perfused hearts [1584], where it is thought to be an important process in several modes of cardioprotection against ischemic injury [1585]. It should be noted that baseline autophagy levels (as

indicated by LC3-II) appear relatively high in the perfused heart, although this may be due to perceived starvation by the ex vivo organ (e.g., the lack of protein in the perfusion medium may result in osmotic stress and edema, which could trigger a starvation-like stress that accelerates autophagy), highlighting the need to ensure adequate delivery of metabolic substrates in perfusion media, which may include the addition of INS (insulin). Another concern may be that the high partial pressure of oxygen of the perfusate (e.g., buffer perfused with 95%:5% [O₂:CO₂]) used in the Langendorff method makes this preparation problematic for the study of autophagy because of the high levels of oxidation (redox disturbances) that could result from the preparation. However, the absence of hemoglobin means that even at a high partial pressure of oxygen these hearts may be at the limit of oxygen availability, and perfused hearts have normal levels of glutathione, NADH and other measures of redox. Due to these potential effects, great caution should be exercised in interpretation of these results. As a guide to correct interpretation of these data, we recommend a review that covers the diverse array of “state of the art” methods to analyze autophagy in cardiac physiopathology [1586].

The role of autophagy in pregnancy has been extensively reviewed [1587,1588], and human placenta represents an organ suitable for ex vivo studies, such as to investigate pregnancy outcome abnormalities. Autophagy has been evaluated in placentae from normal pregnancies [1589-1591] identifying a baseline autophagy level (as indicated by LC3-II) in uneventful gestation. In cases with abnormal pregnancy outcome, LC3-II is increased in placentae complicated by intrauterine growth restriction in cases both from singleton pregnancies [1592] and from monochorionic twins pregnancies [1593]. Moreover, placentae from pregnancies complicated by preeclampsia show a higher level of LC3-II than normal pregnancies [1594]. Finally, placentae from acidotic newborns developing neonatal encephalopathy exhibit a higher IHC LC3 expression than placentae from newborn without neonatal encephalopathy [1595]. For this reported association, further investigations are needed to assess if autophagy protein expression in placentae with severe neonatal acidosis could be a potential marker for poor neurological outcome.

The retina is a very suitable organ for ex vivo as well as in vivo autophagy determination. The retina is a part of the central nervous system, is readily accessible and can be maintained in organotypic cultures for some time, allowing treatment with protease and autophagy inhibitors. This allows determination of autophagic flux ex vivo in adult and embryonic retinas by western blot [1566, 1596,1597] as well as by flow cytometry and microscopy analysis [1567,1597]. Moreover, only 4 h of leupeptin injection in fasted mice allows for autophagic flux assessment in the retina [1567] indicating two things: first, food deprivation induces autophagy in selected areas of the central nervous system; and second, leupeptin can cross the blood-retinal barrier. Accordingly, the intravitreal injection of beta-adrenergic receptor blockers in a mouse model of oxygen-induced retinopathy stimulates autophagic turnover of retinal neurons [1598].

In vivo analysis of the autophagic flux in the brain tissue of neonatal rats can also be performed. These studies use the

intraperitoneal administration of the acidotropic dye monodansylcadaverine (MDC) to pup rats 1 h before sacrifice, followed by the analysis of tissue labeling through fluorescence or confocal laser scanning microscopy (365/525-nm excitation/emission filter). This method was adapted to study autophagy in the central nervous system after its validation in cardiac tissue [1599]. MDC labels acidic endosomes, lysosomes, and late-stage autophagosomes, and its labeling is upregulated under conditions that increase autophagy [1600]. In a neonatal model of hypoxic-ischemic brain injury, where autophagy activation is a direct consequence of the insult [1601], MDC labeling is detectable only in the ischemic tissue, and colocalizes with LC3-II [1602]. The number of MDC- and LC3-II-positive structures changes when autophagy is pharmacologically up- or downregulated [1601,1602]. Whether this method can also be used in adult animals needs to be determined. Furthermore, it should be kept in mind that staining with MDC is not, by itself, a sufficient method for monitoring autophagy in live cells (see *Acidotropic dyes*). A better alternative approach in live cells is the MDC derivative monodansylpentane (MDH) which stains lipid-containing vacuoles such as late autophagic vacuoles [1603]. In formaldehyde-fixed cells MDC and MDH both stain lipid-containing vacuoles/late autophagosomes.

Cell-type specific observation of autophagy flux in vivo in adult brain and spinal cord is possible. Adult mice can be stereotactically injected with lentivirus expressing mRFP-GFP-LC3 under the control of the *Nes* promoter in hippocampus. Using this approach, it was demonstrated that restraint stress increases autophagy flux in adult hippocampal neural stem cells, and induces autophagic death of neural stem cells without signs of apoptosis [1604]. Intrathecal injection of adeno-associated viral vector AAV9rh10, that infects spinal motoneurons, and expressing the mCherry-GFP-LC3 reporter, can be used to demonstrate autophagy flux blockage in the neurodegenerative process after proximal axotomy or nerve root avulsion [1550].

Another approach that can be used in vivo in brain tissue is to stain for lysosomal enzymes. In situations where an increase in autophagosomes has been shown (e.g., by immunostaining for LC3 and immunoblotting for LC3-II), it is important to show whether this is due to a shutdown of the lysosomal system, causing an accumulation of autophagosomes and/or incompletely acidified autolysosomes, or whether this is due to a true increase in autophagic flux. The standard methods described above for in vitro research, such as the study of clearance of a substrate, are difficult to use in vivo, but if it can be demonstrated that the increase in autophagosomes is accompanied by an increase in lysosomes, this makes it very likely that there has been a true increase in autophagic flux [1605]. Conversely, a decrease in lysosomal enzyme levels and activity can indicate that accumulation of autophagosomes is caused by lysosomal damage and a consequent decrease in flux [1606,1607]. Lysosomal enzymes can be detected by IHC (e.g., for LAMP1 or CTSD) or by classical histochemistry to reveal their activity (e.g., ACP/acid phosphatase or HEX/β-hexosaminidase) [1608,1609]. It should be noted, however, that this combination of measures will not exclude a defect in lysosomal acidification, increasingly

reported in several major neurodegenerative diseases [1610]. In this situation, flux is blocked, and incompletely acidified autolysosomes accumulate, which cannot be discriminated from autophagosomes using the mCherry/RFP-GFP-LC3 probe (or other measures of LC3) because both vesicle types will fluoresce yellow. Only by applying a third fluorescent marker for lysosomes (e.g., CTSD, CTSB) by IHC can the deacidified autolysosomes be identified [451]. Lysosomal enzyme activity can be also separately assessed in lysosomes and cytosol following tissue fractionation. In this case, a decrease in enzyme activity in the lysosomal fraction accompanied by an increase in the cytosol can indicate lysosomal membrane permeabilization (LMP) as a potential cause for lysosomal dysfunction. LMP may also be detected in vivo in the brain by comparing the pattern of IHC staining for lysosomal membrane proteins (such as LAMP1/2) to soluble lysosomal enzymes (such as CTSD, CTSB or CTSL) [1606,1611].

Some biochemical assays may be used to at least provide indirect correlative data relating to autophagy, in particular when examining the role of autophagy in cell death. For example, cellular viability is related to high CTSD activity and low CTSB activities [1612]. Therefore, the appearance of the opposite levels of activities may be one indication of the initiation of autophagy (lysosome)-dependent cell death. The question of “high” versus “low” activities can be determined by comparison to the same tissue under control conditions, or to a different tissue in the same organism, depending on the specific question.

Cautionary notes: The major hurdle with most in vivo analyses is the identification of autophagy-specific substrates and the ability to “block” autophagosome degradation with a compound such as bafilomycin A₁. Regardless, it is still essential to adapt the same rigors for measuring autophagic flux in vitro to measurements made with in vivo systems. Moreover, as with cell culture, to substantiate a change in autophagic flux it is not adequate to rely solely on the analysis of static levels or changes in LC3-II protein levels on western blot using tissue samples. To truly measure in vivo autophagic flux using LC3-II as a biomarker, it is necessary to block lysosomal degradation of the protein. Several studies have successfully done this in selected tissues in vivo. Certain general principles need to be kept in mind: (a) Any autophagic blocker, whether leupeptin, bafilomycin A₁, CQ or microtubule depolarizing agents such as colchicine or vinblastine, must significantly increase basal LC3-II levels in control cells or tissues. The turnover of LC3-II or rate of basal autophagic flux is not known for tissues in vivo, and therefore short treatments (e.g., 4 h) may not be as effective as blocking for longer times (e.g., 12 to 24 h). (b) The toxicity of the blocking agent needs to be considered (e.g., treating animals with doses higher than 2 mg/kg bafilomycin A₁ for 2 h can be quite toxic), and food intake must be monitored. If long-term treatment is needed to see a change in LC3-II levels, then confirmation that the animals have not lost weight may be needed. Mice may lose a substantial portion of their body weight when deprived of food for 24 h, and starvation is a potent stimulus for the activation of autophagy. (c) The bioavailability of the agent needs to be considered. For example, many inhibitors such as bafilomycin A₁ or CQ have relatively poor bioavailability to the central

nervous system. To overcome this problem, intracerebroventricular injection can be performed.

A dramatic increase of intracellular free poly-unsaturated fatty acid levels can be observed by proton nuclear magnetic resonance spectroscopy in living pancreatic cancer cells within 4 h of autophagy inhibition by omeprazole, which interacts with the V-ATPase and probably inhibits autophagosome-lysosome fusion [1613]. Omeprazole is one of the most frequently prescribed drugs worldwide and shows only minor side effects even in higher doses. Proton nuclear magnetic resonance spectroscopy is a noninvasive method that can also be applied as localized spectroscopy in magnetic resonance tomography, and therefore opens the possibility of a noninvasive, clinically applicable autophagy monitoring method, although technical issues still have to be solved [1614].

In terms of measuring mitophagy in tissues, recently developed reporter systems represent a more rigorous choice than monitoring any particular pathway. This is especially true for stress-induced PINK1-dependent PRKN phosphorylation, where KO-validated reagents to monitor this signaling pathway in mice have only just become available. It is important to note that despite a plethora of publications, many commercially available anti-PINK1 and anti-PRKN antibodies are not specific; that is, although it is possible to run a western blot with these reagents and detect a band at the predicted size, it is highly likely that this band will also be present in KO tissue (especially for endogenous mouse PINK1). The first endogenous detection of mouse PINK1 from tissues verified using KO controls and mass spectrometry has been published [1231]. Readers should be aware that the detection of bona fide PINK1 is technically challenging, and the current state of the art necessitates an immunoprecipitation-immunoblot approach to ensure optimal results. This approach has been successfully replicated in other mouse cell types. In cells, researchers also use the PINK1-dependent phosphorylation of PRKN or ubiquitin at Ser65 to monitor pathway activation. Monitoring PRKN substrate ubiquitination is another useful approach. While these methods are tractable for *in vitro* paradigms, the activation of this pathway requires substantial levels of stress (often treatment with harsh mitochondrial uncouplers). Thus, PINK1-mediated generation of phospho-ubiquitin, phospho-PRKN or substrate ubiquitination can be difficult to detect without mitochondrial depolarization. Nonetheless, the activation of this endogenous pathway has been performed in mature primary neurons using a combination of ubiquitin-enrichment and highly specific antibodies [1615]. Researchers should also be mindful that while detection of *Pink1* or *Prkn* mRNA may seem like a useful approach, changes in the levels of these genes do not infer any reliable alterations in mitophagy.

When analyzing autophagic flux in vivo, one major limitation is the variability between animals. Different animals do not always activate autophagy at the same time. To improve the statistical relevance and avoid unclear results, these experiments should be repeated more than once, with each experiment including several animals; it may also be important to consider age and gender [1616] as additional variables. Induction of autophagy in a time-dependent manner by fasting mice for different times requires appropriate caution.

Mice are nocturnal animals, so they preferentially move and eat during the night, while they mostly rest during daylight. Therefore, in such experiments it is better to start food deprivation early in the morning, to avoid the possibility that the animals have already been fasting for several hours. The use of CQ is technically easier, because it only needs one intraperitoneal injection per day, but the main concern is that CQ has some toxicity (mouse intraperitoneal LD₅₀: 68 mg/kg). CQ suppresses the immunological response in a manner that is not due to its pH-dependent lysosomotropic accumulation (CQ interferes with LPS-induced *Tnf/Tnf-α* gene expression by a nonlysosomotropic mechanism) [1617], as well as through its pH-dependent inhibition of antigen presentation [1433]. Therefore, CQ treatment should be used for short times and at doses that do not induce severe collateral effects, which may invalidate the measurement of the autophagic flux, and care must be exercised in using CQ for studies on autophagy that involve immunological aspects.

It is also important to have time-matched controls for in vivo analyses. That is, having only a zero-hour time point control is not sufficient because there may be substantial diurnal changes in basal autophagy [989]. For example, variations in basal flux in the liver associated with circadian rhythm may be several fold [989], which can equal or exceed the changes due to starvation. Along these lines, to allow comparisons of a single time-point it is important to specify what time of day the measurement is taken and the lighting conditions under which the animals are housed. It is also important that the replicate experiments are conducted at the same time of day. Controlling for circadian effects can greatly reduce the mouse-to-mouse variability in autophagy markers and flux [1618]. Note, when handling litters, autophagy flux should be analyzed within a restricted range of weight; nursing mothers have a limited production of nutrients, and therefore an increased variability is detected between groups of big and small litter number.

When analyzing the basal autophagic level in vivo using GFP-LC3 transgenic mice [239], one pitfall is that GFP-LC3 expression is driven by the *Cmv/cytomegalovirus* enhancer and *Actb/β-actin* (CAG) promoter, so that the intensity of the GFP signal may not always represent the actual autophagic activity, but rather the CAG promoter activity in individual cells. For example, GFP-LC3 transgenic mice exhibit prominent fluorescence in podocytes, but rarely in tubular epithelial cells in the kidney [239], but a similar GFP pattern is observed in transgenic mice carrying CAG promoter-driven non-tagged GFP [1619]. Furthermore, proximal tubule-specific ATG5-deficient mice [1620] display a degeneration phenotype earlier than podocyte-specific ATG5-deficient mice [1621], suggesting that autophagy, and hence LC3 levels, might actually be more prominent in the former.

One caution in using approaches that monitor ubiquitinated aggregates is that the accumulation of ubiquitin may indicate a block in autophagy or inhibition of proteasomal degradation, or it may correspond to structural changes in the substrate proteins that hinder their degradation. In addition, only cytosolic and not nuclear ubiquitin is subject to autophagic degradation. It is helpful to analyze aggregate degradation in an autophagy-deficient control strain, such as an

autophagy mutant mouse, whenever possible to determine whether an aggregate is being degraded by an autophagic mechanism. This type of control will be impractical for some tissues such as those of the central nervous system because the absence of autophagy leads to rapid degeneration. Accordingly, the use of *Atg16l1* hypomorphs, *Becn1* heterozygotes or *Atg4b* homozygotes, with systemic autophagy impairment, may help circumvent this problem.

Conclusion: Although the techniques for analyzing autophagy in vivo are not as advanced as those for cell culture, it is still possible to follow this process (including flux) by monitoring, for example, GFP-LC3 or mCherry/RFP-GFP-LC3 by fluorescence microscopy, and SQSTM1 and NBR1 by IHC and/or western blotting.

Proteomic readouts of autophagy

An alternate approach for evaluating autophagy is with proteomics, which enables the identification of hundreds to thousands of protein species in a sample. The main advantage of proteomics is that it provides a direct, holistic readout of how autophagic activity affects the protein composition of a cell. Proteomics also avoids an assumption of common “marker-based” autophagy assays (LC3B-based or otherwise)—that dynamic changes to either the abundance or localization of a marker protein is generally reflective of total autophagic activity. Although proteomics requires specialized equipment and data processing, gradual improvements in technology, declining cost, and availability through core facilities and companies are making proteomics increasingly accessible.

Over the last decade, dozens of studies employing proteomics to examine autophagic activity have been published, and the pace of novel publications is accelerating [1622,1623]. While these studies differ significantly in their technical execution (on-label versus label free, instrumentation, sample processing, and quantification), conceptually they can be subdivided into three general experimental approaches. In the first approach, proteomics is used to examine changes to total cellular protein composition in the setting of autophagy inhibition or stimulation. As an example, an on-label proteomic approach known as stable isotope labeling by amino acids in cell culture (SILAC) has been used to analyze cells subjected to autophagy activation by amino acid starvation [1029]. The results indicate that autophagy activation is accompanied by an orderly progression of substrates that are targeted for disposal, starting with cytosolic proteins and followed later by mitochondrial and other organellar proteins. This kind of whole cell proteomics analysis provides a holistic picture of how autophagy affects cellular proteostasis, but it does not distinguish between proteins that are directly degraded by autophagy and proteins whose steady-state levels change through indirect effects (regulation of transcription, translation, or export) or through off-pathway functions of ATG proteins.

Another example is seen from experiments conducted in maize, where the protein composition in autophagy mutants was determined using a label-free MS analysis of the total protein extract [1624]. One remarkable observation was the ~2-fold increase in protein content/fresh weight in the absence of autophagy, which was at least partially due to a

retention of various organelles. Global comparisons between affected transcript and protein abundances, made it possible to pinpoint putative autophagic cargo (solely elevated protein levels) and proteins that are actively engaged (elevated transcript and protein levels). Although protein-transcript comparisons are potentially flawed due to misassigned protein-coding mRNAs (due to homology), or due to differences in translation efficiencies, consistent trends were observed for several protein groups. For example, strong increases of peroxisomal, endoplasmic reticulum, Golgi, ribosomal and proteasomal proteins are evident without any associated transcripts being affected, indicating that these organelles and protein complexes are autophagic targets. In contrast, proteins involved in secondary, amino acid, glutathione and lipid metabolism are elevated in both protein and corresponding mRNA abundances, which strongly correlate with alterations in associated metabolites, indicative of an active response to restore cellular homeostasis.

In the second approach, proteomics is used to catalog the composition of autophagosomes or autolysosomes that are isolated using biochemical fractionation or affinity purification. This approach can identify specific autophagy substrates, and through these substrates it can suggest cellular functions that autophagy is affecting. To cite some examples, label-free proteomics of biochemically fractionated autolysosomes was used to identify the cargo receptor NCOA4 that regulates iron homeostasis by recruiting ferritin to phagophores [1264] (see Ferritinophagy). Another study [1625] used label-free proteomics to compare the substrates of CMA-competent versus CMA-incompetent lysosomes in mouse liver, thereby inferring unique substrate specificity of CMA compared to autophagy. A novel chemical labeling approach [1626] transfected APEX-Atg8-family fusion proteins into cells, which enables the biotinylation and subsequent purification of autophagosome contents using streptavidin resin. Combined with a SILAC-based proteomics analysis, this technique identified a novel PRKN-independent mitophagy mechanism that is dependent on LC3C.

In the third approach, proteomics is used in a quantitative or semi-quantitative manner to measure autophagic flux. This approach enables simultaneous examination of how a stimulus affects the rate of autophagic activity and the composition of the autophagy substrate proteome. For example, SILAC was used to conduct a pulse-chase experiment in human fibroblasts, enabling the proteome-wide calculation of protein half-lives under basal conditions [1627]. By comparing cells with *atg5* or *atg7* deletion to wild-type cells, they were able to infer degradation rates via autophagy in many hundreds of proteins simultaneously. In another example, a label-free approach was used to examine circadian variations in autophagic flux in mouse liver [1618].

Cautionary notes: Current proteomic platforms identify on the order of 10^4 to 10^5 protein spectra (similar in concept to RNA sequencing reads) per sample. By comparison, RNA sequencing provides on the order of 10^7 reads per sample, although it does not specifically address the issue of RNA turnover. The limited sensitivity of proteomics means that the technique favors detection of abundant proteins and is less reliable for reproducibly detecting rarer protein species.

To some extent this can be overcome by reducing the complexity of the sample being analyzed (for example, by analyzing purified autolysosomes rather than whole cell homogenates), but it is routine for non-abundant proteins to be detected in some biological replicates but not in others.

Because cellular material must be homogenized, proteomic readouts do not preserve subcellular localization information precisely, even when samples are carefully biochemically fractionated. Particularly with human biological samples, care must be taken to avoid contamination with exogenous human proteins, especially with samples that have small quantities of protein to begin with [1628].

In proteomics, proteins are identified by matching peptide sequences against a database (akin to RNA sequencing). In some instances, peptides can be misassigned to a protein because the peptide sequence in question maps to a conserved region shared by multiple different protein species. Finally, the sensitivity of proteomic detection depends on the ionizability of different oligopeptides which varies from protein to protein. As a result, the linear relationship between a proteomic metric such as spectral counts, and absolute protein abundance varies in slope from protein species to protein species. What this means is that while shotgun proteomics can distinguish between the relative amounts of a given protein in different samples, it cannot reliably compare the abundances of two different protein species without the addition of reference protein standards of known quantity.

Conclusion: Even with all the technical caveats, proteomics is unique in allowing the application of “omics” approaches to autophagy measurement and can be used to validate the conclusions of marker-based autophagy assays. As the technology continues to improve and as the costs of experiments decline, proteomics is likely to become an increasingly standard approach to examining the role of autophagy in cellular physiology and pathophysiology.

Metabolic markers of autophagy

Metabolites play an essential role in autophagy regulation and therefore constitute key targets for the understanding of biological processes that are involved in autophagy and are misregulated in autophagy-related diseases. Recent metabolomics approaches have been developed in order to identify the key metabolites involved in the regulation of autophagy [1629]. These approaches rely on two main and complementary methods, which are MS and NMR spectroscopy. On the one hand, NMR provides access to unique structural information, is quantitative and highly reproducible. On the other hand, MS is more sensitive than NMR, but suffers from the ambiguity of spectral signatures.

The regulation of autophagy is mediated by various conditions including (a) starvation and (b) protein acetylation status. Under normal growth conditions, associated with abundant nutrients, autophagy is kept at a basal level making it possible to maintain essential cellular processes such as the turnover of damaged cellular organelles and the degradation of proteins. Under conditions of nutrient starvation, autophagy is further induced to provide cells with additional internal nutrient supplies and is associated with a dramatic change in the cellular metabolome profile. Indeed, low glucose levels

result in decreased cellular capacity to convert ATP to cAMP and are therefore linked to a decreased activation of autophagy-related proteins via the PRKA/cAMP-dependent protein kinase A pathway [36,1629]. Therefore, monitoring the levels of glucose and cAMP as well as the AMP:ATP ratio are efficient readouts associated with autophagic capacity, and these can be quantitatively detected using both NMR spectroscopy and MS approaches.

Several studies underlined the role of protein acetylation in the regulation of autophagy, and show that a decreased cellular acetylation level is associated with increased autophagy [996,1630]. For instance, Atg proteins mediate autophagy via formation of autophagosomes only in their de-acetylated state [1631,1632]. Protein acetylation status is regulated by the cellular balance between acetyltransferases and deacetylases, which use acetyl-CoA and NAD⁺ as cofactors, respectively. Therefore, monitoring acetyl-CoA and NAD⁺ metabolites are efficient readouts of protein acetylation marks and associated autophagic flux. Several studies also underline the role of polyamines, spermidine and spermine in the regulation of autophagy via inhibition of histone-acetyltransferases [1633-1636]. Nevertheless, the exact cellular mechanisms linking histone deacetylation and autophagy regulation are still unclear but likely involve a transcription-dependent activation/repression of autophagy-related genes. The cellular NAD⁺ and spermidine levels can be detected by both MS and NMR spectroscopy, whereas, due to its low cellular abundance, acetyl-CoA can only be detected using MS.

Other metabolites also reflect the autophagic capacity of the cell. As previously mentioned, autophagy allows protein turnover via activation of proteolysis. Therefore, levels of free amino acids, which are building blocks of proteins are suitable markers for (in)activation of autophagy and can be quantitatively detected using NMR spectroscopy and MS [1637,1638]. Finally, elevated levels of free fatty acids or triglycerides as well as production of PtdIns3P are linked to induction of autophagy [36]. Detection and quantification of this complex class of lipids is usually performed using MS [1639], as NMR spectroscopy provides mainly information regarding the chemical nature of apolar metabolites.

In conclusion, metabolomics studies provide essential information in the field of autophagy and contribute to the deep-understanding of its complex regulatory mechanisms in living cells and organisms. Given the recent advances in method development using NMR and MS metabolomics approaches, it is to be expected that more metabolites involved in autophagy regulation [1640-1642] will be identified in the coming years.

Clinical setting

Altered autophagy is clearly relevant in neurodegenerative diseases, as demonstrated by the accumulation of protein aggregates and gene dysregulation, for example in AD [1643,1644], adult brain ischemia [1645,1646], PD [1647], Huntington disease (HD) and other polyglutamine repeat expansion diseases [1648,1649], muscle diseases [1650,1651], and ALS [1652]. Elevated levels of autophagosomes or mitophagosomes have been identified ultrastructurally in aging, brain ischemia, vacuolar myopathies, PD, AD and Lewy body dementia [79,1133,1188,1653]. Of note, depending on the disease being

considered, autophagy is not necessarily impaired but could be, in particular conditions, excessively activated (i.e., an increase in the autophagic flux) such as in neonatal models of cerebral ischemia [1608,1654,1655]. Autophagy defects with autophagosome accumulation are also associated with different forms of hereditary spastic paraplegia/HSP [1656]. Of note, the expression levels of ATG5 and the ratio between LC3A and LC3B significantly increase in 3xTgAD mouse brain, following treatment with near infrared light, thus emphasizing the involvement of autophagic machinery in the degradation of dysfunctional MAPT protein [1657]. Further evidence comes from the observations that the stress-inducible mitophagy regulators PINK1 and PRKN show loss-of-function mutations in autosomal recessive juvenile parkinsonism [1658]. Along these lines, it is important to dissociate the clinical significance of these PD-associated loci in patients from the depolarization-induced “PINK1-PRKN signaling pathway” as it is traditionally studied in cultured cells.

A very useful nonspecific indicator of deficient aggrephagy in autopsy brain or biopsy tissue is SQSTM1 IHC [1659,1660]. For clinical attempts to monitor autophagy alterations in peripheral tissues such as blood, it is important to know that eating behavior may be altered as a consequence of the disease [1661], resulting in a need to control feeding-fasting conditions during the analyses. Recently, altered autophagy was also implicated in schizophrenia, with *BECN1* transcript levels decreasing in the postmortem hippocampus in comparison to appropriate controls [1662]. In the same hippocampal postmortem samples, the correlation between the RNA transcript content for ADNP (activity-dependent neuroprotective homeobox) and its sister protein ADNP2 is deregulated [1663], and *ADNP* as well as *ADNP2* RNA levels increase in peripheral lymphocytes from schizophrenia patients compared to matched healthy controls, suggesting a potential biomarker [1662].

Over the past decade, our depth of knowledge and understanding on therapeutic potentials of autophagy inhibition for treating cancer has been vastly improved. Particularly, after tumors have been formed, cancer cells actively undergo autophagy to survive and grow under conditions of nutrient limitation and hypoxia. Therefore, autophagy inhibitors are becoming emerging therapeutics to combat cancer [1664,1665]. To this end, more pharmacological molecules that are designed to suppress autophagy have been examined for clinical use such as 3-MA, wortmannin, LY294002, CQ, and HCQ [1665]. For example, class III PtdIns3K inhibitors including 3-MA, wortmannin and LY294002 prevent autophagosome formation, and thus inhibit autophagy. However, these inhibitors are not specific for inhibiting autophagy and can activate autophagy at higher doses. Thus, the PtdIns3K inhibitors are not suitable for clinical settings. Other commonly used autophagy inhibitors such as CQ and its derivative HCQ that are FDA approved anti-malaria drugs, have been extensively studied and tested in clinical trials. Although CQ and HCQ show moderate anti-neoplastic effects, these largely come from the modulation of pathways other than autophagy inhibition *per se* [1666,1667]. Moreover, the mechanism by which CQ and HCQ inhibit autophagy is still not fully understood. Therefore, developing molecules that specifically regulate autophagy will surely broaden clinical utility in combating cancer.

In addition to neurodegenerative diseases, alterations in autophagy have also been implicated in other neurological diseases including some epilepsies, neurometabolic and neurodevelopmental disorders [1569 [1668-1670]], and inherited autophagic vacuolar myopathies (including Danon disease, acid maltase deficiency/Pompe disease, X-linked myopathy with excessive autophagy/XMEA, etc.), which are characterized by lysosomal defects and an accumulation of autophagic vacuoles [1671]. Autophagic vacuolar myopathies and cardiomyopathies can also be secondary to treatment with autophagy-inhibiting drugs (CQ, HCQ and colchicine), which are used experimentally to interrogate autophagic flux and clinically to treat malaria, rheumatological diseases, and gout [1561]. Autophagy impairment has also been implicated in the pathogenesis of inclusion body myositis, an age-associated inflammatory myopathy that is currently refractory to any form of treatment [1672-1675], along with some muscular dystrophies such as tibial muscular dystrophy [1676]. In all these striated muscle disorders, accumulated autophagic vacuoles can be seen by electron microscopy, or, alternatively, LC3 and/or SQSTM1 can be detected by IHC [1560,1561,1651,1677]. In addition, autophagy defects can also lead to the formation of an eosinophilic cytoplasmic inclusion, which is a round to oval homogeneous cytoplasmic eosinophilic globule composed of protein aggregates and/or organelles; SQSTM1, BECN1, NBR1, LC3 and/or peroxisomes are deposited in the inclusion, and both the proteins and organelles can be detected by IHC, immunofluorescence, or TEM [1678].

Whereas autophagosomes and autolysosomes are not always distinguishable using only morphological methods to confirm whether or not an autophagic structure has fused with a lysosome, “autophagic vacuoles” are easily recognized by electron microscopy in the cardiomyocytes of patients with dilated cardiomyopathy [550]. Autophagic vacuoles are easily observed not only in secondary cardiomyopathy but also in failing cardiomyocytes of dilated cardiomyopathy [550]. These vacuoles display LC3 expression by using the ABC technique for TEM observation (see *Transmission electron microscopy*) [112]. Dilated cardiomyopathy with autophagic vacuoles indicates a good prognosis, confirming that autophagy resists cardiomyocyte degeneration. In dilated cardiomyopathy, it is suggested that autophagy is not always the cause of the disease but also a process that occurs to prevent the disease.

In addition, altered basal autophagy levels are seen in rheumatoid arthritis [1028,1029], systemic lupus erythematosus (SLE) [1679-1681], and osteoarthritis [1682]. Other aspects of the immune response associated with dysfunctional autophagy are seen in neutrophils from patients with familial Mediterranean fever [1683] and in monocytes from patients with TNF receptor-associated periodic syndrome [1684], two autoinflammatory disorders. Aberrant elevation of IL17A plays a critical role in the pathogenesis of pulmonary fibrosis through suppressing the autophagic degradation of collagen in fibrotic lung tissue [1685]. In lung epithelial cells, IL17A-activated PIK3CA inhibits the kinase activity of GSK3B by stimulating its phosphorylation at Ser9, which consequently attenuates activation of an autophagic core complex via inhibiting the ubiquitination-dependent degradation of BCL2 and

its interaction with BECN1 [1686]. ANXA2 is identified as a specific bleomycin target linked to interstitial pulmonary fibrosis as bleomycin binding to ANXA2 impedes TFEB-induced autophagic flux to cause pulmonary fibrosis proliferation [1687].

Moreover, autophagy regulates an important neutrophil function, the generation of neutrophil extracellular traps (NETs) [1674,1688]. The important role of autophagy in the induction of NET formation has been studied in several neutrophil-associated disorders such as gout [1689] and other IL1B autoinflammatory disorders [1690-1692], ulcerative colitis [1693], sepsis [1694], thromboinflammation [1695,1696] and lung fibrosis [1697], including the inflammatory remodeling associated with systemic sclerosis [1698]. The prototypical DAMP and autophagy inducer, HMGB1, released by activated platelets appears to play a role in neutrophil autophagic flux induction [1674,1698,1699], and studies of patients with systemic sclerosis have shown that platelet-derived, microparticle-associated HMGB1 promotes neutrophil autophagy, as evidenced by Cyto-ID labeling, leading to the production of NETs [1698].

Furthermore, there is an intersection between autophagy and the secretory pathway in mammalian macrophages for the release of IL1B [1700], demonstrating a possible alternative role of autophagy for protein trafficking. This role has also been implied in neutrophils through exposure of protein epitopes on NETs by acidified LC3-positive vacuoles in sepsis [1694] and anti-neutrophil cytoplasmic antibody associated vasculitis [1701]. Patients with chronic kidney disease also have impaired autophagy, which results in NLRP3 activation, IL1B release and leukocyte influx. However, autophagy was also shown to play an important role in the development in vitro of giant phagocytes, a long-lived neutrophil subpopulation, derived from neutrophils of healthy individuals [1702,1703]. Recently, evidence from genetic, cell biology and animal models suggests that autophagy plays a pivotal role in the occurrence and development of SLE. For example, altered basal autophagy levels are seen in immune cells, such as B cells, T cells, and neutrophils in SLE [1679]. There is also evidence for altered autophagy in pancreatic beta cells [1704,1705], and in adipocytes [292,396,1706] of patients with type 2 diabetes [1707].

Photodynamic therapy (PDT), an FDA-approved anticancer therapy, is based on electromagnetic radiation and has applications in the selective eradication of delineated tumor lesions and infection sites. It is a two-step process whereby cells are first incubated with photosensitizers and then exposed to light, usually in the red spectral region. Although these components (i.e., photosensitizers and light) are harmless alone, when combined they provide a localized therapeutic archetype avoiding attack to healthy cells and preventing side effects [1708,1709]. This combination results in the generation of singlet oxygen ($^1\text{O}_2$) and other ROS that can cause cancer cell death [1710]. PDT can prompt AKT-MTOR pathway downregulation and stimulate autophagy in eukaryotic cells [1711]. The mechanism of PDT that modulates autophagy depends on several factors, such as photosensitizer molecular properties and concentrations, light dose and the preferential intracellular target of the photosensitizers.

Particularly, photosensitizers that target lysosomes (e.g., chlorophyllin e4, chlorophyllin f, NPe6, WST11, TPPS_{2a}, MB, and DMMB) can modulate autophagy [316, 317 [1712-1715],]. PDT fulfills the need to merge a direct cytotoxic action on tumor cells with potent immunostimulatory effects (i.e., immunogenic cell death, ICD) [1716]. A few photosensitizers, such as Photofrin, hypericin, Foscan, 5-ALA and Rose Bengal acetate, are associated with DAMP exposure and/or release that is a requisite to elicit ICD. Rose Bengal acetate PDT is the first treatment to induce autophagic HeLa cells to express and release DAMPs, thus suggesting a possible role of the autophagic cells in ICD induction [1717]. Similarly, the photosensitizer hypocrellin B-acetate is able to induce autophagy at very low concentrations [1718].

A crucial role for therapy-induced autophagy in cancer cells has recently emerged, in modulating the interface of cancer cells and the immune system [1719]; primarily, by affecting the nature of danger signaling (i.e., the signaling cascade that facilitates the exposure and/or release of danger signals) associated with ICD [1716 [1719-1722],]. This is an important point considering the recent clinical surge in the success of cancer immunotherapy in patients, and the emerging clinical relevance of ICD for positive patient prognosis. Several notorious autophagy-inducing anticancer therapies induce ICD including mitoxantrone, doxorubicin, oxaliplatin, radiotherapy, certain oncolytic viruses and hypericin-based photodynamic therapy (Hyp-PDT) [1709 [1722-1724],]. In fact, in the setting of Hyp-PDT, ER stress-induced autophagy in human cancer cells suppresses CALR (calreticulin) surface exposure (a danger signal crucial for ICD) thereby leading to suppression of human dendritic cell maturation and human CD4⁺ and CD8⁺ T cell stimulation [1724]. Similarly, ATG5- and ATG7-dependent autophagic responses limit the secretion of type I interferon by cancer cells undergoing radiotherapy-driven ICD, largely as a consequence of decreased cytosolic accumulation of mitochondrial DNA and consequent inhibition of CGAS-STING1 signaling [1725].

Conversely, chemotherapy (mitoxantrone or oxaliplatin)-induced autophagy facilitates ATP secretion (another crucial ICD-associated danger signal) thereby facilitating ICD and anti-tumor immunity in the murine system, the first documented instance of autophagy-based ICD modulation [1726]. The role of ATP as a DAMP becomes clear when the extracellular concentration of ATP becomes high and elicits activation of the purinergic receptor P2RX7. P2RX7 is involved in several pathways, including the sterile immune response, and its activation induces cancer cell death through PI3K, AKT and MTOR [1727,1728]. In addition, cells lacking the essential CMA gene *LAMP2A* fail to expose surface CALR after treatment with both Hyp-PDT and mitoxantrone [1729].

Although autophagy has been linked to fibrosis in many tissues, not much is known about it with regard to respiratory diseases *per se*. Initial observations have demonstrated that there is an increased formation of autophagosomes in mesenchymal cells from asthmatic donors with an increase in ATG5 in the lung [1730,1731]. Basal autophagy markers can be measured using IHC in the lung tissue, and with this approach it is possible to measure expression of BECN1, ATG5, LC3B and SQSTM1 in the airway epithelium and

mesenchymal layer (airway wall) of asthmatic and non-asthmatic human tissues in both small and large airways [1732]. The actual expression of these markers may vary in the airway wall and is largely dependent upon cell type as observed in the lung tissue; however, these observations provide a tool to monitor basal autophagy in health *vs* disease and can provide useful information on how it varies from one cell type to another in a clinical setting.

Finally, it is important to note that disease-associated autophagy defects are not restricted to macroautophagy but also concern other forms of autophagy. CMA impairment, for instance, is associated with several disease conditions, including neurodegenerative disorders [307,1733], lysosomal storage diseases [1734,1735], nephropathies [1736] and diabetes [1737]. In addition, it is very important to keep in mind that although human disease is mostly associated with inhibited autophagy, enhanced autophagy has also been proposed to participate in, and even contribute to, the pathogenesis of human diseases, such as chronic obstructive pulmonary disease [1738], adipocyte/adipose tissue dysfunction in obesity [292,396] and bilirubin-induced neurotoxicity [1739]. Along these lines, CQ was reported to decrease diabetes risk in patients treated with the drug for rheumatoid arthritis [1740].

A set of recommendations regarding the design of clinical trials modulating autophagy can be found in ref [1741].

Cautionary notes: Although the protein products of several genes mutated in different neurodegenerative diseases are involved in regulating selective autophagy [1188], several of these gene products also act together to regulate other important aspects of neuronal structure and function. For example, PINK1 (implicated in mitophagy) interacts with VCP/p97 (implicated in ribophagy and granulophagy) to promote the growth and extension of neuronal processes through activation of PRKA/PKA signaling, and not via degradative mechanisms [1742]. To establish a role for autophagy in disease states, whether neurodegenerative or immunological, specific tests need to be performed where genes encoding autophagy-relevant components (e.g., *ATG5*, *ATG7* or *BECN1*) have been knocked down through RNA silencing or other protein- or gene-specific targeting technologies [1724,1726,1729]. Usage of chemical inhibitors such as bafilomycin A₁, 3-MA or CQ can create problems owing to their off-target effects, especially on immune cells, and thus their use should be subjected to due caution, and relevant controls are critical to account for any off-target effects. In the context of ICD, consideration should be given to the observations that autophagy can play a context-dependent role in modulating danger signaling [1724,1726,1729]; and thus, all the relevant danger signals (e.g., surface exposed CALR or secreted ATP) should be (re-)tested for new agents/therapies in the presence of targeted ablation of autophagy-relevant proteins/genes, accompanied by relevant immunological assays (e.g., in vivo rodent vaccination/anti-tumor immunity studies or *ex vivo* immune cell stimulation assays), in order to imply a role for autophagy in regulating ICD or general immune responses.

Cell death and autophagy

Autophagy is often seen in tumor tissue accompanying cell death; however, the function of autophagy mediating cell death

is more limiting, and mostly confined to specific settings [1743-1745]. It is important to carefully establish the contribution of autophagy to the execution of cell death before making claims that autophagy is involved in the cell death process. Published literature often suffer from ambiguous use of the term “autophagic cell death,” which was coined in the 1970s [1746] in a purely morphological context to refer to cell death with autophagic features (especially the presence of numerous secondary lysosomes); this was sometimes taken to suggest a role of autophagy in the cell death mechanism, but death-mediation was not part of the definition [1747]. Recent nomenclature guidelines suggest that autophagy-dependent cell death (ADCD) is a distinct mechanism of cell death, independent of apoptosis or necrosis [1266]. Additional contributions of autophagy to cell death can be: (a) autophagy-associated cell death, where autophagy accompanies other cell death modalities and (b) autophagy-mediated cell death (AMCD), which could involve a standard mechanism of cell death such as apoptosis, but triggered by autophagy. The contribution of autophagy to cell death needs to be established by genetic and pharmacological means where autophagy inhibition blocks or reduces cell death, especially when distinct pathways of cell death appear to be simultaneously triggered by certain events [1748,1749]. However, while evidence for the need of autophagy in the context of cell death alone may support the definition of autophagy-mediated cell death, it is important when establishing ADCD that further proof is required that other established modes of programmed (or regulated) cell death do not contribute to cellular demise. It is preferable to use the term AMCD when it is proven that autophagy is a pre-requisite for the occurrence of cell death, but it is not proven that autophagy mechanistically mediates the switch to cell death [1750].

Inhibition of the full autophagy degradation cycle has also been proposed to lead to specific forms of autophagy-associated cell death, such as karyoptosis, involving the nucleophagy machinery and clearance by expulsion into the extracellular space [1750-1752]. Induction of the autophagy degradation cycle also promotes other cell death pathways, such as apoptosis, and cell cycle arrest [1753,1754]. It is important to note that a stress stimulus can in many circumstances induce different cell death pathways at the same time, which might lead to a “type” of cell death with mixed phenotypes [678,1755-1757]. Here, autophagy can be one of a range of adaptive mechanisms induced in the face of cellular stress, which precedes cell death if the stress cannot be overcome. Furthermore, inhibition of one cell death pathway (e.g., apoptosis) can either induce the compensatory activation of a secondary mechanism (e.g., necrosis) [1758,1759], or attenuate a primary mechanism (e.g., liponecrosis) [1755].

The role of autophagy in the death of plant cells is well established, because plants are devoid of the apoptotic machinery and use lytic vacuoles to disassemble dying cells from inside [1760]. This mode of cell death governs many plant developmental processes, as well as stress-induced cell death in some plant systems [911] and was named “vacuolar cell death” [1761]. Recent studies have revealed a key role of autophagy in the execution of vacuolar cell death, where autophagy sustains the growth of lytic vacuoles [1762,1763]. Besides being an executioner of vacuolar cell death, autophagy

can also play an upstream, initiator role in immunity-associated cell death related to the pathogen-triggered hypersensitive response [1760,1764].

Upon induction by starvation of multicellular development in the protist *D. discoideum*, autophagy (or at least Atg1) is required to protect against starvation-induced cell death, allowing vacuolar developmental cell death to take place instead [1765,1766]. Autophagy may be involved not only in allowing this death to occur, but also, as during vacuolar cell death in plants, in the vacuolization process itself [1767]. *D. discoideum* provides the ability to rapidly identify and characterize defects in lysosomal activity and autophagic degradation in relation to model diseases, such as a non-proteolytic activity for the gamma secretase complex [1768,1769].

The best known physiologically relevant demonstration of cell death that involves autophagy, and not apoptosis, is during *Drosophila* development. *Drosophila* is a powerful genetically amenable model system to study ADCD, as the process of autophagy and the function of *Atg* genes are highly conserved, enabling genetic analysis of the autophagy machinery components and interactions with other pathways (see *D.4. Drosophila melanogaster*). During *Drosophila* metamorphosis temporal increases in the steroid hormone ecdysone trigger the degradation of obsolete larval tissues including the midgut and salivary gland. Larval midgut degradation is dependent on autophagy and not apoptosis, as the inhibition of autophagy significantly delays midgut degradation whereas in the absence of apoptosis degradation occurs normally [375]. Many *Atg* genes are transcriptionally upregulated immediately prior to larval midgut degradation in an ecdysone receptor-dependent manner [375,1770]. Yet only a subset of the multi-subunit complexes that are required for autophagy induced during cell survival are essential for ADCD [1162,1771]. In contrast to the midgut, destruction of the salivary gland requires both caspase-dependent apoptosis and autophagy in parallel [1772-1774]. Inhibition of either autophagy or apoptosis alone results in a partial block in degradation, whereas combined inhibition completely blocks salivary gland degradation [1772]. As in the midgut, in response to ecdysone the expression of several *Atg* and apoptosis genes increase during salivary gland degradation [939,940,1775]. Although larval midgut and salivary gland degradation utilize autophagy for cell death, there are clear differences in the requirement of other cell death pathways between these tissues.

While there are numerous examples where autophagy promotes cell death in cultured cells, evidence for the physiological roles of ADCD in mammals have been more difficult to establish. The first description of autophagic cell death under physiological conditions in mammals is the terminal cell death in keratinocyte lineage cells of the skin [1776]. Under pathological conditions, an authentic case of autophagic cell death is the death of adult hippocampal neural stem cells following chronic restraint stress or injection of corticosterone, a stress-mediating hormone in mice [1777].

Along these lines, recent evidence suggests that ferroptosis is a type of autophagy-dependent cell death with increased autophagic flux [1778]. Mechanistically, NCOA4-facilitated ferritinophagy [1267,1272], RAB7A-dependent lipophagy [1779], BECN1-mediated SLC7A11/system xc⁻ inhibition

[1780,1781], STAT3-induced lysosomal membrane permeabilization [1782], HSP90-associated CMA [1271], and SQSTM1-dependent clockophagy [1249] can trigger ferroptosis through increasing iron accumulation or lipid peroxidation.

Another programmed death pathway, paraptosis [1783], is non-apoptotic in nature and has been linked to autophagy. There are several reports showing continuous increase in the autophagy marker protein LC3 and in SQSTM1 in ER stress-induced paraptosis [1784-1791]; in particular LC3 is indispensable for paraptosis as its knockdown significantly abrogates the cell death process [1784]. Pretreatment with autophagy inhibitors cannot interrupt, but rather enhances, the induction of cytoplasmic vacuolization and cell death during paraptosis. Increased SQSTM1 levels clearly indicate that the autophagy is impaired or inhibited during paraptosis-mediated cell death [1792]. Wheat germ agglutinin- and 8-p-hydroxybenzoyl tovarol-induced autophagy can antagonize paraptosis in cancer cells [1793,1794]. In contrast, a mitophagy-dependent pathway plays a crucial role in paraptosis induction by activating PINK1 [1795]. TEM analysis would be the best way to characterize the big empty vacuoles observed during paraptosis.

Cautionary notes: In brief, rigorous criteria must be met in order to establish a death-mediating role of autophagy (AMCD or ADCD), as this process typically promotes cell survival. These include a clear demonstration of autophagic flux as described in this article, as well as verification that inhibition of autophagy prevents cell death (if using a knockdown approach, multiple ATG genes should be targeted), and that, in the case of ADCD, other mechanisms of cell death are not responsible. It is imperative to assess the genetic inhibition of autophagy using multiple ATG gene ablation, especially given the emerging non-autophagy role of ATG proteins [1796,1797]. Another caution concerns the stability of ATG proteins; for some proteins the half-life may exceed several days, making a 24- to 48-h knockdown experiment problematic. In addition, depending on the experimental model system, appropriate protocols are needed to determine cellular viability or cell death. For example, long-term clonogenic assays should be employed when possible to measure the effective functional survival of cells. Together, care is needed to establish that the cell death is primarily dependent on autophagy rather than contributions from other modes of cell death.

Conclusion: In most systems, ascribing death to autophagy based solely on morphological criteria is insufficient; ADCD can only be demonstrated as death that is suppressed by the inhibition of autophagy, through either genetic and/or chemical means, noting that there are very few pharmacological inhibitors of autophagy induction [1798].

Chaperone-mediated autophagy

The primary characteristic that makes CMA different from the other autophagic variants described in these guidelines is that it does not require formation of intermediate vesicular compartments (autophagosomes or microvesicles) for the import of cargo into lysosomes [1799,1800]. Instead, the CMA substrates are translocated across the lysosomal membrane through the action of HSPA8/HSC70 (heat shock protein family A [Hsp70] member 8) located in the cytosol and lysosome lumen, and the lysosome membrane protein LAMP2A. This machinery makes CMA unique and distinct from the other two major types of

autophagy [1801, 1802]. CMA was originally identified in mammalian cells, and this section refers only to studies in mammals; however, this process has now been investigated in birds [1803], fish [1804,1805], *Drosophila* [1806] and *C. elegans* [1807]; in *C. elegans*, the process may actually be ESCRT-mediated sorting at the endosome, also referred to as endosomal microautophagy (e-MI), because the *lmp-1* and *lmp-2* genes are more closely related to mammalian *LAMP1*. In fact, in a large variety of fish species there exist expressed sequences displaying high homology with mammalian LAMP2A, suggesting that a functional CMA activity might not be solely restricted to mammals and birds, and therefore likely appeared much earlier during evolution than initially thought [1805]. Along these lines, a CMA activity is indeed present in fish [1808]. These data provide new information on the evolution of CMA, and also bring new perspectives on the possible use of complementary genetic models, such as zebrafish or medaka for studying CMA function from a comparative angle.

Furthermore, a complete *in silico* analysis has shed further light on the definition of CMA-competent and -incompetent species. In this case, the authors used two essential features that differentiate the LAMP2A splice variant from the other two LAMP2 variants, which are the presence of (a) three to four basic amino acids in the C-terminal proximal region of the cytosolic tail [1806] and (b) the sequence GYEQF at the C terminus of the LAMP2A protein [1809]. Following these systematic approaches, CMA-competent species include mammals, some types of birds [1810], reptiles [1809] and fish [1808]. Interestingly, not all the mammalian species can perform CMA, such as the Metatheria, which could indicate a diversified evolution for autophagy in this branch of the mammalian kingdom [1809]. It should also be noted that although most teleost fish display the consensus sequence GYXXF, the divergence of that motif in zebrafish, encoding an additional C-terminal amino acid, raises questions about the ability of this species to specifically perform CMA, and deserves special attention. Therefore, CMA-competent species should at present be restricted to mammals, some birds, fish and reptiles, until convincing data are provided regarding the presence of LAMP2A homologs in other species.

The following section discusses methods commonly utilized to determine if a protein is a CMA substrate (see ref [1811], for experimental details):

a. Analysis of the amino acid sequence of the protein to identify the presence of a KFERQ-related motif, which is recognized by HSPA8, and is an absolute requirement for all CMA substrates [1812]. A free web-based resource is available to perform searches for KFERQ-like motifs in proteins [1809]. Modifications by signaling or stress may generate a novel CMA motif in proteins without such a motif and then make them suitable to be degraded via CMA. For example, acetylation can make the lysine (K) mimic a glutamine (Q), leading to a new CMA substrate motif in the protein, which is accessible for recognition by the CMA chaperone protein [1813]. In experimental CMA activity assays, mutation of the KFERQ-related motif in a protein substrate of interest to alter its physical properties for CMA recognition is one of the strategies to elucidate the specificity of CMA-mediated protein degradation [1814].

b. Colocalization studies with lysosomal markers (typically LAMP2A and/or LysoTracker™) to identify a fraction of the protein associated with lysosomes. The increase in association of the putative substrate under conditions that upregulate CMA (such as prolonged starvation) or upon blockage of lysosomal proteases (to prevent the degradation of the protein) helps support the hypothesis that the protein of interest is a CMA substrate. However, association with lysosomes is necessary, but not sufficient, to consider a protein an authentic CMA substrate, because proteins delivered by other pathways to lysosomes will also behave in a similar manner. A higher degree of confidence can be attained if the association is preferentially with the subset of lysosomes active for CMA (i.e., those containing HSPA8 in their lumen), which can be separated from other lysosomes following published procedures [1815].

c. Co-immunoprecipitation of the protein of interest with cytosolic HSPA8. Due to the large number of proteins that interact with this chaperone, it is usually better to perform affinity isolation with the protein of interest and then analyze the isolated proteins for the presence of HSPA8 rather than vice versa.

d. Co-immunoprecipitation of the protein of interest with LAMP2A [1816]. Due to the fact that the only antibodies specific for the LAMP2A variant (the only one of the three LAMP2 variants involved in CMA [133,1817]) are generated against the cytosolic tail of LAMP2A, where the substrate also binds, it is necessary to affinity isolate the protein of interest and then analyze for the presence of LAMP2A. Immunoblot for LAMP2A in the precipitate can only be done with the antibodies specific for LAMP2A and not just those that recognize the luminal portion of the protein that is identical in the other LAMP2 variants. If the protein of interest is abundant inside cells, co-immunoprecipitations with LAMP2A can be done in total cellular lysates, but for low-abundance cellular proteins, preparation of a membrane fraction (enriched in lysosomes) by differential centrifugation may facilitate the detection of the population of the protein bound to LAMP2A.

e. Selective upregulation and blockage of CMA to demonstrate that degradation of the protein of interest changes with these manipulations. Selective chemical inhibitors for CMA are not currently available. Note that general inhibitors of lysosomal proteases (e.g., bafilomycin A₁, NH₄Cl, leupeptin) also block the degradation of proteins delivered to lysosomes by other autophagic and endosomal pathways. The most selective way to block CMA is by knockdown of LAMP2A, which causes this protein to become a limiting factor [133]. The other components involved in CMA, including HSPA8, HSP90AA1, GFAP, and EEF1A/eF1α, are all multifunctional cellular proteins, making it difficult to interpret the effects of knockdowns. Overexpression of LAMP2A [1816] is also a better approach to upregulate CMA than the use of chemical modulators. The two compounds demonstrated to affect degradation of long-lived proteins in lysosomes [1818], 6-aminonicotinamide and geldanamycin, lack selectivity, as they affect many other cellular processes. In addition, in the case of geldanamycin, the effect on CMA can be the opposite (inhibition rather than stimulation) depending on the cell type (this is due to the fact that the observed stimulation of CMA is actually a compensatory response to the blockage of

HSP90AA1 in lysosomes, and different cells activate different compensatory responses) [1819].

f. The most conclusive way to prove that a protein is a CMA substrate is by reconstituting its direct translocation into lysosomes using a cell-free system [1811]. This method is only possible when the protein of interest can be purified, and it requires the isolation of the population of lysosomes active for CMA. Internalization of the protein of interest inside lysosomes upon incubation with the isolated organelle can be monitored using protease protection assays (in which addition of an exogenous protease removes the protein bound to the cytosolic side of lysosomes, whereas it is inaccessible to the protein that has reached the lysosomal lumen; note that pre-incubation of lysosomes with lysosomal protease inhibitors before adding the substrate is required to prevent the degradation of the translocated substrate inside lysosomes) [1820]. The use of exogenous protease requires numerous controls (see ref [1811].) to guarantee that the amount of protease is sufficient to remove all the substrate outside lysosomes, but will not penetrate inside the lysosomal lumen upon breaking the lysosomal membrane.

The difficulties in the adjustment of the amount of protease have led to the development of a second method that is more suitable for laboratories that have no previous experience with these procedures. In this case, the substrate is incubated with lysosomes untreated or previously incubated with inhibitors of lysosomal proteases, and then uptake is determined as the difference of protein associated with lysosomes not incubated with inhibitors (in which the only remaining protein will be the one associated with the cytosolic side of the lysosomal membrane) and those incubated with the protease inhibitors (which contain both the protein bound to the membrane and that translocated into the lumen) [1821].

Confidence that the lysosomal internalization is by CMA increases if the uptake of the substrate can be competed with proteins previously identified as substrates for CMA (e.g., GAPDH [glyceraldehyde-3-phosphate dehydrogenase] or RNASE1 [ribonuclease A family member 1, pancreatic], both commercially available as purified proteins), but is not affected by the presence of similar amounts of nonsubstrate proteins (such as SERPINB/ovalbumin or PPIA/cyclophilin A). Blockage of uptake by pre-incubation of the lysosomes with antibodies against the cytosolic tail of LAMP2A also reinforces the hypothesis that the protein is a CMA substrate. It should be noted that several commercially available kits for lysosome isolation separate a mixture of lysosomal populations and do not enrich in the subgroup of lysosomes active for CMA, which limits their use for CMA uptake assays.

Further to the limitations in purifying CMA-active lysosomes for cell-free assays, CMA activity of these lysosomes may be blocked by proteins that bind abnormally to LAMP2A on the lysosomal surface, e.g., mutant LRRK2 [1733]. Such protein binding, which happens *in vivo*, may be inadvertently removed during stringent washes and centrifugation during the lysosome isolation and purification processes. Hence, assaying the degradation of an artificial CMA substrate in isolated lysosomes may not necessarily reflect the *in vivo* CMA activity [1814].

In other instances, rather than determining if a particular protein is a CMA substrate, the interest may be to analyze possible changes in CMA activity under different conditions or in response to different modifications. We enumerate here the methods, from lower to higher complexity, that can be utilized to measure CMA in cultured cells and in tissues (see ref [1811], for detailed experimental procedures).

a. Measurement of changes in the intracellular rates of degradation of long-lived proteins, when combined with inhibitors of other autophagic pathways, can provide a first demonstration in support of changes that are due to CMA. For example, CMA is defined in part as lysosomal degradation upregulated in response to serum removal but insensitive to PtdIns3K inhibitors.

b. Measurement of levels of CMA components is insufficient to conclude changes in CMA because this does not provide functional information, and changes in CMA components can also occur under other conditions. However, analysis of the levels of LAMP2A can be used to support changes in CMA detected by other procedures. Cytosolic levels of HSPA8 remain constant and are not limiting for CMA, thus providing no information about this pathway. Likewise, changes in total cellular levels of LAMP2A do not have an impact on this pathway unless they also affect their lysosomal levels (i.e., conditions in which LAMP2A is massively over-expressed lead to its targeting to the plasma membrane where it cannot function in CMA). It is advisable that changes in the levels of these two CMA components are confirmed to occur in lysosomes, either by colocalization with lysosomal markers when using image-based procedures or by performing immunoblot of a lysosomal enriched fraction (purification of this fraction does not require the large amounts of cells/tissue necessary for the isolation of the subset of lysosomes active for CMA).

Given that specific LAMP2A antibody is available for immunohistochemistry, comparison of puncta sizes from LAMP2A-positive lysosomes under different conditions provides useful information on the availability of LAMP2A at lysosomal levels. Although LAMP2A plays a key role in CMA activity, an increased LAMP2A level does not necessarily reflect increased CMA activity. Blockage of substrate translocation and disassembly of LAMP2A-binding complexes can result in accumulation of lysosomal LAMP2A, thus impairing LAMP2A turnover and CMA activity [1814].

c. Tracking changes in the subset of lysosomes active for CMA. This group of lysosomes is defined as those containing HSPA8 in their lumen (note that LAMP2A is present both in lysosomes that are active or inactive for CMA, and it is the presence of HSPA8 that confers CMA capability). Immunogold or immunofluorescence against these two proteins (LAMP2A and HSPA8) makes it possible to quantify changes in the levels of these lysosomes present at a given time, which correlates well with CMA activity [1815].

d. Analysis of lysosomal association of fluorescent artificial CMA substrates. Two different fluorescent probes have been generated to track changes in CMA activity in cultured cells using immunofluorescence or flow cytometry analysis [1815]. These probes contain the KFERQ and context sequences in frame with photoswitchable or photoactivated fluorescent

proteins. Activation of CMA results in the mobilization of a fraction of the cytosolic probe to lysosomes and the subsequent change from a diffuse to a punctate pattern. CMA activity can be quantified as the number of fluorescent puncta per cell or as the decay in fluorescence activity over time because of degradation of the artificial substrate. Because the assay does not allow measuring accumulation of the substrate (which must unfold for translocation), it is advisable to perform a time-course analysis to determine gradual changes in CMA activity. Antibodies against the fluorescent protein in combination with inhibitors of lysosomal proteases can be used to monitor accumulation of the probe in lysosomes over a period of time, but both the photoswitchable and the unmodified probe will be detected by this procedure [1822]. As for any other fluorescence probe based on analysis of intracellular "puncta" it is essential to include controls to confirm that the puncta are indeed lysosomes (colocalization with LysoTracker™ or LAMPs and lack of colocalization with markers of cytosolic aggregation such as ubiquitin) and do not reach the lysosomes through other autophagic pathways (insensitivity to PtdIns3K inhibitors and sensitivity to LAMP2A knockdown are good controls in this respect).

e. Direct measurement of CMA using in vitro cell-free assays. Although the introduction of the fluorescent probes should facilitate measurement of CMA in many instances, they are not applicable for tissue samples. In addition, because the probes measure binding of substrate to lysosomal membranes it is important to confirm that enhanced binding does not result from defective translocation. Last, the in vitro uptake assays are also the most efficient way to determine primary changes in CMA independently of changes in other proteolytic systems in the cells. These in vitro assays are the same ones described in the previous section on the identification of proteins as substrates of CMA, but are performed in this case with purified proteins previously characterized to be substrates for CMA. In this case the substrate protein is always the same, and what changes is the source of lysosomes (from the different tissues or cells that are to be compared). As described in the previous section, binding and uptake can be analyzed separately using lysosomes previously treated or not with protease inhibitors. The analysis of the purity of the lysosomal fractions prior to performing functional analysis is essential to conclude that changes in the efficiency to take up the substrates results from changes in CMA rather than from different levels of lysosomes in the isolated fractions. Control of the integrity of the lysosomal membrane and sufficiency of the proteases are also essential to discard the possibility that degradation is occurring outside lysosomes because of leakage, or that accumulation of substrates inside lysosomes is due to enhanced uptake rather than to decreased degradation.

f. Time-course analysis to determine CMA activity in live cells. Cells of interest can be developed to express a photoactivatable fluorescent reporter protein (e.g., PA-mCherry) conjugated to a KFERQ-like recognition motif. Photoactivation induces emission of fluorescence of reporter substrates already expressed in the cells. Any decline in substrate fluorescence levels after photoactivation can be monitored and quantified at different time points using flow cytometry. It is crucial that the culture medium be refreshed prior to photoactivation (typically

2 to 4 h) to minimize the confounding effects of basal autophagy due to depletion of nutrients in the old culture medium. Furthermore, CMA reference substrates may be degraded via non-CMA pathways. To confirm whether the degradation of the substrate is CMA-specific, it is important to include a control assay after *lamp2a* knockdown [1814].

Cautionary notes: The discovery of a new selective form of protein degradation in mammals named endosomal microautophagy [1823] has made it necessary to reconsider some of the criteria that applied in the past for the definition of a protein as a CMA substrate. The KFERQ-like motif, previously considered to be exclusive for CMA, is also used to mediate selective targeting of cytosolic proteins to the surface of late endosomes. For example, MAPT containing the KFERQ-like motifs has been found to be a CMA substrate [1824]; however, it was also revealed to be a substrate of e-MI [1825]. Once there, substrates can be internalized in microvesicles that form from the inward invagination of the limiting membrane of these organelles in an ESCRT-dependent manner. HSPA8 has been identified as the chaperone that binds this subset of substrates and directly interacts with lipids in the late endosomal membrane, thus acting as a receptor for cytosolic substrates in this compartment [1826]; accordingly, e-MI is a variation of the MVB pathway, and as such can be referred to as ESCRT-mediated sorting at the endosome. At a practical level, to determine if a KFERQ-containing protein is being degraded by CMA or e-MI the following criteria can be applied: (a) Inhibition of lysosomal proteolysis (for example with NH_4Cl and leupeptin) blocks degradation by both pathways. (b) Knockdown of LAMP2A inhibits CMA but not e-MI. (c) Knockdown of components of ESCRT-I and ESCRT-II (e.g., VPS4 and TSG101) inhibits e-MI but not CMA. (d) Interfering with the capability to unfold the substrate protein blocks its degradation by CMA, but does not affect e-MI of the protein. In this respect, soluble proteins, oligomers and protein aggregates can undergo e-MI, but only soluble proteins can be CMA substrates. (e) In vitro uptake of e-MI substrates can be reconstituted using isolated late endosomes whereas in vitro uptake of CMA substrates can only be reconstituted using lysosomes. e-MI has also been described in *Drosophila* neuromuscular junctions and fat body. Using photoactivatable PA-mCherry or split-GFP sensors it was shown to genetically depend on Hsc70-4, a homolog of HSPA8, and components of the ESCRT machinery [1806,1827].

Another pathway that needs to be considered relative to CMA is chaperone-assisted selective autophagy (CASA) [1828]. CASA is dependent on HSPA8 and LAMP2 (although it is not yet known if it is dependent solely on the LAMP2A isoform). Thus, a requirement for these two proteins is not sufficient to conclude that a protein is degraded by CMA.

It should also be noted that LAMP1 and LAMP2 share common function as revealed by the embryonic lethal phenotype of *lamp1^{-/-} lamp2^{y/-}* double-deficient mice [1829]. LAMP2 is involved in the fusion of late endosomes and autophagosomes or phagosomes [1830,1831]. LAMP2C, one of the LAMP2 isoforms, can also function as an RNA/DNA receptor in RNautophagy and DNautophagy pathways, where RNA or DNA is taken up directly by lysosomes in an ATP-dependent manner [1395-1398]. Whereas LAMP2A and LAMP2B are expressed in most mammalian cells, LAMP2C is selectively

expressed in different tissues and cell types. Increased expression of LAMP2C is induced in human lymphocytes upon cellular exposure to inflammatory stimuli, with ectopic LAMP2C expression disrupting CMA [1832]. In human melanoma tumors, increased cellular LAMP2C reduces the expression of LAMP2A and LAMP2B, disrupting CMA and autophagy, as well as cell cycle progression and tumor growth in vivo [1833]. Finally, LAMP1 and LAMP2 deficiency does not necessarily affect protein degradation under conditions when CMA is active [1829], and the expression levels of neuronal CMA substrates does not change upon loss of LAMP2 [1397,1834,1835].

Conclusion: One of the key issues with the analysis of CMA is verifying that the protein of interest is an authentic substrate. Methods for monitoring CMA that utilize fluorescent probes are available that eliminate the need for the isolation of CMA-competent lysosomes, one of the most difficult aspects of assaying this process.

Chaperone-assisted selective autophagy

CASA is a specialized form of macroautophagy whereby substrate proteins are ubiquitinated and targeted for lysosomal degradation by chaperone and co-chaperone proteins [1828]. The substrate protein does not require a KFERQ motif, which differentiates CASA from CMA. In addition, in CASA the cargo protein destined for degradation is delivered to the phagophore instead of directly to the lysosome as occurs in CMA. In CASA the substrate protein is recognized by the CASA complex that is formed by the assembly of the co-chaperone BAG3, which forms a multidomain complex with HSPA8, the small heat shock proteins HSPB6 and HSPB8, the ubiquitin ligase STUB1/CHIP, and the receptor proteins SYNPO2/myopodin (synaptopodin 2) and SQSTM1. The co-chaperone DNAJB6 also interacts with the core CASA machinery [1836], although its precise role in the pathway awaits confirmation. Following ubiquitination, the substrate protein is loaded onto the CASA machinery. SYNPO2 and SQSTM1 then bind to core components of the phagophore (VPS18 and LC3, respectively) resulting in sequestration of the substrate protein and associated multidomain complex within the autophagosome, and subsequent lysosomal degradation [1828,1837]. Note that association of BAG1 with STUB1/CHIP and HSPA8, displacing or preventing the association of HSPA8 with BAG3, causes the cargoes to be re-routed from CASA to the proteasome [1838-1841]. Along these lines, BAG3 Pro209 mutants, associated with neuromuscular diseases and peripheral neuropathies, relocate chaperones of the CASA complex to aggresomes; the mutant BAG3 protein traps ubiquitinated client proteins at the aggresome preventing their efficient clearance [1842]. Finally, CASA has been observed primarily in mammalian cells, but is also found in *Aspergillus* [1843]. See also *Filamentous fungi*.

Conclusion: Given that the autophagy machinery involved in CASA is very similar to that in other forms of autophagy there are currently no specific markers or inhibitors available to study this process specifically, but the involvement of HSPA8, BAG3 and ubiquitination of client proteins is highly suggestive of CASA activity.

Microautophagy

Microautophagy is a category of autophagic pathway that is driven by morphological changes of the lysosomal (vacuolar) or endosomal membrane. Protrusion (type 1) or invagination (type 2) of the lysosomal membrane leads to an uptake of the cytoplasmic components, while invagination of the endosomal membrane producing multivesicular bodies is also known to transport cytoplasmic components into the organelle lumen (type 3), and eventually to the lysosomal lumen [1844]. This category encompasses both bulk and selective autophagic pathways; several of the latter, termed micropexophagy (selective microautophagy of peroxisomes) in the yeast *Komagataella phaffii*/*Pichia pastoris*, and PMN in *Saccharomyces cerevisiae*, have been extensively studied [157,1061]. Whereas both micropexophagy and PMN are dependent on “core” Atg proteins [1845] responsible for the biogenesis of autophagic membrane structures [1846,1847], recent studies identified several microautophagic pathways independent of such Atg proteins, that function in selective degradation of lipid droplets (microlipophagy) in the yeast *S. cerevisiae* [1848,1849] or in the formation of anthocyanin vacuole inclusions in *A. thaliana* [1850]. Endosomal microautophagy (type 3) requires ESCRT and HSPA8-family proteins, and similar pathways have been found in *Schizosaccharomyces pombe* [1851] and *D. melanogaster* [1827].

Because microautophagy accompanies incorporation of part of the lysosomal membrane into the organelle lumen together with the cargo (target) components, the most authentic method to monitor microautophagy is detection of transport of lysosomal transmembrane proteins into the lumen. In yeast studies, the vacuolar transmembrane protein Vph1 can be expressed with a C-terminal GFP, and subjected to immunoblot analysis for the detection of the cleaved GFP moiety produced in the vacuolar lumen through microautophagic activity [1849,1852,1853]. For specific monitoring of selective microautophagy, similar detection of free GFP from GFP-tagged, organelle-specific proteins have been utilized for monitoring their activity. For example, Nvj1 or Swl1/Osh1 can be used for monitoring PMN [1847]; and Erg6 [1854,1855], Faa4 [1856], or Ldo16/Osw5 [1849] are useful for the detection of microlipophagy. For *in vitro* detection of bulk microautophagic activity in *S. cerevisiae*, luciferase incorporation into the purified vacuole fraction can be monitored [1857]. In mammalian cells, exosomes correspond to intraluminal vesicles (ILVs) of multivesicular endosomes (MVEs) that are secreted in the extracellular space upon fusion of MVEs with the plasma membrane instead of lysosomes. Exosome analysis can be used as a readout of ILV biogenesis [1858]. Some elements of commonality are achieved between exosome/ILV biogenesis (type 3) and vacuolar microautophagy (type 2), such as lipid domain and ESCRT involvement [1859]. Moreover, a crosstalk exists between the exosomal and autophagic pathways allowing cell clearance of unwanted components [822].

Cautionary notes: It should be noted that these assay systems monitoring the dynamics of organelle-specific proteins other than lysosomal transmembrane proteins, do not discriminate between autophagic and microautophagic activities, and thus the data should be interpreted in combination with other morphological analyses or immunoblot data from the lysosomal membrane protein(s). In monitoring microlipophagy, care should be taken for the choice of the lipid droplet marker proteins for the immunoblot analysis, as several of the marker proteins, e.g., Erg6,

exhibit dual localization to the ER and lipid droplets, depending on culture conditions [1849]; the use of such dual-localized marker proteins makes it difficult to discriminate reticulophagy and (micro)lipophagy. It also should be noted that overexpression of lipid marker proteins easily leads to release of the proteins into the cytosol, which renders the degradation dependent on bulk autophagy and “core” Atg factors, because all of the lipid droplet proteins are peripherally associated with the organelle surface.

Comments on additional topics

Acidotropic dyes

Among the older methods for following autophagy is staining with acidotropic dyes such as MDC [1603], acridine orange [1860], neutral red [1552], LysoSensor Blue [1861] and LysoTracker™ Red [377,1862]. It should be emphasized that, whereas these dyes are useful to identify acidified vesicular compartments, they should not be relied upon to compare differences in endosomal or lysosomal pH between cells due to variables that can alter the intensity of the signal. For example, excessive incubation time and/or concentrations of LysoTracker™ Red can oversaturate labeling of the cell and mask differences in signal intensity that reflect different degrees of acidification within populations of compartments [1863]. Use of these dyes to detect, size, and quantify numbers of acidic compartments must involve careful standardization of the conditions of labeling and ideally should be confirmed by ancillary TEM and/or immunoblot analysis. Reliable measurements of vesicle pH require ratiometric measurements of two dyes with different peaks of optimal fluorescence (e.g., LysoSensor Blue and LysoSensor Yellow), or the use of a molecule with two emission wavelengths that are differentially affected by pH to exclude variables related to uptake and cell size [80,1863,1864]. Another method to validate the fluorescent signal of an acidotropic dye is by defining a cut-off level for the net fluorescence intensity resulting from each dye’s incorporation in acidic lysosomes. Coupling acidotropic dye staining with flow cytometric analysis is highly recommended for a numerically validated and objective determination of autophagy, and the use of a control such as CQ or HCQ will further validate this inexpensive and convenient technique [1865].

Finally, degradation of lysosomal cargo depends on acidification which leads to enzyme activation. Most cathepsins are abundant and activated at the low pH of the lysosomal lumen. For validation of cathepsin activation, and thus validation of functional lysosomes, co-staining with Magic Red dye and a lysosomal marker such as LAMP2 is recommended. Selective inhibitors of cathepsin, such as E64d for cathepsin B, must be included as an experimental control for Magic Red specificity.

Cautionary notes: Although MDC was first described as a specific marker of autophagic vacuoles [1866] subsequent studies have suggested that this, and other acidotropic dyes, are not specific markers for early autophagosomes [439], but rather label later stages in the degradation process. For example, autophagosomes are not acidic, and MDC staining can be seen in autophagy-defective mutants [814] and in the absence of autophagy activation [1867]. MDC may also show confounding levels of background labeling unless narrow bandpass filters are used. However, in the presence of vinblastine, which blocks fusion with lysosomes, MDC labeling increases, suggesting that under

these conditions MDC can label late-stage autophagosomes [1600]. Along these lines, cells that overexpress a dominant negative version of RAB7 (the T22N mutant) show colocalization of this protein with MDC; in this case fusion with lysosomes is also blocked [1510] indicating that MDC does not just label lysosomes. Nevertheless, MDC labeling could be considered as an indicator of autophagy when the increased labeling of cellular compartments by this dye is prevented by treatment with specific autophagy inhibitors.

Overall, staining with MDC or its derivative monodansylpentane [1603] is not, by itself, a sufficient method for monitoring autophagy. Similarly, LysoTracker™ Red, neutral red and acridine orange are not ideal markers for autophagy because they primarily detect lysosomes, and an increase in lysosome size or number could reflect an increase in nonprofessional phagocytosis (often seen in embryonic tissues [1868]) rather than autophagy. These markers are, however, useful for monitoring selective autophagy when used in conjunction with protein markers or other dyes. For example, increased colocalization of mitochondria with both GFP-LC3 and LysoTracker™ Red can be used as evidence of autophagic cargo delivery to lysosomes. Moreover, LysoTracker™ Red has been used to provide correlative data on autophagy in *D. melanogaster* fat body cells (Figure 32) [376,377]. However, additional assays, such as GFP-Atg8-family protein fluorescence and EM, should be used to substantiate results obtained with acidotropic dyes whenever possible to rule out the possibility that LAP is involved (see *Noncanonical use of autophagy-related proteins*). Finally, one important caution when co-imaging with LysoTracker™ Red and a green-fluorescing marker (e.g., GFP-LC3 or MitoTracker™ Green) is that it is necessary to control for rapid red-to-green photoconversion of the LysoTracker™, which can otherwise result in an incorrect interpretation of colocalization [1869].

Some of the confusion regarding the interpretation of results with these dyes stems in part from the nomenclature in this field. Indeed, the discussion of acidotropic dyes points out why it is advisable to differentiate between the terms “autophagosome”

and “autophagic vacuole,” although they are occasionally, and incorrectly, used interchangeably. The autophagosome is the sequestering compartment generated by the phagophore. The fusion of an autophagosome with an endosome or a lysosome generates an amphisome or an autolysosome, respectively [1480]. The early autophagosome is not an acidic compartment, whereas amphisomes and autolysosomes are acidic. As noted in the section *Transmission electron microscopy*, earlier names for these compartments are “initial autophagic vacuole (AVi),” “intermediate or intermediate/degradative autophagic vacuole (AVi/d)” and “degradative autophagic vacuole (AVd),” respectively. Thus, acidotropic dyes can stain late autophagic vacuoles (in particular autolysosomes), but not the initial autophagic vacuole, the early autophagosome.

A recently developed dye for monitoring autophagy, Cyto-ID (Enzo Life Sciences), stains vesicular structures shortly after amino acid deprivation, which extensively colocalize with RFP-LC3-positive structures, while colocalizing partially with lysosomal probes [1870]. Moreover, unlike MDC, Cyto-ID does not show background fluorescence under control conditions and the two dyes colocalize only marginally. Furthermore, the Cyto-ID signal responds to well-known autophagy modulators. Therefore, this amphiphilic dye, which partitions in hydrophobic environments, may prove more selective for autophagic vacuoles than the previously discussed lysosomotropic dyes.

With the above caveats in mind, the combined use of early and late markers of autophagy is highly encouraged, and, when quantifying mammalian lysosomes, it is important to note that increases in both lysosome size and number are frequently observed. Finally, to avoid confusion with the plant and fungal vacuole, the equivalent organelle to the lysosome, we recommend the use of the term “autophagosome” instead of “autophagic vacuole” when possible, that is, when the specific nature of the structure is known.

Conclusion: Given the development of better techniques that are indicators of autophagy, relying entirely on the use of acidotropic dyes to study this process is not acceptable.

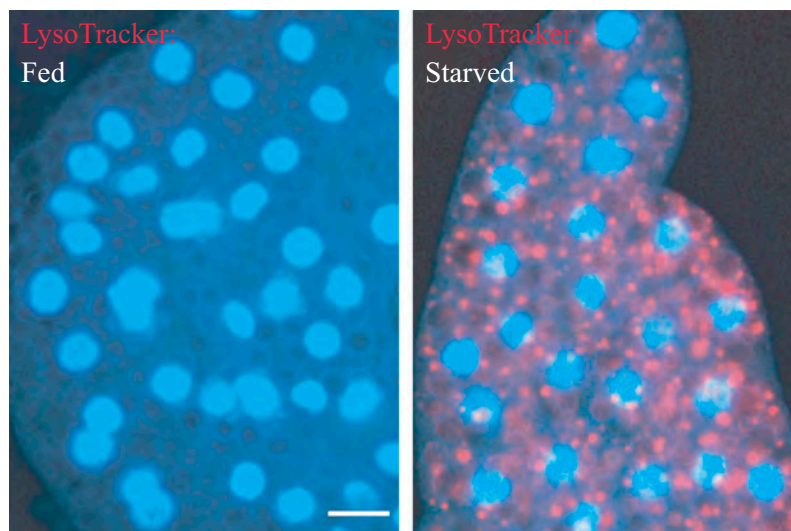


Figure 32. LysoTracker™ Red stains lysosomes and can be used to monitor autophagy in *Drosophila*. Live fat body tissues from *Drosophila* were stained with LysoTracker™ Red (red) and Hoechst 33342 (blue) to stain the nucleus. Tissues were isolated from fed (left) or 3-h starved (right) animals. Bar: 25 μ m. This figure was modified from data presented in ref. [377], Developmental Cell, 7, Scott RC, Schuldiner O, Neufeld TP, Role and regulation of starvation-induced autophagy in the *Drosophila* fat body, pp. 167-78, copyright 2004, with permission from Elsevier.

Autophagy inhibitors and inducers

In many situations it is important to demonstrate an effect resulting from inhibition or stimulation of autophagy (see ref [1871], for a partial listing of regulatory compounds), and a few words of caution are worthwhile in this regard. Most chemical inhibitors of autophagy are not entirely specific, and it is important to consider possible dose- and time-dependent effects. Accordingly, it is generally preferable to analyze specific loss-of-function *Atg* mutants. However, it must be kept in mind that some apparently specific *Atg* gene products may have autophagy-independent roles (e.g., ATG5 in cell death, and the PIK3C3/VPS34-containing complexes—including BECN1—in apoptosis, endosomal function and protein trafficking), or may be dispensable for autophagy (see *Noncanonical use of autophagy-related proteins*) [31, 817,860,1550,1872-1875]. Therefore, the experimental conditions of inhibitor application and their side effects must be carefully considered.

In addition, it must be emphasized once again that autophagy, as a multistep process, can be inhibited at different stages. Sequestration inhibitors, including 3-MA, LY294002 and wortmannin, inhibit class I PI3Ks as well as class III PtdIns3Ks [181,437,1876]. The class I enzymes generate products such as PtdIns(3,4,5)P₃ that inhibit autophagic sequestration, whereas the class III product (PtdIns3P) generally stimulates autophagic sequestration. The overall effect of these inhibitors is typically to block autophagy because the class III enzymes that are required to activate autophagy act downstream of the negative regulatory class I enzymes, although cell death may ensue in cell types that are dependent upon high levels of AKT for survival. The effect of 3-MA (but not that of wortmannin) is further complicated by the fact that it has different temporal patterns of inhibition, causing a long-term suppression of the class I PI3K, but only a transient inhibition of the class III enzyme. In cells incubated in a complete medium for extended periods of time, 3-MA may, therefore (particularly at suboptimal concentrations), promote autophagy by inhibition of the class I enzyme [436,437]. Thus, wortmannin may be considered as an alternative to 3-MA for autophagy inhibition [437]. However, wortmannin can induce the formation of vacuoles that may have the appearance of autophagosomes, although they are swollen late endocytic compartments [1527]. In addition, treatment of human alveolar macrophages with wortmannin or 3-MA in complete medium or HBSS results in increased levels of LC3-I and LC3-II as detected by western blotting. Neither wortmannin nor 3-MA blocks rapamycin-induced conversion of LC3-I to LC3-II in these cells; rather there seems to be an additive effect. Consequently, these inhibitors should be used with caution when investigating autophagy in macrophages (M. O'Sullivan and S. O'Leary, unpublished observation). Furthermore, studies have demonstrated that inhibition of autophagy with 3-MA or wortmannin can have effects on cytokine transcription, processing and secretion, particularly of IL1 family members [1877-1879], but 3-MA and wortmannin also inhibit the secretion of some cytokines and chemokines (e.g., TNF, IL6, CCL2/MCP-1) in an autophagy-independent manner (J. Harris, unpublished observations) [1877,1880]. Moreover, 3-MA inhibits the production of nitric oxide in IFNG-activated bone-marrow derived macrophages [1881]. Thus, in studies where the effect of autophagy inhibition on specific cellular processes is being investigated, it is important to confirm results using other methods,

such as RNA silencing. Due to these issues, it is of great interest that inhibitors with specificity for the class III PtdIns3Ks, and their consequent effects on autophagy, have been described [331,1882,1883]. For instance, the selective class III PtdIns3K inhibitor SAR405 is an efficient blocker of autophagic (LDH) sequestration and (long-lived protein) degradation activity [25,56,302]. Finally, it is important to stress that the efficacy of wortmannin as an inhibitor of PI3Ks and PtdIns3Ks may be decreased by its non-enzymatic covalent binding to free amino acids [1884,1885].

A mutant mouse line carrying a floxed allele of *Pik3c3* has been created [1886]. This provides a useful genetic tool that will help in defining the physiological role of the class III PtdIns3K with bona fide specificity by deleting the class III kinase in a cell type-specific manner in a whole animal using the Cre-LoxP strategy. For example, the phenotype resulting from a knockout of *Pik3c3* specifically in the kidney glomerular podocytes (*pik3c3* [*pdKO*]) indicates that there is no compensation by other classes of PtdIns3Ks or related *Atg* genes, thus highlighting the functional specificity and physiological importance of the class III PtdIns3K in these cells.

CHX, a commonly used protein synthesis inhibitor in mammals, is also an inhibitor of sequestration in vivo [13-15, 113,1522,1887-1890], and in various cell types in vitro [216,660, 1891], and it has been utilized to investigate the dynamic nature of the regression of various autophagic elements [13-15, 28,113,1887,1888]. The mechanism of action of CHX in short-term experiments is not clear, but it has no direct relation to the inhibition of protein synthesis [660]. This latter activity, however, may complicate certain types of analysis when using this drug.

A significant challenge for a more detailed analysis of the dynamic role of autophagy in physiological and pathophysiological processes, for instance with regard to cancer and cancer therapy, is to find more specific inhibitors of autophagy signaling which do not affect other signaling cascades (reviewed in ref [527]). For example, in the context of cellular radiation responses it is well known that PI3Ks, in addition to signaling through the PI3K-AKT pathway, have a major role in the regulation of DNA-damage repair [1891]. However, 3-MA, which is a nonspecific inhibitor of these lipid kinases, can alter the function of other classes of this enzyme, which are involved in the DNA-damage repair response. This is of particular importance for investigations into the role of radiation-induced autophagy in cellular radiation sensitivity or resistance [1892,1893]. CQ, through the induction of ROS, increases DNA damage and can be used to synergistically enhance the therapeutic effect of otherwise toxic NOTCH and gamma secretase inhibitors that target the oncogenic NOTCH signaling pathway [1894].

Most other inhibitory chemicals act at post-sequestration steps. These types of agents have been used in many experiments to both inhibit endogenous protein degradation and to increase the number of autophagic compartments. These chemicals cause the accumulation of sequestered material in either autophagosomes or autolysosomes, or both, because they allow autophagic sequestration to proceed. The main categories of these types of inhibitors include the vinca alkaloids (e.g., vinblastine) and other microtubule poisons that inhibit fusion, inhibitors of lysosomal enzymes (e.g., leupeptin, pepstatin A and E-64d), and compounds that elevate lysosomal pH (e.g., inhibitors of V-ATPases such as

bafilomycin A₁, concanamycin A and concanamycin B [64], and weak base amines including methyl- or propylamine, CQ, and neutral red, some of which slow down fusion). Ammonia is a very useful agent for the elevation of lysosomal pH in short-term experiments, but it has been reported to cause a stimulation of autophagy during long-term incubation of cells in a full medium [1895], under which conditions a good alternative might be methylamine or propylamine [1896]. Along these lines, it should be noted that the half-life of glutamine in cell culture media is approximately two weeks due to chemical decomposition, which results in media with lowered glutamine and elevated ammonia concentrations that can affect the autophagic flux (either inhibiting or stimulating autophagy, depending on the concentration [1897]). Thus, to help reduce experimental variation, the use of freshly prepared cell culture media with glutamine is advised. Alternatively, GlutaMAX is recommended for culture media without glutamine [1898].

A special note of caution is also warranted in regard to CQ. Although this chemical is commonly used as an autophagy inhibitor, CQ may initially stimulate autophagy (F.C. Dorsey, personal communication; R. Franco, personal communication). In addition, culture conditions requiring acidic media preclude the use of CQ because intracellular accumulation of the chemical is dramatically reduced by low pH [1899]. To overcome this issue, it is possible to use acid compounds that modulate autophagy, such as betulinic acid and its derivatives [314,1900-1902]. Betulinic acid damages lysosomal function differing from traditional inhibitors (e.g., CQ, NH₄Cl or bafilomycin A₁) that raise the lysosomal pH; betulinic acid interacts with pure phospholipid membranes [314,1170], and is capable of changing membrane permeability [314,1903,1904]. The lysosomal damage mediated by betulinic acid is capable of compromising autophagy without any incremental damage when lysosomal function is altered by lysosomal inhibitors (e.g., CQ or bafilomycin A₁) [314]; however, betulinic acid is not lysosome specific, and will affect other organelles such as mitochondria.

Other natural compounds, such as sulforaphane (in breast cancer MDA-MB-231 cell line), the *Phellinus linteus* fungus extract (in the breast cancer MDA-MB-231 cell line) and neferine (in the lung adenocarcinoma A549 cell line) combined with anticancer drugs synergistically induce autophagic cell death [1905]. Dehydroandrographolide and polyphyllin G trigger activation of MAPK8/9 and an inhibition of AKT and MAPK/p38, inducing oral cancer autophagic cell death [1906,1907]. Notably, a significant number of natural compounds have been identified to overcome drug-resistant or apoptosis-resistant cancer *via* induction of autophagic cell death: For example, an ATP2A/SERCA inhibitor, saikosaponin-d, N-desmethyldauricine and celastrol [1908-1911]; a group of AMPK activators (liensinine, isoliensinine, dauricine, cepharanthine, hernandezine and thalidezine) [1912-1915]; and the PRKCA/PKC- α inhibitor, tetrandrine [1916]. Other natural small-molecules, such as thonningianin A from *Penthorum chinense* Pursh, steroidal saponin and polyphyllin VI from *Trillium tschonoskii* Maxi were reported to show their anti-oxidative effect *via* autophagy induction [1917].

Some data suggest that particular nanomaterials may also be novel modulators of autophagy, by as yet unidentified mechanisms [1918,1919] (See *Nanoparticles*).

It is worth noting that lysosomal proteases fall into three general groups, cysteine, aspartic acid and serine proteases. Therefore, the fact that leupeptin, a serine and cysteine protease inhibitor, has little or no effect does not necessarily indicate that lysosomal degradation is not taking place; a combination of leupeptin, pepstatin A and E-64d may be a more effective treatment. However, it should also be pointed out that these protease inhibitors can exert inhibitory effects not only on lysosomal proteases, but also on cytosolic proteases; that is, degradation of proteins might be blocked through inhibition of cytosolic instead of lysosomal proteases. Conversely, it should be noted that MG132 (Z-leu-leu-leu-al) and its related peptide aldehydes are commonly used as proteasomal inhibitors, but they can also inhibit certain lysosomal hydrolases such as cathepsins and calpains [1920]. Thus, any positive results using MG132 do not rule out the possibility of involvement of the autophagy-lysosomal system. Therefore, even if MG132 is effective in inhibiting autophagy, it is important to confirm the result using more specific proteasomal inhibitors such as lactacystin or epoxomicin. Finally, there are significant differences in cell permeability among protease inhibitors. For example, E-64d is membrane permeable, whereas leupeptin and pepstatin A are not (although there are derivatives that display greater permeability such as pepstatin A methyl ester) [1921]. Thus, when analyzing whether a protein is an autophagy substrate, caution should be taken in utilizing these protease inhibitors to block autophagy.

As with the PtdIns3K inhibitors, many autophagy-suppressive compounds are not specific. For example, okadaic acid [1922] is a powerful general inhibitor of both type 1 (PPP1) and type 2A (PPP2) protein phosphatases [1923]. Bafilomycin A₁ and other compounds that raise the lysosomal pH may have indirect effects on any acidified compartments. Moreover, treatment with bafilomycin A₁ for extended periods (18 h) can cause significant disruption of the mitochondrial network in cultured cells (M.E. Gegg, personal communication), and either bafilomycin A₁ or concanamycin A cause swelling of the Golgi in plants [1924], and increase cell death by apoptosis in cancer cells (V.A. Rao, personal communication) [216]. Furthermore, bafilomycin A₁ may have off-target effects on the cell, particularly on MTORC1 [781,1925,1926]. Bafilomycin A₁ is often used at a final concentration of 100 nM, but much lower concentrations such as 1 nM may be sufficient to inhibit autophagic-lysosomal degradation and are less likely to cause indirect effects [300,1927]. For example, in pulmonary A549 epithelial cells bafilomycin A₁ exhibits concentration-dependent effects on cellular morphology and on protein expression; at concentrations of 10 and 100 nM the cells become more rounded accompanied by increased expression of VIM (vimentin) and a decrease in CDH1/E-cadherin (B. Yeganeh, M. Post and S. Ghavami, unpublished observations). Thus, appropriate inhibitory concentrations should be empirically determined for each cell type [309]. As elaborated earlier in these guidelines, there is a lacuna in the field due to lack of specific autophagy inhibitors. Nonetheless, a small molecule inhibitor of autophagosome-lysosome fusion, EACC (ethyl [2-{5-nitrothiophene-2-carboxamido} thiophene-3-carbonyl] carbamate), has been identified [1928]. This molecule selectively blocks autophagic flux by inhibiting STX17 translocation onto autophagosomes.

Although these various agents can inhibit different steps of the autophagic pathway, their potential side effects must be considered in interpretation of the secondary consequences of autophagy inhibition, especially in long-term studies. For example, lysosomotropic compounds can increase the rate of autophagosome formation by inhibiting MTORC1, as activation of lysosomally localized MTORC1 depends on an active V-ATPase (as well as RAG GTPases [223]) [1925,1929]. Along these lines, CQ treatment may cause an apparent increase in the formation of autophagosomes possibly by blocking fusion with the lysosome (F.C. Dorsey and J.L. Cleveland, personal communication). This conclusion is supported by the finding that CQ reduces the colocalization of LC3 and LysoTracker™ despite the presence of autophagosomes and lysosomes (A.K. Simon, personal communication). In addition, CQ, but not bafilomycin A₁, blocks autophagosome-lysosome fusion in U2OS, HeLa and MEFs [302]. This mechanism might be cell-type specific, as other studies report that CQ prevents autolysosome clearance and degradation of cargo content, but not autophagosome-lysosome fusion [1930-1933]. Concanamycin A blocks sorting of vacuolar proteins and diverts the route of autophagy in plant cells along with inhibiting vacuolar acidification [1934,1935]. Furthermore, in addition to causing the accumulation of autophagic compartments, many of these drugs seem to stimulate sequestration in many cell types, especially in vivo [114,432,1521,1582,1887,1890,1936-1939]. Although it is clear why these drugs cause the accumulation of autophagic compartments, it is not known why they stimulate sequestration. One possibility, at least for hepatocytes, is that the inhibition of protein degradation reduces the intracellular amino acid pool, which in turn upregulates sequestration. A time-course study of the changes in both the intra- and extracellular fractions may provide accurate information regarding amino acid metabolism. For these various reasons, it is important to include appropriate controls; along these lines, MTOR inhibitors such as rapamycin or amino acid deprivation can be utilized as positive controls for inducing autophagy. In many cell types, as well as in *D. discoideum* [1940], however, the induction of autophagy by rapamycin is relatively slow, or transient, allowing more time for indirect effects.

Amino acid starvation induces autophagy through deactivation of MTOR. Whereas autophagy is induced equally well by pharmacological inhibition of MTOR and amino acid starvation, amino acid starvation additionally causes depletion of intracellular amino acids, which strongly repress protein synthesis. For that reason, the protein expression levels of classical substrates of autophagy (e.g., SQSTM1-like receptors [SLRs]) decrease more rapidly during amino acid starvation than during pharmacological inhibition of MTOR. Additionally, endosomal microautophagy, which also targets SLRs and certain Atg8-family protein homologs, is also active during amino acid starvation contributing to the overall decreased expression of many classical substrates of autophagy [1941].

Several small molecule inhibitors, including torin1, PP242, KU-0063794, PI-103 and NVP-BEZ235, have been developed that target the catalytic domain of MTOR in an ATP-competitive manner [300,802,1942-1945]. In comparison to rapamycin, these catalytic MTOR inhibitors are more potent, and hence are stronger autophagy agonists in most cell lines [453,802,1946]. The use of these second-generation MTOR inhibitors may reveal that some reports of MTOR-independent autophagy may actually

reflect the use of the relatively weak inhibitor rapamycin. Furthermore, the use of these compounds has revealed a role for MTORC1 and MTORC2 as independent regulators of autophagy [1947].

Neurons, however, seem to be a particular case in regard to their response to MTOR inhibitors. Rapamycin may fail to activate autophagy in cultured primary neurons, despite its potent stimulation of autophagy in some cancer cell lines [106,818,1948]. Interestingly, both rapamycin and catalytic MTOR inhibitors do not induce a robust autophagy in either cultured primary mouse neurons or human neuroblastoma SH-SY5Y cells, which can differentiate into neuron-like cells, whereas the drugs do elicit a potent autophagic response in cultured astrocytes (J. Diaz-Nido and R. Gargini, personal communication). This observation suggests a differential regulation of autophagy in neurons. It has been suggested that control of neuronal autophagy may reflect the particular physiological adaptations and metabolic requirements of neurons, which are very different from most peripheral cell types [1949]. For example, acute starvation in transgenic mice expressing GFP-LC3 leads to a potent induction of autophagy in the liver, muscle and heart but not in the brain [239]. Along these lines, glucose depletion may be much more efficient at inducing autophagy than rapamycin or amino acid starvation in neurons in culture (M. Germain and R. Slack, personal communication). Indeed, treatment of cultured primary mouse neurons and human neuroblastoma SH-SY5Y cells with 2-deoxy-glucose, which hampers glucose metabolism and leads to activation of AMPK, results in robust autophagy induction (J. Diaz-Nido and R. Gargini, personal communication). A number of compounds can also be quite efficient autophagy inducers in neurons including the CAPN (calpain) inhibitor calpeptin [1950-1952]. Thus, it has been suggested that autophagy induction in neurons may be achieved by molecular mechanisms relying on AMPK or increases in intracellular calcium concentration [1949]. An example where changes in cytosolic calcium levels, due to the incapacity of the mitochondria to buffer Ca²⁺ release, result in an increase in autophagy is seen in a cellular model of the neurodegenerative disease Friedreich ataxia, based on FXN (frataxin) silencing in SH-SY5Y human neuroblastoma cells [1953].

Finally, a specialized class of compounds with α,β -unsaturated ketone structure tends to induce autophagic cell death, accompanied by changes in mitochondrial morphology. Because the cytotoxic action of these compounds is efficiently blocked by *N*-acetyl-L-cysteine, the β -position in the structure may interact with an SH group of the targeted molecules [1954]. Due to the potential pleiotropic effects of various drug treatments, it is incumbent upon the researcher to demonstrate that autophagy is indeed inhibited, by using the methodologies described herein. Accordingly, it is critical to verify the effect of a particular biochemical treatment with regard to its effects on autophagy induction or inhibition when using a cell line that was previously uncharacterized for the chemical being used. Similarly, cytotoxicity of the relevant chemical should be assessed.

The use of gene deletions/inactivations (e.g., in primary or immortalized *atg*^{-/-} MEFs [814], plant T-DNA or transposon insertion mutants [378,1955], or in vivo using transgenic knockout models [1956,1957] including Cre-lox based “conditional” knockouts [424,425]) or functional knockdowns (e.g., with RNAi against *ATG* genes) is the preferred approach when possible

because these methods allow a more direct assessment of the resulting phenotype; however, different floxed genes are deleted with varying efficiency, and the proportion deleted must be carefully quantified [1958]. Studies also suggest that microRNAs may be used for blocking gene expression [332-335,990,991,1959]. In most contexts, it is advisable when using a knockout or knock-down approach to examine multiple autophagy-related genes to exclude the possibility that the phenotype observed is due to effects on a nonautophagic function(s) of the corresponding protein, especially when examining the possibility of autophagic cell death. This is particularly the case in evaluating BECN1, which interacts with anti-apoptotic BCL2 family proteins [848], or when low levels of a target protein are sufficient for maintaining autophagy as is the case with ATG5 [346]. With regard to ATG5, a better approach may be to use a dominant negative (K130R) version [1875,1948,1960]. Also noteworthy is the role of ATG5 in mitotic catastrophe [818] and several other nonautophagic roles of ATG proteins (see *Noncanonical use of autophagy-related proteins*) [106]. Along these lines, and as stated above for the use of inhibitors, when employing a knockout or especially a knock-down approach, it is again incumbent upon the researcher to demonstrate that autophagy is actually inhibited, by using the methodologies described herein.

Finally, we note that the long-term secondary consequences of gene knockouts or knockdowns are likely much more complex than the immediate effects of the actual autophagy inhibition. To overcome this concern, inducible knockout systems might be useful [346,559]. One additional caveat to knockdown experiments is that PAMP recognition pathways can be triggered by double-stranded RNAs (dsRNA), such as siRNA probes, or the viral vector systems that deliver shRNA [1961]. Some of these, including TLR-mediated RNA recognition [1962], can influence autophagy by either masking any inhibitory effect or compromising autophagy independent of the knockdown probe. Therefore, nontargeting (scrambled) siRNA or shRNA controls should be used with the respective transfection or transduction methods in the experiments that employ ATG knockdown. Another strategy to specifically interfere with autophagy is to use dominant negative inhibitors. Delivery of these agents by transient transfection, adenovirus, or TAT-mediated protein transduction offers the possibility of their use in cell culture or in vivo [1960]. However, because autophagy is an essential metabolic process for many cell types and tissues, loss of viability due to autophagy inhibition always has to be a concern when analyzing cell death-unrelated questions. In this respect it is noteworthy that some cell-types of the immune system such as dendritic cells [440] seem to tolerate loss of autophagy fairly well, whereas others such as T and B cells are compromised in their development and function after autophagy inhibition [1963,1964].

In addition to pharmacological inhibition, RNA silencing, gene knockout and dominant negative RAB and ATG protein expression, pathogen-derived autophagy inhibitors can also be considered for use in manipulating autophagy. Along these lines ICP34.5, viral BCL2 homologs and viral FLIP of herpesviruses block autophagosome formation [848,1418,1965], whereas M2 of influenza virus and HIV-1 Nef block autophagosome degradation [493,1966]. However, as with other tools discussed in this section, transfection or transduction of viral autophagy inhibitors should be used in parallel with other means of autophagy manipulation,

because these proteins are used for the regulation of usually more than one cellular pathway by the respective pathogens. Finally, RavZ is an example of a bacterial protein that blocks autophagy. RavZ is a *Legionella* effector that inhibits host autophagy by irreversible deconjugation of LC3 [1967]. RavZ has 3 LIR motifs in its N- and C-terminal regions for interacting with LC3 [1968] and a catalytic cysteine protease domain that cleaves the peptide bond between the PE-modified C-terminal glycine residue and the adjacent aromatic residue in Atg8-family proteins [1967]. In addition, all *Legionella pneumophila* strains sequenced to date [1969] encode a homolog of the eukaryotic enzyme SGPL1 (sphingosine-1-phosphate lyase 1) that was named LpSPL for *Legionella pneumophila* SPL. This gene was most likely acquired from a protist host [1970]. The translocated LpSPL effector protein targets host sphingosine biosynthesis to curtail autophagy. LpSPL activity alone is sufficient to prevent an increase in sphingosine levels in infected host cells and to inhibit autophagy during macrophage infection [1971].

There are fewer compounds that act as inducers of autophagy, but the initial characterization of this process was due in large part to the inducing effects of glucagon, which appears to act through indirect inhibition of MTOR via the activation of STK11/LKB1-AMPK [1531,1532,1972]. Currently, the most commonly used inducer of autophagy is rapamycin, an allosteric inhibitor of MTORC1 (although as mentioned above, catalytic inhibitors such as torin1 are increasingly being used). Nevertheless, one caution is that MTOR is a major regulatory protein that is part of several signaling pathways, including for example those that respond to INS (insulin), EGF (epidermal growth factor) and amino acids, and it thus controls processes other than autophagy, so rapamycin will ultimately affect many metabolic pathways [744,1973-1975]. In particular, the strong effects of MTOR on protein synthesis may be a confounding factor when analyzing the effects of rapamycin. MTOR-independent regulation can be achieved through lithium, sodium valproate and carbamazepine, compounds that lower the myo-inositol 1,4,5-triphosphate levels [1976], as well as FDA-approved compounds such as verapamil, trifluoperazine and clonidine [1977,1978]. Regarding trifluoperazine, studies have shown that other structurally related antipsychotic phenothiazine derivatives, such as chlorpromazine and thioridazine, induce autophagy in tumor cells in vitro through the inhibition of AKT-MTOR [1979,1980] and by modulating the WNT-CTNNB1/ β -catenin signaling pathway [1981] in glioma cells. The antihistamine phenothiazine derivative promethazine also induces autophagy-associated cell death in a Philadelphia chromosome-positive chronic myeloid leukemia model (K562) mediated by activation of AMPK [1982].

In vivo treatment of embryos with cadmium results in an increase in autophagy, probably to counter the stress, allowing cell survival through the elimination/recycling of damaged structures [1552]. Autophagy may also be regulated by the release of calcium from the ER under stress conditions [216,1922,1983-1987]. Studies have demonstrated that a natural compound, celastrol, inhibits ATP2A/SERCA, a sarcoplasmic/endoplasmic reticulum Ca^{2+} -ATPase pump to induce autophagy-dependent cytotoxicity in rheumatoid arthritis synovial fibroblasts and rheumatoid arthritis fibroblast-like synoviocytes via the CAMK2B (calcium/calmodulin dependent kinase kinase II beta)-AMPK-MTOR pathway [1988]. Conversely, some compounds can

achieve their biological effect by inhibition of calcium-regulated autophagy. For instance, 2-aminoethoxydiphenylborane sensitizes the anti-tumor effect of bortezomib via suppression of calcium-mediated autophagy [1989].

ITPRs as ER-resident intracellular Ca^{2+} -release channels, which also localize at MAMs, have a dual role in autophagy [1990]. In non-starved conditions, ITPRs appear to suppress basal autophagy by funneling Ca^{2+} into the mitochondria, thereby promoting mitochondrial bio-energetics [668]. Upon starvation, ITPRs are involved in the augmented autophagic flux through the CAMK2-OGT-ULK cascade as well as a process that involves ITPR sensitization through the recruitment of BECN1 [1007, 1983]. The essential role of ITPRs and/or intracellular Ca^{2+} signaling to drive autophagic flux has also been observed after treatment with rapamycin [1985], resveratrol [1991] or some chemical inducers of ER stress [1992]. Confluency-induced differentiation of Caco-2 cells increases the expression of the master transcriptional regulator HNF4A/HNF4 α , which in turn induces ER stress via the increased expression of XBP1 and ATF6, accompanied by an increase in the intracellular Ca^{2+} levels and autophagy [1993]. However, additional calcium signals from other stores such as lysosomes could also play an important role in autophagy induction [1994]. The activation of the lysosomal TPCN/two-pore channel (two pore segment channel), by nicotinic acid adenine dinucleotide phosphate (NAADP) induces autophagy through an AMPK-ACAC pathway independently of MTORC1 in neural cells [1995]. Autophagosome formation mediated by NAADP can be selectively inhibited by the TPCN blocker NED-19, by pre-incubation with a cell-permeable acetoxymethyl ester version of BAPTA (BAPTA-AM), or in cells overexpressing TPCN2 mutated within the putative pore region (TPCN2^{L265P}), indicating that lysosomal Ca^{2+} selectively induces autophagy [1996]. Furthermore, a possible NAADP-agonist, glutamate, is able to induce autophagy via a TPC1/2-AMPK-ACAC pathway [1995].

Lysosomal cation-permeable channels such as TPCN2 associate with MTORC1, a key nutrient sensor and upstream control mechanism of autophagy, to regulate autophagy flux [1997]. Lysosomal Ca^{2+} release via TPCN2 occurs upon inhibition of MTOR in response to starvation or rapamycin treatment and is an essential component to drive autophagic flux in these conditions. In addition to MTORC1 control of TPCN2 activity, Ca^{2+} release via TPCN2 also supports MTORC1 activity [1998]. Furthermore, upon starvation, MCOLN1 (mucolipin 1) also contributes to lysosomal Ca^{2+} release. This release results in the Ca^{2+} -dependent activation of PPP3/calcineurin, which dephosphorylates TFEB, triggering its nuclear translocation. In the nucleus, TFEB upregulates several autophagy and lysosomal biogenesis genes. MCOLN1-mediated Ca^{2+} release also contributes to the reactivation of MTORC1 in conditions of prolonged starvation via a mechanism that requires the Ca^{2+} -binding protein CALM (calmodulin) [1999]. As such, the dynamic nature of Ca^{2+} signaling involving ER, mitochondria and lysosomes contribute to the fine-tuned control of autophagic flux [2000,2001]. The use of BAPTA-AM to implicate Ca^{2+} signaling in autophagy comes with a caution, as intracellular BAPTA can also exert Ca^{2+} -independent effects, such as inhibition of the Na^+/K^+ ATPase [2002,2003] as well as autophagy [1994]. Along these lines, it is becoming increasingly clear that BAPTA, and related molecules such as calcium indicator dyes, have cellular effects that are not related to calcium

buffering [2002,2003]. Low-affinity analogs of BAPTA (e.g., dibromo- and difluoro-BAPTA) can inhibit autophagy triggered by PP242 (M.D. Bootman, personal communication).

Cell-penetrating autophagy-inducing peptides, such as Tat-vFLIP or Tat-beclin 1, are also potent inducers of autophagy in cultured cells as well as in mice [1965,2004]. Other cell-penetrating peptides, such as Tat-wtBH3D or Tat-dsBH3D, designed to disrupt very specific regulatory interactions such as the BCL2-BECN1 interaction, are potent, yet very specific, inducers of autophagy in cultured cells [2005].

In contrast to other PtdIns3K inhibitors, caffeine induces autophagy in the food spoilage yeast *Zygosaccharomyces bailii* [2006], mouse embryonic fibroblasts [2007], and *S. cerevisiae* [2008] at millimolar concentrations. In more complex eukaryotes, this is accompanied by inhibition of the MTOR pathway. Similarly, in budding yeast caffeine is a potent TORC1 inhibitor suggesting that this drug induces autophagy via inhibition of the TORC1 signaling pathway; however, as with other PtdIns3K inhibitors caffeine targets other proteins, notably Mec1/ATR and Tel1/ATM, and affects the cellular response to DNA damage.

Another autophagy inducer is the histone deacetylase inhibitor valproic acid [2009,2010]. The mechanism by which valproic acid stimulates autophagy is not entirely clear but may occur due to inhibition of the histone deacetylase Rpd3, which negatively regulates the transcription of *ATG* genes (most notably *ATG8* [2011]) and, via deacetylation of Atg3, controls Atg8 lipidation [2012]. SMER28 is an MTOR-independent inducer of autophagy that acts through largely unknown mechanisms [2013]. Dasatinib, a dual SRC and BCR-ABL kinase inhibitor, also stimulates autophagy through unknown mechanisms to further induce myeloid differentiation of AML cells [2014].

A new promising drug, NeuroHeal, has emerged that activates autophagy through a SIRT1-dependent mechanism [2015,2016]. NeuroHeal treatment protects from ER-stress and promotes in vivo neuroprotection in several models where neurons remain isolated and disconnected from their targets, a common characteristic in any neurodegenerative process [2017,2018]. An efficient high-throughput method for screening of autophagy modulators has been carried out employing a dual-luciferase assay. In this case, degradation of the individual luciferases indicates the degradation of general cytoplasmic contents and the selective degradation of specific cargoes. The levels of cytosolic *Renilla* luciferase, and targeted firefly luciferase, which can be delivered to a specific cargo (such as peroxisomes), is measured and interpreted as rates of general and selective autophagy flux, respectively [2019].

Induction of autophagy can also be involved in virulence mechanisms for infection; the Buruli ulcer causative agent *Mycobacterium ulcerans* produces an exotoxin, mycolactone, that induces autophagy [2020,2021]. The mechanism is most likely a protective response to mycolactone's inhibition of SEC61A1, the major subunit of the SEC61 translocon (R.E. Simmonds, personal communication), which causes the accumulation of mislocalized proteins in the cytosol [2022] and a consequent integrated stress response [2021]. Notably, polymorphisms in autophagy-related genes may be involved in the risk of acquiring *M. ulcerans* infection from the environment [2023].

It is also possible, depending on the organism or cell system, to modulate autophagy through transcriptional control. For example, this can be achieved either through

overexpression or post-translational activation of *TFEB* (see *Transcriptional and translational regulation*), a transcriptional regulator of the biogenesis of both lysosomes and autophagosomes [947,949]. Along these lines, inhibition or genetic deletion of CTSB downregulates MTOR, causing TFEB to activate autophagy [2024]. Similarly, adenoviral-mediated expression of the transcription factor CEBPB induces autophagy in hepatocytes [989]. Either the genetic ablation or the knockdown of the nucleolar transcription factor RRN3/TIF-1A, a crucial regulator of the recruitment of POLR1 (RNA polymerase I) to ribosomal DNA promoters, induces autophagy in neurons and in MCF-7 cancer cells, respectively, linking ribosomal DNA transcription to autophagy [2025,2026]. Likewise, inhibition of POLR1 by the small molecule inhibitor CX-5461 induces autophagy. A growing body of evidence suggests the involvement of nucleolar ribosome biogenesis factors and the so-called nucleolar stress response in autophagy [2027,2028]. A class of diseases connected to impaired ribosome biogenesis, termed ribosomopathies, reveal activation of autophagy (see *Erythroid cells*). Nucleolar-stress induced autophagy seems to engage both TP53-dependent as well as -independent mechanisms. Also, induction of autophagy is commonly connected to MTOR signaling in this context. However, the underlying mechanisms connecting nucleolar stress and autophagy have to be better elucidated in future studies.

Relatively little is known about direct regulation via the ATG proteins, but there is some indication that tamoxifen acts to induce autophagy by increasing the expression of BECN1 in MCF7 cells [2029]. However, BECN1 does not appear to be upregulated in U87MG cells treated with tamoxifen, whereas the levels of LC3-II and SQSTM1 are increased, while LAMP2B is downregulated and CTSD and CTSB activities are almost completely blocked (K.S. Choi, personal communication). Thus, the effect of tamoxifen may differ depending on the cell type. Other data suggest that tamoxifen acts by blocking cholesterol biosynthesis, and that the sterol balance may determine whether autophagy acts in a protective versus cytotoxic manner [2030,2031]. Finally, screens have identified small molecules that induce autophagy independently of rapamycin and allow the removal of misfolded or aggregate-prone proteins [1978,2032], suggesting that they may prove useful in therapeutic applications.

One novel autophagy inducer that does not target MTOR, is KYP-2047, a small-molecule inhibitor for PREP (prolyl endopeptidase), a serine protease belonging to the prolyl oligopeptidase family (clan SC) [2033]. Although the exact mechanism as to how PREP regulates autophagy is not clear, PREP inhibition by KYP-2047 elevates *BECN1* mRNA and protein levels in HEK 293 cells after a 24-h incubation. This inhibition results in decreased aggregation-prone protein levels in several cellular and animal models [2034]. Moreover, removal of PREP from HEK 293 cells induces autophagic flux, and also decreases proteasomal activity [2035]. However, caution should be taken because of the crosstalk between autophagy and the proteasomal system. For example, trehalose, an MTOR-independent autophagy inducer [2036], can compromise proteasomal activity in cultured primary neurons [2037]. Trehalose activates autophagy by inhibiting AKT-mediated phosphorylation of TFEB, thereby promoting TFEB nuclear translocation and subsequent activation of CLEAR-regulated

autophagy and lysosomal genes in cells and *in vivo* [973]. For experiments in cells, it must be considered that at the concentration usually tested (>mM) trehalose effects can be potentially ascribed to hyperosmotic signaling (R. Franco, personal communication). Trehalose treatment also results in subtle lysosomal damage (possibly because of an osmotic shock to this organelle), which causes activation of PPP3/calcineurin, a calcium-dependent phosphatase capable of dephosphorylating and activating TFEB [2038]. This activation permits enhanced lysophagy to degrade damaged lysosomes, but at the same time enhances the overall autophagic capacity of trehalose-treated cells. Lysosomal impairment by trehalose might underlie observations that cell treatment with this disaccharide can decrease degradation of APP in lysosomes [2039], increase GFP:RFP ratios using the GFP-LC3-RFP-LC3ΔG fluorescent probe [494], or result in the accumulation of autophagosomes [2040]. Finally, several disease-causing and aggregation-prone proteins in the secretory pathway that are targeted for autophagy are also targeted for ERAD, which requires proteasome function [2041].

Another autophagy inducer, genistein (trihydroxyisoflavone or 5, 7-dihydroxy-3-[4-hydroxyphenyl]-4 *H*-1-benzopyran-4-one), has been suggested previously to stimulate autophagy in various cancer cell lines, including ovarian cancer [2042], colon cancer [2043], breast cancer [2044], pancreatic cancer [2045], and uterine leiomyoma cells [2046]. Other studies demonstrate that this isoflavone effectively induces autophagy in cellular and animal models of HD and AD, respectively [2047,2048]. Such genistein-mediated autophagy stimulation is responsible for correction of phenotypes of these diseases through degradation of pathological protein aggregates, which otherwise accumulate in cells and organs. In fact, induction of autophagy by this isoflavone has been proposed as a therapeutic approach in various genetic and neurodegenerative disorders caused by accumulation of undegraded proteins or other macromolecules [2049,2050]. The molecular mechanism of genistein-mediated induction of autophagy is not clear, however, it appears that inhibition of MTOR and subsequent activation of TFEB contributes significantly to this process [2051-2053].

While likely to be nonspecific, inhibition of NFκB activation—through either an NFκBIA/IκBα kinase inhibitor or SERPINA1/alpha-1-antitrypsin—may augment autophagy in macrophages infected with mycobacteria [2054,2055]. One possible mechanism is the inhibition of NFκB-mediated induction of TNFAIP3/A20, a deubiquitinating enzyme that normally deactivates BECN1; hence, by sequentially inhibiting NFκB activation and TNFAIP3/A20 expression, a pathway that inhibits BECN1 is mitigated [2054].

Because gangliosides are implicated in autophagosome morphogenesis, pharmacological or genetic impairment of gangliosidic compartment integrity and function can provide useful information in the analysis of autophagy. To deplete cells of gangliosides, an inhibitor of CERS (ceramide synthase), such as a fungal metabolite produced by *Fusarium moniliforme* (fumonisins B1), or, alternatively, siRNA to *CERS* or *ST8SIA1*, can be used [907].

Antimicrobial peptides (AMPs) were originally described for their activity in killing microbes; however, they also have a role in immune system modulation [2056]. Autophagy induction produces AMPs by proteolysis of cytosolic proteins of

infected cells [2057,2058]). Furthermore, three AMPs (indolicidin, and two peptides derived from PYY2/Seminalplasmin) induce autophagy in *Leishmania* cells [2059], and the antimicrobial peptide LL-37 induces autophagy in human cells as a way to eliminate tuberculosis infection [2060].

Finally, in addition to genetic and chemical compounds, it was reported that electromagnetic fields can induce autophagy in mammalian cells. Studies of biological effects of novel therapeutic approaches for cancer therapy based on the use of noninvasive radiofrequency fields reveal that autophagy, but not apoptosis, is induced in cancer cells in response to this treatment, which leads to cell death [2061]. This effect is tumor specific and different from traditional ionizing radiation therapy that induces apoptosis in cells.

Conclusion: Considering that pharmacological inhibitors or activators of autophagy have an impact on many other cellular pathways, the use of more than one methodology, including molecular methods, is desirable. Rapamycin is less effective at inhibiting MTOR and inducing autophagy than catalytic inhibitors; however, it must be kept in mind that catalytic inhibitors also affect MTORC2. The main concern with pharmacological manipulations is pleiotropic effects of the compound being used. Accordingly, genetic confirmation is preferred whenever possible. Alternatively, pharmacological compounds that do not target cell survival and maintenance pathways such as MTOR, can be used for temporal regulation of autophagy [2062].

Basal autophagy

Basal levels of LC3-II or GFP-LC3 puncta may change according to the time after addition of fresh medium to cells, and this can lead to misinterpretations of what basal autophagy means. This is particularly important when comparing the levels of basal autophagy between different cell populations (such as knockout versus wild-type clones). If cells are very sensitive to nutrient supply and display a high variability of basal autophagy, the best experimental condition is to monitor the levels of basal autophagy at different times after the addition of fresh medium. One example is the chicken lymphoma DT40 cells (see *Chicken B-lymphoid DT40 cells*) and their knockout variant for all three ITPR isoforms [668,1990,2063]. In these cells, no differences in basal levels of LC3-II can be observed up to 4 h after addition of fresh medium, but differences can be observed after longer times (J. M. Vicencio and G. Szabadkai, personal communication). This concept should also be applied to experiments in which the effect of a drug upon autophagy is the subject of study. If the drugs are added after a time in which basal autophagy is already high, then the effects of the drug can be masked by the cell's basal autophagy, and wrong conclusions may be drawn. To avoid this, fresh medium should be added first (followed by incubation for 2-4 h) in order to reduce and equilibrate basal autophagy in cells under all conditions, and then the drugs can be added. The basal autophagy levels of the cell under study must be identified beforehand to know the time needed to reduce basal autophagy.

A similar caution must be exercised with regard to cell culture density and hypoxia. When cells are grown in normoxic conditions at high cell density, HIF1A/HIF-1 α

is stabilized at levels similar to that obtained with low-density cultures under hypoxic conditions [2064]. This results in the induction of BNIP3 and BNIP3L and “hypoxia”-induced autophagy, even though the conditions are theoretically normoxic [1170]. Therefore, researchers need to be careful about cell density to avoid accidental induction of autophagy.

It should be realized that in yeast species, medium changes can trigger a higher “basal” level of autophagy in the cells. In the methylotrophic yeast species *K. phaffii*/*P. pastoris* and *Hansenula polymorpha*, a shift of cells grown in batch from glucose to methanol results in stimulation of autophagy [2065,2066]. A shift to a new medium can be considered a stress situation. Thus, it appears to be essential to cultivate the yeast cells for a number of hours to stabilize the level of basal autophagy before performing experiments intended to study levels of (selective) autophagy (e.g., pexophagy). Finally, plant root tips cultured in nutrient-sufficient medium display constitutive autophagic flux (i.e., a basal level), which is enhanced in nutrient-deprived medium [2067-2069].

Conclusion: The levels of basal autophagy can vary substantially and can mask the effects of the experimental parameters being tested. Changes in media and growth conditions need to be examined empirically to determine effects on basal autophagy and the appropriate times for subsequent manipulations.

Experimental systems

Throughout these guidelines we have noted that it is not possible to state explicit rules that can be applied to all experimental systems. For example, some techniques may not work in particular cell types or organisms. In each case, efficacy of autophagy promoters, inhibitors and measurement techniques must be empirically determined, which is why it is important to include appropriate controls. Differences may also be seen between in vivo or perfused organ studies and cell culture analyses. For example, INS (insulin) has no effect on proteolysis in suspended rat hepatocytes, in contrast to the result with perfused rat liver. The INS effect reappears, however, when isolated hepatocytes are incubated in stationary dishes [2070,2071] or are allowed to settle down on the matrix (D. Häussinger, personal communication). The reason for this might be that autophagy regulation by INS and some amino acids requires volume sensing via integrin-matrix interactions and also intact microtubules [2072-2074]. Along these lines, the use of whole embryos makes it possible to investigate autophagy in multipotent cells, which interact among themselves in their natural environment, bypassing the disadvantages of isolated cells that are deprived of their normal network of interactions [1552]. In general, it is important to keep in mind that results from one particular system may not be generally applicable to others.

Conclusion: Although autophagy is conserved from yeast to human, there may be tremendous differences in the specific details among systems. Thus, results based on one system should not be assumed to be applicable to another.

Bimolecular fluorescence complementation

Bimolecular fluorescence complementation (BiFC) may be useful to study protein-protein interactions in the autophagic

pathway [2075] In this assay, a protein of interest is cloned into a vector containing one half of a fluorescent reporter (e.g., YFP), while a second protein is cloned into a different vector containing the other half of the reporter. Constructs are cotransfected into cells. If the two proteins of interest interact, the two halves of the reporter are brought into close proximity and a fluorescent signal is reconstituted, which can be monitored by confocal microscopy. This assay can be used to determine protein interactions without prior knowledge of the location or structural nature of the interaction interface. Moreover, this approach is applicable to living cells, and relatively low concentrations of recombinant protein are required to generate a detectable signal. One issue with BiFC is that once the two halves of the fluorophore interact with each other the binding is extremely stable, which can result in the amplification of weak signals. For the same reason, the localization of the BiFC interaction may not represent the normal physiological site. Conversely, the stable nature of this interaction may be utilized as an alternative to chemical cross-linking for studying protein-protein interactions.

Nanoparticles

Nanoparticles (NPs) are tiny particulate materials, ranging in size from 1 to 100 nm in diameter. Due to their physicochemical properties and small size, some NPs may cross biological membranes and are often used to deliver a cytotoxic agent or as a tool to modulate cellular processes [2076]. NPs may act both as inhibitors and inducers of autophagy [1919]. Indeed, most endocytic routes of NP uptake converge on the lysosome, making this organelle a common site of NP sequestration and degradation [2077]. Autophagy induction is of relevance for NPs due to the similarities in sizes and shapes between NPs and pathogens [2078]. The exact mechanism of autophagy induction by NPs is not well understood, although studies have shown that the surface properties including surface charge, may play a decisive role, as shown in studies using ammonium-functionalized gold NPs [2079]. For example, the positively charged surface of cationic NPs might facilitate their interaction with the negatively charged plasma or endolysosomal membranes harboring the members of the MTOR signaling pathway. Moreover, lysosomal alkalinization by the “proton sponge” effect of cationic NPs could cause lysosomal dysfunction and subsequent defects in lysosomal recruitment and activation of MTORC1 [2080].

NPs also promote autophagy through specific modulation of lysosomal pH. Biodegradable nanoparticles such as photo-activable NPs (paNPs) and poly (lactide-co-glycolide) (PLGA) NPs induce autophagy through acidification of the lysosomal environment in cellular models of type II diabetes [2081,2082], AD [80] and PD [2083,2084]. In pancreatic beta cells under lipotoxicity or PC-12 cells under MPP⁺ neurotoxin treatment, lysosomal pH is elevated and autophagy is inhibited due to impaired fusion between lysosomes and autophagosomes. PLGA NPs and paNPs localize to lysosomes, and lower lysosomal pH in both types of cellular models, thereby restoring autophagy and cellular functions. Of note, the paNPs are stimuli-responsive NPs that can acutely release acids to lower lysosomal pH only upon application of UV light. This allows

for paNPs to be a useful tool that can temporally control the outcomes of autophagy by an external stimulus [2081].

ROS production by NPs may also play a role in autophagy induction [2085,2086]. Furthermore, NPs with ROS-quenching capacity (e.g., non-photo-excited graphene quantum dots) induce subsequent tolerogenic effects in human dendritic cells in an autophagy-dependent manner, and this is reversed by ATG5 silencing [2087]. Conversely, LC3 silencing reduces the oxidative stress-dependent cytotoxicity of photoexcited graphene quantum dots, indicating a role of autophagy in their photodynamic anticancer activity [2088]. Nitrogen-doped TiO₂ NPs can induce autophagy-dependent differentiation or autophagy-associated cell death in leukemia cells, depending on the dose of the NPs, and pre-incubation of leukemic cells with ROS scavengers diminishes the effect of the NPs [2089]. Expansile nanoparticles/eNPs can also induce autophagy-associated cell death through disruption of autophagosomal trafficking, and offer a new opportunity to develop autophagy modulators for cancer therapy when used in conjugation with a chemotherapeutic [2090]. Using a combinatorial library of multi-walled carbon nanotubes (CNTs), it is possible to show that autophagy induction can be “tuned” by varying surface ligands on the CNTs [2091]. Furthermore, the autophagy-inducing activity of certain metallic NPs can be modulated through surface coating with specific peptides [2092]. Size-dependent autophagy induction has also been observed [2093], and it is suggested that quantum dots (i.e., semiconductor crystals) may serve as potentially useful probes for autophagy studies, in light of their unique optical properties [2094].

It should be noted that NPs may also block autophagy, and shape-related targeting of lysosomes may explain NP-mediated inhibition of autophagic flux [2095]. It is important to distinguish between autophagosome accumulation resulting from blockade of autophagic flux as opposed to the induction of autophagy, and, as with other areas of study, the failure to distinguish one from the other may result in the misinterpretation of NP effects on cells [2096]. Silica (SiO₂) NPs are among the most widely produced and most intensively studied nanomaterials, and the persistent presence of enlarged autolysosomes is seen in hepatocytes after exposure to SiO₂ NPs [2097]. This accumulation is due to a defect in the autophagy termination process known as autophagic lysosome reformation (ALR). Similarly, the blockade of autophagic flux by SiO₂ NPs was reported in lung epithelial cells, and evidence was provided for a suppressive effect of the NPs on lysosomal acidification, thereby contributing to the decreased autophagic degradation in these cells [2097]. Others have shown that SiO₂ NPs induce autophagosome accumulation in hepatocytes *via* the activation of the EIF2AK3- and ATF6-dependent UPR pathways [2098]. To further compound the situation, autophagic cell death induction was shown, in a study of single-walled CNTs, to occur through the AKT-TSC2-MTOR pathway. Inhibition of autophagy using both pharmacological and genetic approaches significantly reduces the CNT-induced autophagic cell death as well as the acute lung injury evidenced in mice [2099].

Graphene oxide combined with cisplatin (GO-CDDP) not only elicits autophagy, but induces the nuclear import of cisplatin as well as LC3 [2100]. The nuclear LC3 does not

colocalize with SQSTM1 or LAMP2, and blocking autolysosome formation does not significantly hinder the nuclear import of LC3-CDDP, indicating that autophagosome and autolysosome formation is dispensable. Furthermore, direct binding between silica nanoparticles and LC3 and SQSTM1 was demonstrated in osteoblast cells [2101].

ATG4 proteases are essential enzymes in the autophagic process, and ATG4B appears to be most relevant for autophagy. Several peptide-conjugated polymeric nanoprobe have been developed for real-time monitoring of ATG4B activity *in vitro* and *in vivo*. There is an “in vivo self-assembly”-based nanoprobe that consists of a TFGF peptide (a peptide from LC3, which specifically responds to ATG4B), an aggregation-induced emission molecule and a hydrophilic carrier, that in situ self-assembles into new nanostructures that “turn on” signals in the presence of ATG4B [2102,2103]. These nanoprobe do not induce autophagy at the used dose and can be applied for real-time and quantitative evaluation of ATG4B in living tumor cells, as well as the zebrafish and mouse models. Another probe is a FRET-based nanoparticle that uses the fluorescent dye FITC and the quencher BHQ1 attached to the TFGF peptide, which is nonfluorescent, but fluoresces in autophagy-inducing cells [2104].

To summarize, careful, case-by-case evaluation of the role of autophagy for each NP is required, and a direct interaction between NPs and the cellular autophagic machinery seems possible. In addition, it is important to determine whether each type of NP alters the net autophagic degradation capacity by employing one of the functional assays described in these guidelines. This will provide a more comprehensive picture than merely determining the levels of autophagic markers and the number of autophagosomes.

NPs may provide useful tools with which to study autophagy, as suggested in early work on quantum dots and using photo-activated nanoparticles [2081,2093]. NPs can either induce or inhibit autophagy; thus, the autophagy-inducing/inhibiting efficacy of nanoprobe should be carefully explored before using them *in vivo* or in clinical research.

Another example of the use of NPs to study autophagy is seen with nanotubes (NTs) in the study of ATG3-membrane interaction. As shown in flotation studies with sonicated unilamellar vesicles, ATG3 increases its binding to neutral membranes when vesicle size decreases. To visualize this effect under the microscope, lipid NTs can be generated, starting from a compositionally well-defined unilamellar membrane system, such as SUPER templates [2105]. The formed NTs are thin tubules with high membrane curvature, reported to be a powerful tool to analyze curvature-dependent binding of proteins. ATG3-Alexa Fluor 488 interacts with electrically neutral (PC:DOPE) NTs, whereas GABARAP does not exhibit any binding to NTs with similar curvature [2106].

General considerations for experimental manipulations

One general issue with regard to any assay is that experimental manipulation could introduce some type of stress—for example, mechanical stress due to lysis, temperature stress due to heating or cooling a sample, or oxidative stress on a microscope slide, which could lead to potential artefacts including the induction of autophagy—even maintaining cells in higher

than physiologically normal oxygen levels can be a stress condition [2107,2108]. Special care should be taken with cells in suspension, as the stress resulting from mixing and/or centrifugation can induce autophagy. This point is not intended to limit the use of any specific methodology, but rather to note that there are no perfect assays. Therefore, it is important to verify that the positive (e.g., treatment with rapamycin, torin1 or other inducers) and negative (e.g., inhibitor treatment) controls behave as expected in any assays being utilized.

Similarly, plasmid transfection or nucleofection can result in the potent induction of autophagy (based on increases in LC3-II or degradation of SQSTM1), and certain transfection agents promote selective autophagy [429]. In some cell types, the amount of autophagy induced by transfection of a control empty vector may be so high that it is virtually impossible to examine the effect of enforced gene expression on autophagy (B. Levine, personal communication). It is thus advisable to perform time-course experiments to determine when the transfection effect returns to acceptably low levels and to use appropriate time-matched transfection controls (see also the discussion in *GFP-Atg8-family protein fluorescence microscopy*). This effect is generally not observed with siRNA transfection; however, it is an issue for plasmid expression constructs including those for shRNA and for viral delivery systems. The use of endotoxin-free DNA reduces, but does not eliminate, this problem. In many cells the cationic polymers used for DNA transfection, such as liposomes and polyplex, induce large tubulovesicular autophagosomes (TVAs) in the absence of DNA [2109]. These structures accumulate SQSTM1 and fuse slowly with lysosomes. In addition, these TVAs appear to reduce gene delivery, which increases 8–10 fold in cells that are unable to make TVAs due to the absence of ATG5.

Finally, the precise composition of media components and the density of cells in culture can have profound effects on basal autophagy levels and may need to be modified empirically depending on the cell lines being used. Along these lines various types of media, in particular those with different serum levels (ranging from 0–15%), may have profound effects with regard to how cells (or organs) perceive a fed versus starved state. For example, normal serum contains significant levels of cytokines and hormones that likely regulate the basal levels of autophagy and/or have an impact upon its modulation by additional stress or stimuli; thus, the use of dialyzed serum might be an alternative for these studies. In addition, the amino acid composition of the medium/assay buffer may have profound effects on initiation or progression of autophagy. For example, in the protist parasite *Trypanosoma brucei* starvation-induced autophagy can be prevented by addition of histidine to the incubation buffer [382]. For these reasons, the cell culture conditions should be fully described. It is also important to specify duration of autophagy stimulation, as long-term autophagy can modify signal transduction pathways of importance in cell survival [780].

Methods and challenges of specialized topics/model systems

There are now a large number of model systems being used to study autophagy. These guidelines cannot cover every detail,

and as stated in the Introduction, this article is not meant to provide detailed protocols. Nonetheless, we think it is useful to briefly discuss what techniques can be used in these systems and to highlight some of the specific concerns and/or challenges. We also refer readers to the three volumes of Methods in Enzymology that provide additional information for “nonstandard” model systems [46–48].

Caenorhabditis elegans

C. elegans has a single ortholog of most yeast Atg proteins; however, two nematode homologs exist for Atg4, Atg8 and Atg16 [1477,2110, 2111]. Multiple studies have established *C. elegans* as a useful multicellular genetic model to delineate the autophagy pathway and associated functions (see for example refs. [367,965,1109,1112,1276]). The LGG-1/Atg8 reporter is the most commonly used tool to detect autophagy in *C. elegans*. Similar to Atg8, which is incorporated into the double membrane of autophagic vacuoles during autophagy [204,365,914], the *C. elegans* LGG-1 localizes into cytoplasmic puncta under conditions known to induce autophagy. Fluorescent reporter fusions of LGG-1/Atg8 with GFP, DsRED or mCherry have been used to monitor autophagosome formation *in vivo*, in the nematode. These reporters can be expressed either in specific cells and tissues or throughout the animal [367,1112,2112,2113]. Caution should be taken, however, when using protein markers fused to mCherry in worms. mCherry can accumulate in lysosomes [471] and might aggregate in autophagy-inducing conditions, such as fasting, even if not fused to LGG-1 or other autophagy markers (E. O’Rourke, personal communication); therefore, caution should be employed when using mCherry puncta as a readout to monitor autophagy in *C. elegans*. LGG-2 is the second LC3 homolog and is also a convenient marker for autophagy either using specific antibodies [1111] or fused to GFP [2114], especially when expressed from an integrated transgene to prevent its germline silencing [1111]. The exact function of LGG-1 versus LGG-2 remains to be addressed [1115].

For observing autophagy by GFP-LC3 fluorescence in *C. elegans*, it is best to use integrated versions of the marker [1111,1112,2115] (GFP::LGG-1 and GFP::LGG-2; Figure 33) rather than extrachromosomal transgenic strains [367,2114] because the latter show variable expression among different animals or mosaic expression (C. Kang, personal communication; V. Galy, personal communication [2116]). Integration of the markers requires mutagenesis, and care should be taken to outcross the strains to ensure that any remaining background mutations do not affect the examined phenotypes by, for example, examining the phenotypes in independent integrants. However, it is important to note that some integrated strains overexpress these chimeras because they are driven by heterologous promoters. One approach to overcome this problem is to monitor cleavage of a dual fluorescent protein marker consisting of tandem monomeric RFP (mRFP) joined by a flexible linker and attached to LGG-1 [2117]. Autophagic flux can be monitored as the ratio of free mRFP (mFP) to the uncleaved full-length protein (dFP) normalized to a loading control (i.e., actin or tubulin). However, this readout needs to be used with caution in the adult worm. Although relative

mFP abundance is reported to change in L3–L4 larvae treated with RNAi against essential autophagy genes (i.e., *bec-1*) or CQ, and in 5-days starved L1 larvae [2117], no changes are observed in 6- to 12-h fasted adults, even when increased autophagic flux can be detected in aliquots of the same samples when using anti-LGG-1 antibodies (V.K. Mony, personal communication). Furthermore, the original studies characterizing this readout reported dFP-to-mFP cleavage in animals incubated for 18 h in a concentrated suspension of *E. coli* in M9 with or without CQ, an incubation condition that activates caloric restriction responses including autophagy (V. K. Mony, personal communication). Therefore, further validation of the dFP-mFP readout may be necessary to confidently use it in adult *C. elegans*.

To increase signal to noise, it is also possible to carry out indirect immunofluorescence microscopy using antibodies against endogenous LGG-1 [965,1112], or LGG-2 [1111]; however, anti-LGG-1 and anti-LGG-2 antibodies are not commercially available. In addition, with the integrated version, or with antibodies directed against endogenous LGG-1, it is possible to perform a western blot analysis for lipidation, at least in embryos (LGG-1-I is the nonlipidated soluble form and LGG-1-II/LGG-1-PE is the lipidated form) [965,1112,2115]. In contrast to the yeast and mammalian autophagosomal membrane proteins Atg8 and LC3, lipidation of the *C. elegans* ortholog LGG-1 with phosphatidylethanolamine has rarely been investigated by western blotting; this is likely due to technical problems with separating the nonlipidated from the lipidated LGG-1 protein by gel electrophoresis. A new protocol for western blot analysis, taking advantage of improved antibodies to LGG-1 and SQST-1/SQSTM1, is applicable for both the detection of transgenic and endogenous proteins and provides a quantifiable method to assess autophagic flux [2118].

The LGG-1 precursor accumulates in the *atg-4.1* mutant, but is undetectable in wild-type embryos [1261]. In fact, LGG-1 phenotypes vary in *atg-4.1* and *atg-4.2* mutants, indicative of distinct functions for these two genes [471]. Moreover, the banding pattern of LGG-1 or LGG-1 fused to fluorescent proteins in western blots may not be easy to interpret in larvae or the adult *C. elegans* because enrichment for a fast running band (the lipidated form) is not observed in some autophagy-inducing conditions including fasting (E.J. O’Rourke, personal communication). In the embryos of some autophagy mutants, including *epg-3*, *epg-4*, *epg-5*, and *epg-6* mutants, levels of LGG-1-I and LGG-1-II are elevated [845,965]. In an immunostaining assay, endogenous LGG-1 forms distinct punctate structures, mostly at the ~64- to 100-cell embryonic stage. LGG-1 puncta are absent in *atg-3*, *atg-7*, *atg-5* and *atg-10* mutant embryos [965], but dramatically accumulate in other autophagy mutants [845,965]. The widely used GFP::LGG-1 reporter forms aggregates in *atg-3* and *atg-7* mutant embryos, in which endogenous LGG-1 puncta are absent, indicating that GFP::LGG-1 could be incorporated into protein aggregates during embryogenesis. Immunostaining for endogenous VPS-34 is also a useful marker of autophagy induction in *C. elegans* embryos [1271].

A variety of protein aggregates, including PGL granules (PGL-1–PGL-3–SEPA-1) and the *C. elegans* SQSTM1 homolog

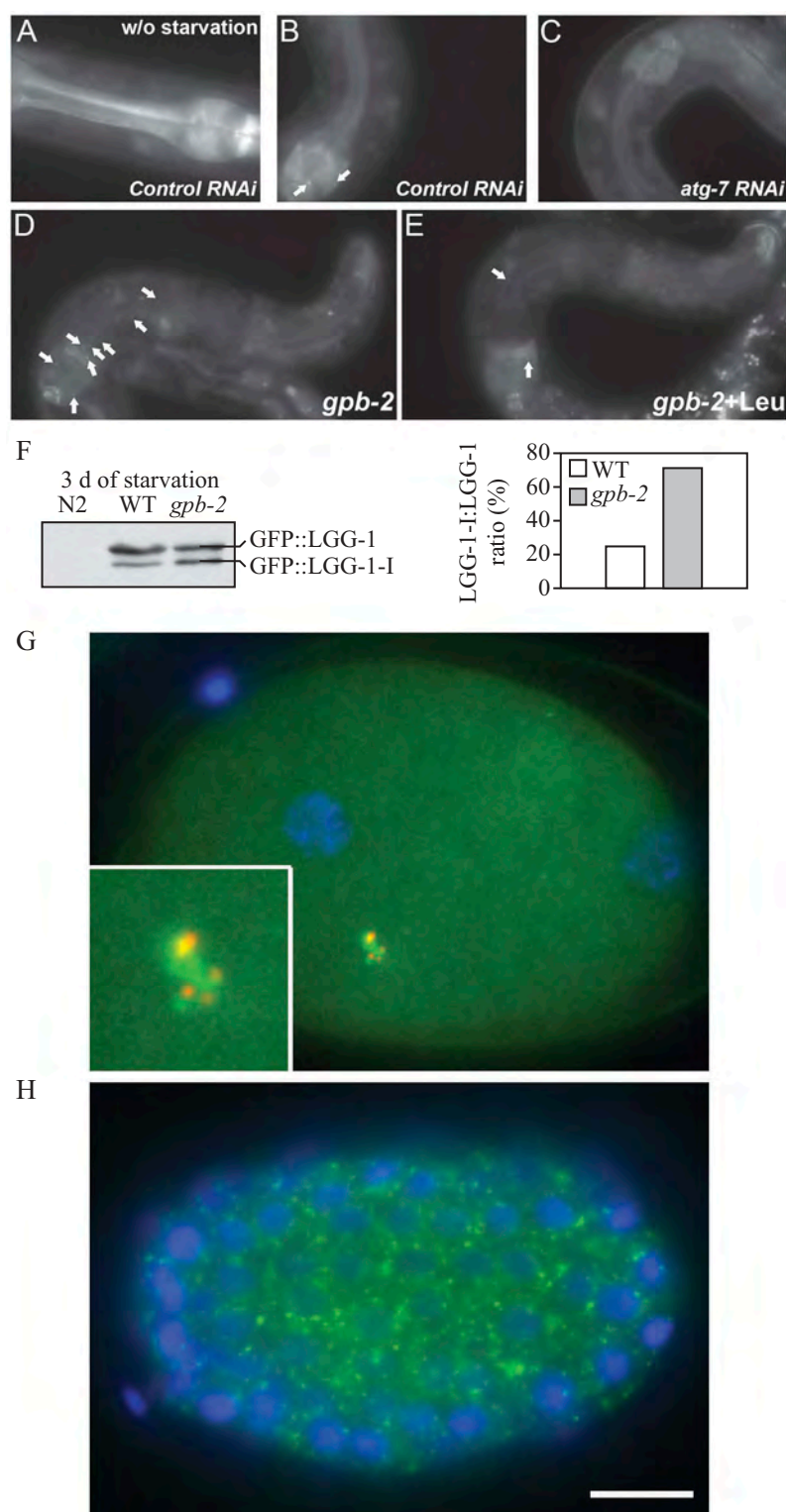


Figure 33. GFP::LGG-1 and GFP::LGG-2 are autophagy markers in *C. elegans*. (A-F) Animals were generated that carry an integrated transgene expressing a GFP-tagged version of *lgg-1*, the *C. elegans* ortholog of mammalian MAP1LC3. Representative green fluorescence images in the pharyngeal muscles of (A) control RNAi animals without starvation, (B) control RNAi animals after 9 d of starvation, (C) *atg-7* RNAi animals after 9 d of starvation, (D) starvation-hypersensitive *gpb-2* mutants without leucine after 3 d of starvation, and (E) *gpb-2* mutants with leucine after 3 d of starvation. The arrows show representative GFP::LGG-1-positive punctate areas that label pre-autophagosomal and autophagosomal structures. (F) The relative levels of PE-conjugated and unconjugated GFP::LGG-1 were determined by western blotting. These figures were modified from data previously published in ref. [2115], Kang, C., Y.J. You, and L. Avery. 2007. Dual roles of autophagy in the survival of *C. elegans* during starvation. *Genes & Development*. 21:2161-2171, Copyright © 2007, *Genes & Development* by Cold Spring Harbor Laboratory Press, and ref. [4086], Kang, C., and L. Avery. 2009. Systemic regulation of starvation response in *C. elegans*. *Genes & development*. 23:12-17, Copyright © 2011, *Genes & Development* by Cold Spring Harbor Laboratory Press, www.genesdev.org. (G-H) GFP::LGG-2 serves as a marker for autophagosomes in early *C. elegans* embryos. (G) GFP::LGG-2 expressed in the germline from an integrated transgene reveals the formation of autophagosomes (green) around sperm-inherited membranous organelles (red). DNA of the two pronuclei is stained (blue). (H) Later during development, GFP::LGG-2-positive structures are present in all cells of the embryo. Scale bar: 10 μ m. Images provided by V. Galy.

SQST-1, are selectively degraded by autophagy during embryogenesis; impaired autophagy activity results in their accumulation and the generation of numerous aggregates [965]. Thus, degradation of these autophagy substrates can also be used to monitor autophagy activity, with similar cautionary notes to those described in section A3 (see *SQSTM1 and related LC3 binding protein turnover assays*) for the SQST-1 turnover assay. Similar to mammalian cells, the total amount of GFP::LGG-1 along with SQST-1::GFP transcriptional expression coupled with its posttranscriptional accumulation can be informative with regard to autophagic flux in the embryo (again with the same cautionary notes described in section A3) [573].

As with its mammalian counterpart, loss of the *C. elegans* TP53 ortholog, *cep-1*, increases autophagosome accumulation [2119] and extends the animal's life span [2120]. *bec-1*- and *cep-1*-regulated autophagy is also required for optimal life-span extension. However, non-autophagic roles for *bec-1* and *cep-1* have been reported. Hence, *bec-1* or *cep-1* inactivation is insufficient to define a longevity mechanism as autophagy dependent. The TFEB ortholog HLH-30 transcriptionally regulates autophagy including the expression of *bec-1* [948,1294], and life-span analyses uncovered an anti-aging role for HLH-30/TFEB in *C. elegans*, and possibly in mammals [573,948,1294]. However, it remains to be definitively demonstrated whether HLH-30/TFEB longevity is exclusively, or even mostly, mediated by activation of autophagy. *bec-1* and *cep-1* are also required to reduce lipid accumulation in response to silencing FRH-1/FXN, a protein involved in mitochondrial respiratory chain functionality [2121]. FRH-1 silencing also induces mitophagy in an evolutionarily conserved manner [1172]. Moreover, the products of *C. elegans* mitophagy regulatory gene homologs (PDR-1/PRKN, PINK-1/PINK1, DCT-1/BNIP3, and SQST-1/SQSTM1) are required for induction of mitophagy (monitored through the Rosella biosensor [2122]) and life-span extension following FRH-1 silencing and iron deprivation [1172]. HLH-30/TFEB transcriptionally regulates autophagy and promotes lipid degradation [948,1294], and life-span analyses uncovered a direct role for HLH-30/TFEB in aging in *C. elegans*, and possibly in mammals [573,948,1294].

C. elegans body wall muscle is a useful tissue for studying autophagy. In addition to the methods discussed above, in this tissue transgenic reporter proteins can be used to monitor rates of protein degradation in specific subcellular compartments [2123], mutations in at least two signaling pathways can be used to modulate autophagy [2124], drugs can be used to inhibit autophagy [2125], and mutations and drugs can be used to inhibit the proteasome [2126], calpains [2125], and caspases [2127] thus allowing both positive and negative controls. Finally, knockdown of a substantial number of kinases [2128] and phosphatases [2129] appears to induce autophagy, potentially enabling further study of the upstream signals that modulate this process.

For a more complete review of methods for monitoring autophagy in *C. elegans* see ref [562]. These approaches can be used to monitor autophagy in embryos, early larval stages, and adult *C. elegans*, including during aging [2130].

Chicken B-lymphoid DT40 cells, retina and inner ear

The chicken B-lymphoid DT40 cell line represents a suitable tool for the analysis of autophagic processes in a nonmammalian vertebrate system. In DT40 cells, foreign DNA integrates with a very high frequency by homologous recombination compared to random integration. This feature was—prior to the CRISPR-Cas9 era—employed in order to generate cellular gene knockouts. Different Atg-deficient DT40 cell lines already exist, including *atg13^{-/-}*, *ulk1^{-/-}*, *ulk2^{-/-}*, and *ulk1^{-/-}ulk2^{-/-}* [693]. Many additional non-autophagy-related gene knockout DT40 cell lines have been generated and are commercially available [2131].

DT40 cells mount an autophagic response upon starvation in EBSS [693], and autophagy can be analyzed by a variety of assays in this cell line. Steady state methods that can be used include TEM, LC3 western blotting and fluorescence microscopy; flux measurements include monitoring LC3-II turnover and tandem mRFP/mCherry-GFP-LC3 fluorescence microscopy. Using *atg13^{-/-}* and *ulk1^{-/-}ulk2^{-/-}* DT40 cells, it was shown that ATG13 and its binding capacity for RB1CC1 are mandatory for both basal and starvation-induced autophagy, whereas ULK1/2 and in vitro-mapped ULK1-dependent phosphorylation sites of ATG13 appear to be dispensable for these processes [693].

Another useful system is chick retina, which can be used for monitoring autophagy at different stages of development. For example, lipidation of LC3 is observed during starvation, and can be blocked with a short-term incubation with 3-MA [1596,2132]. LEP-100 antibody is commercially available for the detection of this lysosomal protein. In the developing chicken inner ear, LC3 flux can be detected in otic vesicles cultured in a serum-free medium exposed to either 3-MA or CQ [2133].

One of the salient features of chicken cells, including primary cells such as chicken embryo fibroblasts, is the capacity of obtaining rapid, efficient and sustained transcript/protein downregulation with replication-competent retrovirus for shRNA expression [2134]. In chicken embryo fibroblasts, nearly complete and general (i.e., in nearly all cells) protein downregulation can be observed within a few days after transfection of the shRNA retroviral vector [231].

Cautionary notes: It is possible that there is some divergence within the signaling pathways between mammalian and nonmammalian model systems. One example might be the role of ULK1/2 in starvation-induced autophagy described above. Additionally, DT40 cells represent a transformed cell line, being derived from an avian leukosis virus-induced bursal lymphoma. Thus, DT40 cells release avian leukosis virus into the medium, and the 3'-long terminal repeat has integrated upstream of the *MYC* gene, leading to increased *MYC* expression [2135]. Both circumstances might influence basal and starvation-induced autophagy.

Chlamydomonas

The unicellular green alga *Chlamydomonas reinhardtii* is an excellent model system to investigate autophagy in

photosynthetic eukaryotes. Most of the *ATG* genes that constitute the autophagy core machinery including the *ATG8* and *ATG12* ubiquitin-like systems are conserved as single-copy genes in the nuclear genome of this model alga. Autophagy can be monitored in *Chlamydomonas* by western blotting through the detection of Atg8 lipidation as well as an increase in the abundance of this protein in response to autophagy activation [397]. Localization of Atg8 by immunofluorescence microscopy can also be used to study autophagy in *Chlamydomonas* because the cellular distribution of this protein changes drastically upon autophagy induction. The Atg8 signal is weak and usually detected as a single spot in non-stressed cells, whereas autophagy activation results in the localization of Atg8 in multiple spots with a very intense signal [397,2136,2137]. A red fluorescent protein (mCherry) tagged-Atg8 has been developed that allows the observation of autophagosomes in living microalgal cells [2138]. Autophagic flux can also be monitored in *Chlamydomonas* by analyzing the abundance and lipidation of Atg8 protein in cells treated with the vacuolar-type ATPase inhibitor concanamycin A. Inhibition of autophagic flux results in the accumulation of total Atg8 and detection of the Atg8 lipidated form [2139]. Finally, enhanced expression of *ATG8* and other *ATG* genes has also been reported in stressed *Chlamydomonas* cells [2136, 2140]. These methodological approaches have been used to investigate the activation of autophagy in *Chlamydomonas* under different stress conditions including nutrient (nitrogen or carbon) limitation, rapamycin treatment, ER stress, oxidative stress, photo-oxidative damage or high light stress [397,2136,2137].

Drosophila melanogaster

Drosophila provides an excellent and highly amenable system for in vivo analysis of autophagy as the machinery is highly conserved with well-characterized functions in several tissues including oocyte, embryo, larval/pupal fat body, midgut, salivary gland and imaginal disc, larval motor neurons and adult neurons [183,1744,2141–2144]. The advantage of using *Drosophila* as a model is the ability to undertake genetic analysis of individual components of the autophagy machinery [1771,2141]. Another major advantage of *Drosophila* is that the problem of animal-to-animal variability can be circumvented by the use of clonal mutant cell analysis [183,2141,2143,2145]. In this scenario, somatic clones of cells are induced that either overexpress the gene of interest, or silence the gene through expression of a transgenic RNA interference construct, or gene mutation/deletion. These gain- or loss-of-function clones are surrounded by wild-type cells, which serve as an internal control for autophagy induction. In such an analysis, autophagy in these genetically distinct cells is always compared to neighboring cells of the same tissue, thus eliminating most of the variability and also ruling out potential non-cell-autonomous effects that may arise in mutant animals (Figure 25). Along these lines, clonal analysis should be an integral part of in vivo *Drosophila* studies when possible.

Multiple steps of the autophagic pathway can be monitored in *Drosophila* due to the development of useful markers, corresponding to every step of the process. Interested readers

may find further information in several reviews with a detailed discussion of the currently available assays and reagents for the study of autophagy in *Drosophila* [183,2141,2146]. For example, the level of autophagy can be examined live *in vivo* using transgenic lines that express fluorescently-tagged specific components of the autophagy pathway. Moreover, fluorescent reporters for components of the autophagy pathway can be used in genetic screens for new regulators of autophagy [2147]. The expression of fluorescently tagged Atg8a from the endogenous *Atg8a* promoter is a useful reporter, that does not require a driver line [375,2148]. In addition, autophagy has been successfully monitored in *Drosophila* expressing various components of the pathway including (but not limited to) human *UAS-GFP-LC3* [123,376,2149], *UAS-GFP-Atg8a* [2150], *UAS-mCherry-Atg8a* [589], *mCherry-Atg18* [2151], *UAS-GFP-Atg5* [376], *UAS-RFP-Atg5* [947], *UAS-GFP-Atg6* [2152], *UAS-GFP-DFCP1* [2153], *UAS-GFP-ref(2)P* (corresponding to the *Drosophila* SQSTM1 homolog) [589], and the tandem fluorescent reporter *UASp-GFP-mCherry-Atg8a* [2154,2155], with an increasing list of addition transgenic fluorescence reagents, including protein traps, that are being made available through the *Drosophila* stock centers.

There are also a limited number of commercially available antibodies, including a rabbit monoclonal anti-GABARAP antibody and a rabbit polyclonal anti-ref(2)P antibody that can be used to detect endogenous levels of *Drosophila* Atg8a and ref(2)P, respectively, in both immunostaining and immunoblotting experiments [560,2141, 2156, 2157]. The advantage of *UAS-ref(2)P-GFP* over the antibody against endogenous ref(2)P is that its accumulation is independent of *ref(2)P* promoter regulation and unambiguously reflects autophagy impairment [557,2155]. Of note, immunoblot analysis of ref(2)P levels should include both soluble and insoluble fractions [557,2157]. Several laboratories have also generated antibodies, including those against Atg8a and ref(2)P [560,2149,2158]. Finally, it is worth noting that a commercial Atg5 antibody can also be used for *Drosophila* [750,2159].

Cultured *Drosophila* (S2) cells can also be stably transfected with GFP fused to *Drosophila* Atg8a, which generates easily resolvable GFP-Atg8a and GFP-Atg8a-PE forms that respond to autophagic stimuli (S. Wilkinson, personal communication); stable S2 cells with GFP-Atg8a under the control of a 2-kb *Atg8a* 5' UTR are also available [2160]. Similarly, cultured *Drosophila* cells (l[2]mbn or S2) stably transfected with EGFP-HsLC3B respond to autophagy stimuli (nutrient deprivation) and inhibitors (3-MA, bafilomycin A₁) as expected, and can be used to quantify GFP-LC3 puncta, which works best using fixed cells with the aid of an anti-GFP antibody [2161].

The selective degradation of cargo can also be used to assay for autophagy in this system. The *Drosophila* components of the IKK complex, key/kenny and IKKβ/ird5, are selectively degraded by autophagy, and transgenic lines are available (*UAS-GFP-key/kenny*, *UAS-mCherry-IKKβ/ird5* and *UAS-mCherry-GFP-IKKβ/ird5*) to follow key and ird5 expression and localization [2162].

With the distinct morphology of autophagy, TEM is also an indispensable and reliable method for monitoring autophagy in *Drosophila*. Finally, in addition to genetic analysis,

pharmacological modulation of autophagy can be examined in *Drosophila*. For example, rapamycin can be fed to larvae or adults to induce autophagy, and CQ can be used to block lysosomal degradation [589,1770,2141].

Cautionary notes: In the *Drosophila* eye, overexpression of GFP-Atg8 results in a significant increase in Atg8-PE based on immunoblot, and this occurs even in control flies in which punctate GFP-Atg8 is not detected by immunofluorescence (M. Fanto, personal communication/unpublished results), and in transfected *Drosophila* Kc167 cells, uninducible but persistent GFP-Atg8 puncta are detected (A. Kiger, personal communication/unpublished results). In contrast, expression of GFP-LC3 under the control of the *ninaE/rh1* promoter in wild-type flies does not result in the formation of LC3-II detectable by immunoblot, nor the formation of punctate staining; however, increased GFP-LC3 puncta by immunofluorescence or LC3-II by immunoblot are observed upon activation of autophagy [616]. Finally, most *Drosophila* food contains the anti-fungal nipagin (methylparaben), which has certain redox and anti-oxidant effects; these could interfere with particular experiments.

Erythroid cells

The unique morphology of red blood cells (RBCs) is instrumental to their function. The bi-concave shape provided by a highly flexible membrane and the absence of organelles is critical to their long lifespan in the peripheral circulation (120 days), allowing unimpeded circulation of the RBC even through the thinnest blood vessels, thereby delivering O₂ to all the tissues of the body. Erythroid cells acquire this unique morphology upon terminal erythroid maturation, which commences in the bone marrow with the release of reticulocytes that become mature RBCs in the peripheral circulation. This process involves extrusion of the pyknotic nucleus through a specialized form of asymmetric division, and degradation of the ribosome and mitochondria machinery along with a reduction in cell volume via a specialized form of autophagy (Figure 34). In the context of RBC biogenesis, autophagy exerts a unique function to sculpt the cytoplasm, with the

mature autophagic vacuoles engulfing and degrading organelles, such as mitochondria and ribosomes, whose presence would impair the flexibility of the cells.

Another unique feature of erythropoiesis is that expression of genes required for autophagosome assembly/function, such as *LC3B*, does not appear to be regulated by nutrient deprivation, but rather is upregulated by the erythroid-specific transcription factor GATA1 [981]. FOXO3, a transcription factor that modulates RBC production based on the levels of O₂ present in the tissues [2163], amplifies GATA1-mediated activation of autophagy genes [981] and additional genes required for erythroid maturation [2164]. Furthermore, lipidation of the cytosolic form of LC3B into the lipidated LC3-II form is controlled by EPO (erythropoietin), the erythroid-specific growth factor that ensures survival of the maturing erythroid cells. The fact that the genes encoding the autophagic machinery are controlled by the same factors that regulate expression of genes encoding important red cell constituents (such as red blood cell antigens and cytoskeletal components, globin, and proteins mediating heme biosynthesis) [2165-2167], ensures that the process of terminal maturation progresses in a highly ordered fashion.

The importance of autophagy for RBC production has been established through the use of mutant mouse strains lacking genes encoding proteins of the autophagy machinery (BNIP3L, ULK1, ATG7) [2168-2171]. These mutant mice exhibit ineffective erythropoiesis with erythroid cells blocked at various stages of terminal erythroid maturation and anemia. Abnormalities of the autophagic machinery are also linked to erythroid disorders such as Diamond-Blackfan anemia or myelodysplastic syndrome, which are characterized by either congenic or acquired loss-of-function mutations of genes encoding ribosomal proteins (ribosomopathies), and involve erythroid progenitors. As in other cell types, in erythroid cells TP53 activation may influence the functional consequences of autophagy—to determine cell death rather than maturation. TP53, through MDM2, is the gatekeeper to ensure normal ribosome biosynthesis by inducing death of cells lacking sufficient levels of ribosomal proteins. In these disorders,

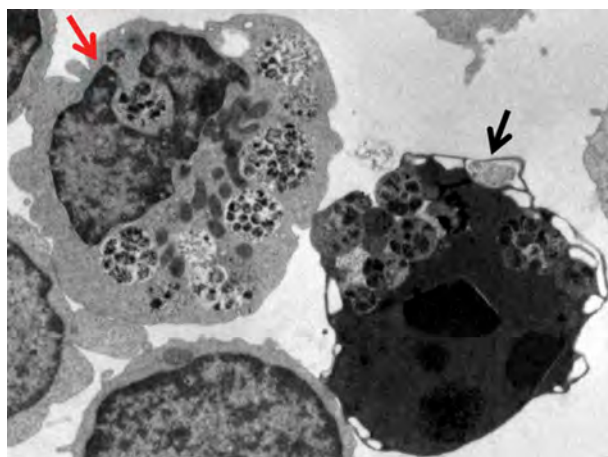


Figure 34. Transmission electron micrograph of erythroblasts obtained from the blood of regular donors after 10 days of culture in the presence of KITLG/SCF, IL3, EPO and dexamethasone. Original magnification 3000X. This figure shows 2 erythroblasts containing autophagic vacuoles. One erythroblast (red arrow) has the morphology of a live cell with several autophagic vacuoles that have engulfed cytoplasmic organelles. The other erythroblast (black arrow) has the electron-dense cytoplasm characteristic of a dead cell and is in the process of shedding its autolysosomes from the cytoplasm to the extracellular space. Image provided by A.R. Migliaccio and M. Zingariello.

activated TP53 and abnormally high levels of autophagic death of erythroid progenitors, promote anemia and bone marrow failure. Glucocorticoids might improve anemia in some Diamond-Blackfan anemia patients by inhibiting TP53 activity. Of note, impairment of autophagy in the late phase of erythropoiesis, involving erythroid precursors, has been reported in hereditary red cell disorders such as β -thalassemic syndromes, characterized by ineffective erythropoiesis [2172,2173], or in chorea-acanthocytosis, a neurodegenerative disorder linked to VPS13 mutations and characterized by circulating acanthocytes containing multivesicular bodies and double-membrane remnants [2174]. Recent evidence also links the abnormal regulation of the redox sensitive transcription factor NFE2L2 to ineffective erythropoiesis and impairment of autophagy, with accumulation in erythroid precursors of non-functional proteins, further amplifying oxidation and promoting cell apoptosis [2175].

13380 *Filamentous fungi*

As in yeast, autophagy is involved in nutrient recycling during starvation [369,373,2176-2182]. In addition, autophagy seems to be involved in many normal developmental processes such as sexual and asexual reproduction, where there is a need for reallocation of nutrients from one part of the mycelium to another to supply the developing spores and spore-bearing structures [369, 1086,2176,2177,2179,2183-2186]. Similarly, autophagy also affects conidial germination under nitrogen-limiting conditions [369]. In *Podospira anserina*, autophagy has been studied in relation to incompatibility reactions between mating strains where it seems to play a prosurvival role [372,2183]. During aging of this long-standing aging model, autophagy is increased (based on numbers of GFP-Atg8 puncta and increased autophagy-dependent degradation of a GFP reporter protein) and acts as a prosurvival pathway [2187]. Moreover, mitophagy has been demonstrated to exert pro-survival effects under mild stress conditions, while displaying Atg1-dependent pro-death features under elevated stress.

In *Sordaria macrospora*, the pexophagy receptor Nbr1 is involved in fruiting-body development and maturation of sexual ascospores [1052]. Of special interest to many researchers of autophagy in filamentous fungi has been the possible involvement of autophagy in plant and insect pathogen infection and growth inside the host [373,1069,1078,2176,2177,2188-2193]. For example, treatment with amiodarone promotes movement of the blast fungus *M. oryzae* between living rice cells during the early biotrophic stage of infection when the fungus inhabits epidermal cells but before symptoms develop, whereas inhibiting autophagy with 3-MA attenuates cell-to-cell movement and disrupts the biotrophic interface between the fungus and living host rice cells. In conjunction with the analysis of a mutant strain impaired in autophagy induction, these results suggest a fundamental role for autophagy in mediating intracellular host-microbe interactions [2193]. Autophagy also appears to be necessary for the development of aerial hyphae [369,2176,2182,2183,2189], and for appressorium function in *M. oryzae*, *Colletotrichum orbiculare* and *Metarhizium robertsii* [373,2188,2189,2191,2194]. In particular, invasion-associated ER stress can promote autophagy to enhance the cell wall integrity-associated MAPK pathway in order to help with infection by *M. oryzae* [2195]. Some of these effects could be caused by the absence of autophagic processing of storage lipids (lipophagy)

to generate glycerol for increasing turgor and recycling the contents of spores into the incipient appressorium, as a prerequisite to infection [2176,2189,2190].

Methods for functional analysis of autophagy have been covered in a review article (see ref [2196]). Most studies on autophagy in filamentous fungi have involved deleting some of the key genes necessary for autophagy, followed by an investigation of what effects this has on the biology of the fungus. Most commonly, *ATG1*, *ATG4*, *ATG8* and/or *ATG9* have been deleted [373,1843,2176,2177,2179,2180,2183,2186,2189,2191,2197, 2198]. To confirm that the deletion(s) affects autophagy, the formation of autophagic bodies in the wild type and the mutant can be compared. In filamentous fungi the presence of autophagic bodies can be detected using MDC staining [373,2176], TEM [373,2177] or fluorescence microscopy to monitor Atg8 tagged with a fluorescent protein [369,2179,2183,2186]. This type of analysis is most effective after increasing the number of autophagic bodies by starvation or alternatively by adding the autophagy-inducing drug rapamycin [369,2176], in combination with decreasing the degradation of the autophagic bodies through the use of the protease inhibitor PMSF [373,2177,2179,2183]. In filamentous fungi it might also be possible to detect the accumulation of autophagic bodies in the vacuoles using differential interference contrast microscopy, especially following PMSF treatment [2179,2183]. Additional information regarding the timing of autophagy induction can be gained by monitoring transcript accumulation of *ATG1* and/or *ATG8* using qPCR [2177].

Autophagy has been investigated intensively in *Aspergilli*, and in particular in the genetically amenable species *Aspergillus nidulans*, which is well suited to investigate intracellular traffic [1843,2199,2200]. In *A. oryzae*, autophagy has been monitored by the rapamycin-induced and Atg8-dependent delivery of DsRed2, which is normally cytosolic, to the vacuoles [369]. In *A. nidulans*, the more “canonical” GFP-Atg8 proteolysis assays have been used, by monitoring the delivery of GFP-Atg8 to the vacuole (by time-lapse microscopy), and by directly following the biogenesis of GFP-Atg8-labeled phagophores and autophagosomes [1843], which can be tracked in large numbers using kymographs traced across the hyphal axis. In these kymographs, the autophagosome cycle starting from a PAS “draws” a cone whose apex and base correspond to the “parental” PAS punctum and to the diameter of the “final” autophagosome, respectively [348]. Genetic analyses revealed that autophagosomes normally fuse with the vacuole in a Rab7-dependent manner. However, should Rab7 fusogenic activity be mutationally inactivated, autophagosomes can traffic to the endosomes in a RabB/Rab5- and CORVET-dependent manner [348]. An important finding was that RabO/Rab1 plays a key role in *A. nidulans* autophagy (and actually can be observed on the phagophore membranes). This finding agrees with previous work in *S. cerevisiae* demonstrating that Ypt1 (the homolog of RAB1) is activated by the Trs85-containing version of TRAPP, TRAPPIII, for autophagy [2201,2202]. This crucial involvement of RabO/Ypt1 points at the ER as one source of membrane for autophagosomes.

In *A. nidulans*, specific misfolded transporters, which are retained in the ER, are degraded by chaperone-assisted selective autophagy. The chaperone involved was identified as

BsdA, which is an ER transmembrane protein acting as an adaptor for the recruitment of the HECT-type ubiquitin ligase Hula (NEDD4/Rsp5 type), which ubiquitinates the misfolded transporter and elicits its recognition by maturing autophagosomes. The process involves Atg8 and Atg9. Epifluorescence microscopy has shown that the misfolded transporter tagged with GFP colocalizes with Atg8-RFP and vacuoles stained with CMAC, revealing a direct translocation from the ER to the vacuole via autophagosomes. Knockout of the gene encoding the BsdA chaperone allows the misfolded transporter to escape autophagy and be sorted to the plasma membrane. Distinct homologs of BsdA might be present in metazoa. Based on the present guidelines the *Aspergillus* example classifies as CASA rather than CMA.

The suitability of *A. nidulans* for *in vivo* microscopy has been exploited to demonstrate that nascent phagophores are cradled by ER-associated structures resembling mammalian omegasomes [348]. The autophagic degradation of whole nuclei that has been observed in *A. oryzae* [1082] might be considered as a specialized version of reticulophagy. Finally, autophagosome biogenesis has also been observed using a PtdIns3P-binding GFP-tagged FYVE domain probe in mutant cells lacking RabB/Rab5. Under these genetic conditions Vps34 cannot be recruited to endosomes and is entirely at the disposition of autophagy [348], such that PtdIns3P is only present in autophagic membranes.

Mitophagy has been studied in *M. oryzae*, by detecting the endogenous level of porin (a mitochondrial outer membrane protein) by western blot, and by microscopy observation of vacuolar accumulation of mito-GFP [1069]. Mitophagy is involved in regulating the dynamics of mitochondrial morphology and/or mitochondrial quality control, during asexual development and invasive growth in *M. oryzae*. Pexophagy has also been studied in rice-blast fungus and it serves no obvious biological function, but is naturally induced during appressorial development, likely for clearance of excessive peroxisomes prior to cell death [2203]. In turn, normal mitochondrial and peroxisomal fission is also essential for mitophagy and pexophagy [2204]. Methods to monitor pexophagy in *M. oryzae* include microscopy observation of the vacuolar accumulation of GFP-SRL (peroxisome-localized GFP), and detection of the endogenous thiolase [2203], or Pex14 levels.

The existence of crosstalk between autophagy and endocytosis has been explored in *M. oryzae*, by analyzing the biological functions of Vps9-domain containing proteins [2205,2206]. *Pyricularia oryzae* (the asexual stage of, and hence essentially a synonym of, *M. oryzae*) Vps9 recruits PoVps34 and targets it to endosomes by activating PoVps21; PoAtg6 is then recruited by PoVps34 under the action of PoVps38 to target endosomes in endocytosis. Additionally, PoAtg6 is recruited to the PAS by PoVps34 to participate in autophagy by activating PoVps21. Methods to monitor the crosstalk include microscopy observation of the endosomes and autophagosomes, affinity isolation and co-IP.

Food biotechnology

Required for yeast cell survival under a variety of stress conditions, autophagy has the potential to contribute to the outcome of many food fermentation processes. For example,

autophagy induction is observed during the primary fermentation of synthetic grape must [2207] and during sparkling wine production (secondary fermentation) [2208]. A number of genome-wide studies have identified vacuolar functions and autophagy as relevant processes during primary wine fermentation or for ethanol tolerance, based on gene expression data or cell viability of knockout yeast strains [2207, 2209-2213]. However, determining the relevance of autophagy to yeast-driven food fermentation processes requires experimentation using some of the methods available for *S. cerevisiae* as described in these guidelines.

Autophagy is a target for some widespread food preservatives used to prevent yeast-dependent spoilage. For example, the effect of benzoic acid is exacerbated when concurrent with nitrogen starvation [2214]. This observation opened the way to devise strategies to improve the usefulness of sorbic and benzoic acid, taking advantage of their combination with stress conditions that would require functional autophagy for yeast cell survival [2006]. Practical application of these findings would also require extending this research to other relevant food spoilage yeast species, which would be of obvious practical interest.

In the food/health interface, the effect of some food bioactive compounds on autophagy in different human cell types has already attracted some attention [2215,2216]. Interpreting the results of this type of research, however, warrants two cautionary notes [2217]. First, the relationship between health status and autophagic activity is obviously far from being direct. Second, experimental design in this field must take into account the actual levels of these molecules in the target organs after ingestion, as well as exposure time and their transformations in the human body. In addition, attention must be paid to the fact that several mechanisms might contribute to the observed biological effects. Thus, relevant conclusions about the actual involvement of autophagy on the health-related effect of food bioactive compounds would only be possible by assaying the correct molecules in the appropriate concentrations.

Honeybee

The reproductive system of bees, or insects whose ovaries exhibit a meroistic polytrophic developmental cycle can be a useful tool to analyze and monitor physiological autophagy. Both queen and worker ovaries of Africanized *A. mellifera* display time-regulated features of cell death that are linked to external stimuli [2218]. Features of apoptosis and autophagy are frequently associated with the degeneration process in bee organs, but only more recently has the role of autophagy been highlighted in degenerating bee tissues. The primary method currently being used to monitor autophagy is to follow the formation of autophagosomes and autolysosomes by TEM. This technique can be combined with cytochemical and immunohistochemical detection of acid phosphatase as a marker for autolysosomes [2219,2220]. Acidotropic dyes can also be used to follow autophagy in bee organs, as long as the cautions noted in this article are followed. The honeybee genome has been sequenced, and differential gene expression has been used to monitor *Atg18* in bees parasitized by *Varroa destructor* [2221].

Human

Considering that much of the research conducted today is directed at understanding the functioning of the human body, in both normal and disease states, it is pertinent to include humans and primary human tissues and cells as important models for the investigation of autophagy. Although clinical studies are not readily amenable to these types of analyses, it should be kept in mind that the MTORC1 inhibitor rapamycin, the lysosomal inhibitors CQ and HCQ, and the microtubule depolymerizing agent colchicine are all available as clinically approved drugs. However, these drugs are not highly selective, having numerous off-targets, and have serious side effects, which often impede their clinical use to study autophagy (e.g., severe immunosuppressive effects of rapamycin; gastrointestinal complaints, bone marrow depression, neuropathy and rhabdomyolysis induced by colchicine; gastrointestinal complaints, neuropathy and convulsions, retinopathy and heart disease induced by HCQ). These side effects may in part be exacerbated by potential inhibition of autophagy itself by these drugs [2222]. In cancer treatment, for example, autophagy-inhibiting drugs are used in combination with other anticancer drugs to increase their potency. Conversely, normal tissues such as kidney induce autophagy in response to anticancer drugs to resist against their toxicity [2223]; additional blockade of autophagy could worsen normal tissue toxicity and cause serious side effects. Therefore, the potential for serious adverse effects and toxicity of these drugs warrants caution, especially when studying a role of autophagy in high-risk patients, such as the critically ill.

Fortunately, it is possible to obtain fresh biopsies of some human tissues. Blood, in particular, as well as samples of adipose and muscle tissues, can be obtained from needle biopsies or from elective surgery. For example, in a large study, adipocytes were isolated from pieces of adipose tissue (obtained during surgery) and examined for INS (insulin) signaling and autophagy. It was demonstrated that autophagy was strongly upregulated (based on LC3 flux, EM, and lipofuscin degradation) in adipocytes obtained from obese patients with type 2 diabetes compared with nondiabetic subjects [396]. In another study utilizing human adipose tissue biopsies and explants, elevated autophagic flux in obesity was associated with increased expression of several autophagy genes [292,927,2224]. Conversely, by using fibroblasts from a patient with X-linked myopathy with excessive autophagy, it was shown that deficiency of VMA21 blocks vacuolar ATPase assembly and causes autophagic vacuolar myopathy due to increased pH of lysosomes, reduced lysosomal protein degradation and enhanced macroautophagy [2225].

The study of autophagy in the blood has revealed that SNCA may represent a further marker to evaluate the autophagy level in T lymphocytes isolated from peripheral blood [2226]. In these cells it has been shown that (a) knocking down the SNCA gene results in increased autophagy, (b) autophagy induction by energy deprivation is associated with a significant decrease of SNCA levels, (c) autophagy inhibition (e.g., with 3-MA or knocking down ATG5) leads to a significant increase of SNCA levels, and d) SNCA levels negatively correlate with LC3-II levels. Thus, SNCA, and in particular the 14-kDa monomeric form, can be detected by

western blot as a useful tool for the evaluation of autophagy in primary T lymphocytes. In contrast, the analysis of SQSTM1 or NBR1 in freshly isolated T lymphocytes fails to reveal any correlation with either LC3-II or SNCA, suggesting that these markers cannot be used to evaluate basal autophagy in these primary cells. Conversely, LC3-II upregulation is correlated with SQSTM1 degradation in neutrophils, as demonstrated in a human sepsis model [1694].

A major caveat of the work concerning autophagy in human tissue is the problem of tissue heterogeneity, postmortem times, agonal state, genetic heterogeneity, premortem clinical history (medication, diet, etc.) and tissue fixation. Time to fixation is typically longer in autopsy material than when biopsies are obtained. For tumors, careful sampling to avoid necrosis, hemorrhagic areas and non-neoplastic tissue is required. The problem of fixation is that it can diminish the antibody binding capability; in addition, especially in autopsies, material is not obtained immediately after death [2227,2228]. The possibilities of postmortem autolysis and fixation artefacts must always be taken into consideration when interpreting changes attributed to autophagy [2229]. Analyses of these types of samples require not only special antigen retrieval techniques, but also histopathological experience to interpret autophagy studies by IHC, immunofluorescence or TEM. Nonetheless, at least one recent study demonstrated that LC3 and SQSTM1 accumulation can be readily detected in autopsy-derived cardiac tissue from patients with CQ- and HCQ-induced autophagic vacuolar cardiomyopathy [1559]. Despite significant postmortem intervals, sections of a few millimeters thickness cut from fresh autopsy brain and fixed in appropriate glutaraldehyde-formalin fixative for EM, can yield TEM images of sufficient ultrastructural morphology to discriminate different autophagic vacuole subtypes and their relative regional abundance in some cases (R. Nixon, personal communication).

The situation is even worse with TEM, where postmortem delays can cause vacuolization. Researchers experienced in the analysis of TEM images corresponding to autophagy should be able to identify these potential artefacts because autophagic vacuoles should contain cytoplasm. While brain biopsies may be usable for high quality TEM (Figures 35, 36), this depends upon proper handling at the intraoperative consultation stage, and such biopsies are performed infrequently except for brain tumor diagnostic studies. Conversely, biopsies of organs such as the digestive tract, the liver, muscle and the skin are routinely performed and thus nearly always yield high-quality TEM images. When possible, nonsurgical biopsies are preferable because surgery is usually performed in anesthetized and fasting patients, two conditions possibly affecting autophagy. Moreover, certain surgical procedures require tissue ischemia-reperfusion strategies that can also affect autophagy level [2230]. An analysis that examined liver and skeletal muscle from critically ill patients utilized tissue biopsies that were taken within 30 ± 20 min after death and were flash-frozen in liquid nitrogen followed by storage at -80°C [2231]. Samples could subsequently be used for EM and western blot analysis.

A major limitation of studying patient biopsies is that only static measurements can be performed. This limitation does not apply, however, for dynamic experiments on tissue biopsies or

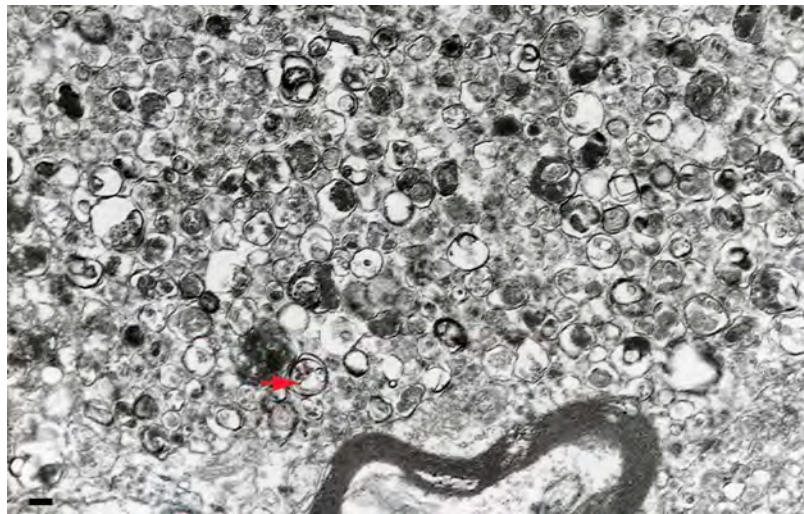


Figure 35. A large dystrophic neurite from a brain biopsy of a patient with Gerstmann-Sträussler-Scheinker disease not unlike those reported for AD [79]. This structure is filled with innumerable autophagic vacuoles, some of which are covered by a double membrane. Electron dense lysosomal-like structures are also visible. The red arrow points to a double-membrane autophagic vacuole. Scale bar: 200 nm. Image provided by P. Liberski.

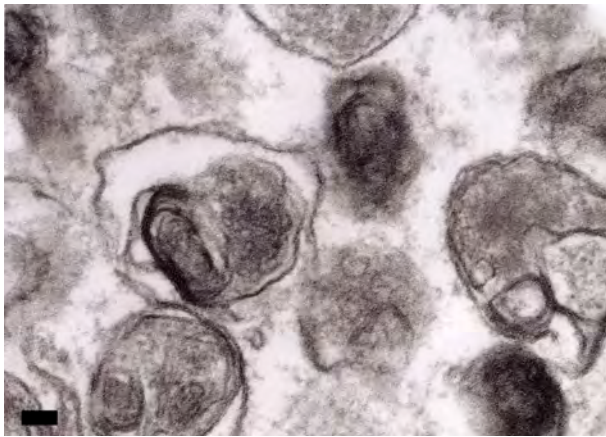


Figure 36. A high-power electron micrograph from a brain biopsy showing autophagic vacuoles in a case of ganglioglioma. Scale bar: 200 nm. Image provided by P. Liberski.

cells derived from biopsies, as described above [396]. Multiple measurements over time, especially when deep (vital) organs are involved, are impossible and ethically not justifiable. Hence, quantitative flux measurements are virtually impossible in patients. To overcome these problems to the extent possible and to gain a more robust picture of the autophagic status, observational studies need to include two different aspects. First, a static marker for phagophore or autophagosome formation needs to be measured. This can be done by assessing ultrastructural changes with TEM and/or on the molecular level by measuring LC3-II protein levels. Second, accumulation of autophagy substrates, such as SQSTM1 and (poly)ubiquitinated proteins, can provide information on the overall efficacy of the pathway and can be a surrogate marker of the consequences of altered autophagic flux, especially when autophagy is insufficient, although these changes can also be affected by the ubiquitin-proteasome system as mentioned above.

In addition, and even more so when problems with selective pathways are suspected (e.g., mitophagy), specific

substrates of these pathways should be determined. Again, none of these measurements on its own provides enough information on (the efficacy of) autophagy, because other processes may confound every single parameter. However, the combination of multiple analyses should be informative. Of note, there has been interest in assessing markers of autophagy and autophagic flux in right atrial biopsy samples obtained from patients undergoing cardiac surgery [2232,2233]. Evidence to date suggests that cardiac surgery may be associated with an increase in autophagic flux, and that this response may protect the heart from perioperative cardiac ischemia-reperfusion injury [2232]. The autophagy deficiency also correlates with the decline of serum testosterone in some hypogonadism patients, as the LC3 expression and puncta number per square micrometer are significantly decreased in the Leydig cells from the patients compared with those of the control group [2234]. In the brain of hypoxic-ischemic encephalopathy human neonates, punctate LC3 labelling combined with increased number and size in CTSD- and LAMP1-positive dots (presumably autolysosomes) and decreased SQSTM1 expression is detected in dying neurons, suggesting that the autophagy flux is enhanced and associated with neuronal death occurring in neonatal brain injury [534,535]. Although still in its infancy with regard to autophagy, it is worth pointing out that mathematical modeling has the power to bridge whole body in vivo data with in vitro data from tissues and cells. The usefulness of so-called hierarchical or multilevel modeling has been demonstrated when examining the relevance of INS (insulin) signaling to glucose uptake in primary human adipocytes compared with whole-body glucose homeostasis [2235].

In contrast to tissue samples, blood samples for autophagy study can be more easily obtained from living donors, from non-diseased donors, and from a wide age range including infants up to adults. However, current medication history is especially important in blood samples, as high concentrations of medications that can alter autophagy may be present. For example, in

patients with cystic fibrosis (CF) repurposed medications such as cysteamine are undergoing clinical trial evaluation. Cysteamine improves autophagy in CF [2236-2238], whereas other chronic medications such as azithromycin may suppress autophagy. Therefore a careful record of daily and study medications should be accounted for when examining human blood cells. Further, many autophagy regulators are differentially expressed across human sample and cell types. This was shown for CF sputum, where high expression of a microRNA cluster that regulates autophagy was found, in contrast to low expression in the blood [2239]. It is recommended that autophagy studies in humans account for multiple biological sources (including cells from the affected tissues or organs) when making definitive conclusions about the state of overall autophagy under- or over-expression. Likewise, therapeutic testing of new compounds in human samples *ex vivo* should be validated in multiple sample types. In the case of CF, this is often done in local tissues such as airway epithelial brushings, and validated in blood cells that are recruited to the local site of action [2240]. Autophagy studies in CF models can be easily adopted for other disease states. Alternatively, several pathologies with an aberrant autophagy process have been identified in humans through genome-wide studies. Cells derived from the affected tissues of such patients could be used for testing the therapeutic potency of new molecules.

A stepwise process can be proposed for linking changes in the autophagic pathway to changes in disease outcome. First, in an observational study, the changes in the autophagic pathway should be quantified and linked to changes in disease outcome. To prove causality, a subsequent autophagy-modifying intervention should be tested in a randomized study. Before an intervention study is performed in human patients, the phenotype of (in)active autophagy contributing to poor outcome should be established in a validated animal model of the disease. For the validation of the hypothesis in an animal model, a similar two-step process is suggested, with the assessment of the phenotype in a first stage, followed by a proof-of-concept intervention study (see *Large animals*).

Hydra

Hydra is a freshwater cnidarian animal that provides a unique model system to test autophagy. The process can be analyzed either in the context of nutrient deprivation, as these animals easily survive several weeks of starvation [2241], or in the context of regeneration, because in the absence of protease inhibitors, bisection of the animals leads to an uncontrolled wave of autophagy. In the latter case, an excess of autophagy in the regenerating tip immediately after amputation is deleterious [2242,2243]. Most components of the autophagy and MTOR pathways are evolutionarily conserved in Hydra [2244]. For steady-state measurements, autophagy can be monitored by western blot for Atg8-family proteins, by immunofluorescence (using antibodies to Atg8-family proteins, lysobisphosphatidic acid or RPS6KA/RSK), or with dyes such as MitoFluor™ Red 589 and LysoTracker™ Red. Flux measurements can be made by following Atg8-family protein turnover using lysosomal protease inhibitors (leupeptin and pepstatin A) or *in vivo* labeling using LysoTracker™ Red. It is also possible to monitor MTOR activity with

phosphospecific antibodies to RPS6KB and EIF4EBP1 or to examine gene expression by semiquantitative RT-PCR, using primers that are designed for Hydra. Autophagy can be induced by RNAi-mediated knockdown of *Kazal1* [2242,2243], or with rapamycin treatment, and can be inhibited with wortmannin or bafilomycin A₁ [2241,2244].

In situ hybridization shows high expression of *ATG12* transcripts specifically in nematoblasts, and of *ATG5* in the budding region and growing buds. The utilization of both knockdown and RNAi approaches indicates a crucial role of autophagy in various developmental and physiological processes, including the regeneration processes in adults [2245].

Induced pluripotent stem cells

Previous studies typically used patient biopsies and post-mortem tissues to investigate the role of autophagy in the pathogenesis of human disease. Nonetheless, the availability, preparation, and fixation of human biopsied tissues and organs, as well as the quantity and quality of biopsies, limit the dynamic measurement of autophagic flux. Furthermore, insufficiency of tissue biopsies from healthy controls for comparison challenges the snapshot results obtained from patient biopsies. To overcome the limitation of sample sources for investigating autophagy in human disease, various animal models and immortalized cell lines have been used to represent these diseases. Valuable results from these model systems have provided a fundamental pathomechanism for the role of autophagy in various human diseases; however, the species discrepancy between animal and human, and the tumorous genetic background of cell lines elicit concerns for the implications of the results as they pertain to humans.

Recently, the development of induced pluripotent stem (iPS) cells provides a valuable experimental system to uncover disease mechanisms and novel therapeutic strategies in human disease [2246,2247]. Diverse tissue-specific cells differentiated from iPS cells offer great potential to model different systemic diseases. Furthermore, the unique genetic and molecular signature of the affected individuals allows researchers to address disorder-relevant phenotypes at a cellular level. Multiple somatic cell sources such as skin, adipose tissues and peripheral blood for reprogramming to iPS cells can be obtained in non-invasive procedures. Thus, both disease and control iPS cells can be made available for comparison.

Emerging studies have reported the application of iPS cells and the corresponding derived tissue-specific cells in unraveling the regulation of autophagy in the pathogenesis of disease. iPS cell-derived neurons from PD patients show elevation of SNCA as well as autophagic and lysosomal defects, and dysregulation of calcium homeostasis [2248]. iPS cell-derived astrocytes from PD patients demonstrate accumulation of SNCA as well as dysfunctional CMA and impaired autophagy, indicating a non-cell autonomous contribution of astrocytes during pathogenesis of this disease [2249]. In a cellular model of ALS harboring a FUS mutation, iPS cell-derived neurons exhibit accumulation of toxic cytoplasmic FUS aggregates and dysregulation of autophagy, recapitulating the ALS pathology observed in patients' spinal cords [2250]. Moreover, iPS cell-derived neurons from beta-propeller protein-associated neurodegeneration/BPAN patients show defects in both autophagy and lysosomal function,

accumulation of iron deposits, elevation of oxidative stress and aberrant mitochondrial morphology [2251]. These findings provide evidence for a link between autophagy and pathogenesis in neurodegenerative disorders.

iPS cells modeling mitochondrial disease have been used for investigating the impact of mtDNA mutation on autophagy [2252]. Both isogenic iPS cell clones with high mutant mtDNA burden and without mtDNA mutation can be isolated simultaneously during cell passages. Thus, the impact of mtDNA heteroplasmy on autophagy involving pathogenesis of mitochondrial diseases can be observed directly. iPS cells with high mutant mtDNA burden modeling mitochondrial encephalomyopathy, lactic acidosis, and stroke-like episodes (MELAS) syndrome show elevated levels of autophagy, superoxide, intracellular calcium and mitochondrial depolarization at basal conditions in comparison with control iPS cells [2252]. It is noted that oxidative stress exacerbates the accumulation of autophagosomes and autolysosomes, increases levels of superoxide and enhances calcium flux into the

cytoplasm, leading to robust depolarization of mitochondrial membrane potential and enhanced mitophagy in MELAS-iPS cells. Mitophagy is very scarce in MELAS-iPS cells at the basal condition, consistent with previous observations that selective elimination of mitochondria containing pathogenic mtDNA is spared in mitochondrial diseases under physiological conditions [2252, 2253].

Moreover, work describing the changes occurring in long-term cultures of iPS cells, suggest this as a suitable model to study aging processes. In this context, autophagy increases in senescent cells (Figure 37), so that identifying autophagic mechanisms triggered by cellular senescence could suggest potential therapeutic strategies against premature aging [150,2254].

Cumulative evidence from emerging research indicates that the iPS cellular model is a useful and promising tool to recapitulate the pathogenesis of human diseases, allowing better understanding of the mechanism, and facilitating development of potential therapeutic targets.

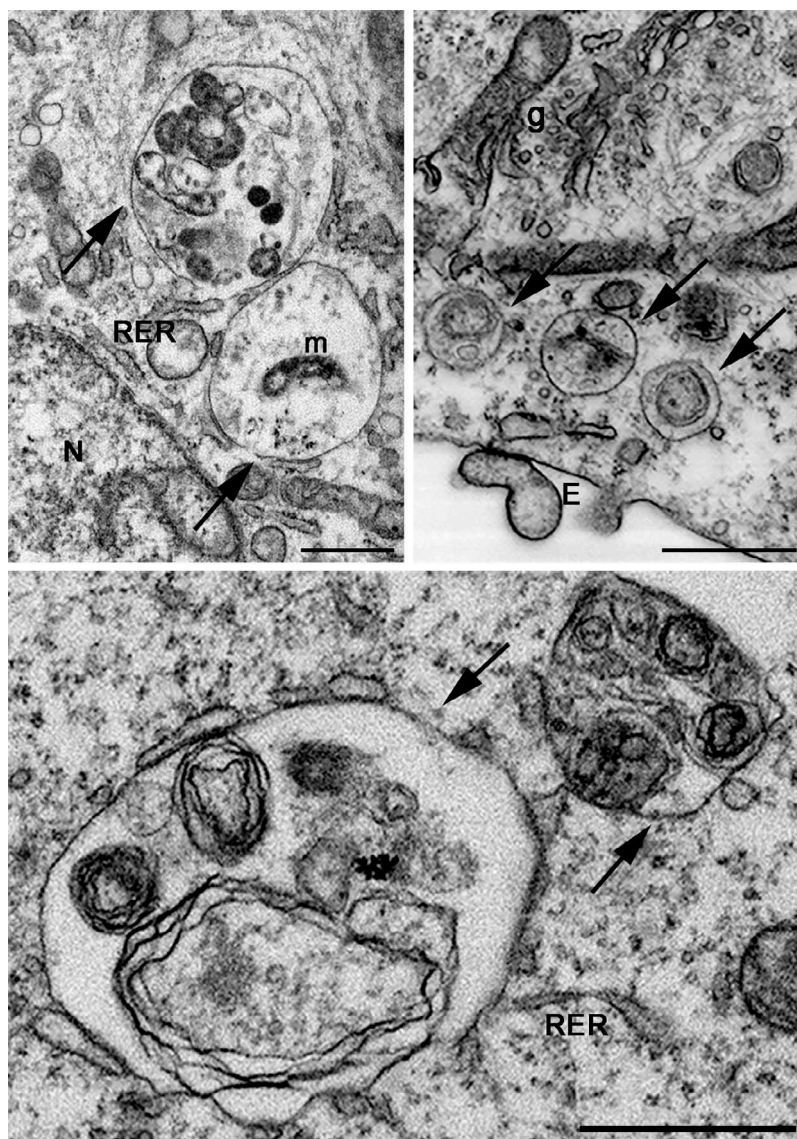


Figure 37. FIB-SEM images showing ultrastructural details of aging iPS cells. Arrows indicate autophagosomes containing mitochondria or other partially digested cytoplasmic material. E, exosomes; g, Golgi apparatus; m, mitochondrion; N, nucleus; RER, rough endoplasmic reticulum. Scale bars: 1 μ m. Image provided by F. Colasuonno, modified from ref. [150].

Large animals and rodents. This section refers in particular to mammals other than humans. Assessment of autophagy (and, in particular, autophagic flux) in clinically relevant large animal models is critical in establishing its (patho)physiological role in multiple disease states. For example, evidence obtained in swine suggests that upregulation of autophagy may protect the heart against damage caused by acute myocardial infarction/heart attack [2255]. Ovine models of placental insufficiency leading to intrauterine growth restriction have shown that there is no change in the expression of markers of autophagy in the fetus in late gestation [2256] or in the lamb at 21 days after birth [2257]. Furthermore, there is an increase in markers of autophagy in the placenta of human intrauterine growth restriction pregnancies [2258]. Studies in rabbits suggest a protective role of upregulated autophagy against critical illness-induced multiple organ failure and muscle weakness [2259,2260], which is corroborated by human studies [2231,2261]. Conversely, autophagy may contribute to the pathogenesis of some types of tissue injury, at least in the lung [2262,2263] and different regions of the CNS [39,86,539]. Similarly, autophagy may play different roles in ischemic stroke as ischemia progresses [2264], or during subsequent reperfusion [2265]. For example, studies in rats demonstrate that activation of autophagy [539] and disruption of autophagosome-lysosome fusion [86] may induce ischemic neuronal damage in the hippocampal CA1 region after transient global cerebral ischemia. The autophagic flux was also demonstrated to be activated, and an autophagic mechanism may contribute to ischemic neuronal injury in rats subjected to focal ischemia [2266] and neonatal cerebral hypoxic ischemia [535,2267]. Dysregulation of autophagy and mitophagy genes with parallel *Casp3* gene expression is observed in rats after complete cerebral ischemia with survival of 2-30 days after ischemia, and post-ischemic studies in rats suggest a lack of a protective role of the dysregulated autophagy in the brain as assessed by the expression of the *Bace1* gene [1645,1646]. In the mouse retina, mitophagy is dramatically impaired during prolonged diabetes, suggesting a pathogenic role in the development of neurovascular complications and premature senescence [39]. Finally, there is an increase in LC3-II in the kidney in normal wild-type mice treated with bafilomycin A₁, but no increase in LC3-II in mice with polycystic kidney disease, suggesting suppressed autophagic flux in *cys1/cpk* mouse kidneys [2268].

Studies in rodent and cellular models have shown a critical role of dysregulated autophagy in pancreatitis [1499,2269]. Experimental pancreatitis stimulates autophagosome formation, but at the same time inhibits autophagic degradation, resulting in impaired autophagic flux evidenced by accumulation of enlarged autolysosomes, decreased rate of long-lived protein degradation in pancreatic acinar cells, and increases in both LC3-II and SQSTM1. Mice with pancreas-specific ablation of *Atg5* or *Atg7*, double knockout of *Tfeb* and *Tfe3*, or *Lamp2* knockout, all develop spontaneous pancreatitis. Further, manifestations of impaired autophagy are prominent in human pancreatitis, such as acinar cell vacuolization (a long-noted, but poorly understood hallmark response of this disease), increases in pancreatic LC3-II and SQSTM1, and decreases in LAMP2 and TFEB.

Autophagy also plays an important role in the development and remodeling of the bovine mammary gland. In vitro

studies with the use of a 3-dimensional culture model of bovine mammary epithelial cells (MECs) have shown that this process is involved in the formation of fully developed alveoli-like structures [2270]. Earlier studies show that intensified autophagy is observed in bovine MECs at the end of lactation and during the dry period, when there is a decrease in the levels of lactogenic hormones, increased expression of auto/paracrine apoptogenic peptides, increased influence of sex steroids and enhanced competition between the intensively developing fetus and the mother organism for nutritional and bioactive compounds [2271,2272]. These studies were based on some of the methods described elsewhere in these guidelines, including GFP-Atg8-family protein fluorescence microscopy, TEM, and western blotting of LC3 and BECN1. Creation of a specific GFP-LC3 construct by insertion of cDNA encoding bovine LC3 into the pEGFP-C1 vector makes it possible to observe induction of autophagy in bovine MECs in a more specific manner than can be achieved by immunofluorescence techniques, in which the antibodies do not show specific reactivity to bovine cells and tissues [2270,2272]. However, it is important to remember that definitive confirmation of cause-and-effect is challenging for studies on large animals, given the lack or poor availability of specific antibodies and other molecular tools, the frequent inability to utilize genetic approaches, and the often prohibitive costs of administering pharmacological inhibitors in these translational preparations.

In contrast with cell culture experiments, precise monitoring of autophagic flux is practically impossible in vivo in large animals. Theoretically, repetitive analyses of small tissue biopsies should be performed to study ultrastructural and molecular alterations over time in the presence or absence of an autophagy inhibitor (e.g., CQ). However, several practical problems impede applicability of this approach. First, repetitive sampling of small needle biopsies in the same animal (a major challenge by itself) could be assumed to induce artefacts following repetitive tissue destruction, especially when deep (vital) organs are involved. In addition, chemical inhibitors of autophagy have considerable side effects and toxicity, hampering their usage. Also, the general physical condition of an animal may confound results obtained with administration of a certain compound, for instance altered uptake of the compound when perfusion is worse.

Therefore, in contrast to cells, where it is more practical to accurately document autophagic flux, we suggest the use of a stepwise approach in animal models to provide a proof of concept with an initial evaluation of sequelae of (in)active autophagy and the relation to the outcome of interest.

First, prior to an intervention, the static ultrastructural and molecular changes in the autophagic pathway should be documented and linked to the outcome of interest (organ function, muscle mass or strength, survival, etc.). These changes can be evaluated by light microscopy, EM and/or by molecular markers such as LC3-II. In addition, the cellular content of specific substrates normally cleared by autophagy should be quantified, as, despite its static nature, such measurement could provide a clue about the results of altered autophagic flux in vivo. These autophagic substrates can include SQSTM1 and (poly)ubiquitinated substrates or aggregates, but also

specific substrates such as damaged mitochondria. As noted above, measurement of these autophagic substrates is mainly informative when autophagic flux is prohibited/insufficient, and, individually, all have specific limitations for interpretation. As mentioned several times in these guidelines, no single measurement provides enough information on its own to reliably assess autophagy, and all measurements should be interpreted in view of the whole picture. In every case, both static measurements reflecting the number of autophagosomes (ultrastructural and/or molecular) and measurements of autophagic substrates as surrogate markers of autophagic flux need to be combined. Depending on the study hypothesis, essential molecular markers can further be studied to pinpoint at which stage of the process autophagy may be disrupted.

Second, after having identified a potential role of autophagy in mediating an outcome in a clinically relevant large animal model, an autophagy-modifying intervention should be tested. For this purpose, an adequately designed, randomized controlled study of sufficient size on the effect of a certain intervention on the phenotype and outcome can be performed in a large animal model. Alternatively, the effect of a genetic intervention can be studied in a small animal model with clinical relevance to the studied disease.

As mentioned above, exact assessment of autophagic flux requires multiple time points, which cannot be done in the same animal. Alternatively, different animals can be studied for different periods of time. Due to the high variability between animals, however, it is important to include an appropriate control group, and a sufficiently high number of animals per time point as corroborated by statistical power analyses. This requirement limits feasibility and the number of time points that can be investigated. The right approach to studying autophagy in large animals likely differs depending on the question that is being addressed. Several shortcomings regarding the methodology, inherent to working with large animals, can be overcome by an adequate study design. As for every study question, the use of an appropriate control group with a sufficient number of animals is crucial in this regard.

Lepidoptera

Some of the earliest work in the autophagy field was carried out in the area of insect metamorphosis. Microscopy and biochemical research revealed autophagy during the metamorphosis of American silkmoths and the tobacco hornworm, *Manduca sexta*, and included studies of the intersegmental muscles, but they did not include molecular analysis of autophagy [2273]. Overall, these tissues cannot be easily maintained in culture, and antibodies against mammalian proteins do not often work. Accordingly, these studies were confined to biochemical measurements and electron micrographs. During metamorphosis, the bulk of the larval tissue is removed by autophagy and other forms of proteolysis [2274]. *Bombyx mori* is now used as a representative model among Lepidoptera, for studying not only the regulation of autophagy in a developmental setting, but also the relations between autophagy and apoptosis. The advantages of this model are the large amount of information gathered on its developmental biology, physiology and endocrinology, the

availability of numerous genetic and molecular biology tools, and a completely sequenced genome [2275]. The basic studies of *B. mori* autophagy have been carried out in four main larval systems: the silk gland, the fat body, the midgut and the ovary.

The techniques used for these studies are comparatively similar, starting from EM, which is the most widely used method to follow the changes of various autophagic structures and other features of the cytosol and organelles that are degraded during autophagy [942,2276-2279]. Immuno-TEM also can be used, when specific antibodies for autophagic markers are available. As in other model systems the use of Atg8 antibodies has been reported in Lepidoptera. In *B. mori* midgut [942,2280], fat body [943] and silk gland [944] as well as in various larval tissues of *Galleria mellonella* [2281] and *Helicoverpa armigera* [2282], the use of both custom and commercial antibodies makes it possible to monitor Atg8 conversion to Atg8-PE by western blotting. Moreover, transfection of GFP-Atg8 or mCherry-GFP-Atg8 has been used to study autophagy in several lepidopteran cell lines [2282]. In addition, an antibody against Sqstm1 was generated, and it is efficient in detecting its autophagic degradation during autophagic processes in *B. mori* [2283,2284]. Activation of MTOR can be monitored with an antibody against p-EIF4EBP1 [943,2280,2284]. Acidotropic dyes such as MDC and LysoTracker™ Red staining have been used as markers for autophagy in silkworm egg chambers, always combined with additional assays [2276,2277]. Acid phosphatase also can be used as a marker for autolysosomal participation in these tissues [942,2278,2285]. Systematic cloning and analysis revealed that homologs of most of the *Atg* genes identified in other insect species such as *Drosophila* are present in *B. mori*, and 14 *Atg* genes have now been identified in the silkworm genome, as well as other genes involved in the TOR signal transduction pathway [2286-2288]. Variations in the expression of several of these genes have been monitored not only in silkworm larval organs, where autophagy is associated with development [942,944,2286,2287,2289], but also in the fat body of larvae undergoing starvation [2286,2290].

In the IPLB-LdFB cell line, derived from the fat body of the caterpillar of the gypsy moth *Lymantria dispar*, indirect immunofluorescence experiments have demonstrated an increased number of Atg8-positive dots in cells with increased autophagic activity; however, in contrast to larval tissues, western blotting did not reveal the conversion of Atg8 into Atg8-PE. In fact, a single band with an approximate molecular mass of 42 kDa was observed that was independent of the percentage of cells displaying punctate Atg8 (D. Malagoli, unpublished results). Thus, the utility of monitoring Atg8 in insects may depend on the species and antibody.

Marine invertebrates

The invaluable diversity of biological properties in marine invertebrates offers a unique opportunity to explore the different facets of autophagy at various levels from cell to tissue, and throughout development and evolution. For example, work on the tunicate *Ciona intestinalis* has highlighted the key role of autophagy during the late phases of development in lecithotrophic organisms (those in which the larvae during

metamorphosis feed exclusively from the egg yolk resources) [374,2291]. This work has also helped in pinpointing the coexistence of autophagy and apoptosis in cells, as well as the beneficial value of combining complementary experimental data such as LC3 immunolabeling and TUNEL detection. This type of approach could shed a new light on the close relationship between autophagy and apoptosis, and provide valuable information about how molecular mechanisms control the existing continuum between these two forms of programmed cell death. Autophagy also appears to play a role in the cell renewal process observed during the regeneration of the carnivorous sponge *Asbestopluma hypogea* [2292].

The identification of a growing number of autophagy-related sequences in different species has opened a much wider scenario for investigating the molecular mechanisms of autophagy and its role in a variety of processes. For example, in the “living fossil”, the sponge *Astrosclera willeyana*, molecular, histochemical, and morphological evidence indicate that specialized cells involved in the formation of a highly calcified skeleton actively degrade their intracellular microbial community using the autophagy pathway (namely ATG8) [2293]. This is the first observation suggesting an association between the process of autophagy and biomineralization in a metazoan. Analysis of the expression patterns of 13 genes involved in autophagy and apoptosis in the sea urchin *Paracentrotus lividus* highlights the simultaneous involvement of both processes in early embryo development [2294].

Bivalve molluscs provide useful models for studying autophagic function [2295]. Autophagy plays a key role in the resistance to nutritional stress as is known to be the case in many Mediterranean bivalve molluscs in the winter. For example, the European clam *Ruditapes decussatus* is able to withstand strict fasting for two months, and this resistant characteristic is accompanied by massive autophagy in the digestive gland (Figure 38). This phenomenon, observed by

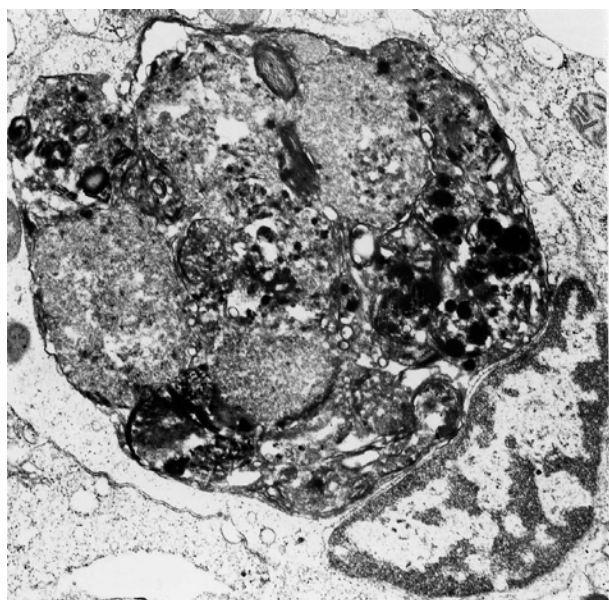


Figure 38. Autophagy in the digestive gland of *Ruditapes decussatus* (Mollusca, Bivalvia) subjected to a strict starvation of 2 months. Image provided by S. Baghdiguian.

TEM, demonstrates once again the advantage of using this classical ultrastructural method to study autophagy in unconventional biological models for which molecular tools may not be operational. Autophagy has been also demonstrated by different types of lysosomal reactions in digestive gland cells in response to a variety of environmental stressors (starvation, salinity change, hyperthermia, hypoxia, pollutant-induced stress). In the Mediterranean mussel *Mytilus galloprovincialis*, dephosphorylation of MTOR, evaluated by immunohistochemistry with antibodies generated to the mammalian protein, contributes to increased lysosomal membrane permeability and autophagy induced by contaminant exposure [2296].

Autophagy also plays a role during pathogen infections, as has been observed in the Pacific oyster, *Crassostrea gigas*. In the mantle of this bivalve mollusc, autophagy is modulated in response to a viral (Ostreid herpesvirus 1 [OsHV-1]) and a bacterial (*Vibrio aestuarianus*) infection [2297]. Autophagy may therefore play a protective role in oysters against infections as suggested by a survival assay when autophagy is inhibited by NH_4Cl treatment or induced by carbamazepine or starvation. Furthermore, autophagy occurs in the hemocytes of the Pacific oyster [502], which are the main effectors of its immune system, and thus play a key role in the defense against pathogens. Hemocyte autophagy activity characterized by flow cytometry, fluorescence microscopy and TEM analysis shows the importance of combining different approaches to investigate autophagy in marine invertebrate models.

Although the different facets of autophagy are increasingly studied, the molecular mechanism of autophagy is still poorly understood in these models. For the first time, an identification of the ATG proteins that constitute the core molecular machinery of autophagy in a bivalve mollusc, *C. gigas*, has been established [502]. The autophagy machinery in this organism is conserved with other eukaryotic organisms. These results will provide new possibilities to better understand the autophagy processes and mechanism in marine invertebrates.

At present, the use of TEM still represents a unique tool to confirm the presence of autophagic structures in bivalves at the subcellular level [502,2297,2298]. In *M. galloprovincialis* hemocytes, rapid autophagosome formation is observed within 5-15 min of in vitro challenge with *Vibrio tapetis* [2298]. This observation, together with increased LC3-II expression, decreased levels of phosphorylated MTOR and of SQSTM1, represents the first direct evidence for modulation of autophagic processes induced in bivalve immune cells by bacterial challenge.

Genome sequencing and transcriptomic data in different bivalve species are revealing a growing number of autophagy-related genes that are involved in the immune response [2299,2300]. Overall, available data in bivalves underlines the point that autophagy is not involved in pathogen degradation, but in protection against viral and bacterial infection.

A relationship between autophagy and resistance to disease has also been described in corals. Comparison of transcriptomics data on the immune response of four coral species, with a range of disease susceptibility, shows activation of apoptosis and autophagic pathways prevailing, respectively,

in susceptible species (*Orbicella faveolata*) and disease-tolerant species (*Porites porites* and *P. astreoides*), indicating that apoptotic and autophagic pathways might have a significant impact on the susceptibility of corals to disease [2301].

In crustaceans, gene expression, miRNA silencing and proteome analysis are revealing the role of autophagy-related mechanisms in immune and stress responses. Different miRNAs play key roles in immunity and host autophagy after infection by white spot syndrome virus, one of the main causes of disease in aquacultured species [2302,2303]. In the crab *Eirocheir sinensis*, EsBECN1 (Vps30/Atg6) is involved in regulating the expression of antimicrobial peptides in the immune responses to bacterial infection [2304]. In copepods, ocean acidification enhances lysosome-autophagy pathway proteomes that are responsible for repairing and removing proteins and enzymes damaged under stress, possibly mitigating mercury-induced toxicity [2305].

The intralysosomal subcellular distribution of C₆₀ fullerene nanoparticles in digestive gland cells of the marine mussel (*M. galloprovincialis*), following experimental exposure to C₆₀ nanoparticles in seawater results in lysosomal membrane permeabilization and inhibition of MTOR, and provokes an excessive induction of autophagy [2296,2306]. The effects of C₆₀ fullerene nanoparticles indicate that moderate to severe ROS production and oxidative damage are not necessary under these conditions to inhibit the MTOR pathways, although lysosomal membrane permeabilization, probably caused by lysosomal overload of foreign material (i.e., C₆₀ fullerene), will result in release of intralysosomal iron that will produce ROS [2077]. Consequently, autophagic induction by C₆₀ (as for other nanoparticles [2077,2094]), may represent a protective degradation in autolysosomes of material that is recognized by the cell as foreign or aberrant, such as pathogens or damaged intracellular proteins and membranes.

The cytoskeletal alterations induced by C₆₀ fullerene nanoparticles may impair the growth of the cells and their organization in the digestive tubules of the digestive gland. Overall, dysregulation of MTORC1 and MTORC2 may reduce the capacity of the cells, and organisms, to properly grow and reproduce. Consequently, MTOR dephosphorylation should be considered a diagnostic biomarker for the toxic effects of the C₆₀ nanoparticles and polycyclic aromatic hydrocarbons as previously demonstrated [2296]; and, under chronic stressful conditions, prognostic for potential harmful effects at the whole animal and population level.

Overall, knowledge on the autophagic machinery in marine invertebrates will help not only in elucidating the molecular networks that regulate autophagy within an evolutionary framework; this information will also contribute to understanding the response to infection of those species that are affected by pathogen-induced mass mortalities or other environmental stressors, also in the context of rapid global changes that affect their survival and distribution in oceans.

Neotropical teleosts

In tropical environments, fish have developed different reproductive strategies, and many species have the potential for use as a biological model in cell and molecular biology, especially for studying the mechanisms that regulate gametogenesis and

embryo development. In these fish, the ovary is a suitable experimental model system for studying autophagy and its interplay with cell death programs due to the presence of postovulatory follicles (POFs) and atretic follicles, which follow different routes during ovarian remodeling after spawning [2307]. In fish reproductive biology, POFs are excellent morphological indicators of spawning, whereas atretic follicles are relevant biomarkers of environmental stress. In addition, many freshwater teleosts of commercial value do not spawn spontaneously in captivity, providing a suitable model for studying the mechanisms of follicular atresia under controlled conditions [2308]. When these species are subjected to induced spawning, the final oocyte maturation (resumption of meiosis) occurs, and POFs are formed and quickly reabsorbed in ovaries after spawning [2309]. Assessment of autophagy in fish has been primarily made using TEM at different times of ovarian regression [2310]. Due to the difficulty of obtaining antibodies specific for each fish species, immunodetection of ATG proteins (mainly LC3 and BECN1) by IHC associated with analyses by western blotting can be performed using antibodies that are commercially available for other vertebrates [546]. Such studies suggest dual roles for autophagy in follicular cells [2307]; however, evaluation of the autophagic flux in different conditions is critical for establishing its physiological role during follicular regression and ovarian remodeling after spawning. Given the ease of obtaining samples and monitoring them during development, embryos of these fish are also suitable models for studying autophagy that is activated in response to different environmental stressors, particularly in studies in vivo.

Odontoblasts

Odontoblasts are long-lived dentin-forming postmitotic cells, which evolved from neural crest cells early during vertebrate evolution. These cells are aligned at the periphery of the dental pulp and are maintained during the entire healthy life of a tooth. As opposed to other permanent postmitotic cells such as cardiac myocytes or central nervous system neurons, odontoblasts are significantly less protected from environmental insults such as dental caries and trauma. Mature odontoblasts develop a well-characterized autophagy-lysosomal system, including a conspicuous autophagic vacuole that ensures turnover and degradation of cell components. Immunocytochemical and TEM studies make it possible to monitor age-related changes in autophagic activity in human odontoblasts [2311]. Tooth pulp cells, in contrast, process minor autophagic activities; however, the autophagy level in those cells can be highly induced in stress conditions [2312]. Furthermore, in the periodontal ligament mesenchymal cells, increased autophagy has a protective role in apoptosis prevention [2313], and it plays a role in healing of the oral mucosa [2314].

Parasitic helminths

Parasitic helminths comprise parasitic flatworms (Monogenea, Trematoda [flukes], and Cestoda [tapeworms] of the class Neodermatans [2315]) that infect vertebrates and cause certain human neglected tropical diseases such as neurocysticercosis and taeniasis (*Taenia* sp.), echinococcosis

(*Echinococcus* sp.), schistosomiasis (*Schistosoma* sp.), fascioliasis (*Fasciola hepatica*), clonorchiasis (*Clonorchis sinensis*) and opisthorchiasis (*Opisthorchis viverrini*) among others [2316]. Although autophagy is a fundamental catabolic pathway conserved from yeast to mammals, it remains understudied in these parasites. Since the 1960s, autophagy and particularly glycophagy have been described via TEM for these parasitic helminths through ultrastructural changes in the syncytial tegument of larval stages and adult worms during *in vitro* and *in vivo* drug chemotherapy [2317-2320]. In addition, data obtained by TEM analysis led to the proposal that specialized biomineralized cells, termed calcareous corpuscles, are the result of continuous cytoplasmic autophagy in tapeworms [2320,2321]. These cells show multi-lamellar structures coincident with the typical ultrastructure of autophagy activation induced by endoplasmic reticulum stress, and different from that seen in cells deprived of nutrients (Figure 39A) [2322]. The calcareous corpuscles play key roles in the physiology of tapeworms; they are involved in bioaccumulation of ions (calcium, magnesium, carbonate and phosphate, and traces of aluminum, boron, copper and iron), metamorphosis of parasitic tissues (the corpuscles are formed, reorganized and resorbed in different hosts) and they correlate with previous or ongoing active metabolic activity (high content of carbohydrate metabolism enzymes and glycogen) [2323]. Studies carried out with confocal IHC using a commercial polyclonal antibody directed against the N terminus of human LC3, make it possible to verify the autophagy activity of calcareous corpuscles in *Echinococcus granulosus* larval stages exposed to arsenic trioxide, metformin and rapamycin (Figure 39B) [2324].

Currently, the availability of genome sequences together with the extensive transcriptomic and/or expressed sequence tag (EST) data allow *in silico* confirmation of the occurrence of the autophagy-related genes for the parasitic flatworms that cause the most serious problems among 50 helminth genome draft assemblies [2325-2328]. Most components of the autophagy core machinery and related key signaling pathways such as those involving AKT, PI3K, TOR, AMPK, FOXO and TFEB are evolutionarily preserved in these parasitic flatworms; however, only in some parasites such as *Echinococcus* sp. has the autophagy pathway been formally analyzed [2324,2329]. Basic studies performed in metacestodes and protoscoleces, larval forms of the cestode *Echinococcus* that can develop in humans, allow the detection of active basal autophagy both in cellular systems and during the vesicular de-differentiation of protoscolex to metacestode [2324]. All Atg homologs (encoded by fourteen genes including two paralogs for *Atg8*) involved in induction, vesicle nucleation, autophagosome expansion and membrane recycling (except *Atg10*, which was also not identified in *D. melanogaster* nor in *Apis mellifera* [2]) have been found in *Echinococcus* sp. [2324]. These autophagy-related proteins conserve all domains corresponding to specific functions, including the key amino acids involved in protein-protein or protein-membrane interactions.

Autophagy in *Echinococcus* can be regulated by transcription-dependent upregulation via FOXO and non-transcriptional inhibition through TOR [2330] (J. Loos and V.

Dávila, personal communication). As in other invertebrates, a single FOXO transcription factor is identified in the cestode. Likewise, the consensus core recognition motif for FOXO binding (TTGTTTAC) is conserved in autophagy genes (*atg8* and *atg12*). Furthermore, it has been demonstrated that rapamycin, metformin and bortezomib are able to induce autophagy, dose-dependent pharmacological effects and death in these parasites even under nutrient-rich conditions. These results were verified by detection of diverse autophagic structures through TEM (including the phagophore, autophagosomes, autolysosomes with lamellar stacks, and glycogen surrounded by double-membrane vesicles), *Atg8* punctate images detected by confocal microscopy, conversion of *Atg8* to the *Atg8*-PE conjugate by western blotting, and an increase in the mRNA levels of autophagy genes (*atg5*, *atg6*, *atg8*, *atg12*, *atg16* and *atg18*) by RT-PCR, proportional to the drug concentration employed [2324,2329-2331]. Although autophagy is predominantly a homeostatic mechanism, drug-induced excessive autophagy might also play a role in cell death. Therefore, from a therapeutic perspective, it will be of great importance to understand how autophagy can be pharmacologically manipulated to favor pro-death signaling in these parasites. The establishment of new molecular tools and studies involving specific related *atg* mutants would be of great value in order to get insights into the role of autophagy in parasitic flatworms.

Planarians

Because planarians are one of the favorite model systems in which to study regeneration and stem cell biology, these flatworms represent a unique model where it is possible to investigate autophagy in the context of regeneration, stem cells and growth. Currently the method used to detect autophagy is TEM. A detailed protocol adapted to planarians has been described [2332,2333]. However, complementary methods to detect autophagy are also needed, because TEM cannot easily distinguish between activation and blockage of autophagy, which would both be observed as an accumulation of autophagosomes. Other methods to detect autophagy are being developed (C. González-Estévez, personal communication), including IHC and western blotting approaches for the planarian homolog of LC3. Several commercial antibodies against human LC3 have been tried for cross-reactivity without success, and three planarian-specific antibodies have been generated. Some preliminary results show that LysoTracker™ Red can be a useful reagent to analyze whole-mount planarians. Most of the components of the autophagy and MTOR signaling machinery are evolutionarily conserved in planarians. Whether autophagy genes vary at the mRNA level during starvation and after depletion of MTOR signaling components is still to be determined.

Plants

As stated above with regard to other organisms, staining with MDC or derivatives (such as monodansylmethylamine) is not sufficient for detection of autophagy, as these stains also detect vacuoles. The same is the case with the use of LysoTracker™ Red, neutral red or acridine orange. The fluorophore of the red fluorescent protein shows a relatively high

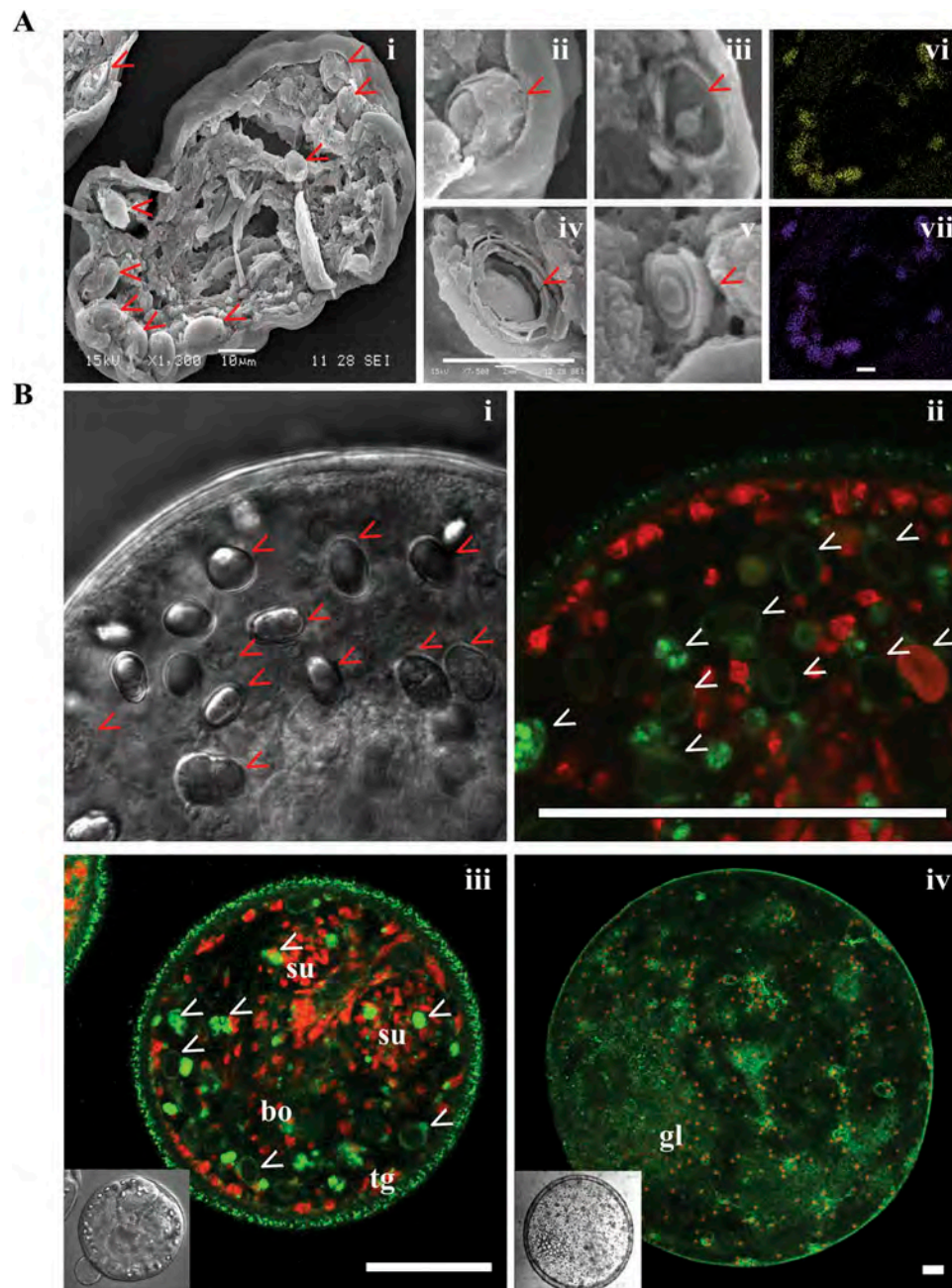


Figure 39. Detection of autophagy in *Echinococcus granulosus* larval stage. **(A)** Scanning electron micrographs of a sectioned larva (or protoscolex) (i) showing big oval-shaped cells named calcareous corpuscles (red arrowheads) developed by cytoplasmic autophagy. Ultrastructural details of different developmental stages of these parenchymatic cells showing a central vacuole (ii-iii) at the initial development phase and concentric membranes that marginalize a thin layer of cytoplasm in mature corpuscles at the end of the autophagic process (iv-v). Energy-dispersive X-ray elemental microanalysis of the calcareous corpuscles in a sectioned protoscolex demonstrates the colocalization of accumulated ions into corpuscles: calcium (vi), phosphorus (vii). Scale bar: 10 μ m. **(B)** Optical transmission (i) and confocal (ii-iv) microscopy images of a protoscolex treated with metformin (10 mM) for 48 h (i-iii) and an untreated microcyst (or metacystode) (iv) incubated with an anti-LC3 antibody and revealed with an antibody conjugated with Alexa Fluor 488 (green fluorescence) and counterstained with propidium iodide (red fluorescence) to observe cell nuclei under optimal contrast conditions. Fluorescent punctate images are often detected in the tegument of rapamycin-treated protoscoleces (ii-iii) and microcysts originated by vesicular de-differentiation from protoscoleces (iv) with high Atg8 polypeptide levels within the free cytoplasmic matrix of these cells, demonstrating pharmacological autophagy induction in corpuscles (ii-iii) and basal autophagy in small cysts in development even under nutrient-rich conditions (iv). Scale bar: 100 μ m. Inset images correspond to TEM. bo, body; gl, germinal layer; su, sucker; tg, tegument. Images provided by A. C. Cumino and J. A. Loos. Only images in panel B were previously published in ref. [327].

stability under acidic pH conditions. Thus, chimeric RFP fusion proteins that are sequestered within autophagosomes and delivered to the plant vacuole can be easily detected by fluorescence microscopy. Furthermore, fusion proteins with some versions of RFP tend to form intracellular aggregates, allowing the development of a visible autophagic assay for

plant cells [2334]. For example, fusion of cytochrome b5 and the original (tetrameric) RFP generate an aggregated cargo protein that displays cytosolic puncta of red fluorescence and, following vacuolar delivery, diffuse staining throughout the vacuolar lumen. However, it is not certain whether these puncta represent autophagosomes or small vacuoles, and

14490

14495

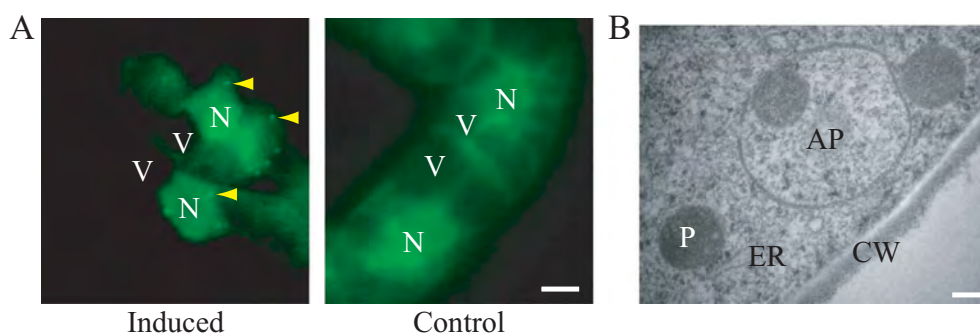


Figure 40. Detection of autophagy in tobacco BY-2 cells. **(A)** Induction of autophagosomes in tobacco BY-2 cells expressing YFP-NtAtg8 (shown in green for ease of visualization) under conditions of nitrogen limitation (Induced). Arrowheads indicate autophagosomes that can be seen as a bright green dot. No such structure was found in cells grown in normal culture medium (Control). Bar: 10 μ m. N, nucleus; V, vacuole. **(B)** Ultrastructure of an autophagosome in a tobacco BY-2 cell cultured for 24 h without a nitrogen source. Bar: 200 μ m. AP, autophagosome; CW, cell wall; ER, endoplasmic reticulum; P, plastid. Image provided by K. Toyooka.

therefore these data should be combined with immuno-TEM or with conventional TEM using high-pressure frozen and freeze-substituted samples [2335].

In plant studies, GFP-Atg8 fluorescence is typically assumed to correspond to autophagosomes; however, as with other systems, caution needs to be exercised because it cannot be ruled out that Atg8 is involved in processes other than autophagy. Immunolabeled GFP-Atg8 can be detected both on the inner and outer membrane of an autophagosome in an Arabidopsis root cell, using chemical fixation (see Fig. 6b in ref [2336].), suggesting that it will be a useful marker to monitor autophagy. Arabidopsis cells can be stably transfected with GFP fused to plant ATG8, and the lipidated and non-lipidated forms can be separated by SDS-PAGE [289]. Furthermore, the GFP-ATG8 processing assay is particularly robust in Arabidopsis and can be observed by western blotting [290,350]. Two kinds of GFP-ATG8 transgenic seeds are currently available from the Arabidopsis Biological Resource Center, each expressing similar GFP-ATG8A transgenes but having different promoter strength. One transgene is under the control of the stronger *Cauliflower mosaic virus* 35S promoter [816], whereas the other uses a promoter of the Arabidopsis *AT4G05320.2/ubiquitin10* gene [2337]. In the GFP-ATG8 processing assay, the former has a higher ratio of GFP-ATG8A band intensity to that of free GFP than does the latter [2337]. Because free GFP level reflects vacuolar delivery of GFP-ATG8, the ubiquitin promoter line may be useful when studying an inhibitory effect of a drug/mutation on autophagic delivery. Likewise, the 35S promoter line may be used for testing potential autophagy inducers. GFP-ATG8CL *Nicotiana benthamiana* seeds are also available upon request² (unpublished). The transgene is under a 35S promoter, and the plants can be used for both confocal microscopy and western blotting to monitor autophagic flux and image autophagosomes in vivo. Immunofluorescence with anti-ATG8 antibodies followed by confocal microscopy imaging has been also used to visualize autophagic structures in plant cells, during developmental events, from tissue differentiation [2338] to senescence [2339], as well as in stress-treated barley microspores [911].

Thus, as with other systems, autophagosome formation in plants can be monitored through the combined use of

fluorescent protein fusions to ATG8, immunolabeling and TEM (Figure 40). A tandem fluorescence reporter system is also available in Arabidopsis [2340]. The number of fluorescent ATG8-labeled vesicles can be increased by pretreatment with concanamycin A, which inhibits vacuolar acidification [1763,2336]; however, this may interfere with the detection of MDC and LysoTrackerTM Red. It is also possible to use plant and fungal homologs of SQSTM1 and NBR1 in Arabidopsis [1052,2340] (the NBR1 homolog is called JOKA2 in tobacco [2341]) as markers for selective autophagy when constructed as fluorescent chimeras. In addition, detection of the NBR1 protein level by western blot, preferably accompanied by qPCR analysis of its transcript level, provides reliable semi-quantitative data about autophagic flux in plant cells [2342].

Another approach for assessing autophagic flux is based on the observation that autophagy mutants in Arabidopsis exhibit peroxisomal abnormalities [2343,2344]. Consequently, peroxisome abundance can provide information on autophagic flux. Peroxisome abundance can be measured in total tissue extracts by spectrofluorometry using the small fluorescent probe Nitro-BODIPY [2345,2346]. This approach demonstrates that knockout of Arabidopsis *ATG5* correlates with both a greater number of peroxisomes per cell and higher Nitro-BODIPY fluorescence in the total extracts from leaves [2345]. Although, low cost and ease of the procedure makes the Nitro-BODIPY assay applicable for the identification of autophagy mutants in large populations, direct markers should be used to examine autophagic flux in the identified genotypes.

Hydrotropism determines the degree of root bending towards the water source, which consequently compensates for the effects of drought. Hydrotropism modulates the development of the root system, and it has an effect on plant support, as well as water and nutrient intake. A water potential gradient system (using a water stress medium [WSM]) [2347] can be used to demonstrate that autophagy is required for the hydrotropic response. Looking for autophagosome accumulation in the root bending zone, 4-days-post germination 35S-ATG8A seedlings [378] are transferred to the WSM, and accumulation of autophagosomes is followed from 0 to 6 h by confocal microscopy using a 40X dry objective in order to avoid manipulation that may affect the root bending.

During this time the root bending is achieved and autophagosome accumulation can be observed in the bending zone. Autophagosomes accumulate in the epidermal cells of the root bending zone 2 h after the transfer of seedlings to WSM. WSM supplemented with CQ can be used to monitor the requirement of autophagy flux. Several ATG mutants do not show hydrotropic curvature in WSM [2348]. Thus, the WSM system also allows the observation of autophagosomes in situ using confocal microscopy without seedling manipulation.

It has been assumed that, just as in yeast, autophagic bodies are found in the vacuoles of plant cells, because both microautophagy and autophagy are detected in these cells [2349]. The data supporting this conclusion are mainly based on EM studies showing vesicles filled with material in the vacuole of the epidermis cells of *Arabidopsis* roots; these vesicles are absent in *ATG4A* and *ATG4B* mutant plants [378]. However, it cannot be excluded that these vacuolar vesicles are in fact cytoplasmic/protoplasmic strands, or that they arrived at the vacuole independent of autophagy; although the amount of such strands would not be expected to increase following treatment with concanamycin. Immunolabeling with an antibody to detect ATG8 could clarify this issue.

The *Phytophthora infestans* RXLR effector PexRD54 has been published as an inducer of ATG8CL autophagosome formation and can be used in *N. benthamiana* as a tool to transiently activate autophagy [2350]. *ATG4* and *ATG9* RNAi constructs can also be used to knock down gene expression of the core autophagy components and transiently suppress autophagy in *N. benthamiana* [2351].

Other methods described throughout these guidelines can also be used in plants [2352]. For example, in tobacco cells cultured in sucrose starvation medium, the net degradation of cellular proteins can be measured by a standard protein assay; this degradation is inhibited by 3-MA and E-64 c (an analog of E-64d), and is thus presumed to be due to autophagy [1862,2353].

Cautionary notes: Although the detection of vacuolar RFP can be applied to both plant cell lines and to intact plants, it is not practical to measure RFP fluorescence in intact plant leaves, due to the very high red autofluorescence of chlorophyll in the chloroplasts. Furthermore, different autophagic induction conditions cause differences in protein synthesis rates; thus, special care should be taken to monitor the efficiency of autophagy by quantifying the intact and processed cargo proteins.

Protists

An essential role of autophagy during the differentiation of some parasitic protists (formerly called protozoa) is clearly emerging. Only a few of the known ATG genes are present in these organisms, which raises the question about the minimal system that is necessary for the normal functioning of autophagy. The reduced complexity of the autophagic machinery in many protists provides a simplified model to investigate the core mechanisms of autophagosome formation necessary for selective proteolysis; accordingly, protist models have the potential to open a completely new area in autophagy

research. Some of the standard techniques used in other systems can be applied to protists including indirect immunofluorescence using antibodies generated against ATG8 and the generation of stable lines expressing mCherry- or GFP-fused ATG8 for live microscopy and immuno-TEM analyses. Extrachromosomal constructs of GFP-ATG8 also work well with less complex eukaryotes [384,385,2354], as do other fluorescently-tagged ATG proteins including ATG5 and ATG12.

The unicellular amoeba *D. discoideum* provides another useful system for monitoring autophagy [1940,2355]. The primary advantage of *D. discoideum* is that it has a unique life cycle that involves a transition from a unicellular to a multicellular form. Upon starvation, up to 100,000 single cells aggregate by chemotaxis and form a multicellular structure that undergoes morphogenesis and cell-type differentiation. Development proceeds via the mound stage, the tipped aggregate and a motile slug, and culminates with the formation of a fruiting body that is composed of a ball of spores supported by a thin, long stalk made of vacuolized dead cells. Development is dependent on autophagy and, at present, all of the generated mutants in *D. discoideum* autophagy genes display developmental phenotypes of varying severity [628, 2356]. *D. discoideum* is also a versatile model to study infection with human pathogens and the role of autophagy in the infection process. The susceptibility of *D. discoideum* to microbial infection and its strategies to counteract pathogens are similar to those in more complex eukaryotes [1460,2357]. Along these lines, *D. discoideum* utilizes some of the proteins involved in autophagy that are not present in *S. cerevisiae* including ATG101 and VMP1, in addition to the core Atg proteins. The classical markers GFP-ATG8 and GFP-ATG18 can be used to detect autophagosomes by fluorescence microscopy [64]. Flux assays based on the proteolytic cleavage of cytoplasmic substrates are also available [40,422].

One cautionary note with regard to the use of GFP-ATG8 in protists is that these organisms display some “nonclassical” variations in their ATG proteins (see *LC3-associated apicoplast*) and possibly a wide phylogenetic variation because they constitute a paraphyletic taxon [2358]. For example, *Leishmania* contains many apparent ATG8-like proteins (the number varying per species; e.g., up to 25 in *L. major*) grouped in four families, but only one labels true autophagosomes even though the others form puncta [384], and ATG12 requires truncation to provide the C-terminal glycine before it functions in the canonical manner. Unusual variants in protein structures also exist in other protists, including apicomplexan parasites, for example, the malaria parasite *Plasmodium* spp. or *T. gondii*, which express ATG8 with a terminal glycine not requiring cleavage to be membrane associated [2359]. Thus, in each case care needs to be applied and the use of the protein to monitor autophagy validated. In addition, due to possible divergence in the upstream signaling kinases, classical inhibitors such as 3-MA or wortmannin, or inducers such as rapamycin, must be used with caution. Although they are not as potent for *T. brucei* [2360] or apicomplexan parasites as in mammalian cells or yeast (I. Coppens, personal communication) [2354]; they are efficient for *T. cruzi* [2361]. Likewise, RNAi knockdown of TORC1 (e.

g., TOR1 or RPTOR) is effective in inducing autophagy in trypanosomes. Conversely, the inhibitory effect of bafilomycin A₁ on trypanosome autophagy seems to occur during formation, resulting in a low number of ATG8-positive compartments, in contrast to what occurs in mammalian cells [2361,2362]. In addition, small molecule inhibitors of the protein-protein interaction of ATG8 and ATG3 in *Plasmodium falciparum* have been discovered that are potent in cell-based assays and useable at 1-10 μ M final concentration [2363,2364]. Note that although the lysosomal protease inhibitors E64 and pepstatin block lysosomal degradative activity in *Plasmodium*, these inhibitors do not affect ATG8 levels and associated structures, suggesting a need for alternate methodologies to investigate autophagy in this model system [2365].

In conventional autophagy, the final destination of autophagosomes is their fusion with lysosomes for intracellular degradation. However, certain stages of *Plasmodium* (insect and hepatic) lack degradative lysosomes, which makes questionable the presence of canonical autophagosomes and a process of autophagy in this parasite. Nevertheless, if protists employ their autophagic machineries in unconventional manners, studies of their core machinery of autophagy will provide information as to how autophagy has changed and adapted through evolution. For example, although lysosome-like structures were not observed initially in the apicomplexa *T. gondii*, it is now clear that this protist harbors an organelle, named the vacuolar compartment/VAC or plant-like vacuole/PLV, with the characteristics of an acidic degradative compartment similar to lysosomes [2366,2367]. Autophagic markers, such as the *T. gondii* ortholog of ATG8 and ATG9, colocalize with the vacuolar compartment markers CPL and CRT, indicating that in *T. gondii* autophagosomes fuse with this lysosome-like organelle [2368,2369]. The ability of *T. gondii* to sustain prolonged extracellular stress relies on a functional autophagic machinery, although autophagy is dispensable for tachyzoite intracellular growth in normal in vitro culture conditions [2368]. The chronic form of this parasite, the bradyzoite stage, requires a basal autophagy flux for survival also when intracellular, perhaps because of reduced access to host cell nutrient due to the thick wall surrounding the vacuole containing the bradyzoites [2369,2370].

The scuticociliate *Philasterides dicentrarchi* has proven to be a good experimental organism for identifying autophagy-inducing drugs or for autophagy initiation by starvation-like conditions, because this process can be easily induced and visualized in this ciliate [2371]. In scuticociliates, the presence of autophagic vacuoles can be detected by TEM, fluorescence microscopy or confocal laser scanning microscopy by using dyes such as MitoTracker® Deep Red FM and MDC.

Finally, a novel autophagy event has been found in *Tetrahymena thermophila*, which is a free-living ciliated protist. A remarkable, virtually unique feature of the ciliates is that they maintain spatially differentiated germline and somatic nuclear genomes within a single cell. The germline genome is housed in the micronucleus, while the somatic genome is housed in the macronucleus. These nuclei are produced during sexual reproduction (conjugation), which involves not only meiosis and mitosis of the micronucleus

and its products, but also degradation of some of these nuclei as well as the parental old macronucleus. Hence, there should be a mechanism governing the degradation of these nuclei. The inhibition of PtdIns3Ks with wortmannin or LY294002 results in the accumulation of additional nuclei during conjugation [2372]. During degradation of the parental old macronucleus, the envelope of the nucleus becomes MDC- and LysoTracker™ Red-stainable without sequestration of the nucleus by a double membrane, and with the exposure of certain sugars and PS on the envelope [2373]. Subsequently, lysosomes fuse only to the old parental macronucleus, but other co-existing nuclei such as developing new macro- and micronuclei are unaffected [2373]. Using gene technology, it has been shown that ATG8 and VPS34 play critical roles in nuclear degradation [1330,2373]. Knockout mutations of the corresponding genes result in a block in nuclear acidification, suggesting that these proteins function in lysosome-nucleus fusion. In addition, the envelope of the nucleus in the *VPS34* knockout mutant does not become stainable with MDC. This evidence suggests that selective autophagy may be involved in the degradation of the parental macronucleus and implies a link between *VPS34* and ATG8 in controlling this event. In *Trypanosoma cruzi*, there is a complex consisting of the PtdIns3K TcVPS34 and the serine-threonine kinase TcVPS15, which participates in autophagy. It has also been observed that TcVPS34 participates in fundamental processes for *T. cruzi* such as endocytosis, osmoregulation and acidification [387,2374].

Rainbow trout

Salmonids (e.g., salmon, rainbow trout) experience long periods of fasting often associated with seasonal reductions in water temperature and prey availability or spawning migrations. As such, they represent an interesting model system for studying and monitoring the long-term induction of autophagy. Moreover, the rainbow trout (*Oncorhynchus mykiss*) displays unusual metabolic features that may allow us to gain a better understanding of the nutritional regulation of this degradative system (i.e., a high dietary protein requirement, an important use of amino acids as energy sources, and an apparent inability to metabolize dietary carbohydrates). It is also probably one of the most deeply studied fish species with a long history of research carried out in physiology, nutrition, ecology, genetics, pathology, carcinogenesis and toxicology [2375]. Its relatively large size compared to model fish, such as zebrafish or medaka, makes rainbow trout a particularly well-suited alternative model to carry out biochemical and molecular studies on specific tissues or cells that are impossible to decipher in small fish models. The genomic resources in rainbow trout are now being extensively developed; a high-throughput DNA sequencing program of ESTs has been initiated associated with numerous transcriptomics studies [2376-2379], and the full genome sequence is now available.

Most components of the autophagy and associated signaling pathways (AKT, TOR, AMPK, FOXO) are evolutionarily conserved in rainbow trout [952,2380-2382]; however, not all ATG proteins and autophagy-regulatory proteins are detected by the commercially available antibodies produced against

their mammalian orthologs. Nonetheless, the EST databases facilitate the design of targeting constructs. For steady-state measurement, autophagy can be monitored by western blot or by immunofluorescence using antibodies to Atg8-family proteins [2380]. Flux measurements can be made in a trout cell culture model (e.g., in primary culture of trout myocytes) by following Atg8-family protein turnover in the absence and presence of bafilomycin A₁. It is also possible to monitor the mRNA levels of *ATG* genes by qPCR using primer sequences chosen from trout sequences available in the above-mentioned EST database. A major challenge in the near future for this model will be to develop the use of RNAi-mediated gene silencing to analyze the role of some signaling proteins in the control of autophagy, and also the function of autophagy-related proteins in this species.

Retinal pigment epithelium

The retinal pigment epithelium (RPE) is a single polarized layer of cells that form the outer blood retinal barrier and play a central role in maintaining metabolic homeostasis in the outer retina through transport of nutrients and waste products. These terminally differentiated cells also phagocytose lipid and protein-rich photoreceptor outer segments (POS) derived from the underlying photoreceptor cells on a daily basis. RPE develops a well-characterized autophagy-lysosomal system as well as a LAP pathway that ensures the turnover and degradation of cell content, and the daily degradation of ingested POS lipids, respectively [2383]. The RPE may be the only example in which autophagy and LAP are regulated in a light- and circadian-dependent manner that is postulated to occur through RUBCN [2384]. Immuno-histochemical, biochemical and TEM studies make it possible to monitor both circadian and age-related changes in autophagy activity in mouse models [2385–2389]. Moreover, lipidomic and metabolism studies have highlighted the critical role played by LC3-associated processes in RPE health and photoreceptor function [2390]. Lowering of lysosomal pH in diseased cells through pharmacological means or using acidic nanoparticles can enhance autophagic turnover [2391–2393]. The P2Y₁₂ antagonist ticagrelor can reduce loss of photoreceptors and visual function when added to food; the decreased lysosomal pH and autofluorescent lipofuscin waste are consistent with enhanced lysosomal function [2394,2395].

Autophagy plays an important role in maintaining retinal functions. Excessive upregulation of autophagy or depletion of key proteins for autophagy will disrupt functions of photoreceptor cells. Haploinsufficiency of TUBGCP4 (tubulin, gamma complex associated protein 4) impairs assembly of TUBG/γ-tubulin ring complexes and disturbs autophagy homeostasis of the retina. TUBGCP4 can inhibit autophagy by competing with ATG3 to interact with ATG7, thus interfering with lipidation of LC3B. Both cytoplasmic and nuclear autophagy have been observed in photoreceptor cell segments [2396,2397].

POS phagocytosis shares functional similarity with efferocytosis, the ingestion and degradation of dead cell corpses (or apoptotic cells). On a molecular level, both processes rely on PS as an “eat me” signal [245,2398]. Upon ingestion, both dead cells and POS stimulate the recruitment of LC3B via

LAP [245,2389,2399,2400]. The extent of LC3B association with phagosomes in the RPE remains unclear, and the percent of LAPosomes is an open question; in vitro [2389] and in vivo studies [2390,2401] suggest that ~ 30–45% of ingested phagosomes are LC3B positive. In those studies, the levels of endogenous LC3B associated with OPN (opsin)-positive phagosomes were analyzed. Higher percentages are observed when GFP-LC3B is expressed in vitro in ARPE19 cells (between 80–90%) or in GFP-LC3B mice overexpressing this tag [2400] where almost 90% of OPN-containing structures are also GFP-LC3B positive. Further studies using DQ-BSA quantified the extent of LAPosome-lysosome association in vitro [2388]. An assessment of LAPosome levels in models of age-related retinal disease would provide valuable insight into the balance between two LC3-requiring processes—stress-mediated autophagosome formation and OS degradation.

Aberrant MTORC1 signaling has been implicated in aging and age-related degeneration of the human RPE [2387]. The phagocytosed POS serve as a physiological stimulus of MTORC1 activation through lysosome-independent mechanisms in the RPE [2402]. Whereas synchronized photoreceptor disk shedding and RPE phagocytosis activate MTORC1 during the morning burst, this is subsequently followed by MTORC1 inactivation and maintenance of retinal homeostasis. Reports suggest that excessive and sustained activation of MTORC1 in response to stress and independent of nutrient stimulation, leads to RPE cell death and senescence. Furthermore, genetic ablation of RPE mitochondrial oxidative phosphorylation in mice activates the AKT-MTOR pathway leading to dedifferentiation and hypertrophy of the RPE [2386], suggesting that inhibition of MTORC1 could protect the RPE against chronic metabolic stress and acute oxidative stress. It is well known that proteins of the autophagic machinery in the RPE participate in POS trafficking through a non-canonical autophagy pathway independent of the ULK1 complex, namely LAP [2400]. These studies showed that the MTORC1-independent interplay between autophagy and phagocytosis in the RPE is critical for POS degradation.

The cancer stem cell biomarker PROM1/CD133 (prominin 1), was demonstrated to play a critical role in maintaining RPE homeostasis through regulation of autophagy flux [2403]. Whereas overexpression of PROM1 increases autophagy flux, genomic deletion of *PROM1* (using CRISPR-Cas9) in the RPE blocks autophagy through both upstream activation of MTORC1/2 and downstream disruption of a macromolecular complex involving PROM1, SQSTM1, and HDAC6 in the forming autophagosome. These findings have important implications because defective autophagosomal-lysosomal-phagocytic pathways can lead to ineffective clearance of POS and damaged organelles, all of which have been linked to the pathogenesis of retinal diseases, including age-related macular degeneration/AMD. Therefore, PROM1-mediated targeting of MTORC1/2 signaling in the RPE, could provide a therapeutic strategy for retinal degenerative diseases.

Sea urchin

Sea urchin embryo is an appropriate model system for studying and monitoring autophagy and other defense mechanisms activated during physiological development and in response

to stress [1552]. This experimental model offers the possibility of detecting LC3 through both western blot and immunofluorescence in situ analysis. Furthermore, in vivo staining of autolysosomes with acidotropic dyes can also be carried out. Studies on whole embryos make it possible to obtain qualitative and quantitative data for autophagy and also to get information about spatial localization aspects in cells that interact among themselves in their natural environment. Furthermore, because embryogenesis of this model system occurs simply in a culture of sea water, it is very easy to study the effects of inducers or inhibitors of autophagy by adding these substances directly into the culture. Exploiting this potential, it has recently been possible to understand the functional relationship between autophagy and apoptosis induced by cadmium stress during sea urchin development. In fact, inhibition of autophagy by 3-MA results in a concurrent reduction of apoptosis; however, using a substrate for ATP production, methyl pyruvate, apoptosis (assessed by TUNEL assay and cleaved CASP3 immunocytochemistry) is substantially induced in cadmium-treated embryos where autophagy is inhibited. Therefore, autophagy could play a crucial role in the stress response of this organism because it could energetically contribute to apoptotic execution through its catabolic role [2404]. Cautionary notes include the standard recommendation that it is always preferable to combine molecular and morphological parameters to validate the data.

Ticks

In the hard tick *Haemaphysalis longicornis*, endogenous autophagy-related proteins (Atg6 and Atg12) can be detected by western blotting and/or by immunohistochemical analysis of midgut sections [2405,2406]. It is also possible to detect endogenous Atg3 and Atg8 by western blotting using antibodies produced against the *H. longicornis* proteins (R. Umekiya-Shirafuji, unpublished results). Commercial antibodies against mammalian ATG orthologs (ATG3, ATG5, and BECN1) can also be used for western blotting. However, when the tick samples include blood of a host animal, the animal species immunized with autophagy-related proteins should be checked before use to avoid nonspecific background cross-reactivity.

In addition to these methods, TEM is recommended to detect autophagosomes and autolysosomes. Although acidotropic dyes can be useful as a marker for autolysosomes in some animals, careful attention should be taken when using the dyes in ticks. Because the midgut epithelial cells contain acidic organelles (e.g., lysosomes) that are related to blood digestion during blood feeding, this method may cause confusion. It is difficult to distinguish between autophagy (autolysosomes) and blood digestion (lysosomes) with acidotropic dyes.

Another available monitoring method is to assess the mRNA levels of tick ATG genes by qPCR [2407,2408]. However, this method should be used along with other approaches such as western blotting, immunostaining, and TEM as described in this article. Unlike model insects, such as *Drosophila*, powerful genetic tools to assess autophagy are still not established in ticks. However, RNAi-mediated gene silencing is now well established in ticks [2409], and is being

developed to analyze the function of autophagy-related genes in ticks during nonfeeding periods (R. Umekiya-Shirafuji, unpublished results) and in response to pathogen infection. Recently, “omics” technologies such as transcriptomics and proteomics have been applied to the study of apoptosis pathways in *Ixodes scapularis* ticks in response to infection with *Anaplasma phagocytophilum* [2410]. *I. scapularis*, the vector of Lyme disease and human granulocytic anaplasmosis, is the only tick species for which genome sequence information is available (assembly JCVI_ISG_i3_1.0; http://www.ncbi.nlm.nih.gov/nuccore/NZ_ABJB000000000). For related tick species such as *I. ricinus*, mapping to the *I. scapularis* genome sequence is possible [2411], but for other tick species more sequence information is needed for these analyses.

Zebrafish (*Danio rerio*)

Zebrafish have many characteristics that make them a valuable vertebrate model organism for the analysis of autophagy. For example, taking advantage of the transparency of embryos, autophagosome formation can be visualized in vivo during development using transgenic GFP-Lc3 and GFP-Gabarap fish [44,2412,2413] and in specific cell types such as neurons [328]. It has been reported that conventional anti-pigmentation strategies including 1-phenyl-2-thiourea/PTU treatment and genetic targeting of TYR (tyrosinase) induce autophagy in various tissues; however, in vivo visualization of later-stage embryos can still be performed using light-sheet fluorescence microscopy, and image quality is only minimally affected by developed pigments (X.K. Chen, J.S. Kwan, R.C. Chang and A.C. Ma, in press). Lysosomes can also be readily detected in vivo by the addition of LysoTracker™ Red to fish media prior to visualization. Additionally, protocols have been developed to monitor the rate of autophagosome accumulation in vivo [328], and Lc3 protein levels and conjugation to PE by western blot analysis using commercially available Lc3 antibodies [44,388]. It should be noted that in addition to Lc3-I and Lc3-II, a third, lower-sized protein product is frequently evident following western blot analysis in zebrafish [2414].

Because of their translucent character and external fertilization and development, zebrafish have proven to be an exceptional choice for developmental research. In situ hybridization of whole embryos can be performed to determine expression patterns. Knockdown of gene function is performed by treatment with morpholinos; the core autophagy machinery proteins Gabarap [2415], Atg5 [2416,2417] and Atg13 [2418], and regulatory proteins such as the phosphoinositide phosphatase Mtmr14 [2419], Rubcn [2418], Raptor and Mtor [2420], have all been successfully knocked down by morpholino treatment. However, a number of papers have raised concerns about the cellular stress pathway inducing, off-target effects of this approach [2421–2423], therefore, validation of these phenotypes in bona fide mutants is necessary. The CRISPR-Cas9 system has been used for efficient targeted gene deletions of *Epg5*, *Sqstm1*, *Optn* and *Snap29* [2424–2426] and should continue to be of great help in future analyses [2427].

It is well known that the aquatic environment is frequently compromised by the action of chemical substances and/or

their metabolites. According to a study that applied a computational model for investigating biocidal compounds, approximately 50–60% of those substances are highly toxic for different aquatic compartments and organisms [2428]. For this reason, zebrafish are ideal organisms for in vivo drug discovery and/or verification because of their relatively small size allowing easy handling, and several chemicals have been identified that modulate zebrafish autophagy activity [388]. Many chemicals can be added to the media and are absorbed directly through the skin. Because of simple drug delivery and rapid embryonic development, zebrafish are a promising organism for the study of autophagy's role in disease including HD [1951], AD [2429], PD [2430] and myofibrillar myopathy [2431–2433]. In the case of infection, studies in zebrafish have made important contributions to understanding the role of bacterially- [2418,2425,2434,2435] and virally [2436–2438]-induced autophagy. In vivo zebrafish studies have also contributed to understanding the role of autophagy in different aspects of development, including cardiac morphogenesis, caudal fin regeneration [2439], and muscle and brain development [2412,2440,2441].

In vitro studies in the zebrafish cell line ZF4 (zebrafish embryonic fibroblast) [2442] show that autophagy is required for fish rhabdovirus (spring viremia of carp virus, SVCV) replication [1351,2443]. In fact, several standardized autophagy blockers (also including cholesterol-related molecules such as C-reactive protein, 25-hydroxycholesterol, methyl-beta-cyclodextrin and cholesterol itself) inhibit SVCV infectivity in this cell line [1351,2444]. Moreover, the glycoprotein G of viral hemorrhagic septicemia (rhabdo)virus/VHSV and SVCV induce a cell's antiviral autophagic program in ZF4 cells [2438,2443]. In this regard, autophagy is also induced in GFP-LC3 transgenic zebrafish that are experimentally infected with SVCV [2436].

Noncanonical use of autophagy-related proteins

Multiple components of the autophagy machinery mediate non-autophagic functions [1797], as described here below.

LC3-associated phagocytosis (LAP)

Although the lipidation of LC3 to form LC3-II is a commonly used marker of autophagy, studies have established that LC3-II can also be present on phagosomes, acting to promote maturation independently of traditional autophagy, in a non-canonical autophagic process termed LC3-associated phagocytosis [2,30,2445,2446]. LAP requires RUBCN and occurs upon engulfment of particles (such as dead cells, and pathogens including *Aspergillus fumigatus*, *Burkholderia pseudomallei*, *Bacteroides fragilis*, and *Yersinia pestis*) that engage a receptor-mediated signaling pathway, resulting in the recruitment of some but not all of the autophagic machinery to the phagosome. LAP requires the association of RUBCN with the UVRAG-containing class III PtdIns3K complex, and it facilitates generation and localization of PtdIns3P. This PtdIns3P then binds and stabilizes the CYBB/NOX2/gp91^{phox} complex resulting in ROS production for processing the engulfed cargo [245,801,2447]. These autophagic components facilitate rapid phagosome maturation and degradation of engulfed cargo,

and play roles in the generation of signaling molecules and regulation of immune responses [244,245,904,2448,2449]. LAP thus represents a unique process that marries the ancient pathways of phagocytosis and autophagy.

Despite overlap in molecular machinery, there currently exist several criteria by which to differentiate LAP from autophagy: (a) Whereas LC3-decorated autophagosomes can take hours to form, LC3 can be detected on LAP-engaged phagosomes as early as 10 min after phagocytosis, and PtdIns3P can also be seen at LAP-engaged phagosomes minutes after phagocytosis [245,247,2448]. (b) EM analysis reveals that LAP involves single-membrane structures [247]. In contrast, autophagy is expected to generate double-membrane structures surrounding cargo. However, this can be confusing if the engulfed structure already possesses a membrane before engulfment, as in the case of cell corpses [244,2450,2451]. (c) Whereas most of the core autophagy components are required for LAP, the two processes can be distinguished by the involvement of the pre-initiation complex. RB1CC1, ATG13, ULK1 and ULK2 are dispensable for LAP, which provides a convenient means for distinguishing between the two processes [245,2448]. (d) LAP requires the WD repeats of ATG16L1, whereas autophagy does not have this requirement [1477,1478]. (e) LAP involves LC3 recruitment in a manner that requires ROS production by the NADPH oxidase family, notably CYBB/NOX2/gp91^{phox}. It should be noted that most cells express at least one member of the NADPH oxidase family. Silencing of the common subunits, CYBB or CYBA/p22^{phox}, is an effective way to disrupt NADPH oxidase activity and therefore LAP. It is anticipated that more specific markers of LAP will be identified as this process is further characterized. (f) In human macrophages infected with *Mycobacterium tuberculosis*, MORN2 (MORN repeat containing 2) is recruited at the phagosome membrane containing *M. tuberculosis* to induce the recruitment of LC3, and subsequent maturation into phagolysosomes. In addition, MORN2 drives trafficking of *M. tuberculosis* to a single-membrane compartment. Thus, in certain conditions, MORN2 can be used to help to make the distinction between autophagy and LAP [2452].

Of note, an ATG5- and CTSL-dependent cell death process has been reported that can be activated by the small molecule NID-1; this process depends on PtdIns3K signaling, generates LC3B puncta and single-membrane vacuoles, and results in the clearance of SQSTM1. Thus, LAP and/or related processes can be co-opted to cause cell death in some cases [2453].

A very similar process to LAP occurs during the cell cannibalism process of entosis. After engulfment of an epithelial cell by a neighboring cell, LC3 is recruited on the single membrane entotic vacuole before lysosome fusion and death of the inner cell [244]. It is worth noting that many lysosomotropic compounds, including CQ, activate a LAP-like non-canonical autophagy pathway that drives LC3 lipidation on endolysosomal membranes and potentially interferes with the interpretation of LC3 lipidation data [2454,2455]. In a zebrafish model, LAP in macrophages is important in clearing intracellular bacteria such as *Salmonella* [2418]. LAP-like non-canonical autophagy is also observed in pancreatic acinar cells and involves LC3-conjugation to the membrane of

endocytic vacuoles (organelles formed as a consequence of compound exocytosis followed by compensatory membrane retrieval) [760].

Mouse models have also been developed to study LAP in vivo. RUBCN stabilizes the CYBA/p22^{PHOX}-CYBB/NOX2/gp91^{phox} complex during LAP [2456] allowing ROS to induce binding of ATG16L1 to endo-lysosome membranes [801]. *rubcn*^{-/-} mice [2457] have systemic loss of LAP and have been useful as a source of LAP-deficient cells for “in vitro” studies, and for “in vivo” studies of autoimmunity and β -amyloid trafficking [2457,2458]. RUBCN is a multidomain adaptor protein that suppresses NFKB signaling and pro-inflammatory responses [2456]. Exaggerated proinflammatory responses mean that *rubcn*^{-/-} mice are difficult to use in infection studies. The mice also fail to gain weight and have defects in the clearance of dying and apoptotic cells, leading to autoimmune disease that resembles systemic lupus erythematosus [2457]. An alternative approach to the study of LAP “in vivo” has targeted pathways downstream of RUBCN [2459]. LAP and autophagy require the E3-ligase like activity of the ATG12–ATG5–ATG16L1 complex, but conjugation of LC3 to endo-lysosome membranes during LAP requires the WD domain of ATG16L1 [1478]. This has led to the generation of mice lacking the WD and linker domain of ATG16L1, which have been developed to study the role played by non-canonical autophagy in vivo. These mice have systemic loss of LAP and LC3-associated endocytosis (termed LANDO) [2459], but retain the N-terminal CCD and ATG5-binding domains of ATG16L1 required for conventional autophagy. This allows the mice to activate autophagy, grow normally and maintain tissue homeostasis. These mice also maintain inflammatory and immunological homeostasis and can be used to study the role played by LAP and LANDO during infection in vivo.

LC3-associated apicoplast

In several important parasitic protists of the phylum Apicomplexa (e.g., *T. gondii* and *Plasmodium spp.*), the single ATG8 homolog localizes to an endosymbiotic nonphotosynthetic plastid, called the apicoplast [2359,2460–2463]. This organelle is the product of a secondary endosymbiotic event, by which a red alga was endocytosed by an auxotrophic eukaryote (the ancestor Apicomplexa); the apicoplast is the main remnant of this red alga. This organelle is approximately 300 nm in diameter, and is composed of four membranes that trace their ancestry to three different organisms. The successive endosymbiotic events that led to its incorporation into an ancestor of the Apicomplexa imply that its outermost membrane could be of phagosomal origin, although it might also have incorporated elements of the host ER. It is possible that ATG8-containing vesicles are generated from apicoplastic membranes to form phagophores, as evidenced in *Plasmodium* liver forms. Interestingly, it has been shown that in a parasite strain of *Plasmodium* overexpressing ATG8, the apicoplast forms an abnormally large, reticulate network that ultimately collapses, leading to poorly infectious parasites [2464]. This finding suggests that ATG8 may supply the apicoplast with lipids, controlling the maintenance and homeostasis of this organelle. On the apicoplast of *T. gondii*,

ATG8 plays a role in the centrosome-mediated inheritance of the organelle in daughter cells during parasite division, which highlights unconventional functions of ATG8 in protists [2465]. Interestingly, both ATG8 and PtdIns3P-binding PROPPINs of the WIPI/Atg18 family are essential for apicoplast function [2466,2467]. Because of this peculiar ATG8 localization and potential morphological similarities between the multi-membrane apicoplast and stress-induced autophagosomes, caution must be taken when identifying these structures by electron microscopy or by fluorescence microscopy with ATG8 labeling in these parasites.

LC3 conjugation system for IFNG-mediated pathogen control

Similar to LAP, LC3 localizes on the parasitophorus vacuole membrane (PVM) of *T. gondii* [246]. The parasitophorus vacuole is a vesicle-like structure formed from host plasma membrane during the invasion of *T. gondii*, and it sequesters and protects the invasive *T. gondii* from the hostile host cytoplasm. The cell-autonomous immune system uses IFNG-induced effectors, such as immunity-related GTPases and guanylate binding proteins (GBPs), to attack and disrupt this type of membrane structure; consequently, naked *T. gondii* in the cytoplasm are killed by a currently unknown mechanism. Intriguingly, proper targeting of these effectors onto the PVM of *T. gondii* requires the autophagic ubiquitin-like conjugation system, including ATG7, ATG3, and the ATG12–ATG5–ATG16L1 complex [2468], although the necessity of LC3-conjugation itself for the targeting is not yet clear [2469]. In contrast, up- or downregulation of canonical autophagy using rapamycin, wortmannin, or starvation do not significantly affect the IFNG-mediated control of *T. gondii*. Furthermore, the degradative function or other components of the autophagy pathway, such as ULK1/2 and ATG14, are dispensable. Many groups have confirmed the essential nature of the LC3-conjugation system for the control of *T. gondii* [2470–2472], and the same or a similar mechanism also functions against other pathogens such as murine norovirus and *Chlamydia trachomatis* [1958,2470]. Although topologically and mechanistically similar to LAP, the one notable difference is that the parasitophorous vacuole of *T. gondii* is actively made by the pathogen itself using host membrane, and the LC3-conjugation system-dependent targeting happens even in nonphagocytic cells. GBP-mediated lysis of pathogen-containing vacuoles is important for the activation of noncanonical inflammasomes [2473], but the targeting mechanism of GBPs to the vacuoles is unknown. Considering the necessity of the LC3-conjugation system to target GBPs to the PVM of *T. gondii*, this system may play crucial roles in the general guidance of various effector molecules to target membranes, as well as in selective phagophore-dependent sequestration, phagophore membrane expansion and autophagosome maturation.

Intracellular trafficking of bacterial pathogens

Some ATG proteins are involved in the intracellular trafficking and cell-to-cell spread of bacterial pathogens by noncanonical autophagic pathways. For example, ATG9 and WIPI1, but not ULK1, BECN1, ATG5, ATG7 or LC3B are required

for the establishment of an endoplasmic reticulum-derived replicative niche after cell invasion with *Brucella abortus* [2474]. In addition, the cell-to-cell transmission of *B. abortus* seems to be dependent on ULK1, ATG14 and PIK3C3/VPS34, but independent of ATG5, ATG7, ATG4B and ATG16L1 [2475].

Exocytosis with LC3-associated membranes

The Atg8-family protein lipidation machinery is also involved in non-canonical secretion and exocytosis of extracellular vesicles [105,106]. This role has been initially described for yeast Acb1 [2476,2477] and IL1B and CFTR in more complex eukaryotes [1700,2478,2479]. In addition to Atg8-family protein lipidation, this pathway seems to require Golgi reassembly-stacking proteins (GORASPs) and components of ESCRT complexes [2480,2481]. The associated release of extracellular vesicles with Atg8-family protein-conjugated membranes is also hijacked by viruses for their efficient exocytosis [2482-2484]. In the filamentous fungus *Aspergillus nidulans*, a protein denoted AN4171/BapH (BAR- and PH domain-containing) is an effector of RAB11 that binds PtdIns(4,5)P₂ and localizes to exocytic membranes. In mutants lacking BapH, basal autophagy under nitrogen-replete conditions is increased, suggesting that it acts as a liaison between exocytosis/endocytic recycling and autophagy [2200].

Other processes

ATG proteins are involved in various other nonautophagic processes, particularly apoptosis, membraneless organelle dynamics, COPII-mediated ER export, and noncanonical protein secretion, as discussed in various papers [31,105,106,818,858,2399,2448,2485-2489]. For example, ATG5 and RUBCN, but not RB1CC1, are required for LC3-associated endocytosis (LANDO), identified in microglial cells and the macrophage RAW264.7 cell line [2458], whereas the requirement of ATG5, RUBCN, and the lack of a requirement for RB1CC1 are well-established for the non-canonical function of autophagy proteins in the LAP pathway. LANDO is also required for the recycling of putative antibody receptors (CD36, TREM2, and TLR4) from internalized endosomes to the plasma membrane.

Interpretation of in silico assays for monitoring autophagy

The increasing availability of complete (or near-complete) genomes for key species spanning the eukaryotic domain provides a unique opportunity for delineating the spread of autophagic machinery components in the eukaryotic world [2490,2491]. Fast and sensitive sequence similarity search procedures are already available; an increasing number of experimental biologists are now comfortable “BLASTing” their favorite sequences against the ever-increasing sequence databases for identifying putative homologs in different species [2492]. Nevertheless, several limiting factors and potential pitfalls need to be taken into account.

In addition to sequence comparison approaches, a number of computational tools and resources related to autophagy have become available online. All the aforementioned

methods and approaches may be collectively considered as “in silico assays” for monitoring autophagy, in the sense that they can be used to identify the presence of autophagy components in different species and provide information on their known or predicted associations.

In the following sections we briefly present relevant in silico approaches, highlighting their strengths while underscoring some inherent limitations, with the hope that this information will provide guidelines for the most appropriate usage of these resources.

Sequence comparison and comparative genomic approaches

Apart from the generic shortcomings when performing sequence comparisons (discussed in ref [2493].), there are some important issues that need to be taken into account, especially for autophagy-related proteins. Because autophagy components seem to be conserved throughout the eukaryotic domain of life, the deep divergent relations of key subunits may reside in the so called “midnight zone” of sequence similarity: i.e., genuine orthologs may share even less than 10% sequence identity at the amino acid sequence level [2494]. This is the case with autophagy subunits in protists [2495,2496] and with other universally conserved eukaryotic systems, as for example the nuclear pore complex [2497]. This low sequence identity is especially pronounced in proteins that contain large intrinsically disordered regions [2498]. In such cases, sophisticated (manual) iterative database search protocols, including proper handling of compositionally biased subsequences and considering domain architecture may assist in eliminating spurious similarities or in the identification of homologs that share low sequence identity with the search molecule [2496-2498].

Genome-aware comparative genomics methods [2499] can also provide invaluable information on yet unidentified components of autophagy. However, care should be taken to avoid possible Next Generation Sequencing artefacts (usually incorrect genome assemblies): these may directly (via a similarity to a protein encoded in an incorrectly assembled genomic region) or indirectly (via propagating erroneous annotations in databases) give misleading homolog assignments [2500]. In addition, taking into account other types of high-throughput data available in publicly accessible repositories (e.g., EST/RNAseq data, expression data) can provide orthogonal evidence for validation purposes when sequence similarities are marginal [2497].

Web-based resources related to autophagy

A number of autophagy-related resources are now available online, providing access to diverse data types ranging from gene lists and sequences to comprehensive catalogs of physical and indirect interactions. In the following we do not attempt to review all functionalities offered by the different servers, but to highlight those that (a) offer possibilities for identifying novel autophagy-related proteins, or (b) characterize features that may link specific proteins to autophagic processes. Two comments regarding biological databases in general also apply to autophagy-related resources as well: (a) the need for regular

updates, and (b) data and annotation quality. Nevertheless, these issues are not discussed further herein.

The THANATOS database. THANATOS (THE Apoptosis, Necrosis, AuTophagy OrchestratorS) is a comprehensive data resource developed by the CUCKOO Workgroup, which contains 191,543 proteins potentially associated with autophagy and cell death pathways in 164 eukaryotes [2501]. THANATOS was started from the manual collection of 4,237 experimentally identified proteins regulated in autophagy and cell death pathways from the literature, whereas potential orthologs of these known proteins were computationally detected. Besides sequence data, known PTMs, protein-protein interactions (PPIs) and functional annotations are also integrated. A simple web interface assists in data retrieval, using keyword searches, browsing by species and cell death type, performing BLAST searches with user-defined sequences, and by requesting the display of orthologs among predefined species. Using the data in THANATOS, an evolutionary analysis demonstrates that the machinery of the autophagy pathway is highly conserved across eukaryotes, whereas statistical analyses suggest human autophagy proteins are enriched among cancer gene products and drug targets. A reconstruction of a kinase-substrate phosphorylation network for ATG proteins supports a critical role of phosphorylation in regulating autophagy. The THANATOS database is publicly available online at the URL <http://thanatos.biocuckoo.org/>.

With the help of THANATOS, a network-based algorithm of in silico Kinome Activity Profiling/iKAP was designed to computationally infer protein kinases differentially regulated by two natural neuroprotective autophagy enhancers, corynoxine (Cory) and corynoxine B (Cory B) [2502]. This algorithm predicted and verified that two kinases, MAP2K2/MEK2 (mitogen-activated protein kinase kinase 2) and PLK1 (polo like kinase 1), are essential for Cory-induced autophagy to promote the clearance of AD-associated APP (amyloid beta precursor protein) and PD-associated SNCA/ α -synuclein (synuclein alpha). The CUCKOO workgroup is mainly focused on PTM bioinformatics, and has developed fourteen PTM site predictors, five tools for biological data analysis, and twelve PTM-related databases at the URL <http://www.biocuckoo.org/>, including DeepPhagy (deep learning for autophagy) for quantitatively analyzing four types of autophagic phenotypes in *Saccharomyces cerevisiae*, including the vacuolar targeting of GFP-Atg8, the targeting of Atg1-GFP to the vacuole, the vacuolar delivery of GFP-Atg19, and the disintegration of autophagic bodies indicated by GFP-Atg8 [2503]. DeepPhagy was implemented in a 5-layer convolutional neural network framework, containing three connected convolutional blocks and two fully connected layers, and is freely available online at the URL <http://deepphagy.biocuckoo.org/>. This workgroup also developed CGDB, the Circadian Gene DataBase at URL <http://cgdb.biocuckoo.org/> [2504] (see *Clockophagy*).

The human autophagy database (HADb). The human autophagy database, developed in the Tumor Immunotherapy and Microenvironment (TIME) group at the Luxembourg Institute of Health, lists over 200 human genes/proteins

related to autophagy [920]. These entries have been manually collected from the biomedical literature and other online resources. An update of the initially published list is currently underway. For each gene there exists information on its sequence, transcripts and isoforms (including exon boundaries) as well as links to external resources. HADb provides basic search and browsing functionalities and is publicly available online at the URL <http://autophagy.lu/>.

The Autophagy Database. The Autophagy Database is a multifaceted online resource providing information for proteins related to autophagy and their homologs across several eukaryotic species, with a focus on functional and structural data [2505]. It is developed by the National Institute of Genetics (Japan) under the Targeted Proteins Research Program of the Ministry of Education, Culture, Sports, Science and Technology (<http://www.tanpaku.org/>). This resource is regularly updated and as of August 2014 contained information regarding 312 reviewed protein entries; when additional data regarding orthologous/homologous proteins from more than 50 eukaryotes is considered, the total number of entries reaches approximately 9,000. In addition to the browse functionalities offered under the “Protein List” and the “Homologs” menus, an instance of the NCBI-BLAST software facilitates sequence-based queries against the database entries. Moreover, interested users may download the gene list or the autophagy dump files licensed under a Creative Commons Attribution-ShareAlike 2.1 Japan License. The Autophagy Database is publicly available online at the URL <http://www.tanpaku.org/autophagy/index.html>.

The Autophagy Regulatory Network (ARN). Another addition to the web-based resources relevant to autophagy research is the Autophagy Regulatory Network (ARN), originally developed at the Eötvös Loránd University and Semmelweis University (Budapest, Hungary) in collaboration with the Quadram Institute and the Earlham Institute (Norfolk, UK). Maintenance and hosting the ARN resource is secured at The Genome Analysis Centre until at least 2022. ARN is an integrated systems-level resource aiming to collect and provide an interactive user interface enabling access to validated or predicted protein-protein, transcription factor-gene and miRNA-mRNA interactions related to autophagy in human [2506]. ARN contains data from 26 resources, including an in-house extensive manual curation, the dataset of a ChIP-MS study [658], ADB and ELM. As of June 2020, a total of more than 15,000 proteins and 800 miRNAs and lncRNAs are included in ARN, including 38 core autophagy proteins with more than 500,000 transcriptional, post-transcriptional and post-translational interactions. Importantly, all autophagy-related proteins are linked to major signaling pathways. A flexible—in terms of both content and format—download functionality enables users to locally use the ARN data under the Creative Commons Attribution-NonCommercial-ShareAlike 3.0 Unported License. The autophagy regulatory network resource is publicly available online at the URL <http://autophagyregulation.org>.

Prediction of Atg8-family interacting proteins. Being central components of the autophagic core machinery, Atg8-family members (e.g., LC3 and GABARAP subfamilies in mammals) and their interactome have attracted substantial interest [658,2507,2508]. During the last decade, a number of proteins have been shown to interact with Atg8 homologs via a short linear peptide; depending on context, different research groups have described this peptide as the LIR [423], the LC3 recognition sequence (LRS) [1020], or the AIM [2509]. Two independent efforts resulted in the first online available tools for identification of these motifs (LIR-motifs for brevity) in combination with other sequence features, which may signify interesting targets for further validation (see below).

The iLIR server. The iLIR server is a specialized web server that scans an input sequence for the presence of a degenerate version of LIR, the extended LIR-motif (xLIR) [2510]. Currently, the server also reports additional matches to the “canonical” LIR motif (WxxL), described by the simple regular expression $x(2)\text{-}[WFY]\text{-}x(2)\text{-}[LIV]$. A position-specific scoring matrix (PSSM) based on validated instances of the LIR motif has also been compiled, demonstrating that many of the false positive hits (i.e., spurious matches to the xLIR motif) are eliminated when a PSSM score >15 is sought. In addition, iLIR also overlays the aforementioned results to segments that reside in or are adjacent to disordered regions and are likely to form stabilizing interactions upon binding to another globular protein as predicted by the ANCHOR package [2511]. A combination of an xLIR match with a high PSSM score (>13) and/or an overlap with an ANCHOR segment gives reliable predictions [2510]. It is worth mentioning that, intentionally, iLIR does not provide explicit predictions of functional LIR motifs but rather displays all the above information accompanied by a graphical depiction of query matches to known protein domains and motifs; it is up to the user to interpret the iLIR output. As mentioned in the original iLIR publication, a limitation of this tool is that it does not handle any noncanonical LIR motifs at present. The iLIR server was jointly developed by the University of Warwick and University of Cyprus and is freely available online at the URL <http://repeat.biol.ucy.ac.cy/iLIR>. A similar web-based AIM prediction tool termed high-fidelity AIM (hfAIM) was also developed by scientists at the Weizmann Institute and Ghent University [2512], and is freely available online at the URL <http://bioinformatics.psb.ugent.be/hfAIM/>.

iLIR database: Using the iLIR server, a database of putative LIR-containing proteins (LIRCPs) has been created. The iLIR database (<https://ilir.warwick.ac.uk>) lists all the putative canonical LIRCPs identified in silico in the proteomes of eight model organisms combined with a Gene Ontology/GO term analysis. Additionally, a curated text-mining analysis of the literature suggests novel putative LIRCPs in mammals that have not previously been associated with autophagy [2513].

iLIR@viral: The iLIR@viral database (<http://ilir.uk/virus/>) lists all the putative canonical LIR motifs identified in viral proteins, using the iLIR server. Curated text-mining analysis of the literature suggests the presence of novel putative LIRCPs in viruses [2514].

The eukaryotic linear motif resource (ELM). The Eukaryotic Linear Motif resource [2515] is a generic resource for examining functional sites in proteins in the form of short linear motifs, which have been manually curated from the literature. Sophisticated filters based on known (or predicted) query features (such as taxonomy, subcellular localization, structural context) are used to narrow down the results lists, which can be very long lists of potential matches due to the short lengths of ELMs. This resource has incorporated four entries related to the LIR-motif (since May 2014; <http://elm.eu.org/infos/news.html>), while another three are being evaluated as candidate ELM additions (Table 3). Again, the ELM resource displays matches to any motifs and users are left with the decision as to which of them are worth studying further. ELM is developed/maintained by a consortium of European groups coordinated by the European Molecular Biology Laboratory and is freely available online at the URL <http://elm.eu.org>.

Molecular modeling of interactions between Atg8-family proteins and LIR-containing proteins. The availability of several sets of experimental data on LIR-containing proteins, the 3-dimensional structure of their complexes, and sequence-based predictors such as iLIR [2513], has been providing the foundations to apply molecular modeling and simulations to the study of the complexes between members of the Atg8-family proteins and LIR-containing proteins. This class of methods can help autophagy research at different levels: i) to provide information on the role of the residues N- and C-terminal from the core LIR motifs for which coordinates are often missing in the available experimental structures; ii) as a guide for experiments to suggest the residue to mutate to

Table 3. Eukaryotic linear motif entries related to the LIR motif.⁴

| ELM identifier | ELM | Description | Status |
|----------------|----------------------------|---|-----------|
| LIG_LIR_Gen_1 | [EDST].{0,2}[WFY]..[ILV] | Canonical LIR motif that binds to Atg8 protein family members to mediate processes involved in autophagy. | ELM |
| LIG_LIR_Apic_2 | [EDST].{0,2}[WFY]..P | Apicomplexa-specific variant of the canonical LIR motif that binds to Atg8 protein family members to mediate processes involved in autophagy. | ELM |
| LIG_LIR_Nem_3 | [EDST].{0,2}[WFY]..[ILVFY] | Nematode-specific variant of the canonical LIR motif that binds to Atg8-family protein members to mediate processes involved in autophagy. | ELM |
| LIG_LIR_LC3C_4 | [EDST].{0,2}LVV | Noncanonical variant of the LIR motif that binds to Atg8 protein family members to mediate processes involved in autophagy. | ELM |
| LIG_AIM | [WY]..[ILV] | Atg8-family protein interacting motif found in Atg19, SQSTM1, ATG4B and CALR (calreticulin), involved in autophagy-related processes. | Candidate |
| LIG_LIR | WxxL or [WYF]xx[LIV] | The LIR might link ubiquitinated substrates that should be degraded to the autophagy-related proteins in the phagophore membrane. | Candidate |
| LIG_GABARAP | W.FL | GABA _A receptor binding to clathrin and CALR; possibly linked to trafficking. | Candidate |

validate structure-based hypotheses; iii) to provide a structure-based rationale of available experimental data and shed light on determinants of specificity towards different members of the Atg8-family proteins; and iv) to help in the identification of the best LIR-containing candidates for experimental validation in case of multi-domain proteins with several predicted LIRs [1258,2516,2517]. In approaching modeling and simulations studies of the Atg8-family protein-LIR complexes, it is important to have a careful design of the modeling and simulation protocol, selection of the physical model (i.e., force field) to employ to describe the complex structure and dynamics, and use, where possible, multiple models with different conformations of the LIR-containing region in the Atg8-family protein binding pockets to avoid limitation due to the sampling of the conformational space accessible to classical molecular dynamics simulations.

The ncRNA-associated cell death database (ncRDeathDB). The noncoding RNA (ncRNA)-associated cell death database (ncRDeathDB) [2518], most recently developed at the Harbin Medical University (Harbin, China) and Shantou University Medical College (Shantou, China), documents a total of more than 4,600 ncRNA-mediated programmed cell death entries. Compared to previous versions of the miRDeathDB [2519-2521], the ncRDeathDB further collected a large amount of published data describing the roles of diverse ncRNAs (including microRNA, long noncoding RNA/lncRNA and small nucleolar RNA/snoRNA) in programmed cell death for the purpose of archiving comprehensive ncRNA-associated cell death interactions. The current version of ncRDeathDB provides an all-inclusive bioinformatics resource on information detailing the ncRNA-mediated cell death system and documents 4,615 ncRNA-mediated programmed cell death entries (including 1,817 predicted entries) involving 12 species, as well as 2,403 apoptosis-associated entries, 2,205 autophagy-associated entries and 7 necrosis-associated entries. The ncRDeathDB also integrates a variety of useful tools for analyzing RNA-RNA and RNA-protein binding sites and for network visualization. This resource will help researchers to visualize and navigate current knowledge of the noncoding RNA component of cell death and autophagy, to uncover the generic organizing principles of ncRNA-associated cell death systems, and to generate valuable biological hypotheses. The ncRNA-associated cell death interactions resource is publicly available online at the URL <http://www.rna-society.org/ncrdeathdb>.

Predicting impact for autophagy-related gene copy number alterations in cancer. Autophagy is tumor suppressive, yet can also exert pro-survival effects once tumors have been established. The HAPTRIG R tool developed at UCSD uses a curated data set of autophagy genes to predict the functional impact of increases and decreases of genes in the autophagy pathway in cancer [2522]. This tool is useful for determining deficiencies in autophagy among tumor types, as well as for individual tumors within a tumor type. The tool also can prioritize which genes most influence autophagy within a dataset based on protein-protein interactions and haploinsufficiency data. These prioritized genes can then be the subject

of further experimentation. The Shiny application of this tool is available at the URL https://delaney.shinyapps.io/haptrig_single_pathway_networks.

KFERQ finder. There is a growing interest in studying CMA due to its fundamental regulatory role in the physiopathology of diverse cellular processes [2523]. Substrate selectivity is one of the main features of CMA, which relies on the recognition by HSPA8 of KFERQ-like motifs in the sequence of the proteins to be degraded [2524]. Therefore, a reliable, quick and high-throughput method has been developed to find these motifs. This tool (KFERQ finder) allows the identification of KFERQ-like motifs in any given protein of the human, mouse and rat proteomes using their Uniprot ID. Furthermore, multiple proteins can be analyzed uploading the Uniprot IDs in a .csv file, and, finally, the search can be also performed in protein sequences [1809]. The KFERQ finder is available at the URL <http://tinyurl.com/kferq>.

Autophagy to Disease (ATD). Autophagy to Disease (ATD) is a comprehensive bioinformatics resource for deciphering the association of autophagy and diseases. The Liao group developed ATD (<http://auto2disease.nwsuafilmz.com>) to archive autophagy-associated diseases. This resource provides a bioinformatics annotation system about genes, chemicals, autophagy and human diseases by extracting results from previous studies with text mining technology. Based on ATD, some classes of disease tend to be related with autophagy, including respiratory diseases, cancer, urogenital diseases and digestive system diseases. In addition, some classes of autophagy-related diseases have a strong association among each other and constitute modules. Furthermore, by extracting autophagy-disease-related genes from ATD, a novel algorithm was generated, Optimized Random Forest with Label model, to predict potential autophagy-disease-related genes. This bioinformatics annotation system about autophagy and human diseases may provide a basic resource for the further detection of the molecular mechanisms of autophagy as they relate to disease.

LysoQuant. A seven-layer convolutional network with U-Net architecture was trained by Molinari's lab to perform segmentation and classification of individual lysosomes from confocal images with human-level accuracy. This approach, termed LysoQuant, offers quantitative analyses of lysosome number, size, shape, position and occupancy with cargo (i.e., proteins or organelles to be cleared from cells). These parameters eventually inform on activity of lysosome-driven pathways including autophagy at the molecular level and on consequences of genetic or environmental modifications [2525]. LysoQuant is freely available at <http://www.imaging.irb.usi.ch/lysoquant>.

Mathematical models of autophagy dynamics

The idea of using mathematical modeling to characterize the population dynamics of autophagosomes and other vesicles involved in autophagy (e.g., autolysosomes) was discussed as early as 1975 [1529,1530]. However, realization of this idea occurred only much later, after methods became available to

precisely monitor changing autophagic vesicle populations in individual cells [2526,2527]. Present and increasing opportunities to generate quantitative data make further modeling work timely, as do compelling needs to better understand the spatiotemporal dynamics of the subcellular structures affected by and mediating autophagy as well as the system-level behaviors of the molecular networks that regulate autophagy, which contain numerous potential drug targets relevant for diverse diseases [2528]. Because even simple mathematical models have proven to be powerful aids for reasoning about biological systems [2529], we strongly encourage greater use of mathematical modeling in studies of autophagy.

In recent years, several autophagy-relevant mathematical models have been developed and analyzed to study a range of subjects, including the cell fate decision between autophagy and apoptosis [2530-2532], the role of feedback loops in cellular regulatory networks and the possibility of bifurcations in qualitative system-level behavior [2533-2535], autophagy-related gene expression dynamics [2536], mitophagy [2537,2538], pexophagy [2539], and the design of drug interventions for manipulating autophagy [2540].

Mathematical modeling can be, and is, pursued through a rich variety of techniques [2541], and new methods, together with enabling software tools [2542], continue to emerge regularly. The method that one selects for a particular study should be well-matched to the question(s) being asked; the appropriate level of abstraction is invariably context-dependent. Methods specialized for modeling dynamic compartments [2543] and biomolecular site dynamics [2544] may be of special interest in autophagy studies.

Although these modeling processes carry limitations in terms of complexity and portraiture of the realistic biological phenomenon, they can simultaneously be used to study a biological system where the goal is to unveil the underlying principles that are veiled at different levels of description. Various types of mathematical models can be used to study the autophagy process that includes ordinary, partial and stochastic differential equations. Ordinary differential equations/ODE are the simplest form to model a biological system where the focus is to study autophagy dynamics with respect to change in the protein/metabolite concentration [2530, 2532, 2540, 2545-2548]. Partial differential equations/PDE can be an important approach to model autophagy-dependent processes such as autophagy-dependent motility, an area yet to be explored in autophagy. To study the randomness imposed by the generation and variability of different stresses and continuous fluctuations in cellular energy levels, stochastic modeling techniques can be applied [2527,2549]. Autophagy dynamics can also be studied in a discrete-based approach using agent-based modeling [2526,2537]. Another useful modeling tool is petri net (place/transition) [2550], which is capable of modeling both discrete and continuous types of autophagy in cellular biochemical reactions [2551].

In brief, some of the most important, general guidelines for good modeling practice are as follows: Whenever possible, model development and analysis should be tightly integrated with experimental efforts [2552], and model analysis should be directed at generating non-obvious insights and testable predictions, not simply at reproducing phenomenology. Of

course, models have purposes beyond prediction, for example, in capturing knowledge and providing explanations, in exposing knowledge gaps, and in determining the logical consequences of assumptions [2553-2555]. Models should be made shareable and reusable—for this purpose, standardized model-definition formats [2556,2557], means for encoding simulation protocols [2558,2559], and online databases [2560] have been developed. The problem of estimating the values of model parameters is an incessant concern of modelers. Some have recommended that this task is best accomplished through curve fitting versus direct measurement [2561,2562]. In any case, uncertainties of parameter estimates and model predictions should be quantified, which is, arguably, best accomplished via Bayesian methods [2563,2564]. These methods are not always practical because of their computational expense; however, alternative, less computationally expensive approaches are available [2565]. Reproducibility of modeling, a growing concern [2566,2567], is enhanced when general-purpose software compatible with established standards is used for simulations, curve fitting, uncertainty quantification, etc.

For the beginner, excellent, fairly comprehensive introductions to systems biology modeling are available [2568, 2569], and short courses are also available [2570].

As one specific example, mathematical models minimizing the membrane bending energy show that phagophore expansion, which elongates the length of the energetically expensive phagophore edge, is sufficient to drive remodeling of the initially flat phagophore into a curved shape [2571]. Furthermore, geometric considerations indicate that several hundred or thousands of vesicles are required to form a single autophagosome [2572]. The absence of comparable vesicle numbers implies that vesicles provide a minor autophagosomal membrane source.

Conclusions and future perspectives

There is no question that research on the topic of autophagy has expanded dramatically since the publication of the first set of guidelines [3]. To help keep track of the field we have published a glossary of autophagy-related molecules and processes [2573,2574], and now include the glossary as part of these guidelines.

With this continued influx of new researchers, we think it is critical to try to define standards for the field. Accordingly, we have highlighted the uses and caveats of an expanding set of recommended methods for monitoring autophagy in a wide range of systems (Table 4). Importantly, investigators need to determine whether they are evaluating levels of early or late autophagic compartments, or autophagic flux. If the question being asked is whether a particular condition changes autophagic flux (i.e., the rate of delivery of autophagy substrates to lysosomes or the vacuole, followed by degradation and efflux), then assessment of steady state levels of autophagosomes (e.g., by counting GFP-LC3 puncta, monitoring the amount of LC3-II without examining turnover, or by single time point electron micrographs) is not sufficient as an isolated approach. In this case it is also necessary to directly

Table 4. Recommended methods for monitoring autophagy.⁵

| Method | Description |
|--|---|
| 1. Atg8-family protein western blotting | Western blot. The analysis is carried out in the absence and presence of lysosomal protease or fusion inhibitors to monitor flux; an increase in the LC3-II amount in the presence of the inhibitor is usually indicative of flux. |
| 2. Atg18 oligomerization | FRET stopped-flow assay, chemical cross-linking, mass spectrometry. |
| 3. Autophagic protein degradation | Turnover of long-lived proteins to monitor flux. |
| 4. Autophagic sequestration assays | Accumulation of cargo in autophagic compartments in the presence of lysosomal protease or fusion inhibitors by biochemical or multilabel fluorescence techniques. |
| 5. Autophagosome quantification | FACS/flow cytometry. |
| 6. Autophagosome-lysosome colocalization | Fluorescence microscopy. and dequenching assay |
| 7. Bimolecular fluorescence complementation | Can be used to monitor protein-protein interaction in vivo. |
| 8. Degradation of endogenous lipofuscin | Fluorescence microscopy. |
| 9. Electron microscopy | Quantitative electron microscopy, immuno-TEM; monitor autophagosome number, volume, and content/cargo. |
| 10. FRET | Interaction of LC3 with gangliosides to monitor autophagosome formation. |
| 11. GFP-Atg8-family protein fluorescence | Fluorescence microscopy, flow cytometry to microscopy monitor vacuolar/lysosomal localization. Also, increase in punctate GFP-Atg8-family protein or Atg18/WIPI, and live time-lapse fluorescence microscopy to track the dynamics of GFP-Atg8-family protein-positive structures. |
| 12. GFP-Atg8-family protein lysosomal | Western blot \pm lysosomal fusion or delivery and proteolysis degradation inhibitors; the generation of free GFP indicates lysosomal/vacuolar delivery. |
| 13. Immunofluorescence for endogenous LC3 | Can be used to identify puncta autophagosomes in cells difficult to transfect with a GFP-LC3 chimera. |
| 14. Keima | Confocal microscopy, flow cytometry, western blotting to monitor transfer of Keima or various Keima fusion variants to acidic and proteolytically active environments |
| 15. MTOR, AMPK and Atg1/ULK1 kinase activity | Western blot, immunoprecipitation or kinase assays. |
| 16. Pex14-GFP, GFP-Atg8, Om45-GFP, | A range of assays can be used to monitor mitoPho8 Δ 60 selective types of autophagy. These typically involve proteolytic maturation of a resident enzyme or degradation of a chimera, which can be followed enzymatically or by western blot. |
| 17. Sequestration and processing assays | Chimeric RFP fluorescence and processing, in plants and light and electron microscopy. |
| 18. SQSTM1- and related LC3-binding protein | The amount of SQSTM1 increases when turnover autophagy is inhibited and decreases when autophagy is induced, but the potential impact of transcriptional and/or translational regulation or the formation of insoluble aggregates should be addressed in individual experimental systems. |
| 19. Tandem mRFP/mCherry-GFP fluorescence | Flux can be monitored as a decrease in microscopy, Rosella green/red (yellow) fluorescence (phagophores, autophagosomes) and an increase in red fluorescence (autolysosomes). |
| 20. Tissue fractionation | Centrifugation, western blot and electron microscopy. |
| 21. Transcriptional and translational regulation | Northern blot, or RT-PCR, autophagy-dedicated microarray. |
| 22. Turnover of autophagic compartments | Electron microscopy with morphometry/stereology at different time points. |
| 23. WIPI fluorescence microscopy | Quantitative fluorescence analysis using endogenous WIPI proteins, or GFP- or MYC-tagged versions. Suitable for high-throughput imaging procedures. |

measure the flux of autophagosomes and/or autophagy cargo (e.g., in wild-type cells compared to autophagy-deficient cells, the latter generated by treatment with an autophagy inhibitor or resulting from ATG gene knockdowns or knockouts). Collectively, we strongly recommend the use of multiple assays whenever possible, rather than relying on the results from a single method.

As a final reminder, we stated at the beginning of this article that this set of guidelines is not meant to be a formulaic compilation of rules, because the appropriate assays depend in part on the question being asked and the system being used. Rather, these guidelines are presented primarily to emphasize key issues that need to be addressed such as the difference between measuring autophagy components, and flux or substrate clearance; they are not meant to constrain imaginative approaches to monitoring autophagy. Indeed, it is hoped that new methods for monitoring autophagy will continue to be developed, and new findings may alter our view of the current assays. This is a dynamic field, much like the process of autophagy, and we need to remain flexible in the standards we apply.

For those on the move, a Quick Guide to autophagy is provided below.

Glossary

2-D08: An inhibitor of protein SUMOylation that induces autophagy-mediated cancer cell death [2673].

2-Methoxyestradiol (2-ME): 2-ME is a natural metabolite of estrogen that prevents angiogenesis and tumor progression. 2-ME regulates autophagy through mechanisms that involve both ROS production [2674] and MAPK/JNK-DRAM pathway activation [2675].

3-MA: See 3-methyladenine, and appear to induce autophagy [3ine].

3-Methyladenine (3-MA): An inhibitor of class I PI3K and class III PtdIns3K, which results in autophagy inhibition due to suppression of class III PtdIns3K [435], but may under some conditions show the opposite effect [436, 437, 1749]. At concentrations >10 mM 3-MA inhibits other kinases such as AKT (Ser473), MAPK/p38 (Thr180/Tyr182) and MAPK/JNK (Thr183/Tyr185) [2676].

3BDO (3-benzyl-5-[2-nitrophenoxy] methyl)-dihydrofuran-2 [3 h]-one): A novel MTOR activator that occupies the rapamycin-binding site and blocks the interaction between rapamycin and FKBP1A, and then activates the MTOR signaling pathway to inhibit autophagy initiation [2677].